

UNCLASSIFIED

AD NUMBER

AD378484

CLASSIFICATION CHANGES

TO: unclassified

FROM: confidential

LIMITATION CHANGES

TO:  
Approved for public release, distribution  
unlimited

FROM:  
Distribution: Controlled: all requests to  
Director of Supersonic Transport  
Development, Federal Aviation Agency,  
Washington, D. C. 20553.

AUTHORITY

30 Sep 1978, Group-4; FAA, per DTIC Form  
55, dtd 20 Dec 2002

THIS PAGE IS UNCLASSIFIED

✓  
**CONFIDENTIAL**

**SUPERSONIC TRANSPORT  
PHASE III PROGRAM**



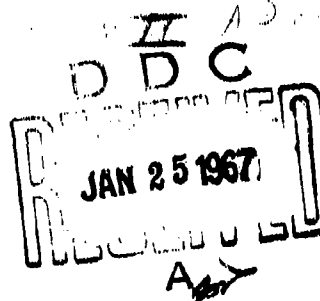
378484

**GE4 SST**

✓ **Volume III — Technical/Engine**

✓ **B. ENGINE DESIGN REPORT**

✓ **PART I — Major Components**



6 September 1966

FAA SECURITY CONTROL  
NO. 67272

FLIGHT PROPULSION DIVISION

**GENERAL  ELECTRIC**

**CONFIDENTIAL**

LYNN, MASSACHUSETTS/CINCINNATI, OHIO

✓  
AUG FILE COPY

### NOTICES

When Government drawings, specifications, or other data are used for any purpose other than in connection with a definitely related Government procurement operation, the United States Government thereby incurs no responsibility nor any obligation whatsoever; and the fact that the Government may have formulated, furnished, or in any way supplied the said drawings, specifications, or other data, is not to be regarded by implication or otherwise as in any manner licensing the holder or any other person or corporation, or conveying any rights or permission to manufacture, use, or sell any patented invention that may in any way be related thereto.

All distribution of this document is controlled. In addition to security requirements which apply to this document and must be met, it may be further distributed by the holder only with specific prior approval of:

Director of Supersonic Transport Development  
Federal Aviation Agency  
Washington, D. C. 20553

The distribution of this report is limited because it contains technology identifiable with items excluded from export by the Department of State (U. S. Export Control Act of 1949, as amended).

ADDITIONAL FOR	
COPY	WHITE & RED <input type="checkbox"/>
ODC	DEF <input checked="" type="checkbox"/>
UNANNOUNCED	
JUSTIFICATION	
BY .....	
DISTRIBUTION/AVAILABILITY	
DIST.	AVAIL. and
15	

CONFIDENTIAL

⑥  
SUPERSONIC TRANSPORT  
PHASE III PROGRAM.

Volume III—Technical/Engine,  
B. ENGINE DESIGN REPORT.  
PART I—Major Components ⑧

⑪⑤ FA-SS-66-6

DOWNGRADED AT 3 YEAR INTERVALS  
DECLASSIFIED AFTER 12 YEARS  
DOD DIR 5200.10

This document contains information affecting the national defense of the United States within the meaning of the Espionage Laws, Title 18 U.S.C., Section 793 and 794, its transmission or the revelation of its contents in any manner to an unauthorized person is prohibited by law.

⑪ 6 Sep 66

⑫ 469p.

FLIGHT PROPULSION DIVISION

GENERAL  ELECTRIC

LYNN, MASSACHUSETTS/CINCINNATI, OHIO

CONFIDENTIAL

mt  
(400 266)



#### **PATENT SECRECY NOTICE**

Portions of information contained herein are under secrecy orders issued by the Commissioner of Patents in accordance with 35 U.S.C. 161-188. Permission has been obtained to disclose this information to authorized persons on a "Need-To-Know" basis. Anyone receiving the information must be of known loyalty and discretion, and must be notified of the existence of the secrecy orders. Disclosure of the information to any unauthorized person is punishable by a fine of up to \$10,000 or imprisonment for up to two years, or both.

**GENERAL ELECTRIC COMPANY**  
**SUPERSONIC TRANSPORT DEVELOPMENT PROGRAM**  
**PHASE III PROPOSAL & SUBSTANTIATING DATA**

**LIST OF BOOKS**

**Proposal**

**Proposal Supplement - Airframe/Engine Contractor Agreement**

**Volume I - Summary**

**Volume III - Technical/Engine - GE4/J5P Engine Specifications - Boeing**

**Volume III - Technical/Engine - GE4/J5M Engine Specifications - Lockheed**

**Volume III - Technical/Engine - GE4/J5P Performance Bulletin - Boeing (R66FPD231)**

**Volume III - Technical/Engine - GE4/J5M Performance Bulletin - Lockheed (R66FPD232)**

**Volume III - Technical/Engine - Component Procurement Specifications**

**Volume III - Technical/Engine - A. Engine Performance Report**

**Volume III - Technical/Engine - B. Engine Design Report - Part I - Major Components**

**Volume III - Technical/Engine - B. Engine Design Report - Part II - Controls and Accessories**

**Volume III - Technical/Engine - B. Engine Design Report - Part III - Fuel and Lube Systems**

**Volume III - Technical/Engine - C. Noise and Suppression Report**

**Volume III - Technical/Engine - D. Installation & Inlet System Report**

**Volume III - Technical/Engine - E. Test and Certification Plan Report**

**Volume III - Technical/Engine - F. Manufacturing Techniques & Materials Report**

**Volume III - Technical/Engine - G. Growth Potential Report**

**Volume IV - System Integration - Part I - Operations and Test**

**Volume IV - System Integration - Part II - Product Assurance**

**Volume V - Management and Manufacturing - Part I - General Management Plans**

**Volume V - Management and Manufacturing - Part II - Manufacturing & Facilities Plans**

**Volume VI - Costs**

# TABLE OF CONTENTS

Section	Title	Page
1.	INTRODUCTION .....	1-1
2.	COMPRESSOR .....	2-1
2.1	INTRODUCTION AND SUMMARY .....	2-1
2.2	DESIGN REQUIREMENTS AND APPROACH .....	2-6
2.3	DESIGN DESCRIPTION .....	2-8
2.3.1	Blading Aeromechanical and Dovetails .....	2-8
2.3.2	Rotor Construction .....	2-27
2.3.3	Disks/Spacers .....	2-29
2.3.4	Cooling .....	2-40
2.3.5	Air Seals .....	2-43
2.3.6	Stator Casing .....	2-47
2.3.7	Blade Containment .....	2-54
2.3.8	Vanes and Shrouds .....	2-57
2.3.9	Actuation System .....	2-66
2.3.10	Maintainability .....	2-72
2.3.11	Reliability .....	2-76
2.3.12	Quality Assurance .....	2-77
2.3.13	Safety .....	2-78
2.3.14	Failure Analysis .....	2-79
2.3.15	Value Engineering .....	2-79
2.3.16	Human Engineering .....	2-79
2.3.17	Standardization .....	2-81
2.4	DEVELOPMENT STATUS .....	2-82
2.4.1	Full Scale Compressor Test .....	2-82
2.4.2	Engine Testing .....	2-87
3.	PRIMARY COMBUSTOR .....	3-1
3.1	INTRODUCTION AND SUMMARY .....	3-1
3.2	DESIGN REQUIREMENTS AND APPROACH .....	3-9
3.2.1	Combustor Inlet and Outlet Conditions .....	3-9
3.2.2	Combustor Liner Durability .....	3-10
3.2.3	Flight Profile, T <sub>3</sub> , T <sub>4</sub> and Durability .....	3-10
3.2.4	Stress Rupture .....	3-13
3.2.5	Thermal Stress and Low Cycle Fatigue .....	3-15
3.2.6	Vibratory Loads and Fatigue .....	3-16
3.2.7	Gas Loads and Maneuver Loads .....	3-20
3.2.8	Buckling Loads .....	3-20
3.2.9	Resistance to Sliding Contact Wear .....	3-23
3.2.10	Fuel Nozzles .....	3-23
3.3	DESIGN DESCRIPTION .....	3-23
3.3.1	Mounting System .....	3-23
3.3.2	Cowl Stiffening Structure .....	3-25
3.3.3	Aft Seals .....	3-25
3.3.4	Cooling Slot Construction .....	3-25
3.3.5	Dome Construction .....	3-35

## TABLE OF CONTENTS (Continued)

*Compressor; primary combustor;*

Section	Title	Page
3.3.6	Skirt Construction .....	3-35
3.3.7	Fuel Nozzles .....	3-39
3.3.8	Material .....	3-39
3.3.9	Maintainability .....	3-43
3.3.10	Reliability .....	3-48
3.3.11	Quality Assurance .....	3-49
3.3.12	Safety .....	3-50
3.3.13	Failure Analysis .....	3-50
3.3.14	Value Engineering .....	3-50
3.3.15	Human Engineering .....	3-53
3.3.16	Standardization .....	3-53
3.4	DEVELOPMENT STATUS .....	3-53
3.5	SUPPORTING TECHNOLOGY .....	3-54
3.5.1	J93 Combustor .....	3-54
3.5.2	J93/SST Turbine Demonstrator .....	3-55
3.5.3	J97 Combustor .....	3-55
3.5.4	High-temperature Turbine Rig .....	3-56
4.	<i>TURBINE; augmentor; exhaust nozzle and thrust reverser;</i> .....	4-1
4.1	INTRODUCTION .....	4-1
4.1.1	Evolution of the Turbine Design .....	4-1
4.1.2	Evolution of the Turbine Vane Design .....	4-1
4.1.3	Evolution of the Turbine Blade Design .....	4-6
4.1.4	Turbine Temperature .....	4-6
4.2	DESIGN REQUIREMENTS AND APPROACH .....	4-9
4.2.1	Gas Temperature - Metal Temperature .....	4-11
4.2.2	Life .....	4-16
4.3	DESIGN DESCRIPTION .....	4-20
4.3.1	Turbine Stator Design .....	4-20
4.3.2	Turbine Rotor Design .....	4-27
4.3.3	Turbine Blades .....	4-34
4.3.3.1	Thermal Fatigue .....	4-34
4.3.3.2	Mechanical Fatigue .....	4-43
4.3.3.3	Erosion and Foreign Object Damage .....	4-48
4.3.3.4	Hole Clogging .....	4-51
4.3.3.5	Containment .....	4-52
4.3.4	Turbine Cooling .....	4-52
4.3.5	Maintainability .....	4-56
4.3.6	Reliability .....	4-64
4.3.7	Quality Assurance .....	4-64
4.3.8	Safety .....	4-67
4.3.9	Failure Analysis .....	4-68
4.3.10	Value Engineering .....	4-68
4.3.11	Human Engineering .....	4-70
4.3.12	Standardization .....	4-71

*⇒ to page iv*


## TABLE OF CONTENTS (Continued)

Section	Title	Page
4.4	DEVELOPMENT STATUS.....	4-71
4.4.1	Review of the Development Program.....	4-71
4.4.2	GE4 Engine Testing.....	4-72
4.4.3	J93/SST Demonstrator Engine Program.....	4-72
4.5	SUPPORTING TECHNOLOGY.....	4-90
4.5.1	Manufacturing and Process Development.....	4-90
4.5.2	Related Development Testing.....	4-93
5.	AUGMENTOR.....	5-1
5.1	MECHANICAL COMPONENTS.....	5-1
5.1.1	Introduction.....	5-1
5.1.2	Comparison with Other Gas Turbine Combustion.....	5-5
5.1.3	General Description.....	5-21
5.1.4	Design Requirements.....	5-25
5.1.5	Design Approach and Criteria.....	5-26
5.1.6	Design Description.....	5-33
5.1.6.1	Spacer Ring Subassembly.....	5-34
5.1.6.2	Exhaust Casing and Cooling Liner.....	5-45
5.1.6.3	Inner Cone.....	5-56
5.1.6.4	Maintainability.....	5-56
5.1.6.5	Reliability.....	5-58
5.1.6.6	Quality Assurance.....	5-60
5.1.6.7	Safety.....	5-60
5.1.6.8	Failure Analysis.....	5-61
5.1.6.9	Value Engineering.....	5-61
5.1.6.10	Human Engineering.....	5-62
5.1.6.11	Standardization.....	5-62
5.1.7	Development Status.....	5-62
5.1.8	Supporting Technology.....	5-70
5.2	FUEL INJECTION SYSTEM.....	5-79
6.	EXHAUST NOZZLE AND THRUST REVERSER.....	6-1
6.1	INTRODUCTION AND SUMMARY.....	6-1
6.2	GENERAL DESCRIPTION.....	6-11
6.3	DESIGN REQUIREMENTS.....	6-22
6.4	DESIGN APPROACH.....	6-23
6.5	DESIGN DESCRIPTION.....	6-25
6.5.1	Primary Nozzle.....	6-25
6.5.2	Thrust Reverser.....	6-33
6.5.3	Secondary Nozzle.....	6-53
6.6	MAINTAINABILITY.....	6-60
6.7	NOZZLE/REVERSER MECHANICAL DESIGN SUPPLEMENT.....	6-67

*from p. iii*

## TABLE OF CONTENTS (Continued)

Section	Title	Page
7.	AUGMENTOR AND EXHAUST NOZZLE COOLING .....	7-1
7.1	INTRODUCTION AND SUMMARY .....	7-1
7.2	GENERAL DESCRIPTION .....	7-7
7.3	DESIGN REQUIREMENT .....	7-9
7.3.1	Component Skin Temperatures .....	7-9
7.3.2	Internal Cooling Air - From Engine Cycle .....	7-10
7.3.3	External Cooling Air - Secondary and Tertiary Airflow .....	7-11
7.4	DESIGN APPROACH .....	7-12
7.5	DESIGN DESCRIPTION .....	7-24
7.5.1	System Summary .....	7-24
7.5.2	Augmentor Liner and Casing .....	7-25
7.5.3	Primary Nozzle .....	7-25
7.5.4	Secondary Nozzle Cooling .....	7-38
8.	MAIN SEALS AND BEARINGS .....	8-1
8.1	SUMMARY .....	8-1
8.2	DESIGN REQUIREMENTS AND APPROACH .....	8-1
8.3	DESIGN DESCRIPTION .....	8-2
8.3.1	Seal Design Philosophy .....	8-2
8.3.2	No. 1 Sump .....	8-4
8.3.3	No. 2 Sump .....	8-10
8.3.4	No. 3 Sump .....	8-10
8.3.5	Rotor Thrust Balance System .....	8-11
8.3.6	Maintainability .....	8-14
8.3.7	Reliability .....	8-19
8.3.8	Quality Assurance .....	8-19
8.3.9	Safety .....	8-20
8.3.10	Failure Analysis .....	8-20
8.3.11	Value Engineering .....	8-20
8.3.12	Human Engineering .....	8-21
8.3.13	Standardization .....	8-21
8.4	DEVELOPMENT STATUS .....	8-22
8.4.1	Work Accomplished .....	8-22
8.4.2	Work in Process .....	8-29
8.5	SUPPORTING TECHNOLOGY .....	8-30
8.5.1	Carbon Face Seals .....	8-30
8.5.2	Bearings .....	8-30
9.	ACCESSORY DRIVES .....	9-1
9.1	SUMMARY .....	9-1
9.2	DESIGN REQUIREMENTS AND APPROACH .....	9-1
9.3	DESIGN DESCRIPTION .....	9-1
9.3.1	Gearbox Accessory Arrangement .....	9-6
9.3.2	Gearbox Mounting System .....	9-7
9.3.3	Bevel and Spur Gears .....	9-7

*frames AND Structure* 

## TABLE OF CONTENTS (Continued)

Section	Title	Page
9.3.4	Splines .....	9-8
9.3.5	Bearings .....	9-8
9.3.6	Oil Seals .....	9-8
9.3.7	Shafts and Miscellaneous Parts .....	9-9
9.3.8	Gearbox Casings .....	9-9
9.3.9	Maintainability .....	9-10
9.3.10	Reliability .....	9-11
9.3.11	Quality Assurance .....	9-11
9.3.12	Safety .....	9-12
9.3.13	Failure Analysis .....	9-12
9.3.14	Value Engineering .....	9-12
9.3.15	Human Engineering .....	9-13
9.3.16	Standardization .....	9-13
9.4	DEVELOPMENT STATUS .....	9-14
9.4.1	Work Accomplished .....	9-14
9.4.2	Work in Process .....	9-14
9.5	SUPPORTING TECHNOLOGY .....	9-14
9.6	AIRCRAFT COMPANY ACCESSORY DRIVE SYSTEM DETAILS .....	9-17
10.	FRAMES AND STRUCTURES .....	10-1
10.1	INTRODUCTION AND SUMMARY .....	10-1
10.2	DESIGN REQUIREMENTS AND DESIGN APPROACH .....	10-5
10.3	DESIGN DESCRIPTION .....	10-6
10.3.1	Compressor Front Frame .....	10-6
10.3.2	Compressor Rear Frame .....	10-13
10.3.3	Turbine Frame .....	10-23
10.3.4	Maintainability .....	10-28
10.3.5	Reliability .....	10-33
10.3.6	Quality Assurance .....	10-32
10.3.7	Safety .....	10-33
10.3.8	Failure Analysis .....	10-34
10.3.9	Value Engineering .....	10-34
10.3.10	Human Engineering .....	10-34
10.3.11	Standardization .....	10-34
10.4	DEVELOPMENT STATUS .....	10-35
10.4.1	Structures Static Load Test .....	10-35
10.4.2	Structures Vibration Survey Test .....	10-35
10.4.3	Structures Destructive Test .....	10-35
10.4.4	Structures Maintainability and Repairability Tests .....	10-37
10.4.5	Front Frame Strut and IGV - Iceball and Bird Impact Tests .....	10-37
10.4.6	System Flow Test .....	10-37
10.4.7	Evaluation of Noise Suppression Materials/or Device Incorporation in the Compressor Front Frame .....	10-37
10.5	SUPPORTING TECHNOLOGY .....	10-37
10.6	ENGINE STRUCTURAL DYNAMICS .....	10-39
10.6.1	Dynamic Analysis .....	10-39
10.6.2	Description of Analytical Method .....	10-39

## TABLE OF CONTENTS (Continued)

Section	Title	Page
10.6.3	Design Criteria .....	10-39
10.6.4	Engine Dynamic Analysis Results .....	10-39
10.7	AIRFRAME COMPANY DESIGN DETAILS .....	10-43

## LIST OF ILLUSTRATIONS

Figure	Title	Page
2-1	Evolution of High-Stage Loading Compressor .....	2-2
2-2	Cross Section of Compressor -- General Features of Construction .....	2-3
2-3A	Comparison of First Stage Blade - GE4, J93 and J79/CJ805 .....	2-9
2-3B	Comparison of Last Stage Blade - GE4, J93 and J79/CJ805 .....	2-10
2-4	Titanium Diffusion Bonded Hollow Blade Stages 1-6 .....	2-11
2-5	Blade Evolution during Manufacturing Process .....	2-11
2-6	Blade Halves Before Bonding .....	2-12
2-7	Microstructure of Bond .....	2-13
2-8	Stem Drilled Blades Stages 7-9 .....	2-14
2-9	Typical Aeroelastic Stability Map; Accel and Different Flight Conditions .....	2-16
2-10	Rotor Inlet to Aeromechanical Test Rig .....	2-17
2-11	Aeromechanical Compressor Wheel Assemblies .....	2-18
2-12	Distortion Screen .....	2-19
2-13	Shroud Configuration 1st Stage Blade .....	2-20
2-14	J93 First-Stage Shrouded Blade After FOD .....	2-21
2-15	Campbell Diagram Stage 3 Titanium Blade .....	2-22
2-16	Campbell Diagram Stage 7 Inco 718 Blade .....	2-23
2-17	Comparison of Stall Stresses - Rotor Blade .....	2-24
2-18	Typical Blade Squealer Tip .....	2-26
2-19	Goodman Diagram Stage 3 Titanium Blade .....	2-27
2-20	Goodman Diagram Stage 7 Inconel 718 Blade .....	2-28
2-21	Copper-Nickel-Indium Coated Dovetails .....	2-29
2-22	Rotor Construction, GE4 .....	2-30
2-23	J79 Compressor Rotor, - Dowel Bolt Construction .....	2-31
2-24	Comparison of J93 and GE4 Rotors .....	2-32
2-25	Slab-head Hook Bolts .....	2-33
2-26	Rotor Flanges .....	2-34
2-27	Disk Rim Comparison .....	2-35
2-28	Bi-axial Disk Bursting Curves .....	2-36
2-29	Uni-axial Disk Bursting Curves .....	2-37
2-30	Disk Thermal Gradients .....	2-39
2-31	Blade Retention and Dovetail Details, Stages 2-9 .....	2-40
2-32	Stage One Blade Retention Design .....	2-41
2-33	Rotor Cooling Configuration .....	2-42



## LIST OF ILLUSTRATIONS (Continued)

Figure	Title	Page
2-34	Vane Tip Shroud and Interstage Seal .....	2-44
2-35	J93 Shroud and Seal Configuration .....	2-45
2-36	Compressor Discharge Seal Configuration .....	2-46
2-37	Fabricated Casing Detail .....	2-48
2-38	J93 Compressor Front Casing, Fabricated Construction .....	2-49
2-39	Casing Cross Section Showing Split Features .....	2-50
2-40	Interstage Bleed Extraction Ports, Manifold and Outlet Ports .....	2-51
2-41	J93 Compressor Stator Liners Having Experienced Rubs .....	2-52
2-42	Liner Configuration and Attachment to Stator Casing .....	2-53
2-43	Blade Containment Experience and Test Data .....	2-55
2-44	Blade Containment Configuration, Stages 1-3 .....	2-56
2-45	Blade Containment Configuration, Stages 4-9 .....	2-58
2-46	Stage 3 Vane Goodman Diagram .....	2-59
2-47	Stage 7 Vane Goodman Diagram .....	2-60
2-48	OGV Configuration .....	2-61
2-49	Low Versus High Boss Variable Vane Stem Configuration .....	2-62
2-50	Stator Vane Stem Configuration - J79 and J93 .....	2-63
2-51	GE4 Vane Stem Geometry .....	2-64
2-52	Variable Stator Vane Stem Bolt, Self-locking Feature .....	2-65
2-53	Stage 2 and 3 Fixed Stagger Angle Stator Vane Mounting and Stator Vane Stem Configuration .....	2-66
2-54	Typical Vane Tip Shroud Configuration .....	2-67
2-55	J93 Compressor Shroud with Honeycomb Forward and Aft Seals .....	2-68
2-56	Lever Arms -- Actuation Ring Assembly .....	2-68
2-57	GE4 Compressor Front Variable Stators Actuation System-Bellcrank Mechanism .....	2-69
2-58	GE4 Compressor Rear Variable Stators Actuation System-Bellcrank Mechanism .....	2-70
2-59	Actuation Ring and Ring Connector .....	2-71
2-60	J93 Compressor Stator .....	2-73
2-61	Maintainability Features - GE4 Compressor .....	2-74
2-62	Maintainability Features - GE4 Compressor Rotor .....	2-75
2-63	Assembly of Rotor - GE4 Compressor .....	2-80
2-64	GE4 475 Lb/Sec Compressor - Measured Blade Stresses During Stall .....	2-83
2-65	GE4 475 Lb/Sec Compressor - Measured Blade Stresses at Operating Line .....	2-84
2-66	GE4 475 Lb/Sec Compressor - Measured Inlet Distortion Effects .....	2-85
2-67	GE4 475 Lb/Sec Compressor - Measured Inlet Distortion Effects .....	2-86
3-1	Forward Quarter View of GE4 Combustor, Phase II-C .....	3-2
3-2	Aft Quarter View of GE4 Combustor, Phase II-C .....	3-3
3-3	Assembly Drawing of GE4 Combustor, Phase III .....	3-4
3-4	Cutaway View of GE4 Combustor, Phase III .....	3-5
3-5	General Electric Annular Combustors .....	3-7
3-6	GE4 Combustor Diffuser Model Velocity Contours, Phase II-C .....	3-10
3-7	Combustor Inlet and Exit Pressures .....	3-11
3-8	Objective Combustor Discharge Temperature Profile - Sea Level Static .....	3-12
3-9	Combustor Discharge Temperature Profiles - SLS - Measured Versus Objective .....	3-13

## LIST OF ILLUSTRATIONS (Continued)

Figure	Title	Page
3-10	Objective Combustor Discharge Temperature Profile - 45,000 ft, $M_p$ 1.5 .....	3-14
3-11	Objective Combustor Discharge Temperature Profile - 65,000 ft, $M_p$ 2.7 .....	3-15
3-12	Combustor Discharge Temperature Profiles - 65,000 ft, $M_p$ - Measured Versus Objective .....	3-16
3-13	Comparison of GE4 Combustor Skin Temperature with other General Electric Combustors .....	3-17
3-14	CJ805 Combustion Liners after 3,000 Hours of Operation .....	3-18
3-15	Effect of Temperature on Stress Rupture Life .....	3-19
3-16	Braze Reinforcement as Applied to the J93 Design .....	3-20
3-17	Set Up for Vibration Test of Combustor .....	3-21
3-18	Gas Load Distribution, SL - 0.6 $M_p$ , Phase II-C Combustor .....	3-22
3-19	Cutaway View of Combustor Mount, Phase III .....	3-24
3-20	View of Combustor Showing Truss in Cowl, Phase II-C .....	3-26
3-21	Combustor/Turbine Air Seals .....	3-27
3-22	Cooling Slot Configuration .....	3-28
3-23	TF39 Liner Temperatures - Measured Versus Calculated (Aft Outer Liner) .....	3-30
3-24	Predicted GE4 Liner Temperatures (Aft Outer Panel) .....	3-31
3-25	Approximate Cooling Air Distribution - GE4, Phase II-C Combustor .....	3-32
3-26	Typical 8-inch-diameter Liner Specimen for Thermal Cycle Endurance Test .....	3-33
3-27	Thermal Cycle Endurance Test Rig .....	3-34
3-28	View of Combustor Swirl Cups, Phase II-C .....	3-36
3-29	Stock Thicknesses of Inner and Outer Combustor Skirts, Phase II-C .....	3-37
3-30	TF39 Combustor Buckling Test .....	3-41
3-31	Air Entry Holes in the Primary Combustion Zone .....	3-42
3-32	GE4 Fuel Nozzle .....	3-42
3-33	Exploded View of the Combustor .....	3-44
3-34	GE4 Disassembly and Replacement Features .....	3-45
3-35	Damage and Repair Sequence Showing Repairability of Combustor Wall .....	3-46
3-36	T64 Take-apart Combustion Liner .....	3-47
3-37	Study Design for Improved Maintenance .....	3-49
3-38	Broscope Inspection Schematic .....	3-51
4.1-1	GE4 Turbine .....	4-1
4.1-2	Family of Turbines .....	4-2
4.1-3	Evolution of General Electric Designs .....	4-3
4.1-4	GE4 Turbine Cooling System .....	4-4
4.1-5	Evolution of Turbine Nozzle Cooling .....	4-5
4.1-6	Airfoil Cooling .....	4-5
4.1-7	Evolution of Turbine Blade Design .....	4-7
4.1-8	Metal Temperature Comparison .....	4-8
4.2-1	Time/Temperature Distribution .....	4-10
4.2-2	Typical Route-Segment Definition .....	4-10
4.2-3	Acceleration and Deceleration Transients .....	4-11
4.2-4	Gas Temperature - Metal Temperature Profiles - Blades .....	4-12
4.2-5	Gas Temperature - Metal Temperature Profiles - Vanes .....	4-13
4.2-6	Turbine Inlet Gas Temperature Pattern .....	4-14
4.2-7	Section Metal Temperature Summary - Blades .....	4-15
4.2-8	Section Metal Temperature Summary - Vanes .....	4-15
4.2-9	Stress - Metal Temperature - Life .....	4-16

## LIST OF ILLUSTRATIONS (Continued)

Figure	Title	Page
4.2-10	Blade Creep Life Summary .....	4-17
4.2-11	Turbine Metal Temperature Summary .....	4-18
4.2-12	Stator Assembly Life Plot .....	4-19
4.2-13	Rotor Assembly Life Plot .....	4-19
4.3-1	Turbine Stator Layout .....	4-20
4.3-2	First-Stage Turbine Nozzle Assembly .....	4-21
4.3-3	Second-Stage Turbine Nozzle Assembly .....	4-21
4.3-4	Turbine Radial Clearance Summary .....	4-22
4.3-5	Turbine Vane Isometric .....	4-23
4.3-6	Turbine Vane Section Temperature .....	4-24
4.3-7	Stator Vane Temperature - Surface Pattern .....	4-25
4.3-8	Stator Shrouds .....	4-26
4.3-9	Shroud Rub Facility .....	4-26
4.3-10	Shroud Rub Test Panel .....	4-26
4.3-11	Oxidation and Erosion Test Panels .....	4-27
4.3-12	Turbine Rotor Layout .....	4-28
4.3-13	Turbine Rotor Materials .....	4-30
4.3-14	Wheel and Blade Stress Summary .....	4-31
4.3-15	Turbine Rotor Rim Detail .....	4-32
4.3-16	Turbine Wheel Cyclic Stress Comparison .....	4-32
4.3-17	Turbine Rotor - Exploded Assembly View .....	4-33
4.3-18	Turbine Blade Details .....	4-35
4.3-19	Turbine Blade Isometric .....	4-36
4.3-20	Turbine Blade Section Temperature .....	4-36
4.3-21	Blade Temperature - Surface Pattern .....	4-37
4.3-22	Blade Cyclic Life .....	4-38
4.3-23	Metal Temperature Response - Solid Versus Impingement-Cooled Edge .....	4-39
4.3-24	Edge to Mid-Chord Temperature Differences .....	4-39
4.3-25	Thermal Stress Temperature Transients on Solid Blades .....	4-40
4.3-26	CJ805 Blade Thermal Fatigue .....	4-40
4.3-27	Thermal Fatigue - Cyclic Life Correlation with Thermal Stress .....	4-41
4.3-28	J93/SST Cyclic Test Blade .....	4-42
4.3-29	GE4/J5 Transient Summary .....	4-42
4.3-30	Cyclic Life Variables .....	4-43
4.3-31	Alternating Blade Stress .....	4-44
4.3-32	Blade Stress-Distribution Testing .....	4-45
4.3-33	Nodal Pattern Determination .....	4-45
4.3-34	Hot-Fatigue Testing .....	4-46
4.3-35	Blade Vibration Test Facility .....	4-46
4.3-36	Second-Stage Blade Shroud .....	4-47
4.3-37	Blade Tip Erosion, Uncoated Airfoil .....	4-48
4.3-38	Blade Tip Erosion, Coated Airfoil .....	4-48
4.3-39	Blade Tip Contour CJ805 Versus GE4 .....	4-49
4.3-40	FOD Impact Damage .....	4-50
4.3-41	Dirt Ingestion Test .....	4-51
4.3-42	Hole Clogging - Turbine Vanes from Dirt Ingestion Engine .....	4-51
4.3-43	Containment Test Facility .....	4-52
4.3-44	Containment Test Results .....	4-52

## LIST OF ILLUSTRATIONS (Continued)

Figure	Title	Page
4.3-45	Cooling Effectiveness .....	4-53
4.3-46	Turbine Cooling Flow Summary .....	4-54
4.3-47	Leakage Control .....	4-55
4.3-48	Maintainability - Borescope Inspection .....	4-56
4.3-49	Maintainability - Turbine Accessibility - Turbine Accessibility - Forward Exposure .....	4-57
4.3-50	Maintainability - Turbine Accessibility - Rear Exposure .....	4-59
4.3-51	Maintainability - Rotor Assembly - Disassembly .....	4-60
4.3-52	Maintainability - Rotor Alignment Dowels .....	4-60
4.3-53	Maintainability - Rotor Balance .....	4-62
4.3-54	Maintainability - Stator Assembly .....	4-63
4.3-55	Maintenance - Turbine Stator .....	4-64
4.3-56	Reliability - System Analysis .....	4-65
4.3-57	Quality Assurance - Procedures and Inspections .....	4-66
4.3-58	Safety - Cooling System .....	4-67
4.3-59	Safety - Containment .....	4-68
4.3-60	Value Engineering .....	4-69
4.3-61	Human Engineering .....	4-70
4.4-1	Design Flow Chart .....	4-73
4.4-2	GE4 Turbine Rotor Parts After Full-Temperature Operation .....	4-75
4.4-3	Turbine Stator Parts After Full-Temperature Operation .....	4-76
4.4-4	Turbine Temperatures - Measured vs Predicted .....	4-77
4.4-5	Turbine Blade Temperatures - Measured vs Predicted .....	4-78
4.4-6	Turbine Vane Temperatures - Measured vs Predicted .....	4-79
4.4-7	J93/SST Demonstrator Engine .....	4-80
4.4-8	J93/SST Turbine Assembly .....	4-80
4.4-9	Accelerated Endurance Rotor Parts .....	4-85
4.4-10	Stator Parts After Extra-severity Testing .....	4-86
4.4-11	Blade Temperatures - J93/SST Measured vs Predicted .....	4-88
4.4-12	Vane Temperatures - J93/SST Measured vs Predicted .....	4-89
4.4-13	Cyclic Test Transients .....	4-91
4.5-1	Electrostream Drilling .....	4-92
4.5-2	Stem Drilling .....	4-92
4.5-3	Electrical Discharge Machining - Slotting .....	4-92
4.5-4	EDM Drilling .....	4-93
4.5-5	Automated Inspection - Wall Thickness .....	4-94
4.5-6	Automated Inspection - Interior Hole Size .....	4-95
5-1	Augmentor Chronological Sequence Chart .....	5-3
5-2	Turbojet Augmentor Simplicity .....	5-5
5-3	J93, GE4 Augmentors .....	5-6
5-4	GE4 Augmentor Two Stage Combustion .....	5-7
5-5	CJ805 Combustor Assembly .....	5-9
5-6	CJ805 Combustor Components .....	5-11
5-7	GE4 Combustor .....	5-13
5-8	GE4 Combustor Components .....	5-14
5-9	GE4 Augmentor .....	5-15
5-10	CJ805 Fuel Nozzle, GE4 Spraybar .....	5-17
5-11	GE4 Augmentor Design Advancements .....	5-20

## LIST OF ILLUSTRATIONS (Continued)

Figure	Title	Page
5-12	GE4 Augmentor Assembly .....	5-22
5-13	GE4 Predicted and Measured Liner Temperature Rise .....	5-22
5-14	GE4 Augmentor Assembly .....	5-23
5-15	GE4 Augmentor .....	5-24
5-16	Augmentor Aerodynamic Design Dimensions .....	5-27
5-17	Rene' 63 Stress Rupture Properties .....	5-28
5-18	Predicted Liner and Exhaust Casing Temperatures .....	5-30
5-19	J93 and GE4 Predicted and Measured Liner Temperature Rise .....	5-30
5-20	GE4 Augmentor (1/5 Scale Drg) .....	5-35
5-21	Fuel Distribution and Flameholder Subassembly .....	5-37
5-22	Spacer Ring .....	5-39
5-23	J79 and J93 Spacer Rings .....	5-40
5-24	Fuel Injector Support Ring .....	5-41
5-25	Comparison of J93 and GE4 Spraybar Support Ring Systems .....	5-42
5-26	GE4 Flameholder .....	5-43
5-27	Flameholder Ring Mounting Arrangement .....	5-44
5-28	Comparison of J93 and GE4 Flameholder Support Linkage Fores .....	5-45
5-29	Flameholder Ring Configuration Comparison .....	5-46
5-30	Reduced GE4 Gradient Yields Low Thermal Stress .....	5-47
5-31	Phase II-C Exhaust Casing and Liner Subassembly .....	5-48
5-32	Phase II-C GE4 Exhaust Casing .....	5-49
5-33	GE4 Exhaust Casing .....	5-50
5-34	J93 Exhaust Casing Hot Section Temperature Gradient .....	5-51
5-35	Cylindrical Augmentor Liner .....	5-52
5-36	Phase II-C Convolute Liner .....	5-53
5-37	GE4 Augmentor Liner Cooling Slot .....	5-54
5-38	GE4 Liner Mounting .....	5-56
5-39	Inner Cone .....	5-57
5-40	Major Augmentor Components .....	5-58
5-41	Size for Easy Maintenance .....	5-59
5-42	J93 Simulator on J79 Engine .....	5-61
5-43	SST Exhaust System Simulator .....	5-62
5-44	Exhaust System Simulator Test Vehicle End View and Side View .....	5-64
5-45	Simulator Envelope .....	5-65
5-46	Exhaust System Simulator Test Vehicle Layout .....	5-67
5-47	Exhaust System Simulator Test Vehicle .....	5-68
5-48	Flameholder Ring Load Test .....	5-69
5-49	Flameholder Ring Test Loading Diagram .....	5-70
5-50	Flameholder Stresses .....	5-71
5-51	Ball Joint Test Set Up (Exploded View) .....	5-72
5-52	Ball Joint Test Set Up Schematic .....	5-73
5-53(B)	Unibal Leakage .....	5-76
5-53(L)	Unibal Leakage .....	5-78

## LIST OF ILLUSTRATIONS (Continued)

Figure	Title	Page
6-1	Supersonic Nozzle Evolution .....	6-2
6-2	GE4 Exhaust Nozzle Progenitors .....	6-3
6-3	Thrust Reverser Evolution .....	6-5
6-4	Exhaust Nozzle Operating Modes .....	6-7
6-5	GE4 Exhaust Nozzle Thrust Reverser and Sound Suppression Configurations .....	6-8
6-6	Nozzle Test at Peebles .....	6-10
6-7	GE4 Exhaust Nozzle and Thrust Reverser .....	6-11
6-8	Multiple Function Star Nozzle .....	6-12
6-9	Flap Seal Configurations .....	6-13
6-10	GE4 Primary Nozzle Assembly .....	6-14
6-11	GE4 Thrust Reverser .....	6-15
6-12	GE4 Thrust Reverser Model .....	6-17
6-13	Shroud and Beam Assembly .....	6-18
6-14	Outer Flap Seal .....	6-19
6-15	Secondary Nozzle Leakage Limits .....	6-20
6-16	Design Criteria .....	6-25
6-17	Primary Nozzle .....	6-26
6-18	J93- J79/10-17 and GE4 Primary Flaps .....	6-27
6-19	GE4 Flap Design .....	6-29
6-20	GE4 Flap and Shield System .....	6-30
6-21	Actuation Ring Structural Design .....	6-31
6-22	Flap Forces .....	6-32
6-23	Flap and Seal Stress Levels .....	6-34
6-24	Ring Loading .....	6-35
6-25	J93 Actuator Ring Construction .....	6-35
6-26	Hinge Ring .....	6-36
6-27	Hinge Ring Support .....	6-37
6-28	Sectional View Cascade Box View in Thrust Reverser Position .....	6-38
6-29	Actuator Mount to Hinge and Ring .....	6-39
6-30	Reverser Actuator Mount .....	6-40
6-31	Forward and Reverse Thrust Load Diagrams .....	6-42
6-32	Actuator Force as a Function of Travel .....	6-43
6-33	Forward to Reverse Thrust Transition .....	6-43
6-34	Cooling Air Inlet Primary .....	6-44
6-35	Hinge Ring and Cascade Box Assembly .....	6-45
6-36	Box Translation and Radial Mounting .....	6-46
6-37	External Door Arrangement .....	6-47
6-38	Cascade Box .....	6-48
6-39	Cascade Box (Photo) .....	6-49
6-40	Cascade Box, Vane and Beam Temperatures .....	6-50
6-41	Hinge Ring Stop .....	6-51
6-42	Adapter Detail .....	6-52
6-43	Adapter, Beam, Exhaust Duct Attachment .....	6-53
6-44	GE4 Secondary Nozzle Configuration .....	6-54
6-45	Material Comparison .....	6-54
6-46	Outer Flap Load Analysis .....	6-55

## LIST OF ILLUSTRATIONS (Continued)

Figure	Title	Page
6-47	J79 Outer Flap .....	6-56
6-48	Inner Flap Cooling .....	6-57
6-49	Shroud .....	6-59
6-50	Inlet Doors .....	6-59
6-51	Nozzle Test at Peebles .....	6-65
6-52(B)	Exhaust Nozzle and Thrust Reverser Configuration .....	6-67
6-53(B)	External Doors on Reverser Cascade .....	6-68
6-54(B)	Thrust Reverser Exit Requirements .....	6-68
6-55(B)	Exhaust Nozzle and Thrust Reverser .....	6-69
6-56(L)	External Door and Reverser Cascade Arrangement .....	6-72
7-1	Augmentor and Exhaust Nozzle Cooling Systems .....	7-1
7-2	Augmentor Cooling Liner Slot Configurations .....	7-2
7-3	Average Augmentor Cooling Liner Temperature Increase Over Dry Operation for Maximum Augmentor Operation .....	7-3
7-4	Effect of Cooling Liner on Casing Temperature .....	7-4
7-5	GE4 Augmentor Liner Metal Temperature Rise .....	7-4
7-6	Cross-Section Primary Flap and Seal Showing Cooling Air Path .....	7-6
7-7	Exhaust Nozzle Metal Temperatures at Maximum Augmentation .....	7-7
7-8	GE4 Augmentor and Exhaust Nozzle Cooling System .....	7-8
7-9	Heat Transfer Analysis Schematic .....	7-13
7-10	J79-10/17 Augmentor Liner Temperatures .....	7-15
7-11	J93 Augmentor Liner Predicted and Actual Temperature .....	7-16
7-12	J93 Nozzle Primary Flap Calculated and Measured Temperatures .....	7-17
7-13	J79 Ejector Nozzle, Measured Primary Flap Temperatures .....	7-18
7-14	J93 Nozzle, Measured Primary Flap Temperatures .....	7-19
7-15	J79-10/-17 Nozzle Measured Primary Flap Temperatures .....	7-20
7-16	J93 Nozzle Metal Temperatures in Flight .....	7-21
7-17	Effect of Secondary Air Flow on J93 Augmentor Liner and Duct Temperatures .....	7-22
7-18	Comparison of Combustor and Augmentor Liner Temperature Gradients .....	7-23
7-19	GE4 Augmentor Liner and Cooling Slot .....	7-26
7-20	Augmentor Liner and Casing Calculated Temperatures .....	7-27
7-21	Predicted Augmentor Liner and Exhaust Casing Temperatures .....	7-28
7-22	Effect of Secondary Air on GE4 Liner and Casing Temperatures .....	7-28
7-23	Cruise Augmentor Temperature Profile .....	7-29
7-24	Max Augmentation Temperature Profile .....	7-29
7-25	Gas Temperature Profile at End of Augmentor for J79 .....	7-30
7-26	Primary Flap Cooling Air Distribution .....	7-31
7-27	Effect of Compressor Discharge Cooling Air .....	
7-28	Effect of Secondary Air Flow and Liner Cooling Air on Primary Flap Temperature .....	7-33
7-29	GE4 Primary Nozzle Measured and Calculated Temperatures - Full Scale Test .....	7-34
7-30	GE4 Primary Nozzle Calculated Temperatures, Sea Level Static .....	7-35
7-31	GE4 Primary Nozzle Calculated Temperatures - Mach 2.7, 55,000 Ft. ....	7-36
7-32	Comparison of Metal Temperatures .....	7-37
7-33	Primary Seal Temperature .....	7-39
7-34	Secondary Nozzle Film Cooling at Cruise and at Take-Off .....	7-40

## LIST OF ILLUSTRATIONS (Continued)

Figure	Title	Page
7-35	Comparison of Secondary Nozzle Cooling Systems .....	7-41
7-36	J79-10 Exhaust Nozzle .....	7-42
7-37	J93 Exhaust Nozzle .....	7-43
8-1	Cross Section of No. 2 Sump Floating Face Seal .....	8-3
8-2	Layout and Schematic of No. 2 Sump .....	8-5
8-3	Layout and Schematic of No. 1 Sump .....	8-6
8-4	Cross Section of Tandem Seal .....	8-7
8-5	Photo of Phase II-C No. 2 Sump Components .....	8-11
8-6	Layout and Schematic of No. 3 Sump .....	8-12
8-7	Cross Section of No. 3 Sump Floating Face Seal .....	8-13
8-8	Corrected Rotor Thrust Versus Corrected Engine Speed .....	8-15
8-9	Major Load Vectors Contributing to the Bearing Axial Load .....	8-16
8-10	Photo of No. 2 Sump Test Facility .....	8-23
8-11	Photo of Component Seal Test Facility .....	8-27
8-12	Photo of Floating Face Seal After 400 Hour Endurance Test .....	8-28
8-13	Photo of Thrust Bearing Test Facility .....	8-29
9-1	Layout of Gearbox Assembly .....	9-3
9-2	Schematic of Gearbox Assembly .....	9-5
9-3	Phase II-C Accessory Gearbox .....	9-9
9-4(B)	Schematic of Gearbox Assembly .....	9-18
9-5(L)	Schematic of Gearbox Assembly .....	9-20
10-4	J79 Compressor Front Frame.....	10-8
10-5	CJ805 Compressor Front Frame .....	10-9
10-6	Anti-Icing, Compressor Front Frame .....	10-10
10-7	Front Frame IGV .....	10-11
10-8	Materials Allowable Stresses, Front Frame .....	10-12
10-9	Compressor Front Frame Stress Range Diagram .....	10-13
10-10	Compressor Rear Frame Assembly.....	10-14
10-11	Turbine Air Conservation Valve, Compressor Rear Frame.....	10-16
10-12	J79, CJ805, and J93 Compressor Rear Frames .....	10-17
10-13	Compressor Rear Frame Cross Section .....	10-18
10-14	Material Allowable Stresses, Compressor Rear Frame .....	10-20
10-15	Compressor Rear Frame Stress Range Diagram at 700°F .....	10-21
10-16	Compressor Rear Frame Stress Range Diagram at 1100°F .....	10-22
10-18	Turbine Frame Assembly.....	10-24
10-19	Turbine Frame Cross Section.....	10-25
10-20	Turbine Frame Outer Casing .....	10-26
10-21	Turbine Frame Hub.....	10-26
10-22	Turbine Frame Outer Liner Support .....	10-27
10-23	Turbine Frame Strut Fairings .....	10-27
10-24	Steady State Stress, Turbine Frame .....	10-29
10-25	Steady State Stress, Turbine Frame .....	10-30
10-26	Turbine Frame Stress Range Diagram .....	10-31
10-27	Turbine Frame Stress Range Diagram .....	10-32
10-28	Compressor Front Frame Radial Spring Rate .....	10-36
10-29	Natural Frequencies of Over-All Engine System .....	10-41



## LIST OF ILLUSTRATIONS (Continued)

Figure	Title	Page
10-1(B)	Definition of Maneuver Modes .....	10-44
10-2(B)	Compressor Front Frame Assembly .....	10-45
10-3(B)	Front Frame Cross Section, Strut Usage, and Tube Sizes .....	10-46
10-17(B)	Compressor Rear Frame Strut Usage and Tube Sizes .....	10-47
10-30(B)	Engine Mount Reactions for Unit Load Input .....	10-48
10-1(L)	Definition of Maneuver Loads .....	10-50
10-2(L)	Compressor Front Frame Assembly .....	10-51
10-3(L)	Front Frame Cross-Section, Strut Usage, and Tube Sizes .....	10-52
10-17(L)	Compressor Rear Frame Strut Usage and Tube Sizes .....	10-53

# 1. INTRODUCTION AND SUMMARY

## 1.1 INTRODUCTION

Volume III-B is the second of seven reports in Volume III, Technical/Engine, of the proposal. This report contains the substantiating data indicated on pages 5-42 through 5-47 of the Request for Proposal for Phase III of the Supersonic Transport Development Program. The presentation is made in three parts, corresponding to the three subject areas identified in the RFP; namely, (1) major components, (2) controls and accessories and (3) fuel and lube systems, and is provided as three separate documents for convenience. Descriptions and discussions of the mechanical designs for all major parts in the engine and many details on operating characteristics are included. The over-all summary below, as given in Volume III-A, is a general review of the GE4 augmented turbojet engine.

## 1.2 OVER-ALL SUMMARY (PERFORMANCE AND DESIGN) - Reference Summary Volume III-A.

# GE4/35 ENGINE DESIGN

## 2. COMPRESSOR DESIGN

### 2.1 INTRODUCTION AND SUMMARY

The selection of the GE4 compressor is based on achieving:

- The highest levels of reliability/durability/safety,
- The highest level of performance,
- Minimum weight,
- Minimum cost, and
- Minimum need for and ease of maintenance

for aircraft turbine engines, and is the result of a systematic compressor development program carried forth by the Flight Propulsion Division since 1959.

The design is based upon the successfully integrated mechanical and aerodynamic configurations of five previous compressors within the family (See Figure 2-1). The objective of this development program has been to reduce the number of stages required in an axial flow compressor and to produce a given pressure ratio while maintaining high efficiency, flow, stall margin, and tolerance to inlet distortion. This advancement in the state of the art also affords significant improvements in length, weight, cost and maintainability through the use of rugged, long-chord blading and fewer parts. When the blades have long chords and very low operational stresses, they can be made hollow with equal or greater reliability than current solid blade compressors.

The X370, four-stage compressor was the first of the higher-stage-loading, aerodynamic family to be developed. This compressor was extremely successful, achieving a design pressure ratio of 4.5 at a weight flow of 350 lb/sec in four stages with a peak efficiency of 86.8 percent. This compressor was tested in 1959 and 1960 with both solid and hollow rotor and stator blading. Considerable aerodynamic and aeromechanical experience was obtained for further development.

The 1963, GE1 eight-stage, 65 lb/sec compressor extended the high-stage loading aerodynamic concept to a higher pressure ratio. This compressor achieved a stall pressure ratio of 11.2 in eight stages with a somewhat lower efficiency. Analysis of the data indicated that an excessive solidity was used, which limited the flow capacity and introduced an axial mismatch of the stages that could not be completely compensated by the variable stators. Aeromechanical experience with blade stresses below 20 percent of limits during steady state and below 50 percent during stall was highly encouraging.

The 1964, eight-stage, 65 lb/sec compressor was designed to attain additional objectives tailored for the GE4 SST turbojet mission. This compressor, reported in Vol. III-A3, was extremely successful in meeting most of the SST mission requirements. A stall taken at full speed revealed that the blade stresses did not exceed 50 percent of the endurance limit.

The 1965, eight-stage, 475 lb/sec compressor, derived from the 1964, 65 lb/sec, compressor and reported in Vol. III-A3, was tested in 1965 and 1966. This compressor demonstrated excellent performance and aeromechanical characteristics and is used on the Phase II-C development engines.

# EVOLUTION OF HIGH STAGE LOADING COMPRESSORS

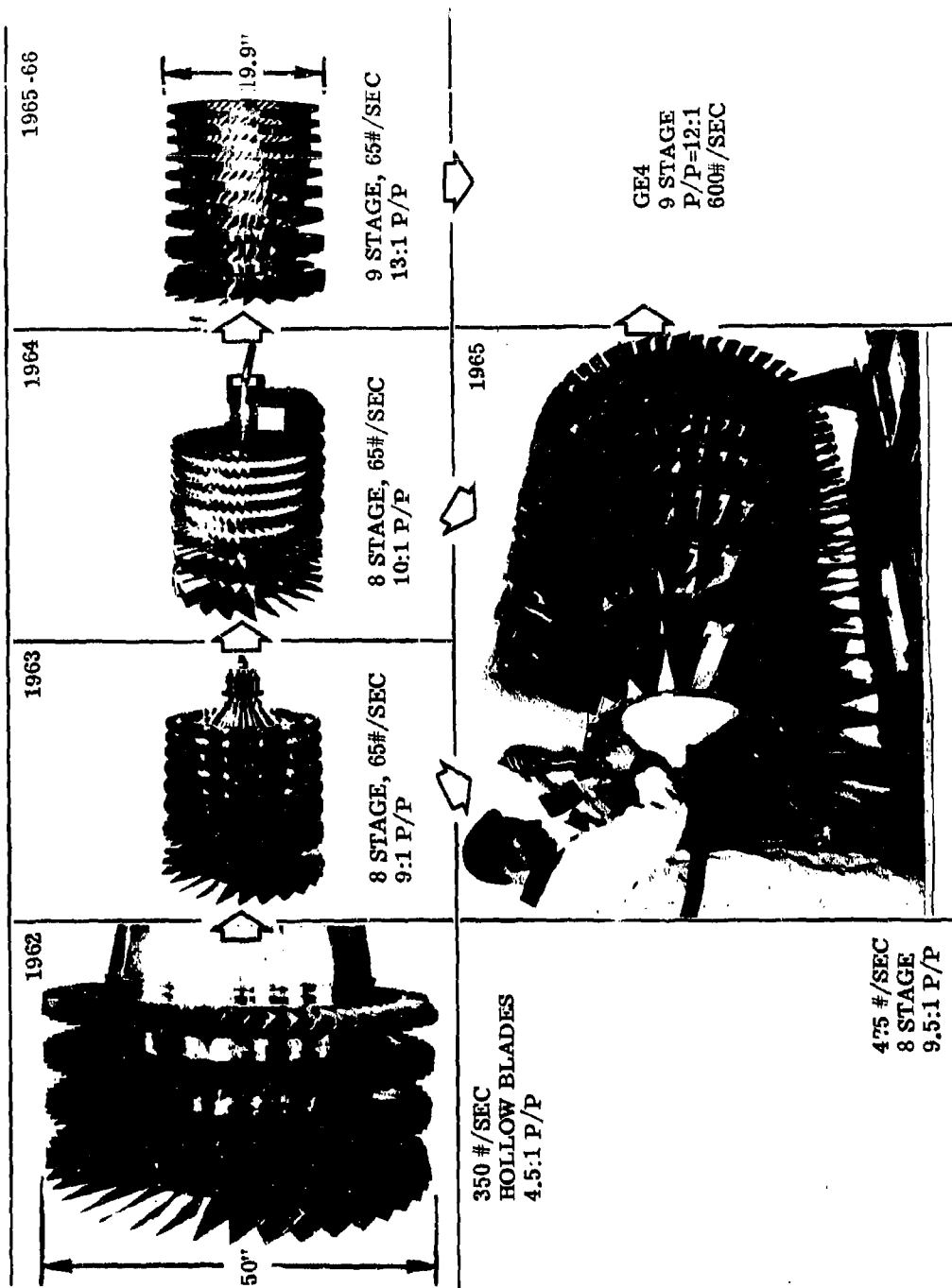


Figure 2-1 EVOLUTION OF HIGH STAGE LOADING COMPRESSORS

A nine-stage, GE1, 65 lb/sec compressor, also developed in 1965, had an operating pressure ratio of 13.0. This compressor offers significant reliability and cost advantages over current aerodynamic-compressor technology and is being used in the advanced GE1 engine programs.

The nine-stage, GE4 compressor with an airflow of 620 lb/sec, described in Vol. III-A3 and proposed for the Phase III engines, is based on the eight-stage, 475 lb/sec and GE1, nine-stage, 65 lb/sec compressors with adaptability to the use of hollow blades as demonstrated by the low stresses observed. This nine-stage compressor has an operating pressure ratio of 12.3, approaching the 17-stage, CJ805 compressor, but has less than half the number of airfoils. Both the magnitude and range in flow and efficiency are considerably higher.

The GE4 compressor features variable stators in the IGV, stages 1 and 4 through 8, for high performance over the wide flight spectrum. The stage-nine outlet guide vanes form a two-position close-off door for an emergency engine-shutdown, windmilling brake. This system, developed by General Electric and successfully used on the J93 engine, is the only practical method of reducing the engine rotor-speed in the aircraft at supersonic speed.

This compressor was selected as a result of intensive aerodynamic and mechanical optimization successively refined by some 40 iterations based on the demonstrated characteristics of the current eight and nine-stage test compressors.

Figure 2-2 is a cross-section of the compressor, showing the general features of construction, including the highly refined General Electric, variable-stator mechanism and internal rotor cooling.

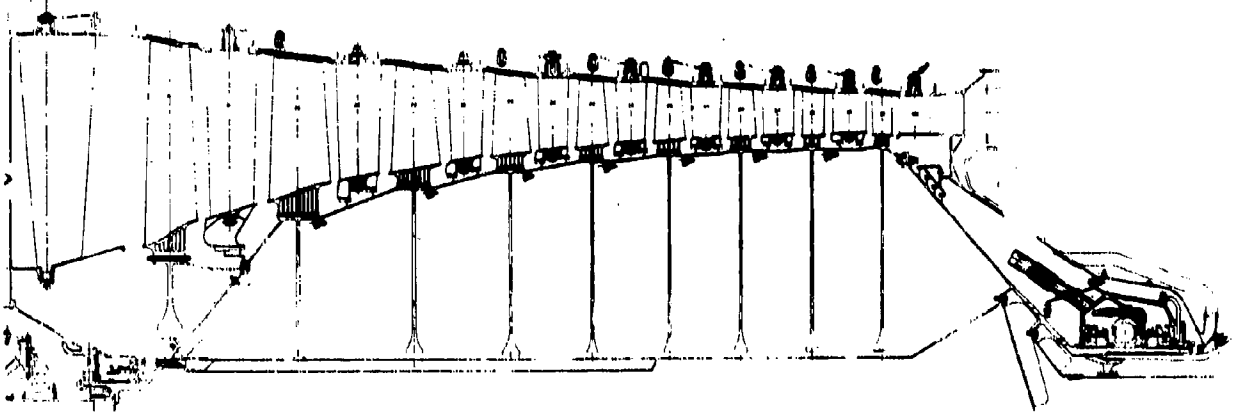


Figure 2-2 CROSS SECTION OF COMPRESSOR - GENERAL FEATURES OF CONSTRUCTION

The following are key features of the compressor design which have been incorporated to satisfy every airline requirement.

A. Reliability/Durability/Safety/Reduced Maintenance

1. Rigidized rotor structure with integral disk and spacer construction

- No bolt holes in disks

- Supported disk rims (low stress concentration)
  - Scalloped flanges to eliminate hoop stress from holes
  - Radiused disk dovetail slot bottoms (high resistance to low cycle fatigue)
  - Spacers integral with disks (fewer joints)
  - Adaptable to Electron Beam or inertia welding
2. Precise rotor balance repeatability through dowelled bolt construction with proven rigidity
  3. Long chord, rugged blades — achieved with low weight through hollow core
    - Low operational stresses
    - More than adequate stall life
    - Low axial deflection
    - Good tolerance to foreign object damage
    - High tolerance to bird and ice ingestion
  4. Shrouded stator vanes with low operating stresses for long life even after damage
  5. Cooled rotor for temperature control
  6. Demonstrated protection from titanium fires with:
    - Rugged low aspect ratio blading
    - Casing liners which protect structural shell and deflect away from blade tip contact during rubs
    - Abradable steel honeycomb stationary seal surfaces to wear away with low heat generation during rubs
  7. Anti-fret coatings on dovetails for long life
  8. Blade retainers — machined part, not deformed at assembly
  9. Blade containment with:
    - Hollow core blades with less impact energy than solid blades
    - Casing liner configuration rigidized with ribbon reinforced honeycomb and bradelloy to absorb impact

- Actuation rings and levers strategically located to absorb possible abnormal damage to compressor casing from multiple blade or disk rim failures.

10. Tungsten carbide stator vane bearings for high strength and low wear rate

11. Highly corrosion resistant materials throughout

#### B. Performance/Weight

1. Hollow core blading results in

- Higher rotor acceleration rate with lower inertia
- 500 lb/engine weight saving with configuration that meets reliability/durability requirements

2. Effective clearance control with:

- Compressor rotor supported with front and rear bearings
- Squealer tips
- Steel honeycomb on seals
- Circumferential ribs on casing

3. Airfoil accuracy with large size profile

#### C. Maintainability

1. Split casings, front and rear, for easy removal, inspection, parts rework or replacement
2. All blades and vanes individually replaceable with casing halves removed
3. 54 percent fewer parts than CJ805 compressor

	<u>GE4</u>	<u>CJ805</u>
Number of blades	499	1271
Number of vanes	697	1332
Total	1196	2603

4. Solid blade leading and trailing edges for liberal repair limits from foreign object damage
5. Replaceable casing liners
6. Actuation system parts individually replaceable without engine removal
7. Rigging of compressor actuation with pre-set links for accuracy and ease of adjustment

8. Provision for inspection of rotor by isotopic X-ray
9. Stator casing borescope ports for inspection of blades and vanes
10. All parts are "foolproof" for correct assembly

The rotor is constructed of integral disks and spacers, which avoids the need for holes for clamping bolts in the stressed disk webs and thereby eliminate a low-cycle fatigue problem. Further, there is then no loss in clamping load from Poisson's Ratio effect which reduces the thickness of the disk web at full speed.

The stage 1 rotor blade incorporates a mid-span shroud so that a shorter blade chord can be used to effect an optimum balance between length, weight, and inlet noise suppression.

The demonstrated success of hollow-cooled turbine blading has been exploited and applied to the GE4 compressor. Blades in stages 1 through 6 are titanium and made by a new molecular bonding process by which the material grains grow together upon the application of heat and pressure. Blades in stages 7 through 9 are Inco 718 and are "hollow-cored" by stem drilling, like the J93, GE1, TF39 and GE4 air-cooled turbine blading.

A variable stator system is used to obtain efficient compressor performance over a broad flight spectrum. This capability has been developed to a high degree of refinement on General Electric engines and is particularly important for the operational extremes of a supersonic engine. The variable stator system provides a means of "tuning" the compressor to obtain the best performance and maintain low blading stresses. This "tuning" is an integral part of the compressor development program and has been used successfully on General Electric turbojets since the J79.

The compressor stator casings consist of forward and aft units that are split along the horizontal center line. This design configuration was perfected for light concentric casings on the J93 engine, and permits ready access for inspection, rework, or replacement of blades and vanes. Liners are used in the casing, as on the J93, to form the flowpath and to isolate the structural shell from possible damage.

All the experience gained by the General Electric Company, the airframe manufacturers, the Military, and the airlines has been collected and applied to the compressor design. Configuration innovations and analytical/experimental techniques have been applied to avoid every mode of failure ever identified.

## 2.2 DESIGN REQUIREMENTS AND APPROACH

The GE4 compressor is designed to meet all the FAA certification and airline requirements, together with the applicable Government and Engine Specifications.

All requirements established by the cycle will be met. The most significant parameter is temperature. During a hot day, the maximum inlet temperature is 1045° R in a transient and 1000° R in steady state. Maximum compressor exit temperature is 1675° R in a transient and 1625° R at steady state. These cycle temperatures are the prime factor in the choice of materials, but the compressor is not limited by time and temperature. However, the last two stages of disks require slight cooling to remove them from the time-temperature region.

The primary consideration in the design of the compressor is high-and low-cycle fatigue. Experience has shown that fatigue is a significant cause of 95 percent of compressor failures. Hence, all



aspects of the design and its environment are carefully considered to avoid conditions that impose the loading or to make certain that the resultant stresses are within limits. For example:

- The compressor parts are designed to meet 22,000 cycles of operation.
- The engine will be free of detrimental stalls in the planned operating range. If a stall does occur, inadvertently, it will have no subsequent effect on performance, vibration, or mechanical integrity. (Stall stress levels will be established by test).
- At constant power settings, the engine will withstand, without mechanical damage, steady state inlet distortions not exceeding  $N_{DI} = 0.20$ . Operation with an index greater than 0.20 can be tolerated in transients.
- The engine will be capable of withstanding without mechanical damage, an instantaneous decrease in inlet total pressure of 50 percent followed by an abrupt return to approximately the original pressure.

In addition to a very careful and detailed analysis (refer to Section 2.3, Blading aeromechanical. . .), a comprehensive test program to evaluate all possible fatigue modes is being pursued. This includes: component and rig tests to establish component strengths, especially in the modes predicted or determined by test; full scale compressor tests to establish the optimum schedule for performance and durability, and instrumented engine tests that establish critical modes and verify component and full scale tests. These are static and simulated flight tests. Tests for endurance and life are also included.

The compressor is designed for an average ultimate life with repair as specified:

Compressor Rotor

Blades and Hardware 18,000 hours

Disks and Shafts 36,000 hours

Stator

Vanes and Actuation System 36,000 hours

Shrouds, hardware, seals 18,000 hours

Bushings and pins 12,000 hours

Casing Unlimited

A windmill brake is provided to retard rotor speed, in the event of a shutdown, to no more than 18 percent rpm at the maximum flight speed. Reset of the stator vanes, after brake during flight is possible.

Special consideration has been given to designing to sustain foreign object damage. The engine is capable of containing any resulting damage. In addition, adequate means are provided for containing a failed rotor blade at normal operating speed.

The engine will be capable of operating transiently up to 105 percent mechanical speed. Demonstration will be made with failure not imminent at 115 percent of maximum rated speed.

## 2.3 DESIGN DESCRIPTIONS

### 2.3.1 BLADING, AEROMECHANICAL AND DOVETAILS

#### 2.3.1.1 Rotor Blading

The GE4 aerodynamic design incorporates relatively long chord, low-aspect-ratio blading to achieve its broad flow range, good stall margin, inlet distortion tolerance, and high-stage pressure ratios. This long chord blading is particularly suited for substantial weight reductions through the use of hollow core blading with its inherently low vibration characteristics and tolerance to stalls and inlet distortion. Hollow core airfoil sections, in turn, permit lighter weight hollow dovetails with correspondingly lighter disks. Table 2-1 is a breakdown of the weights saved on each stage by the use of hollow blades and dovetails.

Table 2-1 Hollow Blade Weight Savings

<u>Stage</u>	<u>Airfoil</u>	<u>Dovetail and Disk Rim</u>	<u>Disk Web</u>
1	—	—	—
2			
3			
4			
5			
6			
7	—	—	—
8			
9			
Totals	136.0	176.0	197.0

Total Rotor Savings over solid design = 509.0 lbs.

The philosophy governing the design of the hollow blades has substantially retained the basic ruggedness of aspect-ratio blades. This has been accomplished by keeping solid sections at least 1/2 inch from the leading edges, trailing edges, and in the tip area. In this way, the areas most susceptible to foreign object damage, erosion, and fatigue failures are not compromised by the hollow core design. Figures 2-3A and 2-3B show comparative aspect ratios and mid span sections of the GE4, J93 and CJ805 first- and last-stage blades. These are typical examples of the relative ruggedness of the GE4 design. The first six stages of blades are of 6-2-4-2 titanium; a light, corrosion-resistant, high-strength alloy suitable for use up to 900°F. The hollow titanium blades are integral structural members with solid leading and trailing edges and a control cavity bridged by button supports joining the concave and convex skins (See Figure 2-4.)

The process for producing these blades, which constitutes a major advance in compressor technology, is a marriage of General Electric's experience in hollow airfoil design and titanium diffusion-bonding technology. Section 1.4 describes the background and details of the manufacturing process. The key to the process is the diffusion bonding of two half-blades together (Figures 2-5 and 2-6) at a precision-ground interface. The resulting composite blade structure is shown in Figure 2-4. Note that the dovetails are also hollowed, resulting in a light-weight, efficient fastener. The microstructure of this bond (Figure 2-7) is indistinguishable from the parent material and result in no loss of mechanical properties.

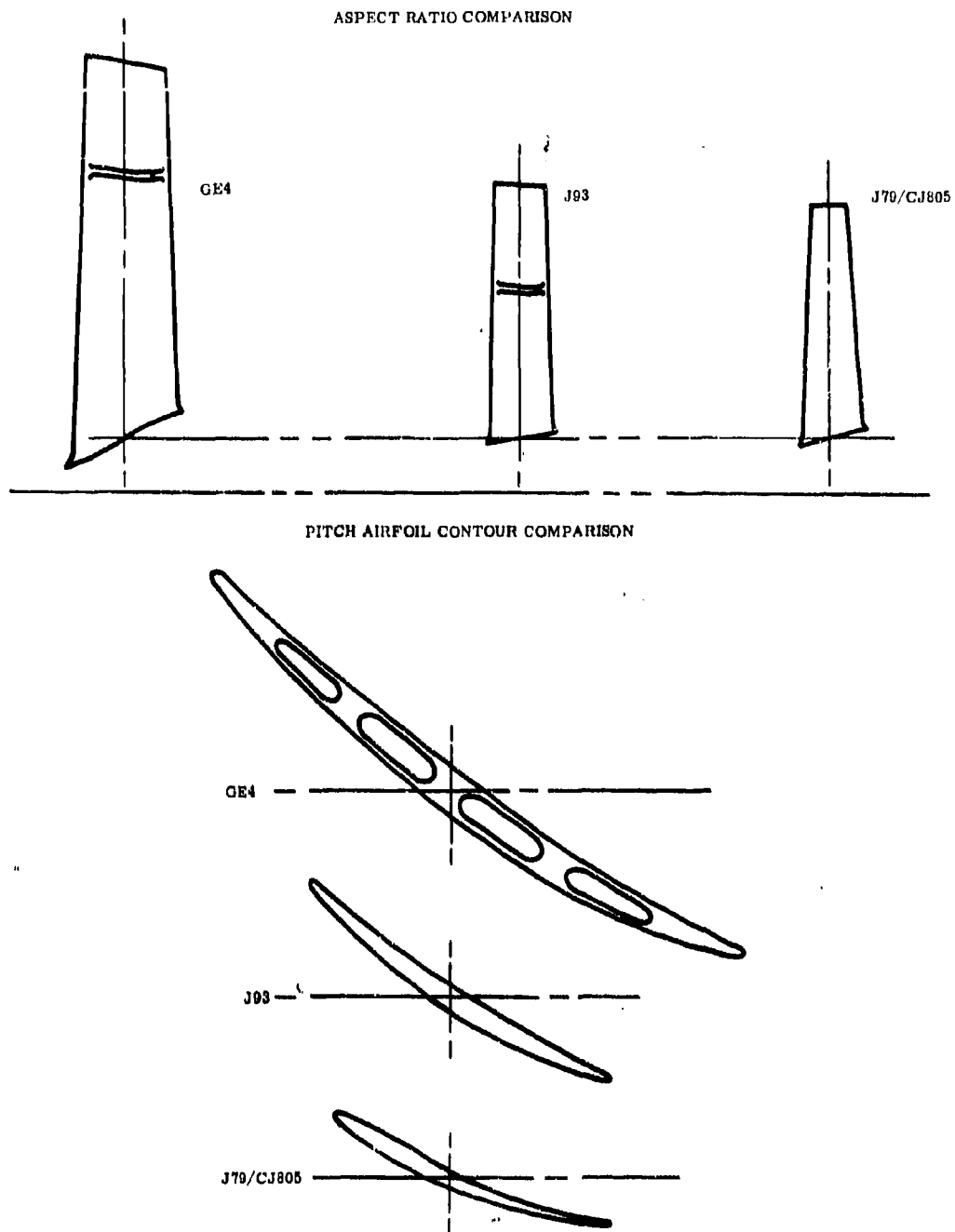
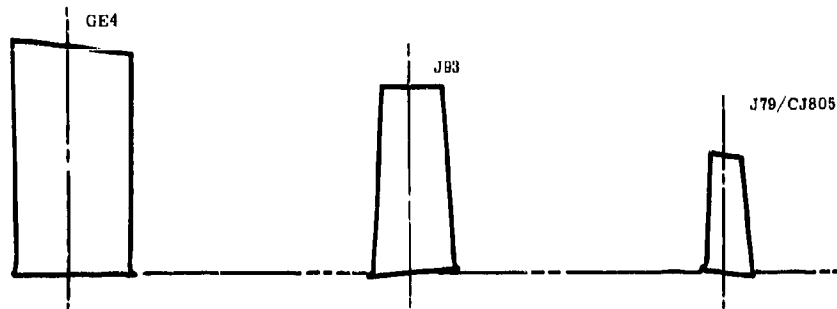


Figure 2-3A. COMPARISON OF FIRST STAGE BLADE - GE4, J93, J79/CJ805

ASPECT RATIO COMPARISON



PITCH AIRFOIL CONTOUR COMPARISON

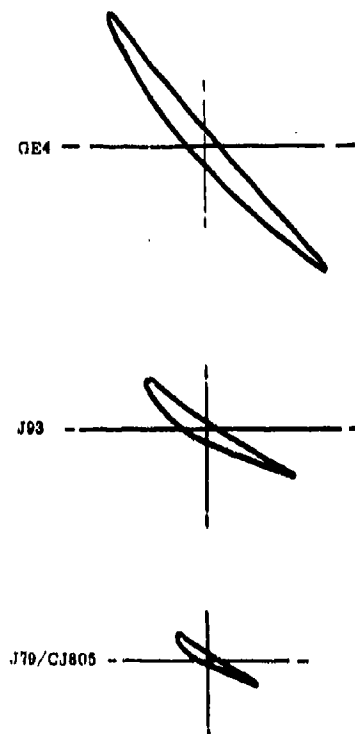


Figure 2-3B. COMPARISON OF LAST STAGE BLADE -- GE4, J93, AND J79/CJ805

SOLID LEADING & TRAILING EDGES & TIP  
& ROOT SECTIONS

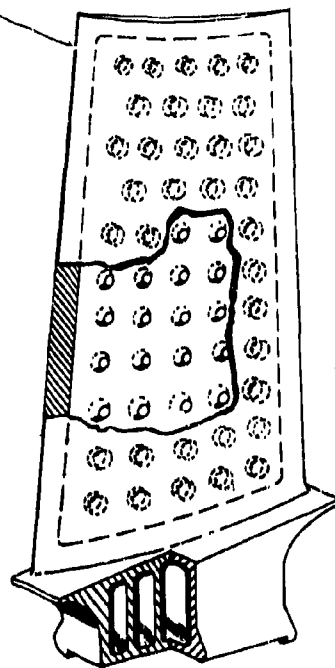
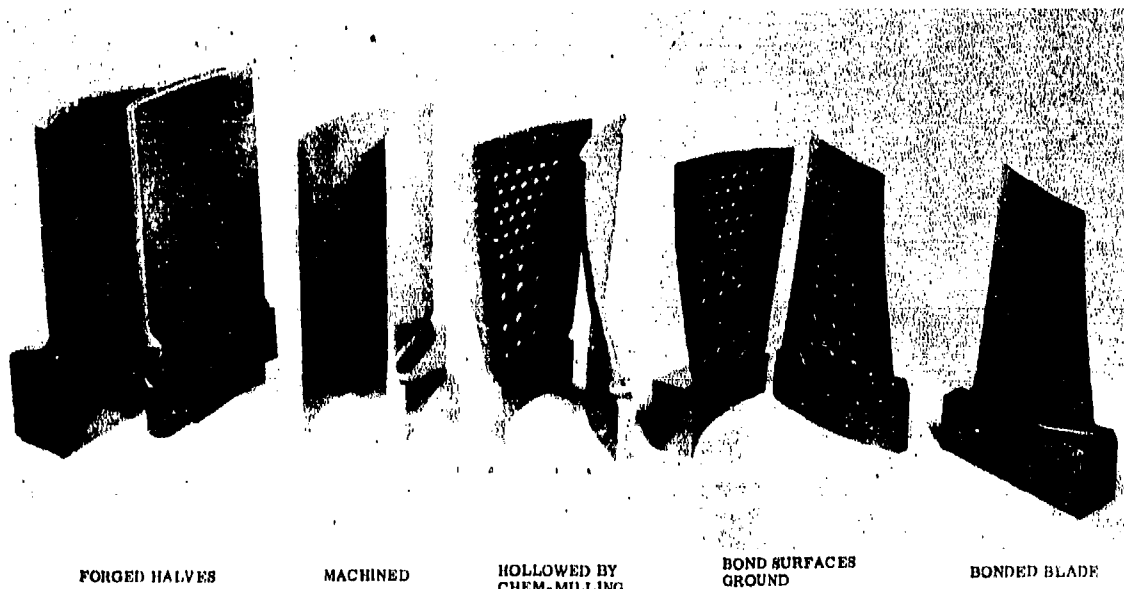


Figure 2-4. TITANIUM DIFFUSION BONDED HOLLOW BLADE STAGES 1-6



FORGED HALVES

MACHINED

HOLLOWED BY  
CHEM-MILLING

BOND SURFACES  
GROUNDED

BONDED BLADE

Figure 2-5. BLADE EVOLUTION DURING MANUFACTURING PROCESS

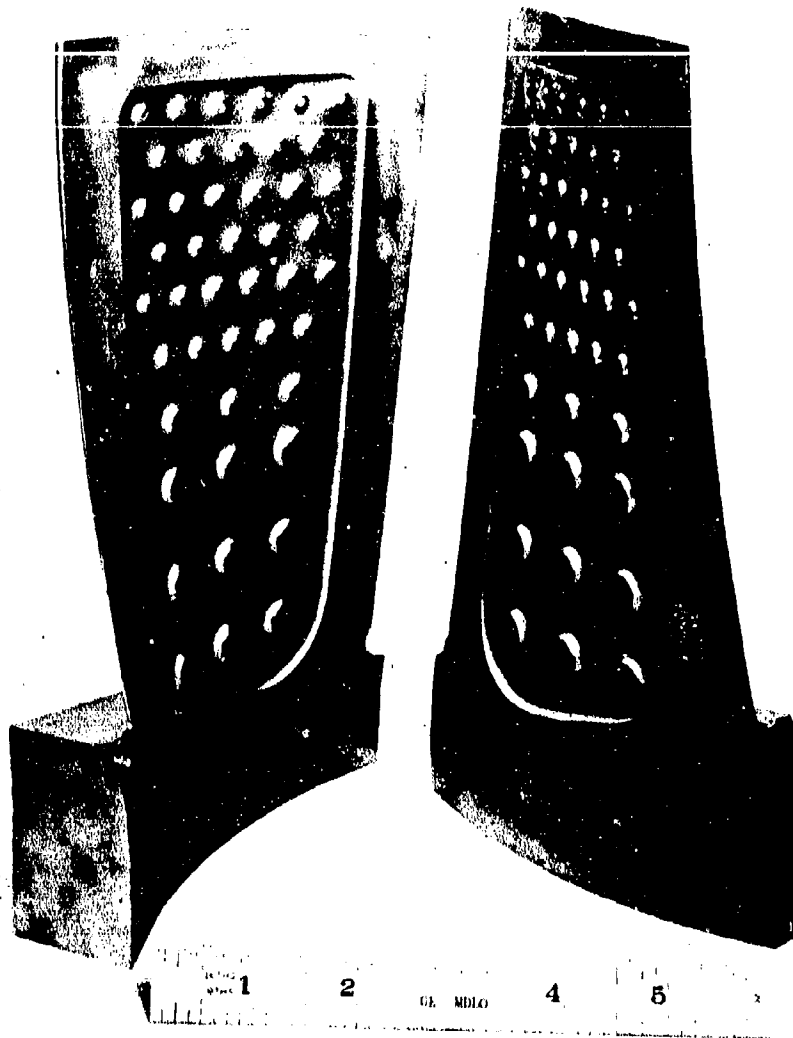


Figure 2-6. BLADE HALVES BEFORE BONDING

An extensive test program has been completed to determine the mechanical properties of diffusion-bonded titanium. These tests included rotating-beam (bending) fatigue, torsion fatigue, low-cycle fatigue, tension, and shear tests on conventional test specimens. In all cases, properties have fallen within the range of the parent material. Combined stress fatigue tests have been conducted on simulated diffusion-bonded airfoils. No failures occurred in the diffusion-bonded areas of the airfoil.

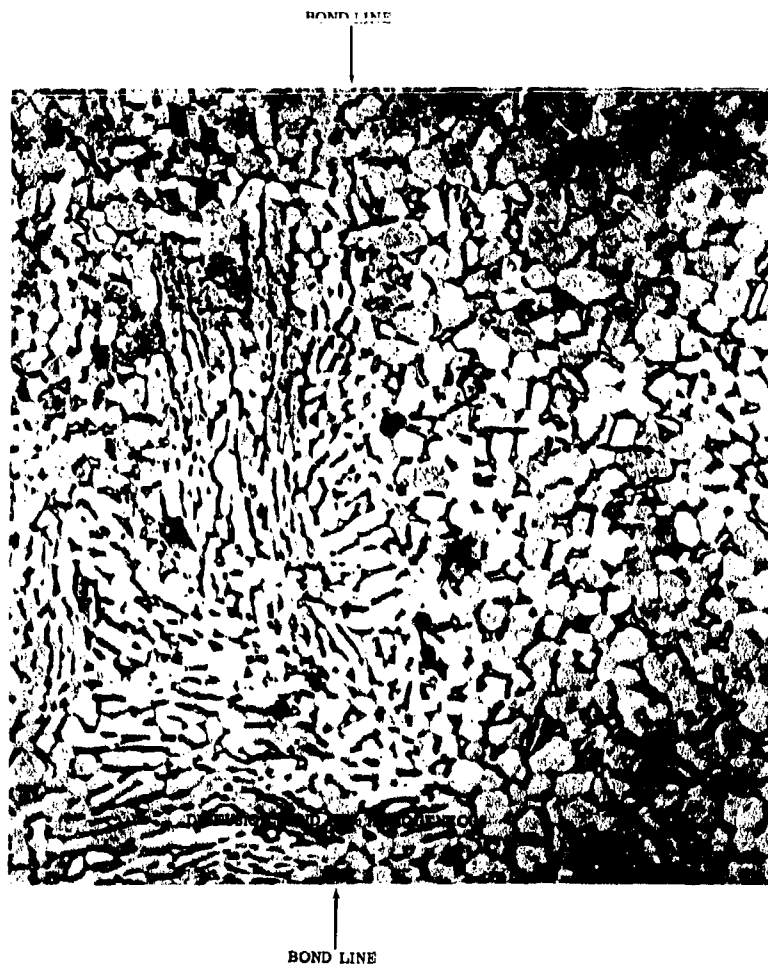


Figure 2-7. MICROSTRUCTURE OF BOND Microstructure Enlarged 1000 Times  
Showing Diffusion Bond Interface

The last three stages of the blades are of Inco 718, a corrosion-resistant, high-strength material suitable for the 900 to 1215°F temperature range encountered in these stages. These blades are lightened by stem drilling multiple holes from the tips down to mid span and from the dovetail outward. This process has been developed by General Electric and is used extensively for drilling turbine-blade holes (Figure 2-8.)

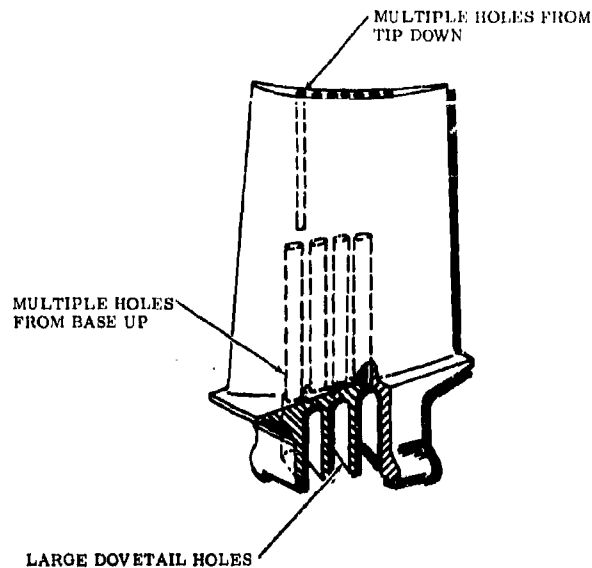


Figure 2-8. STEM DRILLED BLADES, STAGES 7-9

It has also been employed successfully to lighten the outer panel of the TF39 fan blade. Additional lightening is accomplished in the dovetail by stem drilling rectangular holes upward through the shank as shown in Figure 2-8. As in the case of the first six stages, the hollow dovetail configuration is an efficient structural member fulfilling the objective of being stronger than the airfoil in the major modes of vibration.

#### 2.3.1.2 Aeromechanical Design

The variable compressor stator was pioneered in the J79/CJ805 turbojet, successfully employed in the J93, T58 and T64 production engines, and is used on the TF39 and J97. An integral part of the compressor development program (Full Scale Compressor Test) is to "tune" the variable stator schedules as a function of speed, to obtain a high performance over a broad operating range. Minimizing blade vibration is an inherent part of this process. During a two-sided process denoted as "aeromechanical tuning", blade vibration measurements supplement conventional performance instrumentation in defining and refining both local and overall flow characteristics. A by-product of this tuning is a reduction in the intensity of the random-noise-turbulence level throughout the engine flowpath, thereby reducing the level of combustor-shell, vibratory stimulus, as an example, and sensitivity to fatigue. The background level of vibration is thus reduced, and tolerance to foreign object damage or abnormal abusive application is increased. The variable stator approach provides a high degree of flexibility for off-design matching of stage loads at part speed, thereby: 1) holding to a minimum the vibration generated by partial separation, 2) eliminating stimuli associated with rotating stalls by raising their threshold on the compressor map until their onset constitutes the stall line in the same sense as high speed surge, 3) removing dips in the stall line at intermediate speeds so that stall and resulting blade vibratory-distress during transients is avoided, and 4) increasing tolerance to inlet distortion.

The flexibility and adaptability of the variable stator mechanism permits simple design modifications to help overcome problems such as unusual inlet distortions. An example of this is the



"Variable Stator Reset Mechanism" on the CJ805. The variable stator reset mechanism (VSRM) increases the engine stall margin by closing the stator a pre-determined amount whenever thrust is reversed. With the variable stators in the maximum open position, the VSRM partially closes the stator vane angle to accommodate hot exhaust gases ingested by the gas generator.

Tuning the compressor ensures a broad zone of operation for blades, without hazardous vibratory stresses induced by aerodynamic mismatch. However, the basis for a sound compressor, from a blade vibration standpoint, is rigid adherence to resonance and limit-cycle stability criteria, developed from experience on other General Electric engines and supplemented and refined by extensive aeromechanical research tests.

Limit-cycle instability (torsional flutter) is avoided by designing to operate at safe values of the "reduced velocity parameter,"  $V/b\omega$  where  $V$  is the relative air velocity,  $b$  is the semi chord, and  $\omega$  is the first torsional frequency. Plotting this parameter versus incidence angle, as shown in Figure 2-9, gives an indication of the stability margin. The unstable zone boundaries are based on an extensive file of engine and aeromechanical test rig data, and reflect the blade type, air density, and relative airfoil inlet Mach numbers encountered.

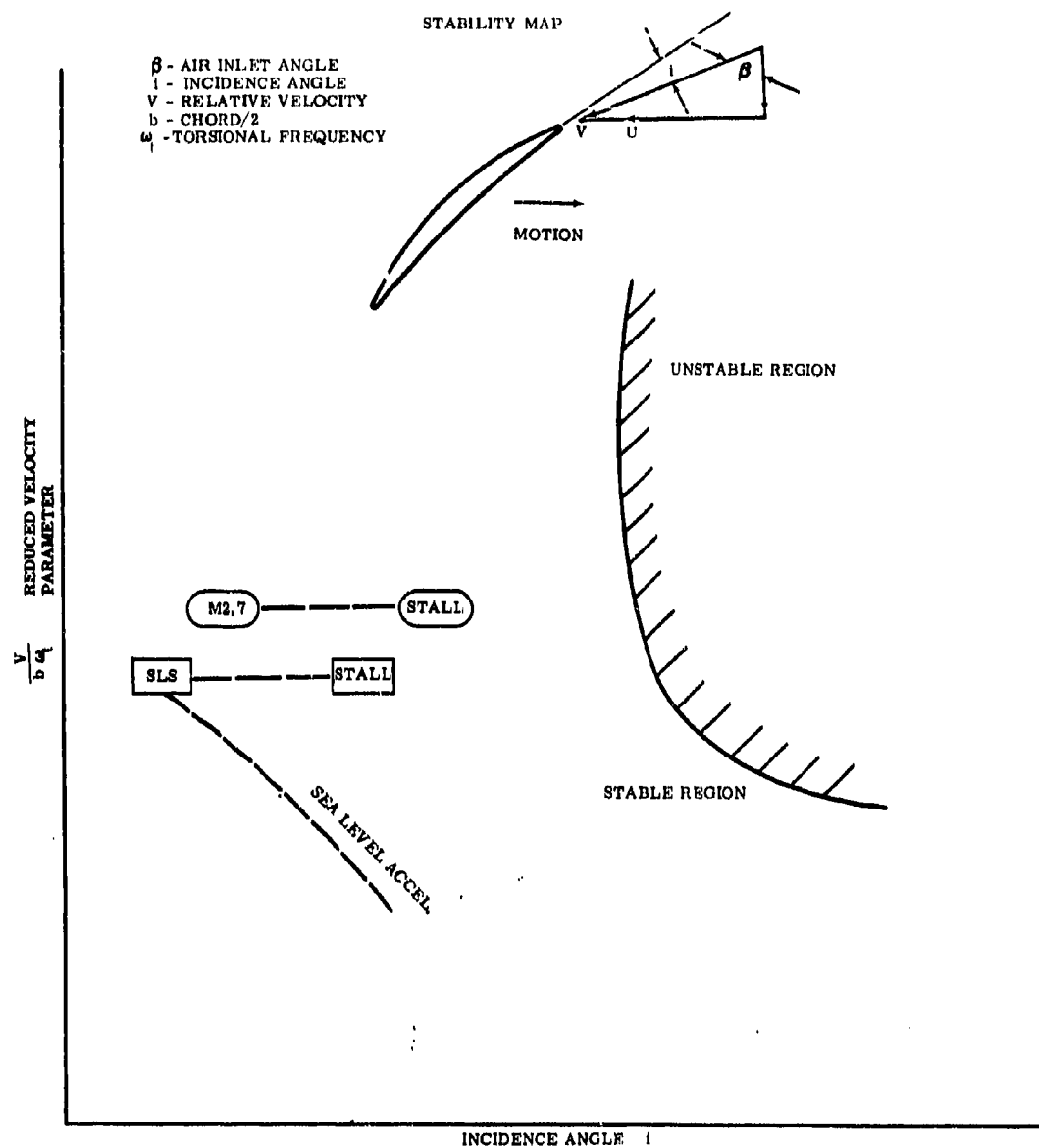
The most comprehensive data was obtained from a systematic series of General Electric Company aeromechanical tests, using the test rig depicted in figure 2-10. These tests isolated the effects of each significant blade design parameter.

Figure 2-11 depicts the range of rotor configurations that were tested. The test rig was equipped with variable inlet and exit guide vanes, making it possible to traverse a wide range of incidence angles at each speed point. Various inlet distortion screens were also arranged in front of the test rig to give precise information as to the effects of distortion on the stability boundary. Figure 2-12 depicts the geometry of these screens.

A primary requirement of the design criteria for the GE4 compressor is to avoid instability at all operating conditions and distortion patterns and consider incidence angles predicted at the compressor stall line. Stages 2 thru 9 have ample margin due to the long chord/low aspect ratio design. The first-stage blade has an interlocking shroud (see Figure 2-13) at 70% span to assure stability. Because of the higher incidence-angle excursion and longer blade, a chord length of nine inches would be required to meet our stability criteria with no shroud. The longer chord and fewer blades would have resulted in potentially higher inlet noise. Therefore, and for reasons of length and weight, a shrouded blade was chosen. In addition to the stability benefits, the shrouded design is more resistant to blade failure resulting from impact damage, since the blades are mutually supporting structurally, through the shrouds - a capability, graphically illustrated by the in-flight failure and separation of a segment of a B70 airframe engine inlet duct. Portions of the failed airframe segment subsequently passed through several of the J93 engines causing extensive compressor damage. An IGV from one engine was torn loose and passed through the compressor. The shroud-supported, first-stage blade bore the brunt of the initial impact without catastrophic failure (Figure 2-14). This engine was operated above 90 percent speed to allow safe landing of the aircraft. General Electric has substantial experience in the design of mid-span shrouds on the J93, GE1, J85-J1A, and TF39 engines.

Serious airfoil resonances were avoided by designing to the following requirements:

- No natural blade modes are in resonance with 1/rev or 2/rev frequencies below 103 percent speed.
- The first flexural mode has a minimum margin of 25 percent over the 2/rev excitation frequency at Mach 2.7 warm day operation.



**Figure 2-9. TYPICAL AEROELASTIC STABILITY MAP. Accel and Different Flight Conditions. GE4 Design Assures Stability Beyond Stall at all Flight Conditions.**

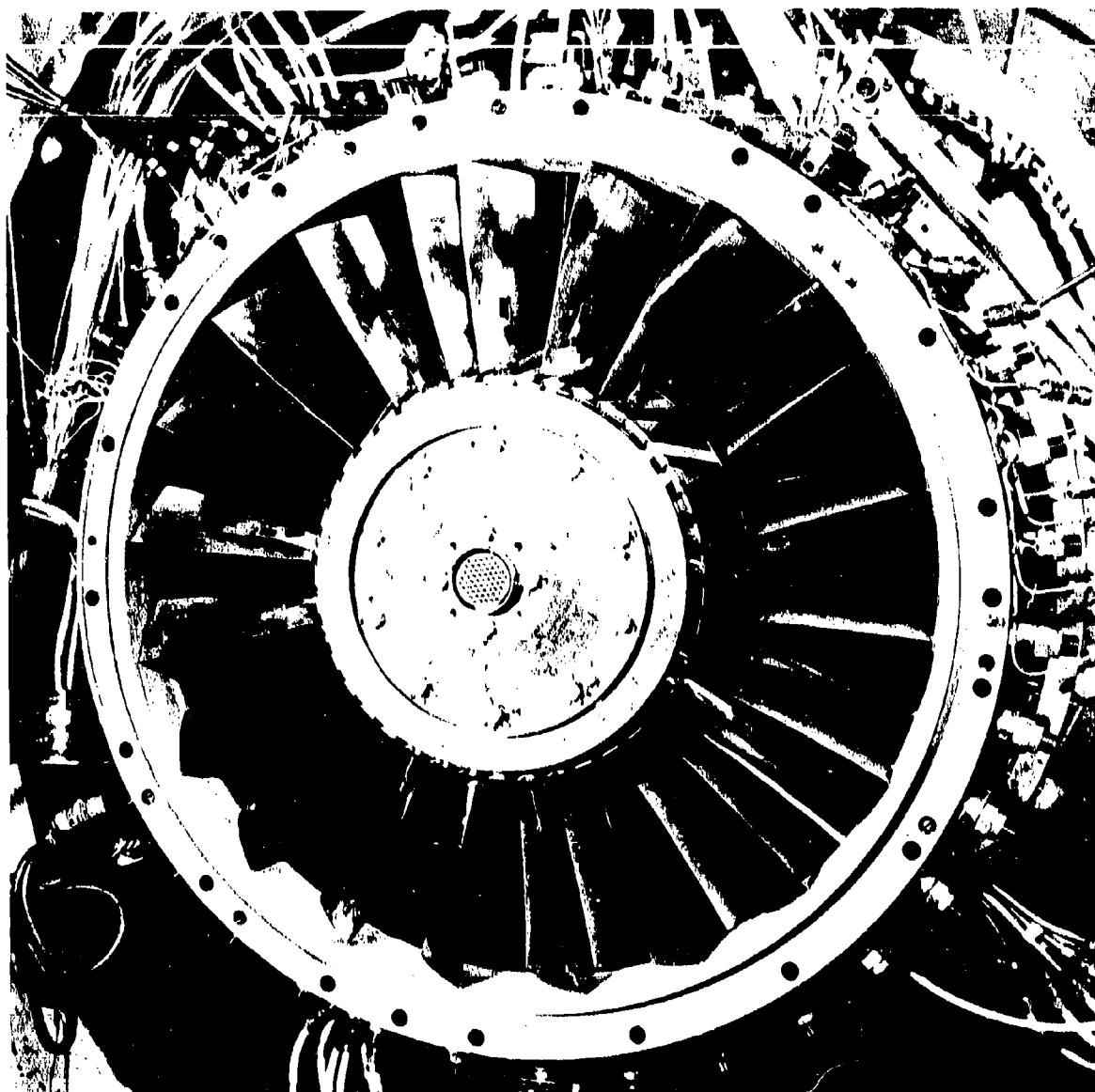


Figure 2-10. ROTOR INLET TO AEROMECHANICAL TEST RIG. Special Configuration MAR-TI-VLS Build-Up used 21 MAR Titanium blades in the 41 slot high solidity disk. Slugs in the unused slots were made from scrap steel and titanium blades and arranged to counter-balance the odd pair of blades at the top of the assembly.

SOLIDITY

HIGH

NOMINAL

LOW

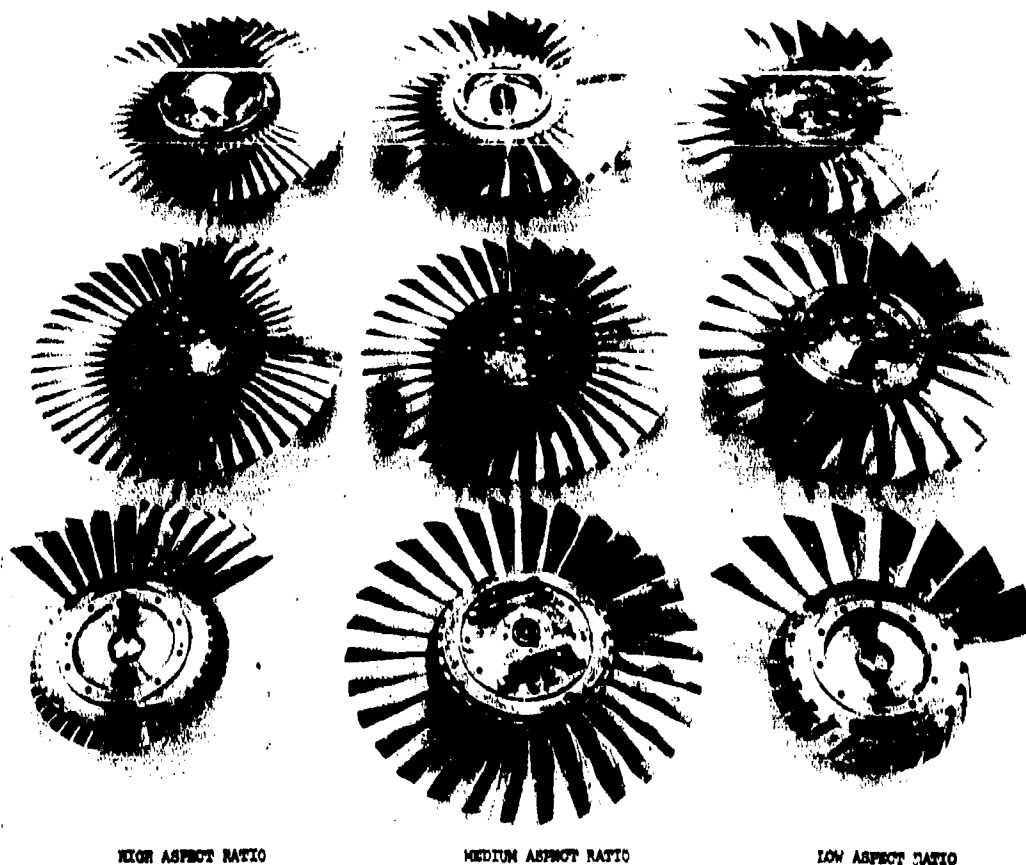
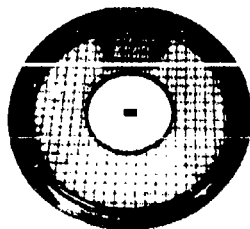


Figure 2-11. AEROMECHANICAL COMPRESSOR WHEEL ASSEMBLIES. Display of Various Airfoils Tested in Aeromechanical Test Rig.

- Coincidence of the first flex mode with 3/rev, and even order-per-revs at steady-state operating speeds, has been avoided.
- Coincidence of blade natural frequencies and stimuli from the front and rear struts has been avoided.
- Button spacing in the titanium blades is such that the titanium panel frequency has a 15 percent margin above the vane-wake frequencies, at least two stages forward and one stage aft.
- Disk-blade coupled modes have also been checked for compliance with the above frequency requirements.



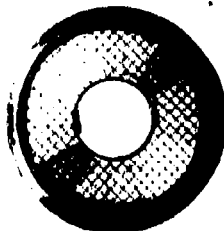
PATTERN #4  
ONE PER REV SINUSOIDAL



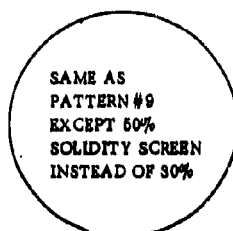
SINGLE IGV OFF ANGLE



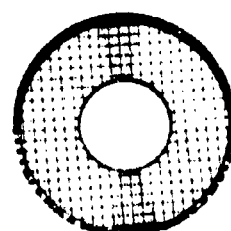
SIMULATED LARGE PROBE



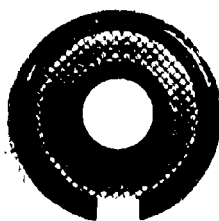
PATTERN #5  
TWO PER REV SINUSOIDAL



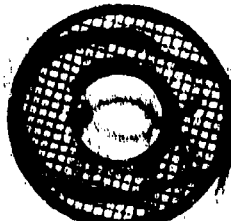
PATTERN #8  
TWO PER REV LOCAL



PATTERN #9  
MILD TWO PER REV LOCAL



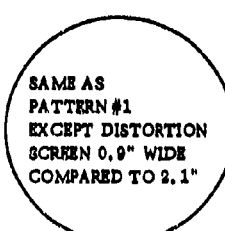
PATTERN #6  
HUB RADIAL LINEAR



PATTERN #3  
HUB LOCAL



PATTERN #1  
SEVERE TIP LOCAL



PATTERN #2  
TIP RADIAL

INLET DISTORTION AND  
LOCAL FLOW DISTURBANCE  
DEVICES TESTED WITH THE  
MEDIUM ASPECT RATIO -  
STEEL - NOMINAL SOLIDITY  
ROTOR.

Figure 2-12. DISTORTION SCREEN

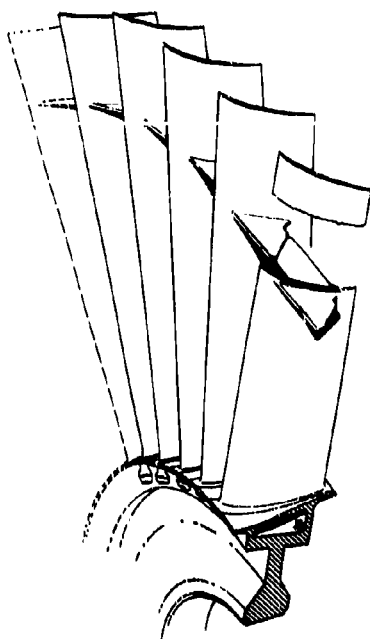


Figure 2-13. SHROUD CONFIGURATION, 1ST STAGE BLADE

Figures 2-15 and 2-16 are Campbell diagrams for stages 3 and 7, which demonstrate graphically the compliance of the blade design to the above criteria. A significant advantage of hollow blades is that they provide an added degree of freedom in adjusting blade frequencies, without compromising the external aerodynamic shape, by varying the internal cavity configuration during the design phase.

An additional criterion that has been observed in the GE4 compressor design is to limit the sea-level-static, uncorrected, gas bending stress (theoretical gas bending stress that would occur without the reduction due to blade-lean and centrifugal effects) to 40,000 psi on stages 1-3 and 45,000 psi on stages 4-9. While this stress does not exist as such, it is a measure of the airfoil flexural strength relative to the aerodynamic loading and has been found to be a good empirical index of general airfoil-vibration stress levels during separated flow and stall. When combined with the frequency and stability criteria, it gives assurance of the low vibration levels required for long life and durability.

Maintaining the uncorrected gas bending stresses below a specified level is also important to the reduction of high stresses during a stall. The GE4 blading is derived from the GE1 high-stage loading compressor, and the resulting "reduced velocity" parameter (Refer to paragraph 2.3.1.2 and Figure 2-6) will have similar values. The highest vibratory stresses recorded on the GE1

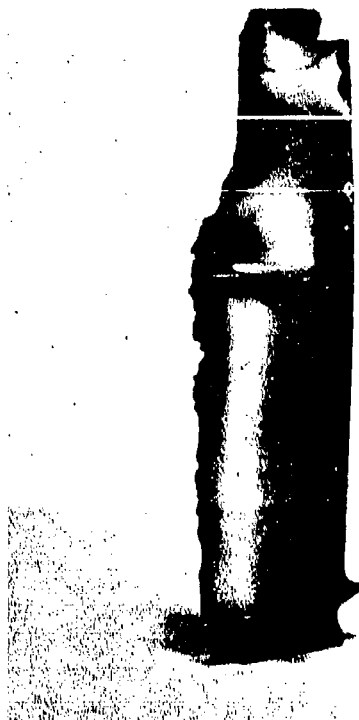


Figure 2-14. J93 FIRST STAGE SHROUDED BLADE AFTER FOD. After Impact from Airframe Inlet Duct and IGV. Engine Continued Operation for Duration of Flight.

during a full scale compressor test are tabulated below (Table 2-2) and reveal that the separated-flow vibration levels on the operating line were largely confined to stage 1 and 2 blades and stage 3 stator (stage 3 stator vane on the GE1 is non-shrouded). This is characteristic of forward stages at part-speed operation:

Table 2-2

<u>Stage</u>	<u>Corrected Speed For Max Separated Flow Vibrations (% <math>N_c</math>)</u>	<u>Vibratory Response (% of Allowable)</u>		<u>Mode of Vibration</u>
		<u>15"Hg</u>	<u>30"Hg</u>	
1R	85	13	18.5	1st Tor. and 1st Flex at outerpanel
2R	75	17	24	1st Flex
3S	75	9	13	1st Flex

No further evidence of separated-flow vibrations were observed on other stages. Since the external airfoil design on the GE4 and GE1 are similar, vibratory stress levels are expected to be similar, except for a small increase due to the hollow section.

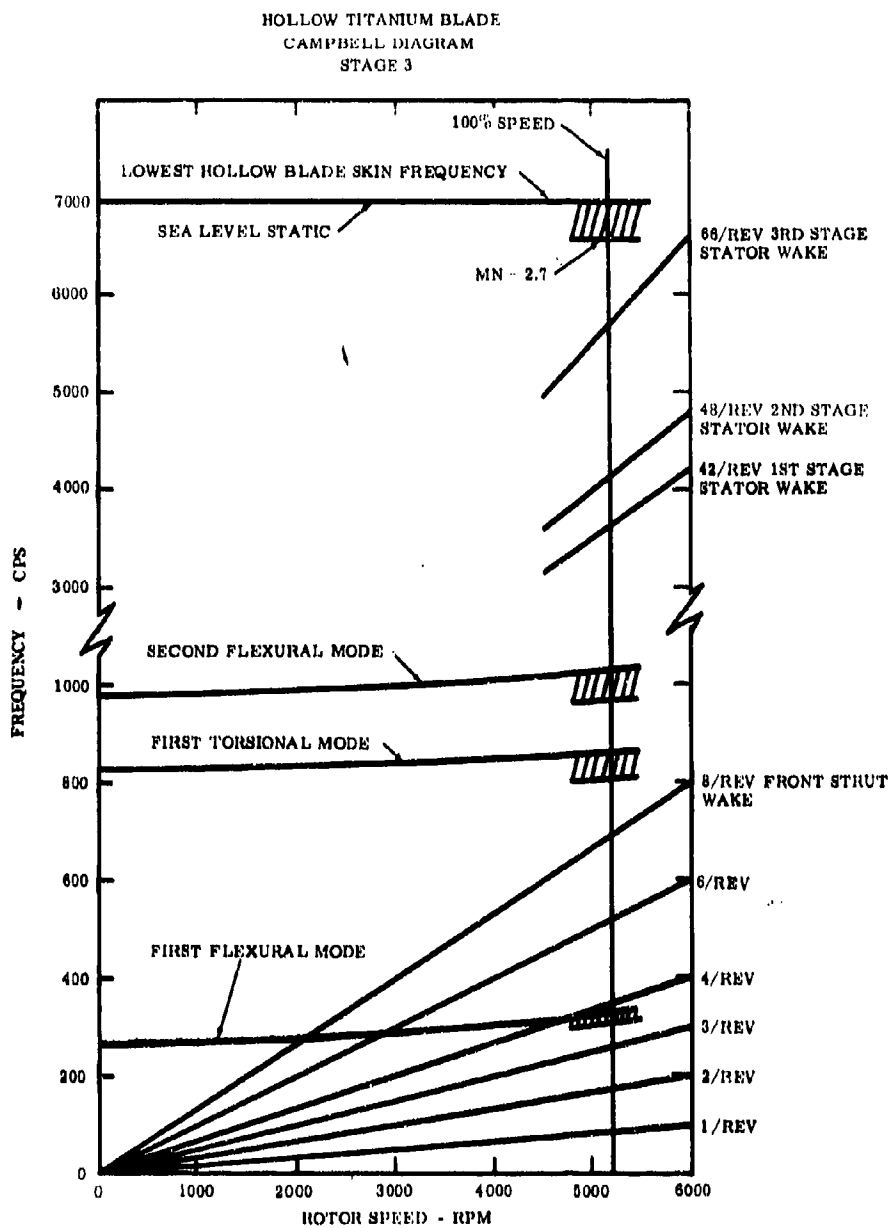


Figure 2-15. CAMPBELL DIAGRAM, STAGE 3 TITANIUM BLADE



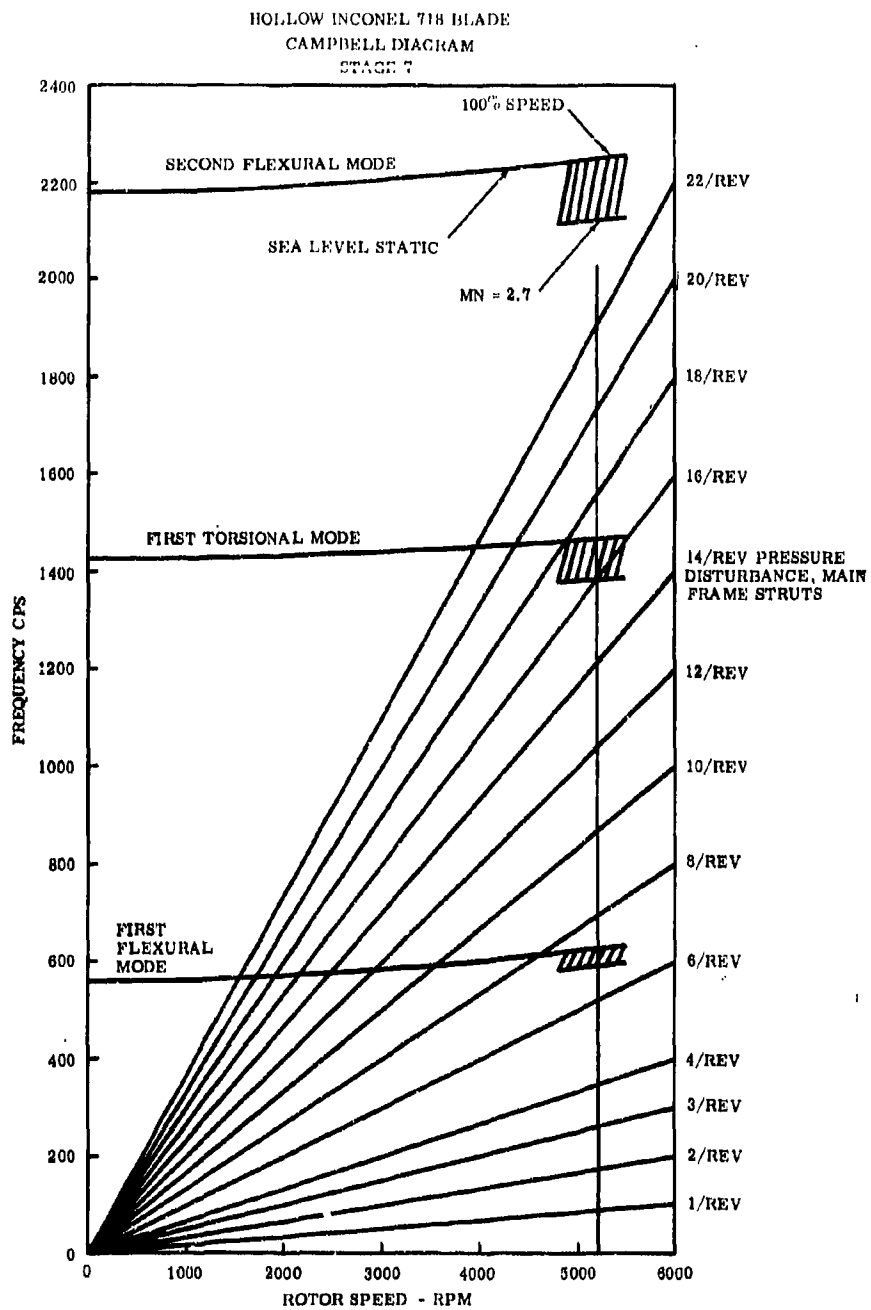


Figure 2-16. CAMPBELL DIAGRAM, STAGE 7 INCO 718 BLADE

Stall stresses recorded at 100 percent speed on the GE4 eight stage, 475 lb per second compressor, show low blade and vane-response. Figure 2-17 is a plot of these stresses compared with J93 stall data. The improvement is obvious.

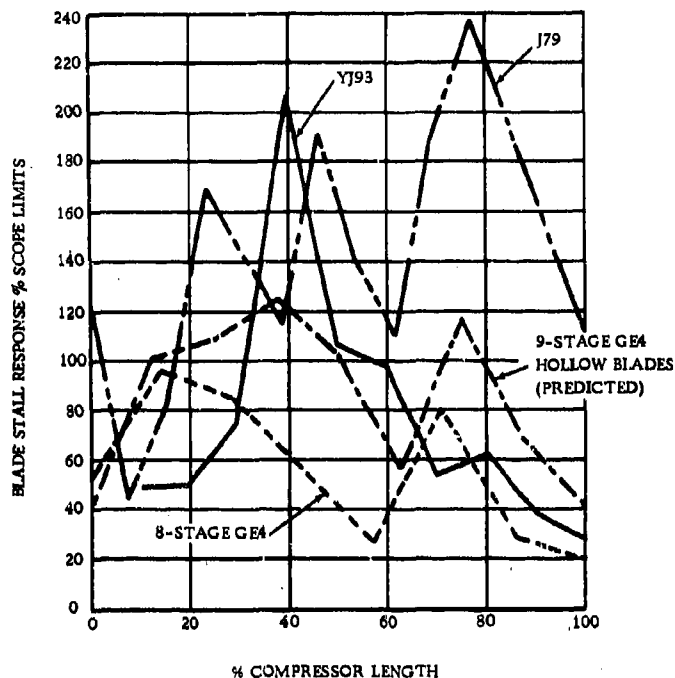


Figure 2-17. COMPARISON OF STALL STRESSES - ROTOR BLADE

Another significant advantage of the GE4 compressor airfoil design is the relative insensitivity of blade vibrations to inlet distortion. This was demonstrated on the GE1 high-stage loading compressor test, (ref. General Electric Report No. R66FPD105) where severe hub-radial, tip-radial, and one-per-rev circumferential patterns were tested. Vibration levels measured with distortion were only slightly higher than the low levels measured with clean inlet. Results of the full scale compressor tests of the GE4, 8-stage, 475lb/sec. compressor are discussed in paragraphs 2.4.1 and 2.4.1.1

No deliberate damping devices are required for blades of this type. The criteria described above result in low, blade-vibration levels with the normal aerodynamic, material and dovetail damping. The stage one shroud, which has a primary function to stiffen the blade, will also serve as a damper to further ensure low vibration levels.

The long chord design with solid leading and trailing edges is tolerant to foreign object damage, capable of absorbing high energy impact with little damage, and provides generous benching limits for repair. Tolerance to FOD is not just a function of size; the low vibratory stresses, characteristic of the GE4 blade design, are much less likely to result in fatigue failure propagating from damaged areas.

Long chord, low aspect ratio blades are more tolerant to erosion and corrosion because of their larger size. Little corrosion is expected on the high strength titanium or Inco 718. The GE4 blade features a squealer tip, as shown in Figure 2-18, to provide assurance that a blade rub will have no detrimental effect on the liners.

The "short chord" J93 compressor revealed that moderate to high aspect ratio blading is unsuitable for long life supersonic engines. The following observations were made on the short chord compressor:

- Inlet distortion was not attenuated with serious effects on performance and flow pattern to the combustor
- Blade vibration levels in stall, resonance, and separated flow were high due to low flexural rigidity
- The performance was exceptionally sensitive to stator schedule and radial clearances.

This development experience resulted in the "long chord" J93 research compressor, which was further improved to the current configuration used in the B-70 aircraft.

#### 2.3.1.3 Dovetail Design

The dovetails (see Figures 2-4, 2-8, 2-31, and 2-32) are designed to be stronger than the airfoil. This criterion is satisfied by assuming that the airfoil is vibrating at its endurance limit in the first flexural mode at all flight conditions. The vibratory and steady state moments and forces that are associated with this assumed condition are applied to the dovetail design analysis.

The General Electric, single-tang dovetail analysis is a comprehensive computerized procedure that enables the designer to apply the exact steady-state and vibratory loadings from the airfoil to the dovetail. This procedure has been verified with whirligig tests and engine failure analysis. The analysis has been modified for the GE4 dovetail to account for the changes in stress distribution when the central portion of the dovetails is hollowed out. Steady state and vibratory stresses are computed along the critical dovetail neck fillet and on the contact surface for various flight conditions and blade vibration modes. In each case vibration of the airfoil at the endurance limit is assumed. The Goodman diagram in Figures 2-19 and 2-20, are examples for stages 3 and 7 at Mach 2.7 flight in the first flexural mode.

The hollow blade and dovetail design results in significantly lower dovetail contact stresses. The contact surfaces have a copper/nickel/indium coating, which has been used extensively on previous General Electric engines such as the J93, GE1, and CJ805 as an anti-fretting medium. This coating, along with the relatively low contact stresses, combines to eliminate dovetail fretting and, at the same time, re-distribute high local peak stresses. The dovetail surface is shot-peened and grit-blasted prior to the coating application in the form of a plasma spray.

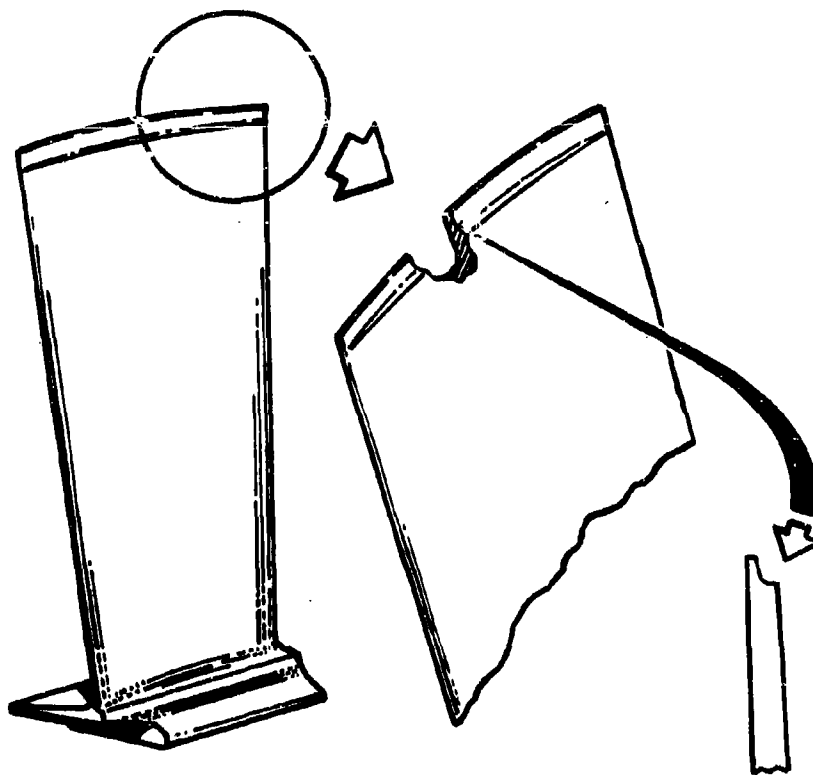


Figure 2-18. TYPICAL BLADE SQUEALER TIP

Figure 2-21 illustrates J93 and GE1 blades coated with copper/nickel/indium. The J93 blades without the coating encountered severe fretting from forced vibration at Mach 3 operation, where the metal temperature reaches 1150F. The coating can be stripped and re-sprayed for economical repair if necessary.

The disk dovetail pressure surfaces are coated with titanium hardcoat for protection against wear. This surface treatment is essentially an anodize process forming a hard surface approximately one-mil deep. This coating is applied by dipping the disk rim with the dovetail pressure surfaces exposed, into a solution. This treatment can be repeated as required.

Extensive testing has been conducted and sponsored by General Electric to perfect dovetail coatings suitable for long life and improved maintenance requirements.

### 2.3.2 ROTOR CONSTRUCTION

The compressor rotor consists of nine stages of disks with integral spacers. These disks are joined together with dowel bolts, giving excellent rotor stability to maintain low vibration levels throughout long periods between overhauls. Construction of the rotor is shown in Figure 2-22. Dowel bolts are used on J79 compressor rotors, as shown in Figure 2-23, and have proven their acceptability for assembly and disassembly and in keeping the rotor parts tightly clamped together. The GE4 rotor design has capitalized on the stability of the dowelled rotor, while locating the bolted joints away from the highly-stressed disk webs for long cyclic life. Also, the Poisson's Ratio effect, which decreases the axial thickness of the bolt pad and reduces the clamping load, is avoided in the disk web. The dynamic clamping load of the bolts is increased by 30 percent when the rotor bolts do not pass through the disk web and when scalloped flanges are used. With the disk flange extensions located below the flowpath boundary, they form a nearly-cylindrical structure which is stiffer than the rim-type spacers of the CJ805, for better control of system criticals and avoidance of rotor whirl.

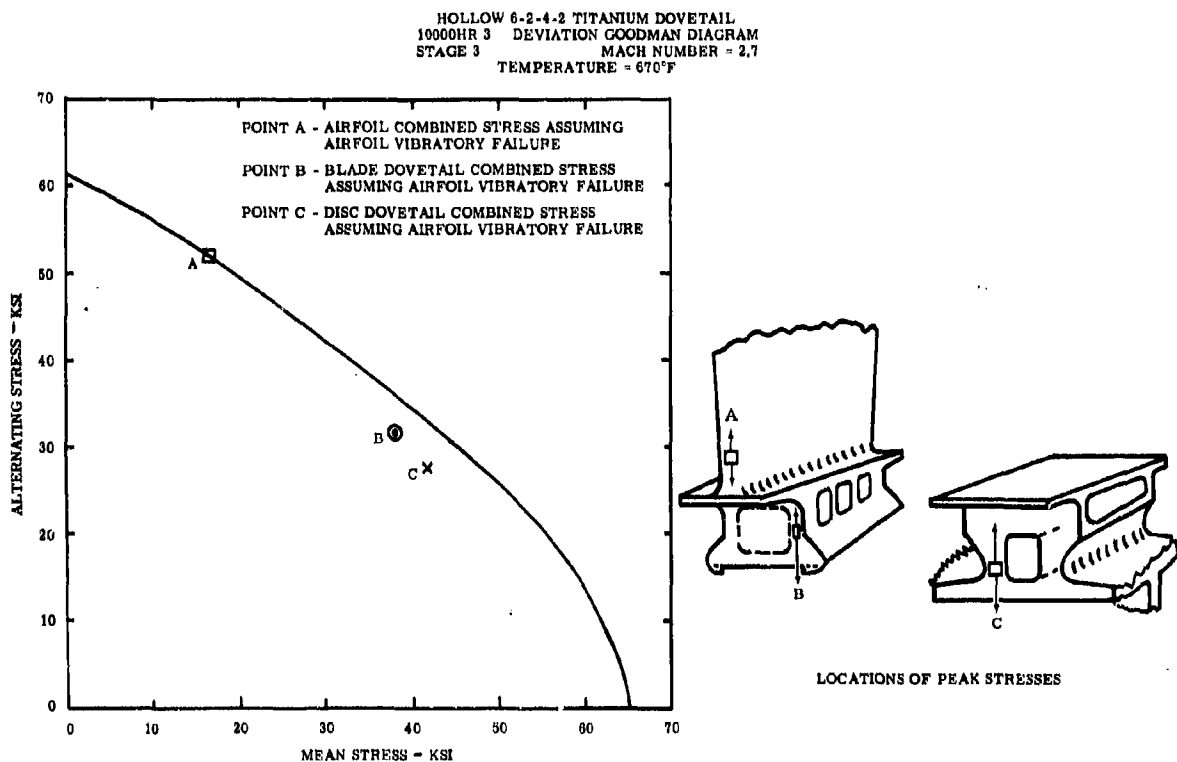


Figure 2-19. GOODMAN DIAGRAM, STAGE 3 TITANIUM BLADE. "Weak link" criteria--blade dovetail stronger than airfoil. Disk dovetail stronger than blade dovetail.

HOLLOW INCONEL 718 DOVETAIL  
10000 HR 3 $\sigma$  DEVIATION GOODMAN DIAGRAM  
STAGE 7 MACH NUMBER = 2.7  
TEMPERATURE = 975°F

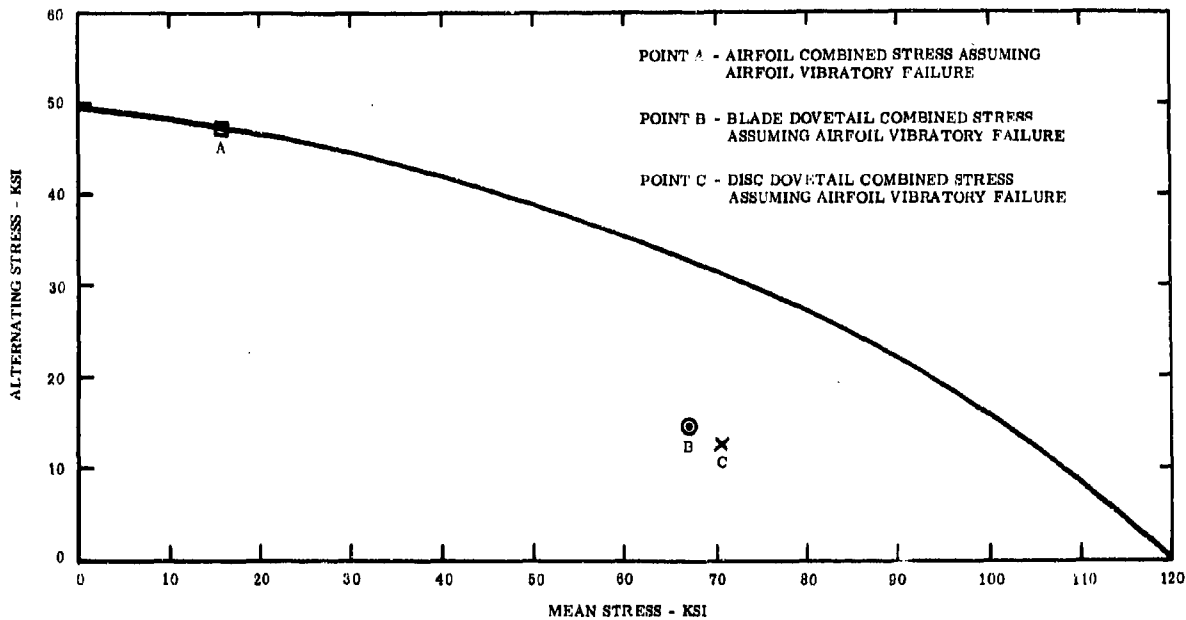


Figure 2-20. GOODMAN DIAGRAM, STAGE 7 INCO 718 BLADE. "Weak link" criteria - blade dovetail stronger than airfoil. Disk dovetail stronger than blade dovetail.

Simplicity of this design concept is evident in Figure 2-24, where the design is compared to the J93 which, while satisfactory, is more redundant.

Corrosion prevention is assured in the GE4 rotor by the use of Titanium 6-2-4-2 in the first four stages and by using Inconel 718 for Stages 5 through 9.

The rotor is firmly supported between two bearings. At the front of the rotor, a conical stubshaft is bolted to the spacer flanges on Stage one and two disks. The No. 1 bearing is mounted on the forward end of the shaft. The aft conical stubshaft is bolted to the stage 9 disk flange. The shafts and integral disk-spacers complete the high stability, structural configuration of the rotor. The rotor thrust bearing is mounted on the aft end of the aft shaft. Turbine torque is transmitted to the compressor rotor through an internal spline on the compressor aft shaft.

The rotor assembly procedure is simple. Beginning with the stage 2 disk, bolts are inserted in forward disk flange and held in place with push-on nuts. With the front stubshaft vertical, flanged end up, the stage 2 disk is positioned, the stage 1 disk aft flange is assembled over the bolts, and the nuts then torqued. Slab-headed hook bolts are used for all flanges and are shown in Figure 2-25. The bolts are inserted in the aft flange of the stage 2 disk and held in place by push-on nuts.

The stage 3 disk, with bolts, is then placed on the adjoining flange, nuts are applied and torqued. A hook on the bolt head engages the flange edge to prevent turning as the nut is tightened. There is ample room for the assembler to reach in through the large disk-bore diameter to torque the nut and inspect the assembly. The assembly proceeds in a like manner back to the aft stubshaft. The central tube is bolted to the aft stubshaft before the aft stubshaft is attached to the stage 9 disk.

Each disk and blade assembly is static-balanced by positioning the blades, which are marked with their moment weights, to facilitate the balancing. The assembled rotor is dynamically balanced by shifting blades and using weights at the bolt circles, which connect the first and ninth stage disk to shaft. (See Figure 2-63)

### 2.3.3 DISKS/SPACERS

Reliability has been of prime concern in the design of the rotor structure. Each disk is integral with flanged spacers, which, when bolted together, make up the backbone of the rotor. Making the spacers integral with the disks eliminates the bolted joint from the disk web, 1) to avoid the potential, low-cycle, fatigue failures associated with bolt holes in a highly-stressed disk and, 2) to avoid potential fatigue cracking in the fillet between disk rim and web. Areas adjacent to bolt holes subjected to repeated high stress will fatigue after a limited number of cycles (start, accel., decel., stop) due, primarily, to the inherently high-stress concentration factor of bolt holes. Positive assurance against low-cycle fatigue is gained only by eliminating the holes from the web area.

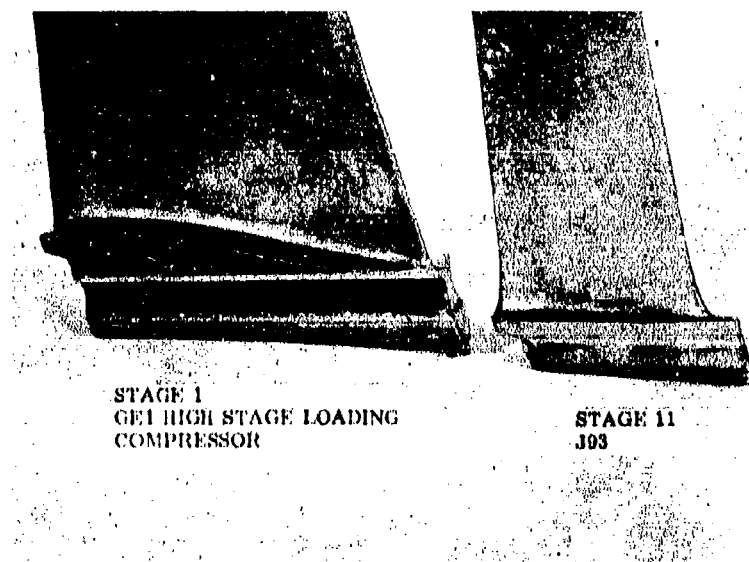


Figure 2-21. COPPER-NICKEL-INDIUM COATED DOVETAILS

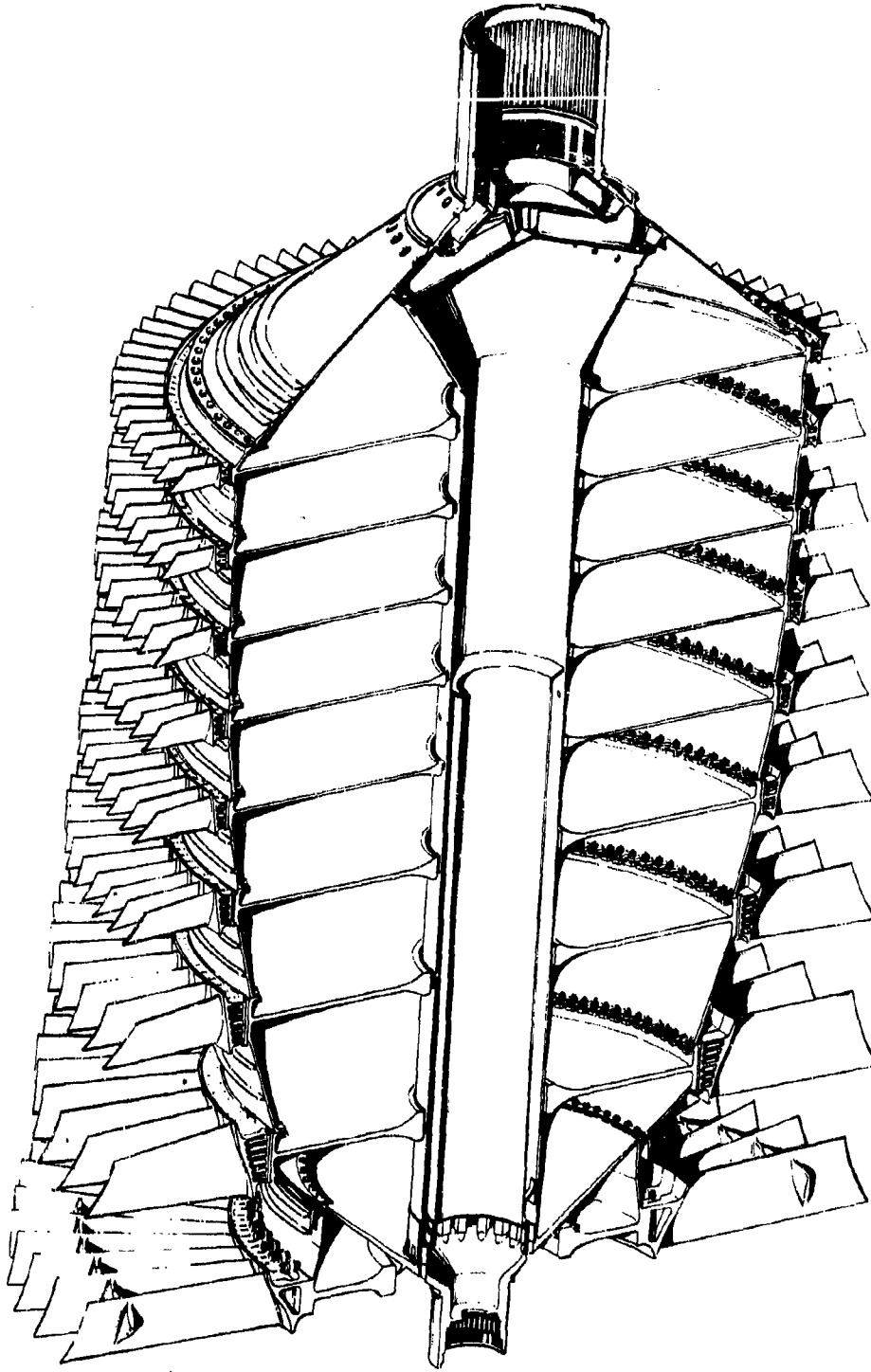


Figure 2-22. ROTOR CONSTRUCTION, GE4. GE4 Compressor Rotor, Showing  
Integral Disk/Spacers Joined With Dowel Bolts



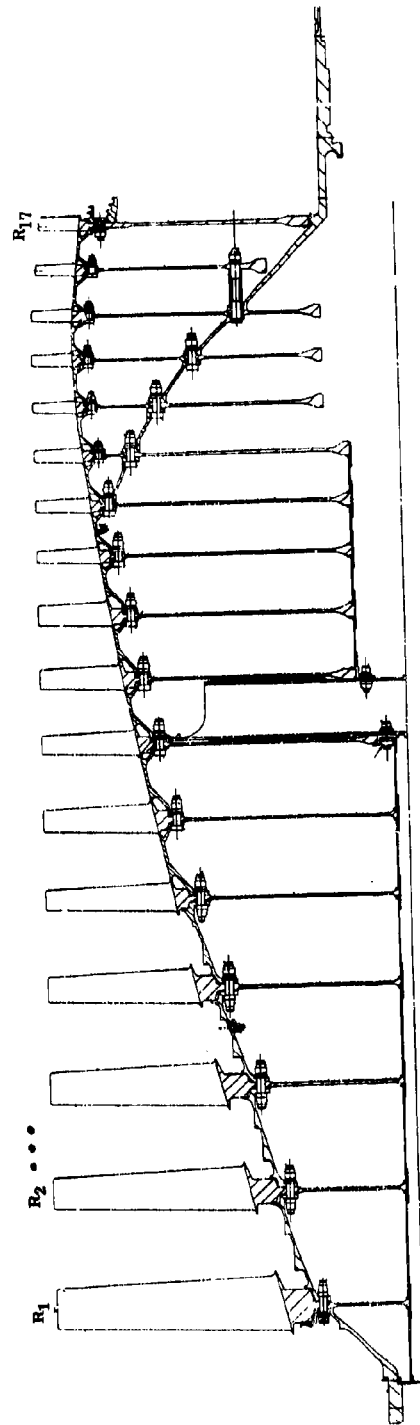


Figure 2-23. COMPRESSOR ROTOR-DOWEL BOLT CONSTRUCTION. J79 Compressor Rotor Showing Dowel Bolt Construction Which, With Modifications, Has Been Adopted for GE4

Low-cycle fatigue of the spacer flange holes has also been considered. By incorporating scalloped flanges, the holes are removed from the high tangential stress area, significantly reducing their stress concentration factors.

Figure 2-26 illustrates the scalloped flanges and the original CJ805 design. Scalloping the flanges of the stage 11 through stage 16 spacers in the CJ805 made a very significant improvement in their low cycle fatigue life, increasing that life by a factor of ten.

Disk rims, supported only by the webs as in the J79, are compared to the GE4 design in Figure 2-27. Vibratory loads of the combined blades and rim may impose a tendency to roll the rim, but the GE4 design takes these moments directly to the spacer extensions and web. In a design with flanges adjacent to the web, the web itself must take the entire moment. Unless the web is made extra thick to resist this moment, it will be subjected to bending stresses in the fillet that will eventually cause fatigue cracks.

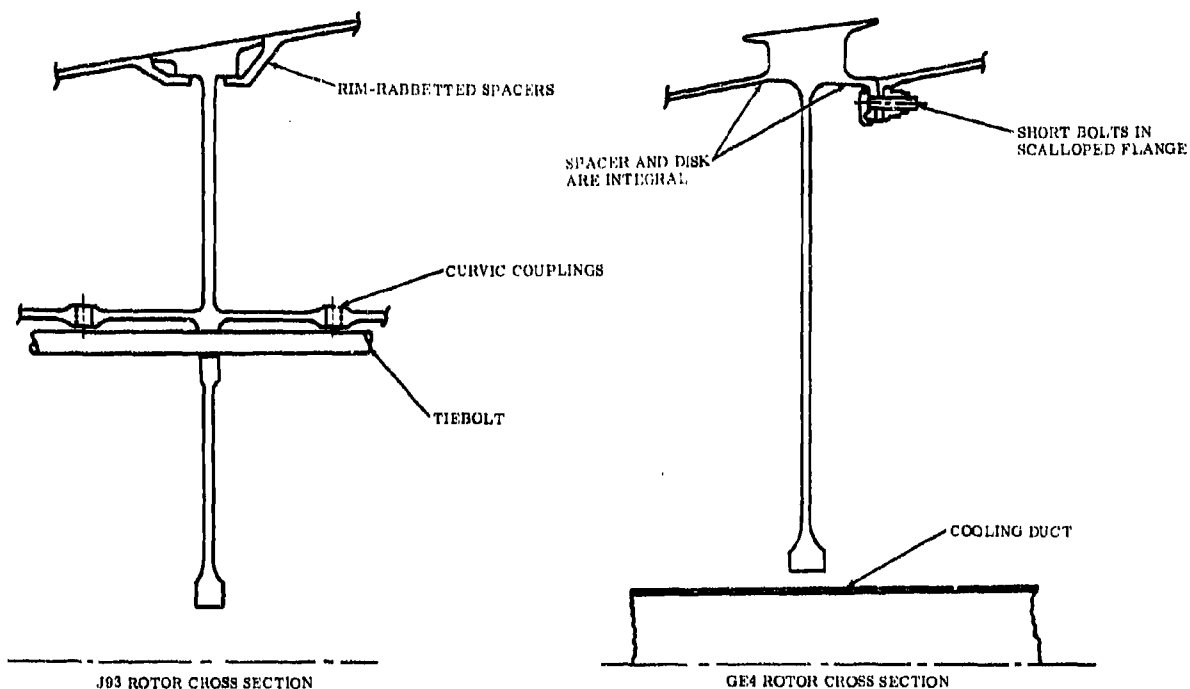
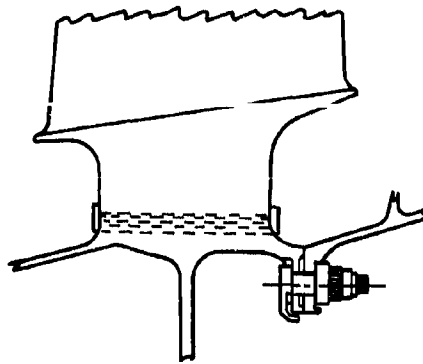
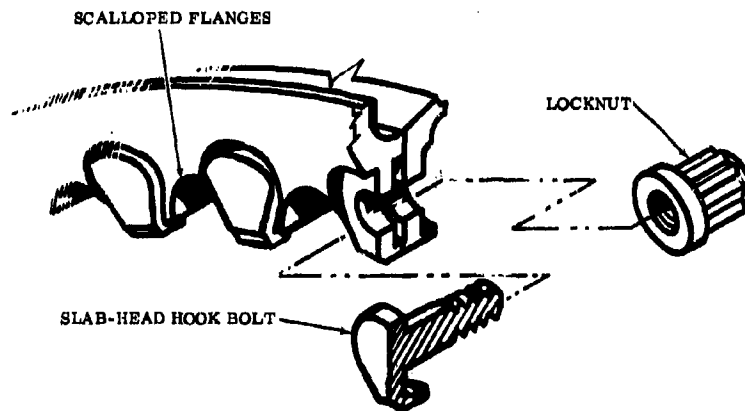


Figure 2-24. COMPARISON OF J93 AND GE4 ROTORS. Simplicity of GE4 Compressor Rotor Design Shown by Comparison With Curvic Extension + Spacers Used in J93 Compressor Rotor



NO BOLT HOLES IN DISK    SCALLOPED FLANGES  
SUPPORTED DISK RIMS    RESISTANCE TO LCF  
HIGH SOLIDITY BOLTING    INCREASED RIGIDITY



**Figure 2-25. SLAB-HEAD HOOK BOLTS. Compressor Rotor Disk/Spacer Flanged Joint Showing Bolts and Scallop Flanges Slab-Headed Hook**

The disks have been designed to provide 36,000 hours of operation. They meet the following stress requirements:

- Steady State -

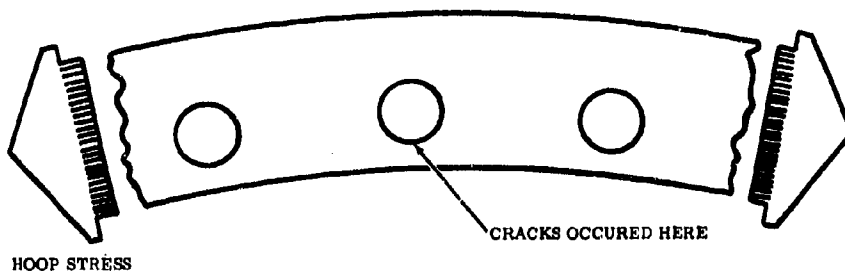
Disks/spacers designed to limit plastic creep to 0.2 percent extension or less, within the more severe condition of either 36,000 hours life while flying typical missions or 30,000 hours life continuous operation at Mach 2.7, standard day. At the same worse condition, average tangential stresses do not exceed 70 percent of master rupture. Stresses include effect of thermal gradients which exist during steady-state operation. Minimum material properties are used for design limits, the minimum being at least three standard deviations lower than the average material property.

- Transient Overspeed (Single Control Malfunction) -

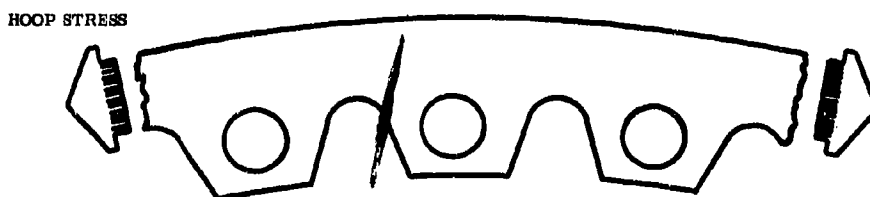
Disk/spacer stresses at 5 percent over the normal operating rpm, are designed to limits that will avoid distortion or growth which would be detrimental to normal reassembly or reduce operating clearances.

- Certification Overspeed -

Disk/spacer stresses at 15 percent over the maximum rated rpm are held to limits that will avoid any possibility of incipient failure after five minutes of engine operation.



ORIGINAL CJ805 ROTOR FLANGE PROFILE  
10:1 INCREASE IN CYCLIC LIFE WAS  
OBTAINED BY SCALLOPING THE FLANGES



GE4 ROTOR FLANGE PROFILE  
SCALLOPS LOWER HOLE STRESS CONCENTRATION

Figure 2-26. ROTOR FLANGES. GE4 Rotor Flange Profile  
(Scallops Lower Hole Stress Concentration)

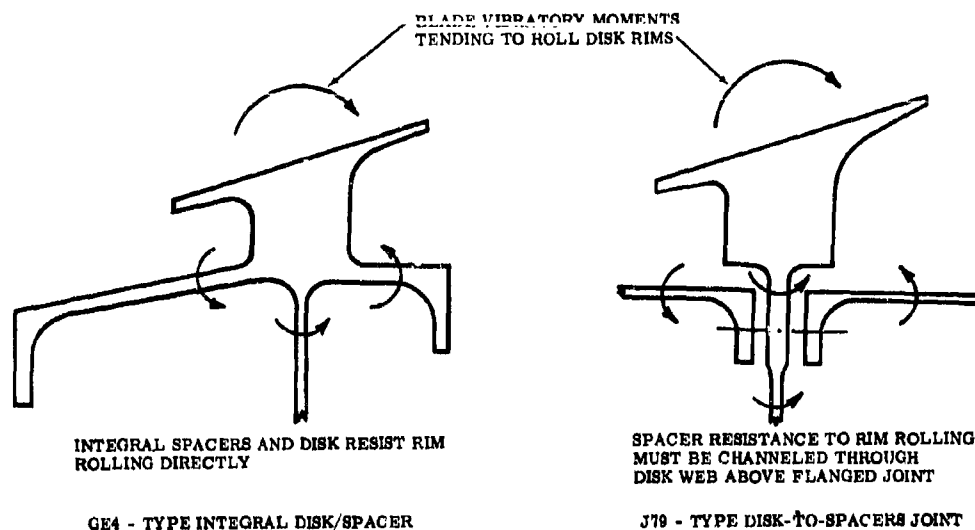


Figure 2-27. DISK RIM COMPARISON. Rim Stiffness of GE4 Integral Disk/Spacers Compared to J79-type Disks with Spacers Bolted to Disk Web

These limits are established by calculating a minimum burst speed, which must be 5 percent greater than the certification overspeed. This experimental/analytical procedure has been developed by General Electric. Calculation of this speed  $N_T$ , is obtained from the expression,  $N_T = S(N_P - N_E) + N_E$ , where:

$N_E$  = speed at which the maximum elastic stress equals the smooth-test-bar ultimate tensile strength of the disk material.

$N_P$  = speed at which the average tangential stress equals the smooth-bar ultimate tensile strength

$S$  = factor obtained from one to two curves, Figures 2-28 and 2-29, depending upon whether the maximum elastic stress is uniaxial or biaxial. Minimum values of  $S$  are used. The parameter, Notch Strength Ratio (NSR), against which values of  $S$  are plotted, is the ratio of notched bar ultimate to smooth bar ultimate. Values of this parameter, NSR, are obtained for the material at the temperature of the wheel at the location of the maximum elastic stress. Use of these parameters for prediction of wheel burst speed have been correlated with actual burst tests of many wheels of materials, varying widely in ductility, as indicated on Figure 2-28 and 2-29.

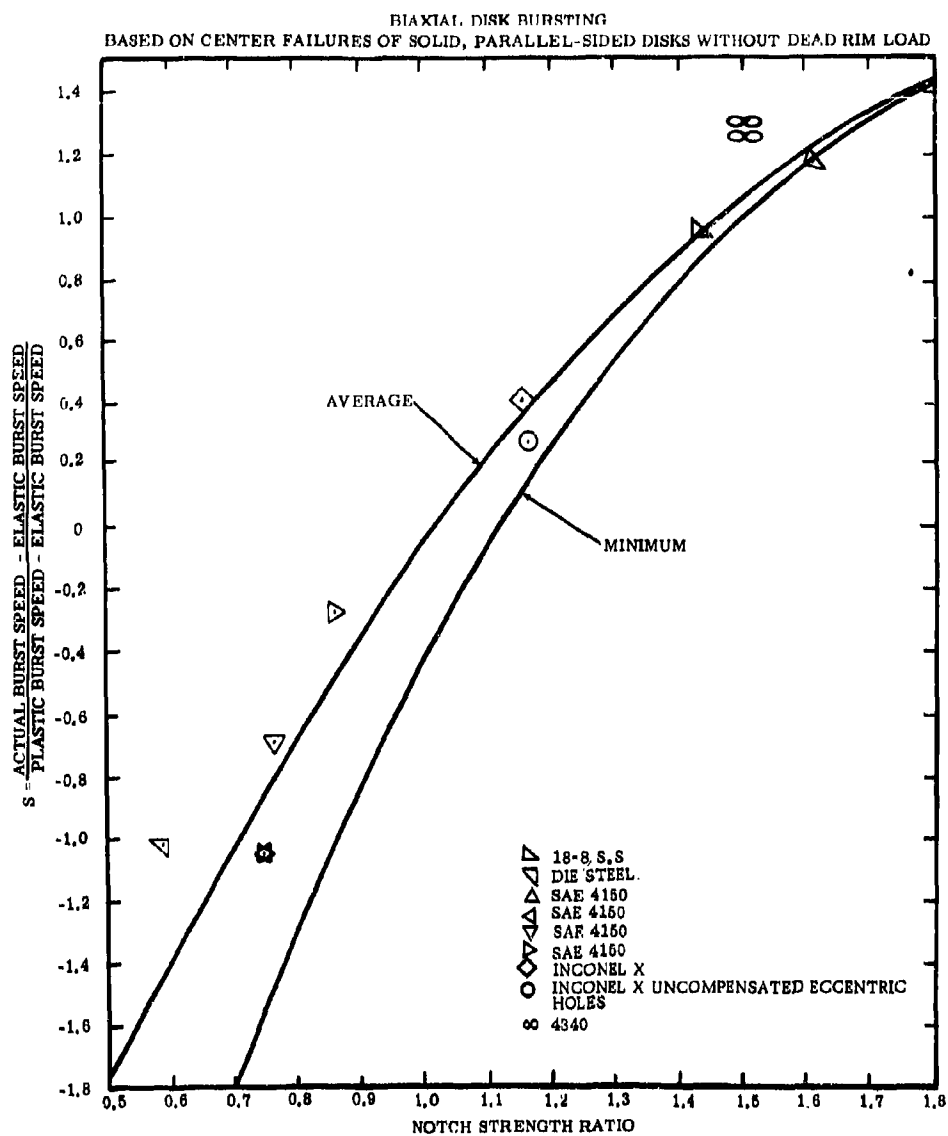


Figure 2-28. BI-AXIAL DISK BURSTING CURVES

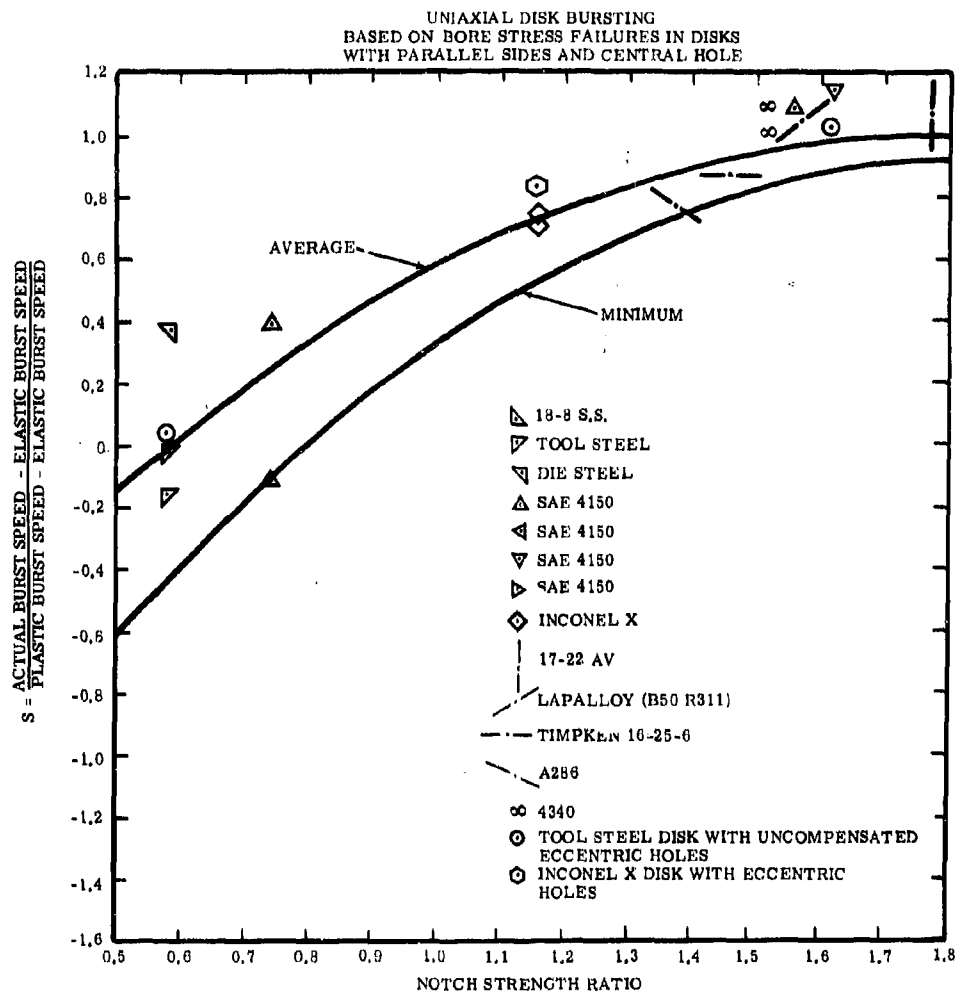


Figure 2-29. UNI-AXIAL DISK BURSTING CURVES

- Cyclic Stresses - Vibratory

Disk/spacer stress levels during steady state operation are set low enough to allow for 10,000 psi alternating stress. High cycle fatigue is avoided by design and testing to assure that this allowable vibratory stress will not be exceeded in any resonances excited by:

Bearing-ball (roller) passing frequencies

Strut-passing frequencies

Vane-passing frequencies

First-or second-engine-order frequencies

- Cyclic Stresses - Engine Starts

For the maximum range of stresses resulting from thermal gradients and engine rpm, the disk/spacers are designed to operate satisfactorily for 22,000 ground start cycles, and 1200 flight start cycles. This objective will be achieved by early investigation of cyclic rupture, a name which has been given to the combined effects of low cycle fatigue and stress rupture. By cyclic tests at high temperatures that included a hold at the peak stress part of the cycle, General Electric research has shown that low cycle fatigue and stress rupture are inter-related. Experimental analysis will permit the design matching of materials and configurations to meet the requirements of the environment.

Disk/spacer thermal gradients will be verified by engine testing in conjunction with heat transfer analysis of the rotor. Design levels for these gradients are illustrated in Figure 2-30, which show the predicted temperature differentials corresponding to maximum stresses at disk bores during the Mach 2.7 cruise condition, and minimum stresses at disk bores after a ground throttle chop.

From the strains corresponding to these maximum and minimum stresses, both a mean strain and an alternating strain, which is half the total strain excursion, are determined. An "A" ratio, defined as alternating strain divided by mean strain, is used to determine from material data curves the number of cycles to failure at the value of alternating strain. In determining low cycle fatigue capability at the disk rim, stress concentration factors for the bottom of the dovetail slots are applied to disk-rim tangential stresses for the maximum stress and minimum stress conditions. The bottom of the dovetail seats are curved to blend with the side radii for minimum concentration of stress. Maximum rim stress occurs at a throttle burst to take off, when the disk is at essentially uniform temperature. Minimum rim stress occurs either during a throttle chop because of rim-temperature, transient-cooling lag or during the Mach 2.7 cruise where the maximum thermal gradient forces the rim into compression.

The blade and disk dovetails have been sized to assure that the disk dovetail is stronger in fatigue than is the blade dovetail, which is, in turn, stronger than the blade airfoil. This reliability approach is used to maintain a rim structure stronger than the airfoil. Material has been removed from the low stressed areas of the rim and blade dovetails to reduce dead load and save weight without impairing the structural integrity.

Figure 2-31 is an exploded view of the rim dovetail area typical of stages 2 through 9. In these stages, the bottom of the blade dovetail is grooved lengthwise. With the blade retainer in this groove, the blade and retainer may be pushed into the disk slot. The ends of the blade retainer project outward on either end of the blade dovetail and project inward on either side of the disk rim



when the retainer is positioned inward. This positioning is provided by a strip of ductile steel inserted between the retainer and the bottom of the blade. The strip is bent outward at each end to keep it in place. The structural retainer itself is not bent during assembly and is made of high tensile strength Inco 718. Only the unloaded positioning spacer is bent to lock the assembly in place. Contact stresses on the dovetail surfaces are low and resulting in minimum fretting action. The blade dovetail surfaces have a coating of copper-nickel-indium to prevent galling and redistribute the higher local contact stresses. The dovetail surfaces of the titanium disks are treated with titanium hardcoat; essentially an anodizing process which has been shown to reduce fretting.

The dovetail has been radiused at the base to reduce the stress concentrations. The original J93 dovetail, as illustrated in Figure 2-31, had a flat base and cracked at the intersection of the radius and flat. A modification (shown in the figure) with a radiused bottom successfully solved the problem.

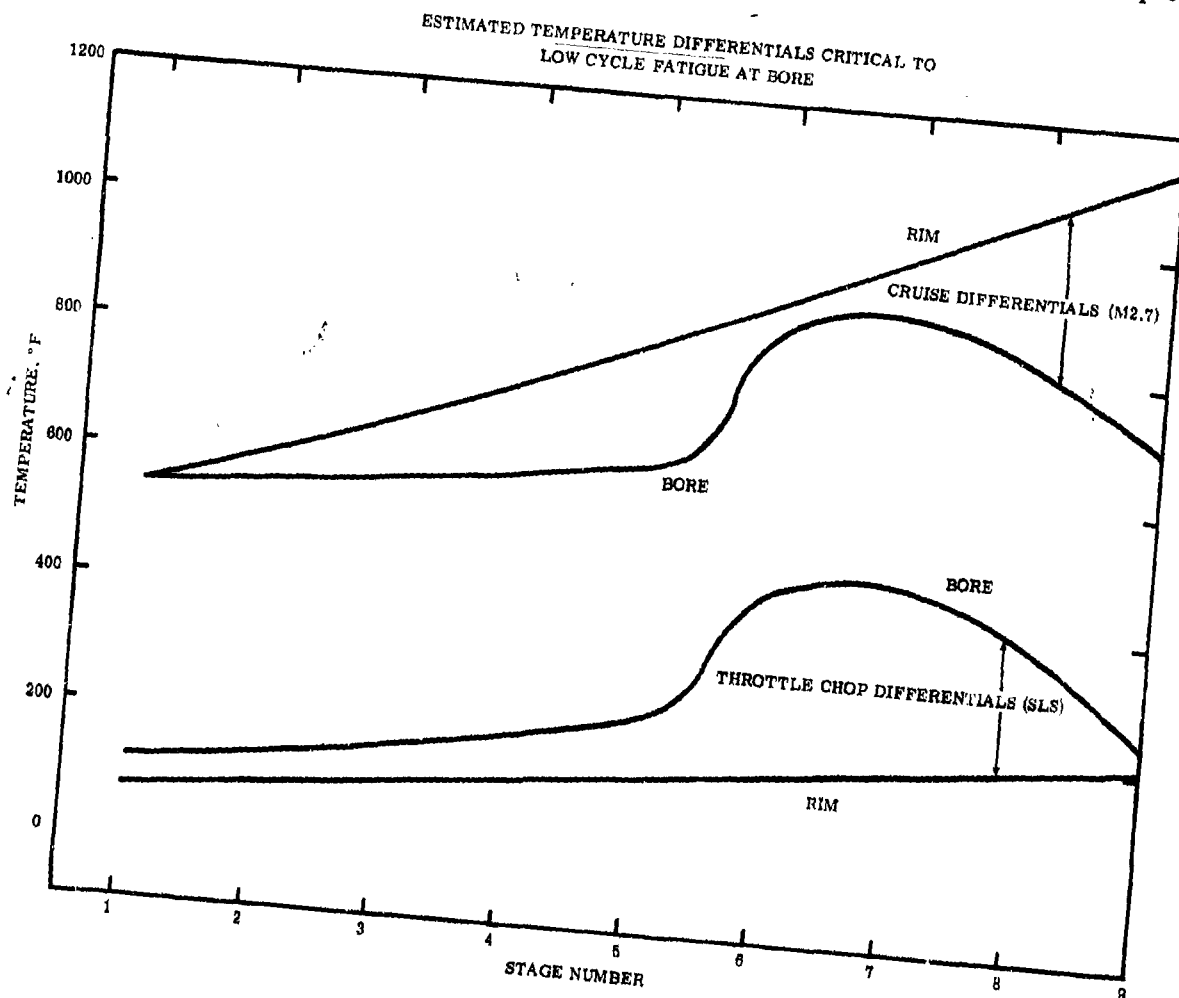


Figure 2-30. DISK THERMAL GRADIENTS

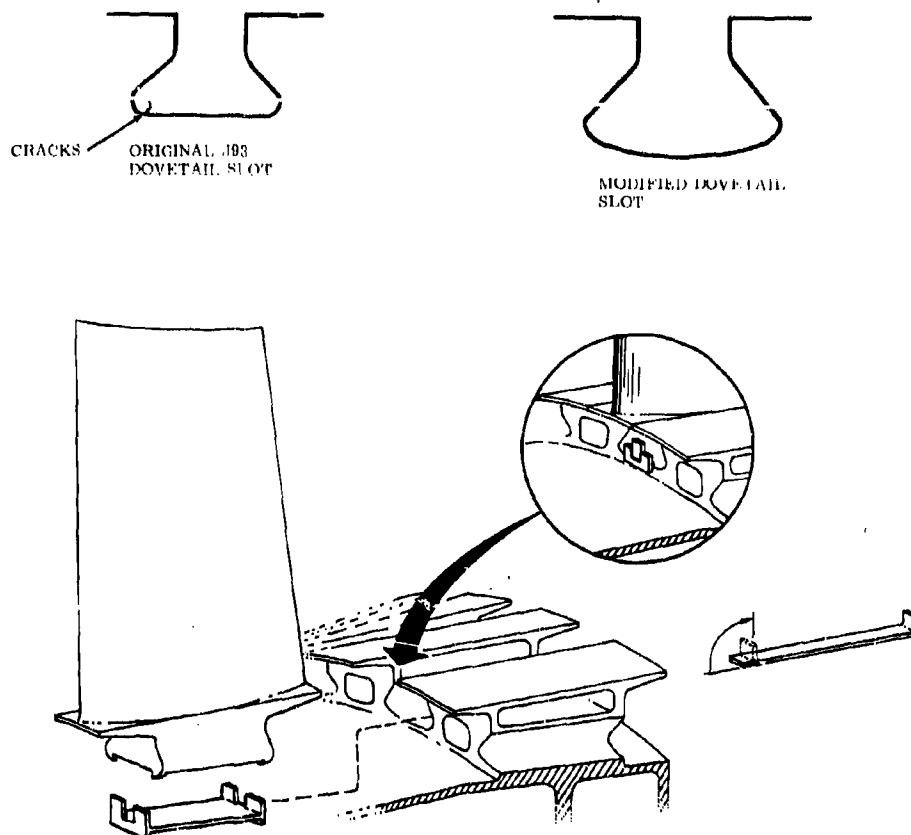


Figure 2-31. BLADE RETENTION AND DOVETAIL DETAILS TYPICAL OF STAGES 2 THROUGH 9

Figure 2-32 shows the improved maintainability for retaining the shrouded blades in stage one. The dovetail slot is deeper than the blade dovetail, permitting installation or removal of an individual blade without disturbing the adjacent blades. The shrouds are engaged when each of the blades is in its outermost radial position in its dovetail slot. The blade is held and locked in position by a bolted, three-piece, retainer assembly. With the blade held radially outward in the disk slot, the outer and inner retainer pieces are inserted and engaged to the blade dovetail ends and disk side faces respectively. The middle spacer is inserted between the inner and outer retainer pieces to hold all parts in position and to seal the slot against air leakage. The three retainer pieces are locked together with a bolt that engages a shank nut in the inner retainer piece.

#### 2.3.4 COOLING

The compressor rotor has been designed to cool internally to save weight and still attain improved durability/reliability levels by maximum use of titanium and to avoid the use of costly turbine-type material in the last two disks. Without cooling, the Inco 718 disks in stages 8 and 9 would be creep limited. An efficient cooling method is provided at a minimum cost to the cycle. This cooling method has an additional important advantage in that thermal stresses during transient are minimized.

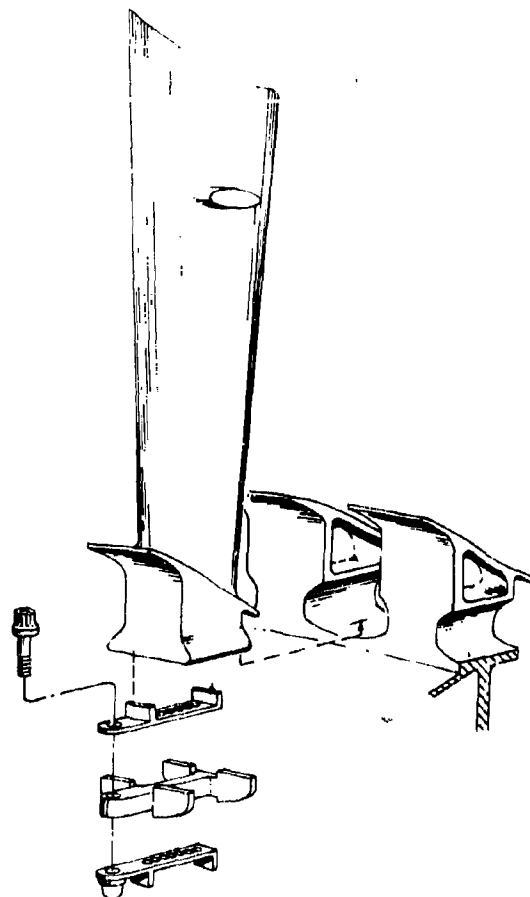


Figure 2-32. STAGE ONE BLADE RETENTION DESIGN

The compressor rotor is cooled internally with a closed loop system (See Figure 2-32). Air is bled from first stage discharge and flows radially inward between the conical stubshaft and the second stage disk. Minimum pressure loss in this cavity is assured by means of radial baffles attached to the inner surface of the front stubshaft cone. The baffles force the air to rotate as a solid body, rather than forming a vortex. Part of the cool air enters the central tube cavity through radial passages and then flows aft. It is emitted radially through holes in the central tube between the ninth stage disk and the rear stubshaft.

The disks and stubshaft are convectively cooled by the higher density, cooler air being centrifuged to the rim and displacing the less dense hotter air, which then flows into the center of the rotor. This mechanism of convective cooling is employed on the J93 compressor forward stages and is effective due to the large surface area of the disk and the low conductive heat path from the rim. Flowing forward between duct and ninth stage disk bore, it enters the cavity forward of the ninth stage disk, where the outward-inward circulation acts by convection to cool the stage 8 spacer and the disks of stages 8 and 9. The cycle is repeated again in each successive rotor cavity as the cooling air flows forward.

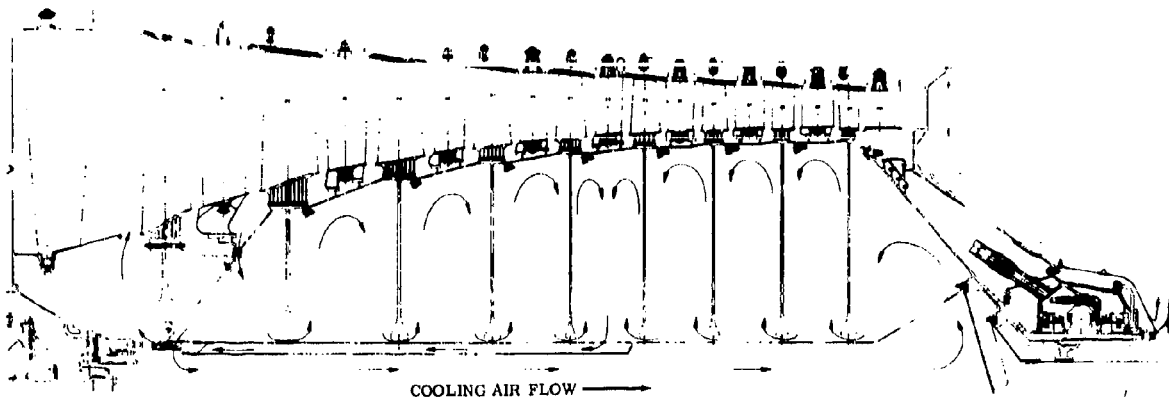


Figure 2-33. ROTOR COOLING CONFIGURATION

Simultaneous with the flow of cooling air from the aft end, another part of the cooling air in the cavity forward of the stage 2 disk flows aft between stage 2 disk bore and the central duct. An outward-inward circulation is set up in each rotor cavity as this cooling air flows aft. In the cavity aft of the Stage 5 disks, the two cooling flows join and mix.

Holes in the central tube aft of the fifth stage disk allow the air mixture to enter an annular passage formed by the central tube and another cylinder concentric with it. The passage conducts the cooling air to the cavity forward of the stubshaft. From this cavity, the air re-enters the flowpath ahead of the first stage.

The cooling air flowing inside the central tube provides high density air where it is needed the most, at the ninth stage cavity. As the air moves forward, it does less cooling on each successive stage until reaching the fifth stage where its temperature is equal to main stream temperature. The air which cools the forward disks is progressively heated as it flows aft past the second, third, fourth and fifth disks, to the cavity between the fifth and sixth disks. There it mixes with the aft cooling air which is at about the same temperature. The only significant cycle loss is in the energy associated with one stage of compression of the cooling air; the pressure ratio of the first stage being the cooling-air source/sink pressure-head. Less than 0.1 percent of total cycle air is required to cool the disks.

Several other advantages obtained with the cooling method are:

- The flow of cool air through the central tube keeps the tube cool enough to be made from titanium and, consequently, have low weight.
- The thermal differentials in the forward disks are substantially reduced, permitting improvements in weight and mechanical integrity.
- The method is well suited to refinement during development and for growth. The quantity of air can be increased or decreased by simply changing the number or size of the metering holes in the cooling circuit.
- Radial clearance control during transients is achieved by substantially improving the thermal cooling rate of the rotor during speed or Mach number changes. Normally, a rotor such as the J93 takes 30 minutes to stabilize after a throttle chop or aircraft

deceleration, during which time the casing shrinks and radial clearances decrease. Temperature measurements for the J79 engine also reveal that the minimum clearances occur some time after the transient. The GE4 internal cooling system offers improvements in clearance control by matching the thermal response rates of the rotor and stator. Clearance changes are thereby minimized during throttle bursts or aircraft accelerations as well as during throttle chops or aircraft decelerations.

- The lower rotor internal-pressure, resulting from being forward venting, decreases the rear spacer stresses by 8 percent and, therefore, improves reliability.

A cap at the aft end of the duct is used to seal the internal compressor air from the turbine cooling air. Duct material is Ti 6-2-4-2. Cap material is Inco 718.

### 2.3.5 AIR SEALS

#### 2.3.5.1 Interstage Seals

To achieve tolerable leakage over the rotor spacers, adequate interstage sealing is provided by the mating honeycomb-and-teeth design incorporated in the GE4 compressor assembly (see Figure 2-34). The sealing in each of the shrouded stators, stages 1 thru 8, is accomplished satisfactorily by two, mating, honeycomb-and-tooth assemblies, positioned forward and aft of the stator vane stacking axis at different radial heights. Essentially, these seals consist of a stationary section, formed by the honeycomb on the inner band of the stator vane shroud, and a rotating section, formed by the circumferential teeth on the rotor spacer at corresponding axial and radial locations. This seal configuration is being used successfully in the J93 engine (Figure 2-35) and has been proven satisfactory for sealing axial flow compressors and turbines.

All the shroud seals forming the stationary section are fabricated from steel honeycomb. The .060 in. cell honeycomb is brazed to a thin sheet metal back-up strip which, in turn, is brazed to the I. D. surfaces of the stator vane shrouds at locations forward and aft of the stator axis and at different radial heights. General Electric engine experiences -- T58, J79, CJ805, J93 -- have proven that honeycomb seals have very good rub tolerance. A direct rub causes instantaneous generation of heat at the honeycomb outer edges, resulting in localized softening, yielding, or melting of the honeycomb foil. This condition effectively reduces heat transference to the rotor. Additionally, there is a constant circulation of air through the honeycomb cells which helps convert rub-induced heat away from the rotor and stator. Since the honeycomb does not machine away in the event of rub but merely mashes down in place, there is no generating of metallic particles to pass downstream and cause erosion or enter critical areas (most particularly, the main bearings) in the engine. Because of its ability to mash down, honeycomb permits much smaller radial clearances than normal; high efficiency and performance is maintained since radial clearance is never greater than actually required at each point. The honeycomb selected for the seals is substantial enough to withstand the gradual effects of gas erosion, and maintain adequate sealing, and is light enough not to damage the rotor seal-teeth in the event of rub.

The rotor spacer teeth forming the seal rotating members are carefully designed with tapered profiles and thin tips in order to achieve the optimum combination of minimum heat conduction, from tip to root, and adequate structural integrity.

The axial locations of the two seals in each stage is an optimization of the effects of transients on the radial position of the circumferential teeth, combined with reliability and simplicity in the design, and the ease of assembly and disassembly of the stator vane shrouds. Thermal transient effects on the compressor are most pronounced at the rotor blade axial locations, and progressively diminished to tolerable levels at the spacer mid-span between rotor stages. Locating the seals at or close to the mid axial span of the rotor stages ensures greatly reduced transient effects on the radial clearances.

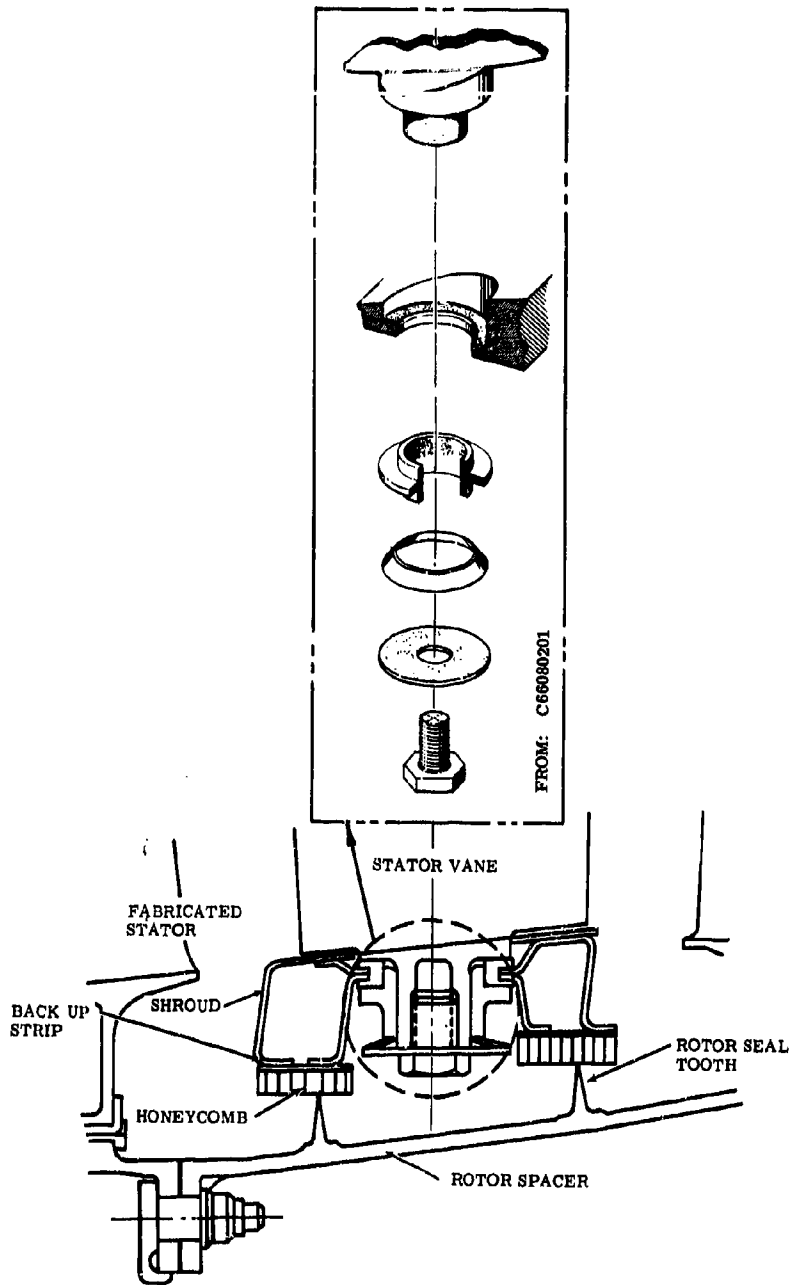


Figure 2-34. VANE TIP SHROUD AND INTERSTAGE SEAL. Typical Vane Tip Shroud Cross Section Illustrating Vane Tip Trunnion and Shroud Configurations and Method of Shroud to Vane Attachment, Interstage Seal Configuration

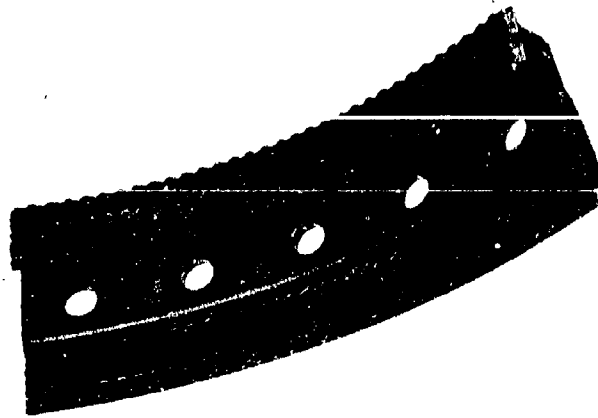


Figure 2-35. J93 SHROUD AND SEAL CONFIGURATION

#### 2.3.5.2 Compressor Discharge Seals

A highly effective seal is necessary at the compressor discharge to minimize flow losses due to leakage air and, hence, prevent a condition detrimental to compressor performance. This is achieved in the GE4 compressor by mating honeycomb and teeth configurations similar to the inter-stage seals. The compressor discharge seal consists of four separate and adjacent sets of honeycomb and tooth combinations, at different radial heights. (See Figure 2-36.) The design of the seals is based on considerations of operational capability, leakage rate, reliability, and seal weight.

Leakage air from the compressor discharge must pass across all four close-clearance seals, with an attendant pressure drop. The stepped configuration of the four seals results in additional pressure drops from seal to seal. The combined overall effect of the design configuration is the attainment of a high performance seal.

Steel honeycomb designed to attain adequate and reliable sealing is the primary member of each seal. Honeycomb is brazed to a support structure, at four different axial locations and radial levels, to form the stationary sections of the seals. The supporting structure for the stationary seal members is a fabricated sheet-metal box section, which is rabbeted and bolted to the compressor-rear-frame internal structure. It is designed with sufficient stiffness and structural integrity to maintain the close clearances, at the seals, during normal engine operation, to provide adequate radial clearances during transients, and to be capable of tolerating vibratory frequency levels such that no damaging resonance could exist between seal members in the engine operating range.

The mating rotating members of the four seals are formed by the circumferential teeth; machined at corresponding axial locations and radial heights integral to the compressor aft stub-shaft. The rotating, seal-teeth structure -- the aft stub shaft -- is designed with sufficient stiffness and structural integrity to maintain seal effectiveness in the engine operating range, as well as to meet the requirements of its primary function adequately.

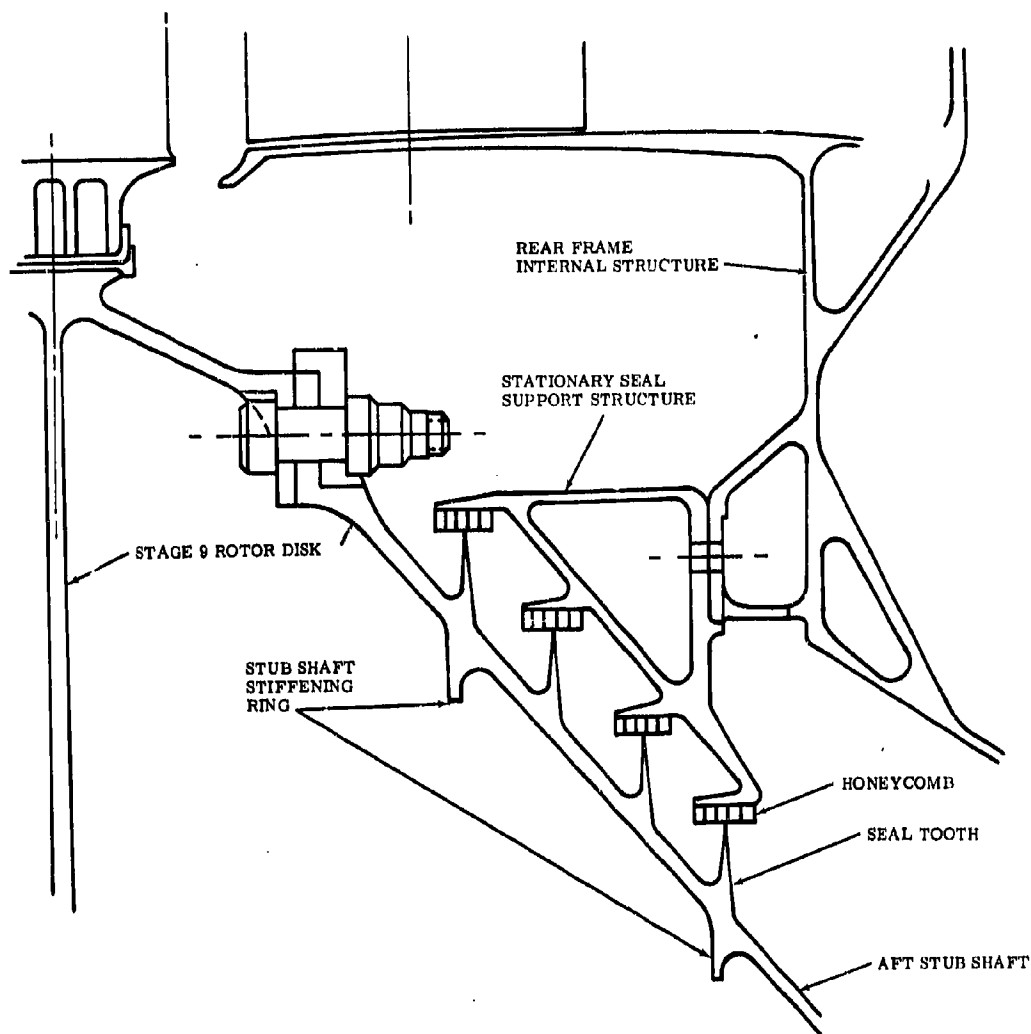


**Figure 2-36. COMPRESSOR DISCHARGE SEAL CONFIGURATION**

Test data, obtained from recent runs of the Phase IIC engine, have shown the effectiveness of the compressor discharge seal of similar design. Maximum leakage through the combined seals was recorded at 0.4% at 90% speed, with a maximum probable of 0.5% at 100% speed to be effective. No rub was observed in the Phase IIC engine through the various accelerations to 100% speed and over.

The design of the seals takes into prime consideration the reliability of the seal members and their supporting structures. In the event of a rub which may occur during severe transients, the honeycomb is light enough not to damage the rotating seal teeth. As with the interstage seals, the



honeycomb will not machine away and, hence, will not generate metallic particles, which could be detrimental to other critical areas downstream of the compressor discharge. The rotating seal teeth are carefully designed to get the best balance between minimum heat conduction from tip to root and the structural integrity of the teeth and the air stub shaft.

General Electric has had many years of experience with honeycomb and mating tooth seals in the T58, J79 and J93 engines. There has never been any failure attributable to these components.

### 2.3.6 STATOR CASING

The stator casing assembly consists of front and rear sections to carry and support nine (9) stages of vanes, actuation system components, and parts necessary for the variable geometry feature of the GE4 compressor. The interface between the front and rear sections is defined by the mating, circumferential flanges, positioned aft of the fourth stage, stator-vane row. The front casing material is titanium 6-2-4-2, a light weight, high strength, corrosion-resistant material. The rear casing material is Inconel 718, a nickel alloy steel with high strength and excellent corrosion resistant properties.

Both front and rear casings are fabricated constructions of successive, circumferentially-ribbed ring and shell sections with welded, axially-oriented flanges (using butt welds on all joints). (See Figure 2-37.) This basic type of construction has been successfully used in the manufacture of the J93, compressor-stator, front casing (see Figure 2-38). The stiffening rings provide the rigidity to maintain roundness of the casings under all conditions, and to limit the axial deflection of the vanes during stall transients. The sheet metal shells forming the casing skin are designed to have maximum stresses within the .02% yield strength and not to exceed 0.2% plastic creep at the M2.7 operating condition which is the limiting condition on a stress-time-temperature basis. The design and construction is quite economical and provides the necessary strength and rigidity to carry the bending moments of an engine main structural member, to support the compressor stator vane loads, and to maintain the roundness and concentricity necessary for close clearance operation on the rotor blade tips.

Each casing section is split in 180° segments, bolted at the axially-oriented, horizontal flanges (see Figure 2-39). This feature is a General Electric method, demonstrated to provide ready access for compressor inspection, for blade and vane rework and/or replacement on the flight line. Minimum time and effort is expended in the removal and replacement of individual blades and vanes, liners, shrouds, and miscellaneous hardware of the stator and rotor sections of the entire compressor.

Extraction of interstage bleed-air from the compressor is provided for sump/pressurization and cooling, for turbine rotor and frame cooling. An axial section, aft of the fifth stage stator row, is provided with radial holes and manifolds circumferentially oriented with scrolled areas to provide required outlets for the bleed air piping (see Figure 2-40).

The casing flanges are designed to have maximum stresses within the .02% yield strength at maximum engine loads and pressures. Bolts are closely spaced and torqued to pre-load levels, designed to maintain true flange contact at the most severe combination of pressure and maneuver loading, thereby maintaining casing structural integrity and roundness and eliminating flange leakage.

The flowpath over the rotor blade tips is formed by removable, circumferentially-segmented liners assembled into tracks machined into the stiffening rings. These liners, a basic design successfully used in the J93 engine, provide a means of sustaining blade rubs during extreme transients thereby avoiding damage to the casing skin. Close clearances on the blade tips are permissible in

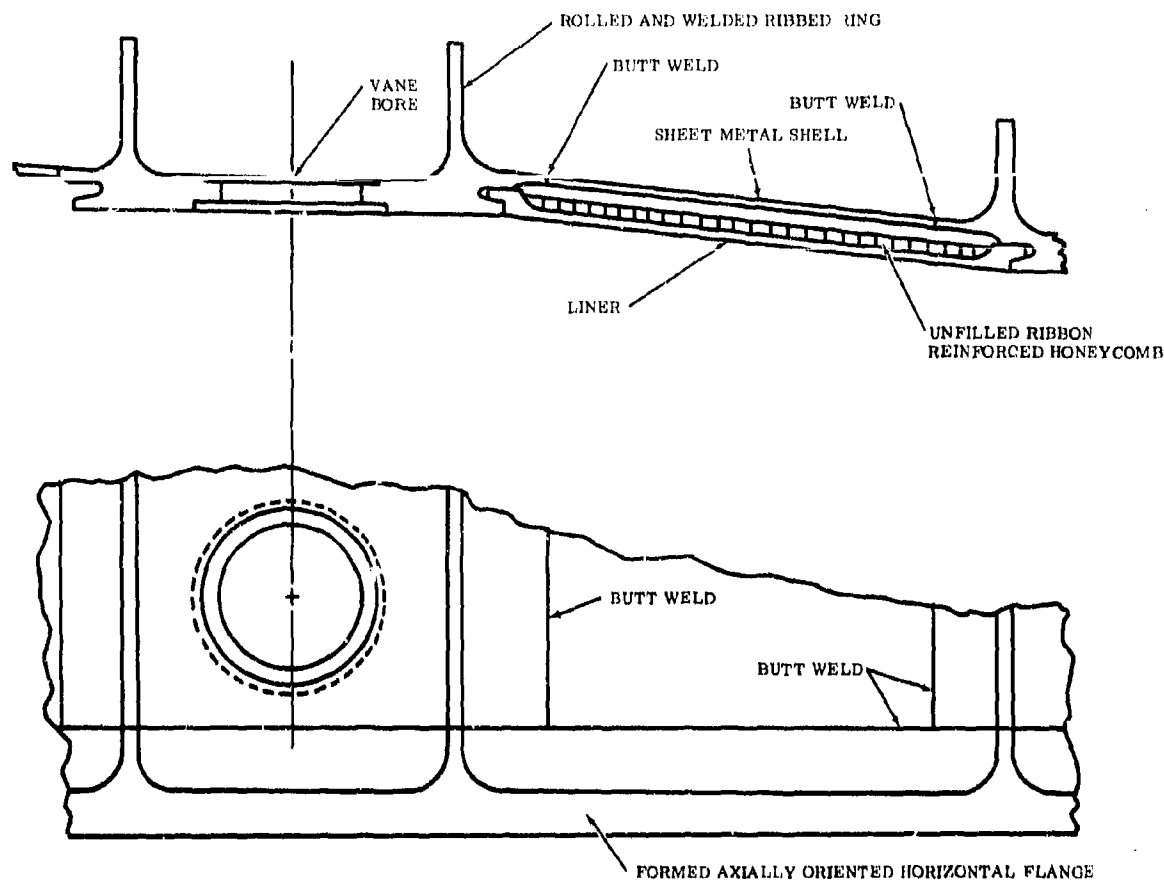


Figure 2-37. FABRICATED CASING DETAIL. Fabricated Casing Detail and Liner Configuration for Stages 4 thru 9

view of the ability of the liners to elastically deflect away from the blade tips during possible rubs. A secondary but equally essential function of these liners is to contribute to containment in the event of rotor blade failures (refer to 2.3.7 for a discussion on blade containment). Figure 2-41 shows J93 compressor liner that has experienced rubs. Additionally, since the liners cover over 50% of the internal surface of the casing, they serve as insulation for the casing wall by moderating the sudden temperature changes that may occur during entrance of the aircraft into rainstorms. This third function effectively minimizes casing distortion and, hence, reduces the possibility of heavy rubs by maintaining adequate operating clearances. Being segmented into 30° arc lengths, these liners are easily removable and replaceable. Liner construction is a basic sheet and honeycomb fabrication. Liners for stages 1 thru 3 consists of double honeycomb layers separated by a sheet steel layer; the honeycomb on the flowpath side has cells filled with nickel-aluminide to form the required smooth flowpath surface and to sustain initial impact loads of a failed blade airfoil; the honeycomb on the casing skin side is unfilled ribbon reinforced honeycomb, to provide liner stiffness and an additional containment barrier (see Figure 2-44). Liners for stages 4 thru 9 are designed with a sheet metal layer rigidized on the casing skin side with ribbon reinforced honeycomb to resist fatigue from panel vibration; the sheet metal layer forms the flowpath surface (see Figure 2-42). It is necessary to have the heavier configuration for the earlier stages in view of the high energy levels at blade impact in stages 1 thru 3. The liners throughout the entire compressor use Hastelloy X as primary material for the sheet and honeycomb.

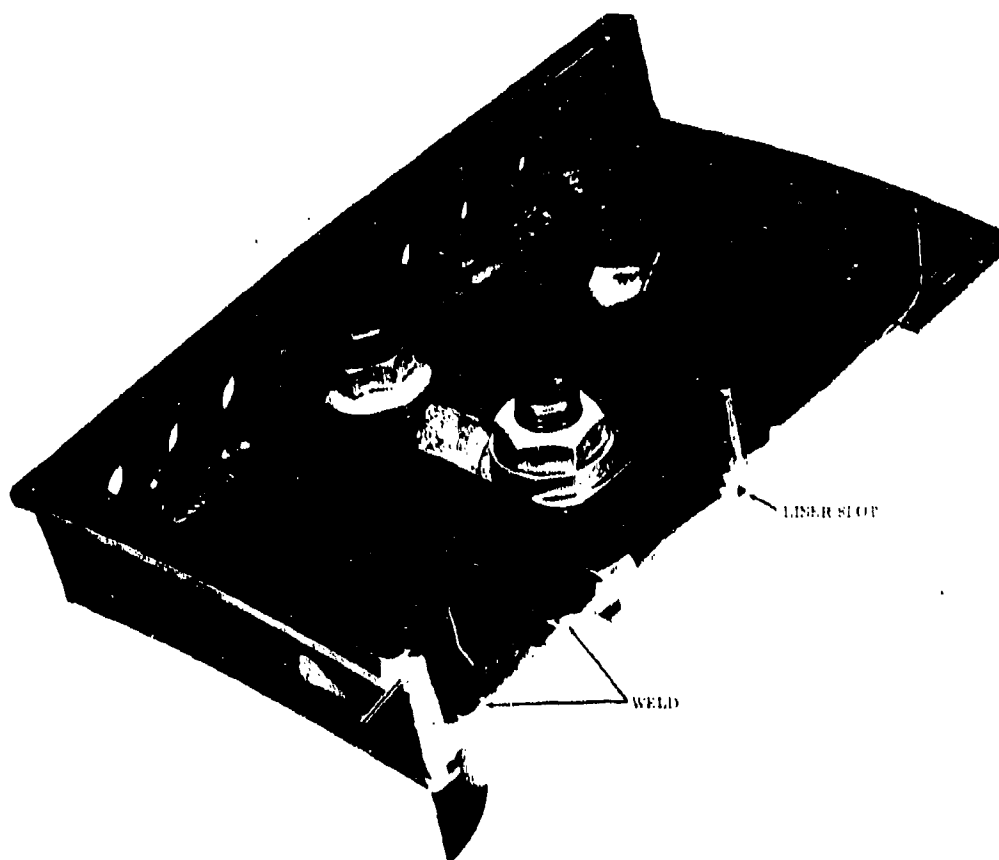


Figure 2-38. J93 COMPRESSOR FRONT CASING, FABRICATED CONSTRUCTION

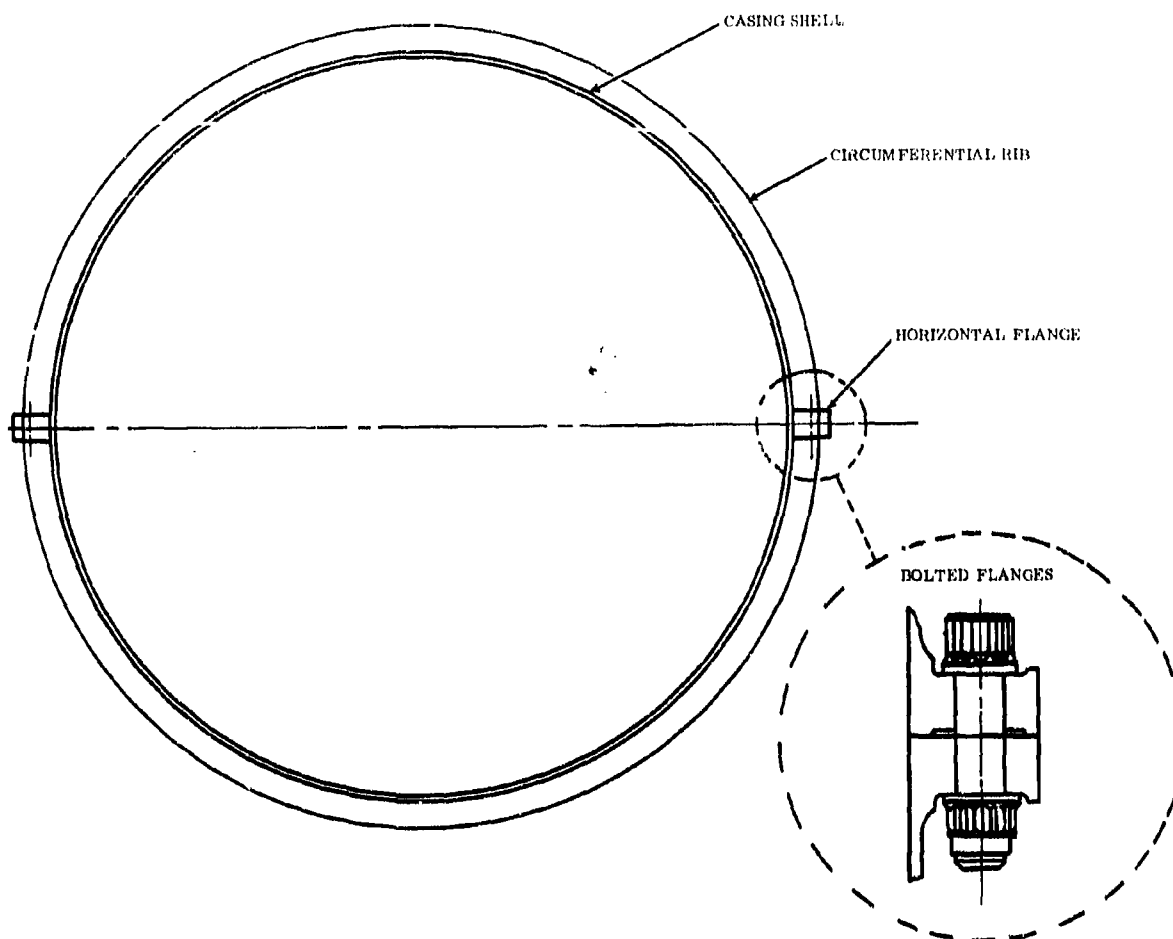


Figure 2-39. CASING CROSS-SECTION SHOWING SPLIT FEATURE FOR ROTOR AND STATOR INTERNAL REWORK

#### 2.3.6.1 Compressor Axial & Radial Clearances

**Axial Clearances.** All axial clearances are established at the most severe transient conditions within the airframe flight envelope and at the worst conditions of engine operation. This includes allowances for blade-and vane-tip, axial, steady-state and stall, vibratory deflections. The magnitudes of the allowable vibratory deflections are determined from parameters based upon recorded blade-and vane-stall stress response during previous testing of J93, J79, GE1, J97 and GE4 compressors. In addition to blade-and vane-stall deflection allowances, axial clearance is provided for the worst combination of the following:

- Arithmetic stackup of all related hardware at their dimensional tolerance limits
- Compressor rotor and stator thermal growths
- Compressor rotor and stator elastic deflections

- Number 2 Bearing, axial-play and elastic deflections of bearing support and rear frame
- Axial running clearance

This provides maximum assurance that adequate axial clearance exists between all blade and vane rows and that overall compressor length is minimized.

**Radial Clearances.** The GE4 compressor is designed for maximum tolerance to blade-tip rubs or seal rubs through the use of replaceable liners in the stator casing opposite all rotor blade tips and through the use of honeycomb seal seats on stator vane shrouds. This assures that even an infrequent rub, severe enough to affect compressor performance, will have no detrimental effect on structural integrity or passenger safety.

The compressor radial clearances are calculated to assure that normal engine operation will not result in rubs severe enough to affect engine performance or to require premature replacement of hardware. Radial clearance calculations consider the worst combination of the following:

- Arithmetic stackup of all related hardware at their dimensional tolerance limits

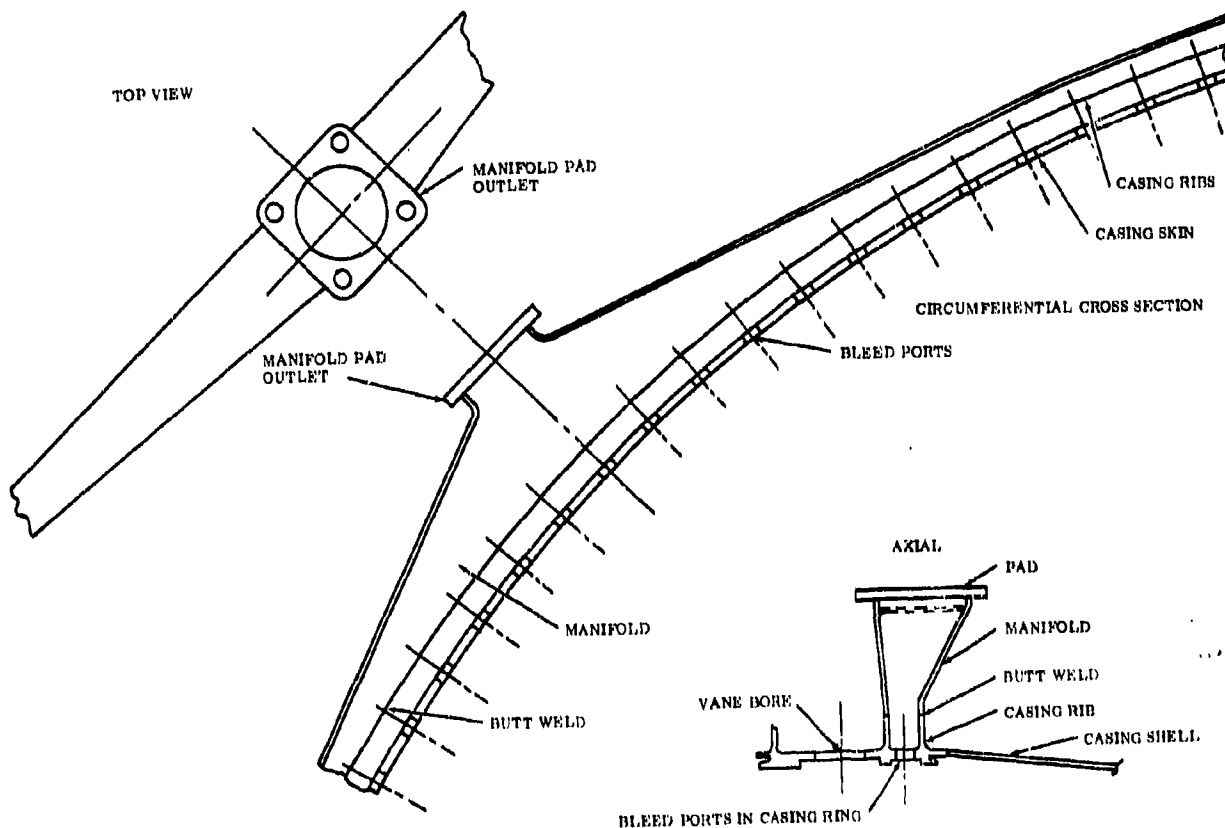


Figure 2-40. INTERSTAGE BLEED EXTRACTION PORTS, MANIFOLD AND OUTLET PARTS



Figure 2-41. J93 COMPRESSOR STATOR LINERS HAVING EXPERIENCED RUBS

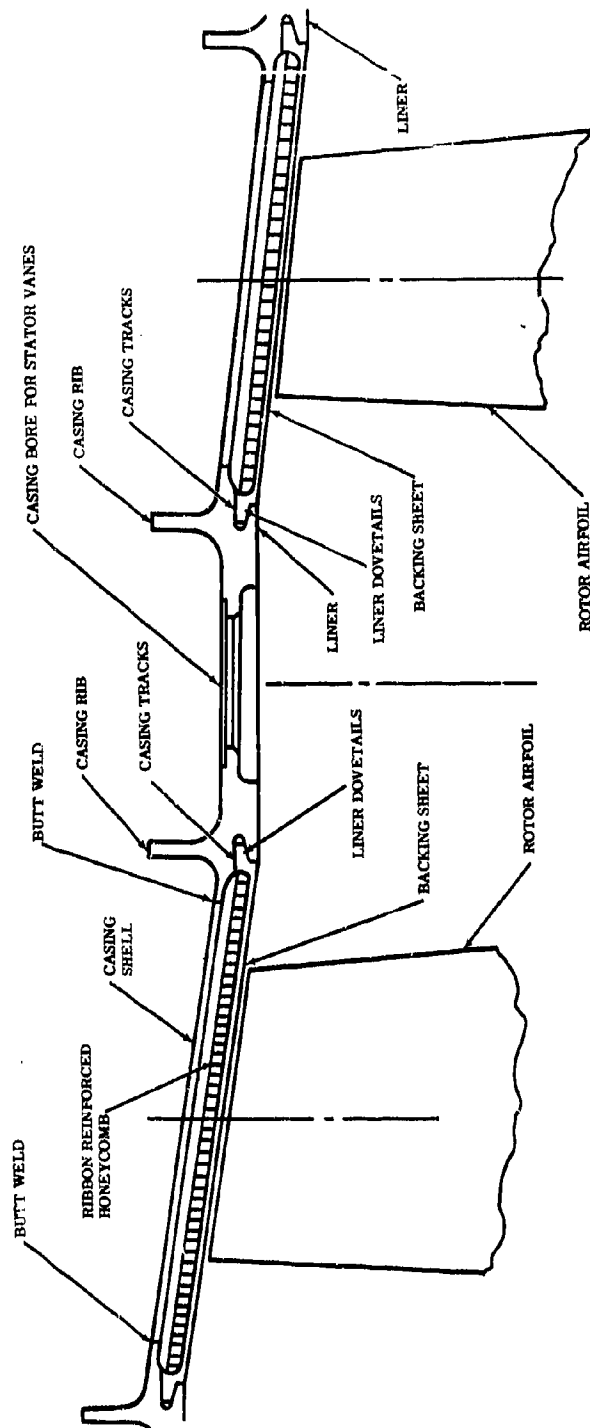


Figure 2-42. LINER CONFIGURATION AND ATTACHMENT TO STATOR CASING. Liner Configuration and Attachment to Stator Casing Stages 4 through 9 Fabricated Casing Cross-Section Delineation

- Rotor and stator thermal growths at the most severe transient conditions within the flight envelope and at the worst conditions of engine operation
- Compressor rotor and stator elastic deflections under the same worst conditions of item 2 and including effects of inlet distortions, flight maneuvers and system vibration criticals

The calculated compressor radial clearances are finally optimized by minor adjustments determined from engine testing. This provides the highest possible levels of compressor efficiency and stall margin consistent with the engine structural integrity required for passenger safety.

### 2.3.7 COMPRESSOR BLADE CONTAINMENT

In the event of a rotor airfoil failure in any stage at maximum rated speed, blade containment is effectively achieved in the GE4 compressor by the multiple layered configurations of the liner, the casing skin and, at certain stages, the actuation rings and lever arms.

The rotor blade attachments are designed to have the disk dovetails stronger than the blade dovetails, and, in turn, to have the blade dovetails stronger than the airfoils. These weak link criteria ensure that blade failure will occur in the airfoil, if at all. Experience has shown that most blade airfoil failures occur as a result of excessive aerodynamic or mechanical excitation, FOD, or both. The philosophy in the design of the blade and its attachment is an important factor in containment design since the impact energy of the separated fragments (i.e., the airfoils) are at reduced levels. The design considerations encompass both steady state and vibratory stress conditions for the dovetails and airfoils at various modes.

The adequacy of the containment features in the compressor stator assembly is based on experience and will be demonstrated by component tests as part of the Phase IIC program. Component tests at Watertown Arsenal have shown a fundamental relationship between the energy absorption capability of a material and its thickness in the form:

$$T = KE^{1/2}$$

Where:

T = required thickness of the material to absorb impact

E = Kinetic energy of the striking object

K = Empirical constant which is a function of shield material and dimensional properties, magnitude and shape of mass.

Figure 2-43 shows experience in the containment of failed blades. Tests have shown that a significant reduction in containment shield thickness, for absorbing a given energy level, is possible when multiple layers of material are used. Ballistic tests have shown that a laminated thickness of steel plate is more effective in containing than a single plate of the same thickness because of the additional resilience of composite structures.

Recent experiences on the J79 engines have further indicated that honeycomb liners with filled cells of nickel-aluminide micro-balloons provide excellent impact resistance.



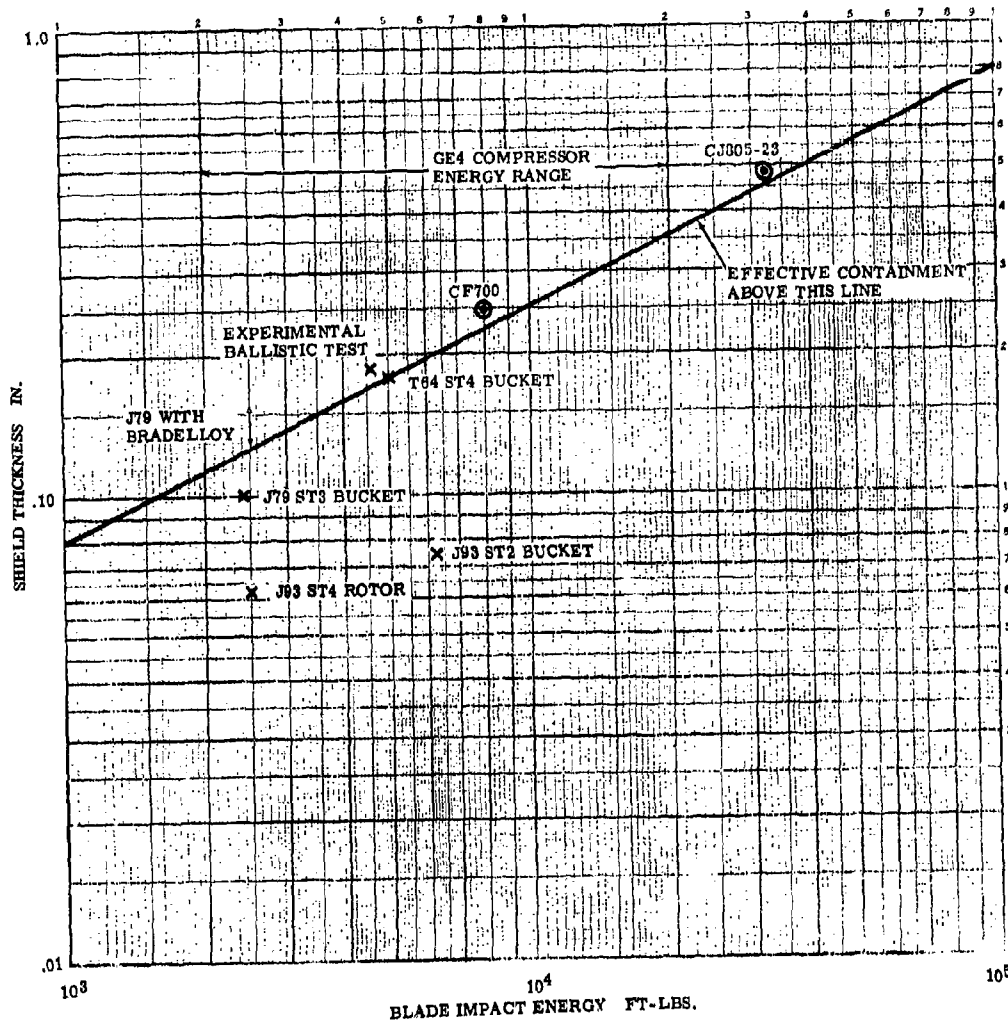


Figure 2-43. BLADE CONTAINMENT EXPERIENCE AND TEST DATA

The above information, together with experience and test data, forms the basis for the design of the satisfactory blade containment capabilities of the GE4 compressor stator. The essential features of the containment capabilities are as follows:

- For stages 1 through 3, blades which have high energy levels (Figure 2-44):
  - Initial layer, composed of honeycomb filled with nickel-aluminide, is designed to sustain initial impact and spread the load, thereby greatly reducing the local peak energy level.
  - A second layer consisting of a steel backing supports the honeycomb and serves as an intermediate barrier.

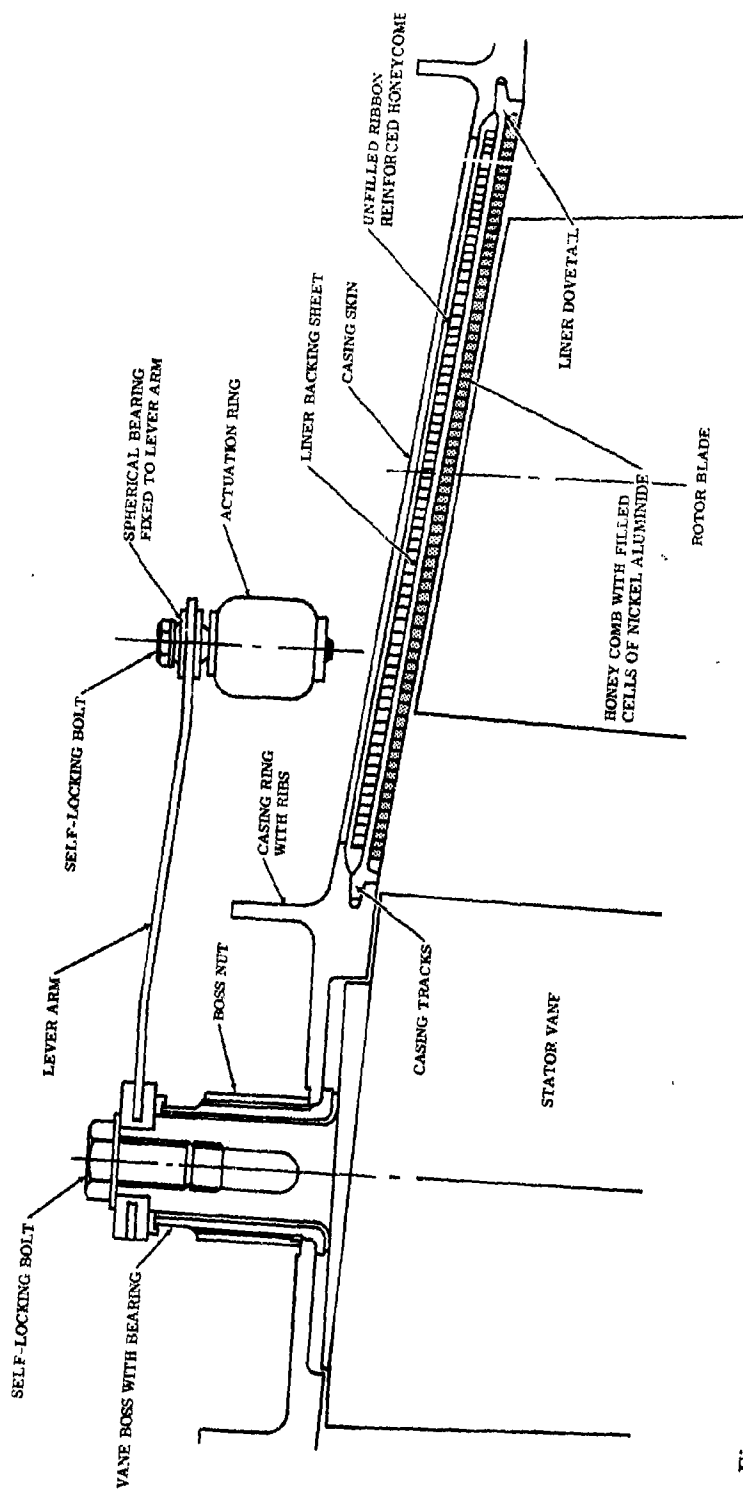


Figure 2-44. BLADE CONTAINMENT CONFIGURATION, STAGES 1-3. Casing - Vane Boss - Lever Arm - Actuation Ring Assembly. Liner Configuration and Attachment to Casing on Stages 1, 2 and 3. Blade Containment Configuration - Stages 1, 2 and 3.

- A third layer, made up of unfilled, ribbon-reinforced honeycomb, for crushing onto the casing wall to absorb further impact energy, is provided.
- A fourth layer, the casing shell, provides back-up for the unfilled honeycomb and acts as the final containment barrier.
- For stages 4 through 9 blades, which have relatively lower energy levels (Figure 2-45):
  - A first layer, formed by a steel-sheet backing for the unfilled honeycomb, is provided to sustain initial impact.
  - A second layer, consisting of unfilled, ribbon-reinforced honeycomb, is present for crushing to absorb thru impact loads.
  - A third layer, formed by the casing shell, provides back-up for the unfilled honeycomb and acts as final containment barrier.
  - A fourth layer is formed by actuation rings and levers, so located as to contain possible fragments penetrating the casing skin.

The dimensions and configurations of the containment layers will vary from stage to stage due, primarily, to varying blade masses and different metal temperatures. Rotor blade masses are on a decreasing level of magnitude from the front to the rear of the compressor. As a general rule, impact resistance of steels and titanium alloys increases with temperature in the range from room temperature to 600°F and then decreases thereafter at higher metal temperatures. The worst combination of temperature and blade mass occurs in the first stage at sea level operating condition. In view thereof, this condition was chosen for component test to demonstrate the containment capabilities of the stator casing assembly. The containment feature incorporated in the design of the GE4 compressor means that a separated airfoil would have to penetrate multiple layers of material to escape the compressor. In stages 4 through 9, fragments which may penetrate the casing would have to pass the actuation rings and levers, which have excellent impact resistant properties, in order to escape the compressor assembly.

## 2.3.8 STATOR VANES & SHROUDS

### 2.3.8.1 Material Selections

The first step in the design of the GE4 stator vanes was the selection of optimum materials for the commercial mission. Titanium 6-2-4-2 was selected for stages 1-6 and Inconel 718 was selected for stages 7-9. These alloys provide the optimum combinations of 10,000 hr. fatigue life, weight, and corrosion resistance at the design temperatures of these stages. Goodman diagrams for the titanium stage-3 vanes and the steel stage-7 vanes are shown in Figure 2-46 and Figure 2-47.

### 2.3.8.2 Overall Approach

The concept of variable compressor stators has been thoroughly proved by extensive G.E. development and production experience with the J79, CJ805, T64, T58 and J93 engines. Variable stators are used on the IGV's, stage 1 and stages 4-8 of the GE4 engine. Stages 2 and 3 are fixed, while stage 9 is variable for the emergency windmill brake closure only. Stator vane shrouds act as effective vibration dampers to minimize stator vane stresses and deflections.

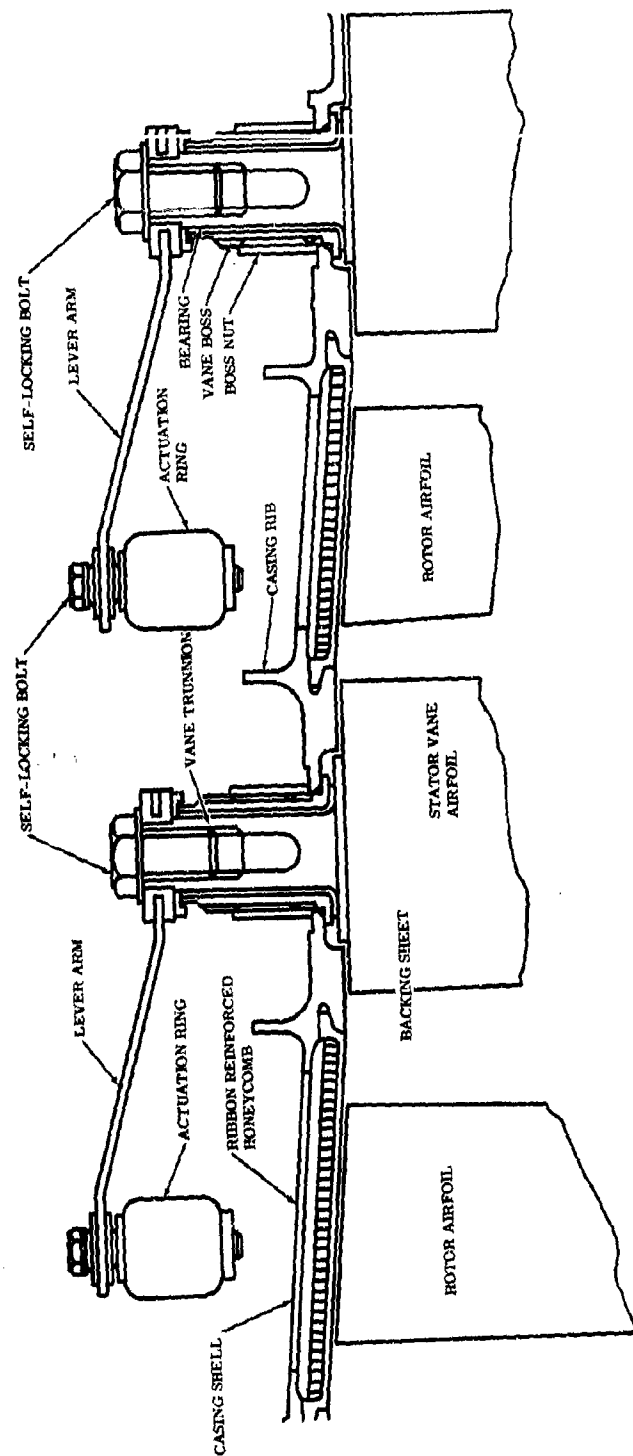


Figure 2-45. BLADE CONTAINMENT CONFIGURATION, STAGES 4-9. Blade Containment Configuration - Stages 4 thru 9. Liner Configuration and Attachment - Stages 4 thru 9. Vane Boss - Casing Assembly - Typical all Variable Stages. Vane - Lever - Actuation Ring Assembly on all Variable Stages

6-2-4-2 TITANIUM STAGE 3 VANE  
 10,000 HR. 3 DEVIATION GOODMAN DIAGRAM  
 MACH NUMBER 2.7 TEMPERATURE 670°F

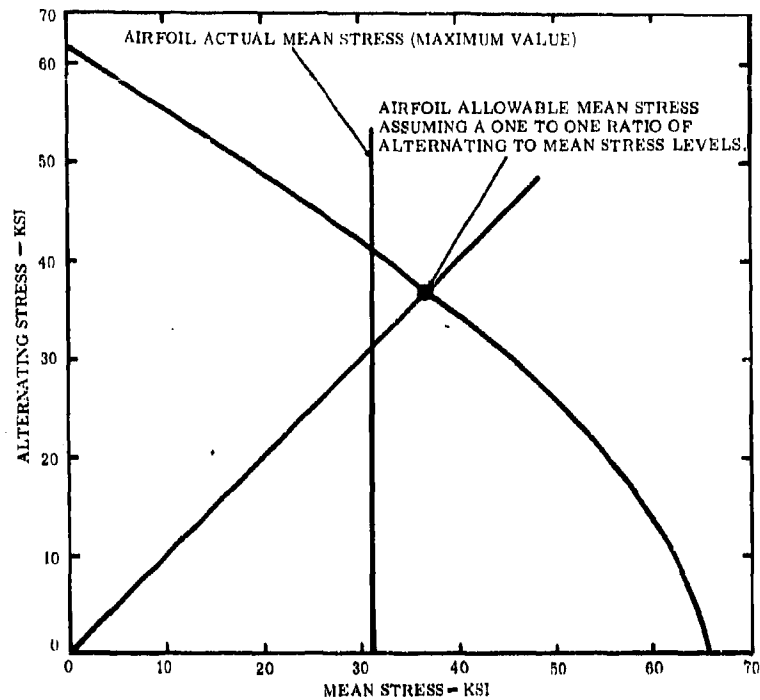


Figure 2-46. STAGE 3 VANE, GOODMAN DIAGRAM

As an example, Table I below is a tabulation of measured GE1, stage 2 and 3 vane, vibratory-stress response during stalls. The shrouded stage 2 vane operates at essentially 30 percent of the stress level observed on the stage 3 unshrouded design.

Table 1

The measured vibratory stress response of the GE1 HSL Stage 2 and 3, compressor stator vane at sea level static 100 percent  $N_c$

Stage	Tip Fixity	Measured/Allowable Stress Ratio
2	Shrouded	0.04
3	Cantilevered	0.13

INCONEL 718 STAGE 7 VANE  
10,000 HR. 3 DEVIATION GOODMAN DIAGRAM  
MACH NUMBER 2.7 TEMPERATURE 975°F

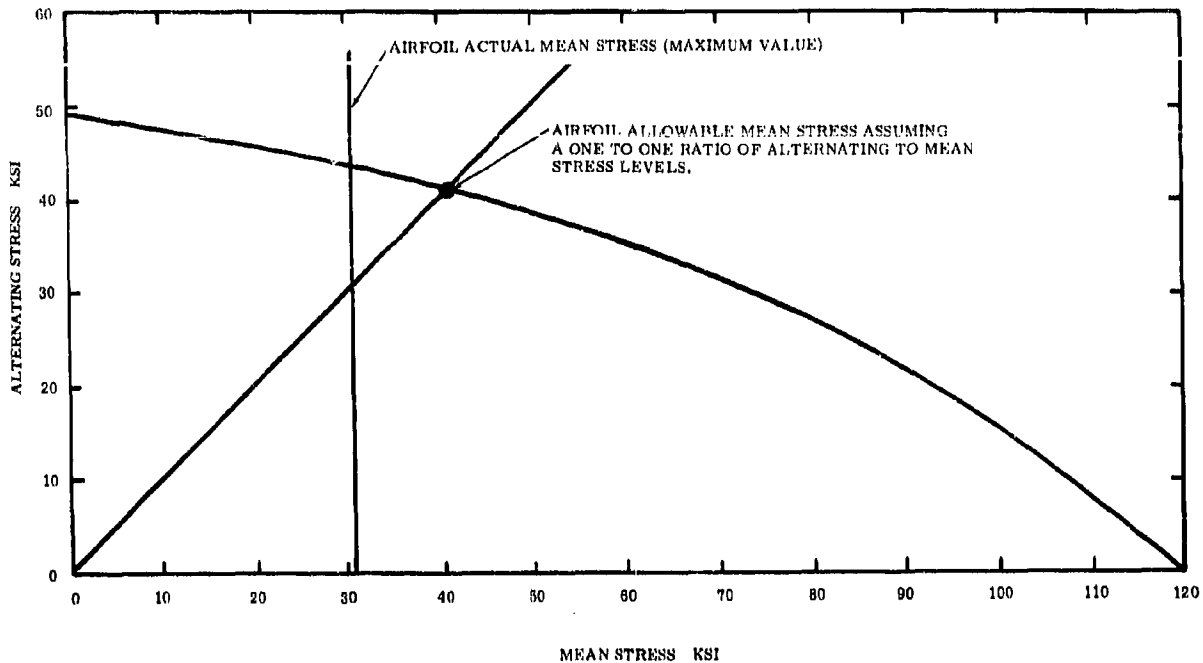


Figure 2-47. STAGE 7 VANE, GOODMAN DIAGRAM

Stator vane shrouds add significantly to resistance to vane fatigue failure from F. O. D. This was graphically illustrated by the recent in-flight ingestion of a portion of a B70 airframe by a J93 engine. The use of vane tip shrouds also accommodates the selected rotor spool design (refer to Rotor Spool Section, Figure 2-22). The Outlet Guide Vanes, OGV's, are unshrouded to preclude binding during emergency closure. The OGV tips are machined with a curvature that matches a like curvature on the portion of the rear frame opposite the OGV's. This curvature is spherical; that is, the center of the arc falls on the engine axial. Therefore, the OGV tip gap does not change as a function of OGV stagger angle. This minimizes air leakage past the vane tips. Figure 2-48 illustrates this.

### 2.3.8.3 Airfoil Design

The design evolution to low-aspect-ratio airfoils has occurred over a seven year period from 1959 to the present. The 620 lb/sec GE4 compressor was evolved from the 475 lb/sec design and has low-aspect-ratio airfoils consistent with this proved design approach.

The GE4 vanes are conservatively designed to attain commercial-mission life requirements. For example, the vanes were designed for vibratory stress levels equal to maximum, steady-state, gas-bending stresses. (See Figure 2-46 and Figure 2-47.) These vibratory stress levels are not expected even during stall. Comparable vanes in the 475 lb/sec FSCT exhibited vibratory stresses of lower magnitude during a full speed stall at ambient operating pressure.

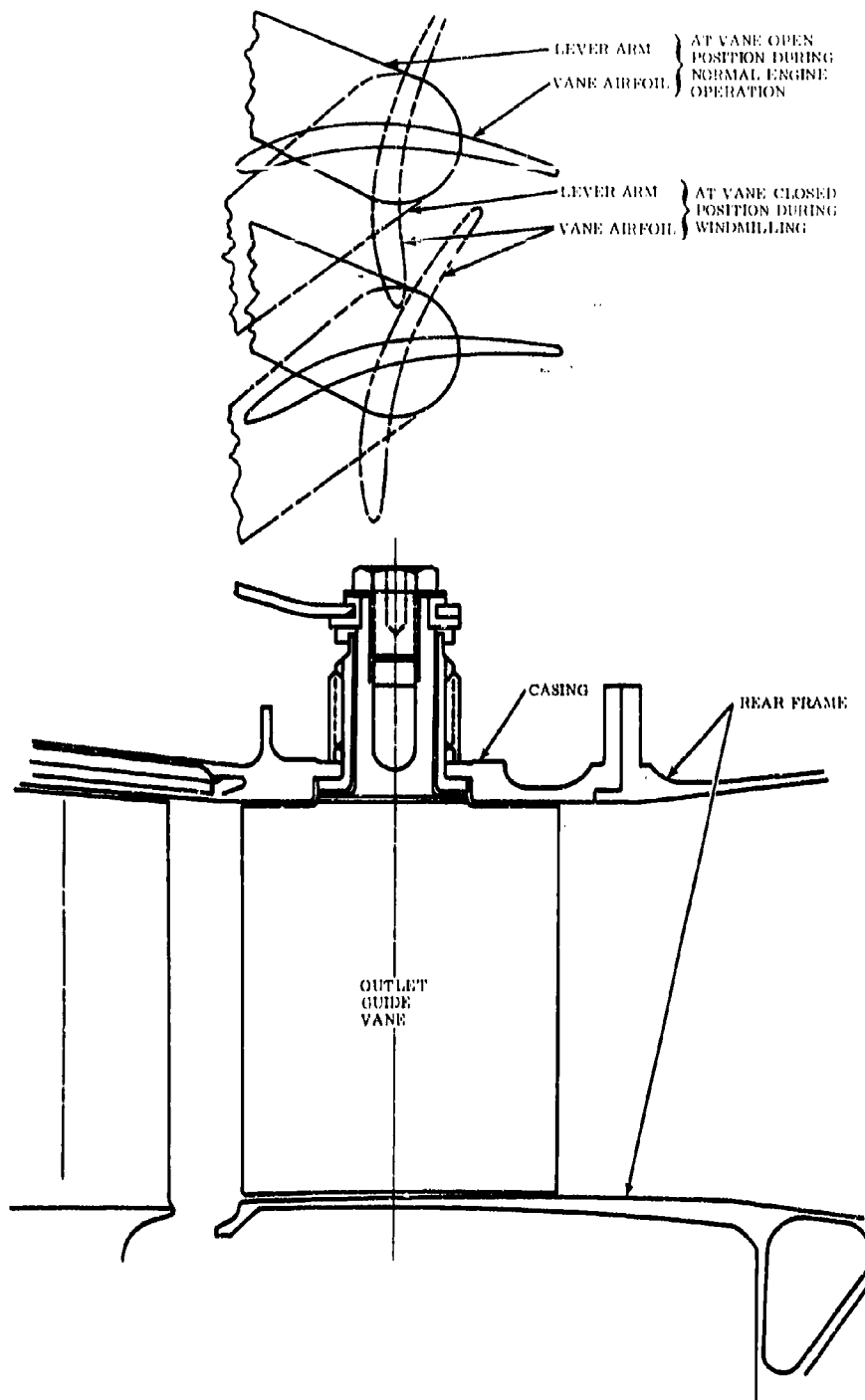


Figure 2-48. OGV CONFIGURATION. Spherical tip curvature for minimum leakage area between the vane tips and the rear frame. Top view shows open and close positions of OGV and Lever Arms.

Limit-cycle vane instability (torsional flutter) is avoided by designing to operate at safe values of the "reduced velocity parameter" -  $V/b\omega$ , where  $V$  is the relative air velocity,  $b$  is the semi chord and  $\omega$  is the first torsional frequency. This is discussed in detail in the section covering rotor-blade aeromechanical design.

#### 2.3.8.4 Stem Design

All of the GE4 variable vane stems are high boss; that is, the vane bearing reactions are perpendicular to the vane of rotation. This is compared in Figure 2-49 with low-boss vane stems. The significant advantage of the low-boss vane stem is that, for a given size vane, more bearing surface area and, subsequently, lower bearing surface loadings can be obtained, than with high boss stems. Low boss stems, illustrated in Figure 2-50, are used on the CJ805 and J79 compressors. The circumferential spacing of the GE4 vane is closer than on the CJ805 and J79 because of substantially higher stator-vane solidities. This dictates the use of high boss stems to obtain the minimum acceptable thickness in the stator casing wall between the vane stem holes. Also, with low-boss vane stems, the stem bearing reactions must be transmitted through the base of the threaded vane spindle, as illustrated in Figure 2-49. If proper vane spindle pre-load is applied by torquing the vane stem locknuts, no fatigue stresses at the spindle base are induced. However, threaded titanium stems heavily pre-loaded demand close dimensional control of all related parts and precise assembly techniques to prevent premature failures. By contrast, high-boss vane spindles require zero preload for proper functioning, since the threaded fastener is isolated from stem bearing reactions. High boss vane stems used on the J93, J97 and GE1 engine have externally threaded studs. (See Figure 2-50).

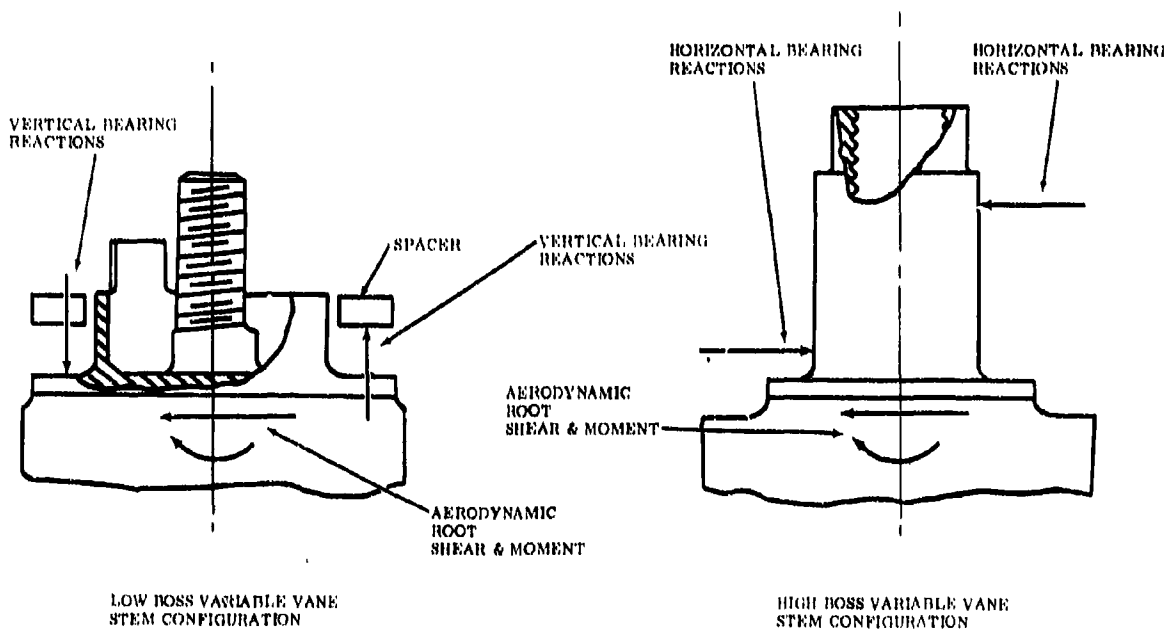


Figure 2-49. LOW VS. HIGH BOSS VARIABLE VANE STEM CONFIGURATIONS.  
Vertical vs. Horizontal Bearing Reactions



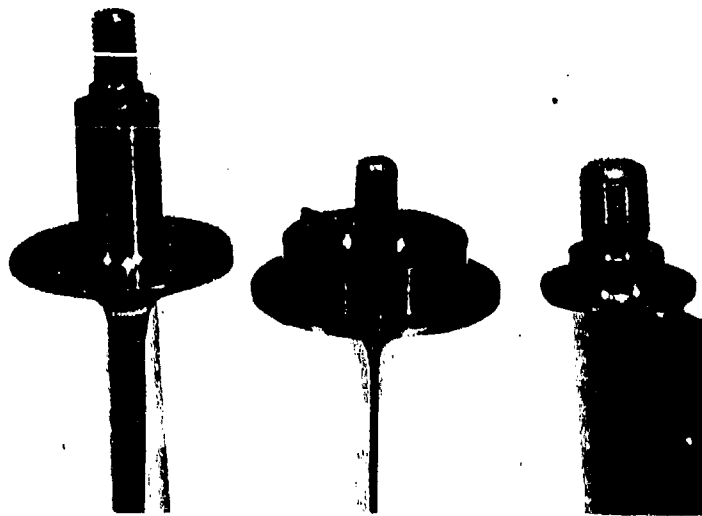


Figure 2-50. STATOR VANE STEM COMPARISON

Left - Typical J93 High Boss Variable Stator Vane Stem  
Center - Typical J79 Low Boss Variable Stator Vane Stem  
Right - Typical J93 Fixed Stagger Angle Vane Stem

The GE4 vane stems have internal threads for use with bolts instead of locknuts. (See Figure 2-51). This is possible because of the relatively large sizes of the GE4 vane stems. Internal threads offer the following advantages over threaded studs: 1) lower overall height and weight and, 2) threads protected from handling damage. A resilient, self-locking feature is provided for the variable-stator-vane stem bolts, as shown in Figure 2-52. Self-locking is obtained by expanding several bolt threads locally. The expanded area does not include the first few threads and the basic thread profile is not altered. This ensures easy starting of the bolts and that the self-locking area will cause no vane-thread damage. The bolt threads are coated with a moly-disulfide dry-film lubricant for additional protection of the vane thread. Vibration tests verify that this locking device will perform satisfactorily with a torque of less than half the specified maximum. Re-use tests indicate torque within the limits of MIL-F-18240B can be maintained for four times the minimum 15 cycles specified.

The stage two and three vanes are held at a fixed stagger angle. These vanes are bolted directly to the casing as on the J93 stage 4, 5 and 6 vanes (see Figure 2-53), with 1/2" diameter, rolled, vane-stem threads and self-aligning nuts. This method of mounting non-variable vanes achieves optimum durability/reliability and ease of maintenance. Since the vane is firmly fastened to the casing, relative vibratory motion between the vane end and the casing is non-existent, thereby eliminating galling and fretting problems and possible extraneous vane excitations caused by "chatter". Rework and replacement of the individual vane is accomplished by disengaging the shroud segment and removing the particular vane. Removal of adjacent vanes is not required. Self-aligning nuts prevent mis-alignment between the locknut seating surface and the spindle thread axis and avoid bending moments in the threaded vane spindle. Self-aligning nuts were originally incorporated into the threaded titanium vanes of the J93, to ensure that the vane stems were loaded in tension only. The threaded titanium vanes of all J93, GE1, J97, GE4 and TF39 now have self-aligning nuts.

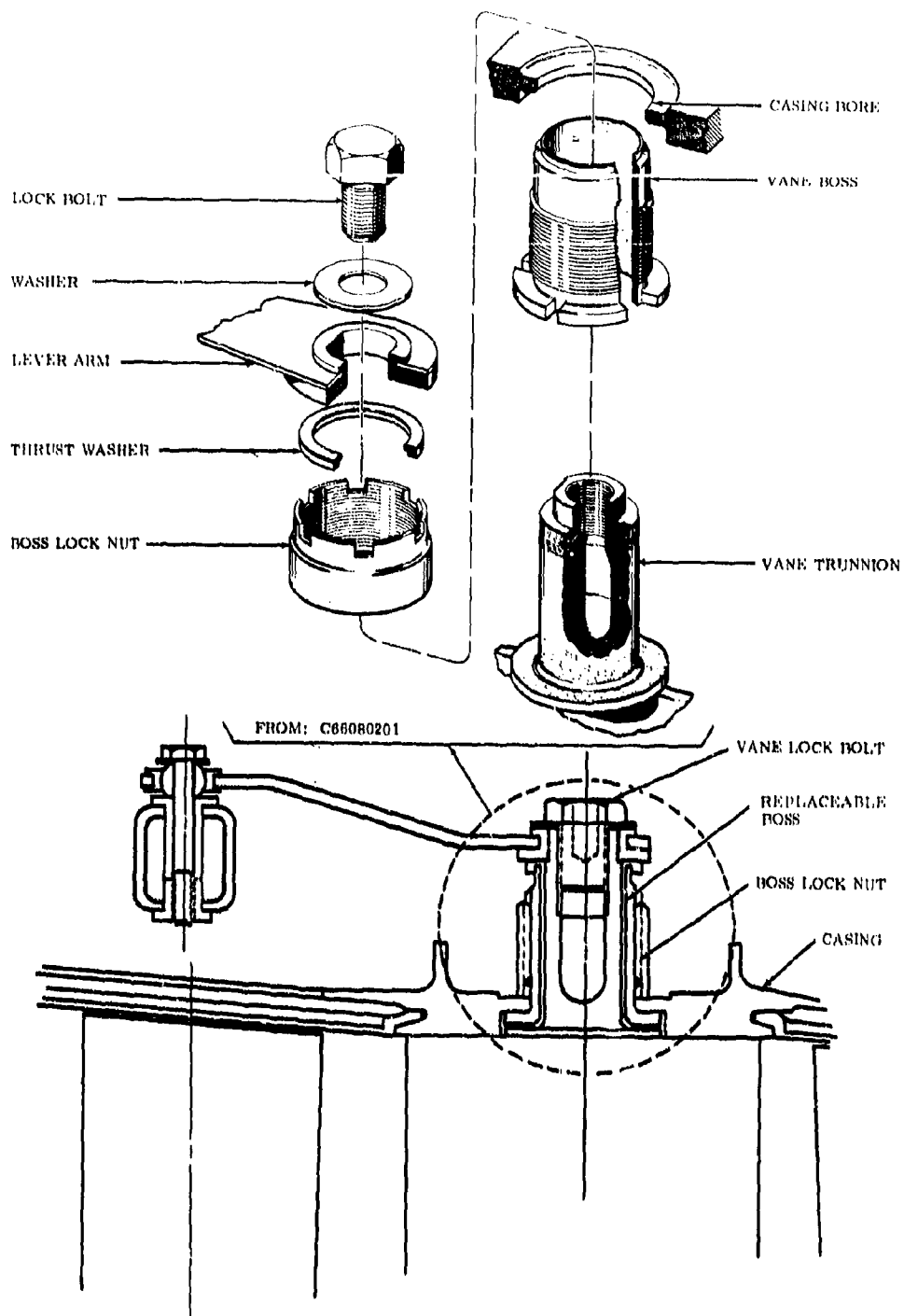


Figure 2-51. GE4 VANE STEM GEOMETRY  
 Typical GE4 Vane Stem Geometry with Internal Stem Threads  
 Top Trimetric Showing Vane Mounting Hardware

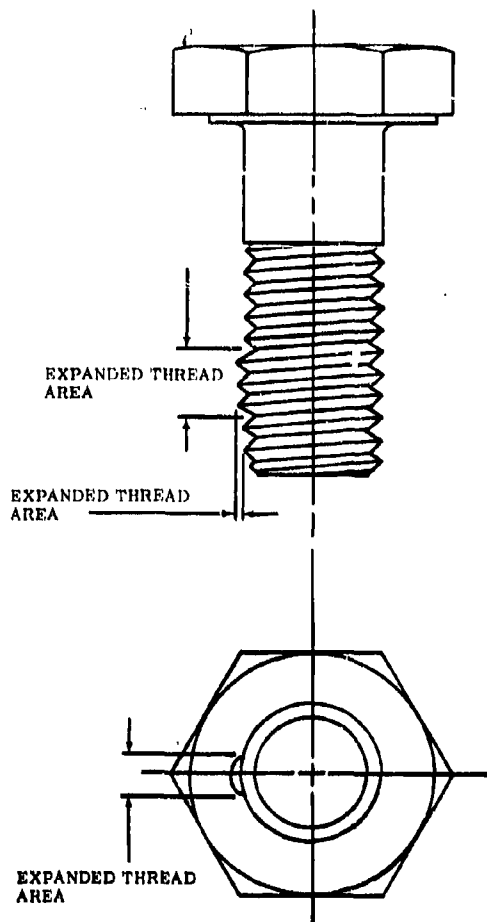


Figure 2-52. VARIABLE STATOR VANE STEM BOLT, SELF-LOCKING FEATURE

#### 2.3.8.5 Stator Vane Shrouds

A cross section of a typical GE4 stator vane shroud is shown in Figure 2-54. Figure 2-55 shows a typical J93 shroud. The evolution of the GE4 shrouds from the J93 shrouds is evidenced in a comparison of Figures 2-54 and 2-55; as shown in Figure 2-54, both shrouds have the following general construction:

- Fabricated (brazed) sheet metal segments, Item #1
- Flowpath surface formed by the outer skin, Item #2
- Inner skin to form a closed box cross section, Item #3
- Honeycomb seals mounted forward and aft, Item #4

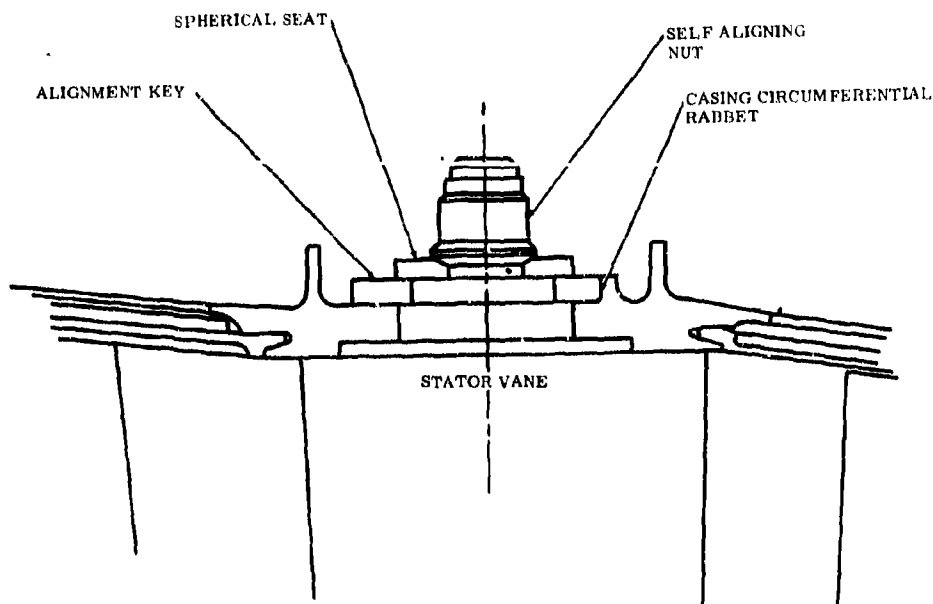


Figure 2-53. STAGE 2 & 3 FIXED STAGGER ANGLE, STATOR VANE STEM CONFIGURATION

- Vane bearing grommets mounted near the center of the cross section and positioned around each vane stem, Item #5
- Spring washers to prevent binding and provide maximum vibration damping, Item #6
- A separate bushing to provide the necessary wear capability for commercial mission, Item #7

J93 engine experience has demonstrated the reliability and durability of this type of shrouds. The GE4 shrouds have been designed to take the maximum advantage of the J93 experience. In addition, the GE4 shrouds have dimensional and manufacturing changes, based on lessons learned with the J93 shrouds, which minimize costs.

These shrouds can be easily removed as individual segments. Therefore, all stator vanes, except the IGV's, are individually replaceable after removal of casing halves and shroud segments.

### 2.3.9 ACTUATION SYSTEM

The variable geometry feature incorporated in the GE4 compressor requires varying orientations of the airfoil stagger angle with respect to corrected speed. The actuation system encompasses the mechanisms to satisfy the motion requirements of the variable stator vanes. The entire compressor system consists of three main groups; the front group, which is designed to move and control the Inlet Guide Vanes and Stage 1 Vanes simultaneously; the rear group, which is designed to move and control the vanes in stages 4 thru 8 simultaneously; and the OGV, which minimizes rotor windmilling rpm for emergency shut-down.

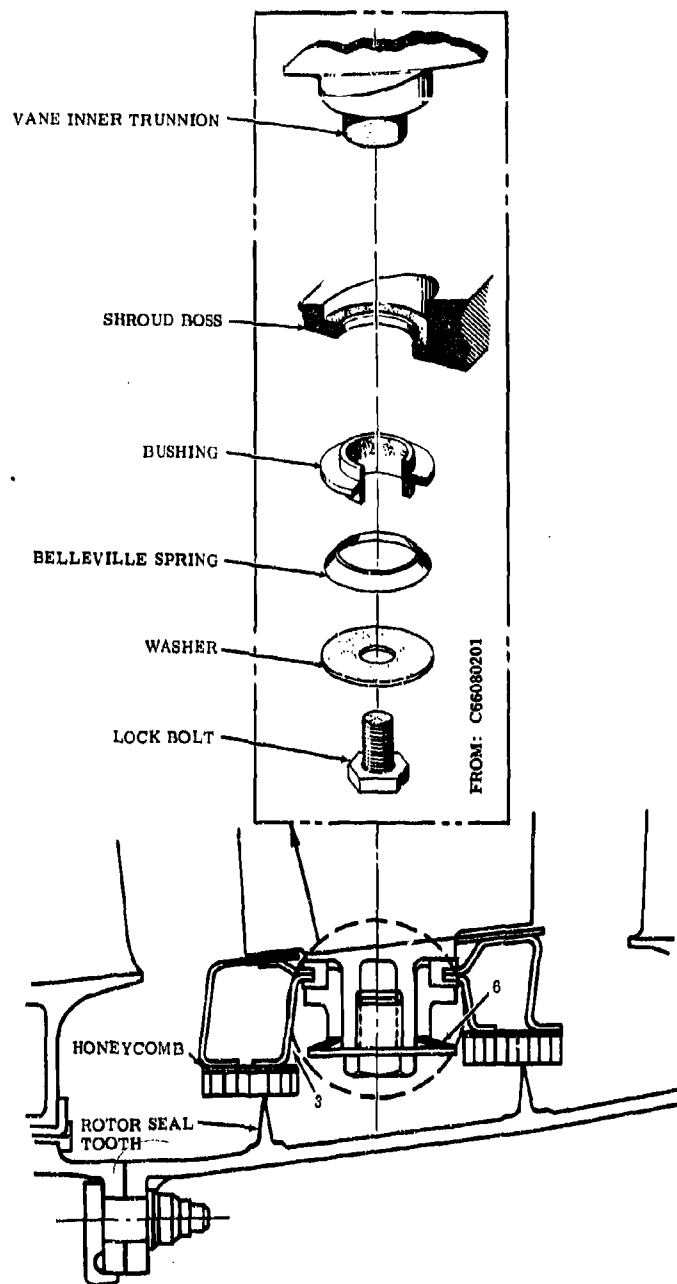


Figure 2-54. TYPICAL VANE TIP SHROUD CONFIGURATION  
Vane Tip Trunnion & Shroud Configurations and Method of Shroud  
to Vane Attachments

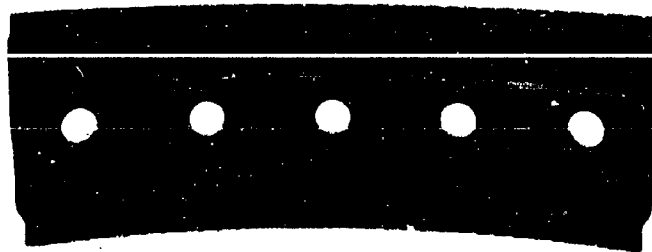


Figure 2-55. J93 COMPRESSOR SHROUD WITH HONEYCOMB FORWARD AND AFT SEALS

Each of the above groups consists of sub-systems comprised of the vane-lever arm-actuation, ring loop and the main actuation linkage loop, which collectively and simultaneously move the vanes in all stages within the group.

Each variable vane is attached at the outer trunnion to a lever arm (see Figure 2-48) in a positive manner that does not permit incorrect assembly and ensure proper orientation of the lever arm with the vane airfoil. The lever arm hole configuration and the mating section on the vane outer trunnion are designed to permit engagement in one direction only. All the lever arms in each stage are, in turn, assembled to a unison ring (see Figures 2-56, 2-57, and 2-58) designed to move the lever arms and vanes in each stage to equal magnitudes of travel simultaneously. Each actuation ring is composed of two half-ring segments joined by bolted segments which bridge the horizontal

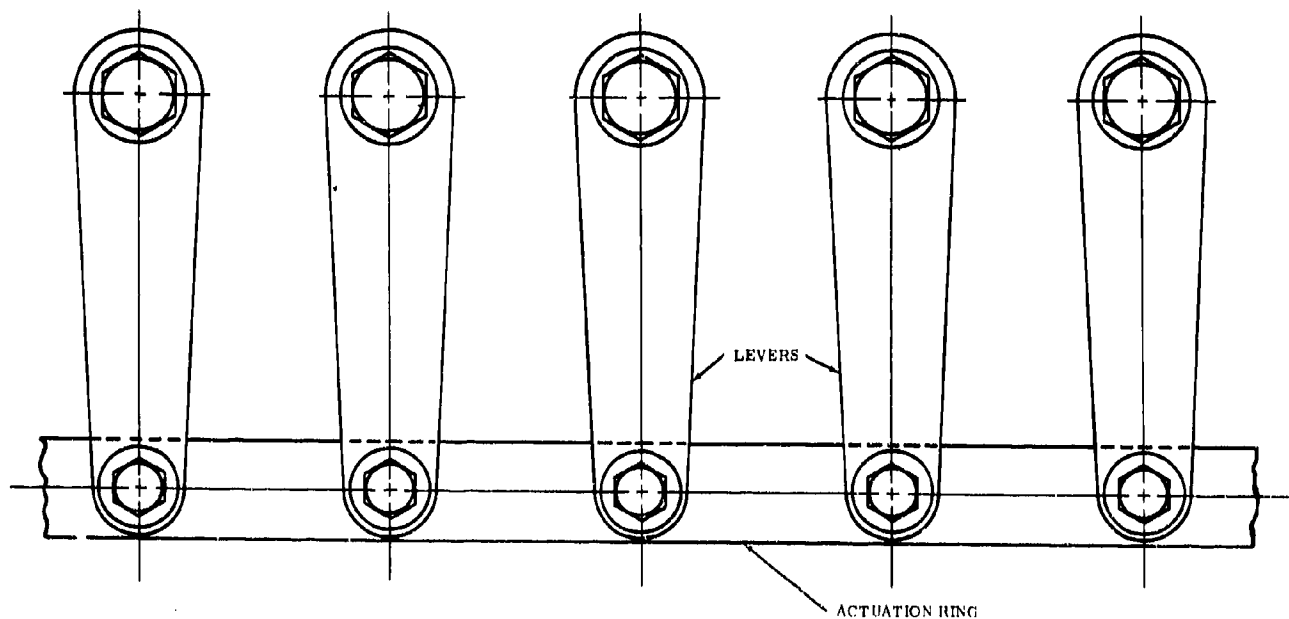
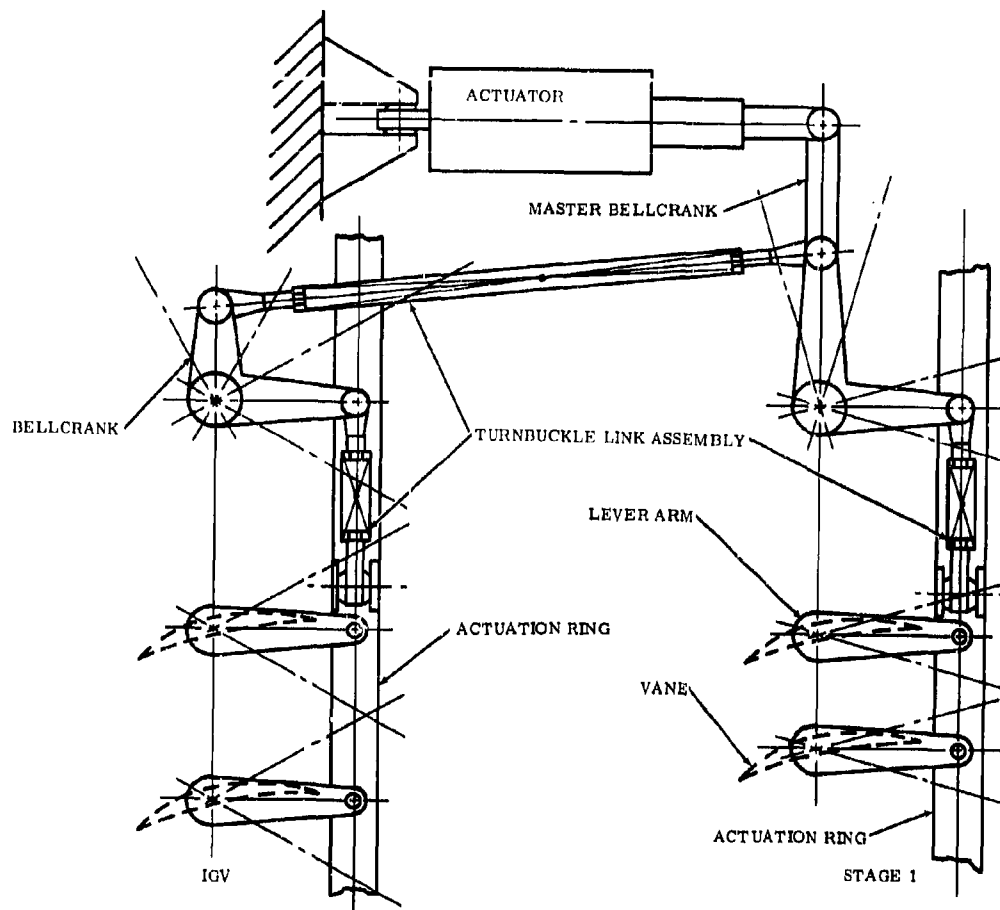


Figure 2-56. LEVER ARMS - ACTUATION RING ASSEMBLY



**Figure 2-57. GE4 COMPRESSOR FRONT VARIABLE STATORS ACTUATION SYSTEM-BELLCRANK MECHANISM**

flanges of the casing. This bolted segment configuration (see Figure 2-59) permits easy assembly and disassembly of the ring/lever system and allows assembly and disassembly of the upper and lower halves of the casings for ready access into the compressor internal area. Significant features of the design of the vane-lever arm-actuation ring loop are:

- Vane to lever arm attachment precludes incorrect assembly
- Lever arms are designed for normal bending and buckling loads with adequate margin for stall pulse loads.
- The fit of the vane trunnion engagement to the lever arm hole is closely controlled to minimize circumferential variation in vane positioning.

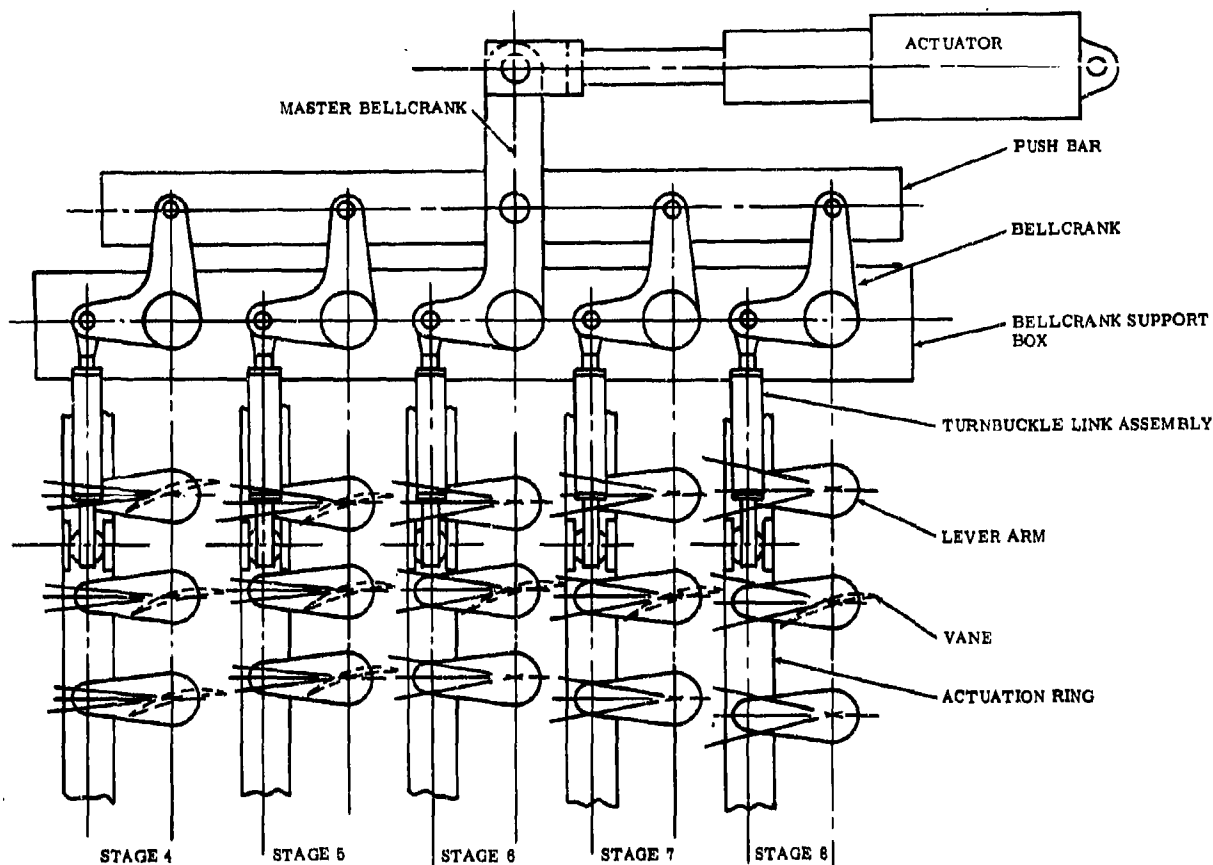
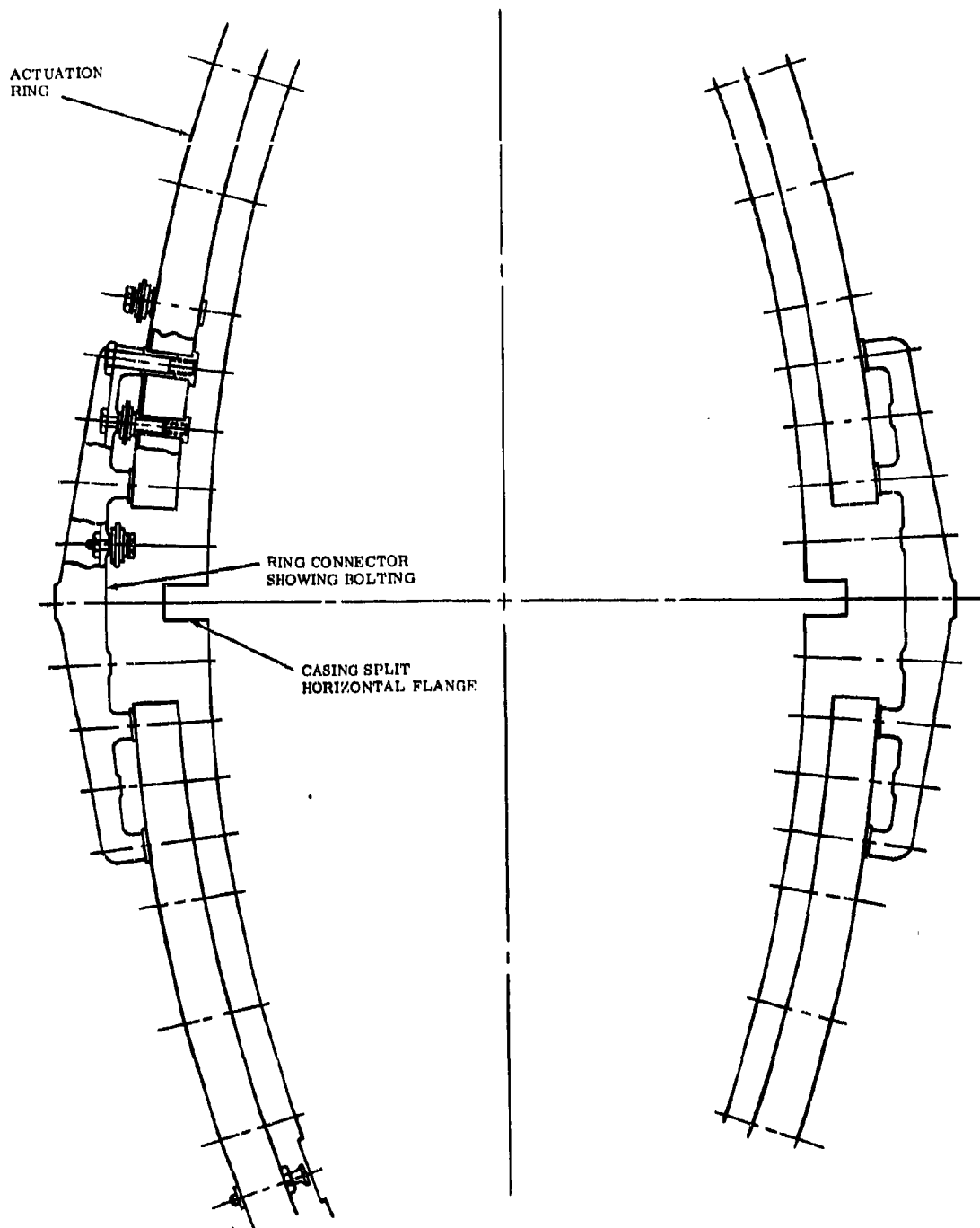


Figure 2-58. GE4 COMPRESSOR REAR VARIABLE STATORS ACTUATION SYSTEM-BELLCRANK MECHANISM

- Lever arms are fitted with spherical bearings at the ring-joint end to permit free motion and, hence, eliminate twist of the lever arms during ring rotation.
- Actuation rings are supported on the casing at eight equally spaced, circumferentially oriented pads to minimize ring distortion during actuation, control the stresses in the lever arms and rings, and minimize vane positioning inaccuracies, which might occur during distortion.
- Actuation rings in the ganged, variable stages are driven at two diametrically opposite points for proper distribution of loads and to ensure free operation.
- Lever-arm spherical bearing is clamped to the actuation ring, allowing relative motion in the bearing only and avoiding wear, galling, and initial looseness in the joint of the lever arm and ring.





**Figure 2-59. ACTUATION RING AND RING CONNECTOR.** Segmented/Bolted Actuation Ring easily disassembled for compressor internal rework and actuation system parts replacement.

- Titanium 6-2-4-2 material is used for the lever arms and actuation rings to gain the advantage of light weight and high strength.
- Spherical bearings have Inconel 718 balls and A286 races for long life and high load capabilities at high temperatures.
- Linkage lengths are pre-set and lockwired prior to assembly. Vane interstage relationships are checked only at assembly to verify that all linkages are properly assembled. This procedure reduces rigging time and eliminates the possibility of rigging errors.

The main actuation linkage loops designed for the groups have the following significant features:

- The bellcrank mechanism is an established and proved General Electric variable-stator actuation system. The high reliability of this system is evidenced by its long and successful use in T58, T64, J79, CJ805 and J93 (Figure 2-60) engines. The front and rear variable stator groups of the GE4 compressor use bellcrank mechanisms. (See Figures 2-57 and 2-58.)
- Each bellcrank is connected to the actuation ring drive-point by a precision turnbuckle-link assembly with pre-set length to ensure properly rigged mechanisms.
- The windmilling brake system employs a direct drive concept wherein the actuator rod-end attaches directly to the ring at a single drive point. The system is designed to hold the vanes at nominal design point during normal operation and to close down the OGV's for reduced windmilling speed at emergency shut down (Figure 2-48).

All the linkages and components are designed to satisfy the following prime requirements:

- Withstand stall loads
- Meet accuracy requirements in vane positioning at all normal operating conditions
- Meet durability requirements without failure and with minimum wear

### 2.3.10 MAINTAINABILITY

The GE4 compressor design incorporates the following primary objectives pertinent to maintainability:

- Designing for highest levels of durability and reliability to achieve a minimum need for maintenance.
- Provisions for ease of detecting and monitoring fault and deterioration
- Ease of required maintenance
- Repairability of components

Following is a summarized listing of the features illustrated in figures 2-61 and 2-62.

- A prime feature which provides ease of maintenance is the split casing configuration. This permits inspecting and working on the interior of the stator and rotor.

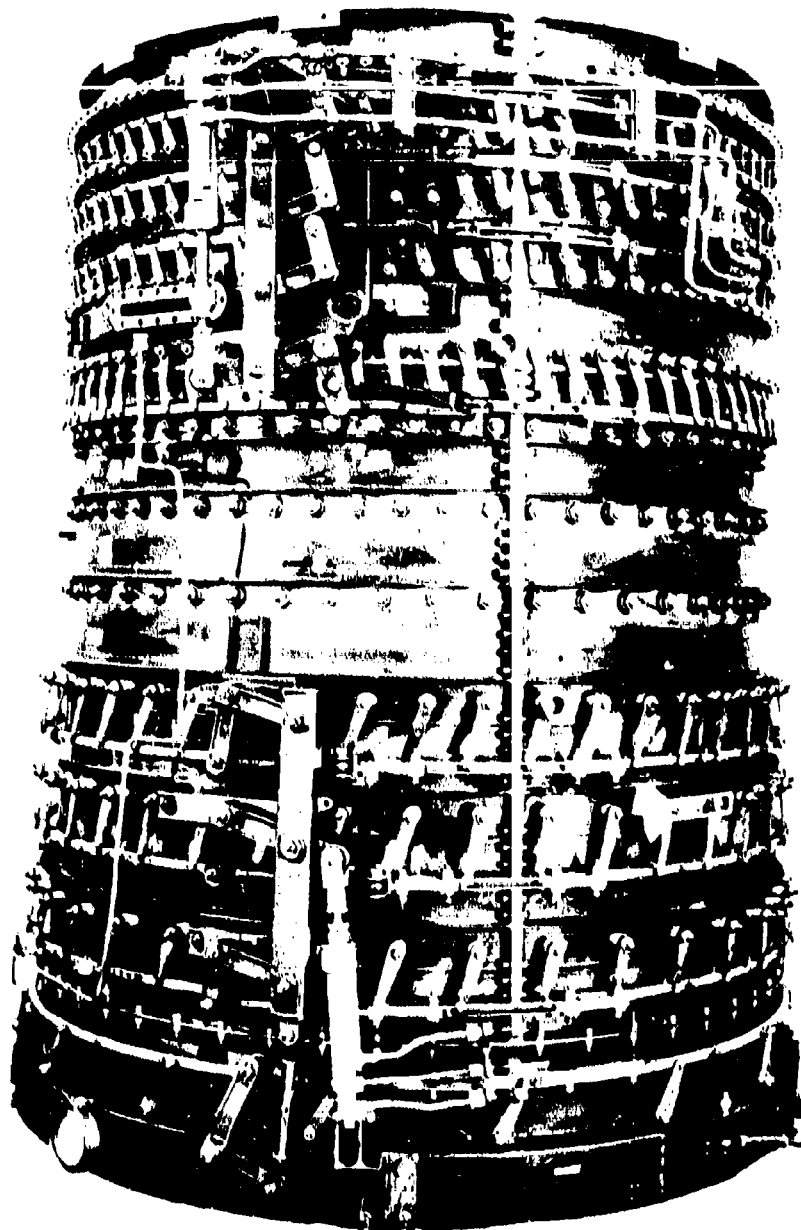
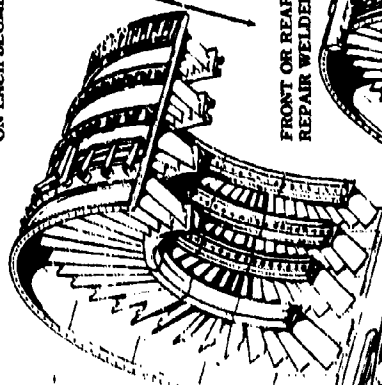


Figure 2-60. J93 COMPRESSOR STATOR  
J93 Compressor - Stator Actuation System (Bellcranks)  
- Fabricated Stator Casing  
- Split Casing

SEGMENTED/BOLTED ACTUATION RING  
EASILY DISASSEMBLE FOR COMPRESSOR  
INTERNAL REWORK AND ACTUATION  
SYSTEM PARTS REPLACEMENT.

HONEYCOMB SEALS PERMIT HEAVY  
RUBS WITHOUT REPAIR OR REPLACEMENT  
OF EITHER HONEYCOMB OR ROTATING  
SEAL -- HONEYCOMB MAY BE REPLACED  
ON EACH SEGMENT.



HUSKY, STURDY VANES AND BLADES -  
LIBERAL DAMAGE AND REPAIR  
LIMITS

NO BLADE OR VANE TIP ADJACENT TO  
STRUCTURAL MEMBER -- LESS REPAIR REQUIRED.

REPLACEABLE LINERS - 30"  
SEGMENTS - RUB DAMAGE LESS  
SEVERE ON BLADE TIP AND LINER  
THAN IF BLADE TIP WAS ADJACENT  
TO CASING.



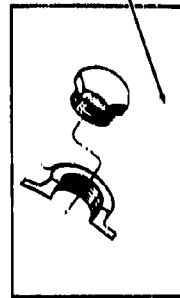
FRONT OR REAR CASING MAY BE  
REPAIR WELDED.

BLADES AND VANES MAY BE REPLACED  
WITH HALF CASINGS REMOVED.

ALL ACTUATION PARTS - BEARINGS,  
ARMS, HAI DWARE ETC MAY BE  
INDIVIDUALLY REPLACED.

INDIVIDUAL VANES MAY BE REPLACED -  
REQUIRES DETACHING FROM LEVER ARM  
AND REMOVAL OF SHROUD SEGMENT.

INSPECTION PORTS -- USED FOR  
BORESCOPE INSPECTION OR CHECKING  
BLADE TIP CLEARANCES.



- MINIMUM NEED FOR MAINTENANCE BY DESIGNING FOR HIGHEST LEVELS OF DURABILITY AND RELIABILITY
- PROVISIONS FOR EASE OF DETECTION AND MONITORING OF FAULT AND DETERIORATION
- REPAIRABILITY OF COMPONENTS
- EASE OF MAINTENANCE WHEN REQUIRED

CASINGS SPLIT FOR ACCESSIBILITY.  
CASINGS MAY BE REMOVED INDIVIDUALLY OR TOGETHER PROVIDING EASY  
ACCESS TO INTERNAL COMPRESSOR FOR INSPECTION OR REPAIR.

Figure 2-61. MAINTAINABILITY FEATURES - GE4 COMPRESSOR

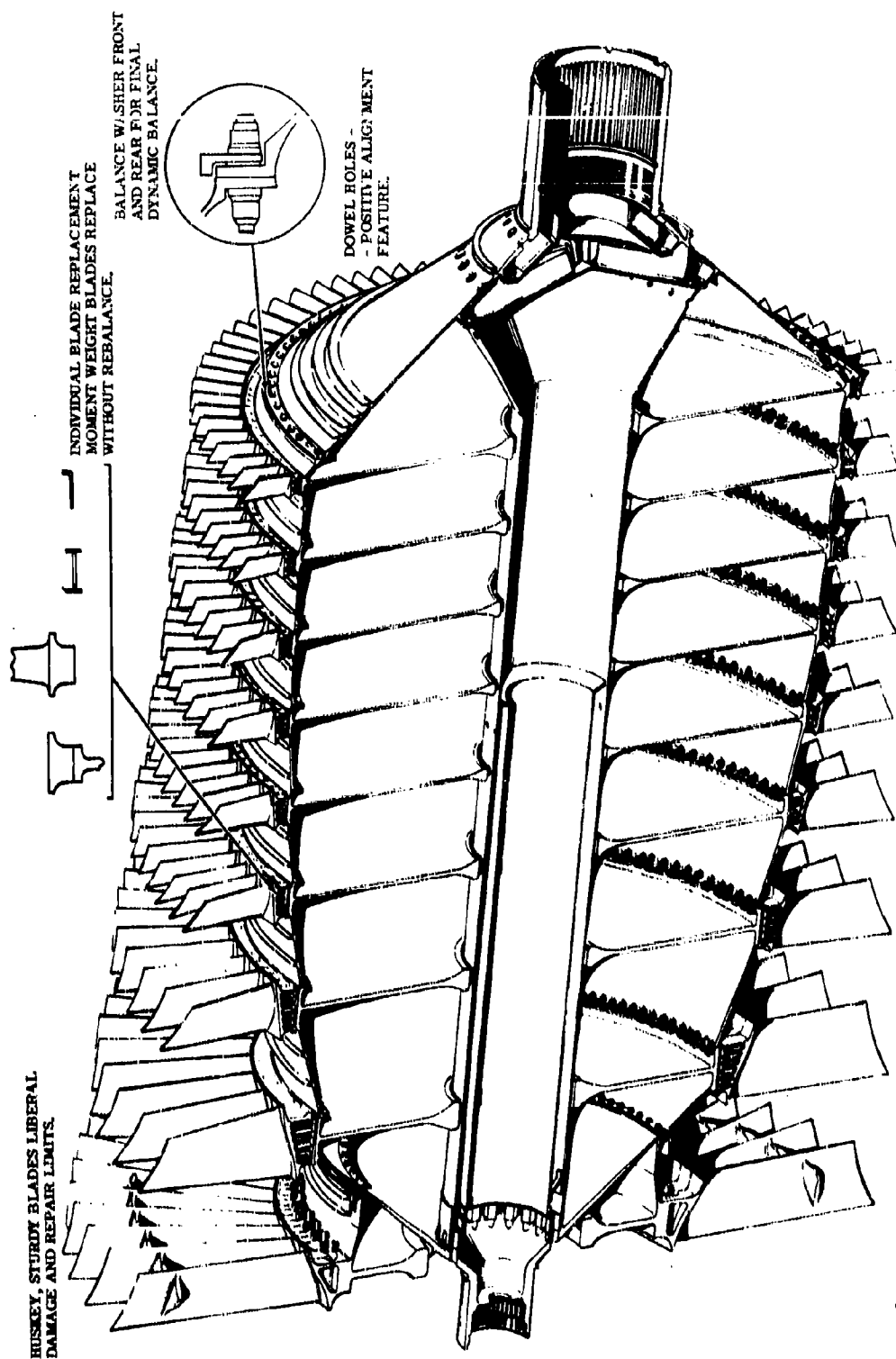


Figure 2-62. MAINTAINABILITY FEATURES--GE4 COMPRESSOR ROTOR

- The above feature is further enhanced by some key features: 1) rotor blades may be individually replaced with casing half removed -- the blades are moment weighed so that rebalance is unnecessary, 2) the vanes and shroud segments are individually replaceable, 3) the blades and vanes are sturdy and permit liberal limits for damage and rework, 4) the liners over the blade tips are easily replaceable by sliding the damaged out and the new in. The liners are non-structural and are designed to allow heavy rubbing before replacement becomes necessary. Squealer tips, which further minimize rub and the likelihood of replacement, are used on the blades.
- A simple rotor structure that has high-solidity, doweled bolts, which provide positive alignment, facilitating assembly and balance. The simple construction, with mid-stage flange and doweled bolts, provides a very stable rotor which is assured of long life without the necessity of rebalance. The rotor is dynamically balanced by use of balance washers at the front and rear. Balancing procedure is easy and effective; disks and blades are static balanced by selective assembly of the moment-weighted blades.
- No hand work or special fitting is required in the assembly of either the rotor or stator. Parts are interchangeable.
- Ports for borescope inspection and rotor tip clearance check have been provided, so that quick and comprehensive check of the blades may be made without casing removal.
- All parts of the variable stator mechanism are individually and easily replaceable. Vane arms are replaced without re-rigging.
- Position indicators are permanently attached at each stage for checking vane position.
- The rotor-blade locking device is a machined part which is re-usable. There is no tab bending of the prime locking device.
- Honeycomb seals permit substantial rub before replacement; honeycomb replacement technique has been proved.
- Casings may be welded in repair.
- Corrosion resistant materials are used throughout
- All rotor and stator contact surfaces with relative movement are treated with anti-fretting material.

A durability and maintainability analysis for the Compressor has been completed and is contained in a special appendix entitled "GE4 Durability and Maintainability Analysis", which is available on request as back up material to the substantiating data submitted.

### 2.3.11 RELIABILITY

A component or assembly with a high level of reliability implies a very thorough analysis of all the factors affecting its structural integrity. A prime example of the thorough analysis required to design for reliability in compressors is the treatment given to the area of fatigue; the failure mode which is responsible for 95 percent of all compressor failures.

An extremely sophisticated and detailed analysis of all components is combined with a very thorough component and engine test program to provide positive assurance that all vibratory modes are avoided or controlled. A systematic approach, similar to a failure mode and effect analysis, is utilized to establish all modes and to ensure that a complete consideration has been given each in the design. To obtain fatigue-resistant compressor parts, the following features have been incorporated in the design:

- Oscillatory loads are controlled; frequencies reaching from 25 cycles per second to blade harmonics surpassing 50 thousand cycles per second are considered. The vibratory response to these excitations are held to levels well below the endurance limits.
- Local design point steady stresses are limited to levels consistent with required engine start/stop cycles.
- Transient thermal responses are controlled.
- The interaction of these stress components locally (throughout a given part) has been allowed for.

More specifically, parts have been made insensitive to fatigue by:

- Selecting the correct material for the life and environment
- Systematic refinement of the details to avoid stress concentrations, inadequate fillets, and fretting in high stress zones.
- Ensuring that linked parts are dynamically consistent; that, for example, dovetails have the strength of the parts they support.
- Establishing the natural frequencies of parts to provide margins tolerant of the unusual, infrequent, or abnormal modes of operation, thus avoiding the "surprise" resonant vibrations that induce fatigue failure.
- Intensive design verification by heavily-instrumented tests of the compressor under severe off-design conditions; deliberately induced stall, inlet distortion, and control malfunction.
- Limiting thermal stresses to the levels consistent with required number of flights in all parts.
- Taking cognizance of the start/stop cycles as it affects the conventional distinctions between low cycle fatigue and steady-stress plus vibration.

This very thorough approach in the area of fatigue is typical of analysis in all critical areas.

#### **2.3.12 QUALITY ASSURANCE (refer to Vol. IV, Sec 4.3)**

The design of the compressor makes use of proven concepts. Quality control procedures and techniques are well developed and have been proved successful on production engines. Tolerances, finishes, non-destructive testing, records, and methods of dimensioning are all standard and are typical of established practices.

A new quality control process has been added for the inspection of diffusion-bonded blade joints. Inspection of diffusion bonded blades is critical in ensuring a structurally effective bond. Using

the conventional inspection process, with mating parts of an unbonded joint in intimate contact, the particle motion of the sound waves tend to be transmitted through the joint to erroneously indicate the existence of a good bond. General Electric has developed equipment achieving propagation of shear sound energy in any desired direction.

The sound wave can be made to impinge upon an interface in such a manner that the particle of motion of the wave is parallel to the interface. Shear-mode sound is transmitted basically as a function of the shear modulus of rigidity of the material. This modulus of rigidity (shear modulus) is closely related to the quality of the joint. An effective joint having a shear modulus of the parent material will reflect the wave differently than will an unsatisfactory joint. Interpretation of the data is relatively simple.

Sophistication and advancement in quality control techniques are constantly being made to meet the design and manufacturing growth. For example, the leading-edge contour of the blade and vane must be carefully controlled since it has a significant effect on engine performance. The microscope (Taylor Hobson) has been an effective means of providing a visual check of the leading edge, but a recent advancement has been made using television to project the image, for comparison with a master, on a screen at 80 times size. This provides the operator with a greater magnification (Taylor Hobson - 40X) and, hence, more accurate readings. In addition, this method reduces operator fatigue, a significant factor in good quality control. This method (television) will be applied also to dovetail contours.

Many features of the design make the quality assurance task much simpler. For example:

- Blades and vanes are husky and sturdy. Their large size permits more generous tolerances; especially in the blade- or disk-dovetail area and in the fillets. The larger sizes make inspection less tedious and less susceptible to error. Handling damage is less likely to occur.
- Blade and vane tips are not adjacent to rotor, or stator, structural members. Thus, there is more tolerance to rub in the design and blade and vane tip measurements are less critical.
- The split casings simplify assembly inspection. For example, axial clearances can be taken with only half of the casing removed.

### 2.3.13 SAFETY

Inherent in the design of any engine component is consideration for safety. There are specific areas pertinent to safety worth recounting:

- The casing is specifically designed to contain a compressor blade. This prevents the failed blade from cutting fuel lines, engine structure, and from entering the cabin. Experience and tests at Watertown Arsenal have shown that the compressor, as now designed, will meet the containment requirement. Proof will be demonstrated during the program.
- A windmill brake is provided to limit rotor windmill speed at high Mach numbers by closing the outlet guide vanes. This system is provided in case the rotor becomes unbalanced and must be slowed to prevent more serious failure.
- Reliable disk and shaft design.
- Highest levels of durability/reliability in the stator and rotor structures.



### 2.3.14 FAILURE ANALYSIS

The complete spectrum of failure analyses to be conducted on the compressor, as well as all other major parts of the engine described in this volume, will include up to six distinct phases. These begin with a comparative failure analysis based on extensive prior experience with other turbojet engines and proceed through: Failure Mode and Effect Analyses, reliability estimates, probabilistic life modelling, major systems analyses, and failure analyses as a result of testing. These phases are fully described in Volume IV, Reliability.

The initial FMEA has been completed on the compressor. A systematic study of each mode on each part of the compressor was made. All items which showed a possibility of early or premature failure was redesigned. For example; these analyses revealed that improvements were required in blade retention and more adequate support of the internal rotating duct. Corrective action was taken on these items.

A very thorough failure analysis was initiated on a stator inner shroud seal problem encountered on the full scale compressor test. This led to the incorporation of important design detail changes of the seals in the Phase III configuration.

### 2.3.15 VALUE ENGINEERING

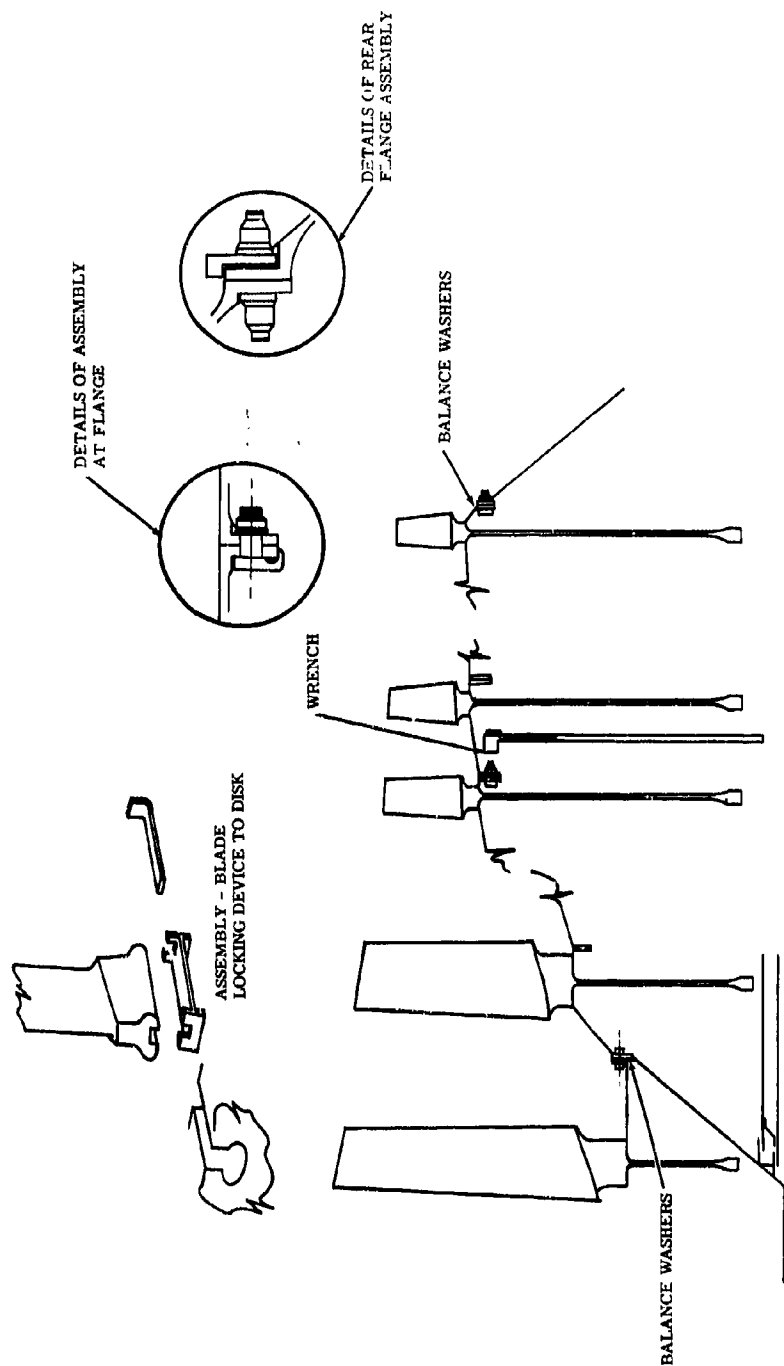
Careful consideration has been given in designing the compressor to value engineering factors. Some of these considerations are:

- Development of a friction welding process for the rotor is planned. A first step to a welded construction will be to use the Electron Beam Welding technique to weld the spacer extensions to the disks. A final step will be to weld the disk and spacers together completely, eliminating all flanges except where the material changes (Titanium to Inco 718). The results will be a less expensive, better quality, structurally stronger, and more rigid rotor.
- Development of the simple, internal, rotor cooling system, using inexpensive cycle air, permits use of Inco 718 material in stage 8 and 9 disks, instead of the more exotic and costly turbine material.
- Vane airfoils are rolled with diffusion bonded trunnions.
- Fabricated compressor casings meet strength, weight, and cost requirements.

Value Engineering effort has also precipitated combined design and manufacturing programs. One such program is the development of a technique to generate the leading edge of the blades and vanes without costly hand work.

### 2.3.16 HUMAN ENGINEERING

The compressor for the GE4 engine uses assembly techniques that have been developed and demonstrated on earlier engines. The rotor assembly is similar to the TF39 power turbine rotor assembly. The rotor will be stacked from rear to front as shown in Figure 2-63. Visual inspection will be possible and assembly procedure sheets will be written to provide a systematic control.



BLADES ASSEMBLED TO DISKS AND STATIC BALANCED. FIRST STG. DISK, SHAFT AND 2ND STG. DISK ASSEMBLED BOLTS INSERTED FORWARD THRU FLG. OF 2ND STG. DISK. SHAFT AND FIRST STG. DISK. NUTS TORQUED WHILE HOLDING BOLT WITH WRENCH. 2ND STAGE DISK THRU 9TH STG. ASSEMBLED IN SAME MANNER - BOLTS INSERTED IN FLANGE AND HELD IN PLACE BY PUSH ON NUTS. NEXT DISK AFT DROPPED ON OVER BOLTS. NUTS TURNED ON BY HAND AND TORQUED UP WITH WRENCH - VISUAL INSPECTION TO ASSURE NO LOOSE NUTS. THE DUCT IS ASSEMBLED TO THE REAR STUShaft AND WHOLE ASSEMBLY DROPPED IN PLACE. THE DUCT IS HELD BY A SLIP FIT TO THE FRONT STUShaft. DYNAMIC BALANCE USING BALANCE WASHERS.

Figure 2-63. ASSEMBLY OF ROTOR - GE4 COMPRESSOR

Features that have been incorporated, specifically to ensure error-free assembly and handling, are:

- Blade locking device is a machined part which is not bent or formed at assembly. A non-critical strip which positions the locking device is the only part formed at assembly.
- Vane lever can be assembled to vane stem in only one way.
- Vane stems, inner and outer, have internal threads to avoid handling damage. The locking feature is applied to the bolt.

The compressor design also has inherent tolerance to mishandling:

- Sturdy blades and vanes are not as susceptible to damage at the leading or trailing edge.
- Honeycomb seals can be assembled with under size clearances without serious effect.
- Blade tip clearances are not a serious problem when small, since rubbing strips (liners) permit damage-free rubs during normal engine operation.

The stator assembly is completed in halves prior to bolting the engine and simplifies assembly. The general procedure for stator assembly and rigging the variable stator mechanism is similar to all production engines.

#### 2.3.17 STANDARDIZATION

Design reviews were held specifically to minimize the number and types of hardware items. The following are examples of this effort:

- Inner and outer trunnions and mounting hardware have only three different sizes each for the six stages of variable vanes, including the outlet guide vane outer trunnion.
- Lever arms are limited to three different sizes.
- One size of lever spherical bearing is used throughout.
- One size of circumferential flange bolt serves on three flanges.
- Six dovetail sizes for all nine stages.

## CONFIDENTIAL

### 2.4 DEVELOPMENT STATUS

#### 2.4.1 FULL SCALE COMPRESSOR TEST

The 8 stage, 475 lb/sec design, airflow compressor has been tested for a total of 202 hours in the Lynn test facility. During this testing, the following objectives were successfully attained.

- Compressor performance map (reference Volume III-A, Section 3)
- Verified variable stator vane schedule for engine operation (reference Volume III-A, Section 3)
- Blade and vane vibration response
- Inlet distortion effects on performance (reference Volume III-A, Section 3) and airfoil vibration response.
- Compressor inlet noise level measurements (reference Volume III-C).

Observation of the vibratory response of the blading during testing confirmed the durability and ruggedness of the design. Figure 2-64 illustrates the measured blade vibratory response in stall at 74 percent  $N_C$ , corrected speed (Mach 2.7), and 100 percent  $N_C$  (SLS). Figure 2-65 illustrates the blade vibratory level observed on the engine operating line at sea level and Mach 2.7. During stall, the blade stresses did not exceed 95 percent of limits at speeds up to 100 percent  $N_C$ . Stator vane vibration was below measurable levels and is not shown.

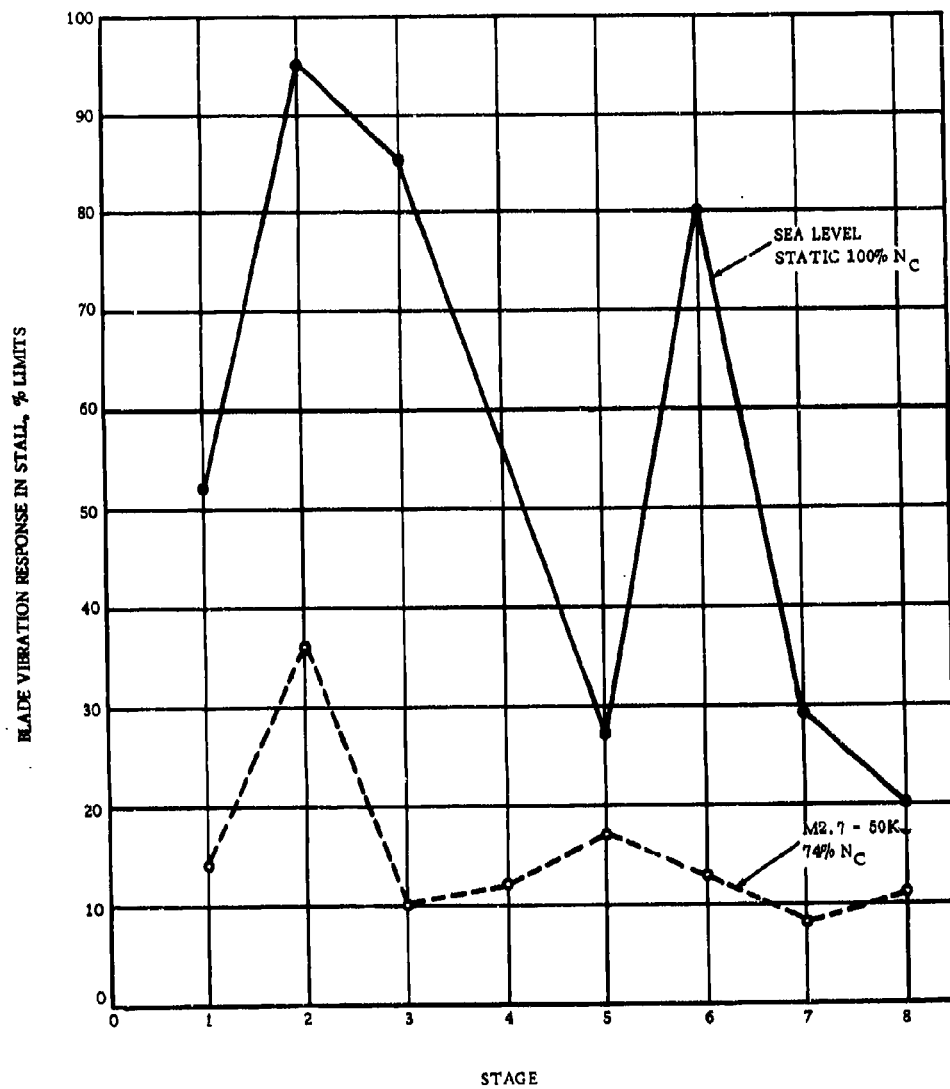
A summary of performance at sea level and Mach 2.7 is as follows:

	<u>Sea Level</u>	<u>Mach 2.7</u>
Corrected Speed, $N_C$ percent	100	74
Operating Pressure Ratio	10	4.65
Corrected airflow, lb/sec	505	300
Efficiency, percent	85.7	84.2
Stall Margin, percent	16.3	19.9

##### 2.4.1.1 Inlet Distortion Testing

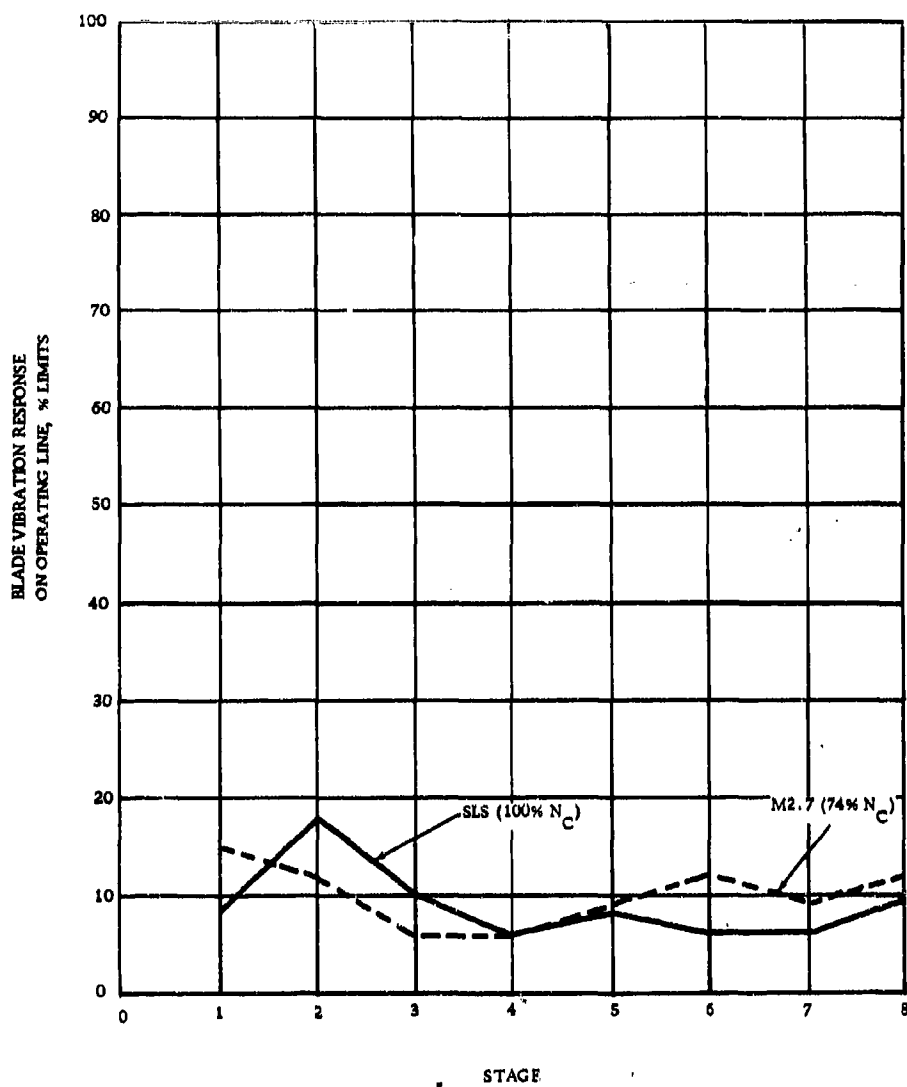
Inlet distortion tests with hub and tip radial and both 1/rev and 2/rev circumferential distortion patterns have been completed. The compressor performance under these conditions of inlet distortion is reported in Volume III-A, Section 3. Figures 2-66 and 2-67 show the effect of inlet distortion on blade vibration response during stall.

The blading absorbed all inlet distortions imposed without mechanical damage or loss in life. The testing revealed that any variety of inlet distortion up to an  $NDI=0.2$  can be absorbed without using up fatigue life of the compressor blading. The highest stress level observed was 155 percent of limits for 30 cycles at 90 percent  $N_C$  with 39.9 percent hub radial inlet distortion. This momentary high degree of overstress under extremely adverse conditions verifies the durability of the blading. The compressor is capable of taking 1000 stalls of this variety and intensity before using up the fatigue life in the blading.



# GE4 COMPRESSOR BLADE VIBRATORY RESPONSE INSTALL

Figure 2-64

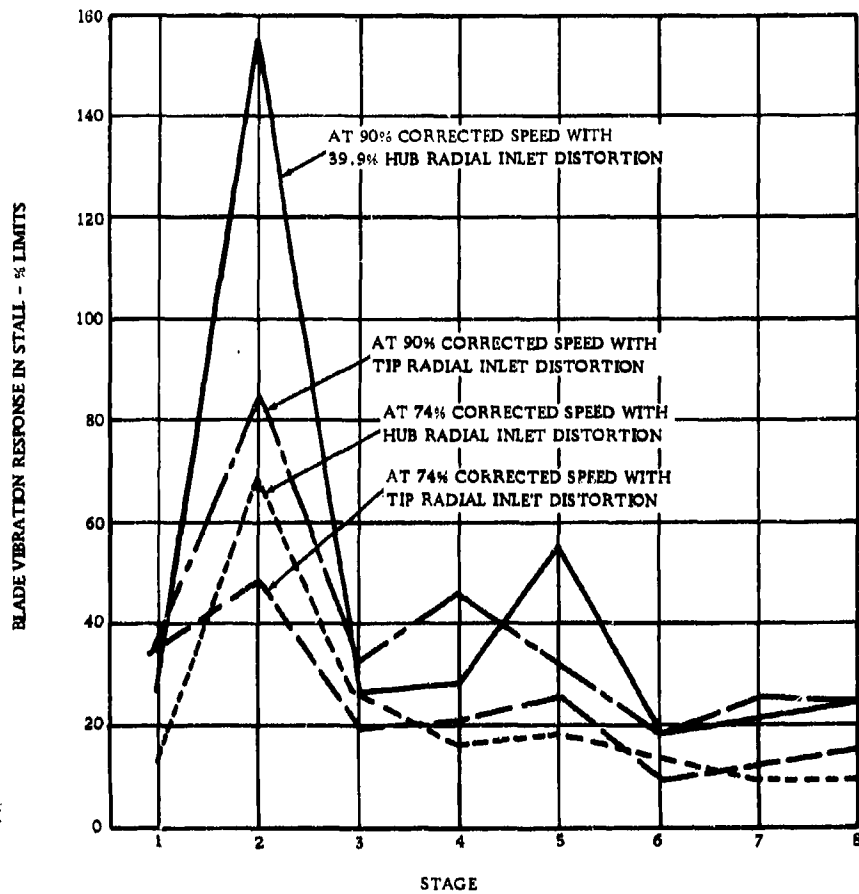


GE4 COMPRESSOR BLADE VIBRATORY RESPONSE ON OPERATING LINE

Figure 2-65

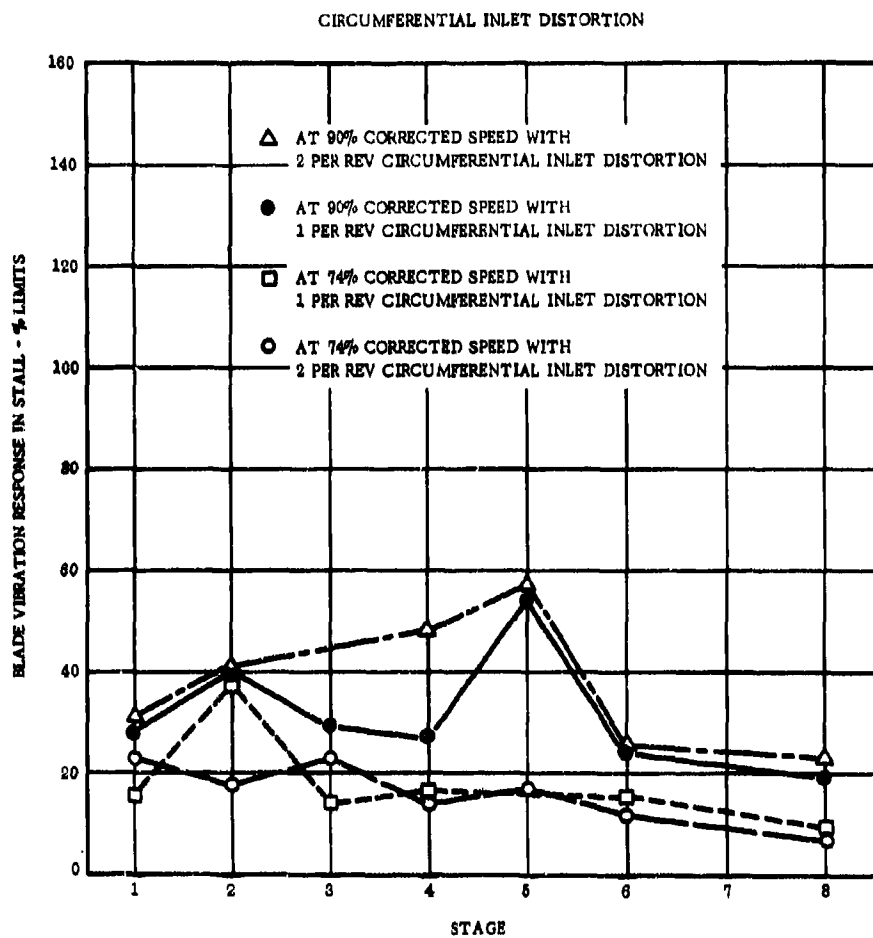
MEASURED INLET DISTORTION EFFECTS  
ON BLADE VIBRATION DURING STALL

~ RADIAL INLET DISTORTION ~



GE4 COMPRESSOR BLADE VIBRATORY RESPONSE INSTANT DURING  
DISTORTED INLET OPERATION

Figure 2-66



GE4 COMPRESSOR BLADE VIBRATORY RESPONSE INSTALL DURING  
DISTORTED INLET OPERATION

Figure 2-67



#### 2.4.2 ENGINE TESTING

A Phase II-C fully instrumented engine with an 8 stage, 475 lb/sec design, airflow compressor similar to the full scale compressor test vehicle discussed in 2.4.1 is being tested at the Evendale test facility.

Observations made during the tests conducted to date show low vibratory stresses in the blades, vanes, disks and ducts. The variable stators are operating and tracking accurately, maintaining scheduled vane positions at all corrected speeds up to 100 percent  $N_c$ .

The compressor, in general, has been operating satisfactorily. Compressor performance is discussed in Volume III-A, Section 3.

2-87/2-88

K

## CONFIDENTIAL

### 3. COMBUSTOR DESIGN

#### 3.1 INTRODUCTION AND SUMMARY

The GE4 combustor design emphasizes durability. Experience has shown that combustor life is often limited by severe oxidation, cracking, and mechanical distortion. These problems are substantially reduced in the GE4 combustor by effective use of cooling air and advanced mechanical design. Sufficient quantity and accurate distribution of cooling air maintains metal temperatures at conservative levels and minimizes thermal gradients. Advanced mechanical design minimizes thermal stresses.

The combustor is of a high-performance annular design, based on annular combustor operating experience of more than three million hours. This experience has been obtained in both large and small General Electric engines during the past 10 years. Only General Electric has had supersonic experience with annular combustors. Photographs of the GE4 Phase II-C design are shown in Figures 3-1 and 3-2. An assembly drawing and a trimetric section of the Phase III design are shown in Figures 3-3 and 3-4, respectively. Figure 3-5 shows the GE4 combustor in comparative scale with other General Electric annular combustors. The T58, J85, T64 and J93 combustors shown are for engines currently in service. The J97 and TF39 combustors are for engines now in development phases.

The selected GE4 design provides a short, compact combustor envelope with associated endurance advantages of relatively small surface areas to be cooled and high structural stability of the shell. The GE4 combustor will ultimately operate for a minimum of 4000 hours between maintenance stops and will have a minimum useful service life of 12,000 hours. These requirements are similar to those of the TF39. Combustor durability requirements will be met because of the following GE4 advantages.

- The annular combustor design is inherently easier to cool. Local hot spots caused by cross-fire tubes and separate cans are eliminated. Also, there is less surface to cool.
- A very active General Electric cooling development program for annular combustors has produced highly refined and effective cooling air distribution techniques. An almost ideal continuous cooling slot design has been devised during the past eight years of this program. This design limits maximum metal temperature to 1500°F, and virtually eliminates thermal stresses from transverse temperature gradients.
- The weld-plus-braze fabrication method applied to cooling slots provides resistance to vibration and thermal fatigue.
- Application of new analysis techniques for thermal stress and cyclic fatigue, complemented with flame tunnel cyclic fatigue endurance testing, is providing further advances for durable mechanical design.
- A friction-grip combustor-mounting system eliminates vibratory motion and wear at the 14 mounting points.
- A truss in the forward end of the cowl prevents structural failure in this region.
- Variable-area fuel nozzles overcome gum build-up and plugging problems, and provide accurate reliable fuel-flow for extended operating periods.

**CONFIDENTIAL**

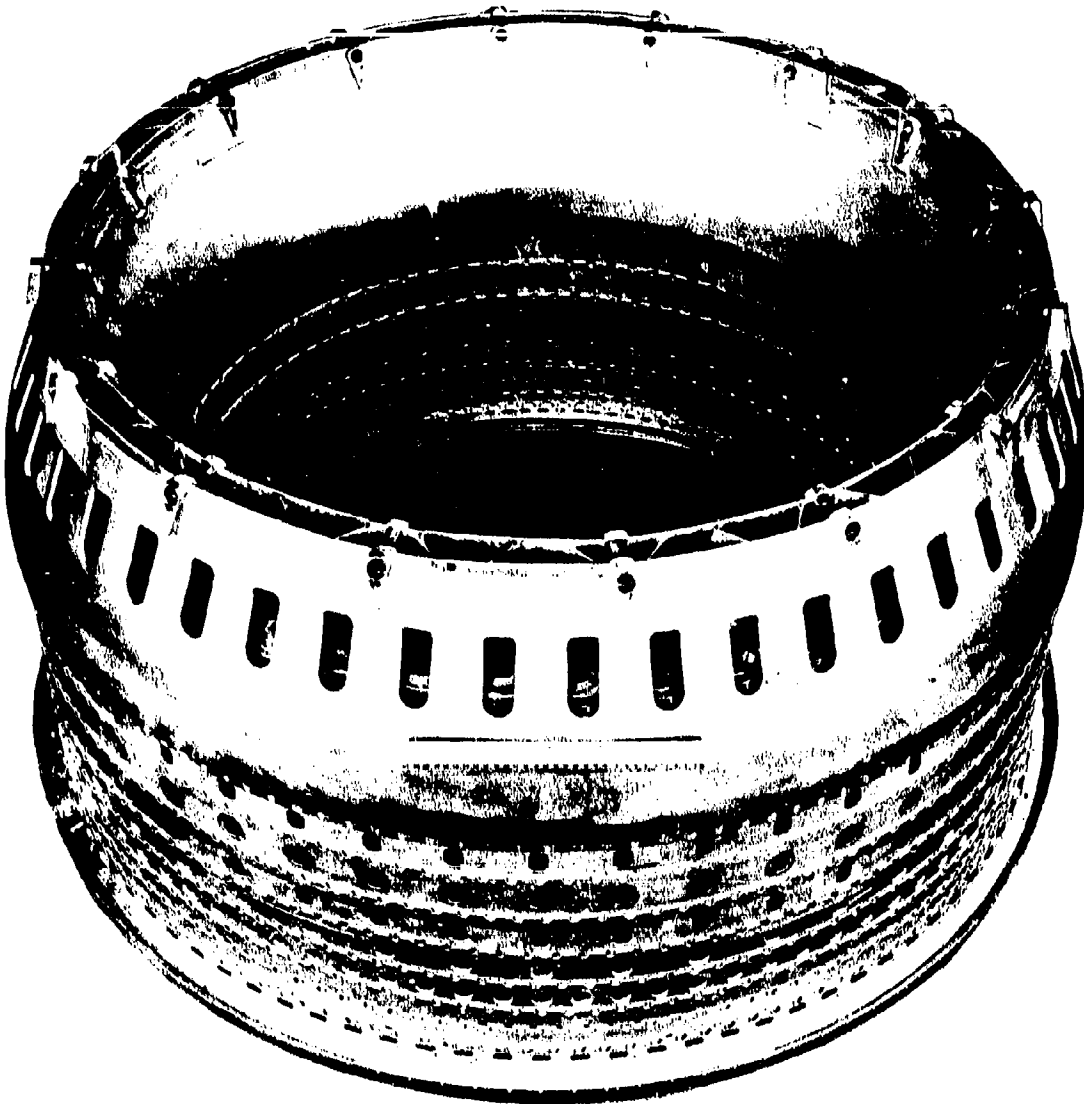


Figure 3-1. GE4 PHASE II-C COMBUSTOR

3-2

**CONFIDENTIAL**

K

**CONFIDENTIAL**

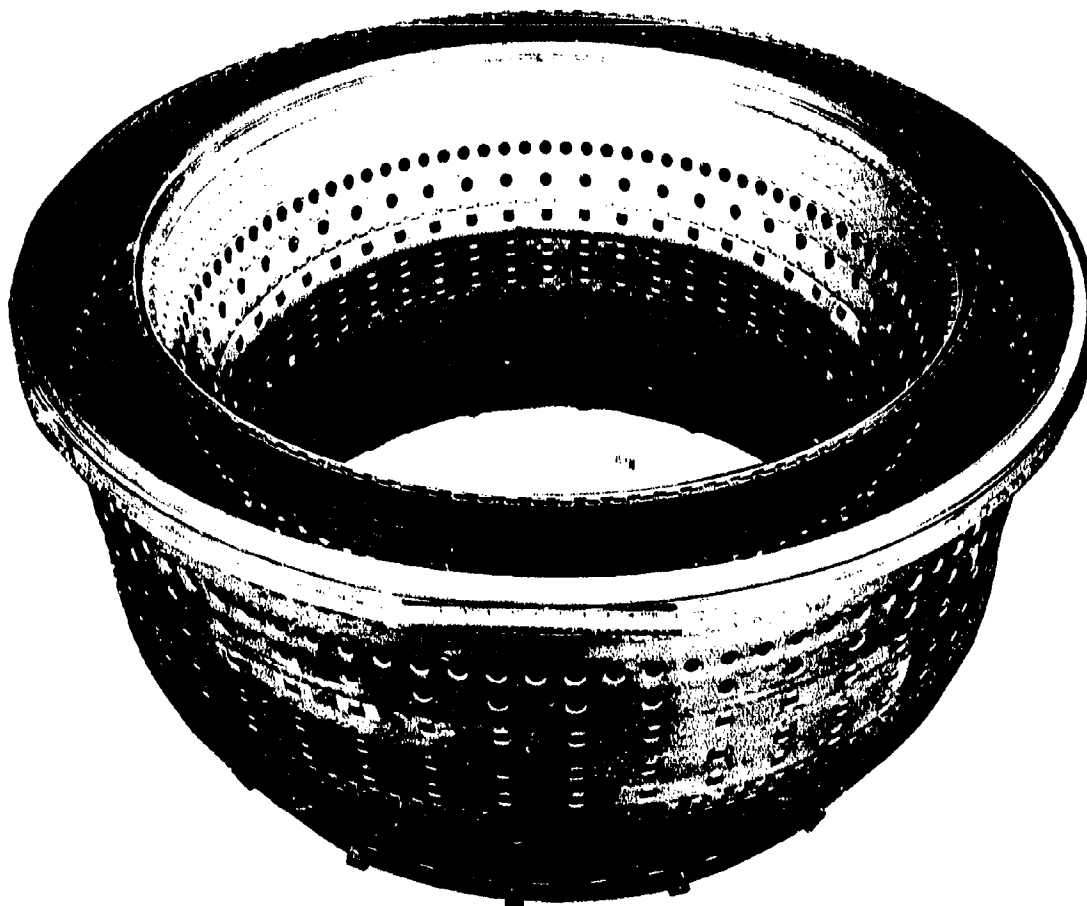


Figure 3-2. GE4 PHASE II-C COMBUSTOR

3-3

**CONFIDENTIAL**

K

CONFIDENTIAL

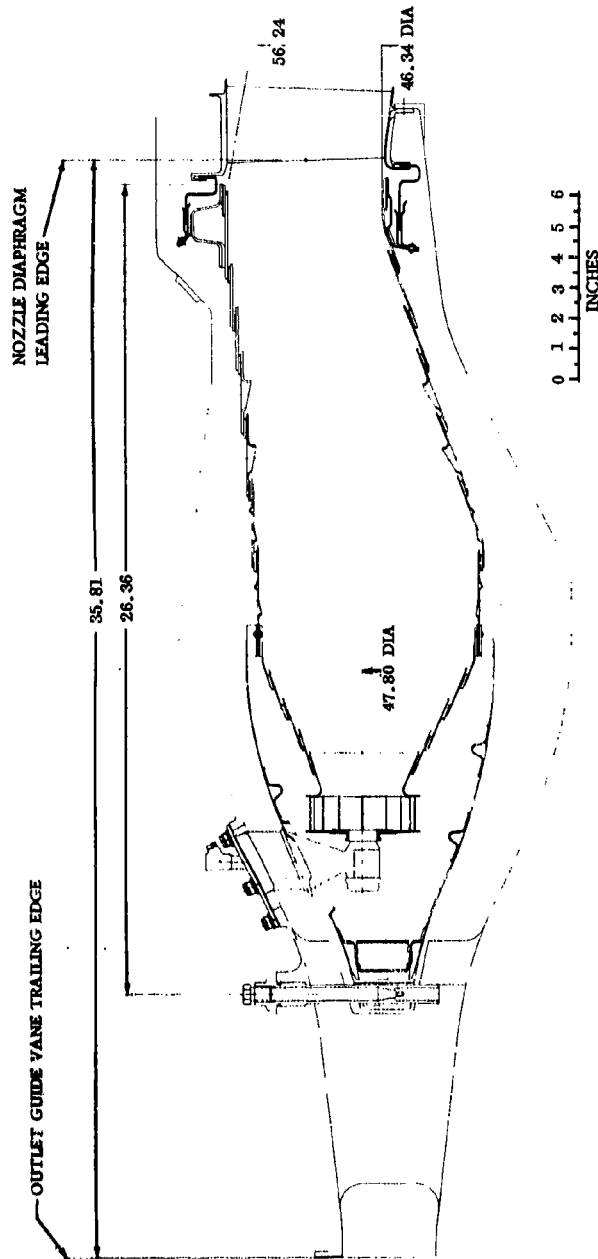


Figure 3-3. GE4 PHASE III COMBUSTOR CROSS SECTION

3-4

CONFIDENTIAL

K

**CONFIDENTIAL**

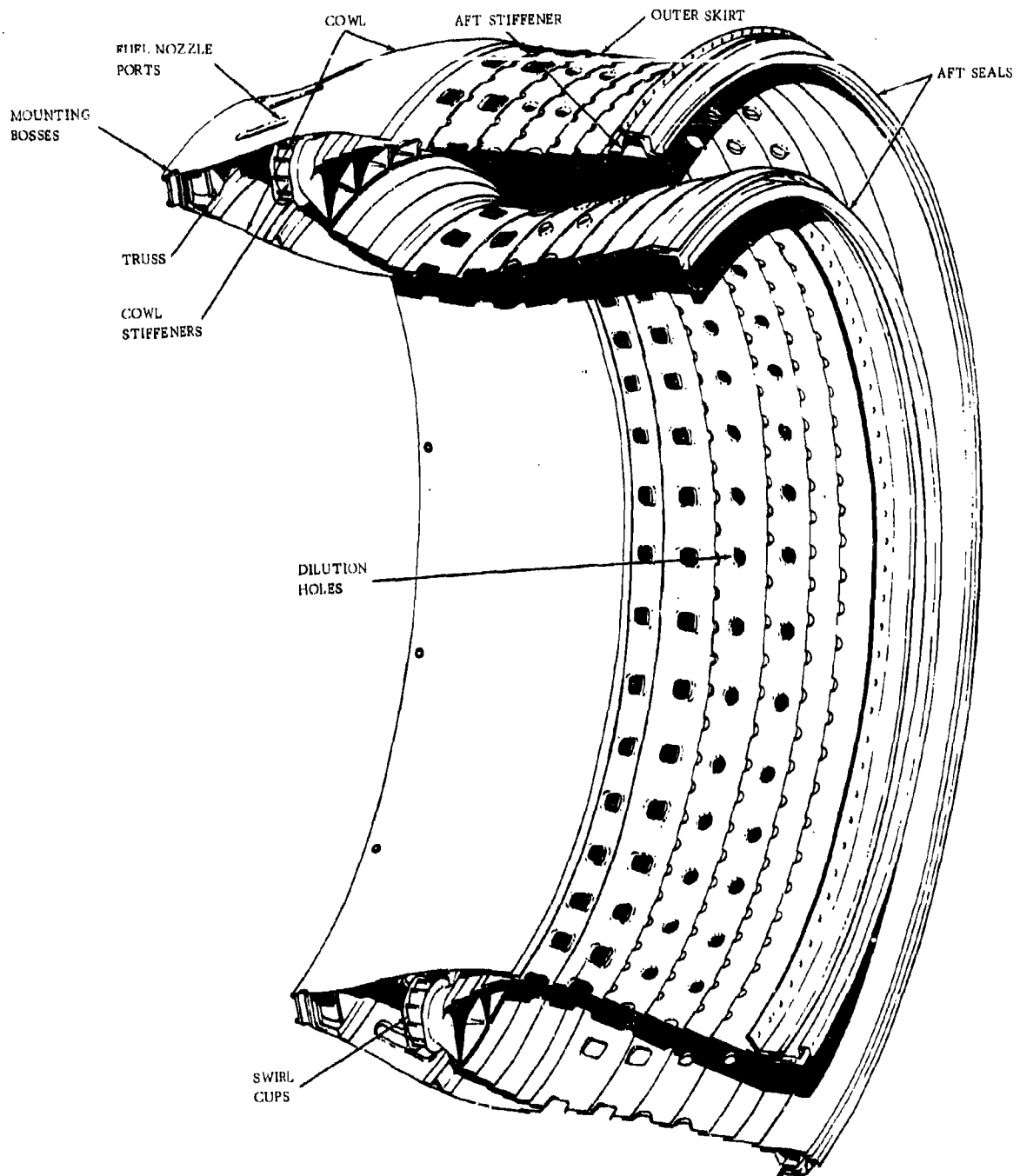


**Figure 3-4. GE4 PHASE III COMBUSTOR**

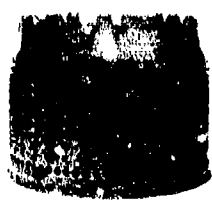
3-5/3-6

**CONFIDENTIAL**

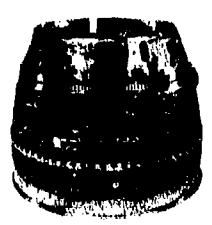
K



T58  
CT58



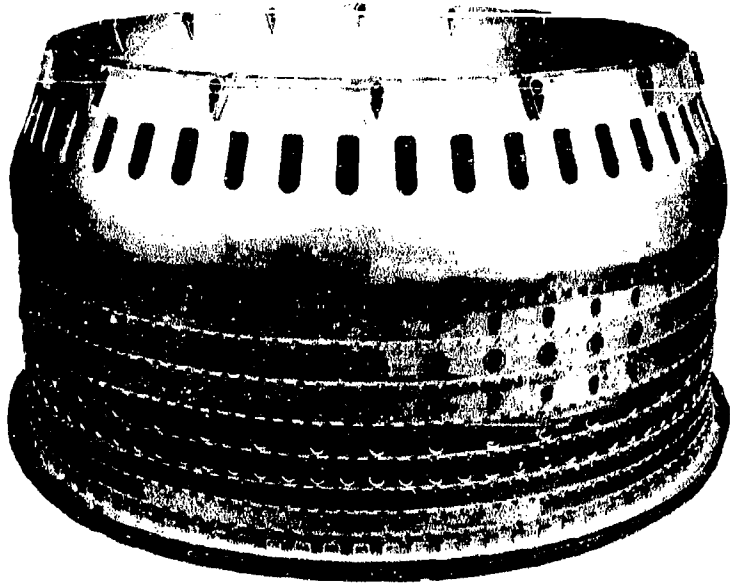
J85  
CJ610



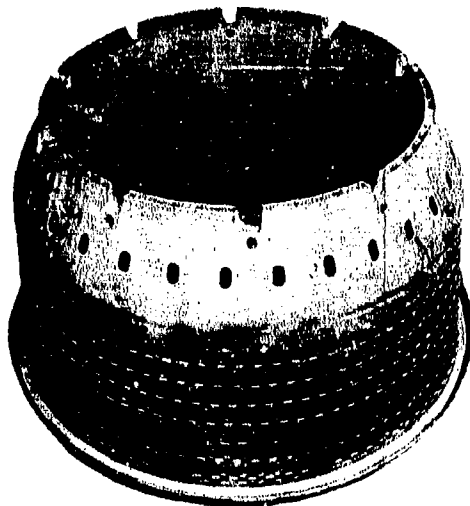
164

1

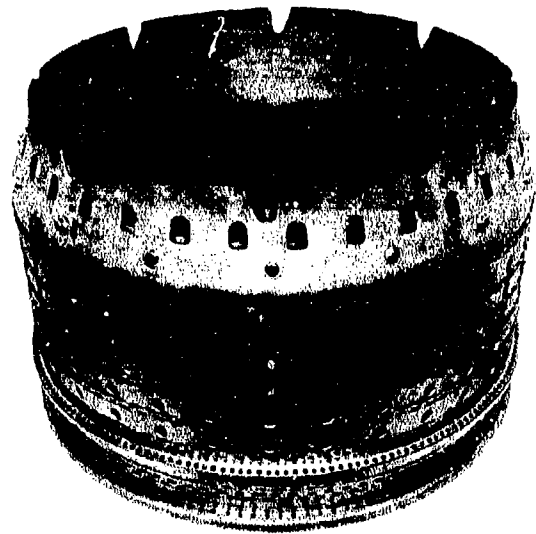
**CONFIDENTIAL**



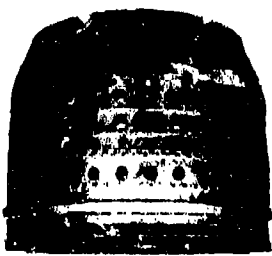
GE4



TF39



J93



J97

Figure 3-5. GENERAL ELECTRIC ANNULAR COMBUSTORS

2

3-7/3-8

**CONFIDENTIAL**

K



- Hastelloy-X material used in combustor construction has excellent oxidation resistance, and high ductility and high-temperature strength.
- The diffuser design essentially eliminates strut wakes. The combustor air inlet holes and cooling slots have low sensitivity to ram effects. The combustor is, therefore, very tolerant of non-uniform diffuser exit velocities.

The above durability features provide important contributions to safety, reliability, maintainability, and economy of operation.

Need for combustor maintenance is substantially reduced with the annular design. However, excellent maintainability is achieved by use of riveted joints that permit disassembly and replacement of the major components. The rivets are located in cool regions to prevent rivet failure from oxidation or over-temperature. All parts subject to wear by sliding contact are individually replaceable. In addition, design studies are being made to provide a circumferential slip joint at the junctions between the skirts and dome-cowl assembly. This will permit replacement of the skirts after removal of the turbine, and can be done without removing the fuel nozzles, mounting pins, or ignitors.

Most annular combustor development work at General Electric has been done with 360 degree, full-scale combustors. This provides a much higher fidelity of stress duplication, and, therefore, identifies design weakness much more readily than sector testing. Initial GE4 combustor development has been done on a full-scale, 360-degree atmospheric test rig.

The General Electric Company is in a unique position to make major contributions, in terms of combustor design, to the over-all success of the SST Program and to commercial aviation. In the TF39 Program, General Electric is already well along toward developing a combustor with durability and outlet temperatures similar to the combustor required for the GE4. General Electric's wealth of supporting technology related to annular combustor design and high combustor outlet temperatures is unmatched in the industry. These important factors deserve careful consideration in the selection of an engine for the Supersonic Transport.

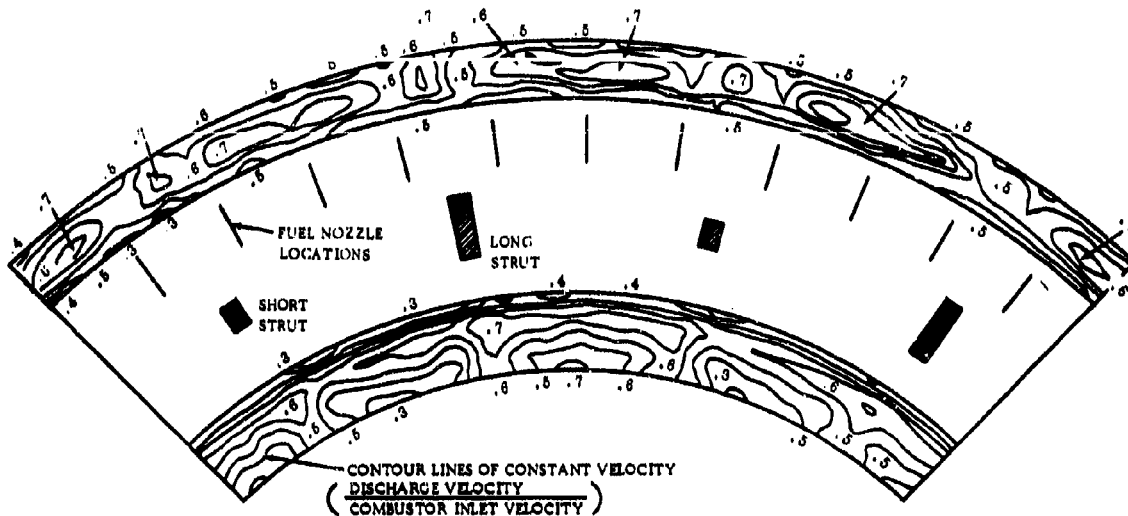
### 3.2 DESIGN REQUIREMENTS AND APPROACH

#### 3.2.1 COMBUSTOR INLET AND OUTLET CONDITIONS

Figure 3-6 is a typical plot of air velocity contours at the discharge end of the inner and outer diffuser channels. The data was obtained from a diffuser model of the GE4 Phase II-C combustor. Effects of strut wakes are essentially eliminated, and the general distribution is very uniform. The air inlet holes of the combustor skirt have low sensitivity to wake effects. The combination of small strut wakes and low sensitivity of air inlet holes to ram effects help to ensure uniform combustor exit-temperature distribution with low peak temperature factors. This stability has been demonstrated by excellent performance of the GE4 Phase II-C combustor on the combustion test stand.

Figure 3-7 shows combustor inlet and exit pressures for take-off, acceleration, and cruise conditions. Figure 3-8 shows objective combustor discharge temperature profiles at sea level static conditions.

Figure 3-9 compares data obtained from full-scale tests of the Phase II-C combustor at sea level static conditions with objectives. Figure 3-10 shows objective combustor discharge temperature profiles during acceleration. Figures 3-11 and 3-12 show equivalent data for 65,000 ft,  $M_p$  2.7.



TYPICAL SECTOR FROM HALF SCALE ANNULAR MODEL OF GE4 DIFFUSER  
(LOOKING DOWNSTREAM)  
THIS SHOWS THAT STRUT WAKES ARE ESSENTIALLY ELIMINATED AND  
THAT GENERAL DISTRIBUTION IS VERY UNIFORM

Figure 3-6. AIR VELOCITY CONTOURS

### 3.2.2 COMBUSTOR LINER DURABILITY

The combustor design has been evolved from the successful, and very capable  $M_p$  3.0 J93 combustor, with cooling-slot improvements already demonstrated in the J97 and TF39 engine programs. Additional advancements are being made to improve mechanical durability of the liner by application of new analytical and testing techniques. Results of this program will be used to define a design for 12,000 hours operating service, and 4000 hours between sectionalized maintenance. (Refer to Section 3.3.4.)

### 3.2.3 FLIGHT PROFILE, $T_3$ , $T_4$ AND DURABILITY

The Supersonic Transport flight profile and engine operating requirements specify that 64 percent of the engine operating time is spent at supersonic cruise. During this portion of the flight segment, the compressor discharge and turbine inlet temperatures produce higher combustor metal temperatures than at any other portion of the flight. Durability and performance at supersonic cruise, in addition to thermal cycle fatigue resistance, must be major characteristics of a successful SST combustor.

CONFIDENTIAL

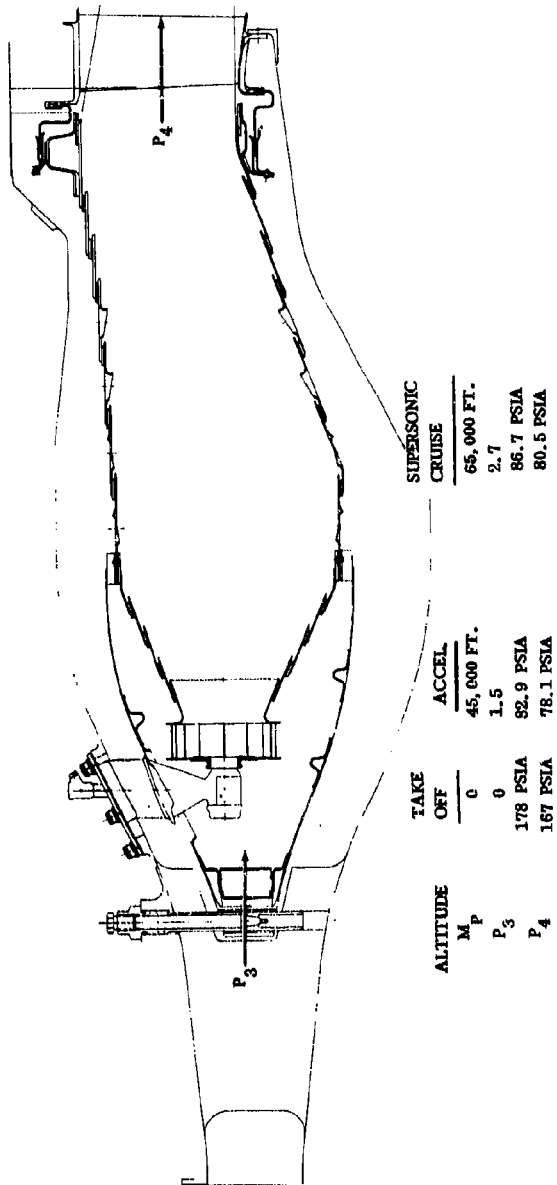
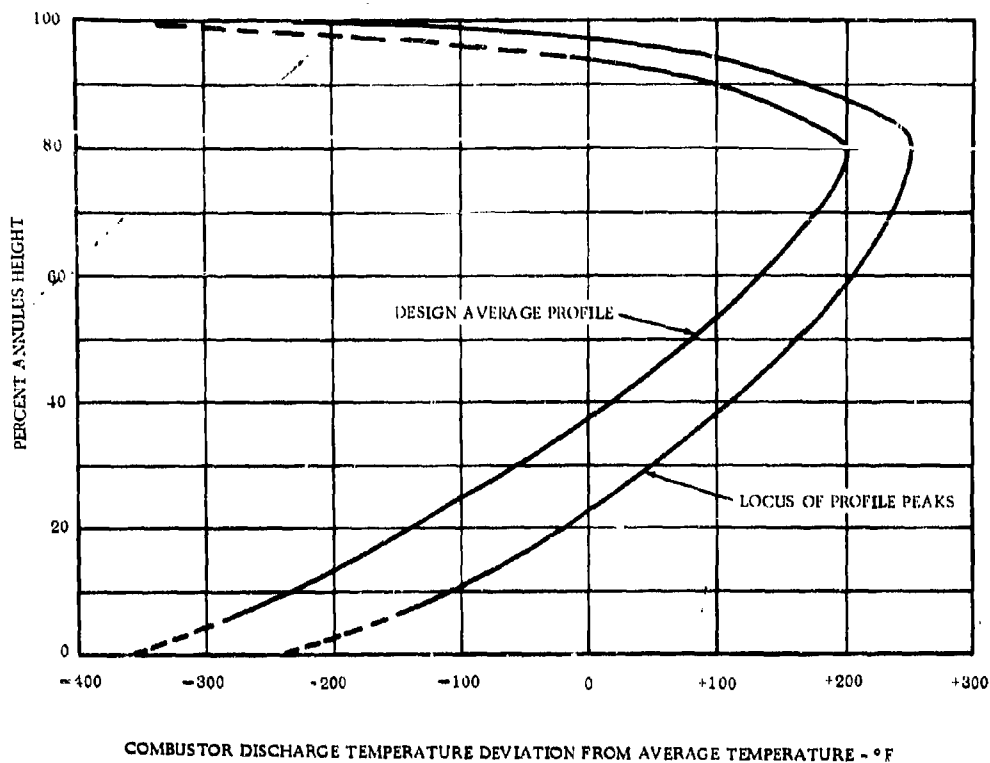


Figure 3-7. COMBUSTOR INLET AND EXIT

CONFIDENTIAL

**CONFIDENTIAL**



**Figure 3-8. COMBUSTOR DISCHARGE TEMPERATURE DEVIATION FROM AVERAGE TEMPERATURE - °F, SLS**

Maximum metal temperature is of prime importance in determining service life during steady-state operation. Local "hot spots" can be drastically detrimental to durability. This reemphasizes the importance of adequate cooling air to protect each square inch of combustor wall. The importance of skin temperature has been the basis of an intensive development effort to achieve a 1500°F maximum skin temperature. This cooling development has been a major element of the annular combustor design and development work at General Electric for the past eight years. Figure 3-13 shows the principal improvements made during this time. As the figure shows, the CJ805 louvered cans have transverse thermal gradients as high as 1200°F. The J93 design reduces this value to 100°F. Recent advancements used in the TF39 and GE4 design further reduce the gradient to 30°F.

The CJ805 cannular combustors, which now have an excellent airline record, have shown that the louver-cooled combustion liners give trouble-free service for 3200 to 3500 hours. Ultimate service time, with replacement of the hottest parts, is estimated to be two to three times this amount. Figure 3-14 shows the CJ805 cans after 3000 hours of operation, including an estimated 4800 thermal cycles.

The high local temperatures and large thermal gradients of the small diameter louvered cans are somewhat compensated by the very low hoop stresses (compared to the large diameter annular combustors), and by the low percentage of total time at maximum temperature conditions (take-off only). However, the GE4 combustor with the following advantages should substantially exceed CJ805 durability.

**CONFIDENTIAL**

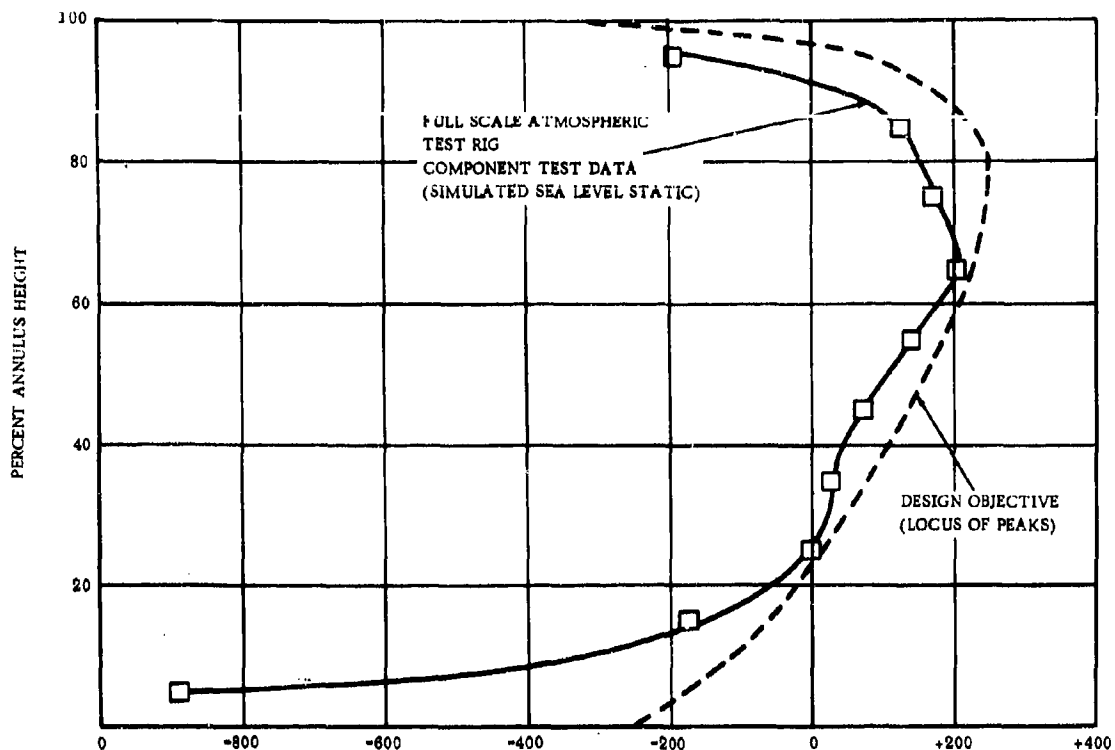


Figure 3-9. COMBUSTOR DISCHARGE TEMPERATURE DEVIATION FROM AVERAGE TEMPERATURE - °F

- Continuous cooling slots that produce low transverse thermal gradients.
- Less complex annular design, with none of the discontinuities of the separate cans and cross-fire tubes, eliminates hot spot problems.
- Lower metal temperatures.

#### 3.2.4 STRESS RUPTURE

The aft sections of the combustor skirts must be designed to resist stress rupture from higher pressure loads at the aft end of the combustor. (Refer to Section 3.3.6 for a more detailed discussion of stresses.) The stress rupture criteria relate the time for metal to rupture with temperature and stress, and are used on high-temperature parts when time-temperature relationships dictate a lower allowable stress than yield strength or other criteria. Figure 3-15 shows the effect of temperature on stress rupture life. It shows that 100°F variation in metal temperature is equivalent to a factor of 10 on theoretical stress rupture life.

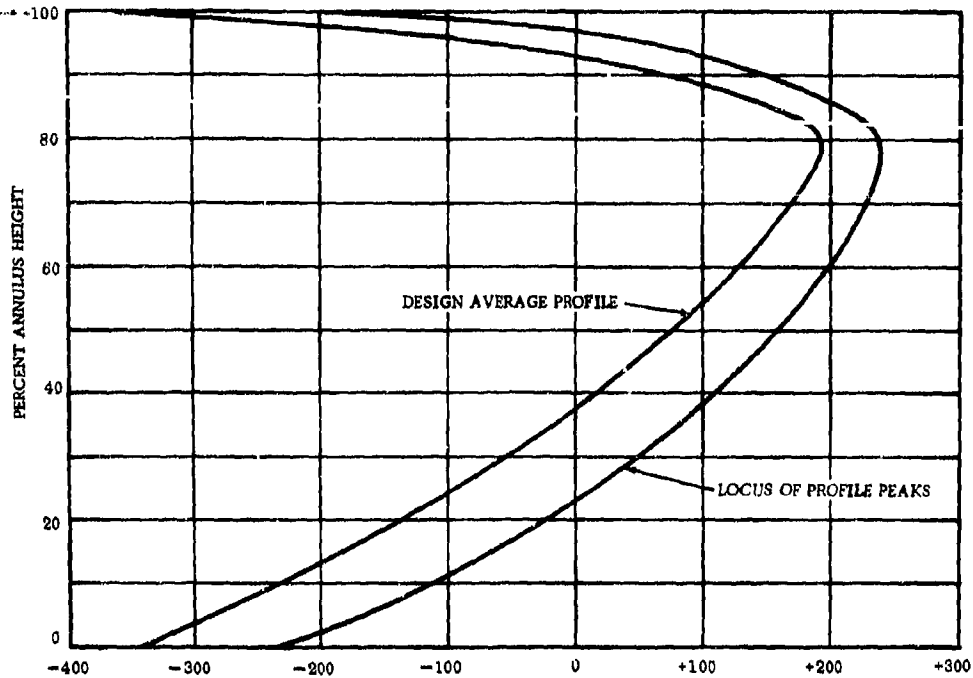


Figure 3-10. COMBUSTOR DISCHARGE TEMPERATURE DEVIATION FROM AVERAGE TEMPERATURE - °F, ACCEL.

The combustor has various combinations of temperatures and stresses imposed upon it, depending on the aircraft flight condition and the engine power setting. Each of the operating conditions of the flight profile consumes stress rupture life at a different rate. The rate of life consumption is higher with increased temperature and stress. For combustor parts that must be designed to resist stress rupture, the supersonic cruise portion of the flight profile consumes 100 times as much theoretical stress rupture life as all of the other conditions combined. This operating mode, however, produces highly reliable thermal conditions with very predictable and stable metal temperatures. This occurs because the relatively low combustor temperature-rise is accompanied by low radiation effects, and by metal temperatures that are largely controlled by the compressor discharge air temperatures.

Stress rupture life will be attained on a reliable basis by holding peak metal temperatures to 1500°F. Metal temperature will be adequately controlled by the cooling air system. See Section 3.3.6 for further details of design for stress rupture resistance.

**CONFIDENTIAL**

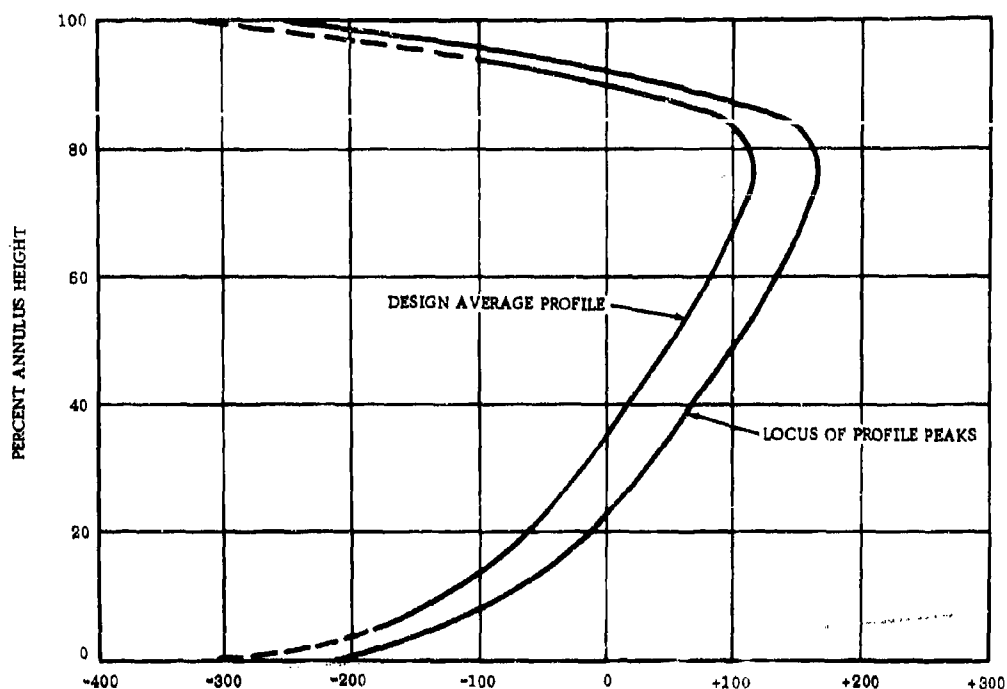


Figure 3-11. COMBUSTOR DISCHARGE TEMPERATURE DEVIATION FROM AVERAGE TEMPERATURE - °F, Mp 2.7, 65K

### 3.2.5 THERMAL STRESS AND LOW-CYCLE FATIGUE

Convection and film cooling protect the metal walls of the combustor from the high-temperature products of combustion. The cooling configuration must be carefully integrated with the mechanical design to avoid thermal stresses that cause low-cycle fatigue. Thermal stresses develop during both steady-state and transient conditions, as one or more regions of the structure attain different temperatures than adjacent regions. The stresses are caused by differential expansion of the metal. High stresses cause the metal to creep or yield. Subsequently, when the parts are cooled, the plastic deformation reverses. Repetition of this cycle causes cracking and eventual failure of the part. Thermal gradients of 1500°F per inch of circumference have been measured on the previously employed louvered liners. The cooling arrangement for the GE4 combustor will limit the circumferential metal temperature gradient to 30°F per inch. The resulting stress in the sheet metal of the combustor is insignificant. The mechanical design must minimize stresses from thermal gradients, both in radial and axial directions. This is done by providing highly efficient heat transfer paths (conduction) in the metal, and by avoiding sharp radii. The addition of braze to resistance (spot) welded joints contributes substantially to both of these objectives. The braze provides additional heat transfer area, and forms structural fillets at the sheet metal overlap joints. The braze application to the J93 design is illustrated in Figure 3-16. The GE4 combustor uses the same principle.

**CONFIDENTIAL**

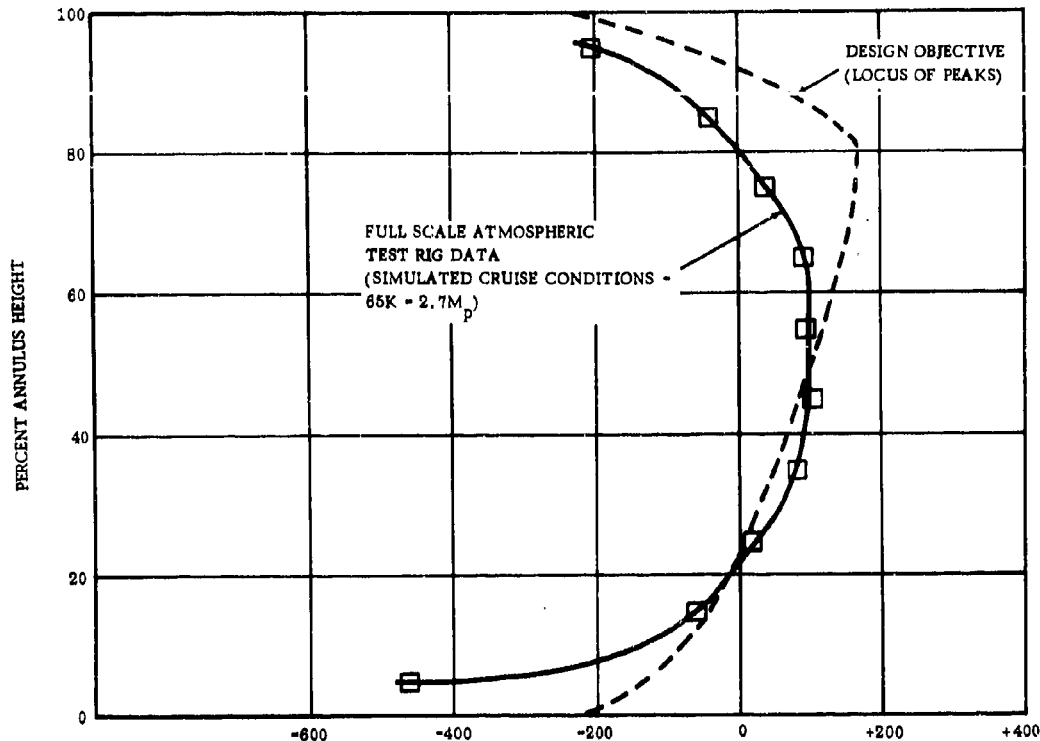


Figure 3-12. COMBUSTOR DISCHARGE TEMPERATURE FROM AVERAGE TEMPERATURE - °F

### 3.2.6 VIBRATORY LOADS AND FATIGUE

The combustor is a relatively large diameter sheet metal structure, and is subjected to vibratory loads. These loads are induced by random pulsations in the inlet air stream, and by the combustion reaction. In an annular combustor, the entire forward structure, or cowl, can vibrate in a radial direction as a ring. Also, portions of the combustor can vibrate locally as panels. Excessive vibratory stresses cause fatigue failures. To stiffen the cowl, the forward end incorporates a structural truss, as described in Section 3.3.1. Extensive General Electric military and commercial experience has shown that structural defects and failures in combustion liners have been largely associated with stress concentrations such as sheared edges, small sheet metal bend radii, and abrupt changes in section. These are avoided in the GE4 design as indicated by:

- Continuous slot cooling construction is employed rather than louver cooling. (Refer to Section 3.3.4.)
- Resistance welded joints are reinforced with braze to reduce the usual stress concentrations. (Refer to Section 3.3.6.)
- All circumferential ring elements are continuous, with no interruptions, and have exact repetitive sequence of structure.



**CONFIDENTIAL**

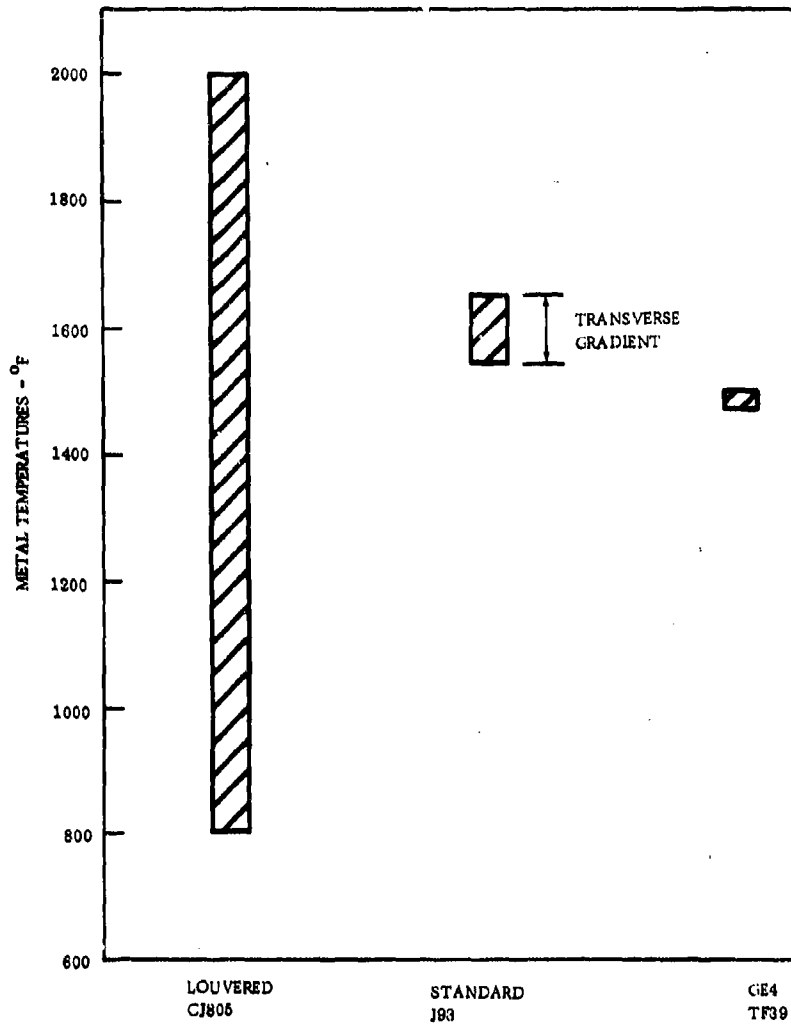
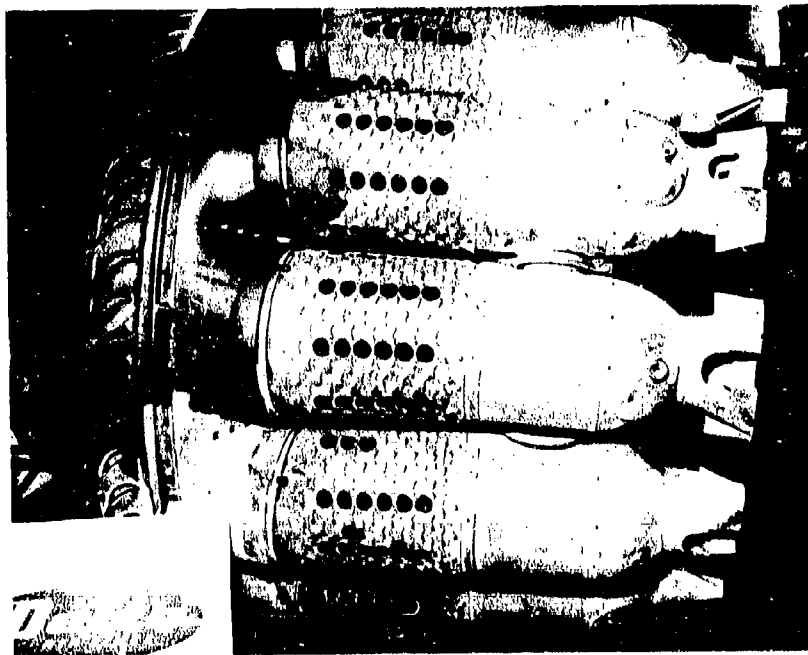
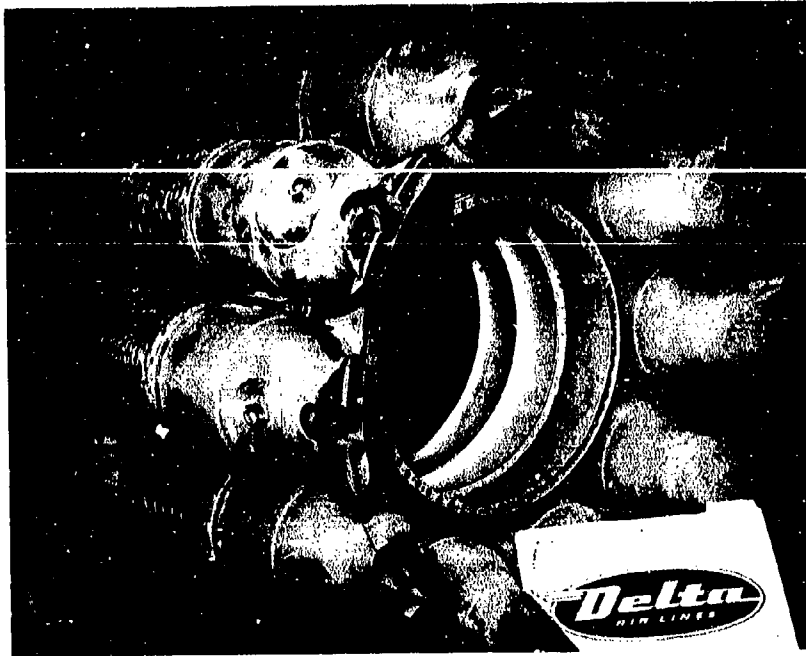


Figure 3-13. PROGRESS IN THERMAL GRADIENT REDUCTION

**CONFIDENTIAL**



- AFTER 3000 HRS ON WING - NO INTERMEDIATE INSPECTION
- ALL LINERS REINSTALLED AFTER TACK WELDING RIVETS
- NEXT INSPECTION AT 4000 HRS

Figure 3-14. CJ805 COMBUSTOR AFTER 3000 HOURS OPERATION

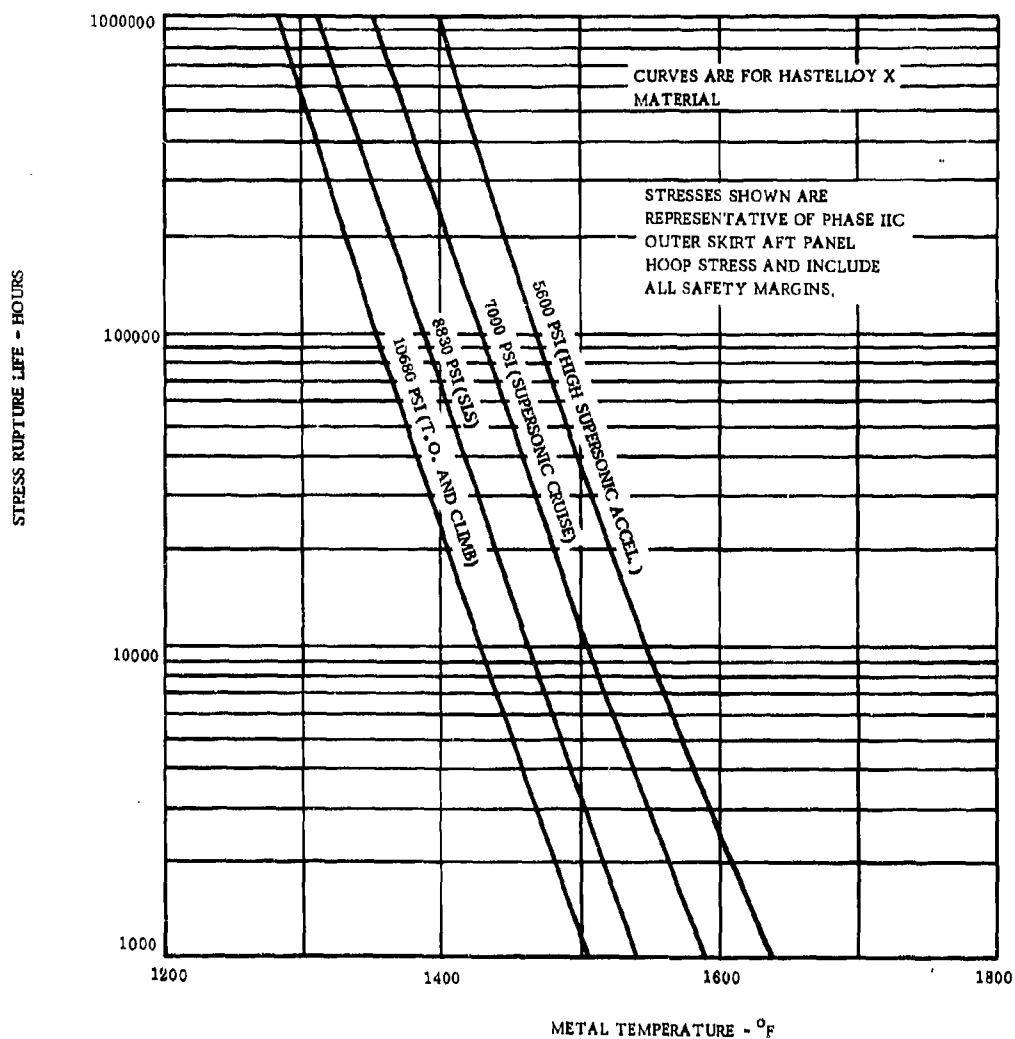


Figure 3-15. EFFECT OF TEMPERATURE ON STRESS RUPTURE LIFE

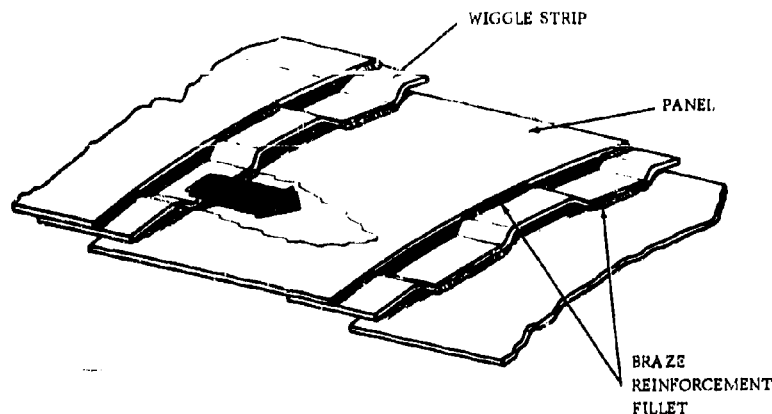


Figure 3-16. BRAZE APPLICATION TO J93 DESIGN

- Sheet metal bend radii have been maintained at a minimum of two times the stock thickness.
- Changes in cross-section are gradual.
- Holes are "eyeletted" for crack resistance, and for additional stiffness of the shell.

The GE4 combustor will be thoroughly vibration tested to determine natural frequency, nodal pattern, and endurance characteristics. Natural frequency and nodal pattern testing has already been performed on the Phase II-C design. Figure 3-17 shows the test set-up. An air siren is used for excitation, as shown.

### 3.2.7 GAS LOADS AND MANEUVER LOADS

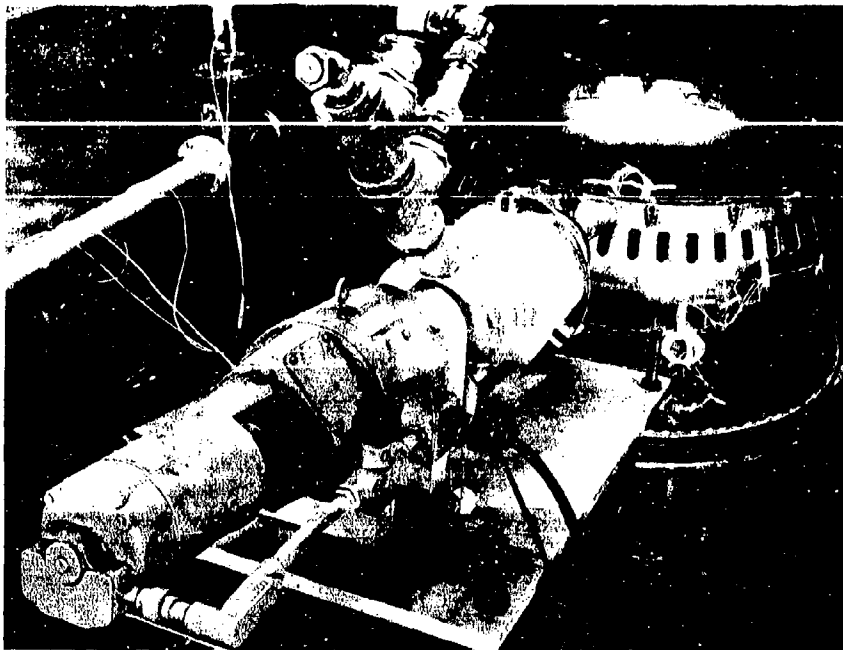
The GE4 combustor and combustor mounting system are designed to withstand gas loads and aircraft maneuver loads. The gas load distribution for the Phase II-C combustor is shown in Figure 3-18. Maximum steady-state gas load occurs at SL-M<sub>p</sub> 0.6 -- Power Setting No. 1. The maximum transient design gas load is 138 percent of the maximum steady-state load. Maximum aircraft maneuver load for the combustor occurs from a six g down load.

### 3.2.8 BUCKLING LOADS

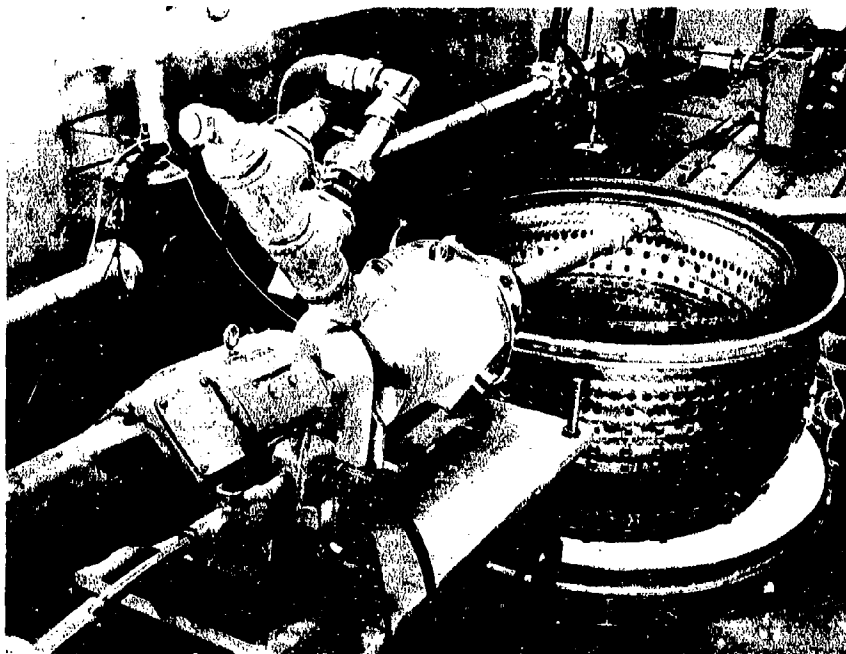
Due to compressive hoop stress resulting from the inward pressure loading, the combustor outer skirt must be designed with sufficient margin in elastic stability to prevent buckling. The applied design procedure provides assurance that the skirt resists buckling in three modes:

- Mode No. 1 Buckling of the entire structure as free ring
- Mode No. 2 Buckling of the panel structure between the relatively stiff cowl and the aft stiffening ring
- Mode No. 3 Individual panel buckling between successive cooling slots.

**CONFIDENTIAL**



View A



View B

Figure 3-17. COMBUSTOR VIBRATION TEST SETUP

3-21

**CONFIDENTIAL**

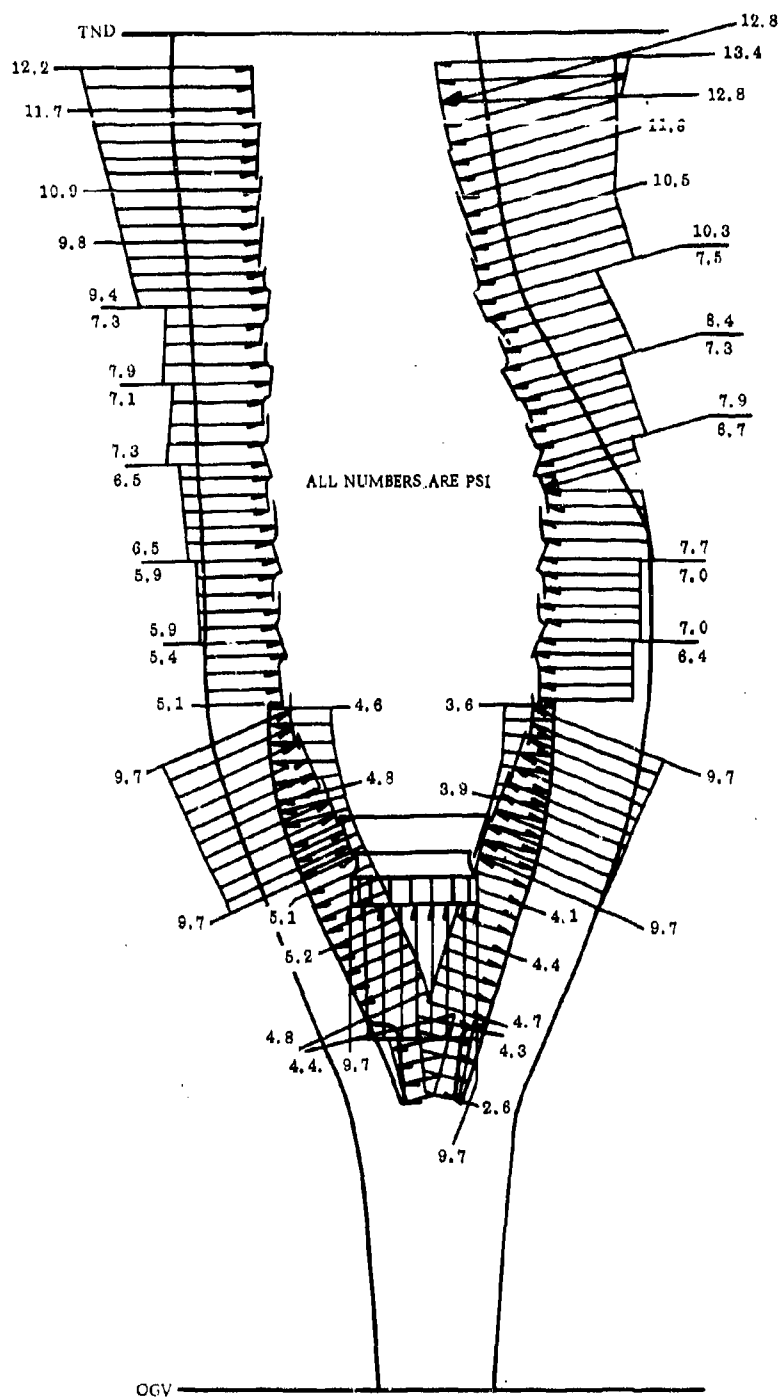


Figure 3-18. GE4 PHASE II-C COMBUSTOR GAS LOADS

## CONFIDENTIAL

Buckling resistance for Mode No. 1, is obtained by use of a stiffening ring at the aft end of the outer skirt, and by support at the forward end of the skirt from the relatively stiff dome and snout. Buckling by Mode No. 2 is prevented by the periodic stiffening effect of the cooling slot structure. Limited length of the individual panels between successive cooling slots prevents Mode No. 3 buckling.

### 3.2.9 RESISTANCE TO SLIDING CONTACT WEAR

All surfaces exposed to wear by sliding contact are out of the high-temperature combustion region. The durability required of these wear surfaces is obtained by maintaining metal temperatures below 1200°F. The relatively low temperature of the wear elements also contributes to elimination of distortion and binding. Mounting pin wear is virtually eliminated by the use of a pin design that prevents vibratory motion, as described in Section 3.3.1. L605 material, with wear-resistant characteristics proved superior in identical applications, is used for other parts exposed to wear. These include nozzle ferrules and turbine inlet junction air seals. Extensive wear tests are planned to prove the required wear resistance, and to identify even more wear-resistant materials and coatings.

### 3.2.10 FUEL NOZZLES

The main fuel nozzles must atomize fuel over a flow range of 60 to 1, with 1200°F (maximum) ambient air flowing over the nozzle stem and tip. The fuel temperature may reach 325°F at the nozzle inlet, and an additional 50°F increase may occur during the flow to the tip.

Present operational engine fuel nozzles are of the dual-orifice type, with either a central flow-divider to serve all of the fuel nozzles, or with an integral flow-divider in each nozzle. Both types have small passages that can clog with fuel gum, and, therefore, neither could provide the required 3500-hour life with high fuel and ambient temperatures. The GE4 fuel nozzle design approach was selected to deal specifically with these problems. The design features a single, variable-area slot. The high actuating forces available from fuel pressure are used to operate the variable-slot mechanism. Thus, positive and accurate area settings are provided. The variable slot maintains high fuel velocity at all fuel flows, and the maximum area is large enough to permit flushing. These characteristics prevent gum formation.

## 3.3 DESIGN DESCRIPTION

### 3.3.1 MOUNTING SYSTEM

Concentricity and axial positioning of the combustor assembly is maintained by a mounting system consisting of 14 radial pins. The pins attach the combustor to the compressor rear frame in double shear. Each pin passes through one of the 14 compressor rear frame struts near the aft end, through the forward end of the combustor, and back into the strut. The J93 engine and subsequent designs have demonstrated the use of the radial pin approach for combustor mounting. Mounting pin wear problems are solved in the GE4 (Phase III) system by an advanced design that eliminates continual vibratory motion. Using the collet principle, the pin grips the combustor snout by means of friction. The design is illustrated in Figure 3-19: the mounting pin is hollow, and is slotted near the mid-point of the pin. The slots run in a direction axial to the pin so the pin will expand when pressure is applied to the inside diameter. Pressure is applied to the inside diameter by engagement of a taper fit between the inside diameter and a solid center pin that screws into the hollow mounting pin. The outside diameter of the hollow mounting pin is thus expanded into the inside diameter of the bushing in the snout. The tightness of the fit can be controlled by the torque applied to the center pin. The friction grip prevents motion between the pin

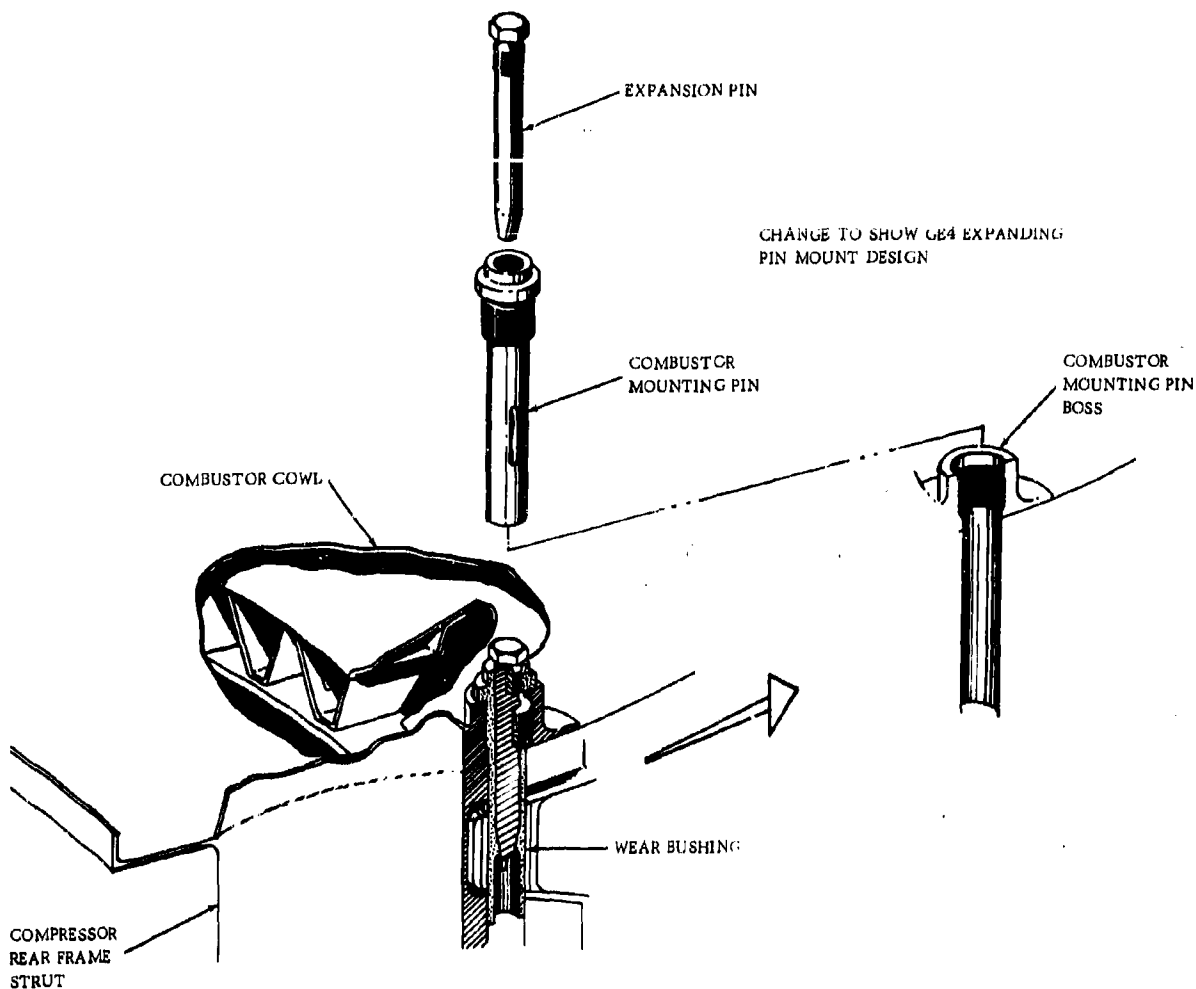


Figure 3-19. GE4 PHASE III COMBUSTOR MOUNTING SYSTEM

and bushing from relatively low vibratory forces (high cycle), but will permit slippage from thermal expansion forces (low cycle). The use of hard, wear-resistant materials, and exposure to only very low frequency thermal cycle motion will overcome previous wear problems of combustor mounting pins. Extensive low cycle endurance testing of the design is planned to confirm durability. To correct possible wear with long service, replaceable wear bushings in the mountings are provided. This permits low-cost replacement of the mounting pins and bushings to the extent necessary during sectionalized maintenance.

The mounting system, in addition to solving the pin wear problem, has advantages as follows:

- Combustor support loads are transmitted directly into basic structural members (struts) of the compressor rear frame rather than to sheet metal casings.
- The combustor is supported from the forward end of the cowl where the truss and other features combine to form the most favorable structure, and where metal temperatures are lowest.



- The mounting structure is buried in the frame strut airfoils to maintain clean aerodynamic flowpaths in the diffuser.

The mounting system is designed to support gas loads and maneuver loads as stated in Section 3.2.7.

### 3.3.2 COWL STIFFENING STRUCTURE

Vibration resistance and high structural integrity of the forward portion of the cowl is obtained by incorporation of a truss in the diffuser section of the center flow passage. The J93 engine experience indicated the need for, and effectiveness of, a stiff truss structure for stabilization of the inner and outer cowl surfaces to resist the flutter forces in the high-velocity compressor discharge air stream. The GE4 truss is integrated with diffuser partitions arranged in an angular fashion. The forward edge of the partitions may be seen in Figure 3-19, and in the photograph of the Phase II-C combustor cowl shown in Figure 3-20. The truss provides radial stiffness, and solidly interconnects the inner and outer cowl. To control panel vibration of the cowls, one circumferential stiffener is used on the outer cowl, and two are used on the inner cowl. Stock thickness, used on the inner and outer cowls, is 0.032 to 0.036 inch.

### 3.3.3 AFT SEALS

Leakage of compressor discharge air into the flow path, at the junction of the combustor outlet and turbine inlet, is positively controlled by the use of sliding seals. The combustor aft seals are designed to accommodate thermal expansion, and out-of-position tolerance in both radial and axial directions. This prevents distortion and damage to parts. Wear elements with surfaces subject to relative motion are attached with AN rivets and are completely replaceable. (Refer to Section 3.3.9.) L605 material is used for high wear resistance. The stock thickness is 0.036 to 0.040 inch. The seal arrangement is shown in Figure 3-21.

### 3.3.4 COOLING SLOT CONSTRUCTION

Both structural and cooling requirements of the GE4 combustor are satisfied by using a three-element cooling slot design as shown in Figure 3-22. This design was evolved from the J93 combustor. Early General Electric experience, in 1958, with J93 annular combustors that used sheared louvers for film cooling, revealed severe temperature gradients in areas between the louvers. Because louvers have a finite circumferential length, the cooling film is interrupted and produces local uncooled areas. The most effective louver pattern never approaches a continuous circumferential cooling film. A louver density sufficient to provide uniform cooling results in inadequate fatigue strength due to lack of cross-section (cracks propagate between the stress concentrations formed by the corners of adjacent louvers). Conversely, reducing the number of louvers produces a part with adequate cross-section but with strength reduced by excessive metal temperatures. Consequently, when louvers are used, the design becomes a compromise as metal temperature and fatigue strength are balanced. This compromise may be accepted when the combustor is small in diameter with high inherent stiffness, as is the case with the cannular or small annular combustors of the J85, T58, and T64 type engines. For diameters corresponding to the GE4 dimensions, the available fatigue strength becomes an acute problem due to panel and ring vibration.

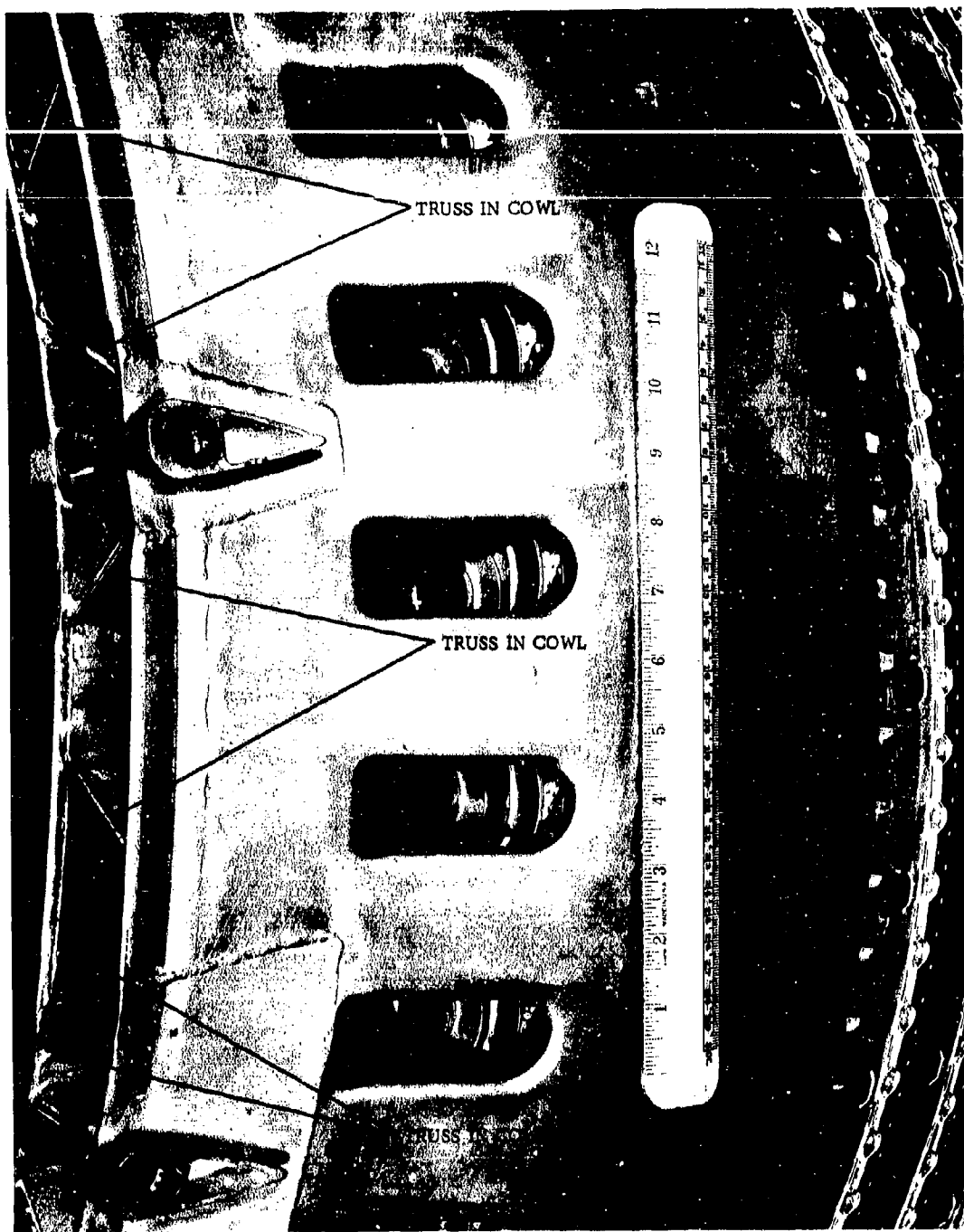


Figure 3-20. GE4 PHASE II-C COMBUSTOR COWL

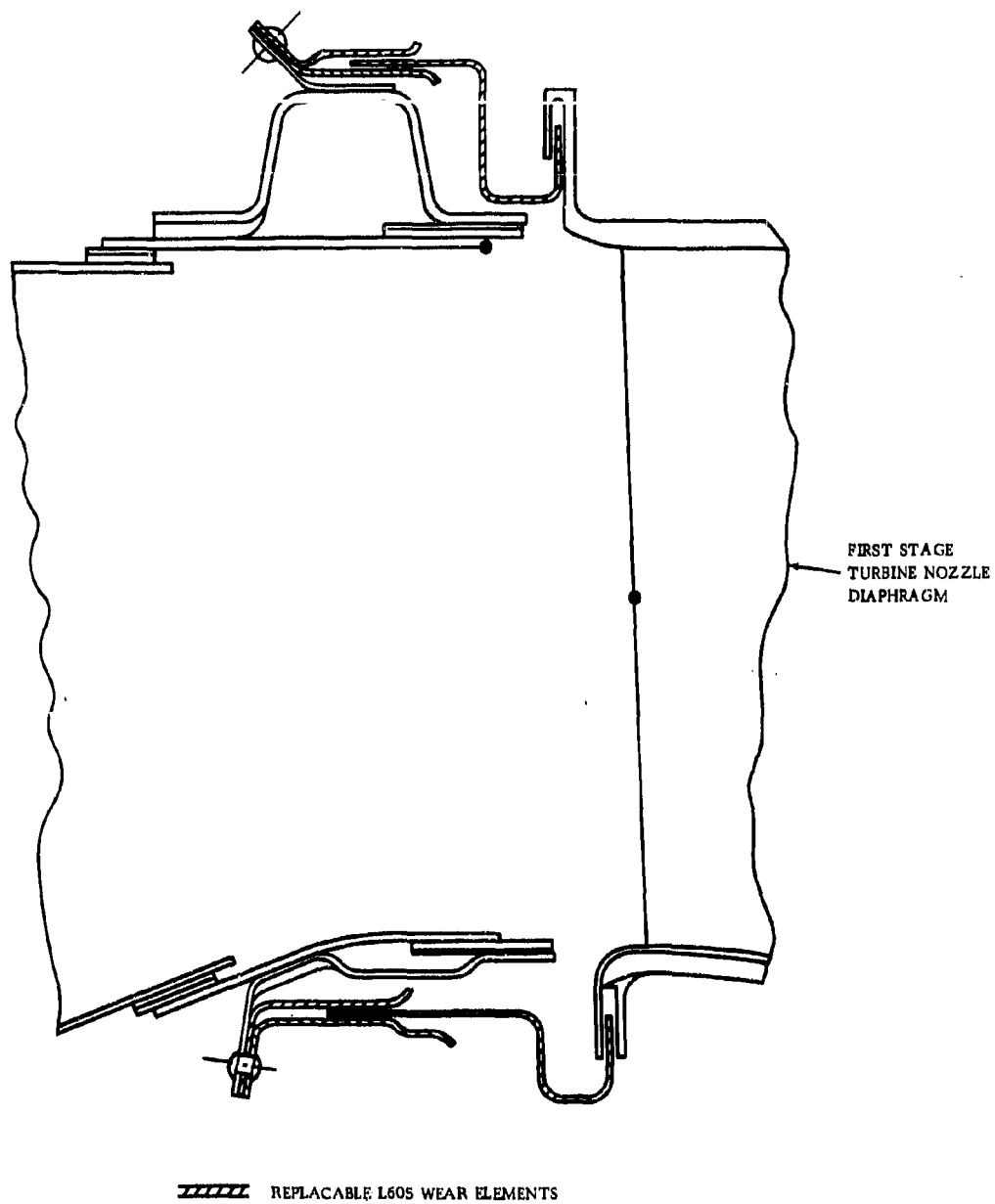


Figure 3-21. GE4 COMBUSTOR AFT SEAL ARRANGEMENT

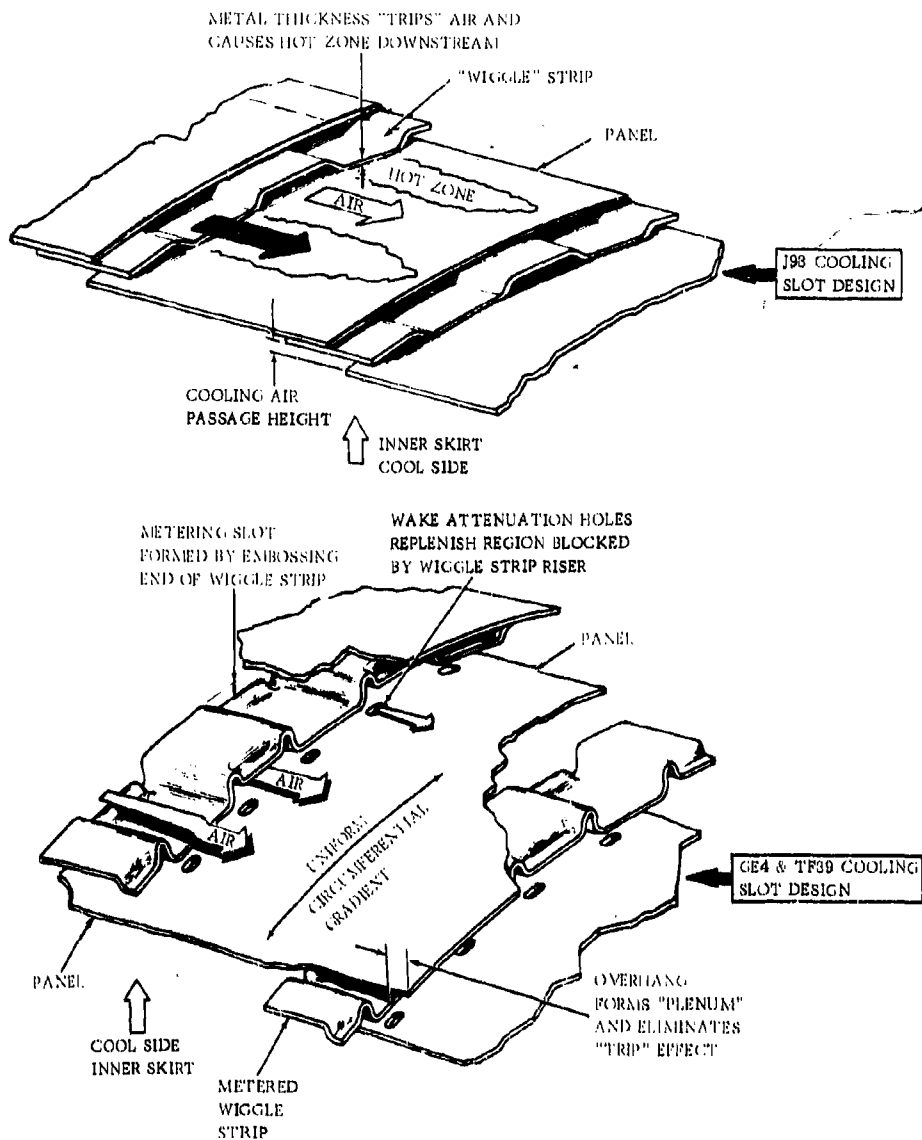


Figure 3-22. GE4 COMBUSTOR COOLING SLOT DESIGN

## CONFIDENTIAL

The three-element cooling slot design was developed and proved for the severe temperature requirements of the J93 combustor, to eliminate the compromise between cooling and strength. This design provides independent control of cooling and structural strength, and produces a continuous uninterrupted circumferential cooling film. Cooling air flow is controlled by the wiggle strip metering height; variation of this height has no effect on the structural band strength because structural section and stress concentrations are not affected. The cooling slot design approach has been satisfactorily proved on J93 combustors operating at compressor discharge temperatures up to 1125°F, and has been subsequently applied to all advanced General Electric engine combustors.

Further cooling development for the GE4 resulted in the panel overlap and metered-slot (with transition wake attenuation) hole is shown in Figure 3-22. This arrangement is used on the TF39 engine. The J93 design shows some hot streaking aft of the wiggle strip edge where the wiggle strip is attached to the hot side of the wall being cooled. The sudden expansion caused by the metal thickness ledge "trips" the flow and renders the cooling film less effective at this location. This is illustrated in Figure 3-22. The problem was eliminated in the GE4 and TF39 design by extending the hot side panel to overhang the downstream end of the wiggle strip. The overhang forms a plenum in which the cooling flow is diffused and re-established as a film. A further change in the GE4 and TF39 design meters the cooling flow for most effective use and distribution. This is done by alternately embossing the leading and trailing edges of the wiggle strip convolutions to form metering slots which locally limit the cooling-air flow-area. Testing of the cooling slot showed that blockage of the wiggle strip risers, or transitions, caused minor hot streaks in the wake of the risers. These hot streaks were eliminated by addition of wake attenuation holes. All of these features are shown in Figure 3-22.

Figure 3-23 shows TF39 calculated and measured metal temperatures for various axial positions along a panel near the aft end of the outer skirt. Figure 3-24 shows corresponding predicted temperatures for the GE4 at several operating conditions.

Figure 3-25 is a schematic drawing showing approximate cooling air distribution in the GE4 Phase II-C combustor, based on the percentage of the total airflow at any operating condition.

The cooling slot design provides effective skin temperature control by maintaining the maximum metal temperature at 1500°F, and the circumferential thermal gradients less than 30°F. This basic approach will meet the required 12,000-hour durability for the GE4 combustor. Actual environmental testing of the proposed design has been in process in the TF39 engine since late 1965, and in the GE4, Phase II-C, engine since July 1966. Careful evaluation and analytical work is being done to develop maximum tolerance to realistic engine operation variables such as:

- Dimensional tolerance extremes
- Variations in uniformity of diffuser exit flow (Refer to Section 3.2.1.) (The cooling slot air-flow is relatively independent of ram effects and therefore not sensitive to diffuser exit velocity variations)
- Possible warping and distortion of cooling slots
- Oxidation or soot deposits and their effect on local heat transfer coefficients.

Thermal cycle tests are being run in a flame tunnel on combustor wall designs for continued development of long-life combustors. A typical eight-inch diameter liner specimen is shown in Figure 3-26. A general view of the test rig is shown in Figure 3-27. To date, 379 test hours have been completed. This work is complemented by the application of advanced thermal stress analysis and thermal fatigue prediction techniques. These techniques are similar to those successfully applied to General Electric's turbine blade design. The high accuracy of the thermal fatigue analysis was substantiated by thermal cyclic endurance tests.

CONFIDENTIAL

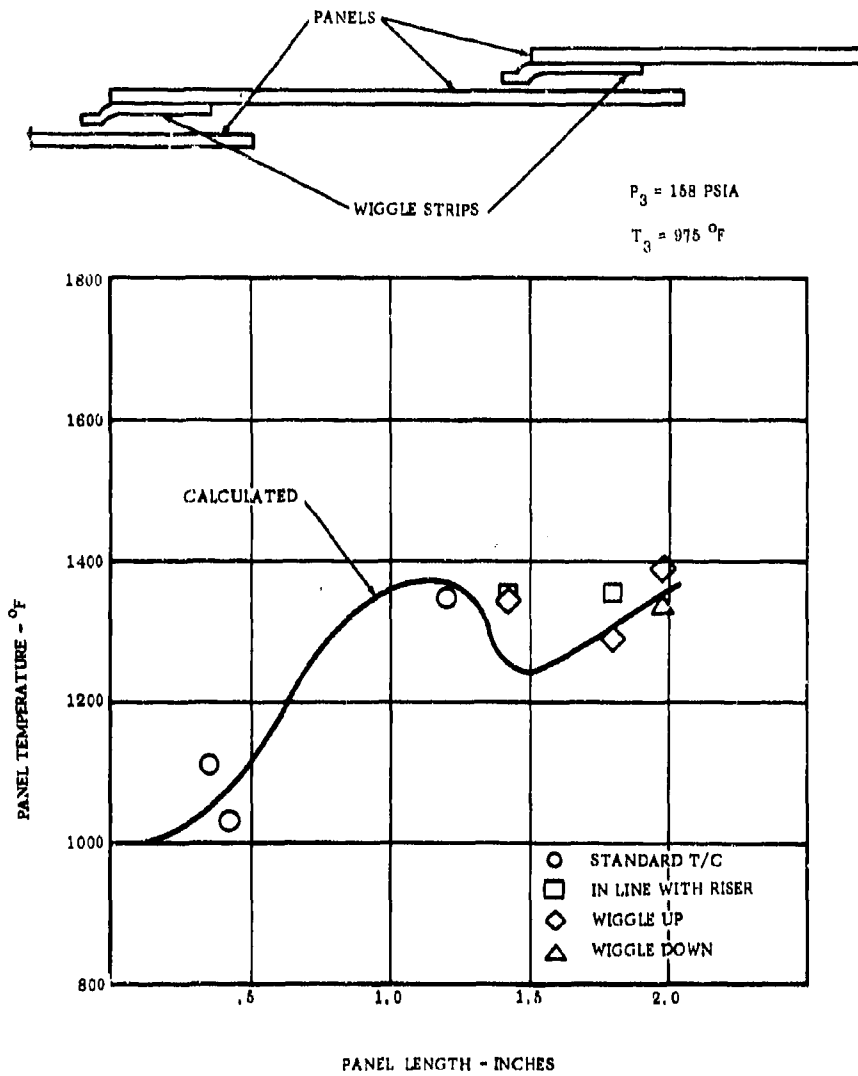


Figure 3-23. TF39 METAL TEMPERATURES

CONFIDENTIAL

**CONFIDENTIAL**

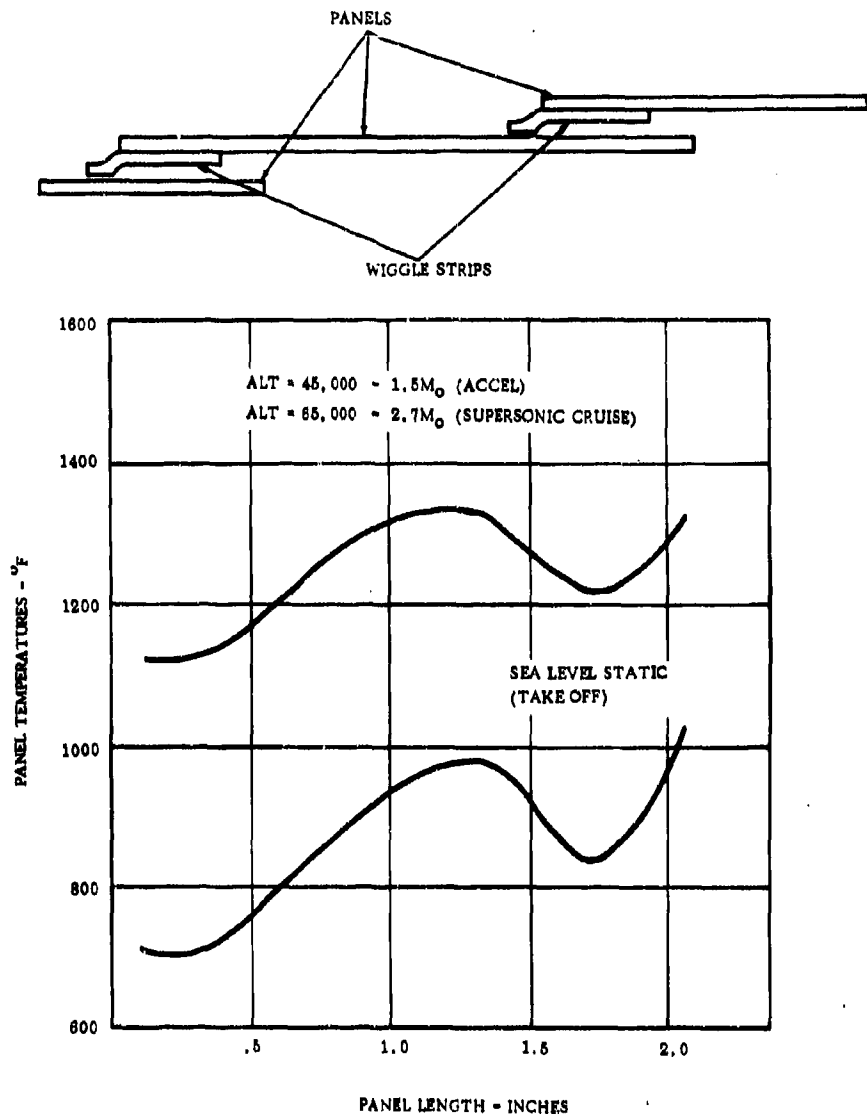
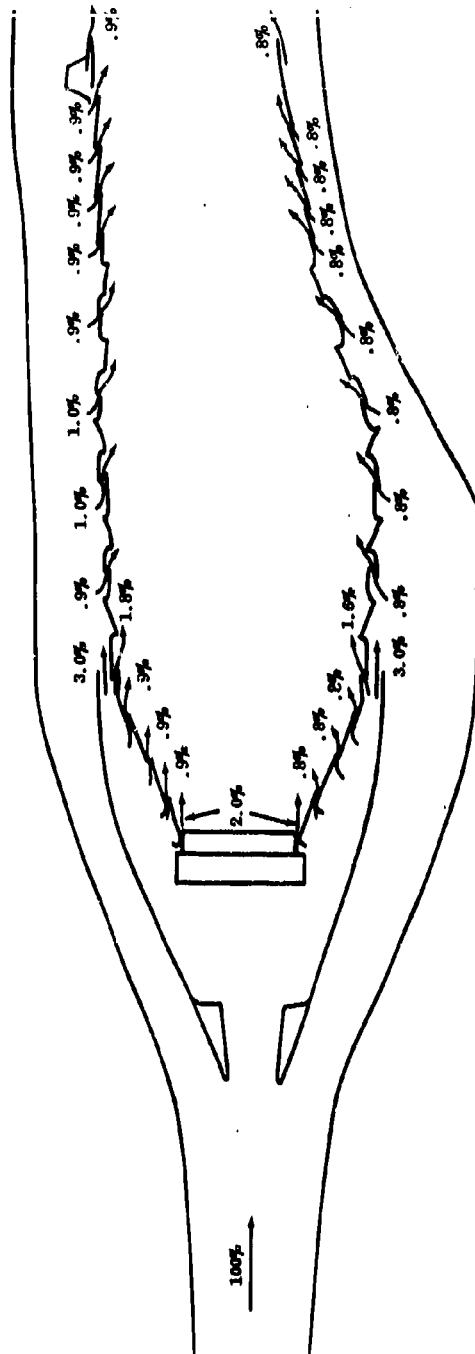


Figure 3-24. GE4 COMBUSTOR PREDICTED METAL TEMPERATURES

**CONFIDENTIAL**

CONFIDENTIAL



COOLING FLOW PERCENTAGES ARE ESSENTIALLY THE SAME FOR TAKEOFF, ACCEL., & SUPERSONIC CRUISE

Figure 3-25. GE4 PHASE - C COMBUSTOR - COOLING AIR DISTRIBUTION

CONFIDENTIAL





Figure 3-26. TYPICAL LINER SPECIMEN



Figure 3-27. THERMAL CYCLE ENDURANCE TEST RIG

## CONFIDENTIAL

### 3.3.5 DOME CONSTRUCTION

The combustor dome incorporates 42 swirl cups (one for each of 42 fuel nozzles). Each swirl cup utilizes 12 separate swirl vanes, tangentially arranged about the circular cup periphery. This design provides a relatively clean aerodynamic path, and imparts a high spin to the air flowing into the swirl cup. Stock thickness of the vanes is 0.028 to 0.032 inch. The vanes are connected to end plates perpendicular to the axis of the cup. Structural integrity is attained by fitting the vanes into slots in the end plates, tack welding, and brazing, in sequence. The forward plate also supports the fuel nozzle ferrule. Adequate radial travel of the ferrule, relative to the forward plate, is provided to accommodate dimensional tolerance stack-up and differential thermal expansion between the fuel nozzle and the dome. Axial positioning of the ferrule is such that under the most adverse stack-up and differential thermal expansion conditions, a minimum of 0.125 inch axial engagement of the fuel nozzle and ferrule will be maintained.

The aft swirl cup is welded to a transition piece that aerodynamically fairs the round swirl cup into a corresponding annular portion of the dome. The Phase II-C combustor swirl cups are shown in Figure 3-28. As the picture shows, the Phase II-C combustor has oval swirl cups (in contrast to the Phase III round cups) because of the closer spacing in the 48 cup design. The annular portion of the dome is constructed of panels and wiggle strip cooling slots like the combustor skirt construction (Refer to Section 3.3.6.).

### 3.3.6 SKIRT CONSTRUCTION

The combustor skirts incorporate the improved cooling liner design, and are composed of a series of circumferential bands and corrugated wiggle strips joined by the combination of resistance weld and braze. The bands and strips are first joined by resistance welding. High-temperature braze is sequentially added to overcome the susceptibility of resistance welded structures to fatigue cracking. This susceptibility is caused by stress concentrations at the termination of the weld. The problem is more acute with combustors because of thermal cycles and gas induced vibration. General Electric's experience has shown that the high-temperature braze reinforcement eliminates this problem. The braze alloy flows around the spot-weld and provides three major functions:

- It repairs internal weld defects or cracks that are not discernable by available inspection techniques.
- It removes the stress concentrations that would otherwise exist at the outer periphery of the spot-weld.
- It increases the area of attachment between adjacent parts to make a stronger and larger heat flow path, thereby reducing thermal gradients.

The J93 engine experience has proved that the spot weld and braze combination is a consistently satisfactory and reliable design. The introduction of braze reinforcement during the J93 development increased crack-free life by a factor of 30.

The combustor skirts are protected from the high convective and radiant heat flux generated from the combustion reaction by continuous circumferential film cooling, and further augmented by coolant-side convective heat transfer. Details of the cooling design are included in Section 3.3.4. The circumferential cooling slots are constructed as previously shown in Figure 3-22.

**CONFIDENTIAL**

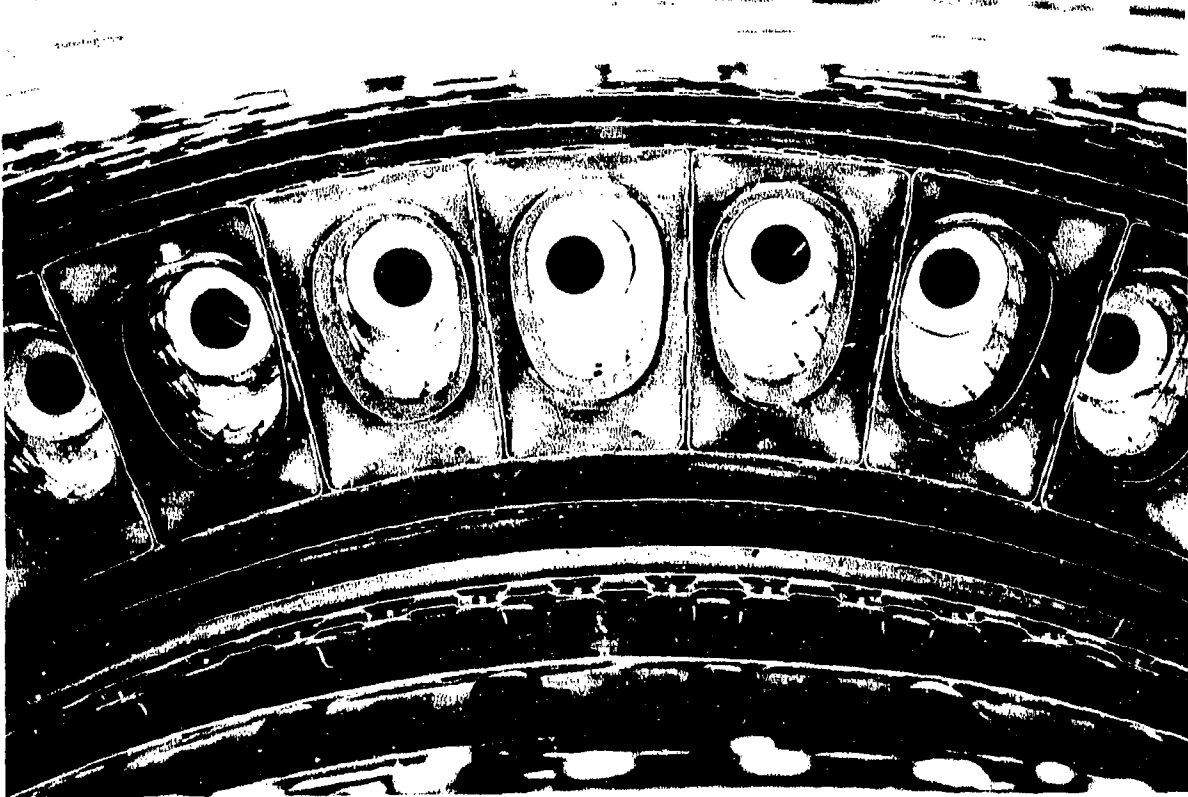


Figure 3-28. GE4 PHASE II-C COMBUSTOR SWIRL CUPS

**CONFIDENTIAL**

Stock thicknesses of the panels on the aft portion of the skirts are established by the requirement to resist stress rupture. In the forward portion of the skirts, the pressure load is low and stock sizes are based on requirements for elastic stability and fatigue resistance. Figure 3-18 shows the pressure-load distribution around the Phase II-C combustor. Table 3-1 shows the method used to determine the stress rupture durability of a panel for the range of temperatures and loads imposed on it by the various operating conditions of the flight profile. The numbers are based on the Phase II-C design. The stresses shown are based on minimum stock thickness permitted, and are increased 25 percent to account for minimum material properties and by 25 percent to provide an additional safety factor. Plots of the required stock thickness to resist stress rupture at various axial locations along the inner and outer skirts are shown in Figure 3-29. This figure also shows the actual stock thickness used in the design.

Buckling of the outer skirt, as discussed in Section 3.2.8, is prevented by the addition of a stiffener at the aft end of the outer skirt, and by the relatively short panel lengths between cooling slots. Although the cooling slot arrangement is designed for best cooling, it also provides a structural advantage for the outer skirt in that the bending moment of inertia of the shell is increased by virtue of the radial separation of the structural bands. This design results in a structure that has increased buckling resistance. The aft stiffener is constructed so that cooling air passes under the stiffener to maintain convective cooling on the liner skin, and, thus to hold temperatures and gradients at design values in this region.

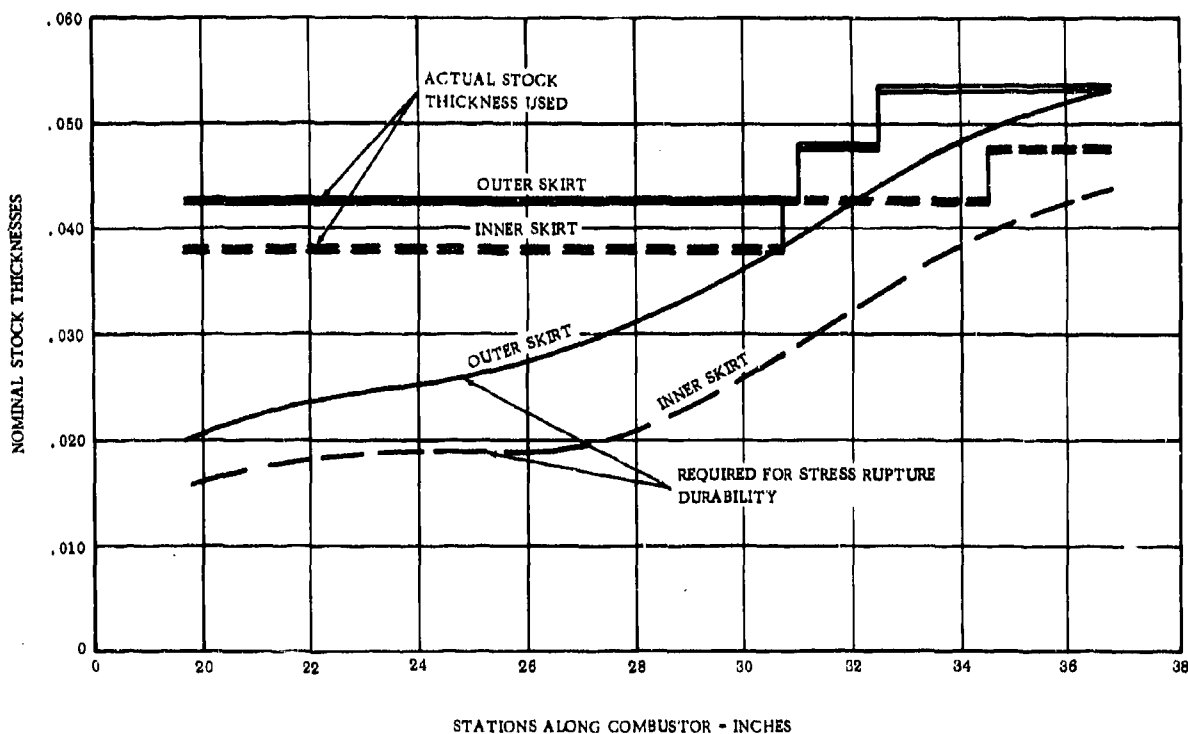


Figure 3-29. GE4 PHASE II-C COMBUSTOR LINER REQUIRED STOCK THICKNESS

# CONFIDENTIAL

Table 3-1  
Method Used to Determine The Stress Rupture  
Durability of Combustor Wall Panels  
(Phase II-C Outer Skirt Aft Panel)

Operating Condition	Power Setting	% Time	Atmospheric Conditions	ΔP across Liner - psi	Liner Metal Temp - °F	Hours	Min Stock Thickness 0.050 (Nominal 0.053)		
							Hoop Stress with deviation & SF (1.25 x 1.25 = 1.562)	Hours to Rupture	% Life Used
Run Up	1	0.5	↑ Used Standard Day Data Only ↓	10.1	1270	60	8,830	1,000,000+	0
T/O & Climb	1	1.5		12.2	1297	180	10,680	500,000	0.036
Min Climb	4	7.6		10.5	1290	912	9,180	1,000,000	0.091
Max Augmentor Climb	1	7.1		7.2	1269	852	6,300	1,000,000+	0
Low S.S. Accel	1	2.4		5.0	1303	288	4,375	1,000,000+	0
High S.S. Accel	1	1.4		6.4	1396	168	5,600	800,000	0.021
Max Cruise	2.5	17.0		7.9	1500	2040	6,915	12,000	17.00
Normal Cruise	4	40.0		8.0	1500	4800	7,000	11,000	43.63
High M <sub>p</sub> Descent	12.4	5.4		8.9	1178	648	7,790	1,000,000+	0
Low M <sub>p</sub> Descent	12.4	3.4		5.0	458	408	4,375	1,000,000+	0
Loiter	9	4.7		7.0	740	564	6,125	1,000,000+	0
Landing	12.4	2.8		5.9	559	336	5,165	1,000,000+	0
Ground Idle & Taxi	12.4	5.7		4.1	884	684	3,475	1,000,000+	0
Reverse Thrust	5	0.4		10.7	1276	48	9,360	1,000,000+	0
Diversion	8	0.1		6.3	847	12	5,515	1,000,000+	0
TOTALS		100.0				12,000			60.778

Table 3-2 shows outer skirt buckling calculation results with the TF39 calculation and test results for comparison. Proof tests will be made to confirm the calculations. Figure 3-30 shows the TF39 combustor in the buckling test rig, and the same combustor after buckling test to failure.

Air entry holes in the primary combustion zone are shown in Figure 3-31. The aft lip of the holes is embossed in the direction of the cool side of the combustor wall rather than the hot side. This design eliminates problems of thimble-hole overtemperature, oxidation, and burning in the region of the aft lip. The configuration has been successfully demonstrated in the J93 and subsequent combustors.

### 3.3.7 FUEL NOZZLES

The fuel nozzle is flange-mounted on the compressor rear frame. The nozzle spray tip enters the combustor dome through a floating ferrule. The ferrule accommodates mechanical stack-up and differential thermal expansion. (Refer to Section 3.3.5.) An external photo of a fuel nozzle in Figure 3-32 shows the long, thin cross-section of the stem. The stem provides the required flexural characteristics without detrimental airflow wakes. An oval-shaped sheet metal cover on the fuel nozzle stem serves as an aerodynamic cover over the installation port in the combustor cowl.

The GE4 fuel nozzle with a variable-slot area (Section 3.2.10) has important advantages when compared to current designs as described below:

- Safety — conservative bellows design and fail-safe features, such as welded closures.
- Component Life — lower pressure-drop of variable-area design reduces erosion and leakage possibility.
- Reliability — actuation forces five times greater than current designs ensure positive valve operation in hot fuel environments.
- Variable-slot Area — slots open to large areas for flushing, and high velocity at all flows prevents gum build-up

### 3.3.8 MATERIAL

Two proven high-temperature alloys, Hastelloy X and L605, are used in the combustion liner. All parts exposed to high temperature are fabricated with Hastelloy X. Hastelloy X has demonstrated excellent oxidation resistance in J79 and J93 applications. This material can sustain temperatures in excess of 2200°F before actual burnout is encountered. It combines the most favorable characteristics for combustion system application: excellent oxidation resistance, high ductility, high temperature strength, formability, and weldability. Oxidation tests on Hastelloy X in a dynamic cyclic flame tunnel, are now in progress at General Electric. Data obtained at this time shows a metal loss of 0.0002 to 0.0004 inch after 100 hours at 2000°F. Depth of corrosion was 0.0012 to 0.0019 inch. Hastelloy X exhibits a minimum of embrittlement (overaging) after long exposure to high-temperature environment, and has been extensively proved in J79, CJ805, J93, and J97 combustors and other hot section applications. L605, because of its demonstrated qualities of wear resistance, is used in combustor parts exposed to mechanical wear. The use of these materials for their specific applications has been substantiated by many hours of military and commercial service. Both alloys can be readily repaired by welding.

CONFIDENTIAL

Table 3-2  
Buckling Calculation and Test Results

Potential Buckling Mode

Failure of Aft Stiffening Ring on Outer Skirt (Prevents Buckling of Entire Structure as free Ring)

Buckling of the Panel Structure Between the Relatively Stiff Cowl and Aft Stiffening Ring

Individual Panel Buckling Between Successive Cooling Slots

Comparison Criteria	Moment of Inertia of Ring Cross-section	Axial Average of Pressure Load	Pressure Load on Most Critical Panel
Theoretical Requirements	GE4 TF39	11.85 psi 15.80 psi	11.68 psi 21.0 psi
Theoretical Capacity	GE4 TF39	24.2 psi 30.0 psi	23.9 psi 60.0 psi
Theoretical Capacity Relative to Requirements	GE4 TF39	204% 190%	205% 286%
Test Capacity	TF39	30.7	(TEST RESULTS CORRECTED TO OPERATING TEMPERATURE)
Test Capacity Relative to Requirements	TF39	194% +	194%

CONFIDENTIAL



**CONFIDENTIAL**

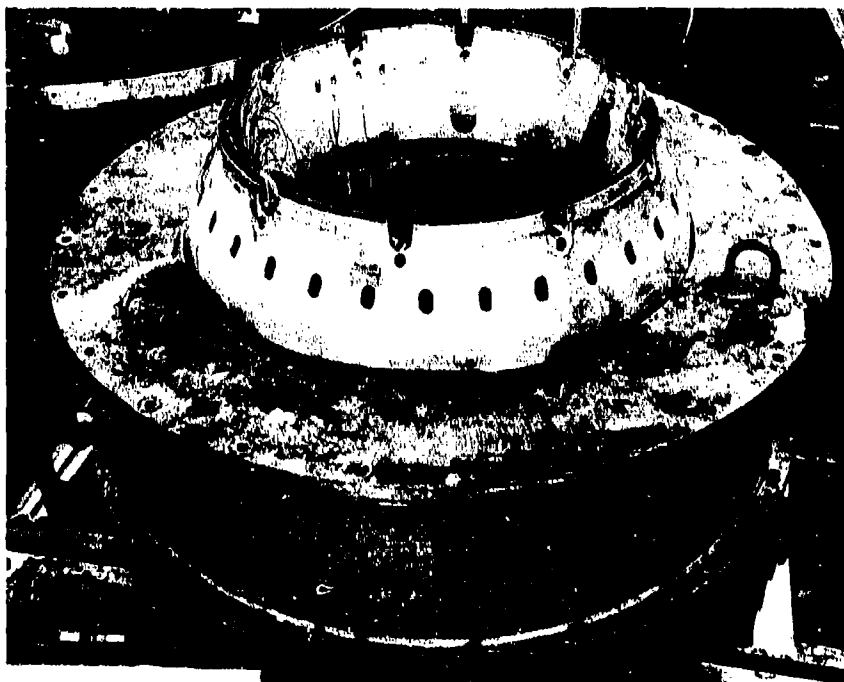
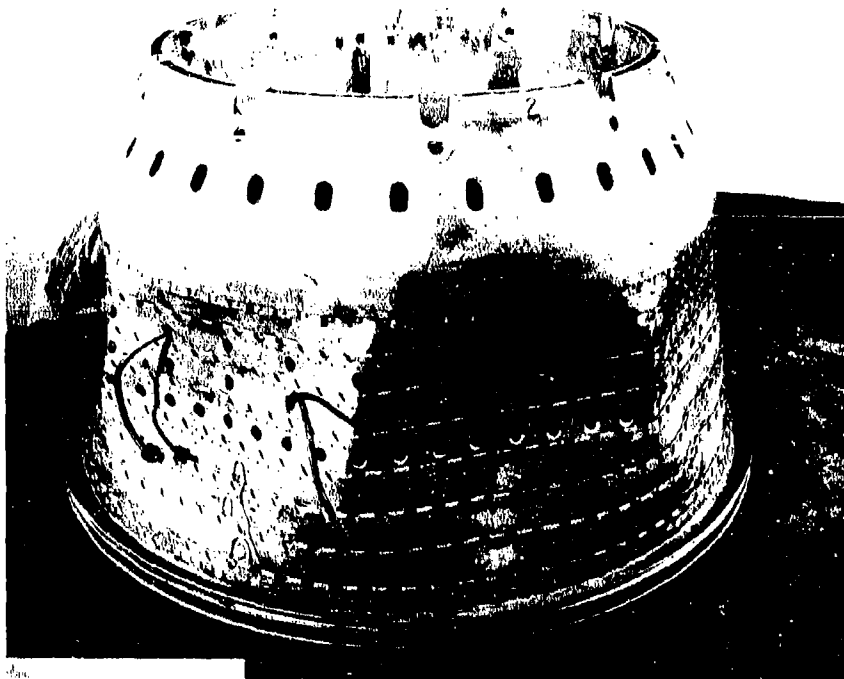


Figure 3-30. TF39 COMBUSTOR IN TEST RIG

3-41

**CONFIDENTIAL**

K

**CONFIDENTIAL**

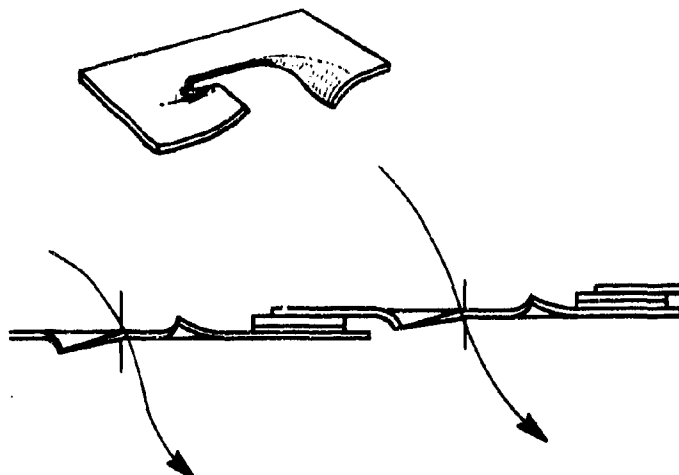


Figure 3-31. AIR ENTRY HOLES IN PRIMARY COMBUSTION ZONE

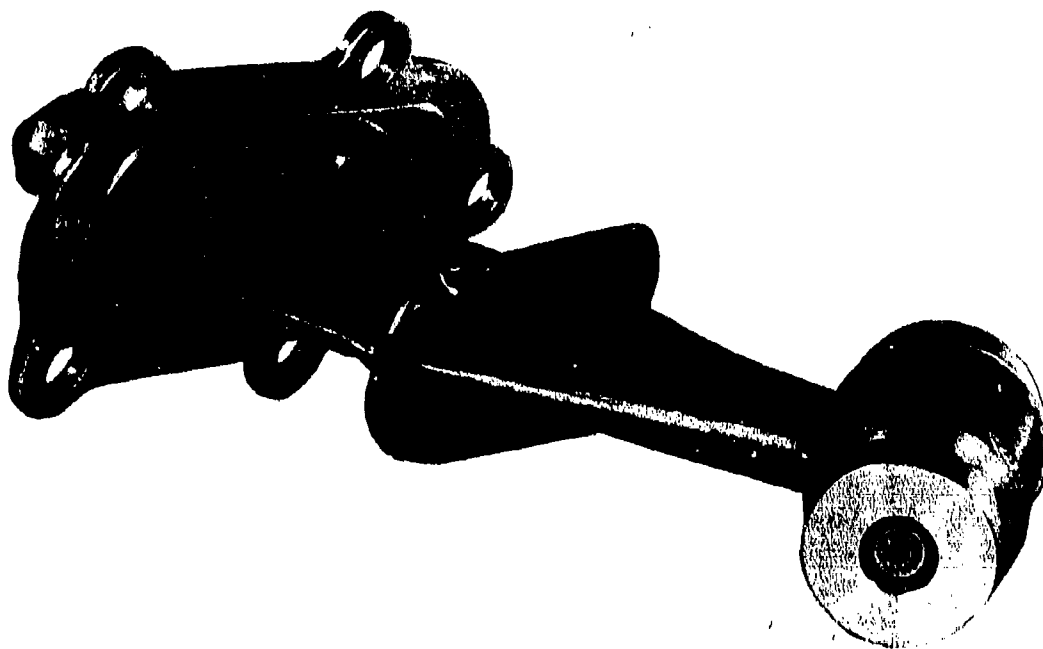


Figure 3-32. GE4 FUEL NOZZLE

3-42

**CONFIDENTIAL**

K

### 3.2.9 MAINTAINABILITY

The combustion liner is a riveted assembly composed of four sub-components: cowl, dome, inner skirt, and outer skirt, like previous General Electric designs on the T58, T64, J85, J93, and J97 engines. Only two rows of rivets are used in the assembly of these parts. The rivets facilitate disassembly for repair and/or replacement of interchangeable, individual sub-components without compromise to the structural reliability of the system. Rivets are located in the cooling air stream to prevent the possibility of rivet failure because of oxidation or overtemperature. (Refer to Section 3.3.10.) Figure 3-33 illustrates the buildup and assembly sequence. The relative ease with which the parts can be assembled and disassembled has been extensively demonstrated in the previous J93 development program. Skirts and domes were frequently interchanged and revised for experimental configuration changes, effecting substantial savings in labor and hardware costs. Other repairable features of the combustor design are:

- Fuel nozzle ferrule assemblies are individually replaceable in the swirl cup. This may be required if relative motion between the fuel nozzle and dome causes excessive wear. Replacement is made by cutting out the worn ferrule and flaring the new ferrule in position. The flaring process is similar to that used for flaring the end of a tube.
- Combustor-turbine air seal parts are riveted to the aft end of the inner and outer skirts. The seals may, therefore, be replaced by removal of the rivets and by re-riveting.
- Bushings in the forward end of the cowl that mate with the mounting pins are held in position by a press fit and tack welds. If it becomes necessary, any of the bushings can be replaced easily.

The disassembly and replacement features are illustrated in Figure 3-34. Borescope ports are provided for easy inspection of the combustor during service. This is discussed in Section 3.3.12.

The construction of combustion liner components lends itself readily to field repair. Demonstration of a typical repair is illustrated in Figure 3-35. In this instance, a welded and brazed J93 outer skirt was locally burned with a cutting torch to simulate a failure. The skirt selected for this demonstration had accumulated over 200 hours of engine operation, including over 36 hours of simulated Mach 3.0 operation during two official PFRT endurance tests. The damaged area was removed and fitted with a replacement section. The new section was fusion-welded into place. No special techniques or procedures were used other than normal inert gas "back-up" of the reverse side of the weld. Braze repair in the affected area is not required. Fluorescent-penetrant (Zyglo) inspection of the external surface, and radiographic inspection of the internal structure at the repaired joint confirmed that the repair weld was free of defects. A small sample in the weld region was removed and subjected to a comprehensive metallurgical examination that further verified the soundness of the repair. A component repaired by these techniques is capable of continued service without further processing.

The integral (one-piece) combustor assembly provides "off engine" maintainability advantages proven in J85, T58, and J93 service. Although the need for combustor maintenance is substantially reduced with the annular design, various "take-apart" features for easy removal of the combustor from the engine have been carefully considered. Studies have been made of designs that would permit removal of the combustor from the engine without turbine disassembly. A radial take-apart design was evaluated as part of the T64 engine program. In this design, the inlet cowl was permanently integrated with the compressor rear frame, rather than with the combustor. The dome's inner and outer skirts were separable in halves and were assembled by bolted connections. This configuration is illustrated in Figure 3-36. The take-apart features were demonstrated in the test cell for combustor replacement. The T64 design was developed to a successful 50-hour flight qualification, and accumulated limited flight testing time.

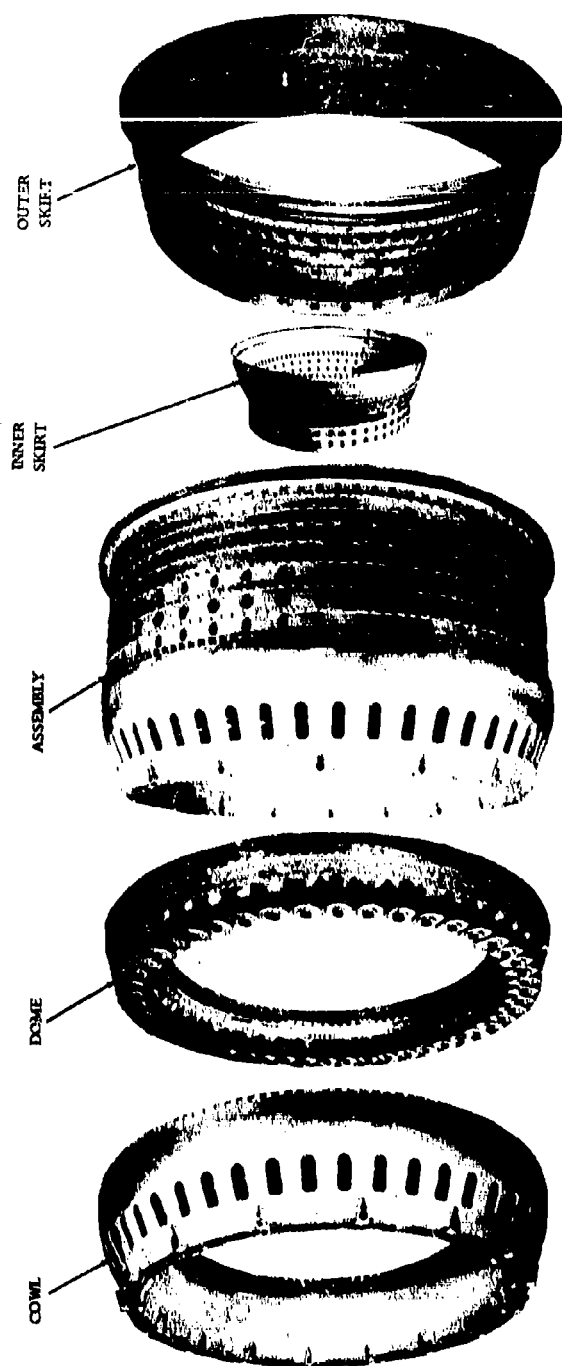
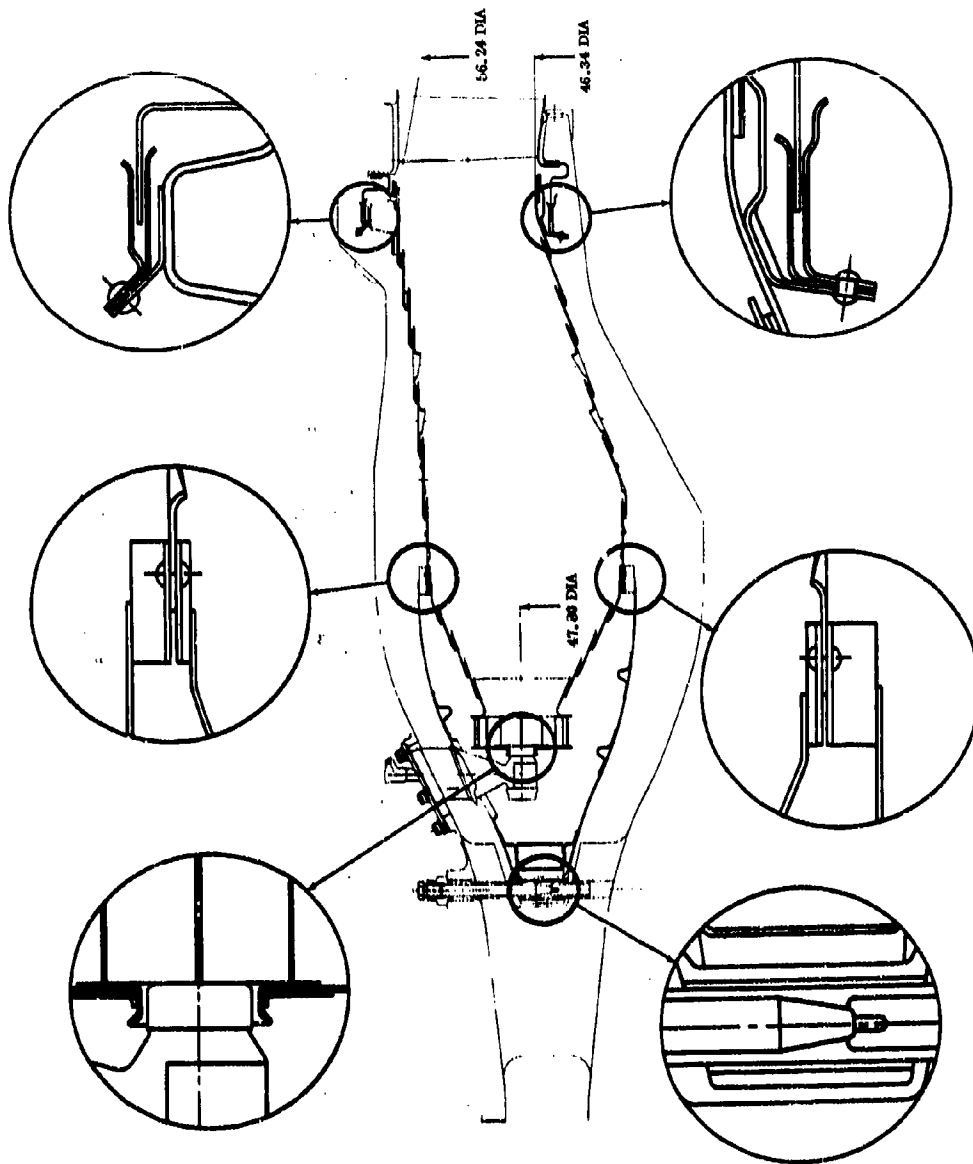


Figure 3-33. GE4 COMBUSTOR ASSEMBLY AND COMPONENTS

**CONFIDENTIAL**

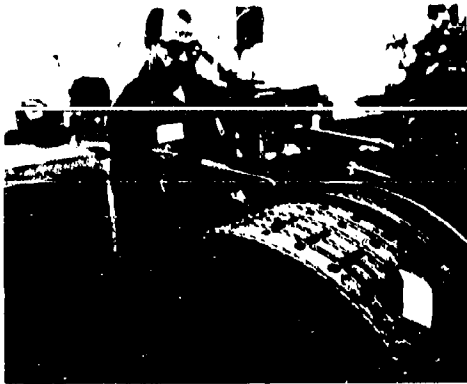


**Figure 3-34. GE4 COMBUSTOR DISASSEMBLY AND REPLACEMENT FEATURES**

**3-45**

**CONFIDENTIAL**

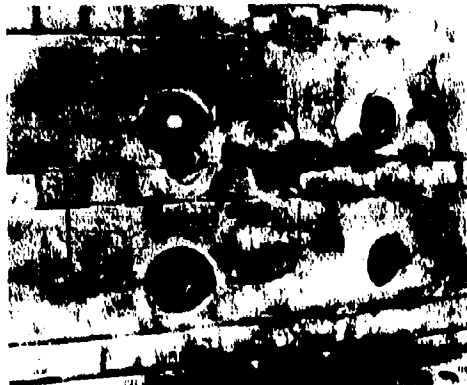
**K**



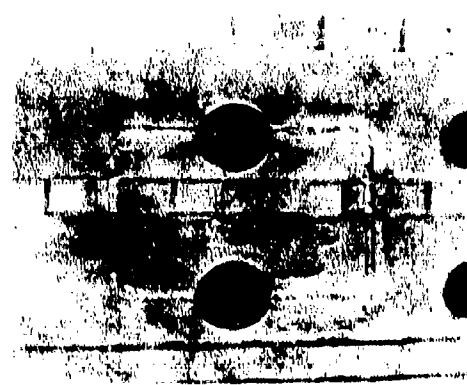
1. SIMULATED "BURN-OUT" BEING  
INFLECTED ON LINER SKIRT



4. NEW SECTION FITTED INTO POSITION PRIOR  
TO CLEANING AND WELDING



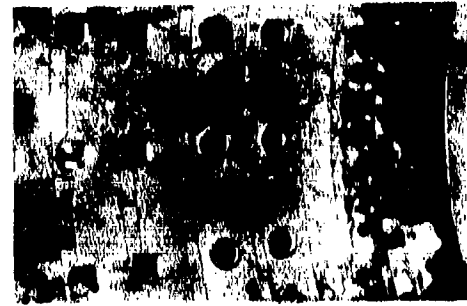
2. CLOSE-UP OF DAMAGE AREA. NOTE: BRAZE  
RESIDUE AT WIGGLE STRIP ENTRANCE



5. REPAIR AREA AFTER CLEANING  
AND WELDING



3. DAMAGE AREA REMOVED AND A REPLACEMENT  
SECTION CUT TO FIT



6. INSIDE REPAIR AREA SHOWING COMPLETE  
PENETRATION OF WELD

Figure 3-35. DAMAGE AND REPAIR SEQUENCE SHOWING THE REPAIRABILITY OF  
BRAZED COMBUSTION COMPONENTS

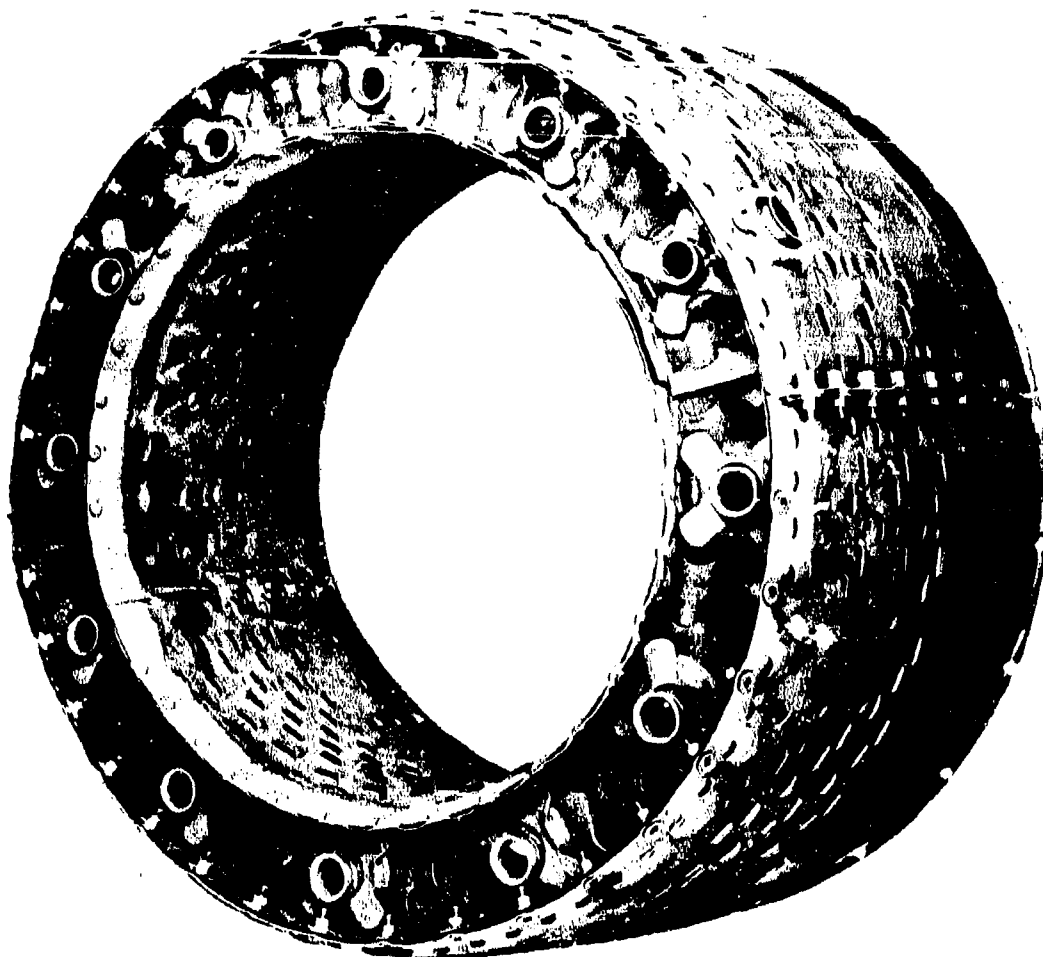


Figure 3-36. T64 TAKE-APART COMBUSTION LINER

The notable problems experienced were:

- Circumferential gap variations between the diffuser/cowl and combustor dome. The gap varied from minus 50 percent to plus 100 percent of design intent. This resulted in variations in performance from one combustor to another.
- Cooling joint overtemperature and leakage.

- Local stiffening due to the axial flanges caused out-of-roundness in the skirts.
- Mechanical fasteners disengaged (the bolts loosened and disengaged, the nut portion was permanently attached to the flange). In several instances following test, missing bolts were found at the bottom of the casing.

Based on these results, the take-apart design was abandoned in favor of the full annular assembly now in production use.

More recently, design studies have been initiated to provide a circumferential slip-joint at the junctions between the skirts and dome assembly. This would permit replacement of the skirts after removal of the turbine section, and could be done without removing the 42 fuel nozzles, 14 mounting pins, and two ignitors; therefore, a substantial maintenance advantage would be achieved. A design approach to provide this feature is shown in Figure 3-37. Design studies including cost and weight trade-offs, are planned.

A durability and maintainability analysis for the GE4 Combustor has been completed and is contained in a special appendix entitled "GE4 Durability and Maintainability Analysis," which is available upon request as backup material to the substantiating data submitted. The frequency of checking deterioration will be determined during the GE4 development program. The combustor is designed for advantageous use of borescope inspection. (Refer to Section 3.3.12.)

### 3.3.10 RELIABILITY

The annular combustor system has inherent reliability advantages over the cannular systems. These include:

- The parts are fewer and simpler in the annular system because separate cans, cross-fire tubes, and transitions are eliminated.
- A reliable and effective cooling-air distribution system is easier to achieve because of design symmetry.
- The area to be cooled is reduced.
- Discontinuities of the separate cans and cross-fire tubes cause cooling problems and troublesome hot spots. These are avoided in the annular design.
- Annular designs eliminate the need for transition (from round to annular) sections, with special thermal problems, at the combustor outlet.

The reliability of resistance welds in the GE4 is ensured by the addition of brazing to all resistance welded joints. (Refer to Section 3.3.6.)

All rivets are located in cooling air streams to prevent overtemperature or oxidation. This is illustrated by Figure 3-37 (present combustor). The reliability of the rivets on the J93, J97, and TF39 combustors in similar applications has been perfect; there have been no reported cases of rivet failure due to either overtemperature or load.

### 3.3.11 QUALITY ASSURANCE

Periodic performance and dimensional checks will be made on production hardware. These checks will include a 100 percent dimensional inspection of the combustor, and performance checks on



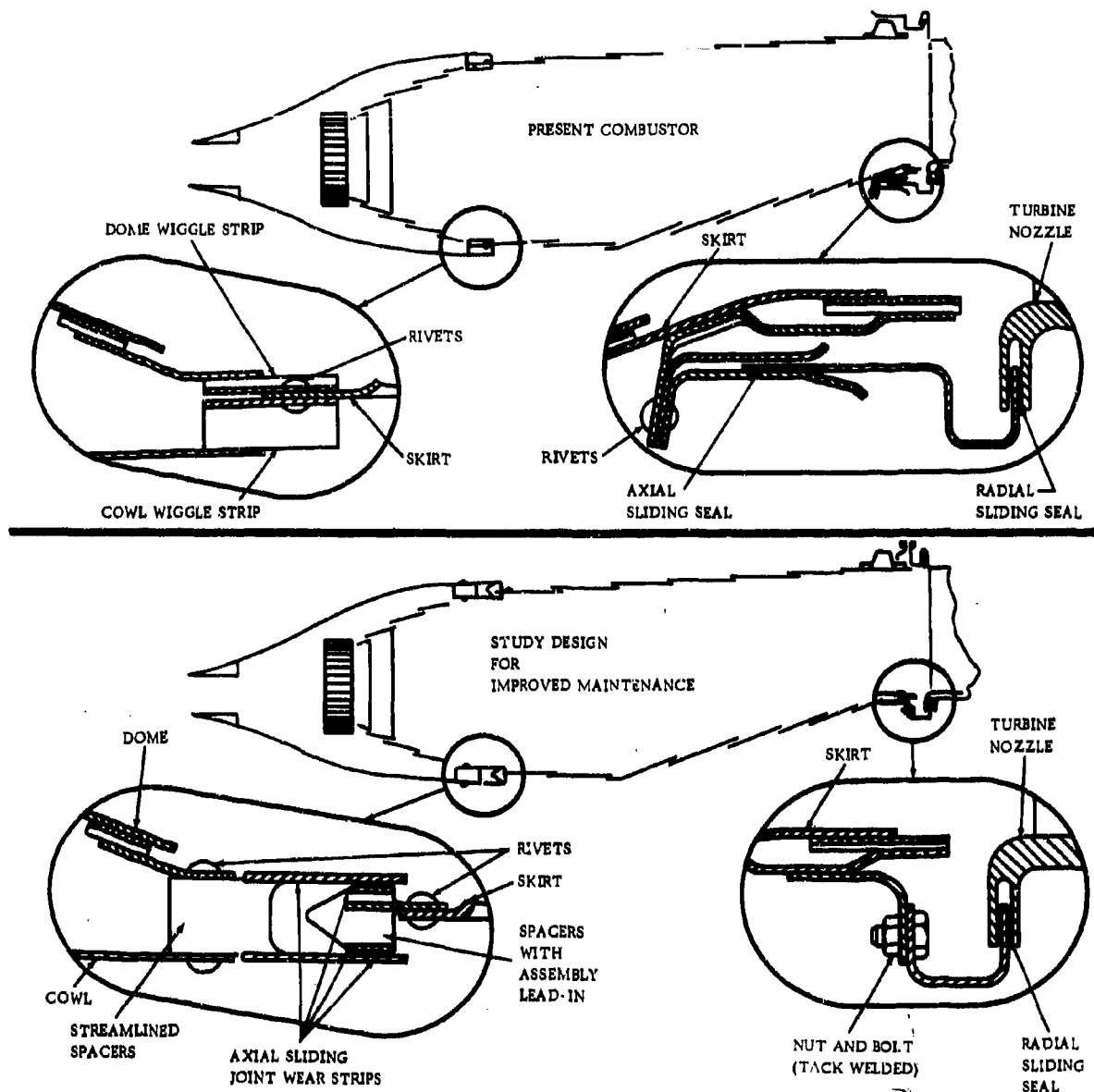


Figure 3-37. CIRCUMFERENTIAL SLIP JOINT DESIGN APPROACH

both full-scale component test stands and on the engine. These procedures will promptly identify any changes in tooling and manufacturing procedures that might adversely influence safety or function. In addition, influences on external performance will be detected by engine test.

### 3.3.12 SAFETY

Combustor safety is primarily achieved by good, dependable, and well proven designs. The reliable cooling air distribution system is essential to safety by minimizing the possibility of burn-through. The reliability features discussed in Section 3.3.10 also apply to safety.

Combustor liner integrity may be ensured visually at routine maintenance inspections. Borescope ports in the combustor case (part of the compressor rear frame) are provided for this purpose. These ports are located at combustor thimble holes so that the borescope may be inserted into the combustor. This is shown schematically in Figure 3-38. Complete visual inspection of the combustor may be made by use of a number of such ports. Figure 3-39 shows typical pictures of a combustor through a borescope. Fuel nozzle and ignitor ports may also be used for closer borescope viewing of swirl cups.

Other safety features of the combustor include:

- Fuel nozzles have welded closures.
- Fuel nozzle engagement in respective fuel nozzle ferrules has been ensured under all conditions by careful stackup studies.
- Fuel nozzles cannot be bolted to their flanges if they are not engaged in the ferrules.

### 3.3.13 FAILURE ANALYSIS

Intensive failure mode and effect analysis work is being performed on the GE4 combustor. An objective of this work is to consider and understand all possible failure modes of the combustor, and the effect of each on the safety and the economy of the aircraft. The ultimate purpose is to identify all design development and assurance test programs needed to prevent potential failures, and to provide assurance that durability requirements will be met before GE4 engines are put into production. Other phases of failure analysis to be conducted on the combustor are described in Volume IV, Reliability.

### 3.3.14 VALUE ENGINEERING

Value Engineering has been systematically applied to the GE4 combustor by a team consisting of Design Engineering, Value Engineering, and Manufacturing Engineering.

Redesigns for increased value include the following:

- A simpler way to provide a wear resistant combustor mounting system has been developed. It is planned to change from the hinge mount, used in Phase II-C, to a friction grip, expanding pin mount in Phase III. This reduces cost, improves maintainability, and reduces weight.
- A simpler cowl truss for ease of manufacture has been designed for the Phase III combustor. The Phase II-C truss consisted of individual triangular boxes that formed both the diffuser

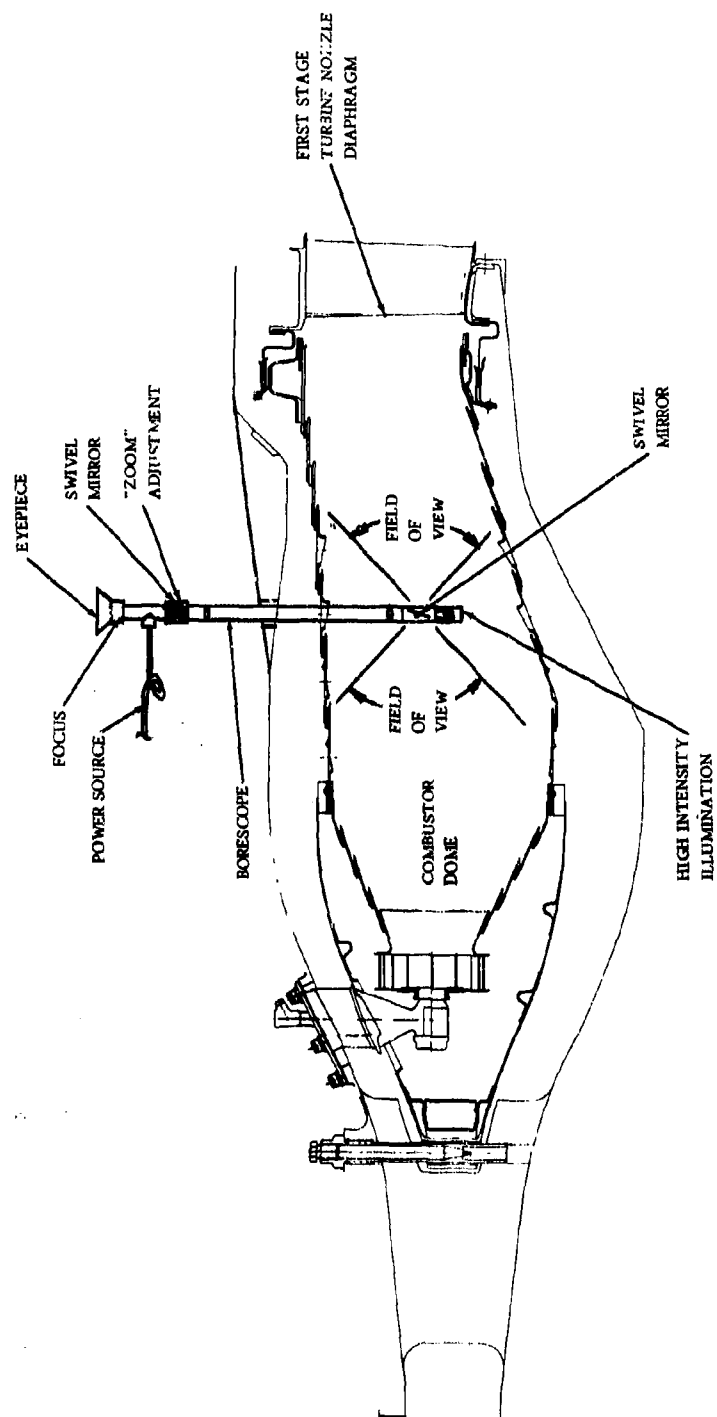


Figure 3-38. BORESCOPE INSPECTION PORT

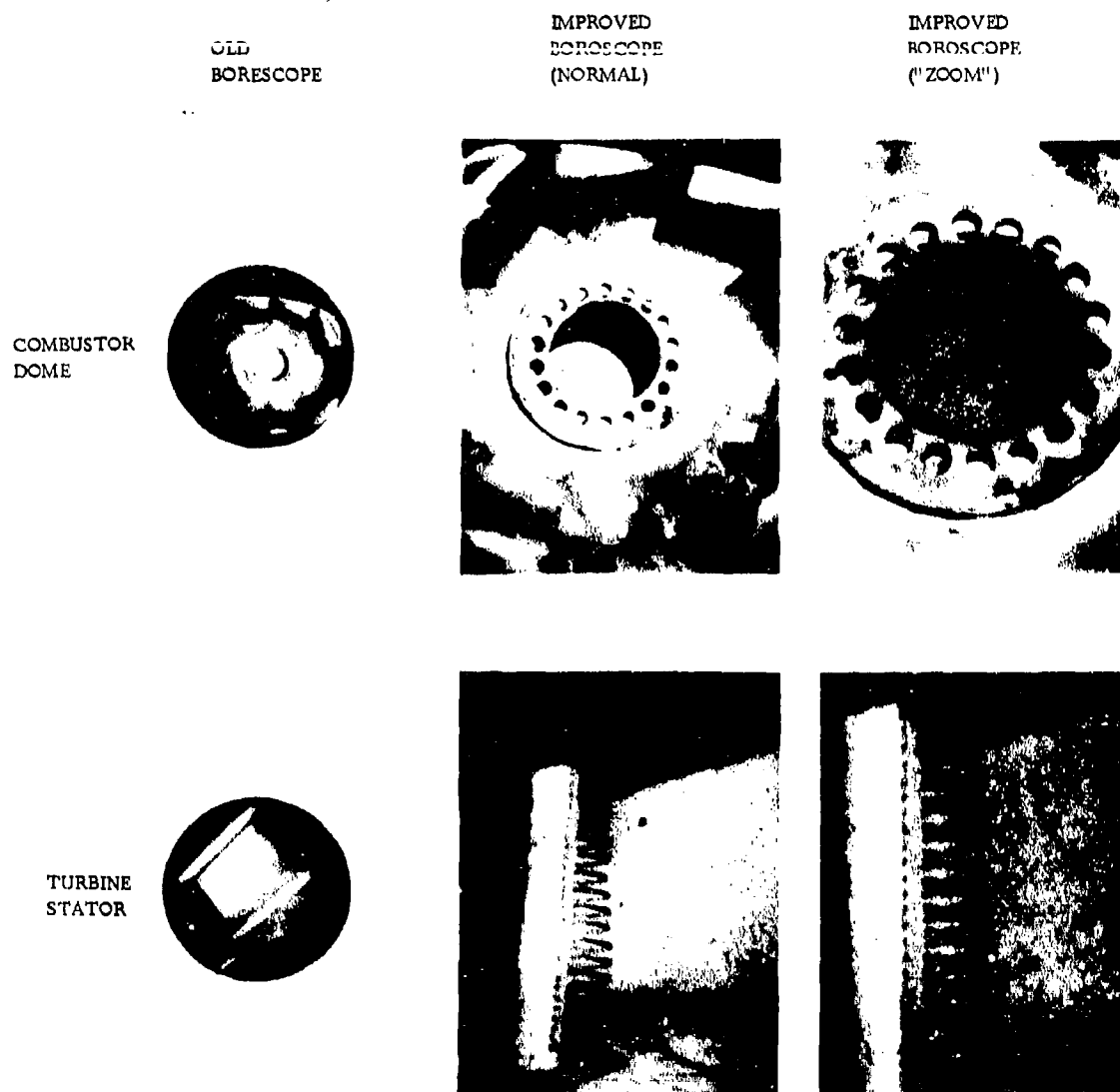


Figure 3-39. BORESCOPE VIEW INSIDE COMBUSTOR

## CONFIDENTIAL

passage, and the truss members. These boxes had to be fitted carefully into the truss before welding. In the Phase III design, the conical diffuser walls are continuous, and the diagonal members of the truss are formed from a continuous convoluted strip. A cleaner mechanical design is obtained and cost is reduced.

- Component test of the Phase II-C combustor showed that fuel nozzle spacing can be increased without deterioration of performance. The number of fuel nozzles and swirl cups is reduced from 48 to 42 in Phase III. This simplifies the swirl cup design, because its shape can be changed from elliptical to round. Cost and weight are also reduced by the change.

Fabrication costs will remain low because present manufacturing technology can be used. Specifications permit conventional materials, tolerances, forming, welding, and inspection techniques. New manufacturing techniques and processes are being studied to improve quality, and to further reduce cost. Full advantage of these new methods will be taken as appropriate.

Production manufacturing processes for annular combustors have been thoroughly developed at General Electric. The majority of the parts are full ring elements, processed separately, and assembled into major sub-components by resistance welding. The brazing is done on the entire assembly after all forming and welding are complete, and before riveting. The process is straightforward, highly repeatable, and well suited for low cost production.

### 3.3.15 HUMAN ENGINEERING

The GE4 combustor design has been carefully studied to avoid structures that can be improperly assembled to cause infant mortality or a dangerous situation through human error. Examples are:

- Fuel nozzles will not seat on their respective pads if the nozzle spray tip is not properly engaged in the nozzle ferrule on the combustor dome.
- Fuel nozzles cannot be put in backwards or sideways because of the bolting pattern and manifold connections.
- Igniters will not assemble unless the combustor is properly oriented in the compressor rear frame.

All assembly or disassembly can be performed by assembly personnel with normal skills and abilities. There are no sharp edges or other features that would constitute unusual hazards.

### 3.3.16 STANDARDIZATION

Combustor cowls, domes, skirts, and replaceable wear elements are designed for complete interchangeability. Standard AN rivets are used in all riveted joints. See Section 3.3.9.

### 3.4 DEVELOPMENT STATUS

The combustors in the first GE4, Phase II-C engine has operated for a total of 18 hours as of August 25, 1966. Rated turbine inlet temperature of 2200°F has been achieved. At this point, maximum combustor metal temperature measured was 1150°F. No mechanical difficulties have been observed.

Two full-scale GE4 combustors has been development tested in an atmospheric combustor test stand for a total of 180 hours. This time included 34 runs to optimize pattern factors and turbine inlet temperature profile. Eighteen hours were run with combustor inlet heated to 1065°F to simulate supersonic cruise conditions. Maximum combustor outlet temperature tested was 2332°F.

### 3.5 SUPPORTING TECHNOLOGY

General Electric's annular combustor experience as of July, 1966 includes the following:

	T64	J85	T58 (All Models)	J93 & *J93/SST Demo.	J97	TF39	Totals
Factory & Field Engine Test	19, 826	31, 017	24, 813	8223	328	188	84, 395
Flight Test	3385	4943	19, 469	1, 092	-	-	28, 889
Customer Use	14, 744	1, 699, 112	1, 116, 761	-	-	-	2, 800, 617
Component Test	2545	5522	3217	2694	752	855	15, 585
Totals	40, 500	1, 710, 594	1, 164, 260	12, 009	1080	1043	2, 929, 486

\*J93 Size GE4 Demonstrator

The following paragraphs discuss some of these combustors and test experience which have contributed most to the GE4 design.

#### 3.5.1 J93 COMBUSTOR

J93 experience provides an excellent platform from which the GE4 combustor design has evolved. The J93 operates at a  $T_4$  of 2100°F. The liner mechanical construction utilizes the basic three-element cooling slot design.

More than 9300 hours of engine testing including 276 hours of simulated Mach 3.0 operation have been accumulated as of July, 1966 on the J93 annular combustor. Individual combustors have accumulated 292 hours, including two successive Preliminary Flight Rating Tests and 38 hours of simulated  $M_p$  3.0 operation. Life requirement for these (YJ) parts was 68 hours.

Combustor mechanical condition after engine operation has been excellent. The step wall cooling system effectively eliminates metal burning and oxidation; and the parts are generally free of cracks, distortion and other structural defects. One minor structural fault produced cracks at the terminations of the cooling slot wiggle strips after extended operation. This deficiency has been corrected by joining the ends of adjacent wiggle strips with axial butt welds. This eliminated all circumferential discontinuities of the wiggle strips. The fix was proven in subsequent combustor designs.

### 3.5.2 AIR COOLED ENGINE VEHICLE

The Air Cooled Engine Vehicle is a test facility that was used to demonstrate the GE4 turbine design in the J93 engine size. The first combustor used was a modified J93 combustor, shortened by 0.65 inch to accommodate the increased-chord turbine rotor and stator design.

Over 435 hours of engine operation were demonstrated. This includes 227 hours at a  $T_4$  of 2200°F and 40 hours of heated inlet (simulated High-Mach) operation. Furthermore, one test included 1000 thermal cycles of operation with throttle bursts from idle to military power. The J93/SST Demonstrator combustor was operated at atmospheric pressure during component testing at discharge temperature of 2700°F. In a high pressure component test, the combustor was tested with the turbine stators. Average discharge temperatures up to 2572°F were achieved.

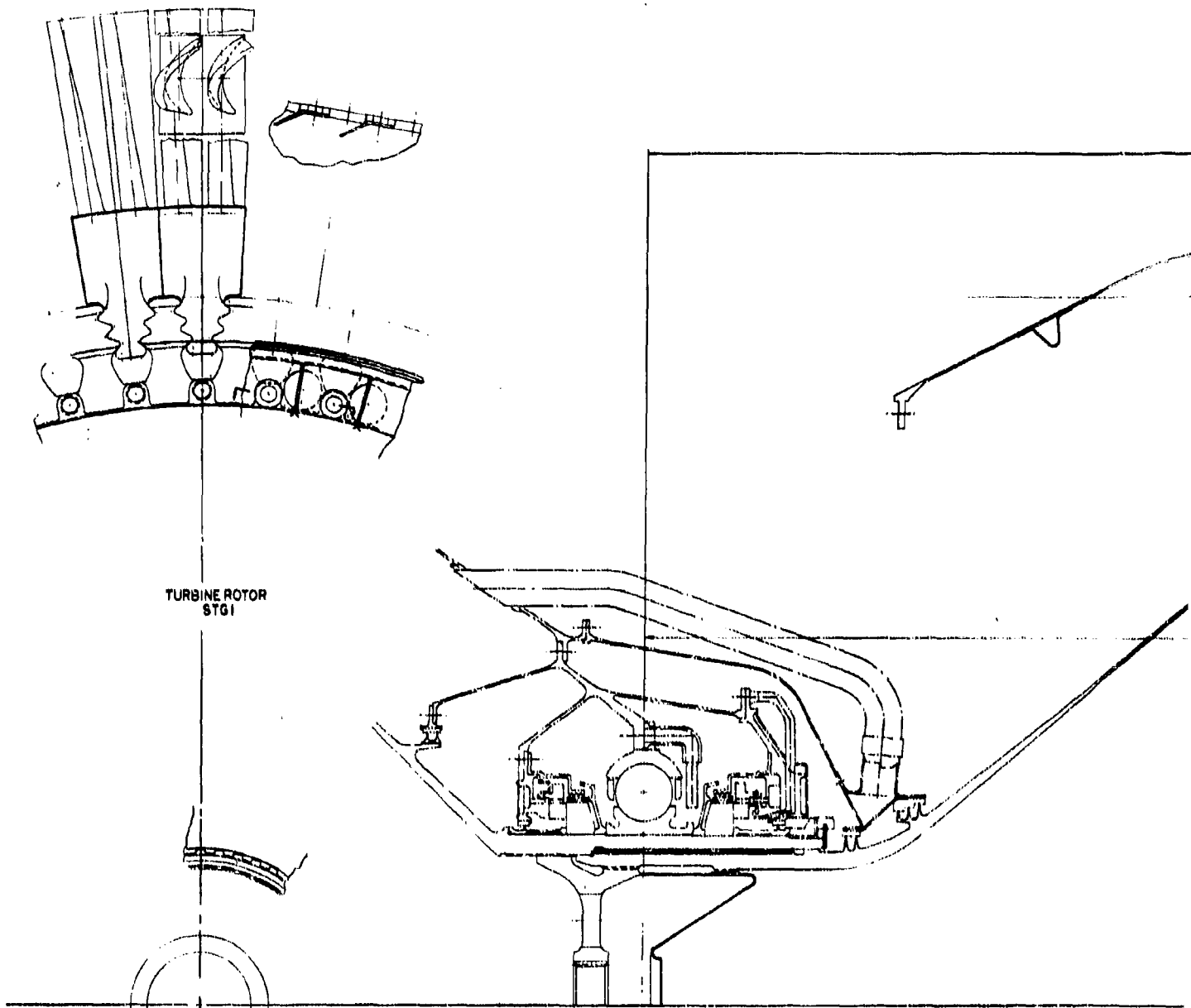
### 3.5.3 J97 COMBUSTOR

The J79 combustor has demonstrated excellent performance and durability in component and engine tests. The GE4 combustor is similar to the J97 in major aero-thermodynamic and mechanical respects.

The J97 annular combustor has accumulated approximately 230 hours of engine test as of July, 1966 without major difficulty. Excellent turbine inlet temperature distribution performance has been consistently achieved at or above 2100°F. This was shown by temperature measurements and overall condition of the turbine hardware. The combustor liners have encountered relatively minor local skin overtemperature problems. Dome carbon accumulation has been limited. Cooling improvements incorporated in J97 problem areas have been applied to the GE4 system. Approximately 200 hours of full annular component combustion tests as well as numerous sector and cold flow investigations have been conducted. Margin testing has shown that the design has significant growth potential. Average discharge temperatures in excess of 2700°F have been achieved in the Atmospheric Combustor Test Rig.

### 3.5.4 AIR COOLED TURBINE TEST

The Air Cooled Turbine Test Rig is a component test facility for evaluating the hot section of engines in the J97 size. It has been used for thermal cyclic endurance testing. During initial testing, combustion performance was satisfactory; however, aft liner temperatures exceeded objectives. For the second test this was corrected; local cooling slots were increased and improved cooling slots were introduced. These changes substantially reduced the liner temperature. Maximum operating conditions included  $P_3 = 200$  psia,  $T_3 = 700^\circ\text{F}$  and discharge temperature = 2500°F. The inner liner exhibited some local overtemperaturing and one small burned area near the aft seal. The procedures applied to the outer skirt to improve the convective cooling were applied to the inner skirt. An additional circumferential cooling slot was added at the inner liner in the region of the local overtemperature. The revised hardware was manufactured and cyclic endurance testing was resumed. After 300 thermal cycles the combustor was in good condition and could have been further tested without repair.



1



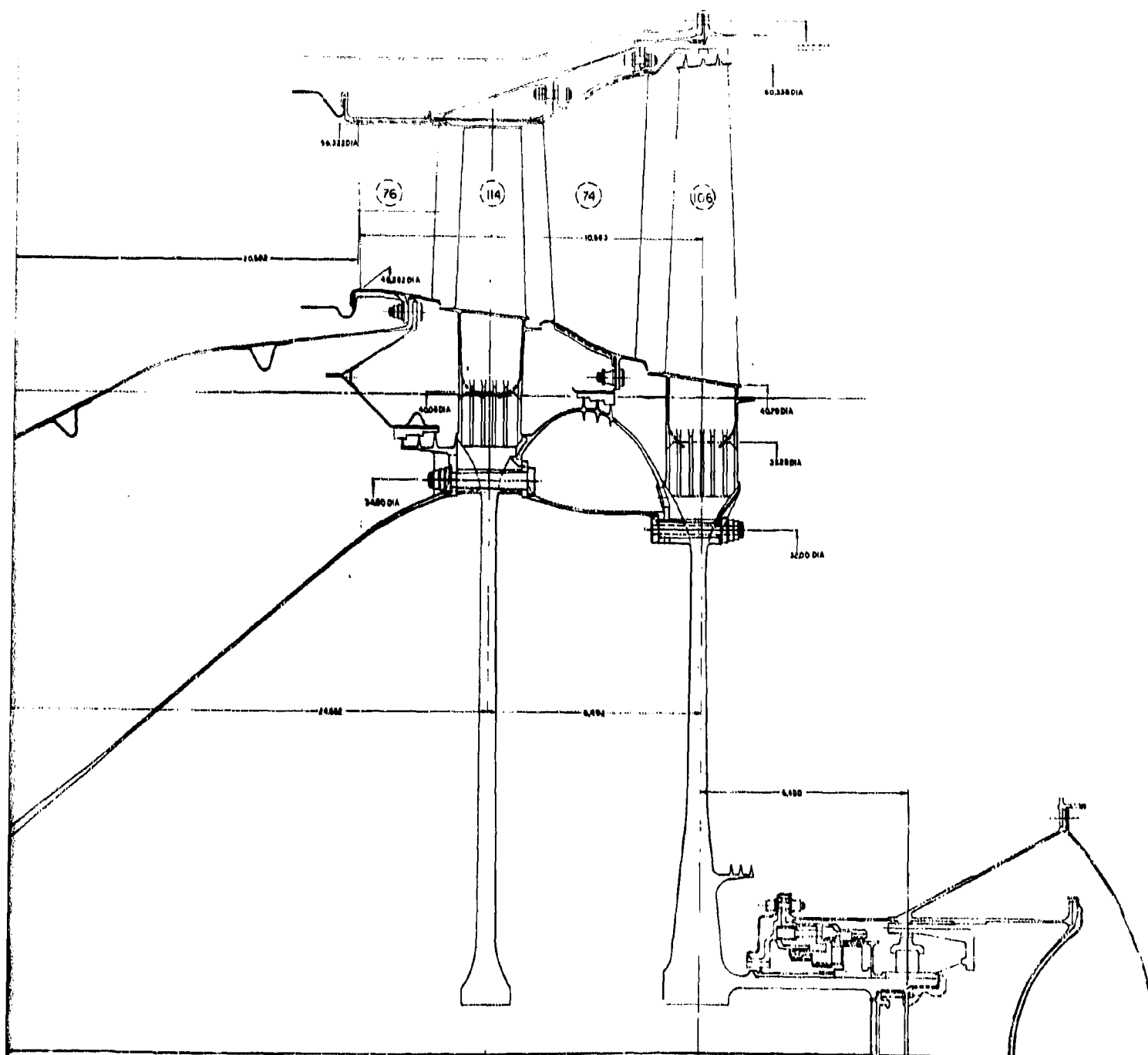


Figure 4.1-1 GE 4 TURBINE - Layout drawing of the General Electric SST Turbine showing the overall configuration and basic dimensions.

4-0

2

K

## CONFIDENTIAL

### 4. TURBINE

#### 4.1 INTRODUCTION

The GE4/J5 Turbine (Figure 4.1-1) is patterned after current proven General Electric designs. It will achieve a useful life much longer than the best of today's commercial engines, through the use of improved cooling techniques. The long life will be achieved by pursuing a conservative design approach based on the following policies:

- Build upon the foundation of successful past design and experience
- Maintain conservative metal temperature levels which make it possible to achieve creep lives far longer than those currently attainable
- Reduce transient temperature cyclic strain to the point where low-cycle fatigue does not affect the life of the turbine.
- Use better materials than in today's commercial engines.

The GE4 engine is rated at 2200°F turbine inlet gas temperature for supersonic cruise, and at 2275°F for take-off and transonic operation. The two stages of turbine vanes and the two stages of blades are cooled - like those of the 2100°F J93 engine, which cools the vanes and the blades of both stages. The J93 was designed to cruise at Mach 3.0 at 2000°F, the GE4 will cruise at Mach 2.7 and 2200°F.

#### 4.1.1 EVOLUTION OF THE TURBINE DESIGN

Figure 4.1-2 shows the evolution of the General Electric family of turbines. The J79/CJ805, J93, J93/SST, TF39, and the GE4 turbines all include such proven features as the large, stable front shaft, paired damped buckets, convection and film cooled nozzles, low-temperature wheel and spacer cooling. The J93, J93/SST, TF39, and the GE4 have air-cooled blades and the catenary heat shield. Cross-section drawings, Figure 4.1-3, show some of the details of these important similarities. All of the turbines are shielded by the large front shaft which seals low-temperature cooling air around the wheels. All have the stable outboard bearing support arrangement.

#### 4.1.2 EVOLUTION OF THE TURBINE VANE DESIGN

Hot parts in turbine engines have been air-cooled for many years. From the first jet engines, sheet metal shells of combustors have been film-cooled, and they have been successful despite gas temperatures greater than 3000°F in the dome region. The turbine vanes in all General Electric engines since the J47 have been cooled. The J47 and J73 use convection cooling; the J79, J85, T64, J93, GE1, TF39 and GE4 use a combination of film and convection cooling. Figure 4.1-4 shows the evolution of cooled vanes from the J79/CJ805 to the GE4. Refinements in manufacturing techniques have made important temperature and life breakthroughs possible, but the basic cooling principles are essentially unchanged. Convection and film cooling combine to control metal temperature locally, ensuring the strength and dimensional stability required for long-life service.

Figure 4.1-6 shows how the airfoil edges and surfaces of the modern turbine are protected. Continuous rows of precision holes provide a blanket of protection which make it possible to maintain metal temperatures many hundreds of degrees cooler than the surrounding gas temperature. End walls, as well as the airfoils, receive this cool shielding treatment.

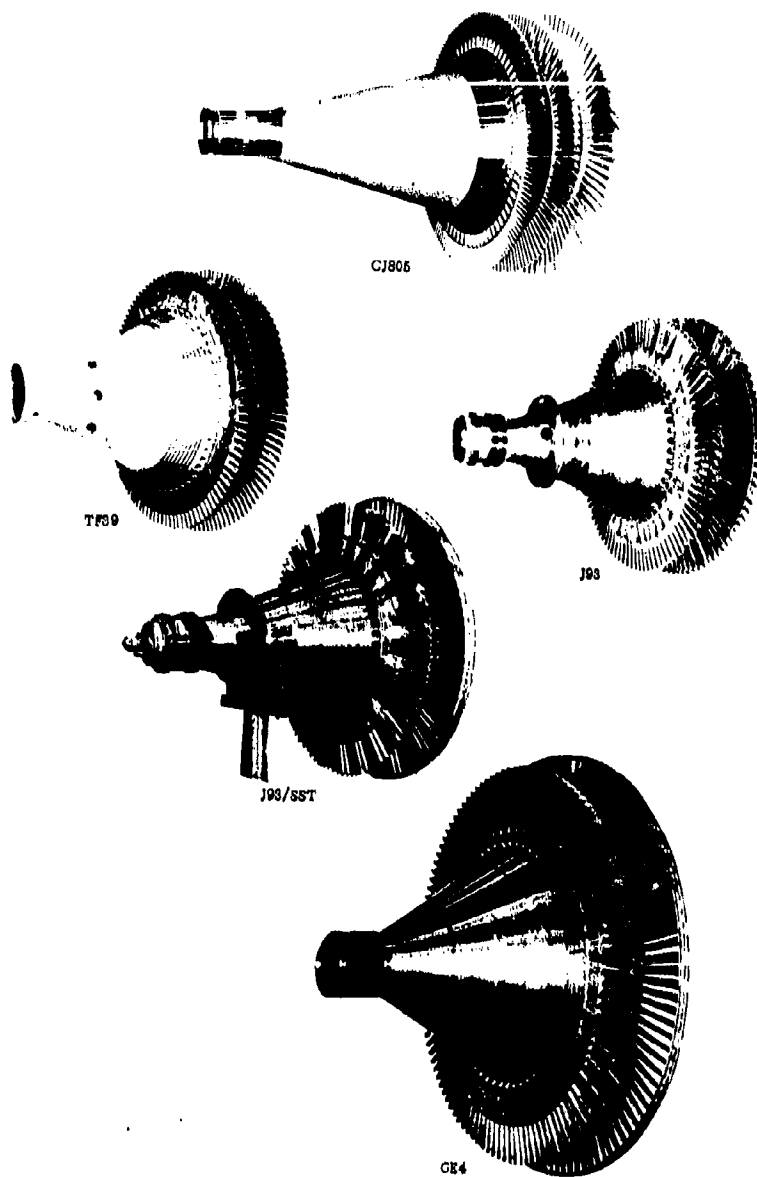
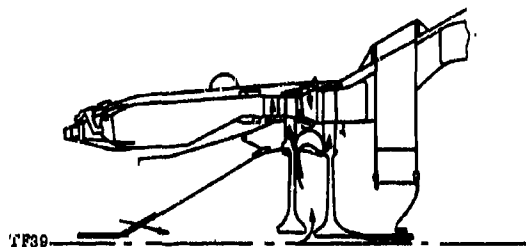
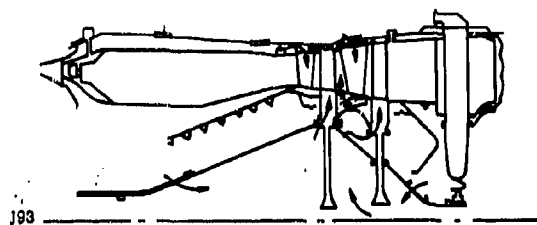
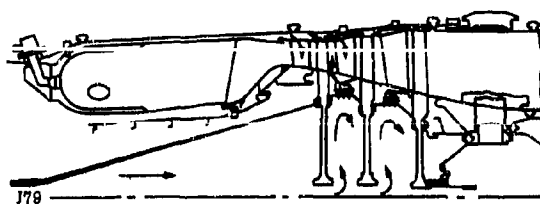


Figure 4.1-2 FAMILY OF TURBINES. GE4 turbine is based on proven General Electric design. Structural and cooling similarities between the CJ805, J93, TF39, J93/SST and GE4 design assure integrity and long life of the SST turbine.

**CONFIDENTIAL**



**Figure 4.1-3 EVOLUTION OF GENERAL ELECTRIC DESIGNS.** Sectional views show the similarity of design and cooling system between the J79, J93, TF39 and GE4 Turbine and Combustor. All have the proven outboard bearing support system, large stable front shaft and the internally cooled rotor concept. Cooling techniques proven on the J79 and refined on the J93 are used throughout the GE4 design.

**CONFIDENTIAL**

**CONFIDENTIAL**



**Figure 4.1-4 EVOLUTION OF TURBINE NOZZLE COOLING.** Views show the manner in which vane cooling design has been refined over the years. Proven J79/CJ805 film cooling techniques are used on the newer engines. Refinements in convection cooling are made possible on the newer designs by advances in casting and hole drilling techniques. Metal temperature levels and temperature gradients show important improvements even in the face of higher gas temperature levels.

4-4

**CONFIDENTIAL**

K

**CONFIDENTIAL**

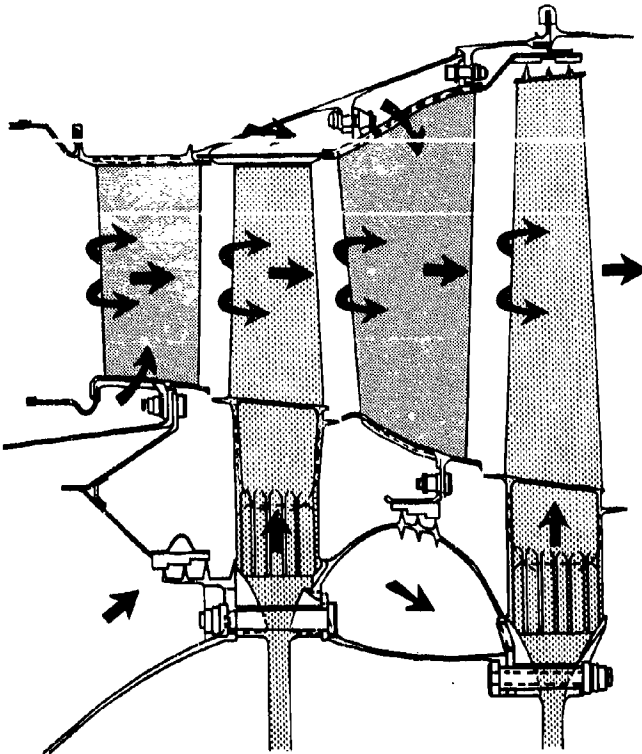


**Figure 4.1-5 GE4 TURBINE COOLING SYSTEM.** A close view of the GE4 cooling air path, showing how the cooling air blankets all surfaces of the turbine. A controlled protective film of cooling air shields each component, while major structural elements like the wheels and vane support rings have the double protection afforded by metal shielding and cooling-air barriers.



**Figure 4.1-6 AIRFOIL COOLING.** Close up photograph shows the manner in which a continuous blanket of cooling air is directed over the airfoil and band surfaces. This protective film covers all of the gas passage surfaces. Edges receive special treatment. Holes through the trailing edges provide efficient convection cooling.

4-5

**CONFIDENTIAL**

K

#### 4.1.3 EVOLUTION OF THE TURBINE BLADE DESIGN

Turbine wheels have been air cooled since the first jet engine. The extension of these life prolonging cooling techniques to the rotating blading was the next logical step. This step was taken in the J93 Program - starting in 1957 - and has been pursued aggressively ever since.

Figure 4.1-7 pictures the evolution of the turbine blades from the J79/CJ805 to the GE4. All blades have the same twin dovetail concept so important in the control of vibration. The convection cooling system first successfully demonstrated on the J93 has been refined as new processes for casting and machining have been developed. The introduction of film cooling on the blades, like that used for many years on the vanes, made important temperature/blade-life gains possible. The GE4 design in detail is similar to the J93/SST demonstrator design on which extensive testing has been successfully completed.

Like the vanes, the key to the success of the film/convection cooled bladed lies in the economical manufacture of the precision, stress-free, film and trailing edge holes. These new processes, initially developed for the J93/SST, have been refined and improved on the GE4 with the result that machining on the GE4 blades has been almost completely without rejection due to processing variations or machining errors.

#### 4.1.4 TURBINE TEMPERATURE

The goal in effective cooling is lower metal temperature and lower thermal gradients. These qualities in the GE4 turbine result in stress and temperature combinations that give longer life than previously possible. Figure 4.1-8 compares important metal temperatures of current engines with those of the GE4. Note that while both turbine inlet temperatures and coolant temperatures have increased, the metal temperatures have not increased proportionately, and that actually the gradients have decreased substantially.

Metal temperature control is the key to reliability and long life. It is of fundamental importance in the substantiation of creep life, rupture life, and low-cycle-fatigue tolerance in all turbine parts. It is the basis for design credibility where stress margin and reliability are concerned. Both steady-state and transient metal-temperature levels are set by the life requirements, duty cycle, material properties, and design margins. Since the turbine is cooled, these temperature levels are far below the main gas stream temperatures, permitting the engine to use proven materials at conservative temperatures and, at the same time, achieving the important performance benefits of the higher cycle gas temperature.

**CONFIDENTIAL**

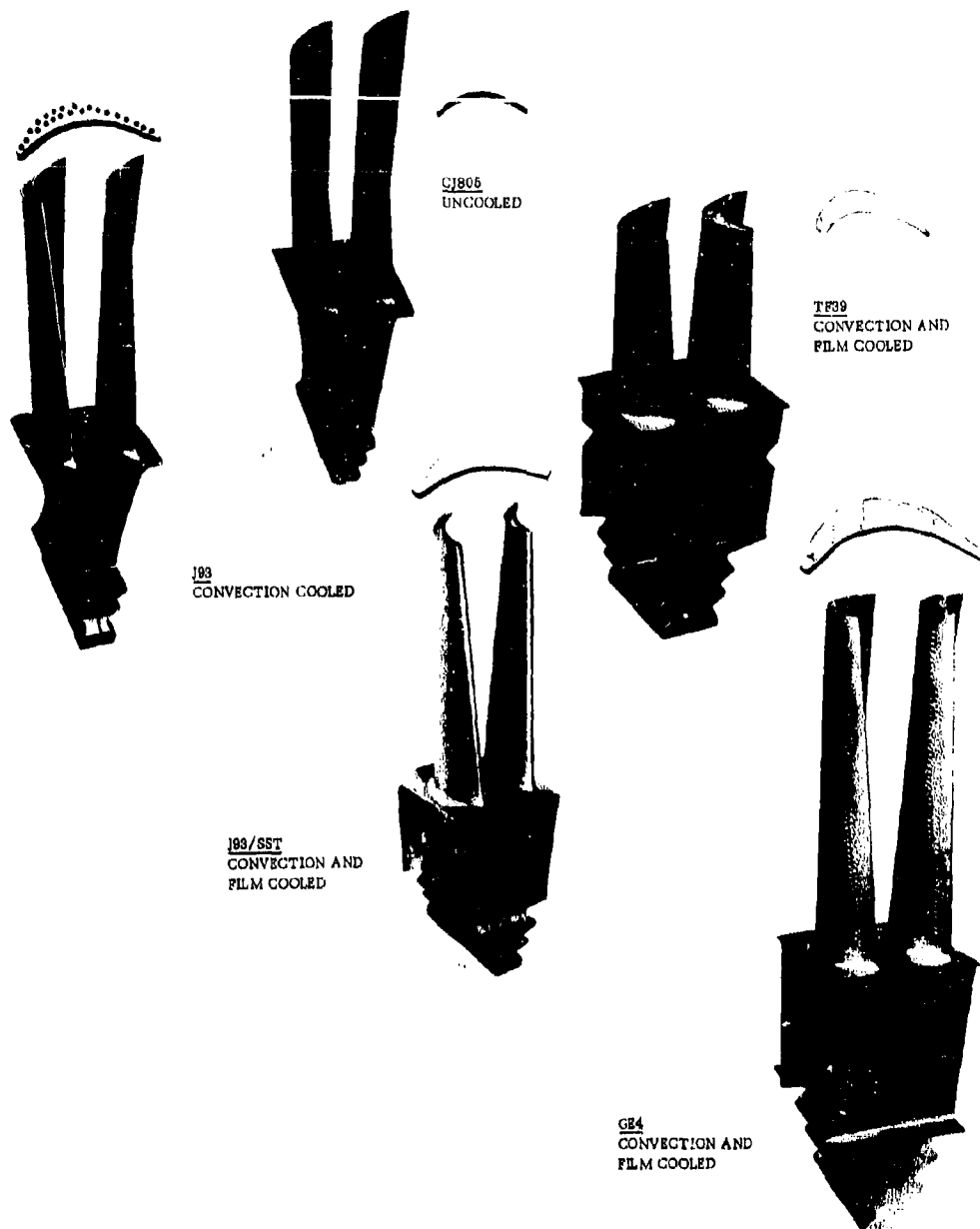
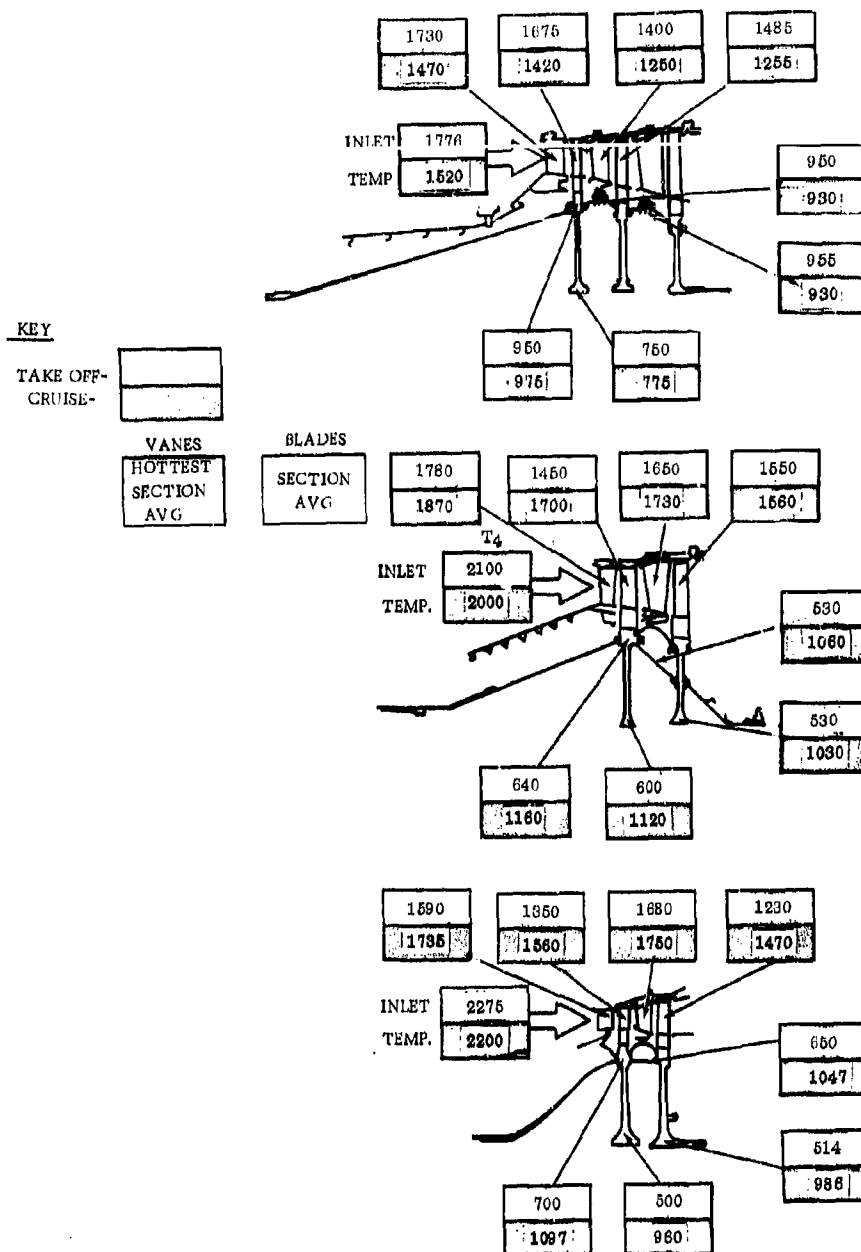


Figure 4.1-7 EVOLUTION OF TURBINE BLADE DESIGNS. Photographs show the progression in General Electric turbine blade design. The twin blade concept of the J79/CJ805 is followed on the J93, TF39, J93/SST and GE4 air cooled blades. The twin blade concept provides important vibration damping and tight manifolding for the airfoil cooling air.

**CONFIDENTIAL**



**CONFIDENTIAL**



**Figure 4.1-8 METAL TEMPERATURE COMPARISON** - Plots of key temperature points show how CJ805 and J93 turbine temperatures compare with the GE4 metal temperature levels. Keeping metal temperatures at the cruise point low makes long creep life possible. Keeping temperature gradients low (both steady-state and transient) makes it possible to have parts with unrestricted cyclic life.

**CONFIDENTIAL**

## 4.2 DESIGN REQUIREMENTS AND APPROACH

Figure 4.2-1 breaks down a typical route structure into its important flight segments. The plot shows the percentage of time spent and the turbine inlet temperature at each condition. About 64-percent of the time is spent at the cruise condition. Creep life of the cooled components is used at this cruise condition only. No other flight condition has stress or temperature levels that could materially affect the life of the material.

Turbine inlet temperature, rpm and compressor discharge temperature levels are shown throughout the typical route segment in Figure 4.2-2. This plot summarizes the temperature exposure (creep and rupture life limiting conditions) and the transient requirements (low-cycle fatigue) to which the GE4 engine is designed. A typical 36,000-hour part, for example, will be subjected to the equivalent of 13,500 such missions. The turbine blades and vanes are designed to complete more than 4500 typical missions, and to last the equivalent of 9000 hours at Mach-2.7 temperatures, before being retired from service.

Figure 4.2-3 expands the transient portions of the typical route segment plot to show gas temperature and rpm-response characteristics. These are nominal transient plots. Some will be slower and some will be faster, just as the engine's emergency response capability is considerably faster.

- The components in the turbine are designed to the following life requirements.

Table 4-1. Life Requirements

Component	Life (Hours)	Cycles (Route Segments)
Blades	12,000	7,000
Vanes	12,000	7,000
Wheels	36,000	20,000
Heat Shield	36,000	20,000
Spacer	36,000	20,000
Front Shaft	36,000	20,000
Vane Support Rings	36,000	20,000
Seals	36,000	20,000
Shrouds	36,000	20,000

- The turbine is designed to the 115-percent FAA overspeed requirements, and this overspeed capability will be demonstrated in the Phase III test program.
- The turbine stator structure will contain the damage resulting from the failure of single blades thrown at full engine speed at any point in the flight envelope. (See Section 4.3.3.5.)
- The GE4 turbine is designed to meet all the FAA certification requirements, applicable Government Specifications and Engine Specifications.

# CONFIDENTIAL

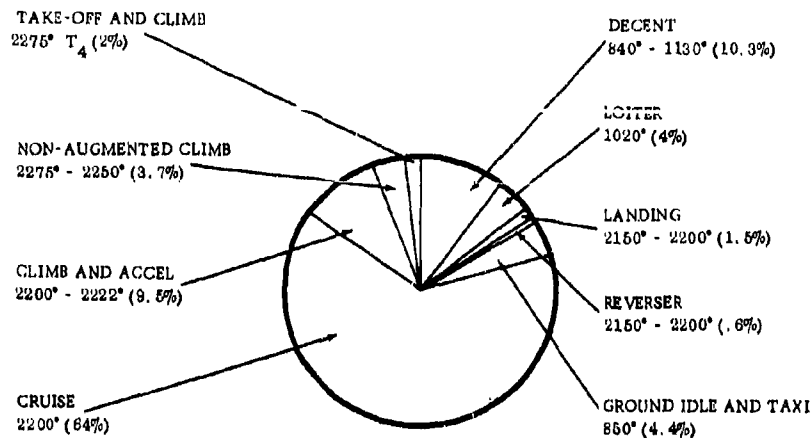


Figure 4.2-1 TIME/TEMPERATURE DISTRIBUTION - TYPICAL SST ROUTE STRUCTURE

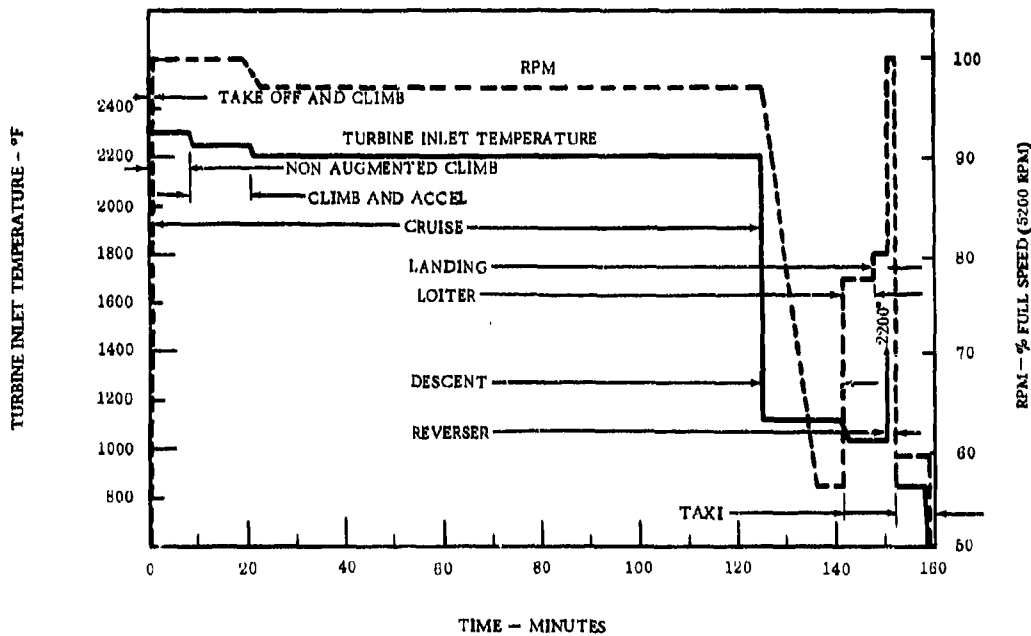


Figure 4.2-2 TYPICAL ROUTE SEGMENT DEFINITION. An average 2.65 hour route segment is broken down to show turbine inlet temperature and RPM at the various points in the flight map.

## CONFIDENTIAL

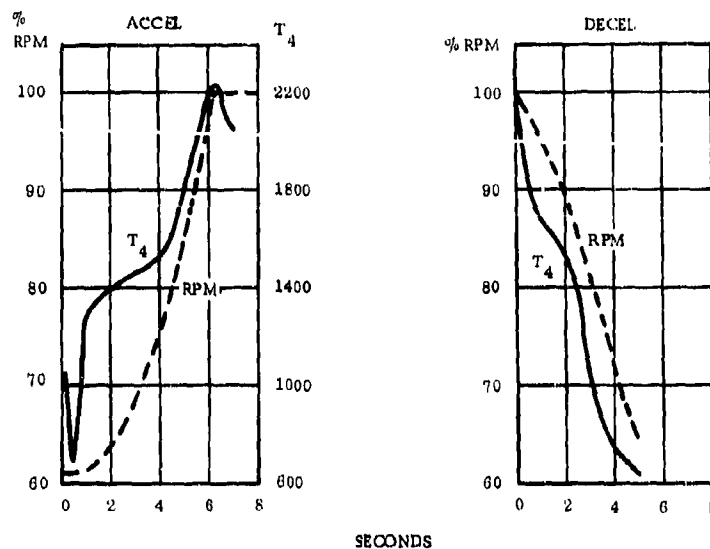


Figure 4.2-3 ACCELERATION AND DECELERATION TRANSIENTS. Expanded time scales show how turbine inlet temperature and RPM respond during typical transient modes. These rates of acceleration and deceleration are not representative of the engine capability, but are rather best estimates of the average for day-in day-out service.

### 4.2.1 GAS TEMPERATURE - METAL TEMPERATURE

Effective cooling keeps the turbine metal temperatures well below the gas temperature levels. The cooling air temperatures are highest at the high Mach-number conditions. This makes the metal temperatures at the Mach 2.7 flight points higher than other flight conditions, even though the turbine inlet temperature is lower than take-off and acceleration levels. A close examination of the gas and metal temperatures at cruise is important to a good understanding of the turbine design.

Figure 4.2-4 and 4.2-5 plot the gas and metal temperatures seen in the turbine at the Mach-2.7 cruise point. These curves relate the turbine inlet gas temperature, the local airfoil gas temperature and the average section airfoil temperature, at each radial position along the airfoil.

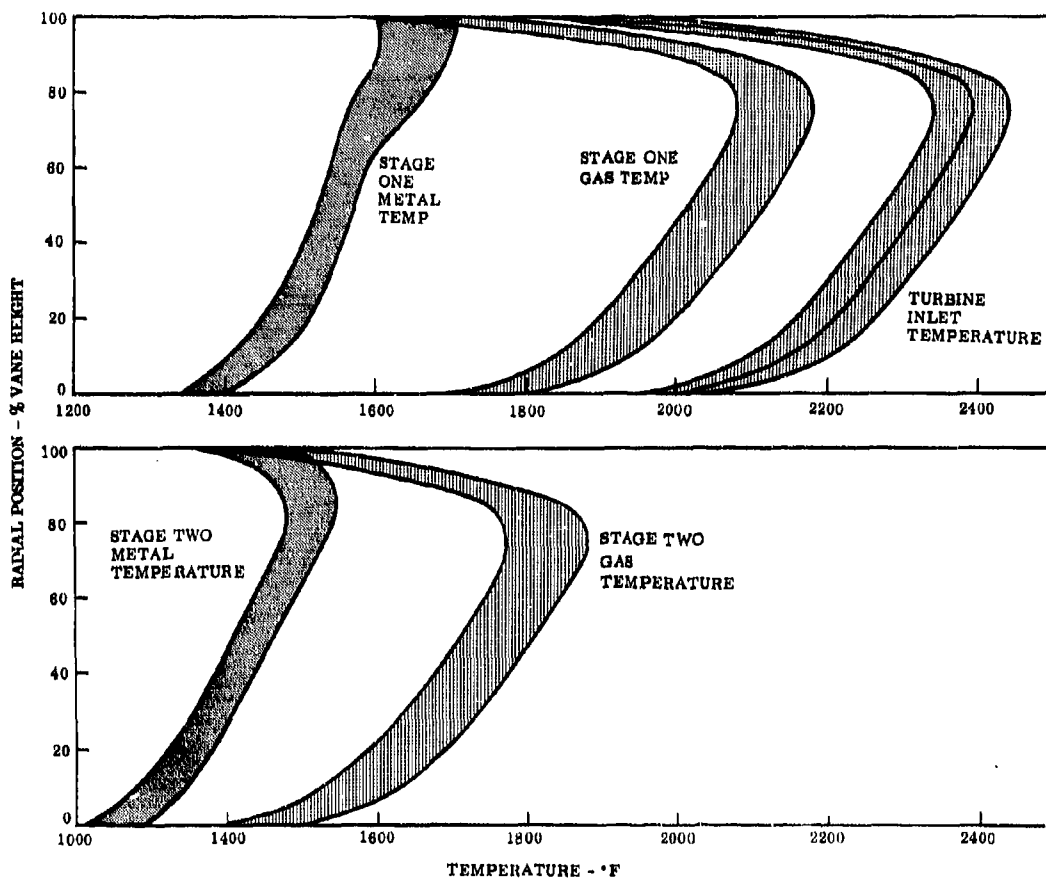
This composite picture on the blades (Figure 4.2-4) shows the range of inlet gas and local gas temperatures seen when integrated circumferentially. The shape of the combustor profile will fall somewhere in the gas profile band and, although the shape may change from engine to engine, the peak values will not exceed the upper limits plotted.

Figure 4.2-5 shows a similar plot for the vanes, but here the combustor tolerance band is wider, since each local hot spot must be considered. Accordingly, the range of anticipated metal temperatures is wider on the vanes than on the blades. It is nevertheless true that the 42-nozzle annular combustor gives substantially better inlet gas temperature patterns than possible with earlier cannular designs.

## CONFIDENTIAL

Figure 4.2-6 shows a typical test section of CJ805, J93 and GE4 combustor temperature patterns. The lines of constant temperature show clearly how much improvement in temperature contour is possible with the newer combustor designs. These improved temperature patterns result in greatly improved turbine stator life and reduced cooling air requirements.

Blade and vane section temperatures for other design conditions are plotted in Figures 4.2-7 and -8. Thus, the average section temperatures and percentage cooling flows for each of several important operating points is observed. A tolerance band comparable to that shown in Figures 4.2-4 and -5 should be added to these average values to obtain the predicted range of metal temperatures for these new flight points. The Mach-2.7, 85,000-foot, idle, flight point is not plotted since it is too low in temperature to be of comparative interest. Turbine inlet temperature for this condition is 882°F, while compressor discharge temperature is 855°F.



**Figure 4.2-4 GAS TEMPERATURE - METAL TEMPERATURE PROFILES - BLADES.** The Mach-2.7 turbine inlet temperature profile is plotted together with the local gas temperature bands and the average section blade metal temperatures. The range on gas and metal temperature reflects the design variation in combustor profile.

**CONFIDENTIAL**

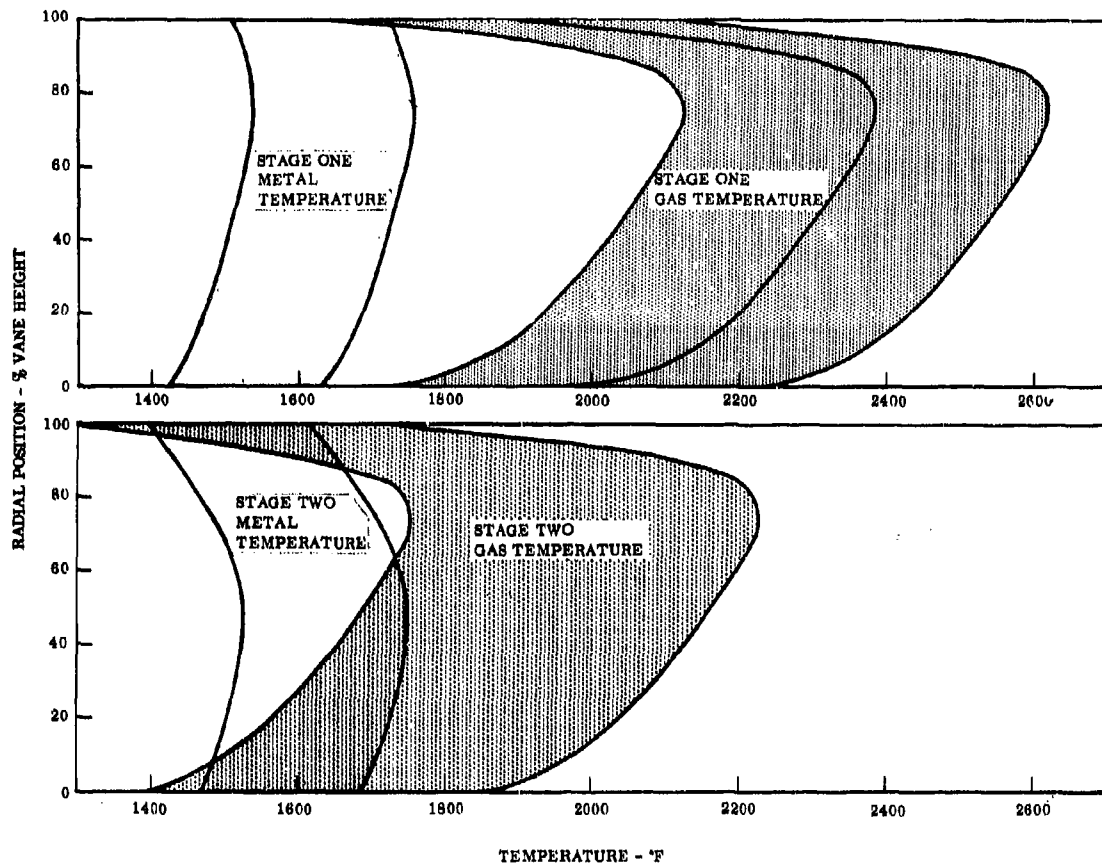
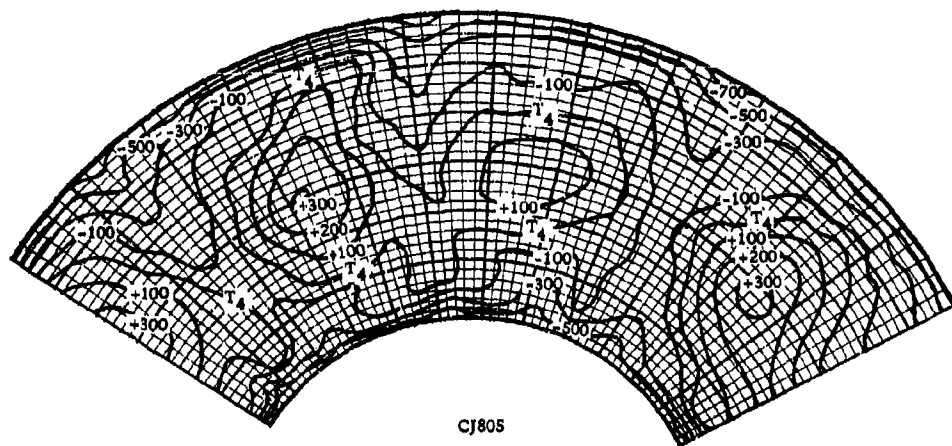
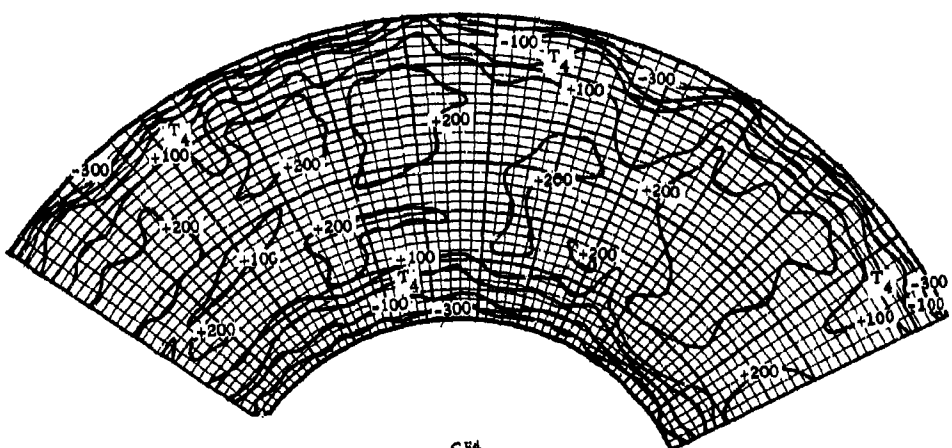


**Figure 4.2-5 GAS TEMPERATURE - METAL TEMPERATURE PROFILES - VANES. M2.7**  
Turbine gas and metal temperature profiles are plotted to show the range of predicted levels. The stationary vanes are subjected to a wider range of temperature variation than the buckets.

**CONFIDENTIAL**



CJ805



GE4

**Figure 4.2-6 TURBINE INLET GAS TEMPERATURE PATTERN.** Plots of full-scale test data compare the CJ805 and GE4 combustor temperature patterns encountered by the first-stage nozzle vanes. The cannular combustor shows the 10-fuel-nozzle pattern and has relatively steep circumferential temperature gradients. The GE4 pattern is more evenly dispersed in the center portion and has an even radial temperature distribution at the inner and out surfaces.

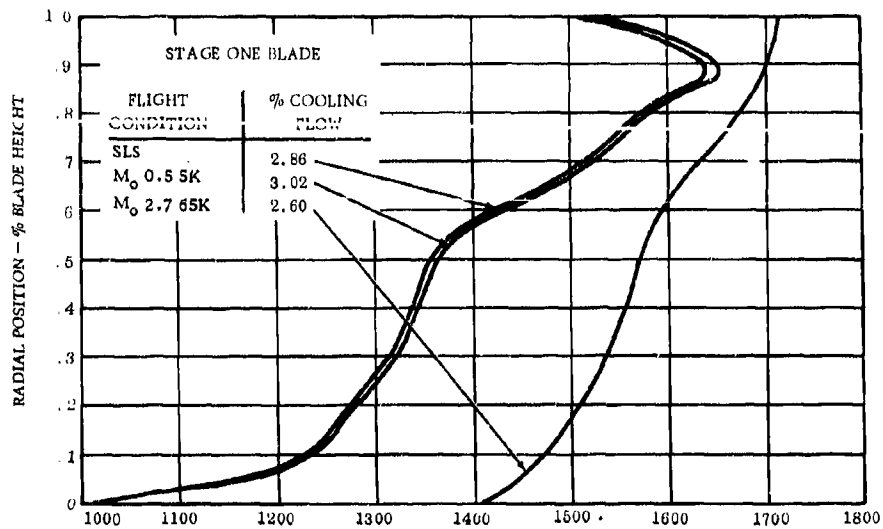


Figure 4.2-7 SECTION METAL TEMPERATURE SUMMARY - BLADES. Radial temperature distribution plots showing the average area metal temperature distribution predicted for various flight conditions. Percentage coolant flows through the first-stage blades are also shown.

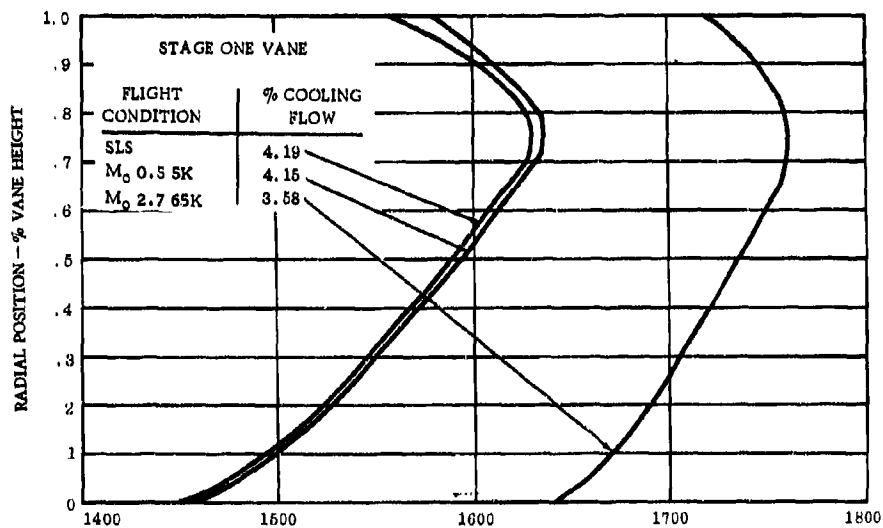
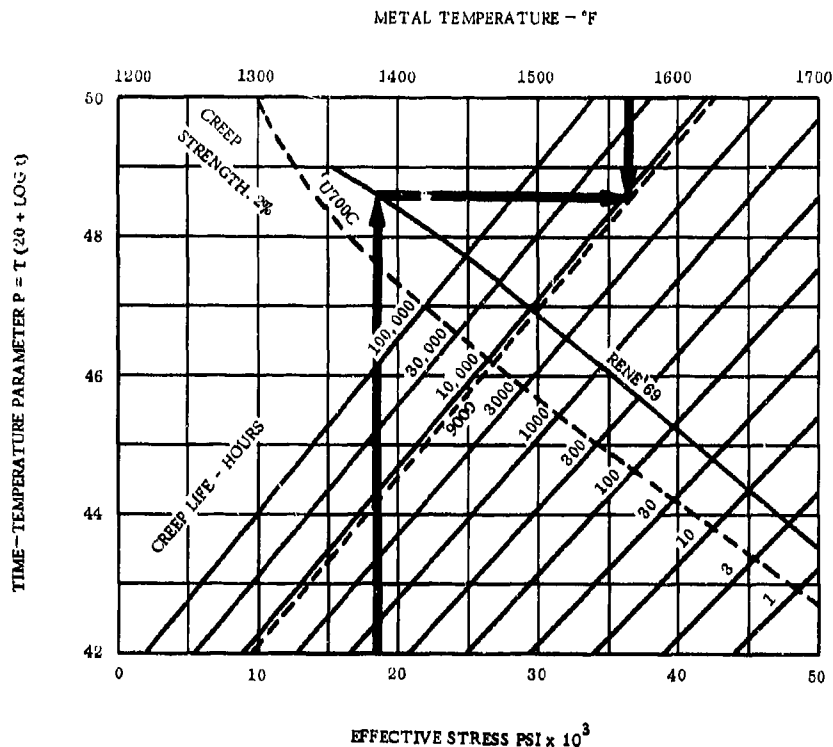


Figure 4.2-8 SECTION METAL TEMPERATURE SUMMARY - VANES. Average area weighted metal temperatures for the first-stage vanes for various flight points. Percentage coolant flows at each flight point are tabulated.



#### 4.2.2 LIFE

The component-life capability listed under paragraph 4.2 refers to a wide variety of life-limiting wearout modes. Each component, for example, must withstand all of the wear and failure modes including erosion, corrosion, hot corrosion, oxidation, low-cycle fatigue, mechanical fatigue, surface contact wear, yield, creep and rupture. The designers objective is to make creep the life-limiting factor in his design. Creep which results in airfoil untwist or in measurable radial growth is predictable and easily monitored. It is, therefore, desirable that all other life-limiting factors fall outside of the creep-life limits. Figure 4.2-9 shows the manner in which stress and metal temperature are related to creep life on the blades.



**Figure 4.2-9 STRESS-TEMPERATURE-LIFE.** Plot relates stress and metal temperatures to creep life. Creep life is predicted on the basis of this graph by following the intersection that effective stress makes with the blade material curve, along a constant parameter (P) line to the predicted metal temperature. The intersection of temperature and parameter denotes the creep life of the design. Effective stress in the case of turbine blades is the centrifugal stress divided by 0.7 for unshrouded blades and 0.85 for shrouded blades. These corrections account for the effect of chordal temperature gradients on airfoil creep life.

This kind of a plot is useful in determining the effect that changes in stress or temperature have on life-limited parts, as well as the effect that changes in materials can have on component life. It is possible, for example, to construct the creep life summary curves of Figure 4.2-10 from Figure 4.2-9 with the stresses of Figures 4.3-14 and temperatures from 4.2-4.

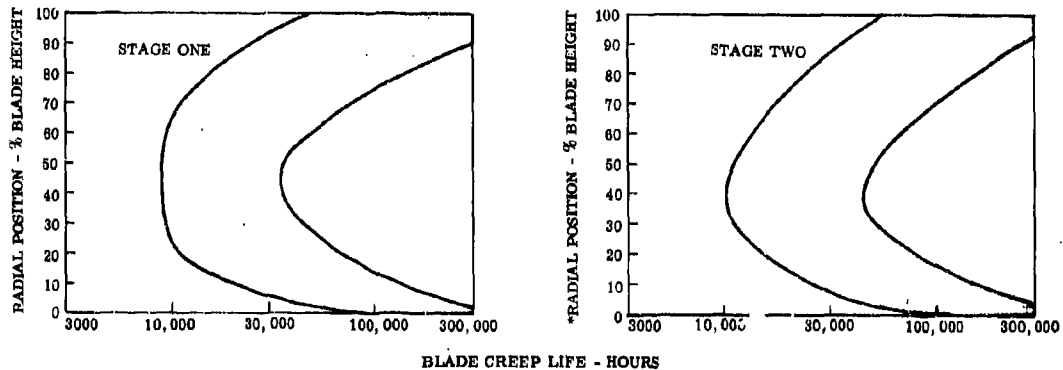


**Figure 4.2-10 BLADE CREEP LIFE SUMMARY** - The creep life range at each section is shown for both stages of blades. Cooling airflow rates that will achieve metal temperature levels required for a minimum life of 9000 hours are selected. The 9000 hours at the Mach-2.7 temperature level is equivalent to 12,000 hours of typical route-structure operation. Metal temperatures from Figure 4.2-4 are used with Figure 4.2-9 to determine creep-life for the René 69 blades.

To the extent possible, the cooling air is distributed along the airfoils to try to obtain a constant-life airfoil, so that the design is balanced and best use is made of the available cooling air.

Most of the turbine has unlimited life. This is true because air cooling makes it possible to cool the main structure of the design to the point where creep or rupture are not design-limiting factors. This means that the disks, spacer and shaft become prime reliable structures with temperatures that are almost independent of gas stream temperatures and with lives that far exceed design requirements. Figure 4.2-11 plots Mach-2.7 rotor temperatures in some detail. From the stresses that exist at each of these points a cross-plot of resultant lives can be made. Figures 4.2-12 and -13 depict this resultant life picture. This picture shows that the prime reliable structural parts have extremely long design lives during which dimensional stability, balance, leakage and performance are not effected in the 36,000-hour life span.

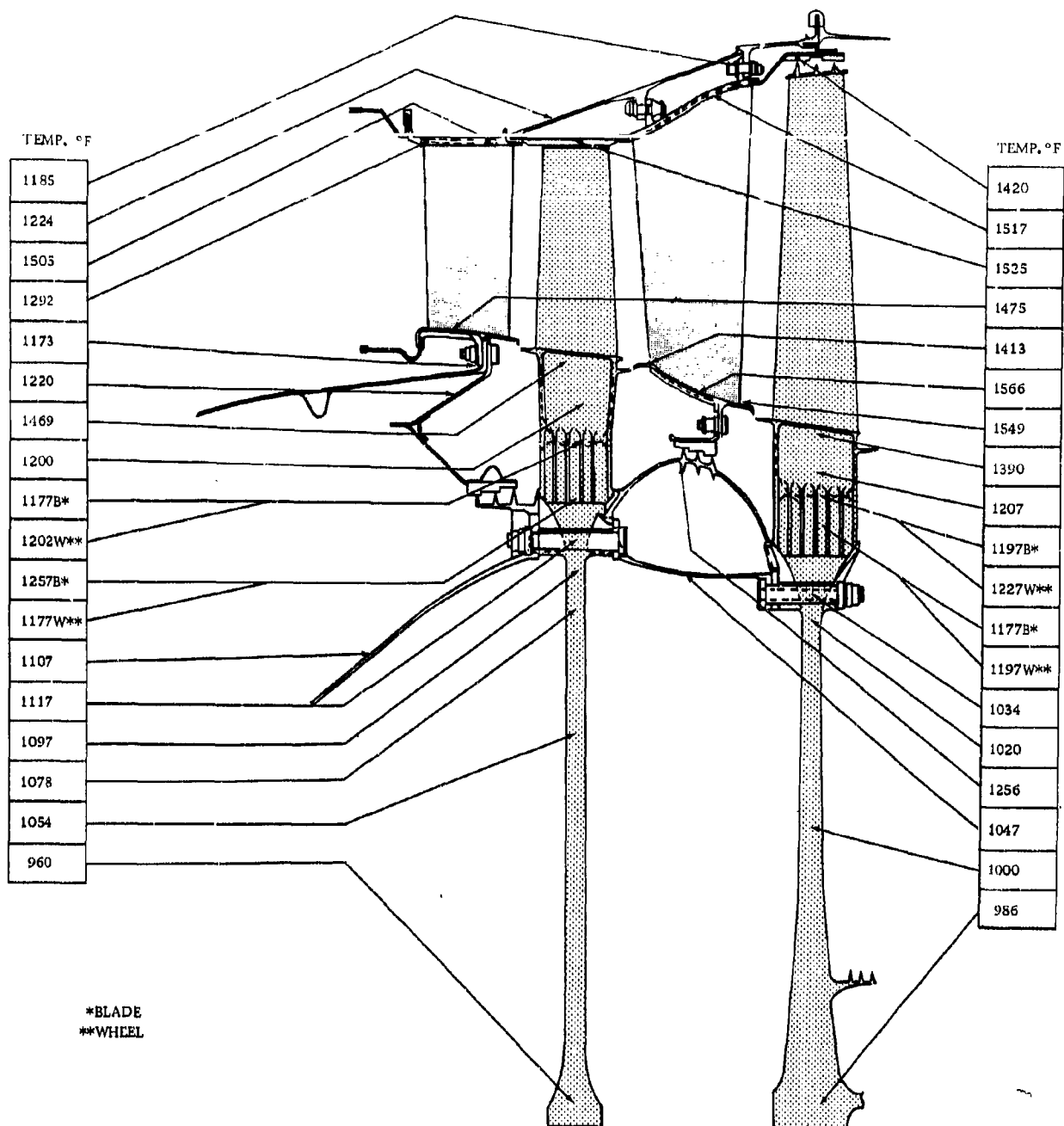


Figure 4.2-11 TURBINE TEMPERATURES - Mach-2.7 25,000 FEET. Detailed plot of Predicted cruise metal temperatures show the uniform distribution and low gradients in the GE4 turbine.

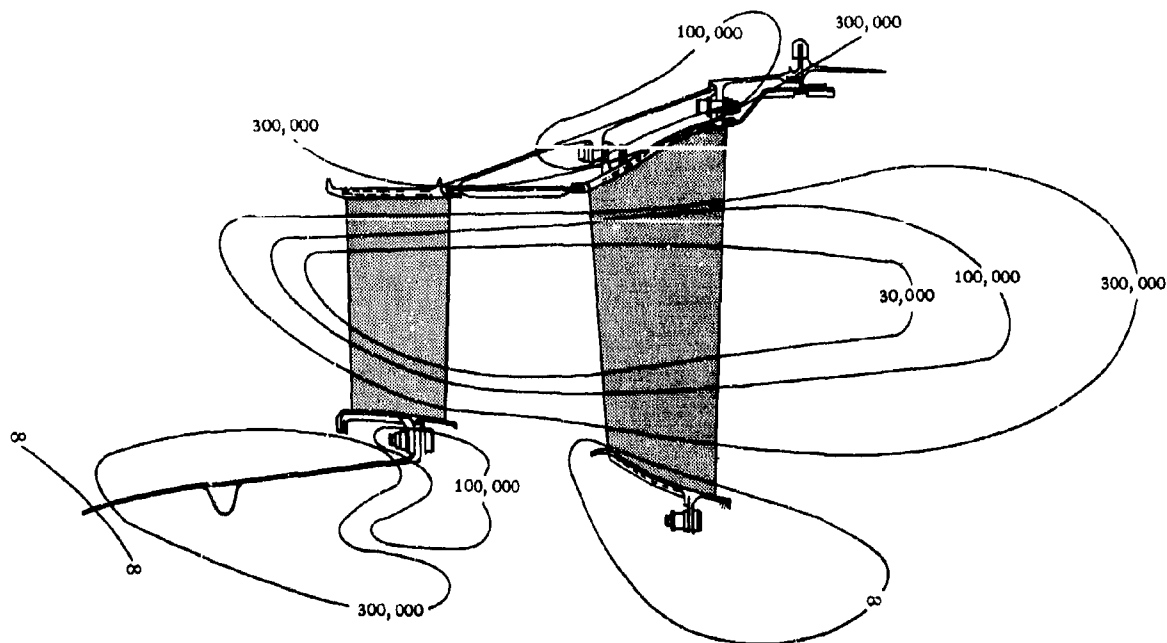


Figure 4.2-12 STATOR ASSEMBLY LIFE PLOT. Lines of constant creep life are identified.

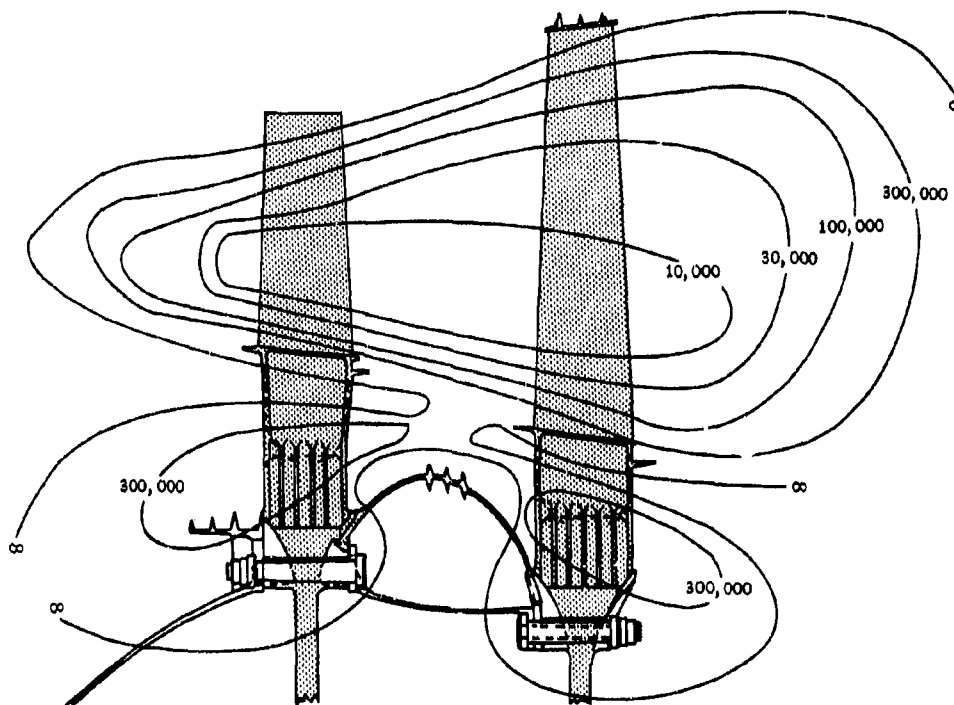


Figure 4.2-13 ROTOR ASSEMBLY LIFE PLOT. Temperature levels assure long life on prime reliable rotor components.

### 4.3 DESIGN DESCRIPTION

The following descriptive information covers the turbine stator, turbine rotor, turbine cooling system and related maintainability, quality and durability factors.

#### 4.3.1 TURBINE STATOR DESIGN

Figure 4.3-1 shows the turbine stator in cross-section. Key features that make possible its inherent simplicity, durability and maintainability include:

- Replaceable vanes. Bolted attachment makes replacement easy and eliminates band thermal stress
- No weldments, brazed-assemblies, or sheet metal in the structure of the stator.
- Continuous, cooled, machined rings support vanes, and ensure long-life dimensional stability.
- Smooth abradable shrouds improve performance, minimize blade wear.
- Provides blade containment capability.
- No split-line structural discontinuity. Roundness, clearance and leakage control.

The materials used in the turbine stator are summarized on the drawing in Figure 4.3-1. Vanes are coated with aluminum diffusion coating, Codep, to resist erosion, corrosion, and oxidation.

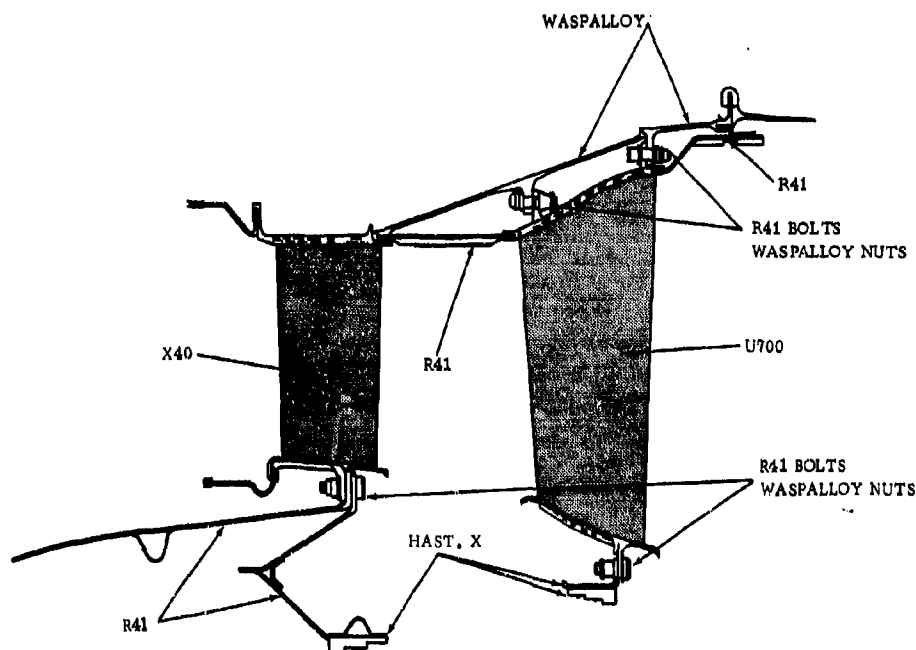


Figure 4.3-1 TURBINE STATOR LAYOUT. Cross-section drawing of the GE4 turbine stator showing details of the continuous ring, replaceable vane, stator system.

## CONFIDENTIAL

The edges of shrouds and seals that ride in retention grooves are sprayed with wear-resistant coatings of nickel aluminide. These soft coatings prevent wear and provide tight seals at interfaces where cooling air leakage might otherwise be a problem.

Figure 4.3-2 shows the first-stage diaphragm assembly of the GE4 engine. Each individual vane is bolted to the load-carrying inner cone, which is designed to maintain the concentricity and dimensional stability of the assembly. The second-stage diaphragm assembly is pictured in Figure 4.3-3 together with the continuous support ring that holds the vanes in precision alignment. Both the outer support ring and the first-stage inner cone ring respond quickly and uniformly to transient temperature changes, giving close clearance control and resulting performance advantages.

The manner in which the transient growth of the stator matches the radial movement of the rotor is an important design feature of the GE4 turbine. Figure 4.3-4 is a summary plot of the important turbine clearances during acceleration and deceleration transients. The curves show two key points.

- Response characteristics of the rotor and stator are well matched. There are no points of severe inequity between rotor growth and stator growth where radial interferences could cause heavy rubs or restrict the rates of transient engine operation.
- Take-off and cruise clearances are close but consistent with build-up tolerance and maneuver excursion requirements.

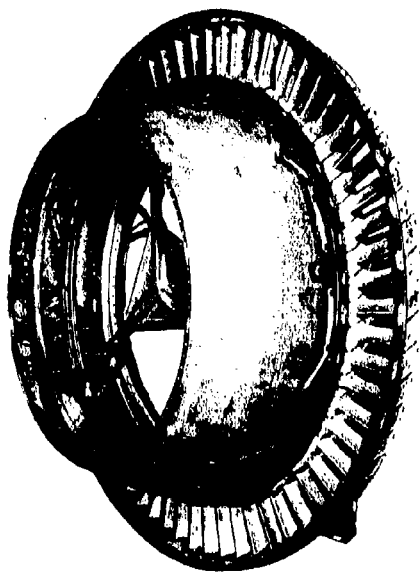


Figure 4.3-2 STAGE ONE TURBINE NOZZLE ASSEMBLY - Photograph of the GE4/J5 stage one turbine stator assembly prior to initial development engine testing.

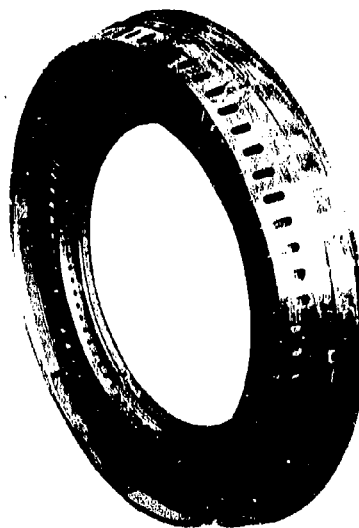


Figure 4.3-3 STAGE TWO TURBINE NOZZLE ASSEMBLY - View of the second stage GE4/J5 turbine vane assembly before buildup into the first development engine.

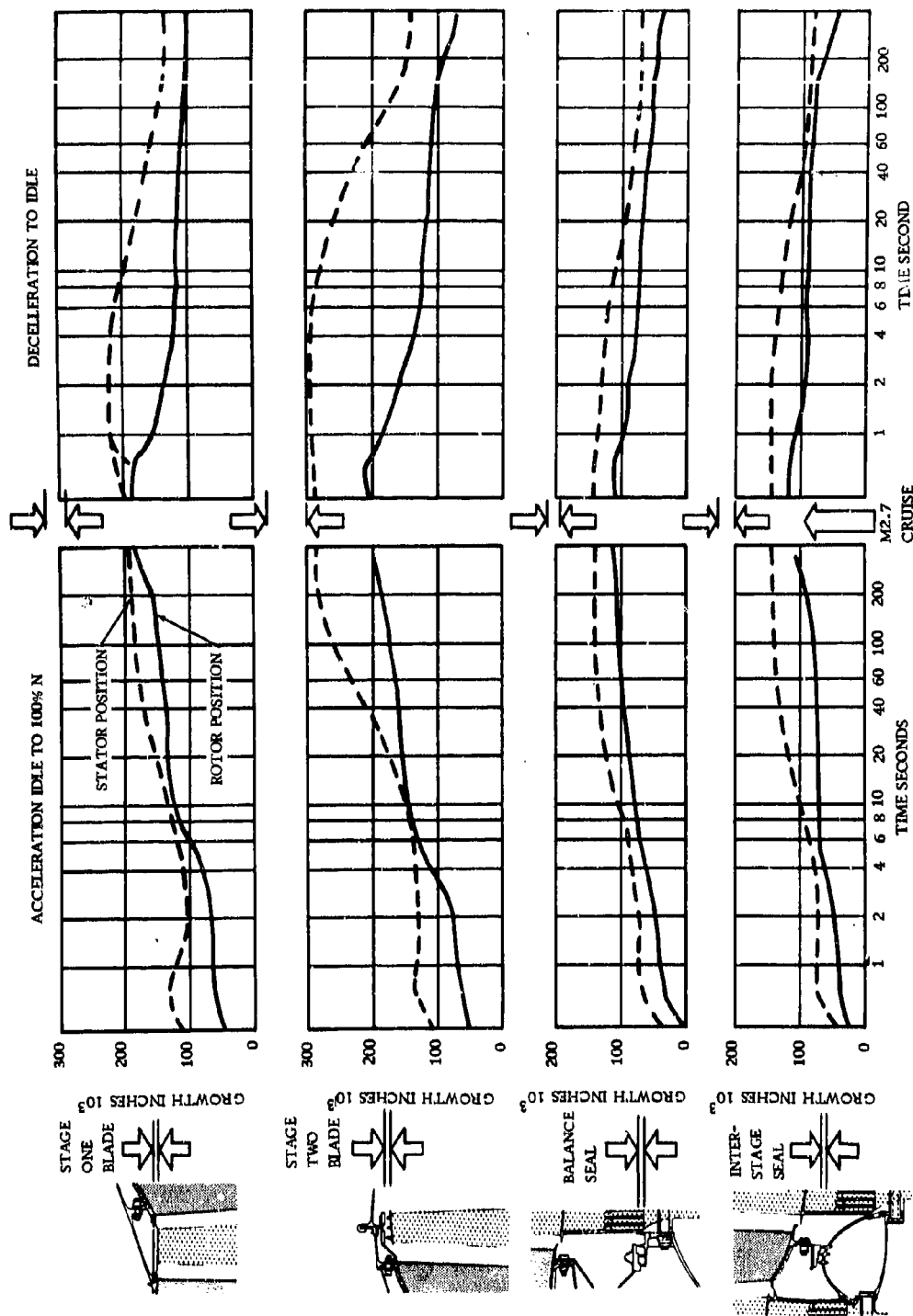


Figure 4.3-4 TURBINE RADIAL CLEARANCE SUMMARY. Plots of transient and cruise radial clearances in the GE4 turbine. The turbine cooling system is designed to make the response of the stator match that of the rotor. This feature is a key item in the maintenance of close cruise clearances and high performance levels.

## CONFIDENTIAL

The clearances predicted here are actually closer than those used in the performance section, Volume III-A, Section 5.3. There would be no difference if the turbine were perfectly round and concentric. Performance clearances, however, relate to nominal values with reasonable out-of-round assumptions, while the clearances shown in Figure 4.3-4 are calculated on the basis of nominal values with round and concentric components.

### 4.3.1.1 Turbine Vanes

Figure 4.3-5 shows cutaway views of the vanes. The exposure shows the internal cooling flowpath and the strong spar-like structure of the airfoil. Internal passages are sized to give high internal velocities and good convection cooling. All internal webs and holes are cast to size with precision molded insert cores. Dimensional reliability is assured. The drawings show the row of internal holes just behind the leading edge through which the forward cavity cooling-air flows. This air impinges on the inside of the leading edge, and cools it before it is discharged out of the side film holes.

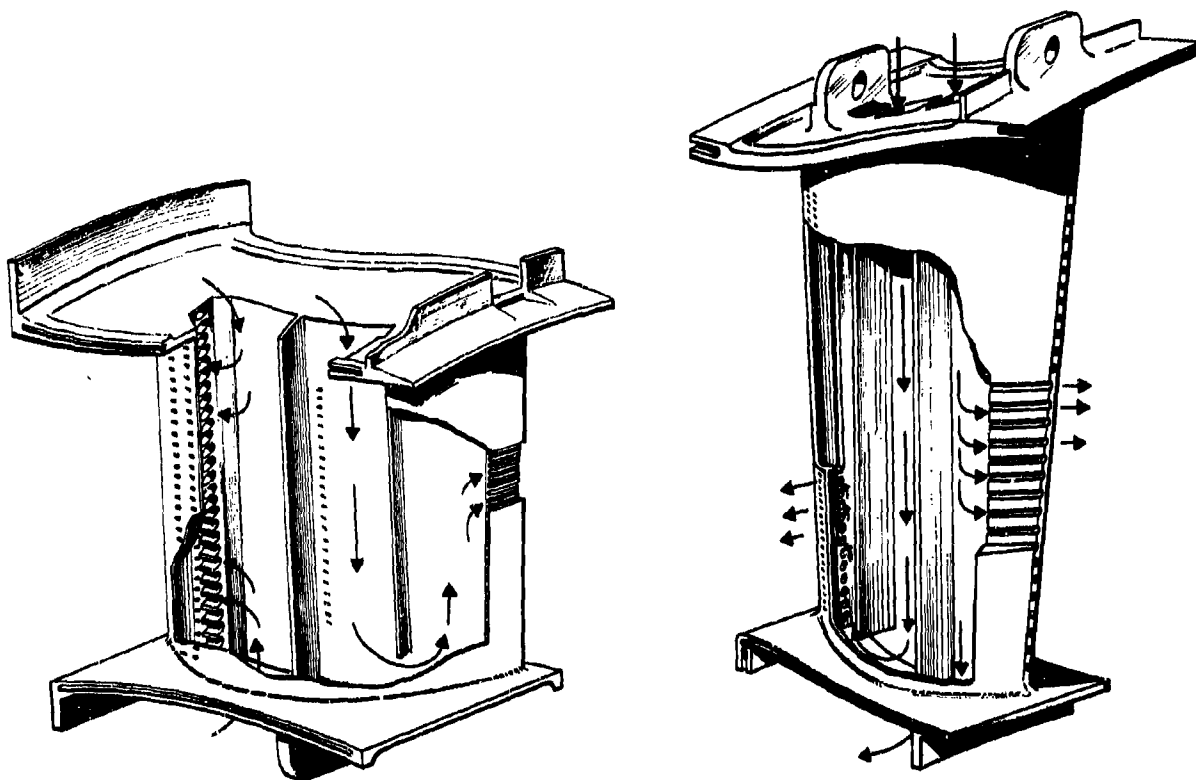


Figure 4.3-5 TURBINE VANE. Cutaway drawings show the interior passageway configuration and the coolant flow-path of the first- and second-stage nozzle vanes. Precision casting techniques ensure uniformity and quality of the cooled stator vane.



The holes out the sides of the leading edge are machined at an angle with the surface of the finished casting. These film or gill holes are simultaneously drilled with accurate electrical discharge machining techniques described in more detail in Section 4.5.1.

Temperatures of the vanes at take-off and cruise conditions are shown in Figure 4.3-6. Lines of constant temperature show the temperature levels and temperature gradients present in the pitch sections of the stator vanes. Figure 4.3-7 shows these lines of constant temperature as viewed on the surface of the unfolded airfoil. Temperatures in both Figures 4.3-6 and 4.3-7 show the temperatures predicted in the hottest section of the gas profile.

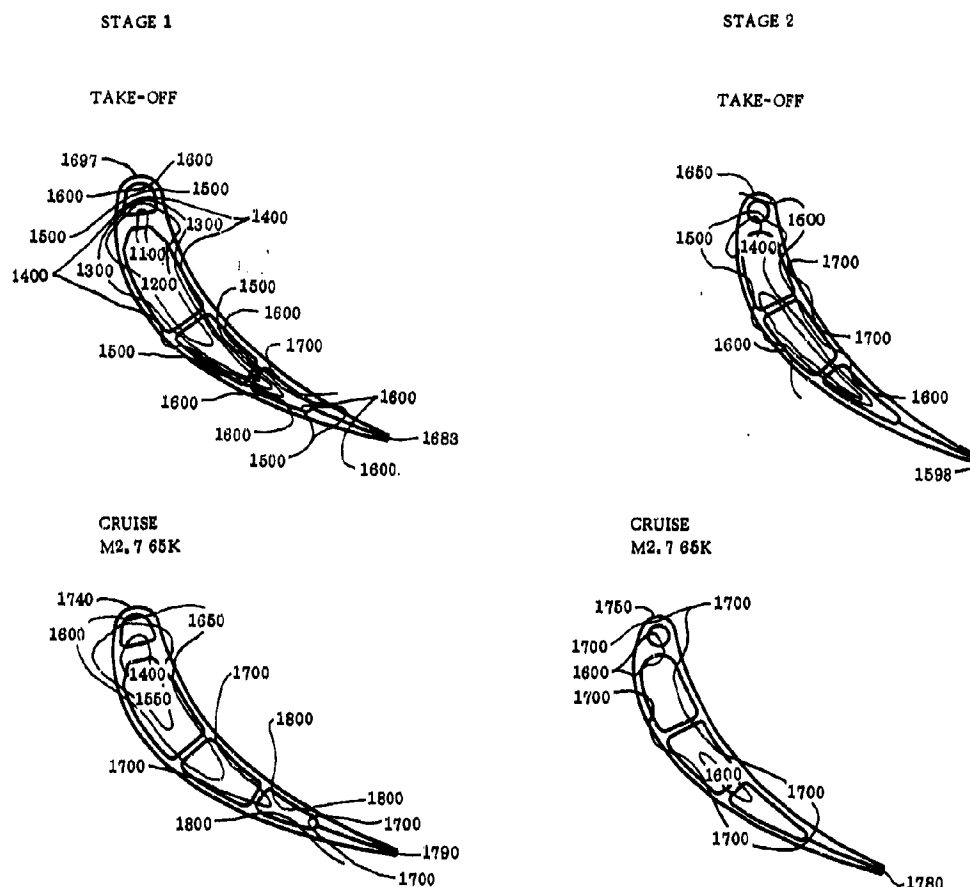


Figure 4.3-6 TURBINE VANE SECTION TEMPERATURE. Pitch section temperatures as seen at the hottest portion of the gas stream. (See Figures 4.2-5 and 4.2-6.)

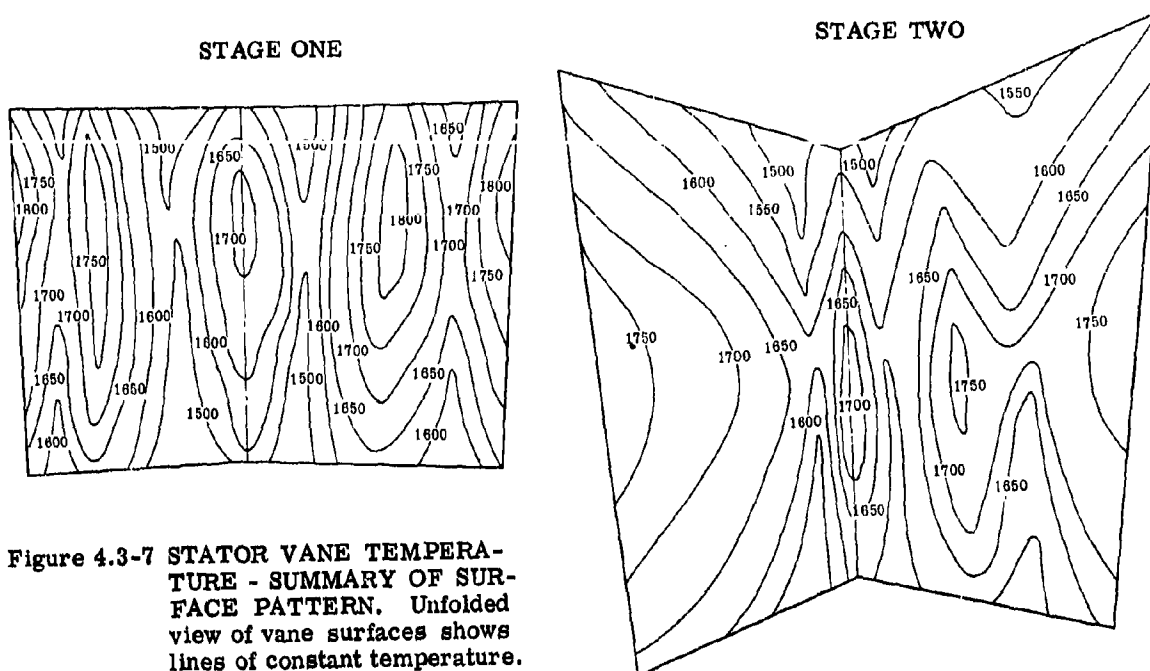


Figure 4.3-7 STATOR VANE TEMPERATURE - SUMMARY OF SURFACE PATTERN. Unfolded view of vane surfaces shows lines of constant temperature.

#### 4.3.1.2 Stator Shrouds

Smooth-surfaced shrouds over the tips of the rotating blading provide important turbine performance advantages. (Refer to Volume III-A, Section 5.3.) These abrasion-resistant shrouds cut down secondary performance losses and allow for closer running clearances than would otherwise be possible if light tip-rubs during off-design operation were not permissible. Figure 4.3-8 is a close-up of the shrouds showing the wear surface and the simplified design of the backing member.

The rub surfaces of the shroud are made of a sintered-wire matrix designed to localize the heat generated during transient blade rubs. The surface must also withstand the oxidation and erosive effects of thousands of hours of service response. Rubs, when they occur, should wear the shroud surface rather than the blade, since the change in tip clearance area is more than three times (pi-times) as high with blade wear as it is with shroud wear.

Figure 4.3-9 shows the wear test facility on which the full-speed blade-rub tests and shroud evaluations have been made. Dozens of shroud structures and material combinations have been tested on this facility. Controlled depths of interference and rates between the shroud test specimen and blade tip are possible at speeds which duplicate the GE4 conditions. Figure 4.3-10 shows a deep 0.050-inch rub in the material selected for one of the GE4 shroud designs. This shroud is the powder-filled, sintered-wire matrix shown in Figure 4.3-8. The rub is deeper than any anticipated in the actual engine. There is no evidence of temperature distortion of the backing or distress in the bond with the backing. There was no measurable wear on the tip of the blades.

Besides good rubbing characteristics, the shrouds must tolerate long-time exposure to oxidation and erosion effects. Special laboratory tests have been designed to measure the effect of oxidation and erosion on the various material under consideration. Figure 4.3-11 shows sample

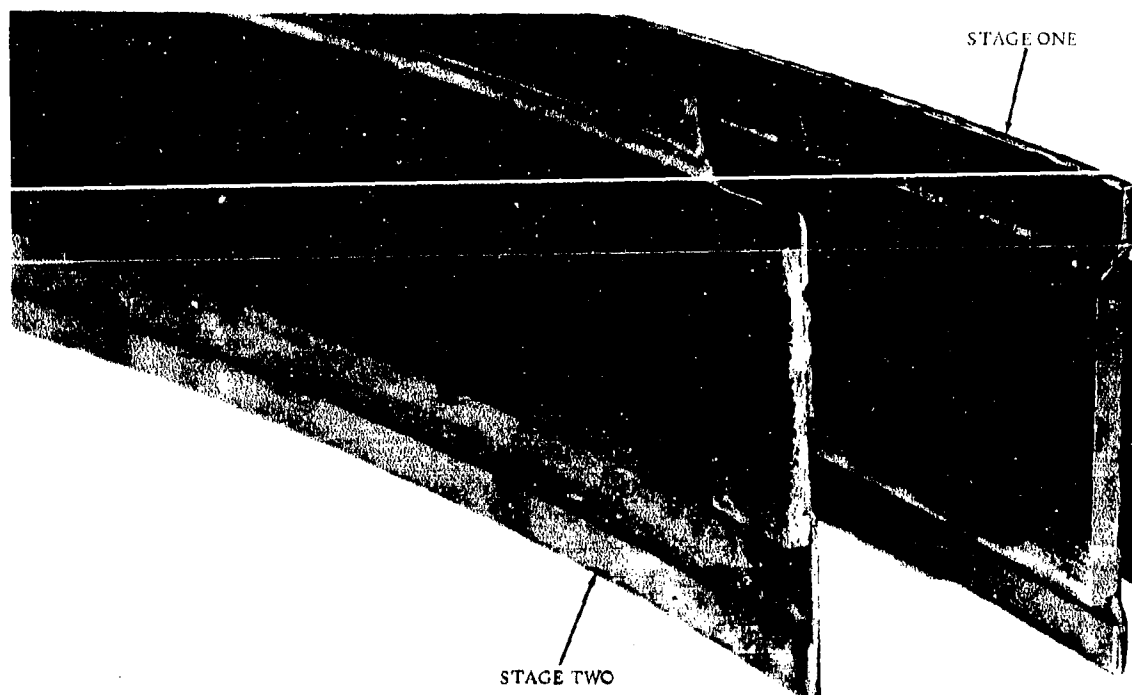


Figure 4.3-8 STATOR SHROUDS. Smooth surfaced abrasible shrouds permit close blade-tip clearance and high turbine performance. Tip-rubs occurring during maneuver or transient conditions do not harm the blades or depreciate performance.



Figure 4.3-9 SHROUD RUB FACILITY. Full speed, controlled rub test facility for wear studies and smooth shroud development.



Figure 4.3-10 SHROUD RUB TEST PANEL. Sintered-wire abrasible shroud after 0.050-inch deep intentional blade rub.

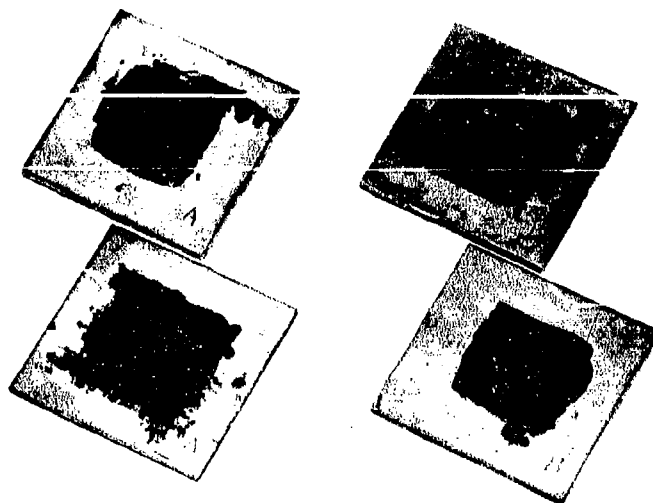


Figure 4.3-11 OXIDATION AND EROSION TEST PANELS. Laboratory test panels show very little effect from extra severity oxidation and erosion test exposure. Several thousands of hours of engine running are simulated in a few hours of controlled flame-tunnel testing.

sections after exposure to these wear-out tests. Oxidation tests are run first at temperatures that exceed engine conditions (1450°F) by several hundreds of degrees. The panels are then subjected to a controlled blast of 50-micron alumina particles to simulate extended service-life exposure to the erosive effects of the combustor gas stream. Results show the GE4 shrouds to have good balance between the requirements of rubbing capability and oxidation/erosion resistance.

#### 4.3.2 TURBINE ROTOR DESIGN

The GE4 turbine rotor is shown in cross-section in Figure 4.3.12. Simplicity of design is obtained by minimizing the number of parts, eliminating separate or loose pieces, and combining functions wherever possible. There is no sheet metal in the structure. There are no points of surface contact where premature wear will foreshorten the full service life.

This prime reliable design is patterned closely after the CJ805 and J93 turbine, and includes all the features which make the J93 design an advancement in both temperature capability and inherent reliability. The entire assembly is simply supported between bearings. The structural torque spacer is protected from the hot gases by the low-stressed catenary heat shield. The blades are held in pairs in the deep slot dovetails. The blade shanks, which completely enclose the cooling air in a leak proof chamber, isolate the wheel rims from the gas stream temperatures. The twin shanks also provide damping to help maintain low vibratory stresses. The side plates on the shanks eliminate loose baffles and provide a smooth surface on the rotor rim to minimize pumping losses.

The rotor assembly is held together by close-tolerance dowel bolts, a design technique that has proved to be thoroughly successful in the CJ805, and that has achieved recognition from the airline



service shops for its superior balance stability. In the GE4 turbine, the dowels are tapered to ease the alignment and assembly - disassembly forces, but are otherwise the same as the CJ805 bolts. There is no hand fitting or line reaming at assembly. In the rim region, only the heat shield has rabbet fits; hence, there are no critical rabbet fits to complicate assembly or to require rework after long-time service.

The rotor consists of few elements, and based on CJ805 experience, will require little maintenance or overhaul. Dovetail wear has never been a problem on the CJ805. Stresses in the GE4 dovetails are only 60 percent of the CJ805 stresses. Stresses on the compressor/turbine spline are about half of the CJ805 levels, and spline wear is not expected ever to be a GE4 life-limiting problem. Seal teeth are designed so that necessary rework caused by foreign objects passing through the teeth, will not necessitate replacement of any of the seal members. All sheet metal, such as baffles, have been eliminated from the rotor to minimize the number of parts which can wear.

Figure 4.3-13 summarized the materials selected for the turbine. Materials that provide the highest margin of design safety factor without extension of today's material technology are used. There have been no manufacturing difficulties in making the GE4 turbine parts in any of the materials selected.

The concept of a design based on best past practices, coupled with well developed materials, working well within their capabilities of stress and temperature, gives assurance of the durability and reliability of the GE4 turbine rotor.

The structural elements of the turbine rotor are designed to conventional CJ805 and J93 stress criteria, with the actual stresses in the GE4 falling below either the CJ805 or the J93. Figure 4.3-14 shows the stress levels in the wheels and blades, together with various material strength curves. Margins shown are well within those required to demonstrate overspeed capability and prime reliability of the rotor system.

Primary importance is attached to those features in the turbine that are designed to eliminate the problems of low-cycle fatigue. This mode of potential failure deserves closer attention in the long-life rotor design than any other single consideration. Three features are of particular importance in achieving prime reliable design.

- Low radial temperature gradients. Transient and steady-state temperature differences between the rim and hub are minimized by the manner in which the wheels are encapsulated by the shaft and spacer in the low-temperature atmosphere of fifth-stage air.
- No web stress concentrations. There are no holes or sharp changes of section in the wheels. The bolt holes are actually extensions of the dovetail slots; not holes in the disc web. (See Figure 4.3-15.)
- No hot wheel rims. Because of the convective cooling effect of the blade cooling air the bilateral stress area of the wheels is thermally isolated almost completely from the hot gas stream. Changes in gas stream temperatures are not sensed by the working portion of the wheel. Transient thermal strains are almost eliminated.

Figure 4.3-16 plots the transient wheel stress picture for the rim and hub of the CJ805 and the GE4. The curves show how rim air cooling serves to reduce the cyclic strain range with the deep slot dovetail concept. The magnitude of the GE4 improvement over the already successful CJ805 design gives confidence that low-cycle fatigue will not be a problem on the GE4 turbine.

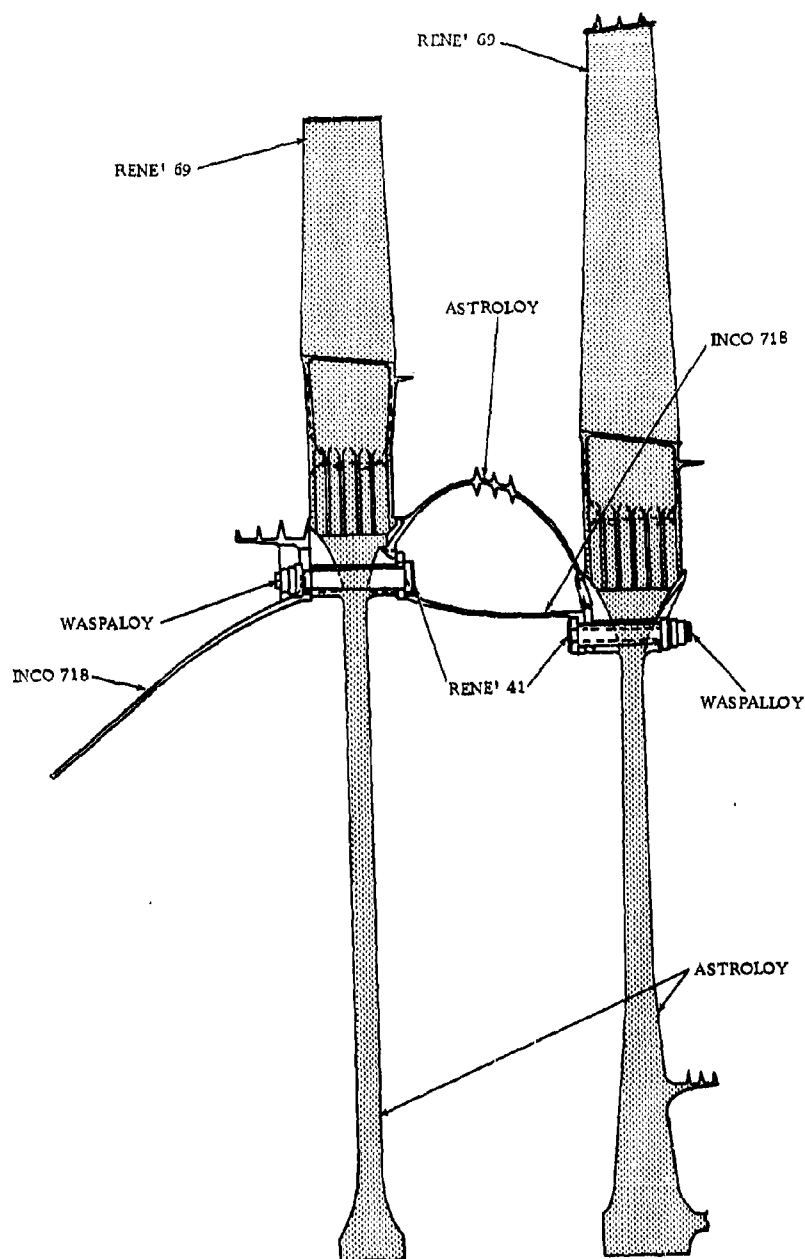


Figure 4.3-13 TURBINE ROTOR MATERIALS

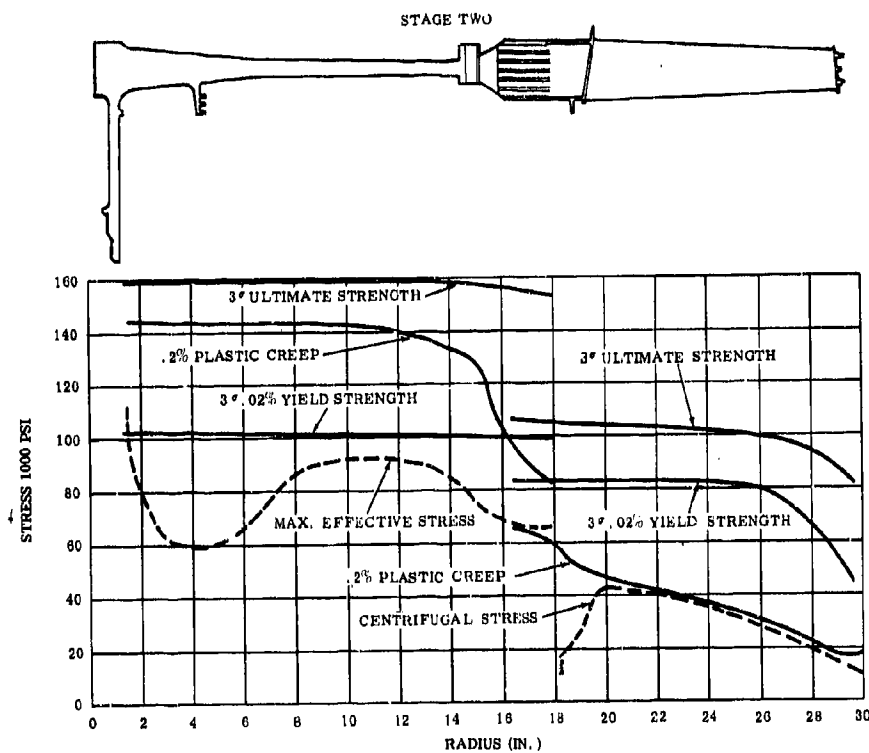
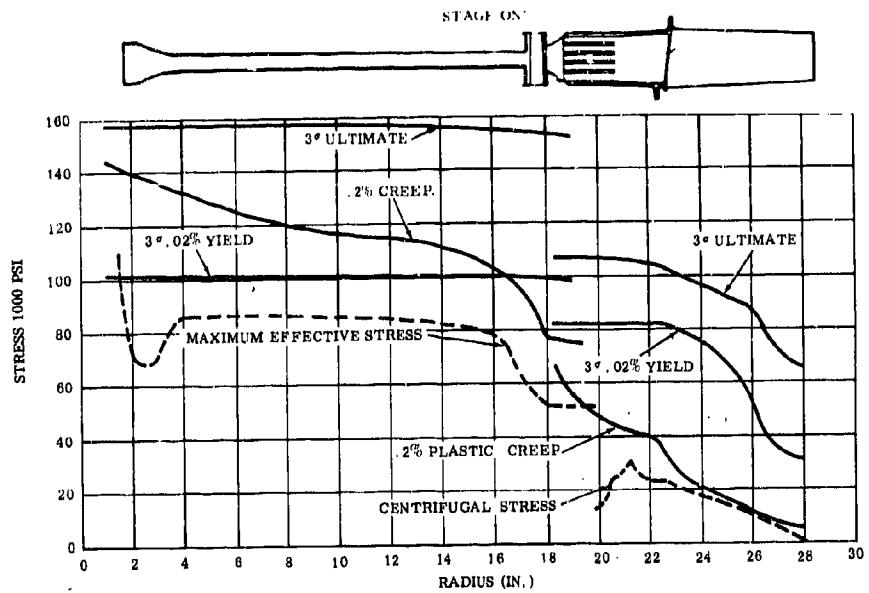


Figure 4.3-14 WHEEL AND BLADE STRESS SUMMARY



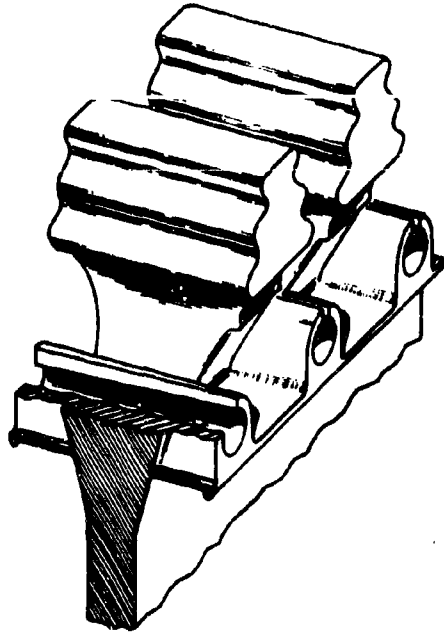


Figure 4.3-15 TURBINE ROTOR RIM DETAIL

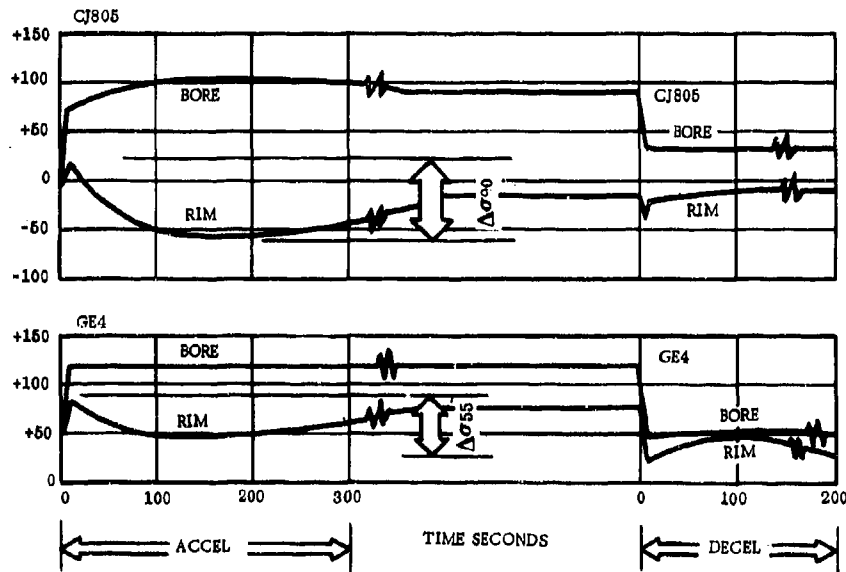


Figure 4.3-16 TURBINE WHEEL CYCLIC STRESS - CJ305 AND GE4 TRANSIENT WHEEL STRESS. Lower cyclic stress is the key to unlimited low cycle fatigue life in the GE4 turbine wheels.

Figure 4.3-17 shows the prime reliable structural portion of the turbine rotor. Simplicity for long-life reliability and easy maintenance is emphasized. With the "marriage" of the bolts with the spacer and heat shield, there are only four structural pieces that require handling during assembly and maintenance.

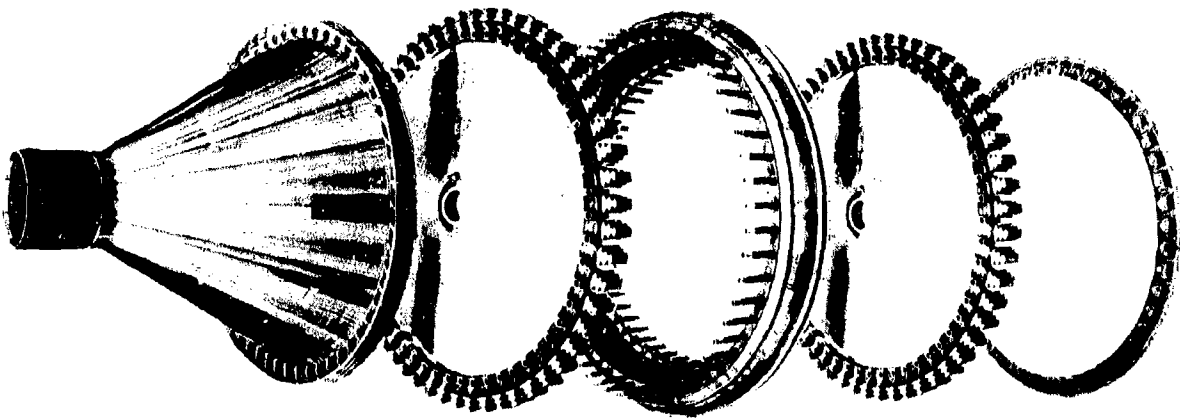


Figure 4.3-17 TURBINE ROTOR EXPLODED ASSEMBLY VIEW. Photographs of the GE4 turbine rotor drum. Fewer parts and large diameter, stiff structure assure ruggedness and durability for thousands of hours of continuous service.

### 4.3.3 TURBINE BLADES

GE4 turbine blades, like the vanes, are precision castings with a ribbed spar section. This design provides important structural beam strength to the airfoil, in addition to forming the cooling path labyrinth. This kind of section offers a maximum of strength and stiffness for a minimum of airfoil weight. Ruggedness of the blading is an important consideration in attaining the long life required. Figure 4.3-18 shows some of the blade details not readily observed.

X-Ray photographs show a side view of the rib structure together with the internal cross-connection passages and edge-cooling holes. Photographs of a cutaway airfoil show the rib and cross-hole pattern. All internal cavities are cast from precision die molded cores. Accuracy and repeatability of the cooling circuit is ensured.

Holes in the surface are machined by advanced electrochemical machining techniques. These electrochemical processes result in stress-free surfaces and smoothly rounded edges, as can be seen in Figure 4.3-18.

A close up view of a cross-section of a hole shows the manner in which the Electrostream process rounds both the entrance and exit edges of the hole. This radius feature plus the stress-free, metallurgically clean surface makes this process ideal for the airfoil film-cooling holes. Tapered holes, ideal from the standpoint of film effectiveness, are easily made by this new process.

Figure 4.3-19 shows a cutaway drawing of the blade with the cooling path defined. Both stages use the same system. There are two circuits. The forward path convectively cools the main airfoil; impingement cools the leading edge and provides the film-flow over the outside surface of the airfoils. The rear circuit cools the trailing edge convectively. Convective, impingement, and film-cooling techniques are balanced to give as flat a temperature profile as possible.

Temperatures at take-off and cruise are summarized in Figure 4.3-20. Temperature levels at take-off are lower than at cruise. Temperature gradients are lower at the cruise operation point. The level of temperature at cruise is the controlling factor as far as the amount of cooling air used is concerned. Cooling flows to the blade are set to give metal temperatures that meet creep life requirements adequately. Figure 4.3-21 is a plot of lines of constant temperatures on the unfolded airfoils of the first and second-stages at Mach 2.7.

#### 4.3.3.1 Thermal Fatigue

Blade thermal fatigue or low-cycle fatigue of the turbine blade edges has received close attention during the design and initial development of the GE4 turbine. Greatly improved analytical techniques and extensive component and engine testing have provided the tools for predicting blade thermal fatigue life with high confidence.

Figure 4.3-22 plots the thermal fatigue life of the leading edge of the first-stage blade as currently predicted.

The distribution of blade life shows the effects of important material property and temperature variables, but it is noted that the average life is 97,000 cycles or 200,000 hours, and the minimum life is 20,000 cycles. These levels of cyclic life far exceed that of today's solid airfoils, and lead to the conclusion that there will be no need for costly edge husking to remove surface cracking on the GE4 blades.

**CONFIDENTIAL**

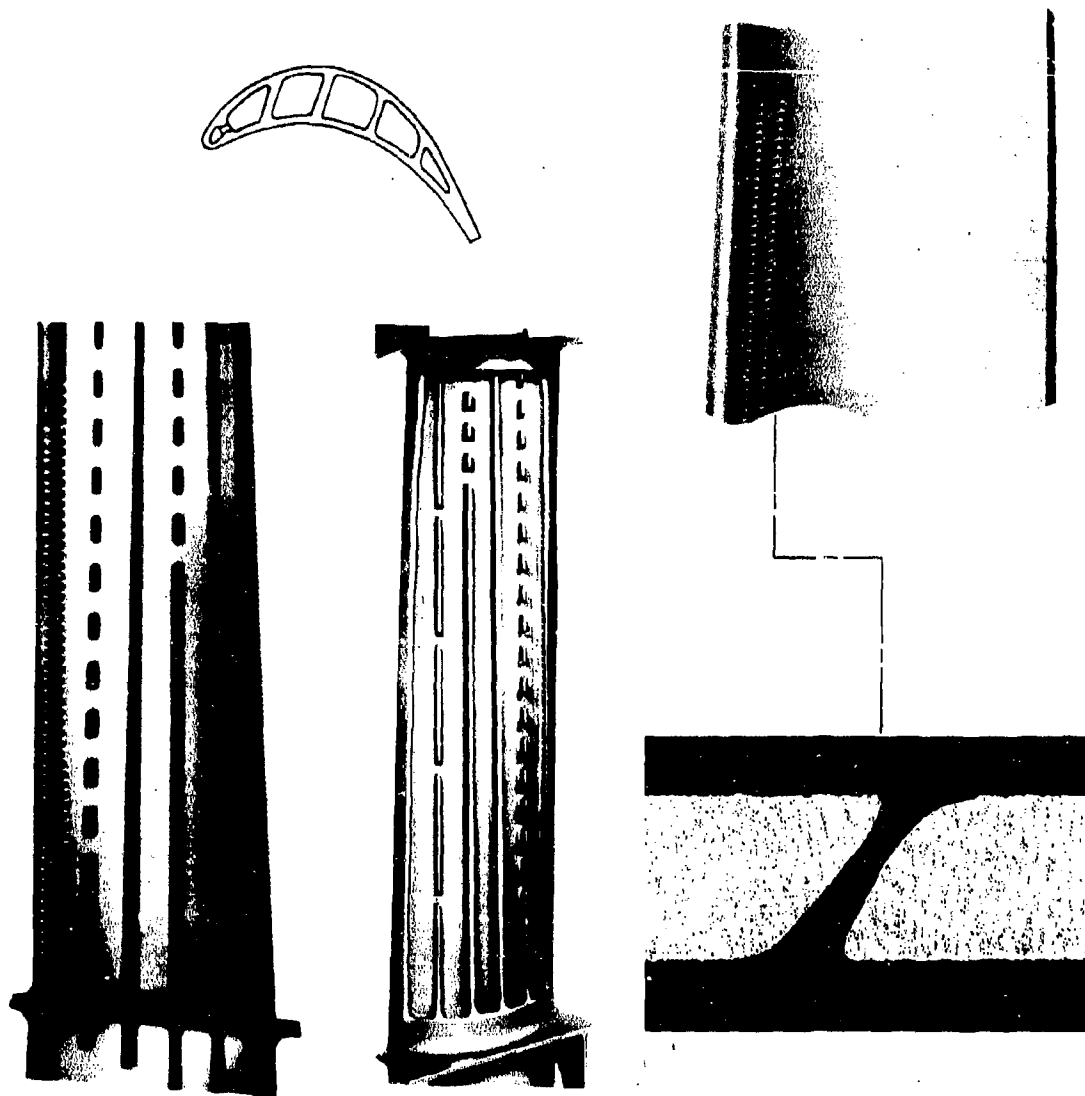


Figure 4.3-18 TURBINE BLADE DETAILS

4-35

**CONFIDENTIAL**

K

**CONFIDENTIAL**

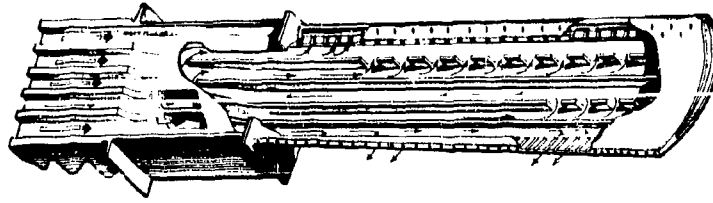


Figure 4.3-19 TURBINE BLADE, CUTAWAY. Cutaway drawings show the interior passageway configuration and the coolant flow path. Convection, impingement, and film-cooling techniques are combined to give very high cooling effectiveness and low temperature gradients.

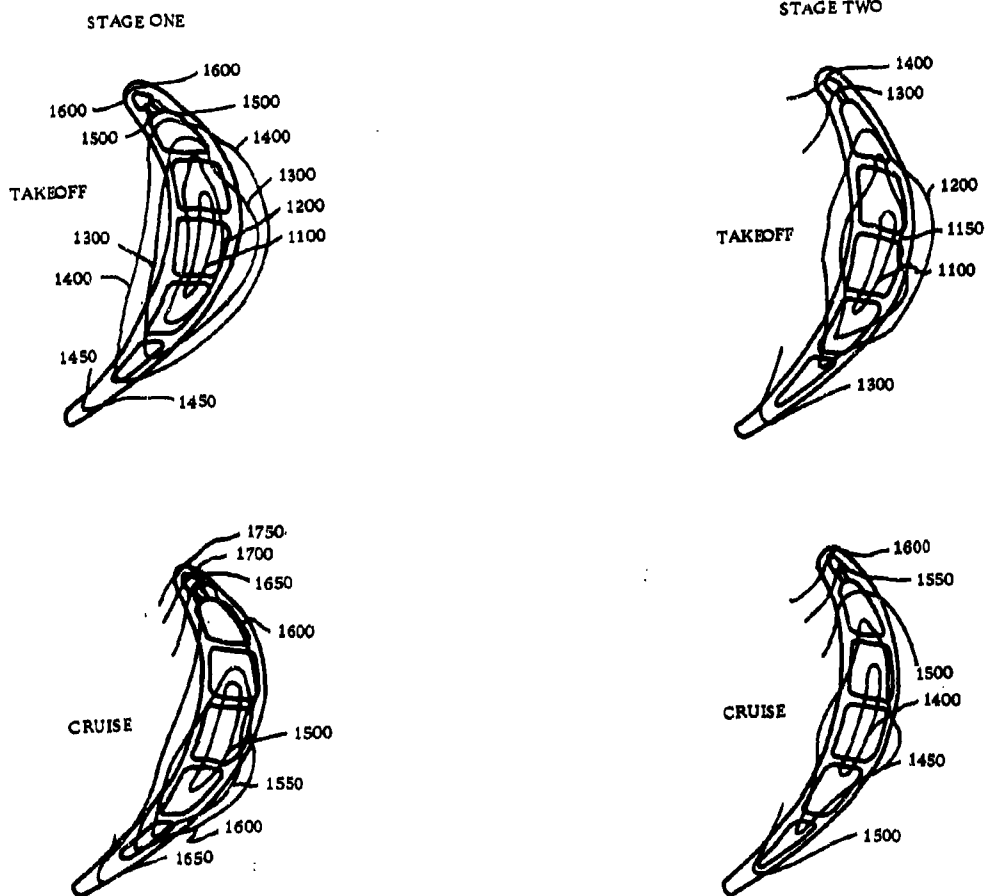


Figure 4.3-20 TURBINE BLADE SECTION TEMPERATURE. Blade section temperature (pitch line) as predicted for the hottest temperature profile limit. Reference Figure 4.2-4

**CONFIDENTIAL**

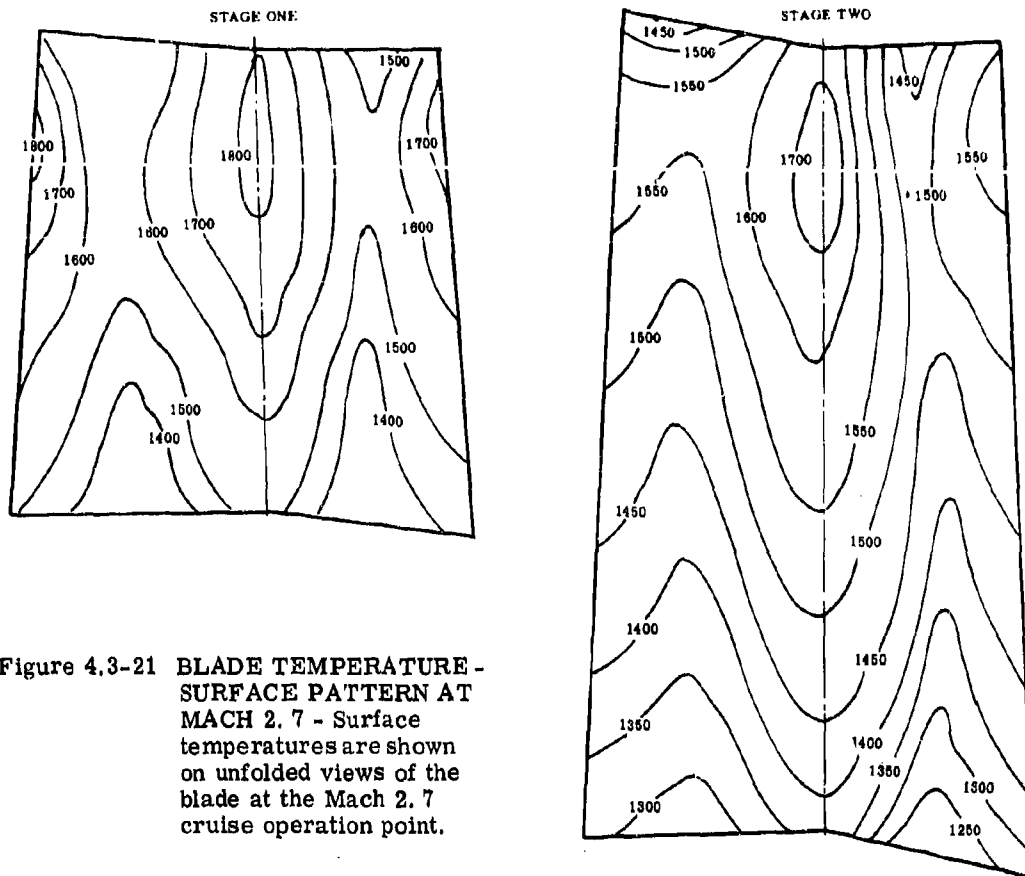


Figure 4.3-21 **BLADE TEMPERATURE - SURFACE PATTERN AT MACH 2.7** - Surface temperatures are shown on unfolded views of the blade at the Mach 2.7 cruise operation point.

In general, air-cooled airfoils are more tolerant of rapid transient operation than are solid blades and vanes. With the same rate of gas temperature change, the metal temperature response rate is slower for the air-cooled blade than for the solid one. Better mass distribution and larger nose radii also work to make the air-cooled blade more tolerant to cyclic operation. Figure 4.3-23 shows a typical example of the transient metal temperature response of the leading edge of the CJ805 and J93/SST first-stage blade.

Temperature differences across each section are the most influential factors in the generation of stresses that can cause low-cycle fatigue cracking. These temperature differences reverse during normal start and stop operation, and cyclic strains result. The magnitude of the temperature differences, together with geometry effects and material properties, set the fatigue life level of each design. Figure 4.3-24 compares the leading edge to mid-chord temperature differences for the CJ805 and the J93/SST. Note that the range of temperature change is smaller for the air-cooled airfoil than for the solid design. This is illustrative of the effect that slower response rates and internal cooling have on the air-cooled design. It is these effects that lend confidence that the GE4 blades will have thermal fatigue lives that exceed the best of the current solid-blade designs.

PROBABILITY DENSITY FUNCTION  
FOR TURBINE BLADE LEADING EDGE  
CRACKING

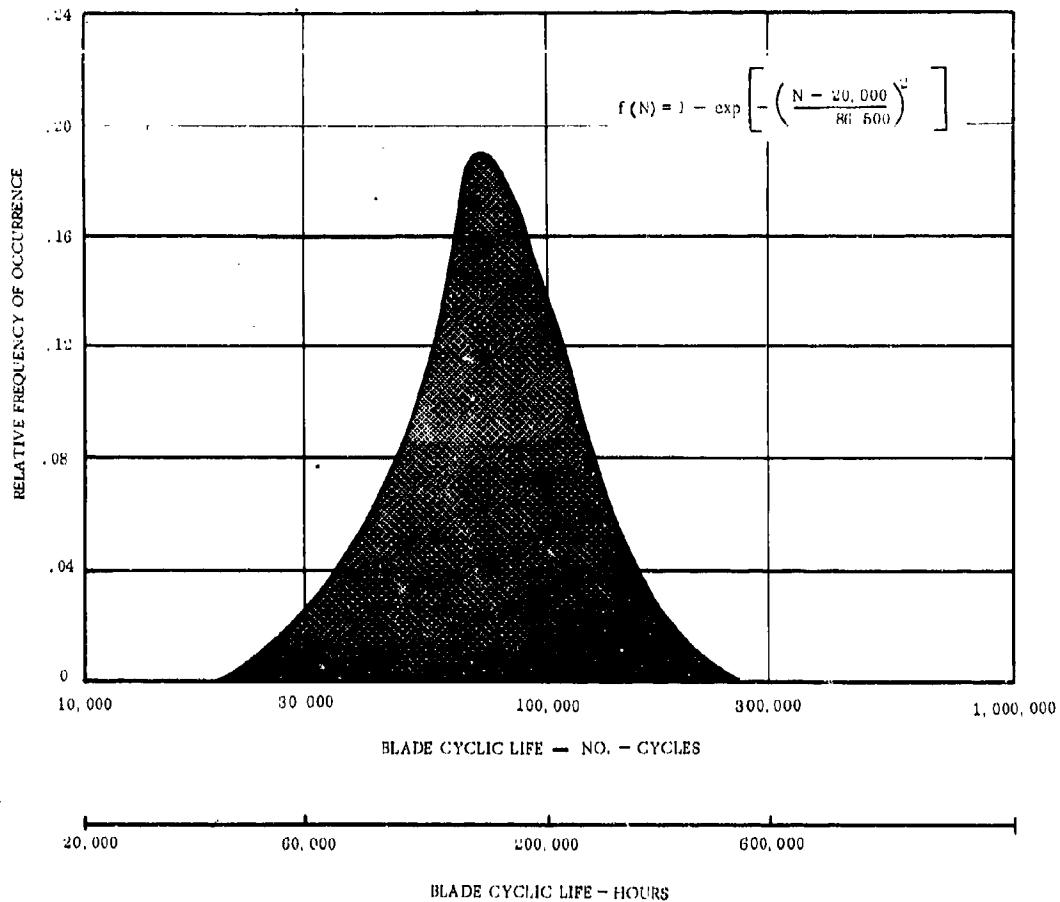


Figure 4.3-22 **BLADE CYCLIC LIFE.** First-stage blade cyclic life distribution plot showing the predicted range of crack-free edge life. Chart shows the distribution of the point of crack initiation predicted by statistical analysis of the full spectrum of important life limiting variables. Minimum life is 20,000 cycles against a design objective of 7000 cycles.

Figure 4.3-25 is a plot of leading-edge temperature response on the J79/CJ805 blade before and after a design change to reduce the severity of the cyclic thermal strain. Cracks were observed at 1000 cycles before the change. Since the change was made, more than 6000 cycles have been run without any edge cracking. Analytical techniques predicted failure on the original blade at 883 cycles and unlimited life on the new design. Figure 4.3-26 shows the original CJ805 blade after 1000 cycles of operation. This cracking started in the range of 800 cycles as predicted by the analysis.

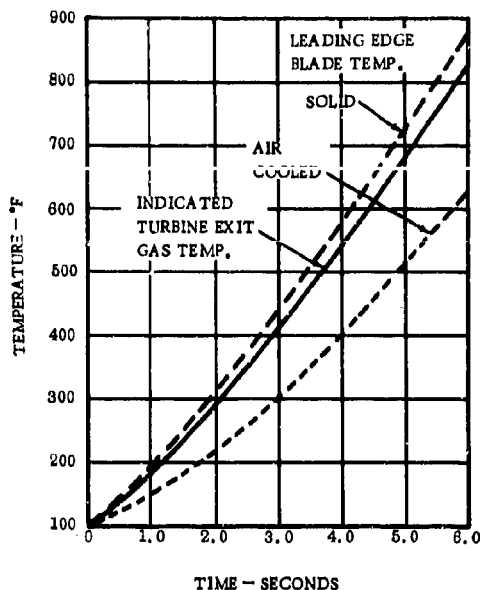


Figure 4.3-23 METAL TEMPERATURE RESPONSE - SOLID VS. IMPINGEMENT COOLED LEADING EDGE. Blade leading-edge metal temperature response rate for both the solid CJ805 and film/impingement cooled J93/SST designs. Because of the cooling effect, the air cooled design responds slower than the un-cooled solid design. Slower transient response means lower cyclic stresses and longer low-cycle fatigue life.

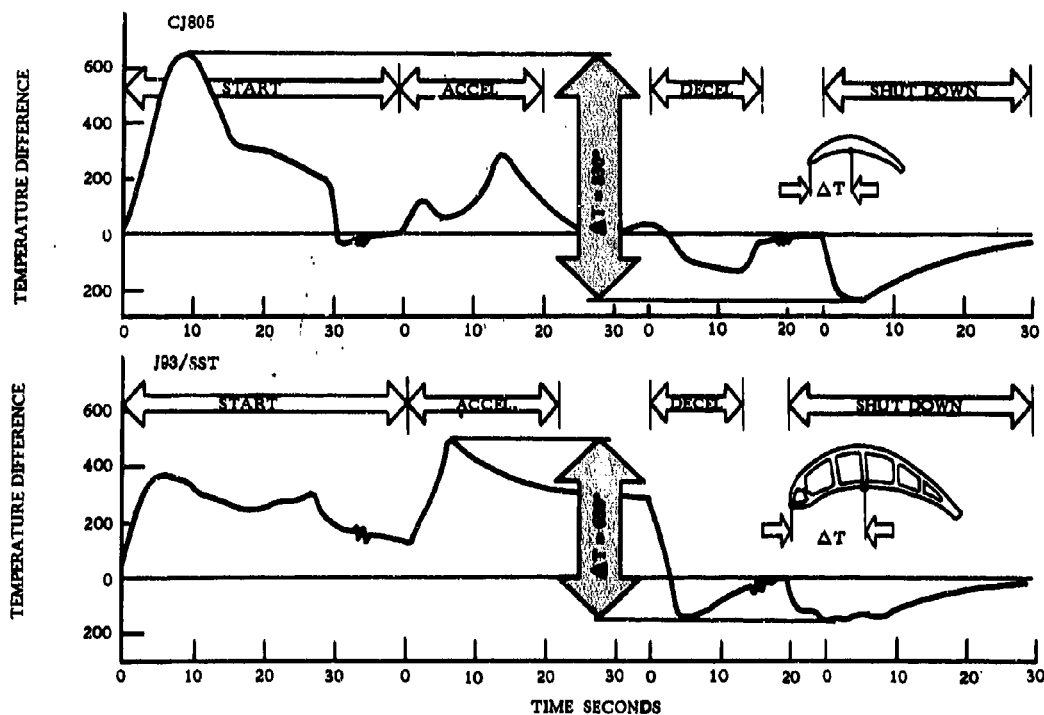


Figure 4.3-24 EDGE TO MIDCHORD TEMPERATURE DIFFERENCES. The maximum temperature difference between the leading edge and the midchord of a solid and air cooled design are compared. Slower edge response rates relieve the starting severity on the air cooled blades.



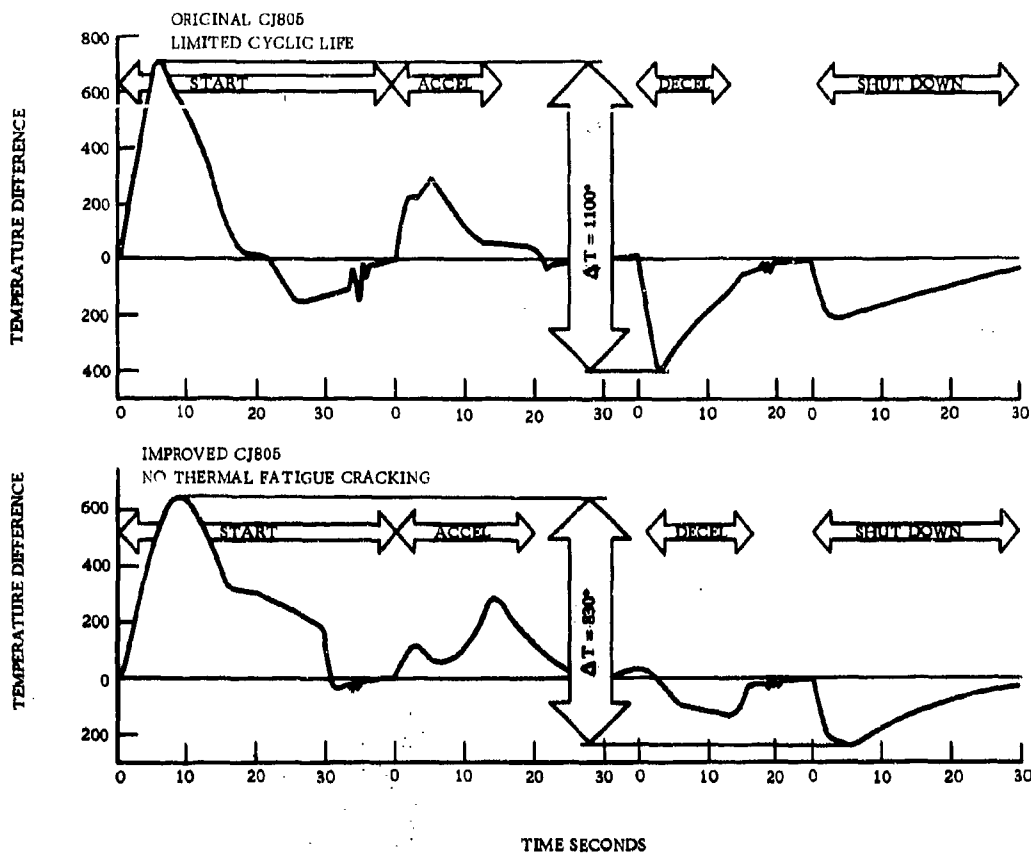


Figure 4.3-25 THERMAL STRESS TEMPERATURE TRANSIENTS ON SOLID BLADES. The original CJ805 had cracks requiring rework at about 1000 cycles. Reducing the severity of the temperature transients eliminated the cracking. Important analytical correlations made here provide confidence in GE4 thermal fatigue prediction capability.

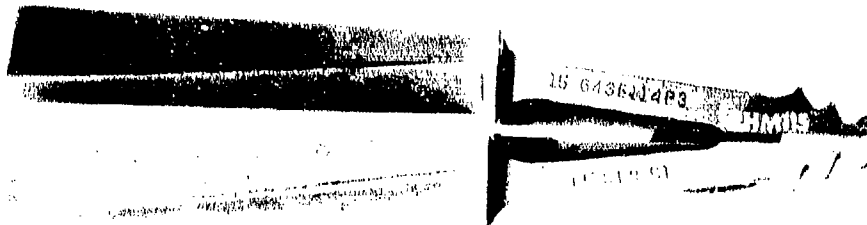


Figure 4.3-26 CJ805 BLADE THERMAL FATIGUE. View of the leading edge of the old CJ805 blades showing cracking observed after 1000 cycles. Cracks are predicted to occur at 883 cycles.

Figure 4.3-27 summarizes some of the key data used in the analytical prediction of thermal fatigue life of the CJ805, J93/SST and GE4 blades. The table compares calculated life with running experience.

	MATERIAL	CRITICAL TEMP. $T_c$	ENDURANCE LIMIT E	STRESS RANGE $\sigma_e$	ELASTIC MODULUS	MATERIAL DUCTILITY % RED. OF AREA	PREDICTED CYCLES N	OBSERVED CYCLES
ORIGINAL CJ805	U500C	1241	35.0	134.5	23.5	12.0	883	800
REVISED CJ805	U500C	1207	37.5	93.5	23.7	11.4	$\infty$	NONE OBSERVED
J93/SST	U700C	1723	26.4	116.5	21.3	11.8	444	540
GE4	R89	1548	37.5	79.8	23.6	6.6	26,660	--
GE4	R89	1548	37.5	79.8	23.6	13.2	117,640	---

Figure 4.3-27 THERMAL FATIGUE CRACK PREDICTION - SUMMARY OF KEY DATA

Test experience has shown that crack initiation in a variety of blade configurations, acceleration gradients, gas temperatures and materials closely match analytical predictions. Moreover, with the analytical correlation extra-severity testing to foreshorten test time is a legitimate approach to initial testing on new designs.

The J93/SST testing represents this kind of extra-severity testing. Figure 4.3-28 shows a pair of blades that have been run through 1000 engine transients. Fluorescent-penetrant inspection showed that initial edge-cracking started at about 500 cycles. This matches the predicted life of 444 cycles very closely. The same prediction analysis shows the GE4 blade life to be 26,660 cycles. On this basis, the J93/SST running is 50 times more severe than the GE4, as far as thermal fatigue is concerned, and it can be said that important long-life thermal fatigue assurance testing has already been accumulated. (Refer to Section 4.4.3.3).

Figure 4.3-29 summarizes the transient stress conditions on which the cyclic life predictions of Figure 4.3-22 are based. These transients are representative of normal operating conditions and average engine performance. As engine acceleration rates change, or as material properties or engine temperature levels vary, the cyclic life of the blade varies. Figure 4.3-20 shows how the cyclic life changes with each of these variables. All these variables are statistically considered in the cyclic life distribution plot of Figure 4.3-22.

It is concluded that for normal and extremes of engine operating conditions and material properties, thermal fatigue cracking of the edges of the blades will not be a problem on the GE4 turbine. This conclusion does not preclude extensive component and engine testing of production blading, for it is on these tests that the final assurances will be obtained.

**CONFIDENTIAL**

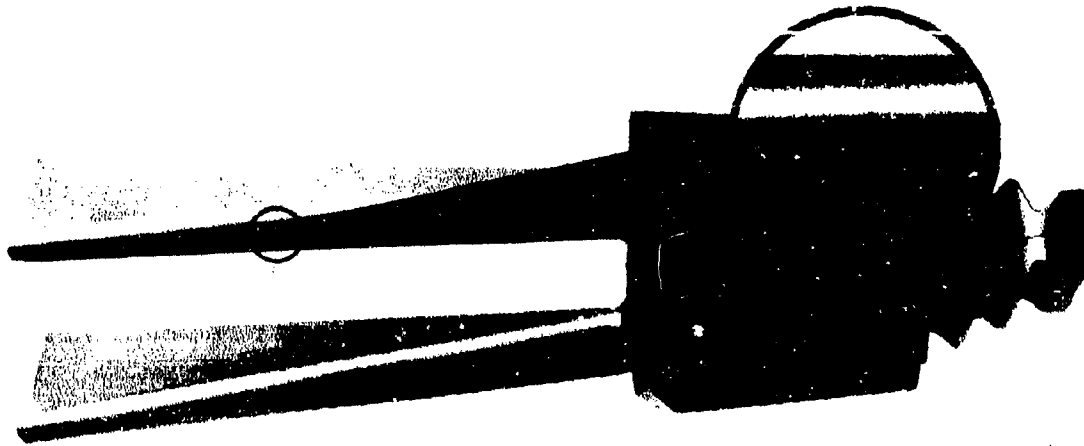


Figure 4.3-28 J93/SST CYCLIC TEST BLADES. Film-cooled blades like the GE4 blades after 1000 rapid cycles of transient engine operation. Crack initiation has started in the predicted range of 450 to 500 cycles.

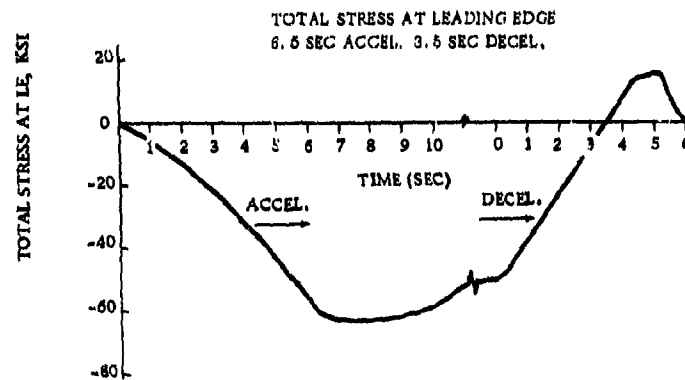


Figure 4.3-29 GE4/J5 TRANSIENT SUMMARY. Calculated stress transients are plotted for typical repeated route-structure operation.

4-42

**CONFIDENTIAL**

K

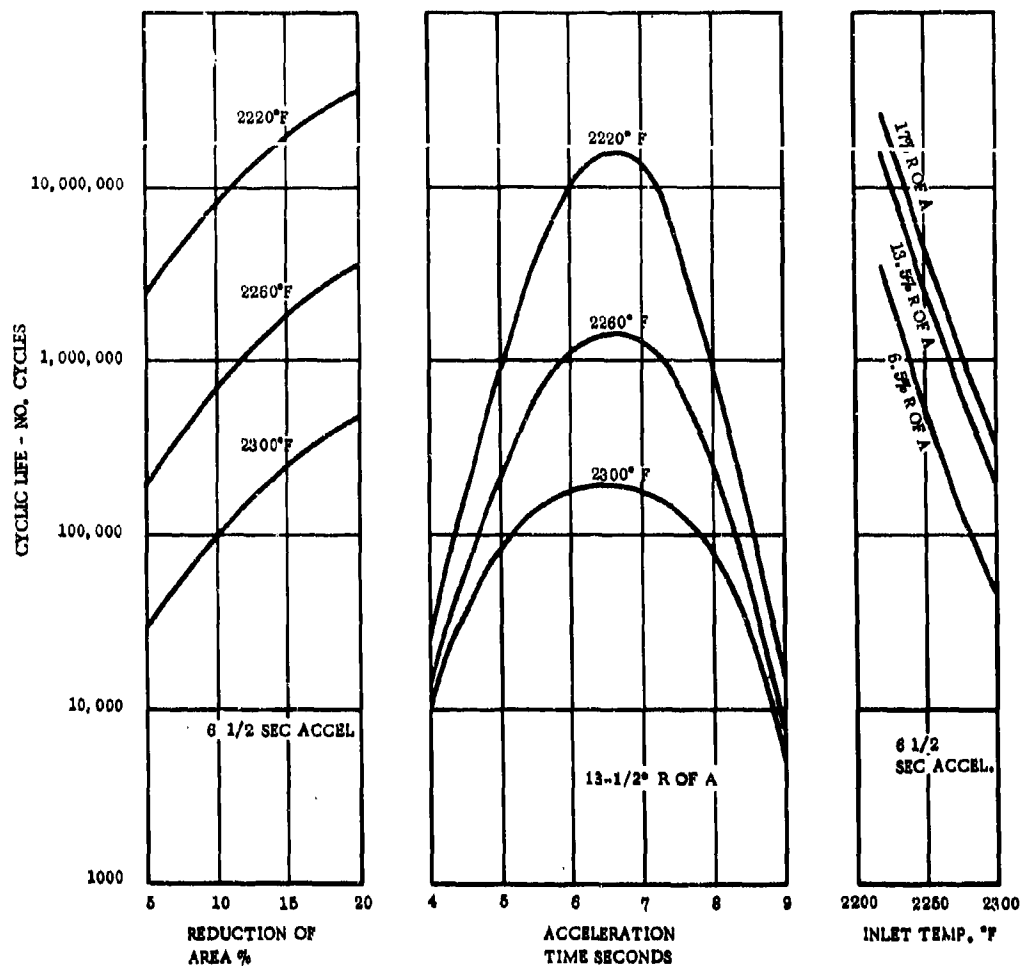
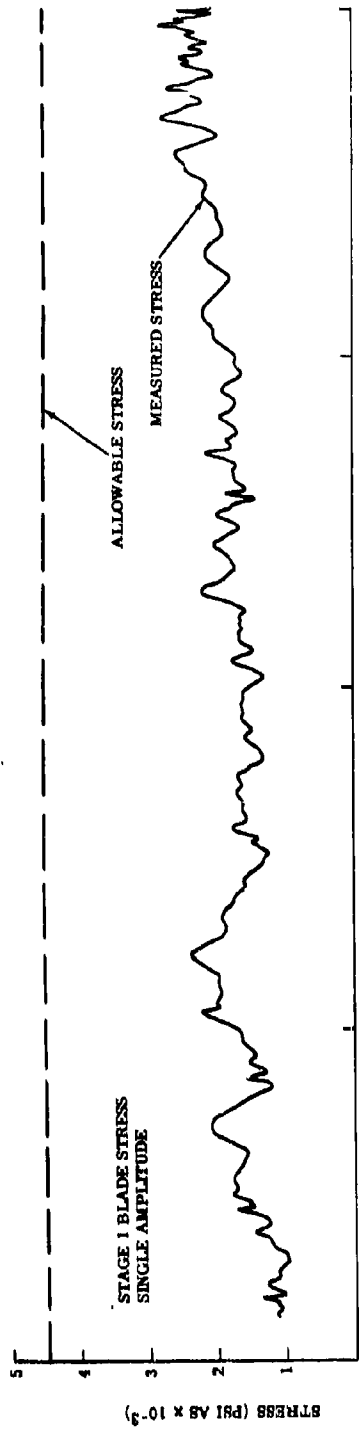


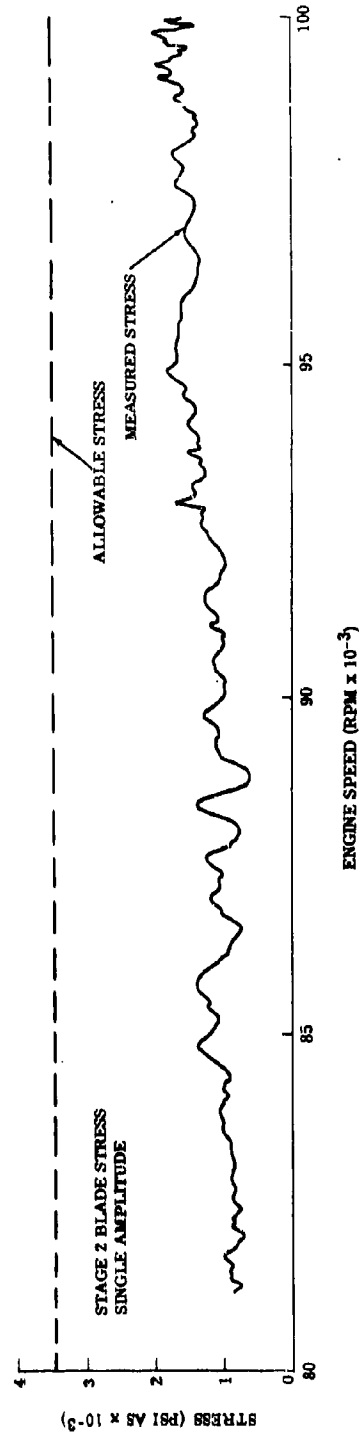
Figure 4.3-30 CYCLIC LIFE VARIABLES. Blade cyclic life is plotted as a function of the three variables that have the greatest influence. Speed of transients, material ductility and engine temperature level are shown as independent variables.

#### 4.3.3.2 Mechanical Fatigue

Figure 4.3-31 shows the level of alternating turbine blade stresses observed in the initial full-speed running of the GE4 engine. The stresses plotted are at the roots of the first- and second-stage airfoils, with strain gages oriented to sense both flexural and torsional vibration modes. The stresses peak at 50 percent of the established gage limits. The gage limits reflect the effect of stress distribution, local stress concentration at the cooling holes, blade to blade geometry/frequency variations, and gage tolerance.



ENGINE SPEED (RPM  $\times 10^{-3}$ )



ENGINE SPEED (RPM  $\times 10^{-3}$ )

Figure 4.3-31 ALTERNATING BLADE STRESS. Observed vibratory stress of the first- and second-stage blades recorded during the first full-speed run of the GE4 turbine. Comparisons of the measured and allowable stress levels provide encouragement that infant mortality due to blade vibration will not be a GE4 problem.

The low levels of stresses observed are attributable to several design considerations.

- Important passing frequencies are avoided in the design of fundamental response modes.
- Nominal gas bending loads are set to be consistent with successful past experience.
- The twin blade design provides good base-damping and resonant vibration control which minimizes sharply tuned stress responses.
- The effect of the airfoil cooling holes on blade endurance strength is minimized by the manner in which they are machined and their location.
- Local cooling effects act to reduce the effective stresses at the cooling holes.

Stress distribution and frequency tests provide the background information on which the engine gage limits are based. (See Figures 4.3-32 and 4.3-33.) In addition, hot bench fatigue tests (Figure 4.3-34) are run to determine the endurance limits of the blades experimentally. Adequate margin between the combined stress endurance limit and the highest engine operating stress is the



**Figure 4.3-32 BLADE STRESS DISTRIBUTION TESTING.** Blade stresses throughout the surface are experimentally and analytically related to the engine gages. Monitoring frequency during the test permits on-the-spot determination of allowable stress limits.

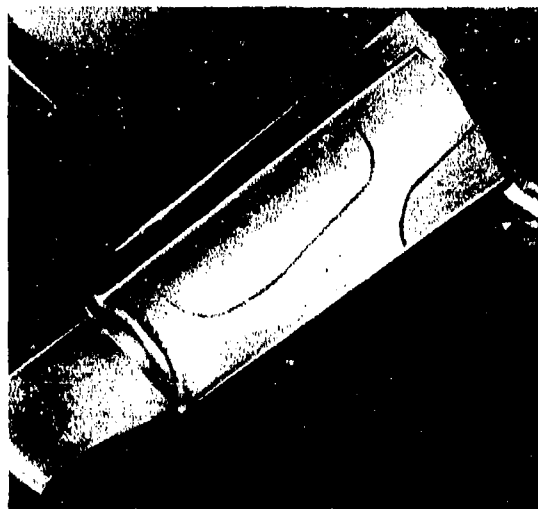


**Figure 4.3-33 NODAL PATTERN DETERMINATION.** Bench tests predetermine nodal patterns and frequencies helpful in the location of engine strain gages and in the identification of engine test response modes.

key to the elimination of "infant mortality" in the turbine blading. Component and engine testing is continuing, but test results to date promise that blade vibratory stress will not be a problem on the GE4 turbine.

In considering blade fatigue and in setting allowable stress limits of Figure 4.3-31, it is important to understand and account for the effect of local temperature gradients around the cooling holes in the airfoil. The blade edges where the holes are located are hotter than the body of the airfoil and are, therefore, compressively loaded throughout most of the life of the blade. In this state of stress, the local temperature gradients (hole edges cooler than the surrounding metal) serve to reduce the stress at the edge of the holes. Mechanical concentrations are considered separately. These effects are determined experimentally and the appropriate stress concentration corrections are incorporated the allowable stress limit, which is shown in Figure 4.3-31.

The most meaningful series of component tests for verification of the reliability and durability of the turbine blading is the full scale GE "whirligig" program. Figure 4.3-35 shows one of the facilities in which wheel and blades are fatigue-tested to failure. This type of instrumented



**Figure 4.3-34 HOT FATIGUE TESTING.** Full-temperature vibration tests determine the endurance limits of the blades of their natural frequencies. Amplitude location of failure, and local stress determinations thus obtained provide substantiation of vibration margins of safety.

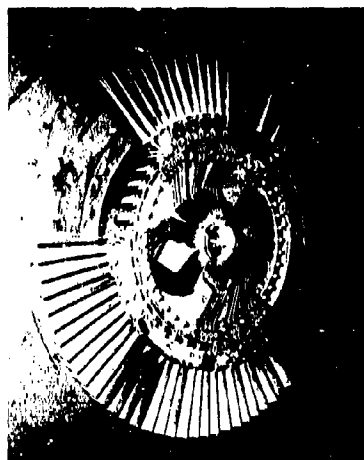


**Figure 4.3-35 BLADE VIBRATION TEST FACILITY.** Full scale "Whirligig" test facility for vibration response testing and blading system reliability testing.

testing gives quantitative information on stress distribution and relative response sensitivity throughout the speed range. The blading is excited at every foreseeable "per rev" frequency in a comprehensive evaluation of response characteristics. Subsequent over-stress tests are run to failure to confirm the relative airfoil-to-dovetail strength ratios. Concurrently, design information is obtained on dovetail and shroud wear characteristics with coating and wear prevention design treatments.

Figure 4.3-36 pictures the second-stage blade-tip shrouds. This double interlock design is specially configured to increase the interlock contact area significantly and to reduce the surface stresses. By doubling the number of interlocks and by increasing both the width and depth it has been possible to make fourfold reductions in shroud interlock loading. With larger contact areas and with the latest surface wear treatments, GE4 shroud interlock wear is not expected to be a problem. Because of difficulty in obtaining quantitative predictions of shroud life, the Whirligig component test will be used to give early insight into the long life adequacy of the design. Moreover, special shroud treatments, including the welding of paired blades at the tip will be studied on the Whirligig facility. The twin-blade concept provides an ideal arrangement for electron-beam-welded shrouds. In the event that shroud wear proves to be a problem, the welded shroud design will already have been evaluated in the blade development test program.

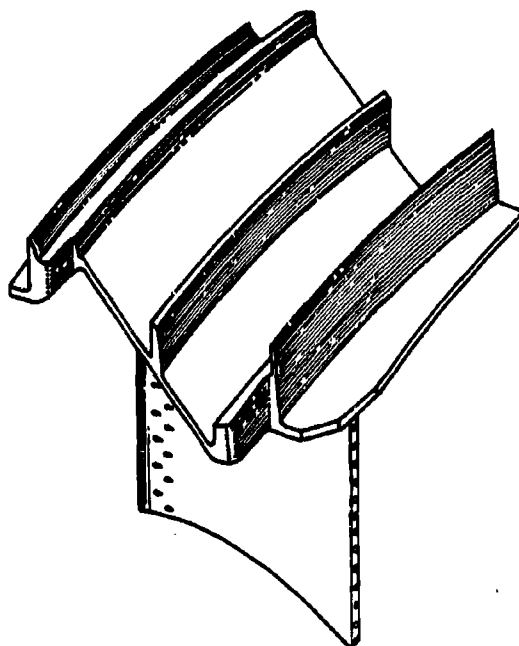


Figure 4.3-36 SECOND-STAGE BLADE SHROUD. The double interlock shroud design is pictured with the provisions made to increase the interlock area and to increase wear life.



#### 4.3.3.3 Erosion and Foreign-Object Damage

Turbine blade erosion and FOD during airline service has, in given instances, limited the useful life because of excessive wear and damage. Some early CJ805 first-stage blades were retired in as few as 3300 hours. Blades intended for 12,000 hours of service must represent a substantial improvement over current airline experience which is in the 6000- to 10,000-hour range. The fact that steady progress to extend blade life in airline operation is being made leads us to believe that 12,000 hours is a realistic goal. The problem is being attacked at its source in the combustor, and also by increasing the resistance to erosion within the blade itself.

- Design changes will reduce the formation of hard carbon in the combustor. Almost all wear on turbine blades today is attributable to the impingement of hard carbon particles on the leading edges of the airfoil at the outer diameter. Active and encouraging design progress is being made in fuel nozzle, swirl cup, and dome design to improve the carbon formation problem materially.
- Coatings reduce the erosion problem a great deal. Figure 4.3-37 shows the leading edge of an uncoated CJ805 airfoil after 1789 hours of service. The 50X picture shows 0.007 inch of wear on the convex side. Figure 4.3-38 shows a coated blade from the same engine. There is only 0.0015 inch of wear. The coating (CoDep) is about worn through, indicating



Figure 4.3-37 **BLADE TIP EROSION - UN-COATED AIR FOIL.** 50X photograph shows the amount of blade tip erosion experienced on the CJ805 stage one blade in 1789 hours of commercial service. This is uncoated U500 material. The dotted line is the original airfoil. A total of .007" is worn from the original contour.

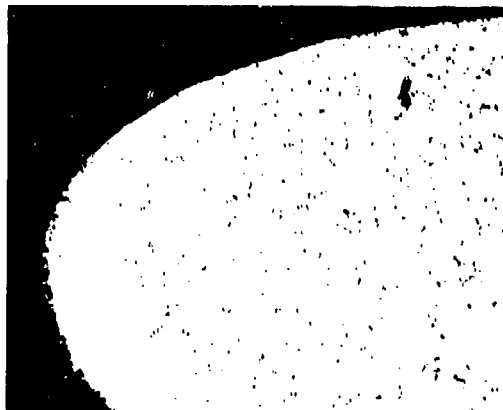
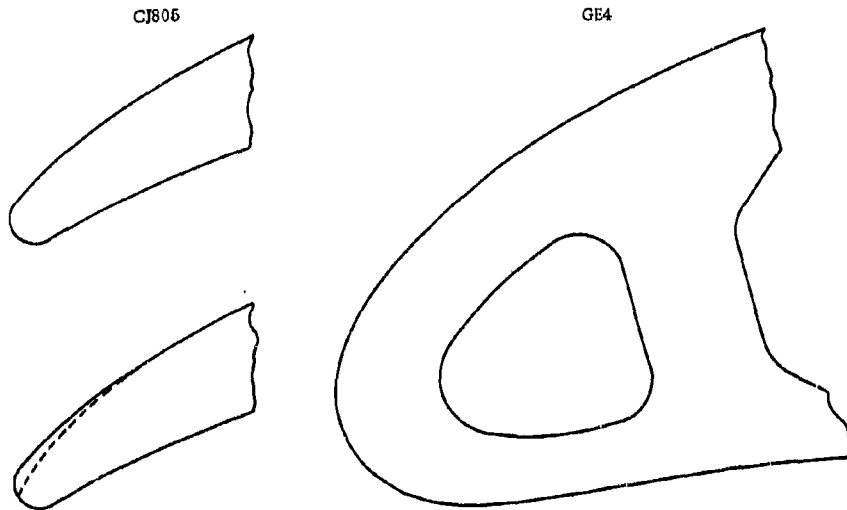


Figure 4.3-38 **BLADE TIP EROSION - COATED AIR FOIL.** 50X photograph of a coated blade in the same turbine as that of figure 4.3-37. After 1789 hours of operation only .0015" of the contour is worn. At this point the coating is worn through, indicative that for this type of service the coating life is about 2000 hours. Recoating is necessary to extend the life.

that the coating life is about 2000 hours. Today's coatings would be replaced at about this time. New developments, however, hold promise that thicker and more ductile coating will be available to help extend the life of the coatings.

- Actual size of the airfoils makes the GE4 much more resistant to erosion and FOD than most solid blades now in production. Figure 4.3-39 shows the relative size of the leading edge of the CJ805 and GE4 first-stage blades. There is 0.05 inch of wall thickness in the high wear area of the GE4. Based on the wear rates observed in Figure 4.3-37, this is enough material to last many times longer than today's longest life blades, even without coatings.



**Figure 4.3-39 BLADE TIP CONTOUR - CJ805 VS GE4.** Comparative 10X drawings show the relative size of the nose of the CJ805 solid blade airfoil and the GE4 cooled airfoil. The extra ruggedness afforded by the size of the GE4 design is apparent. Extra material is added to the convex side of the nose (.050" total thickness) as resistance against erosion and foreign object impingement. The 2000 hour uncoated wear pattern is shown on the bottom CJ805 for comparative purposes.

- Controlled laboratory testing shows that the larger air-cooled airfoils withstand impact damage that will tear a smaller solid blade. Figure 4.3-40 shows a CJ805 blade that has been damaged beyond repair limits with a 300 foot-pound impact of a 1/4-inch round test pin. Damage on the larger air-cooled blade at the 300 and 400 foot-pound level did not tear the blade and did not restrict the cooling system in any way. It is important to note that, because there is no radial coolant flow in the leading edge cavity, a local restriction will not effect the cooling effectiveness detrimentally. The blade is safe for continued service.

**CONFIDENTIAL**

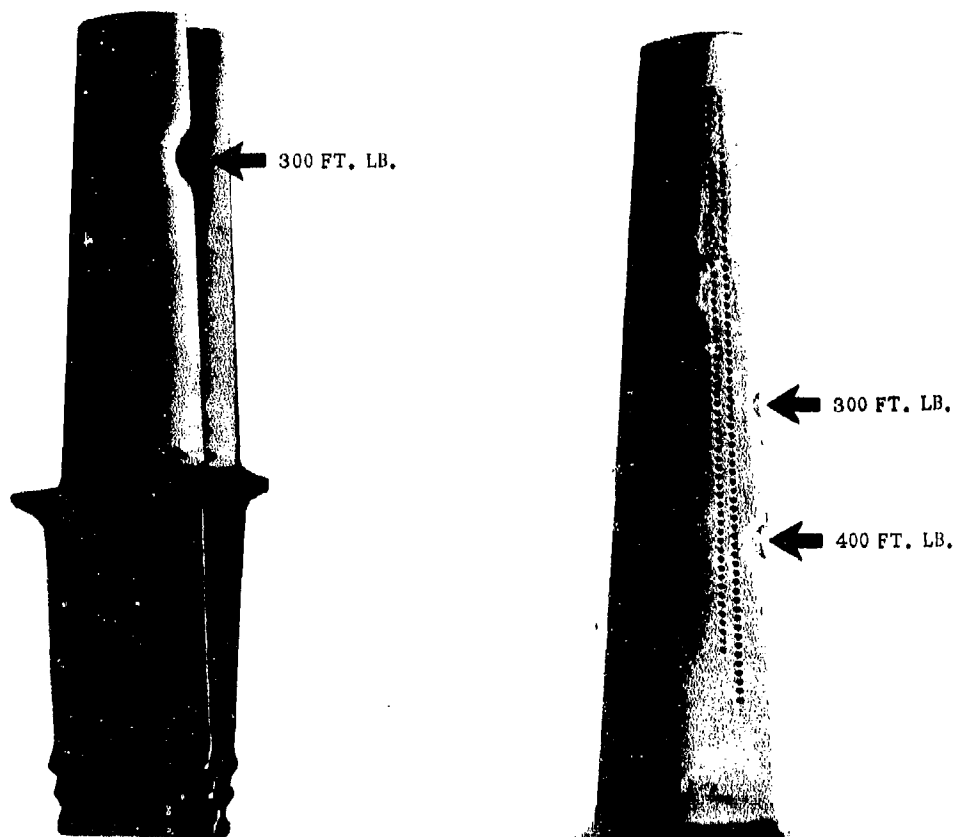


Figure 4.3-40 FOD IMPACT DAMAGE - Izod impact tests with a 1/4" diameter rod anvil shows relative impact damage to solid and hollow air cooled air-foils. The greater mass of the air cooled blade resists damage at an energy level which tears the smaller solid blade beyond repair limits.

**CONFIDENTIAL**

## CONFIDENTIAL

### 4.3.3.4 Hole Clogging

Extensive engine and component testing shows that hole clogging from either internal or external sources will not be a problem on the film-cooled airfoils.

- Clogging tests on the J79 engine show that neither large particle injection or small particle buildup will cause hole clogging on the GE4 turbine. Figure 4.3-41 shows the CJ805 erosion test engine on which accelerated wear tests were run to simulate thousands of hours of typical service operation. Special rows of holes were machined in the sides and leading edges of the first-stage vanes. Holes from 0.032 inch down to 0.016 inch in diameter showed no sign of clogging from either contaminated cooling air or dirt-laden hot gas impingement. The smallest holes on the GE4 turbine are 0.016 inch diameter.
- Vent holes at the tip of each blade prevent a long-time buildup of internally deposited extremely fine dust. Despite the low concentration, it has been found desirable for long-time service to provide these small relief holes in the tips of the blades. This system is the same that has proved so successful on the Conway and Tyne engines.

In summary, hole clogging is not expected to be a problem in the turbine. It is nevertheless true that the design is tolerant of local hole reductions which may come as a result of FOD damage. Tests on the J93/SST engine show only nominal increases in airfoil temperature when holes are intentionally blocked.



Figure 4.3-41 HOLE CLOGGING - DIRT INJECTION TEST. CJ805 engine shown during injection of 500 pounds of hard particle road dust in an accelerated erosion/clogging test.

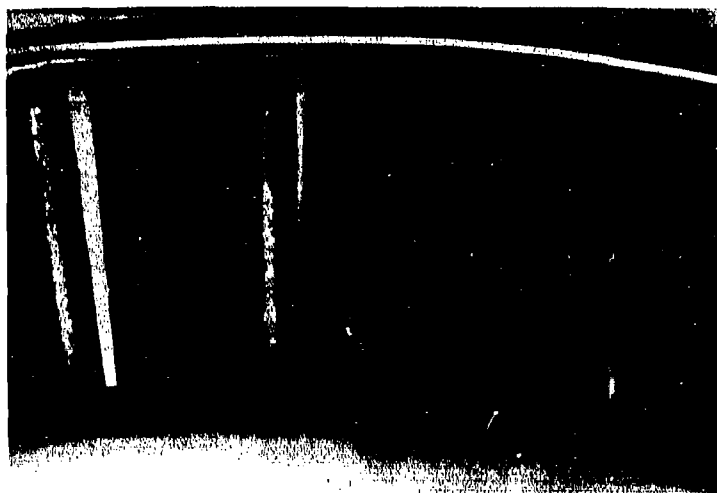


Figure 4.3-42 HOLE CLOGGING. Close up photograph of vane leading edges. None of the .032 inch to .016 inch holes clogged. Film cooled vanes unaffected.

#### 4.3.3.5 Containment

Spin pit tests have been completed which demonstrate the blade containment capability of the turbine. Figure 4.3-43 shows the blade failure test facility in which actual air cooled J93/SST blades are failed inside the J93/SST turbine stator. These tests are run to the same kinetic energy level (8075 foot pounds) as the GE4 turbine blade at full speed.

Figure 4.3-44 pictures the stator and blade airfoil after failure. The blade is shown contained between the shroud and combustor casing skin. The close structural similarity between the J93/SST and the GE4 blades give these tests important significance. It is concluded that the GE4 turbine will safely contain blade failures without the need for additional protective shielding.



Figure 4.3-43 CONTAINMENT TEST FACILITY

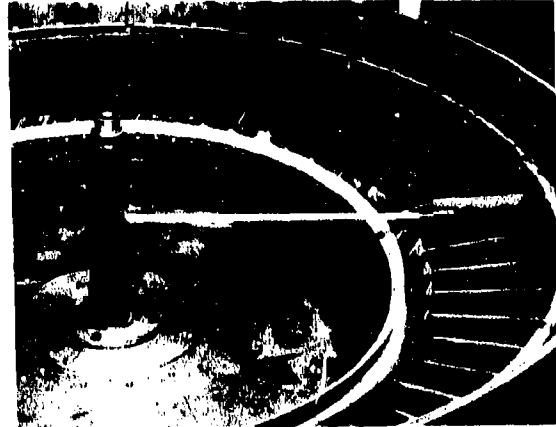


Figure 4.3-44 CONTAINMENT TEST DEMONSTRATION

#### 4.3.4 TURBINE COOLING

From both engine performance and metal temperature considerations it is important that the turbine cooling system make effective use of the air that is allocated for cooling. The GE4 considers the following important influences.

- The effect that cooling flow and cooled flow holes have on performance is understood and accounted for. (Refer to Volume III-A, Section 5.3.)
- The cooling circuit is prime reliable. Failure of shrouds, wear seals, airfoil FOD or other secondary part failure cannot materially affect the cooling efficiencies or the safety of the airfoils, dovetails, wheels or other structural engine components.
- The local effectiveness of cooling film is understood, and flows are equitably distributed in terms of both quantity and location of cooling air.
- Leakage paths receive special tongue and groove treatment as well as nickel aluminide caulking for positive sealing between mating parts.
- System pressure losses have been carefully evaluated so that coolant distribution will not be adversely affected by tolerance variables or off-design flight conditions.

Extensive work on cascade cooling effectiveness has been completed. These are hot cascade tests which show the related effects of configuration and cooling flow on the metal temperature distribution. These tests are the basis of engine test temperature predictions and are continually updated as new and more precise experience is accumulated. Figure 4.3-45 plots some recent cascade test results for the most important GE4 cooling modes. These charts are used to select the correct quantity of air to achieve the level of metal temperature required. Figure 4.3-46 shows a summary of the percentage of cooling air used at various points in the GE4 turbine. Take-off, cruise, and idle points are selected. Chargeable total flows are also listed. Chargeable flow is all cooling flow that enters the main gas stream downstream of the inlet to the first rotor stage. The Turbine Performance Section 5.3 of Volume III-A discusses the question of coolant flow and leakage in more detail.

Interfaces between mating parts where leakage could be a problem receive special treatment. Every such point in the turbine has a double overlap sealing arrangement. Figure 4.3-47 illustrates four examples of the tongue and groove principle.

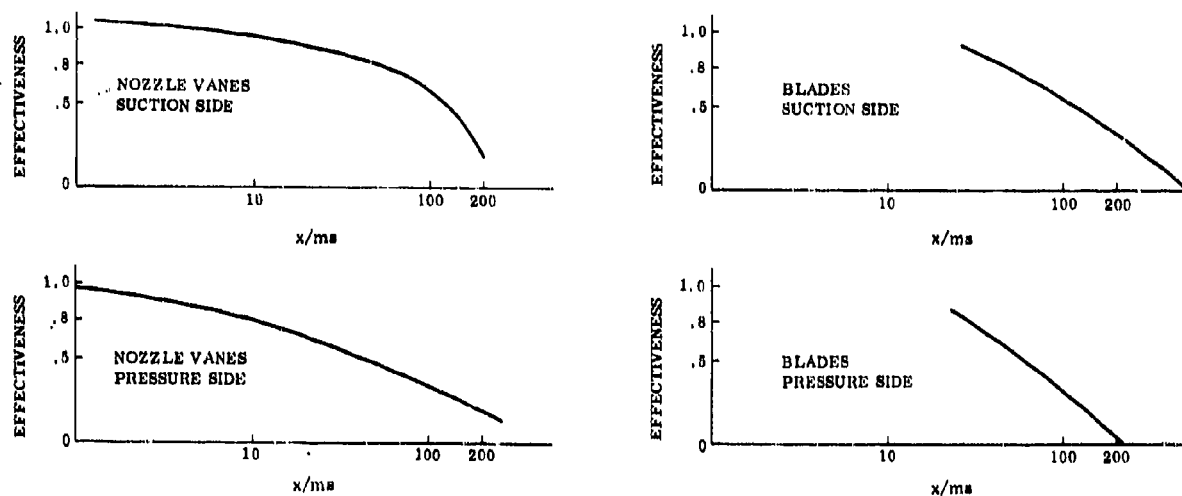
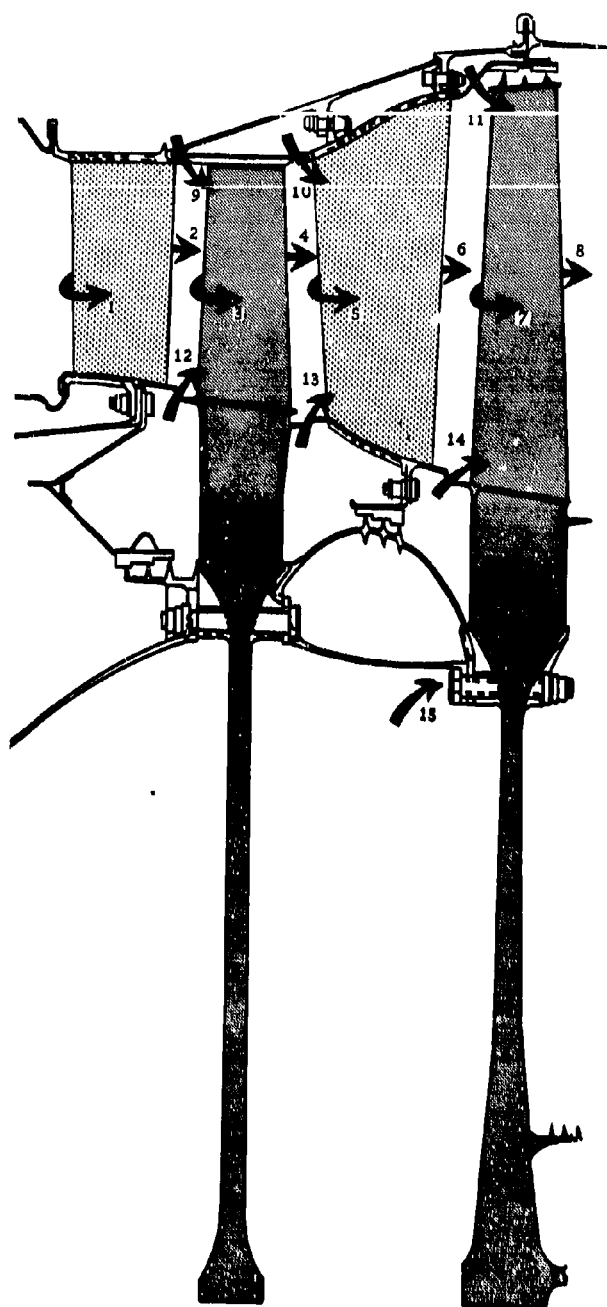
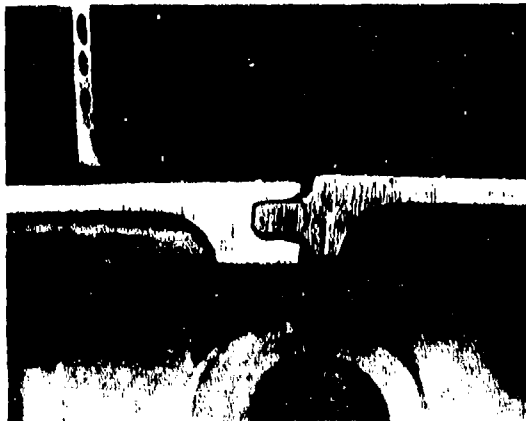


Figure 4.3-45 COOLING EFFECTIVENESS. Plots show the design curves on cooling effectiveness obtained from cascade tests of typical air cooled airfoils.  $X$  is the distance from the film holes,  $M$  is the coolant to gas stream mass velocity ratio and  $S$  is the equivalent slot height.

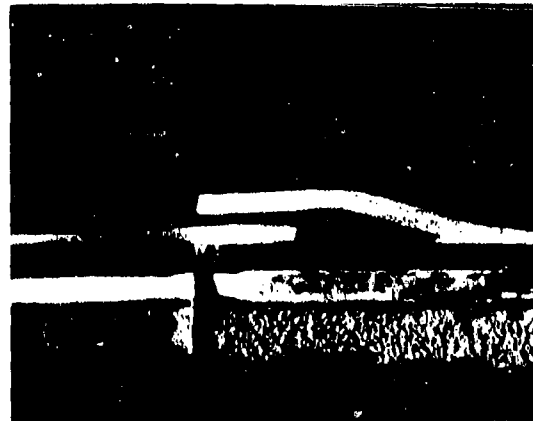


	TAKE OFF	M2.7 CRUISE	M2.7 IDLE
1	3.02	2.58	2.80
2	1.17	1.00	1.08
3	2.25	1.92	2.08
4	.79	.68	.74
5	1.20	1.03	1.12
6	.75	.64	.70
7	1.75	1.50	1.62
8	.58	.50	.54
9	.21	.18	.19
10	.32	.27	.29
11	.35	.30	.32
12	.69	.50	.65
13	.24	.20	.22
14	.34	.30	.32
15	.25	.20	.22
TOTAL COOLANT FLOW	13.39	11.80	12.89
CHARGEABLE COOLANT FLOW	8.81	7.72	8.36

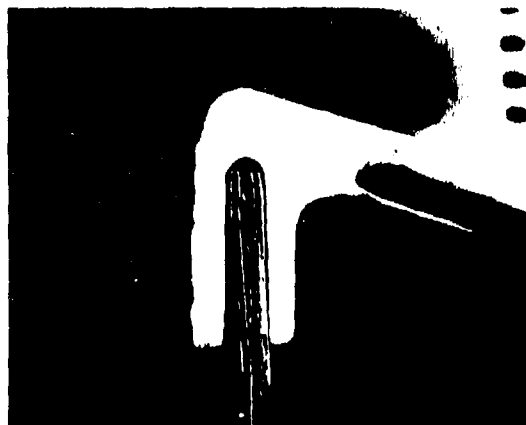
Figure 4.3-46 TURBINE COOLING FLOW SUMMARY. Location and quantity of turbine cooling flow for the various flight conditions. Standard and hot day cooling flow percentages are the same.



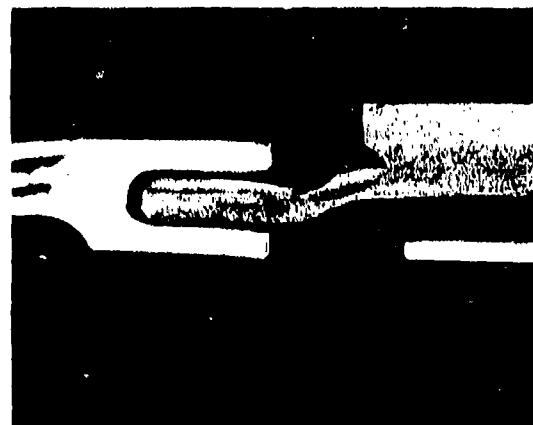
VANE BAND TO VANE BAND



SHROUD TO SHROUD



VANE TO INTERSTAGE SEAL



VANE TO SHROUD

**Figure 4.3-47 LEAKAGE CONTROL.** Each interface between mating parts is closed with a double or overlapping sealing system. Shrouds, bands, and seals throughout the turbine use this controlled leakage area design to ensure tight containment of the cooling air.



## CONFIDENTIAL

### 4.3.5 MAINTAINABILITY

Maintenance features included in the design of the GE4 turbine are:

- Complete and comprehensive borescope access is provided for close vane and blade inspection (Figure 4.3-48).
- The turbine is quickly accessible from either the front or the rear, depending on the choice of engine breakpoints. (See Figure 4.3-49 and -50.)
- Both rotor and stator are easy take-apart units with provisions for complete interchangeability of old and new parts.
- Individually replaceable stator vanes.

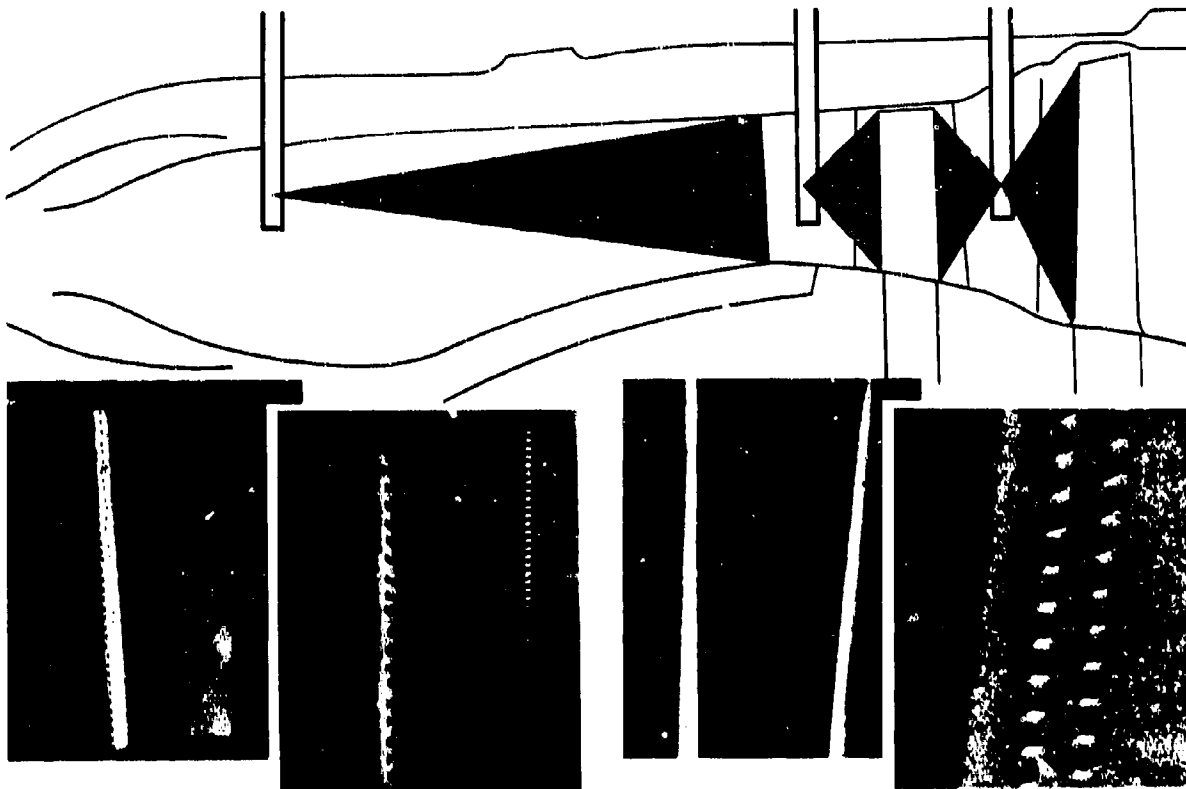
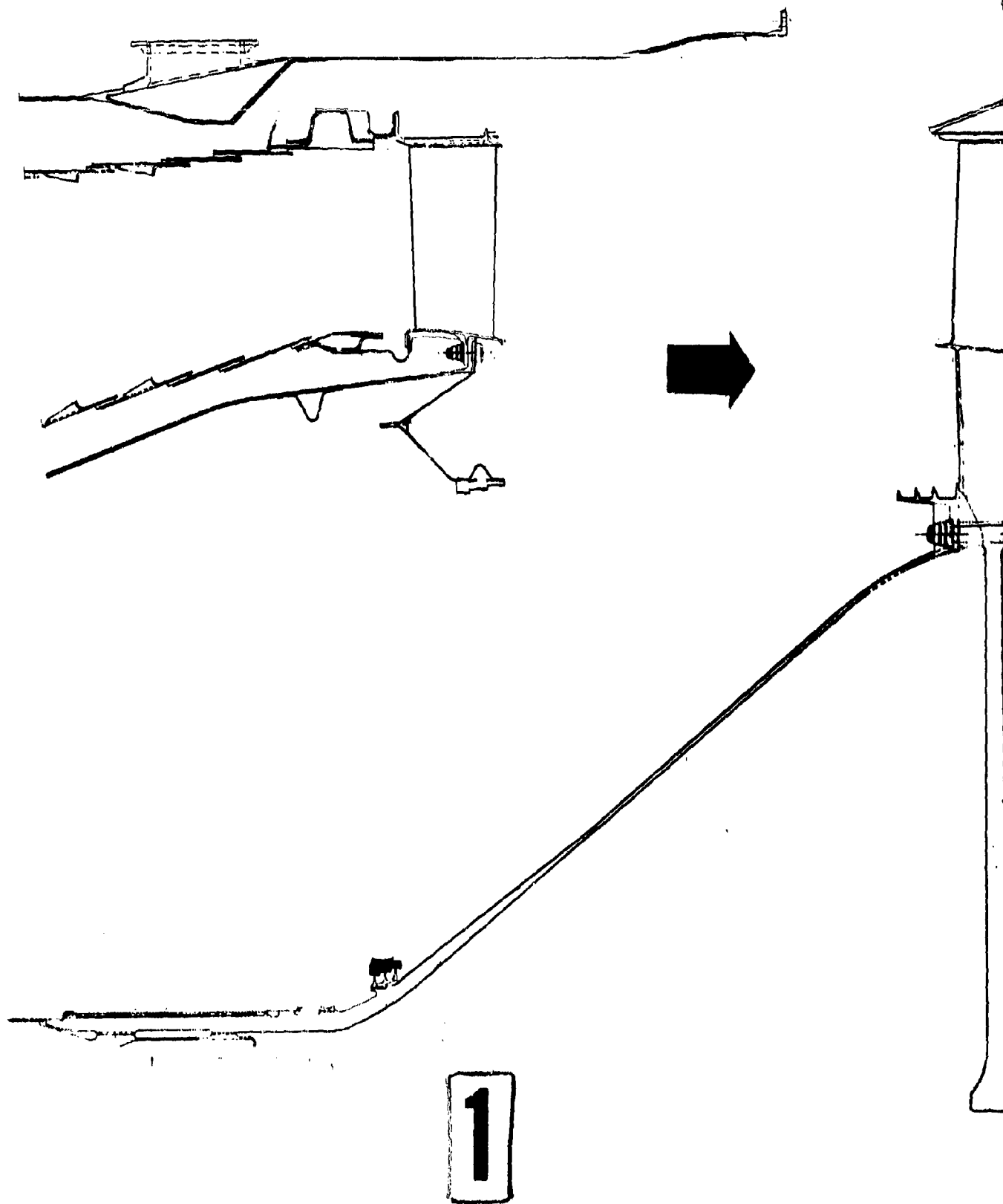


Figure 4.3-48 MAINTAINANCE -BOREScope INSPECTION. Borescope inspection provisions are provided around the periphery of the combustor and in the first- and second-stage diaphragm assemblies. These access ports make it possible to view the most critical parts of the turbine without engine disassembly. The leading edge of the first-stage vanes and the leading and trailing edges of the blades are brought into close perspective with improved wide-angle borescope equipment.



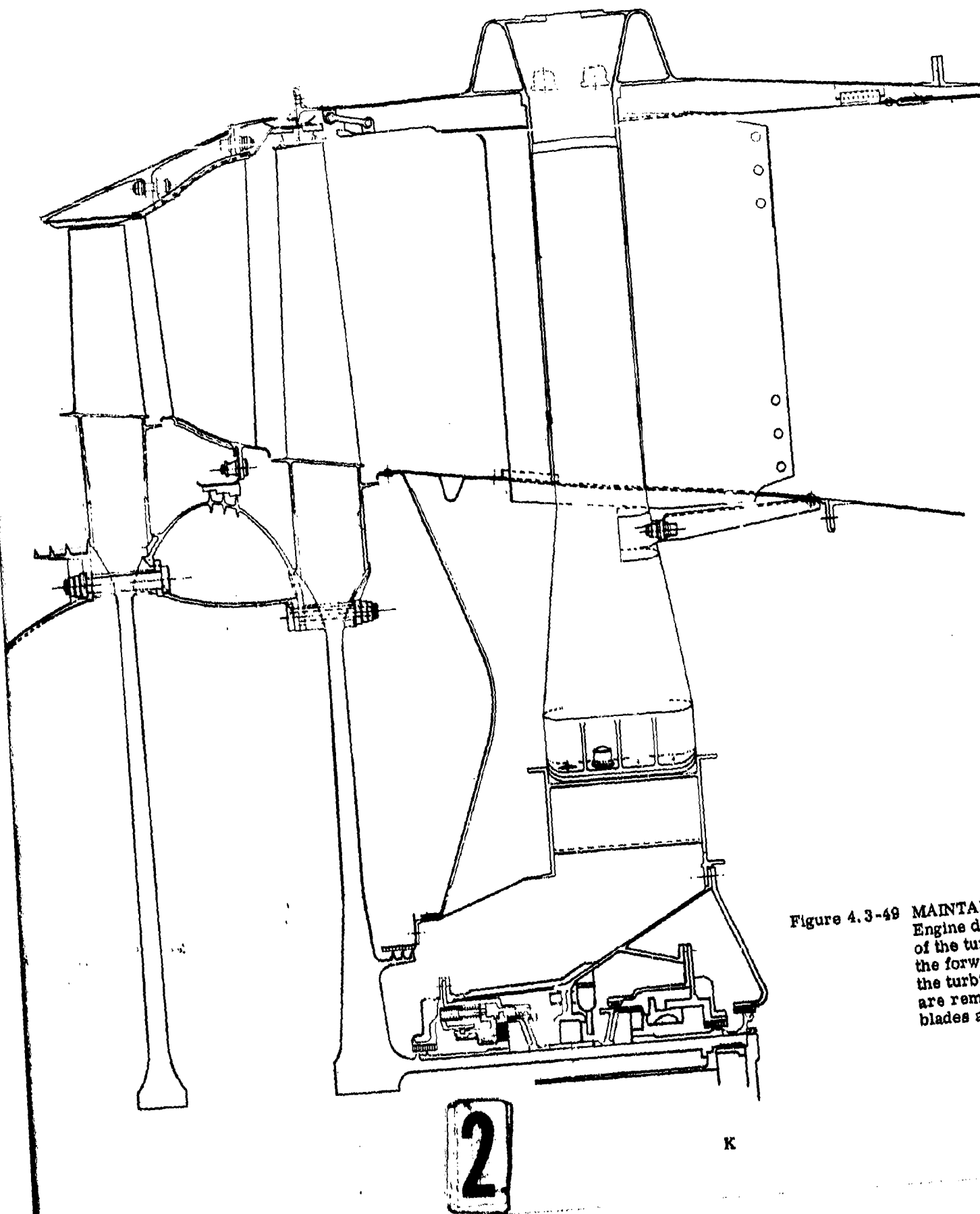
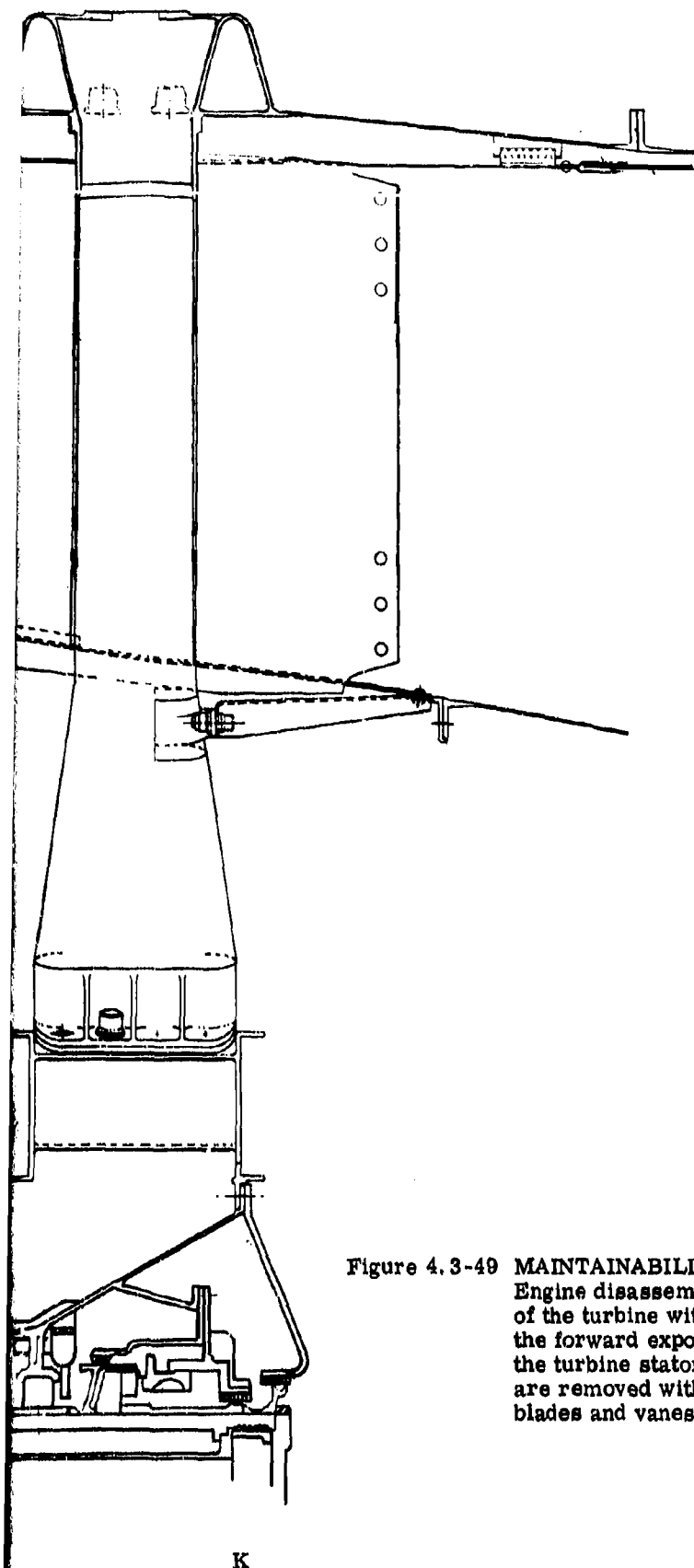


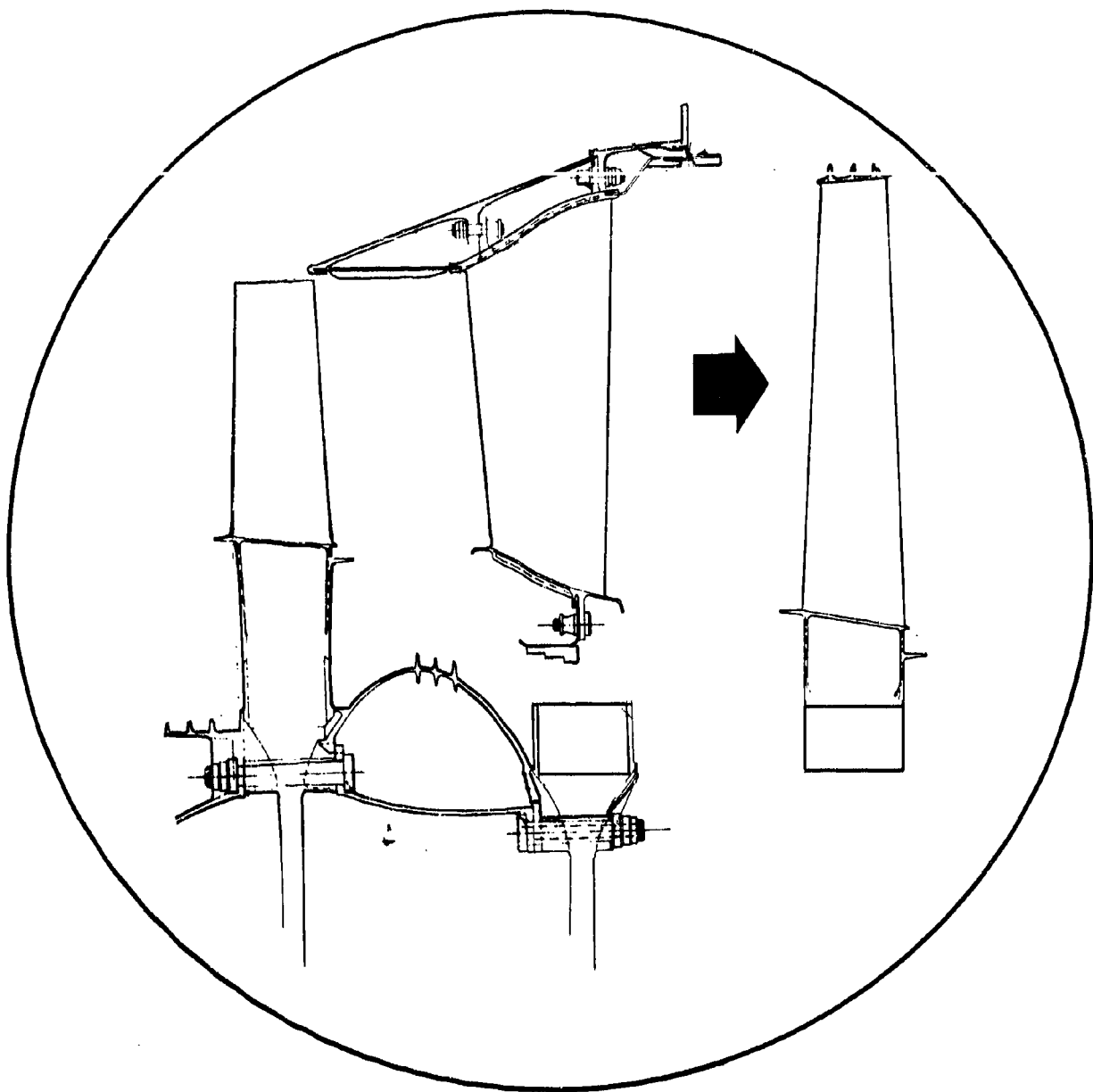
Figure 4.3-49 MAINTAINABILITY  
 Engine disassembly  
 of the turbine with  
 the forward exposure  
 the turbine stator  
 are removed with the  
 blades and vanes.



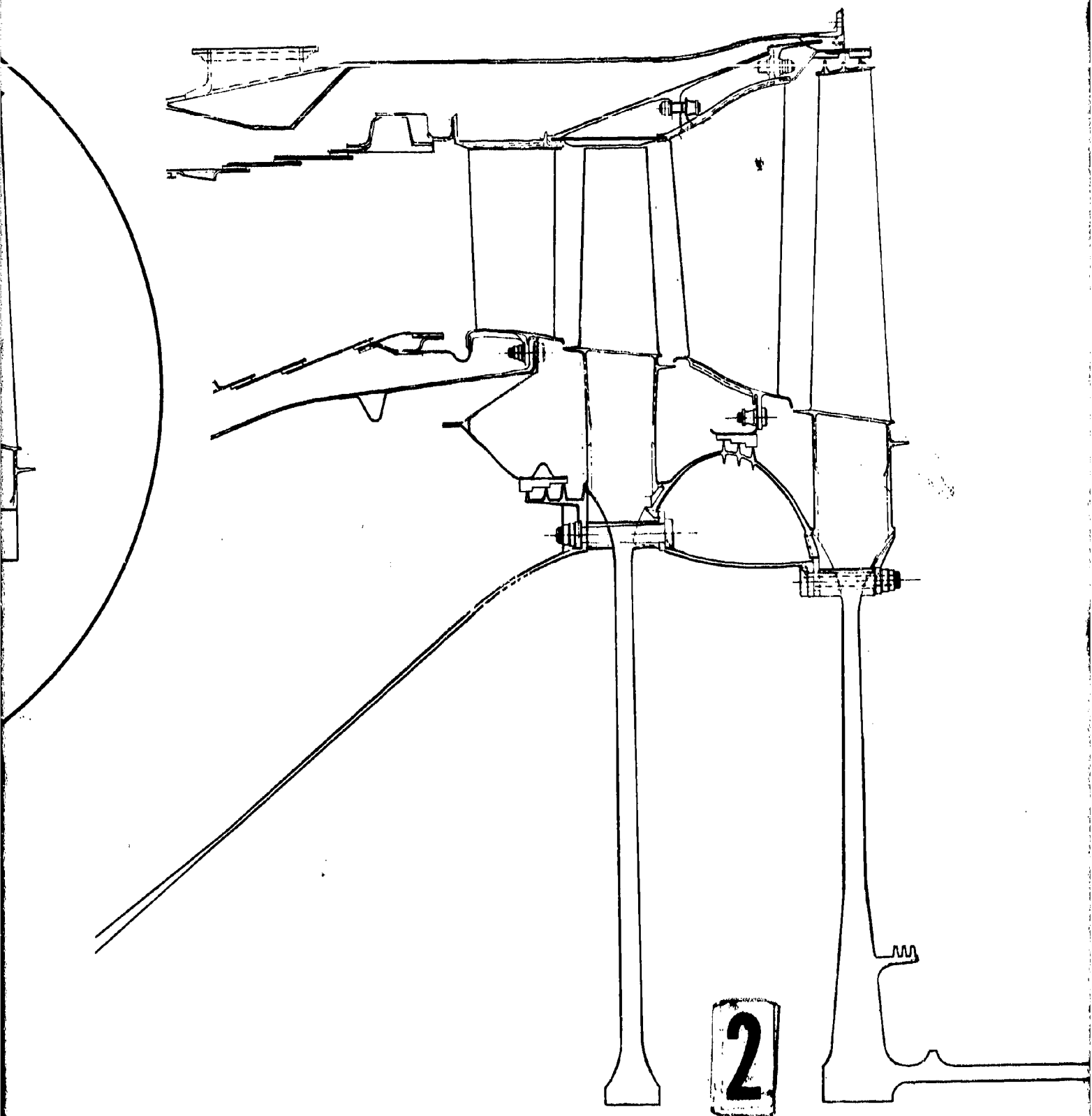
**Figure 4.3-49 MAINTAINABILITY - TURBINE ACCESSABILITY FORWARD EXPOSURE.** Engine disassembly can be planned to expose either the front or the rear of the turbine with a minimum amount of effort. The drawing above shows the forward exposure made possible by separating the center coupling and the turbine stator flange. The rotor and second stage diaphragm assembly are removed with the rear portion of the engine exposing the first stage blades and vanes.

**3**

4-57/4-58



1



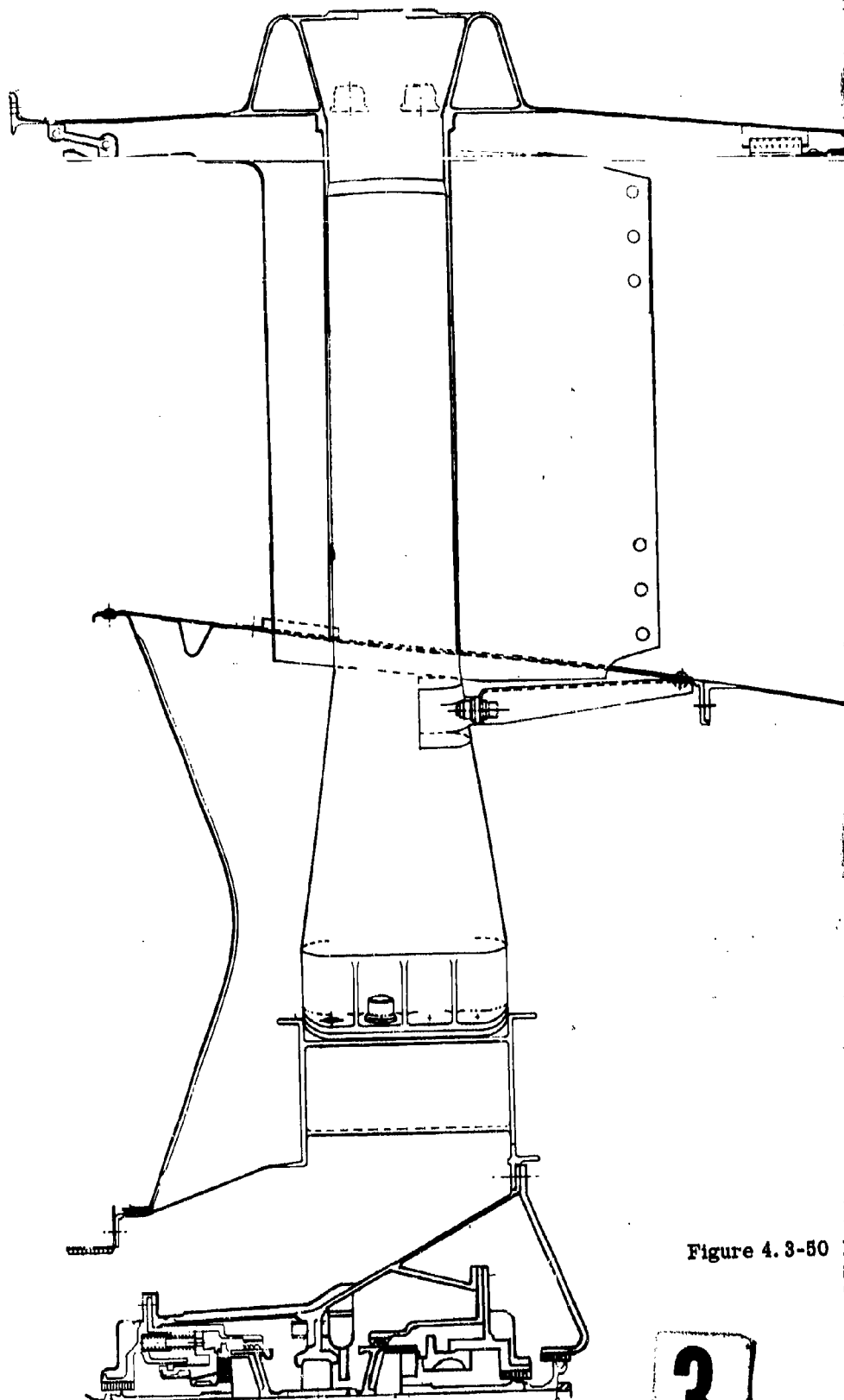
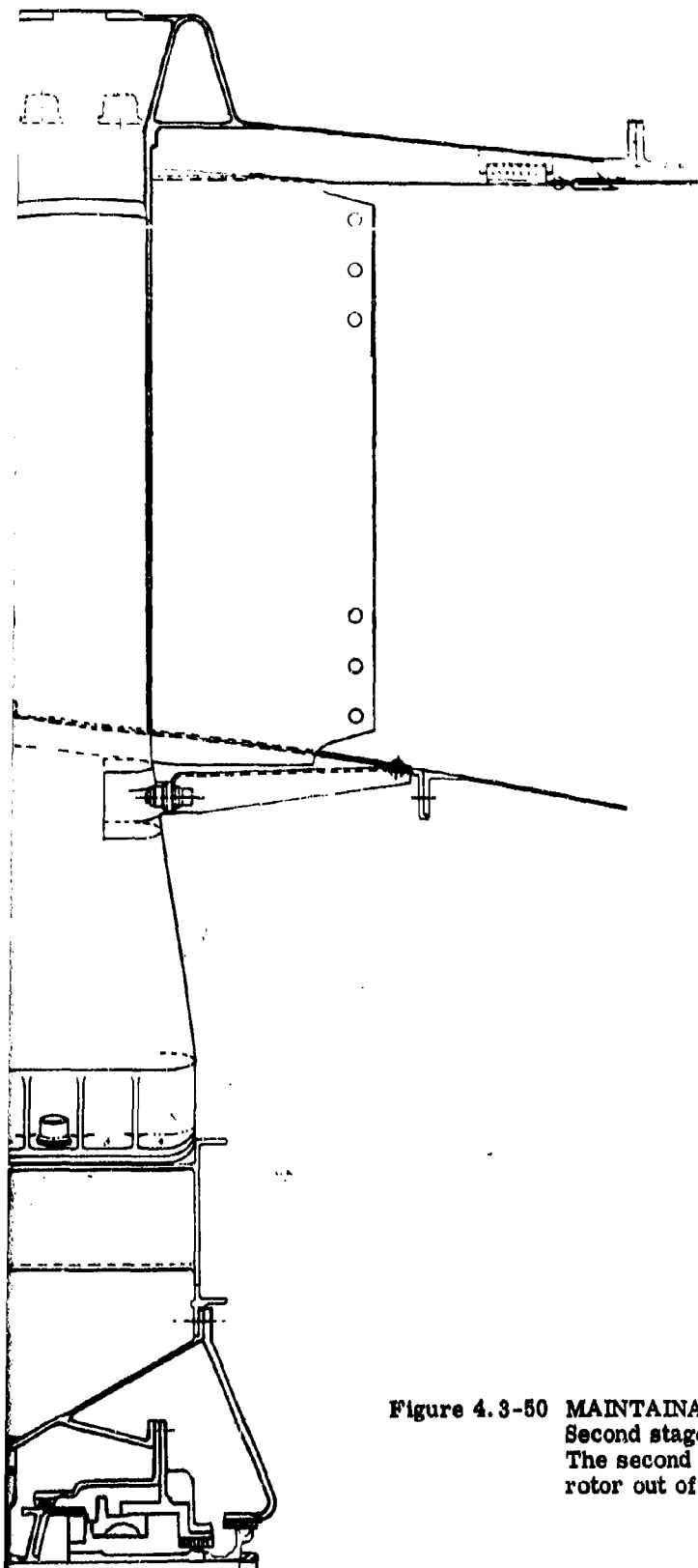


Figure 4.3-50

3



**Figure 4.3-50 MAINTAINABILITY - TURBINE ACCESSABILITY - REAR EXPOSURE.**  
Second stage blades are exposed by removing the turbine rear frame.  
The second stage nozzle assembly can be removed without taking the rotor out of the engine by removing the second stage blades.



- No hand work or special fitting is required at assembly. Torquing standard nuts is the only assembly operation.
- Every effort has been made to simplify maintenance and handling by minimizing the number of parts and eliminating loose parts.
- Wear contact points are eliminated wherever possible. In spots where moving contacts are necessary, special motion and wear prevention coatings are used.

#### 4.3.5.1 Turbine Rotor Assembly and Maintenance

The key feature leading to ease of maintenance on the turbine rotor is the precision tapered dowel construction. This alignment method permits parts to be put together and taken apart with the ease of a gear engagement. Heating or cooling of mating parts is not necessary. There are no hand fitting, interference fitting, or special inspection requirements. The dowels are a semi-permanent part of the spacer assembly and, as such, are handled as a unit. (See Figures 4.3-51 and -52.) Consequently, there are no loose bolts or separate bolt retention parts to contribute to assembly costs and error.

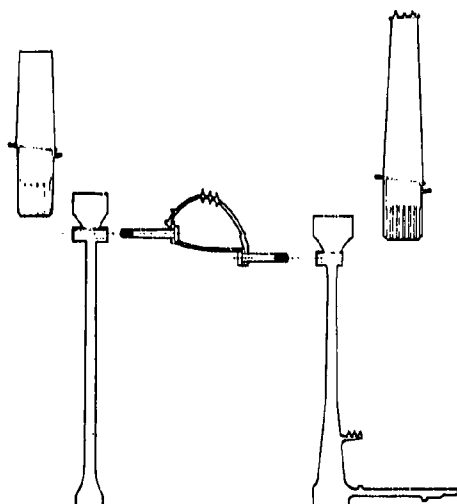


**Figure 4.3-51 MAINTAINABILITY - ROTOR ASSEMBLY - DISASSEMBLY.** The rotor can be assembled or disassembled from the front or rear. The heat shield/spacer assembly is a self contained semi-permanent assembly which retains the tapered dowels during handling and assembly and disassembly. There is easy access to all nuts and complete interchangeability of parts is assured. There is no requirement for any hand work at assembly other than standard self locking nut torquing.

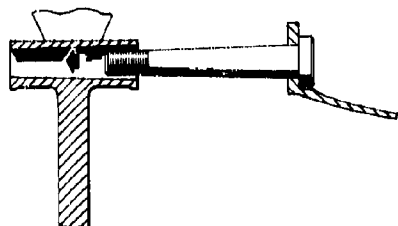


**Figure 4.3-52 MAINTAINABILITY - ROTOR ALIGNMENT DOWELS.** Tapered dowels which are press fit into the turbine spacer provide a positive alignment feature which is easily assembled and taken apart. Accuracy of the taper is built into the assembly. There is no hand reaming or fitting at assembly. There is no requirement for heating or cooling parts to get them together or apart.

There are no individual blade retention fasteners in the rotor and, therefore, no riveting, tab bending or other operations required to ensure proper blade assembly. Blades in the first stage are accessible individually or in total when the front shaft is uncoupled. Second-stage blades are interlocked at the tip, and are removed as a stage assembly. The tapered dowel construction makes disassembly of the shaft or second-stage retention ring a simple operation. There is no need for subsequent balancing in the case of normal reblading.

Balancing is initially corrected by the selective assembly of moment-weighted blades. Programmed analysis methods accurately tell how the blades should be oriented to obtain a good initial dynamic balance. The final correction is achieved with balance washers placed under the nuts in both the first and second stages. (See Figure 4.3-53.)

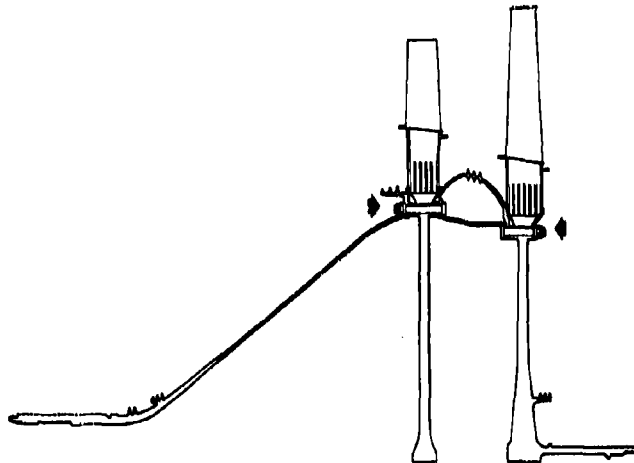


**Figure 4.3-53 MAINTAINABILITY - ROTOR BALANCE.** Rotor balance is achieved by selective assembly of the moment weighed blades, before the turbine shaft is assembled. Final balance is achieved by a dynamic balance correction made in the planes of stage one and two by the addition of balance washers under the nut of the alignment dowels.

#### **4.3.5.2 Turbine Stator Assembly**

The turbine stator is a take-apart structure in which any part or group of parts can be easily removed for repair or replacement. Like the rotor, there is complete interchangeability between parts. There is no requirement for any special hand-fitting operations at assembly.

There is no stator casing in this simplified design. The vanes, instead, are bolted to continuous ring members with standard 5/16-inch bolts. The vanes retain the shrouds, combustor seals and interstage seals without separate retention devices. All contact surfaces receive special motion- and wear-prevention treatment consisting of a surface deposit of nickel aluminate.

Figure 4.3-54 is a cutaway view of the stator, showing the manner in which the parts are matched together. The first-stage assembly is tied through the front inner cone to the No. 2 bearing support for concentricity and gas-load restraint. Figure 4.3-55 is an exploded view of the stator.

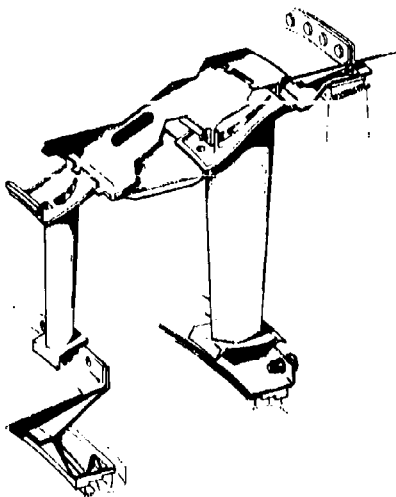


**Figure 4.3-54 MAINTAINABILITY - STATOR ASSEMBLY.** The stator vanes are bolted to machined support rings and as such are easily replaceable. When the vanes are unbolted the shrouds and seals are free to be repaired or replaced as necessary. All contact surfaces in the stator are treated with special wear treatment which prevents gauling, looseness and eventual wear-out.

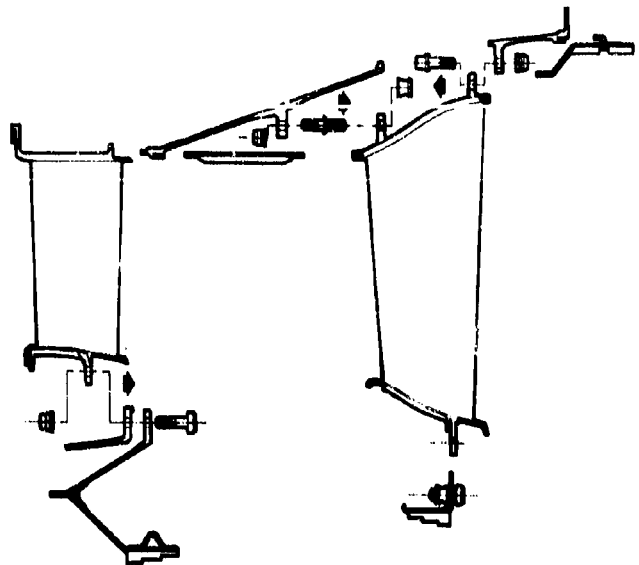


**Figure 4.3-55 TURBINE STATOR.** Exploded drawings show details of the Turbine Stator Assembly. Simplicity and maintenance are stressed. Vanes are replaceable in this take-apart design. Shrouds and seals are easily removed for inspection, repair or replacement. Wear surfaces are specially treated to assure proper alignment and long life.

The second-stage assembly matches with the first stage at interlocking lugs near the trailing edge of the first-stage vanes. The second-stage diaphragm can be assembled as a unit with the turbine rotor or after the turbine rotor is assembled. In the latter case, the second-stage blades are assembled after the stator assembly is moved into position. The entire stage assembly can, accordingly, be removed from the engine for maintenance without loosening the center coupling nut or removing the turbine rotor. The first-stage vane assembly can be quickly removed and replaced by breaking the engine in the forward turbine mode as shown in Figure 4.3-49.

#### **4.3.5.3 Durability and Maintainability Analysis**

A durability and maintainability analysis for the turbine has been completed and is contained in a special appendix entitled "GE4 Durability and Maintainability Analysis", which is available on request as back up material to the substantiating data submitted.

#### 4.3.6 RELIABILITY

Many interrelated variables affect life and life margin in the turbine. The most advanced mathematical modeling techniques are used in the Reliability analysis of the GE4 turbine. These techniques involve the assignment of known statistical variations to each important parameter (stress, gas temperature profile, gas temperature level, coolant temperature, material strength, etc.) and combine them in statistically selected random samplings. The analysis provides life-distribution curves for each failure mode under consideration. Such an approach provides a number of very important facts:

- The correlation of the analysis model with actual current engine experience
- The predicted level of nominal, minimum and maximum GE4 lives
- The effect that changes in each variable have on the ultimate life or life margin.
- The disclosure of information important to the selection of approaches for growth designs or durability improvement programs.

Figure 4.3-56 shows a composite picture of a typical Reliability model showing the variables studies and their interrelation in the systems concept. Blade creep, shown in this figure, is a key item as far as GE4 Reliability modeling is concerned. The work initiated on this study is typical of the kinds of failure mode studies that are providing important new insight into analysis and evaluation planning.

#### 4.3.7 QUALITY ASSURANCE

In order to ensure parts of uniformly high quality in the GE4 turbine, it has been necessary to develop many new inspection and quality control procedures. These Quality Assurance breakthroughs involve rapid and repeatable methods of inspecting dimensions and cooling system characteristics of each component. Figure 4.3-57 illustrates some of the more important tools now available or under development. They include:

- Tooling for inspecting airfoil wall-thickness or hollow castings. Eddy current equipment measures and records metal thicknesses within 0.001 inch.
- Equipment that measures the location and diameter of blind internal cross-holes. The impingement holes near the nose of each airfoil are inspected to within .007 inch with automatically recording photoelectric instrumentation.
- Airflow checks are made on each airfoil to check the pressure-drop in each cavity system, which ensures adequate total flow through the blade or vane.
- Water-flow checks are made on each blade to make certain that all holes are open and that they are flowing properly.
- New functional testing systems that will actually check metal temperature levels when the airfoils are heated on the outside and cooled on the inside are being developed. These systems, when perfected, will make it possible to make assurance checks much faster than would be possible with even the latest of today's dimensional inspection equipment.

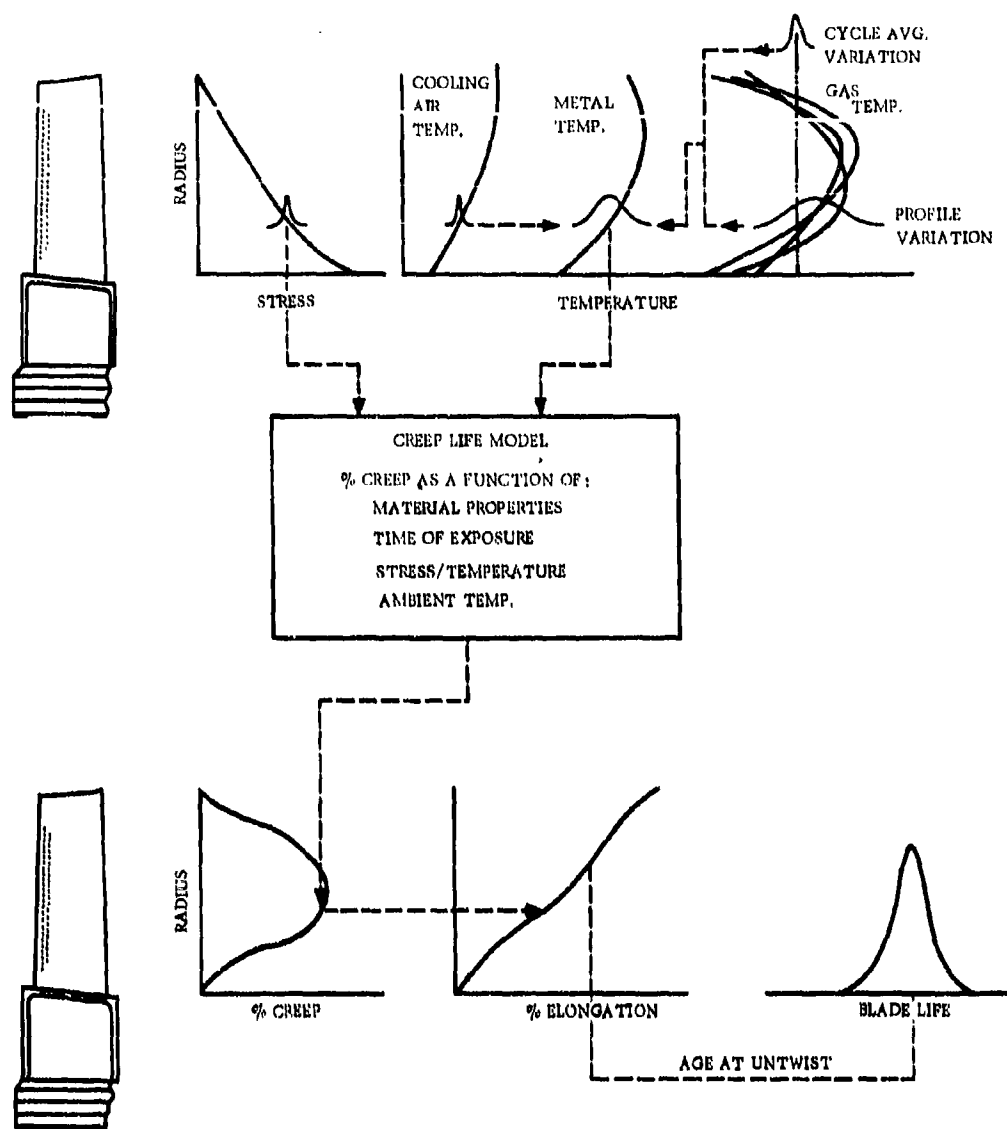
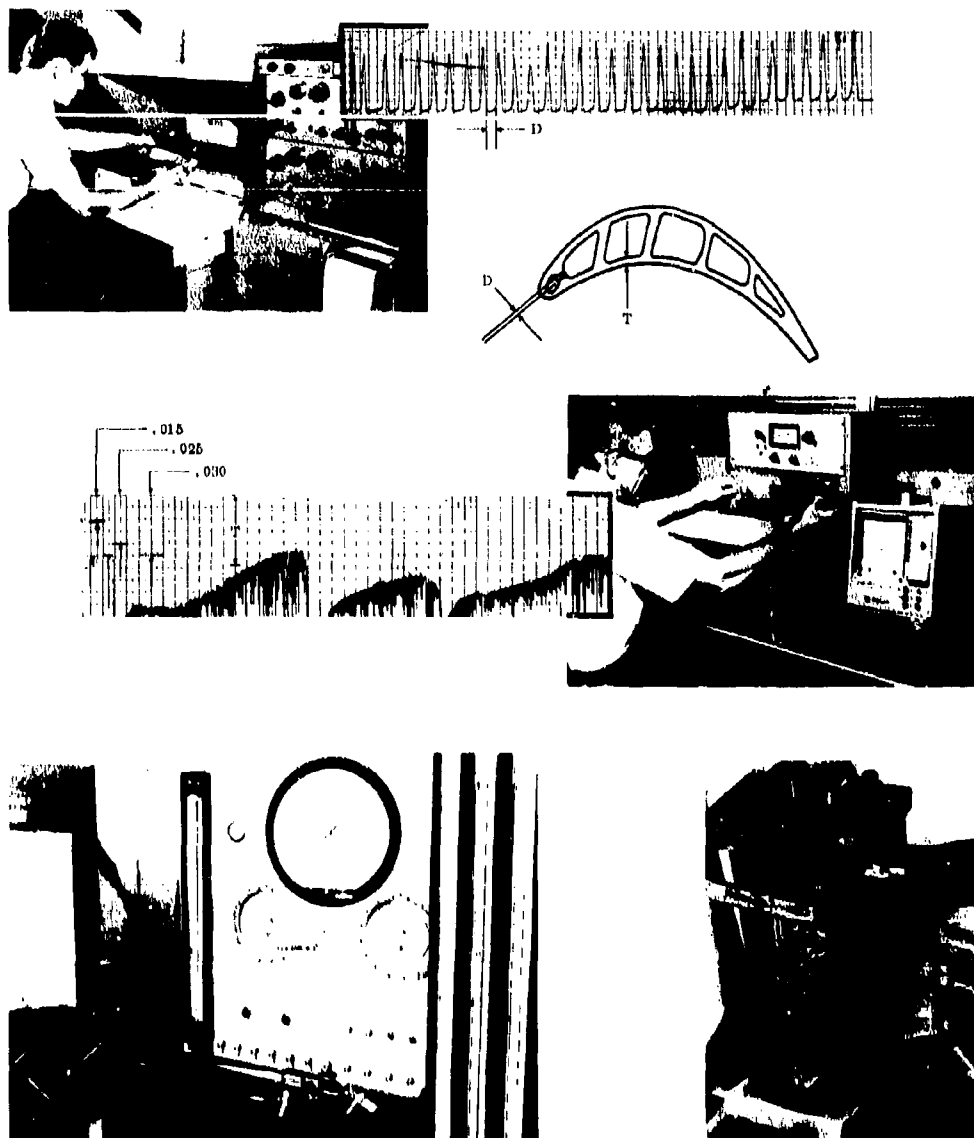


Figure 4.3-56 **RELIABILITY - SYSTEM ANALYSIS.** Design as a complete system is analyzed with regard to the effect of each system variable on metal temperature. This mathematical modeling considers combustor system variables, stress variations, fluctuations in cooling flow and cooling temperature for every foreseeable system malfunction as well as expected ranges of normal variation.



**Figure 4.3-57 QUALITY ASSURANCE.** Special inspection techniques have been developed to provide the high level of quality assurance inherent in the GE4 turbine design. (A) Internal cross hole inspection, location, number and diameter information on the blind internal impingement holes is automatically plotted with recording photoelectric instrumentation. Diameter readings accurate to .003 inches are recorded. (B) Wall thicknesses are measured with eddy current instrumentation and plotted in a clear visual presentation of the thickness of the airfoil along its length. (C) Final air flow checks record local and overall pressure drops to assure correct function of the cooling system. (D) Water flow checks provide a backup to assure that all holes are clear and flowing correctly.

#### 4.3.8 SAFETY

The GE4 turbine includes built-in safety features designed to limit the extent of initial damages, regardless of the cause, and to prevent failure of any of the prime structure of the turbine. Special items include:

- Cooling System - Pressurized coolant supply. Cooling air surrounding the gas side components and on the inside of all the airfoils is at a higher pressure than the hot gas in the turbine. In the event that holes or leakage points develop in the turbine, cooler air will always flow into the gas stream. Hot air will never flow against the coolant supply pressure and cannot, therefore, cause secondary distress to the turbine structure. (See Figure 4.3-58.)

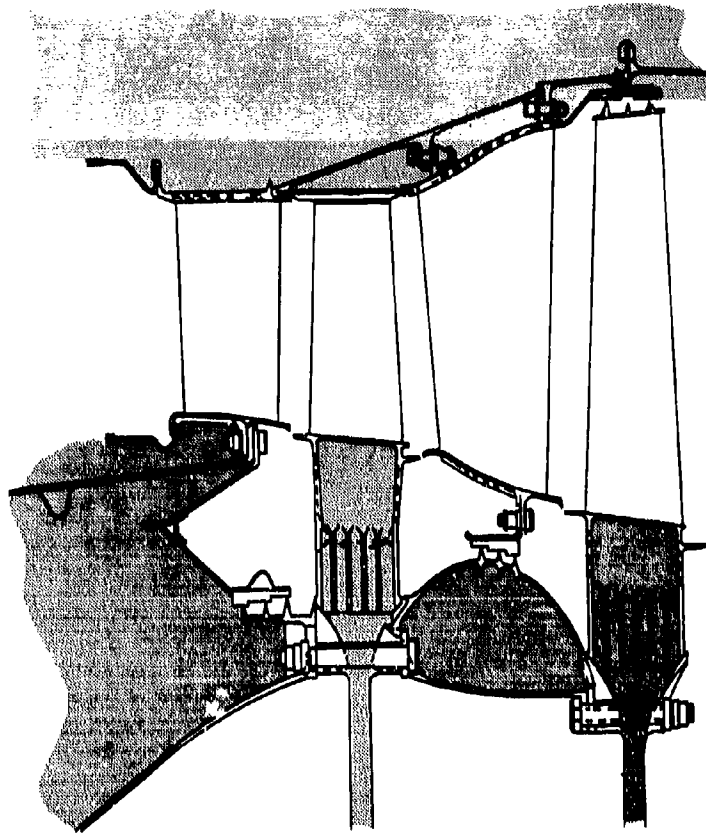


Figure 4.3-58 SAFETY - COOLING SYSTEM. Prime reliability of the Turbine cooling system is assured by surrounding the turbine with cooling air at a higher pressure than any other point in the turbine. Leakage paths which may develop result in cooler air leaking into the gas stream. There is no possibility of main stream air backflowing into the airfoils or onto structural surfaces. Flow limiting areas are provided which safely balance the cooling system in the event of seal or shroud failures. Loss of individual vane or blade cooling air does not effect the safe flow of air to the remaining airfoils.

- Cooling System - Seal failure tolerance. Regulatory flow areas throughout the engine are set so that a loss of seal honeycomb or failure of a shroud will not upset the coolant flow to the blades, vanes, stator structural rings or the rotor drum or wheels. (See Figure 4.3-59.)
- Failure containment - The stator vane support ring design and flame flange location are set to provide positive containment of failed blade airfoils.
- The rotor wheels are prime reliable components operating in a protected atmosphere which is insulated from the hot gas stream. The wheels are designed to tolerate abnormal variations in rotor speed. Temperatures of the wheel are almost totally independent of the blade coolant flow. (See Section 4.3.2.)

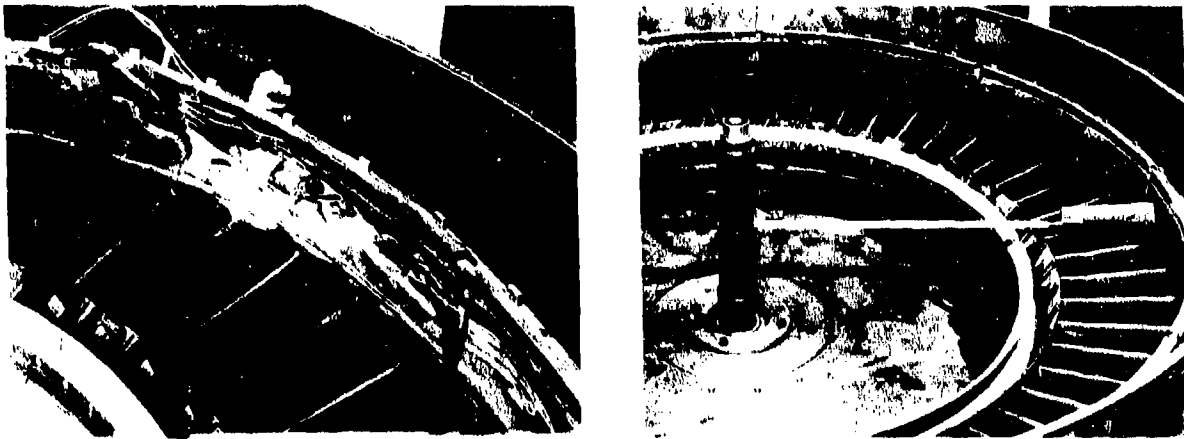


Figure 4.3-59 SAFETY — CONTAINMENT. Actual blade airfoil spin tests have demonstrated the engine structure containment capability. Here the J93/SST blade and casing structure are shown when tested to the same kinetic energy level as the larger GE4 blade at full engine speed.

#### 4.3.9 FAILURE ANALYSIS

A detailed comprehensive failure analysis has been completed on all components of the GE4 turbine. This analysis forms a basis for further test requirements, further development requirements, or for design modification studies. Life-limiting factors have been identified in a detailed part-by-part failure mode and effects analysis. From this detailed analysis, specific design or test action has been taken. Particularly complex failure modes are selected for complete mathematical model analysis to obtain a better understanding of the interrelated effects of complex variables. Refer to Section 4.3.3.1, 4.3.6 and the turbine reliability section of Volume IV.

#### 4.3.10 VALUE ENGINEERING

New processes and manufacturing techniques are used through the turbine to reduce cost and improve quality. Many of these processes were specifically developed in the GE4 turbine development program. They include techniques for multiple hole drilling, contour machining, small hole drilling, automatic finishing, as well as optimum use of the latest more conventional process



capabilities. For example, maximum use is made of the latest precision casting techniques where intricate and yet accurate internal cavities are produced with minimum cost. Figure 4.3-60 summarizes some of the more important features introduced on the GE4 turbine as a result of Value Engineering considerations.

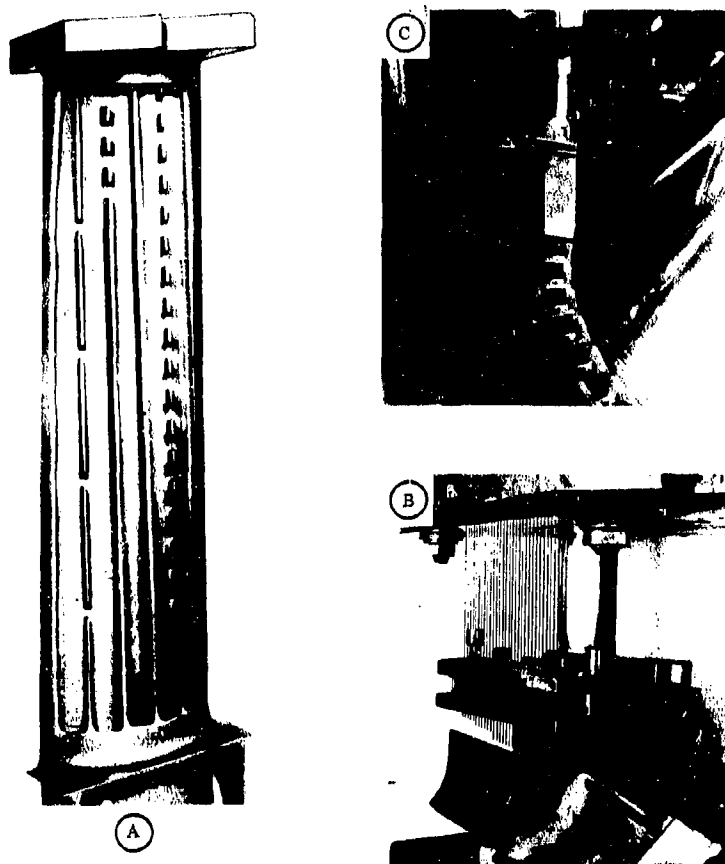


Figure 4.3-60 VALUE ENGINEERING. Careful consideration has been given to Value Engineering factors at each step in the design. Some of these features are illustrated above. A. Cast contoured interior airfoil cooling passages for low cost precision control of the hidden portions of the cooled airfoils. B. Multiple hole drilling techniques for simultaneous processing of precision cooling holes. C. Contour machining with simultaneous EDM electrodes eliminate costly band operations and assures repeatable and reliable dimensional control.

#### 4.3.11 HUMAN ENGINEERING

There are important features in the turbine design that concern human engineering and the prevention of human error. Whenever possible, the design makes it impossible to assemble parts in the wrong direction or orientation. Bolts, if they are different at all, are so sized that they cannot be used in the wrong hole. Taper on the wheel hole makes it impossible to put the wheel on in the wrong direction, etc.

- Complete interchangeability is maintained so that, except for balancing operations, like parts assemble in any order at any position without need for match marking, hand fitting, or special operator skills.
- The unitized sub-assembly concept which minimizes the number of loose pieces has important error and fatigue prevention implications. Loose pieces are eliminated and cannot, therefore, be left out. Bolts are pre-assembled into the sub-assembly units so that they help rather than hinder the assembly makeup problem.
- Tapered engagements ease the alignment problem and make precision and repeatable builds possible. There are no requirements for special assembly and inspection operations requiring special equipment or operator judgments.

Figure 4.3-61 illustrates some of the features important to the human engineering considerations in the turbine design.

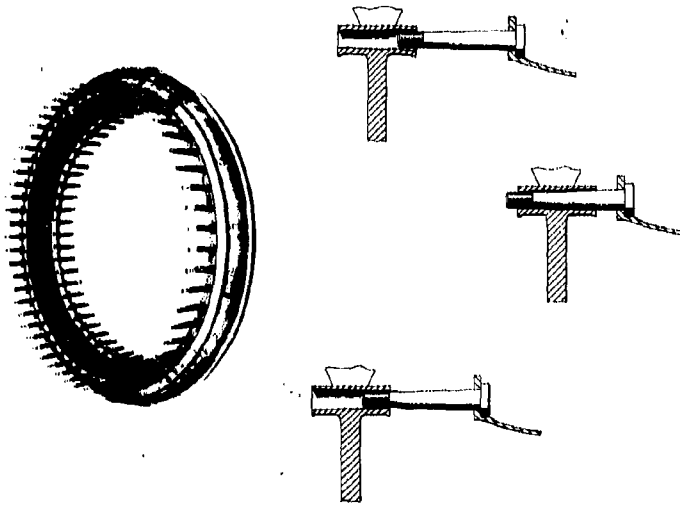


Figure 4.3-61 HUMAN ENGINEERING. Factors effecting handling ease, personnel safety and error free performance are considered at each step in the turbine design. Some of the features designed into the palls are illustrated above. A. Bolts cannot be assembled into the wrong holes. B. Bolts are rigidly pre-positioned easing handling and torquing. C. Wheels will not assemble when improperly oriented. D. Tapered engagement of heavy assemblies for ease of alignment and seating.

#### 4.3.12 STANDARDIZATION

The entire turbine, rotor and stator, is assembled with standard threaded fasteners. No special nuts, non-standard fasteners or non-standard tooling are required. All use 12-point box wrench heads and standard wrench clearances. Materials are standardized so that it is impossible to assemble a part in the wrong position. Torques, lubricants, and assembly and disassembly procedures are set to accepted operation standards, and careful consideration has been given to the benefits of standardization at every step in the design process.

#### 4.4 DEVELOPMENT STATUS

##### 4.4.1 REVIEW OF THE DEVELOPMENT PROGRAM

The key to the success of the turbine design lies in the wealth of background experience and testing that has gone into the development of General Electric's cooled turbine. Because of the broad scope of this development, it has been a complex program requiring many interrelated studies and many important consolidations of findings. Figure 4.4-1 shows how the cooled turbine design has developed, and the manner in which the various component tests have contributed to the final design solutions. This design flow chart is divided into six basic development areas:

- Performance - Performance testing and the evaluation of the effects of cooling on performance levels
- Component Test and Analysis - Stress and fatigue verification testing, and temperature and life analysis programs
- Engine Testing - Full-scale engine testing of the complete design, and important supporting technology.
- Durability Testing - Component testing to evaluate all possible failure modes
- Producibility Development - Conception and development of manufacturing processes, quality control methods, and cost breakthroughs.
- Quality Control - Development of new inspection and quality control equipment to reduce cost and improve quality of air-cooled components.

The Design Flow Chart serves as a convenient cross-reference to further information in the proposal, but more important it brings into perspective a number of key factors. These key points are the important development program findings on which are based the high level of confidence placed in the GE4 cooled turbine.

- Performance - The effect of air cooling on turbine performance has been thoroughly tested and is well understood
- Metal Temperature Prediction - Cooling effectiveness testing, both in cascades and on the engine, give high confidence in temperature prediction techniques
- Stress - Fatigue - Extensive component stress, high - and low-cycle fatigue testing shows that the properly designed cooled airfoil is every bit as reliable as its solid counterpart and can be designed to lives exceeding that of today's solid airfoils.

- **Engine Testing** - Important verification testing has been obtained on the J93/SST engine. Extensive cyclic testing and extra-severity cruise endurance testing that simulate 1000 hours of SST route structure operation have been completed. Thousands of hours of J93 testing are applicable to the SST structural and cooling concepts, while long life, erosion, wear, and hole clogging tests on the J70 ensure significant SST design life.
- **Durability** - Assurance of durability against the wide range of premature or life-limiting wear-out modes has been obtained through extensive component testing.
- **Producibility** - Many essential and dramatic breakthroughs have been accomplished in the area of stress-free drilling, multiple drilling, and value assurance developments.
- **Quality Control** - Important equipment design advances which make it possible to achieve highly reliable and accurate inspection on even the most sophisticated air cooled designs have been made.

The following text describes the more important of these development programs in some detail.

#### 4.4.2 ENGINE TESTING

The GE4/J5 engine has completed its initial test phase including full speed running to 2274° turbine inlet temperature. Running was completely satisfactory. Figure 4.4-2 shows close-up views of the turbine rotor and blading after the first 10 hours of tests. Photographs of the stator from the same engine are shown in Figure 4.4-3.

The engine was extensively instrumented for temperature and stress information with the primary emphasis on data which was important for safety of running. Figure 4.4-4 shows the measured temperature at 2200°. A close correlation between predicted and measure temperature is noted.

Figures 4.4-5 and -6 show the airfoil temperature measured and predicted. Here again, there is a good correlation between the two numbers.

Stresses observed were low and within 50% of gage limits. Further testing will emphasize more extensive temperature instrumentation and heated inlet running to obtain verification of the predicted levels of cruise metal temperatures.

#### 4.4.3 J93/SST ENGINE DEMONSTRATOR PROGRAM

The J93/SST Engine Demonstrator Program is a two-engine development in which scaled versions of the GE4 turbine and combustor components are tested. As configured, these engines test the critical hot and engine component under conditions precisely simulating take-off and cruise design points. This includes the proper cooling system (source, pressure, temperature and flow), as well as the appropriate gas temperature level and actual temperature profile as developed by the high-temperature combustor system. Table 4-2 tabulates the engine test program running time and test accomplishments.

The engines have accumulated hundreds of hours of operation at inlet temperatures in the range of 2000° to 2685°F, during which over 100,000 individual temperature readings have been recorded.



CONFIDENTIAL

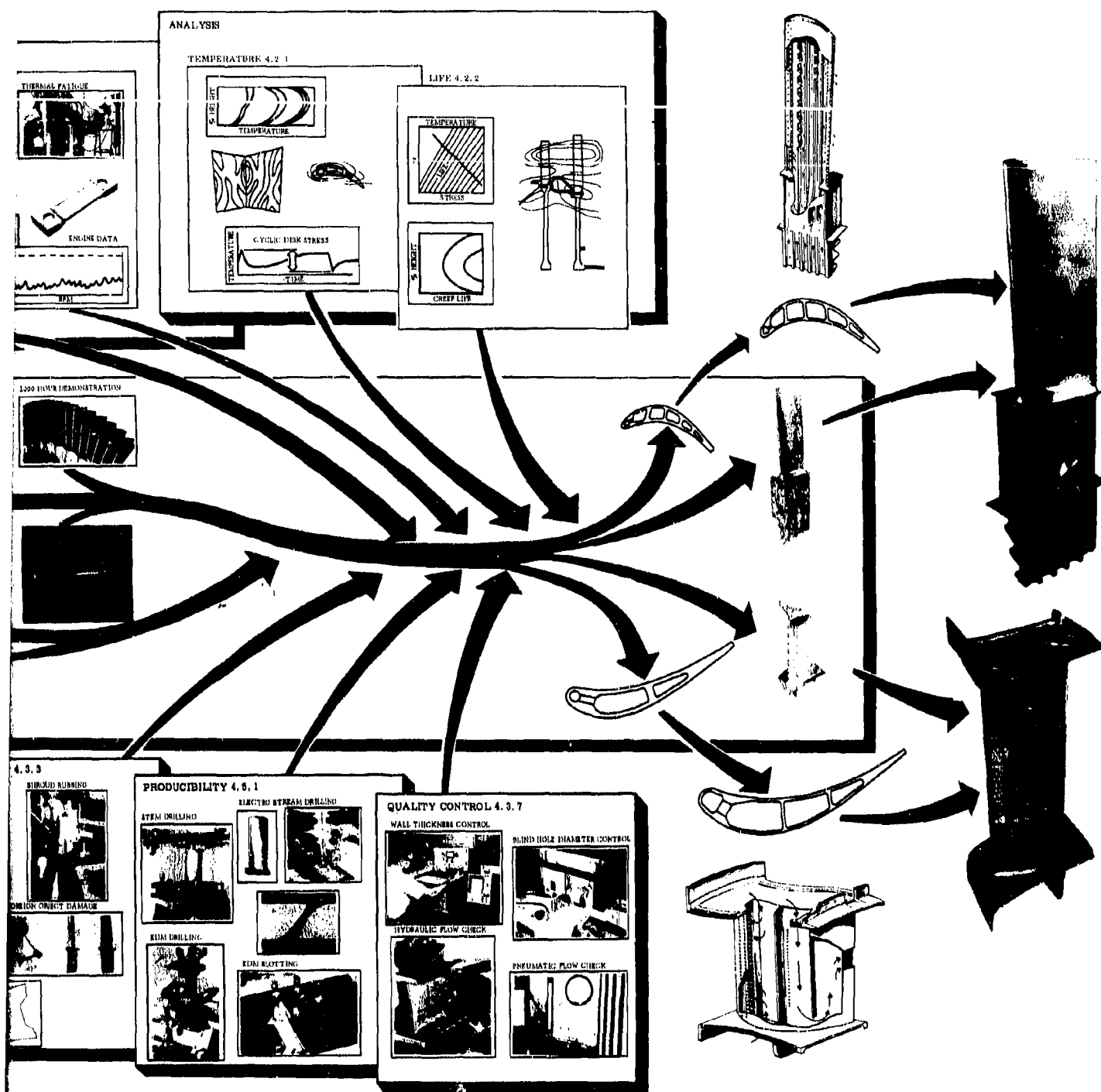


Figure 4.4-1 DESIGN FLOW CHART. Summary Flow Chart showing the Integration of the Various Interrelated Turbine Testing Programs into the Final Design. Cross references are listed where Detailed Discussions of each particular Program can be found.

K

CONFIDENTIAL

4-73/4-74

2

**CONFIDENTIAL**

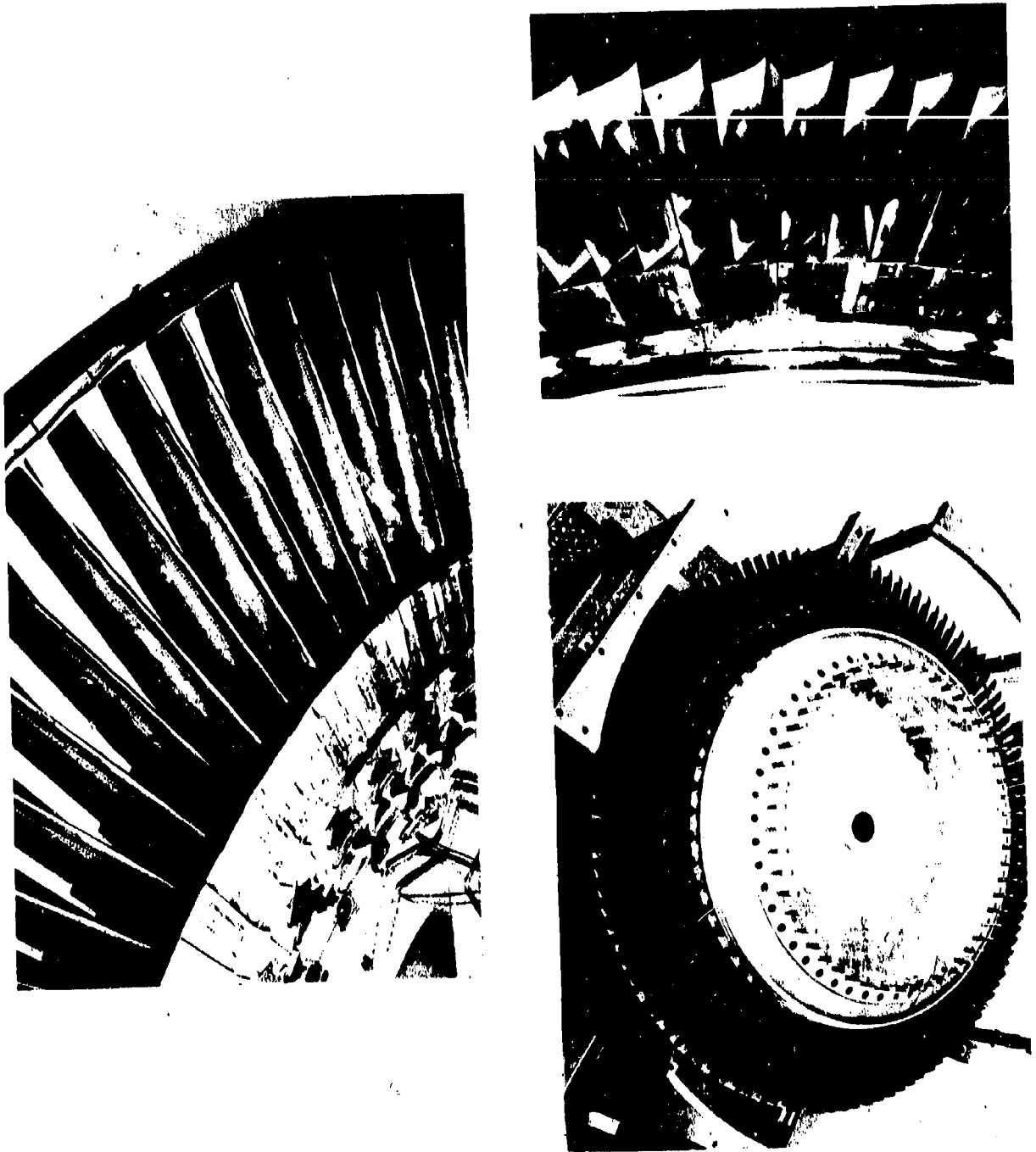


Figure 4.4-2 GE4 TURBINE PARTS AFTER INITIAL FULL SPEED TESTING. Photographs show the turbine parts to be in good condition after initial engine testing.

4-75

**CONFIDENTIAL**

K

**CONFIDENTIAL**

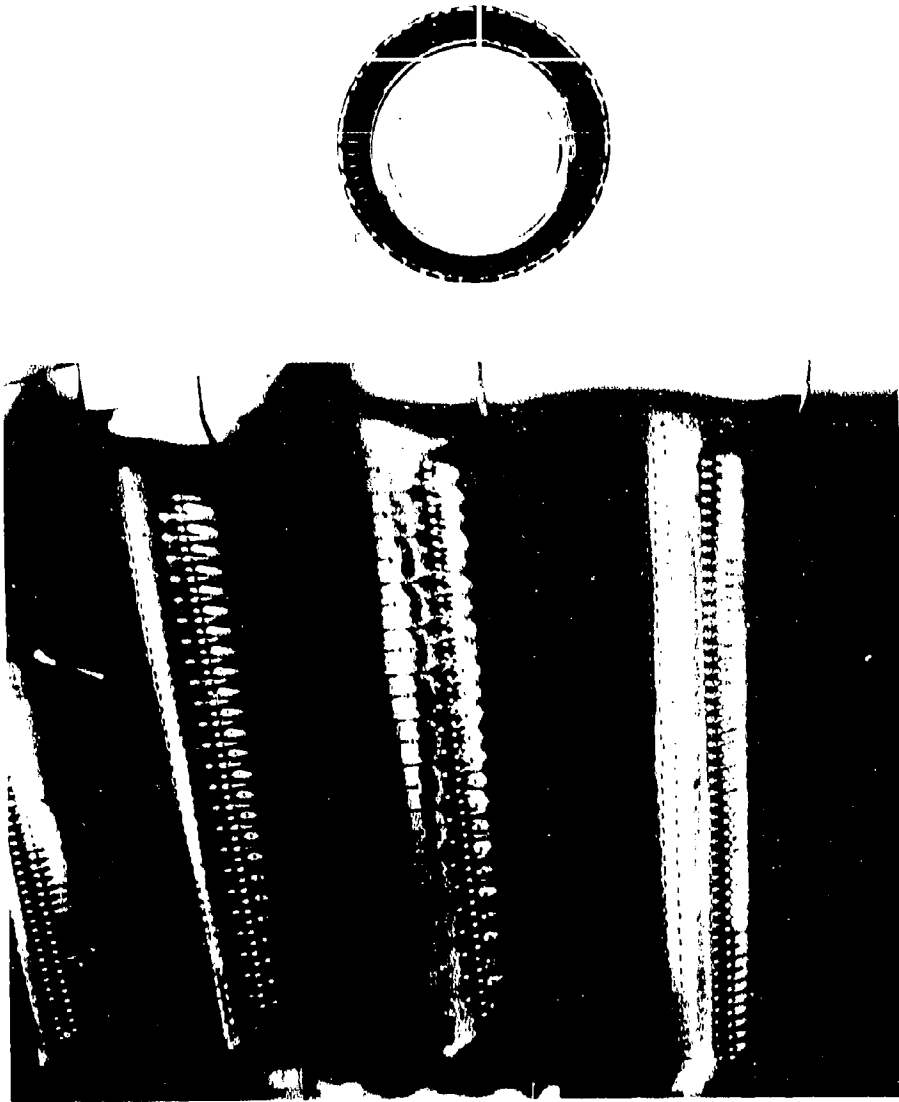


Figure 4.4-3 TURBINE STATOR AFTER FIRST ENGINE TESTING. The first stage nozzle diaphragm and a close view of the leading edges of the vanes are shown after initial full speed testing.

**CONFIDENTIAL**



# CONFIDENTIAL

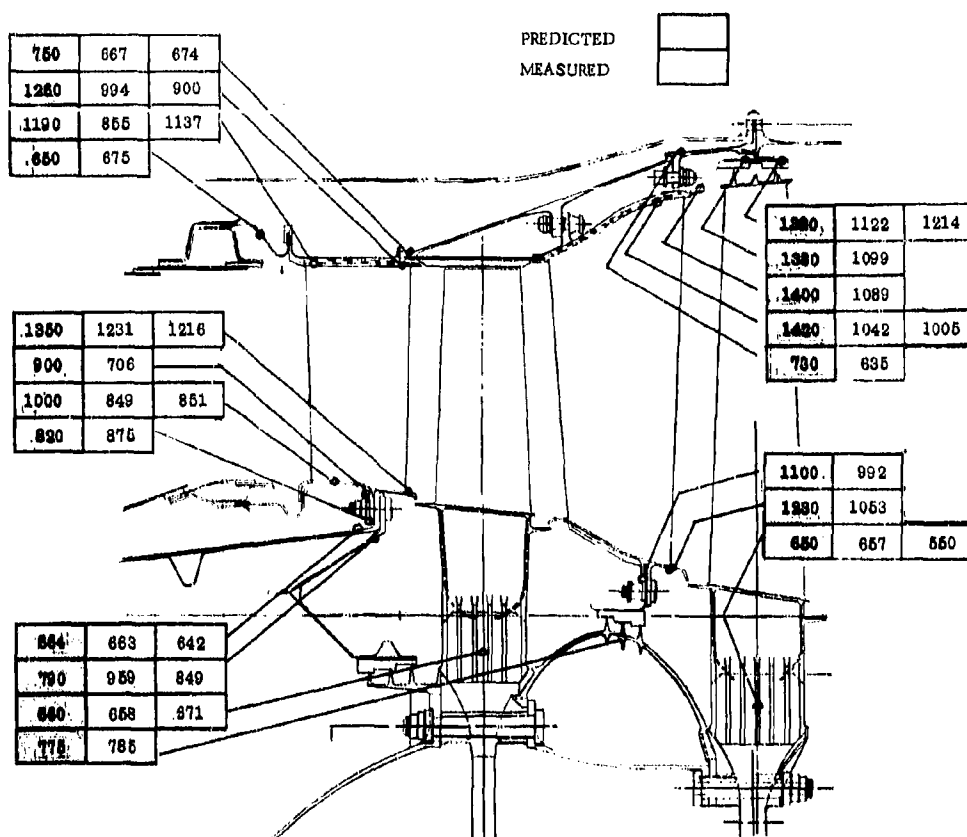


Figure 4.4-4 TURBINE TEMPERATURES - MEASURED vs PREDICTED. Engine temperatures as observed and as predicted at 2200° take off operation. Predicted levels in the flow path are based on the hottest gas temperature assumptions and are in general higher than measured.

Three types of testing have been completed.

- Engineering analysis testing to prove out design features and to confirm cooling effectiveness and soundness of the cooling techniques.
- Endurance testing at take-off and high-temperature cruise operation points.
- Cyclic endurance testing, in which typical accelerations and throttle chops are repeated over and over again, to study tolerance to low-cycle fatigue.

The key accomplishment in the J93/SST engine program is the completion of the test runs simulating 1000 hours of typical SST route segment operation. This testing included accelerated cruise testing at extra-severity temperature conditions and repeated cyclic transient testing. Figures 4.4-9 and 4.4-10 show the rotor and stator parts after the accelerated endurance and cyclic endurance portions of the engine test program. Photographs show the parts to be in excellent condition after the completion of the simulated 1000 hours of SST operation.

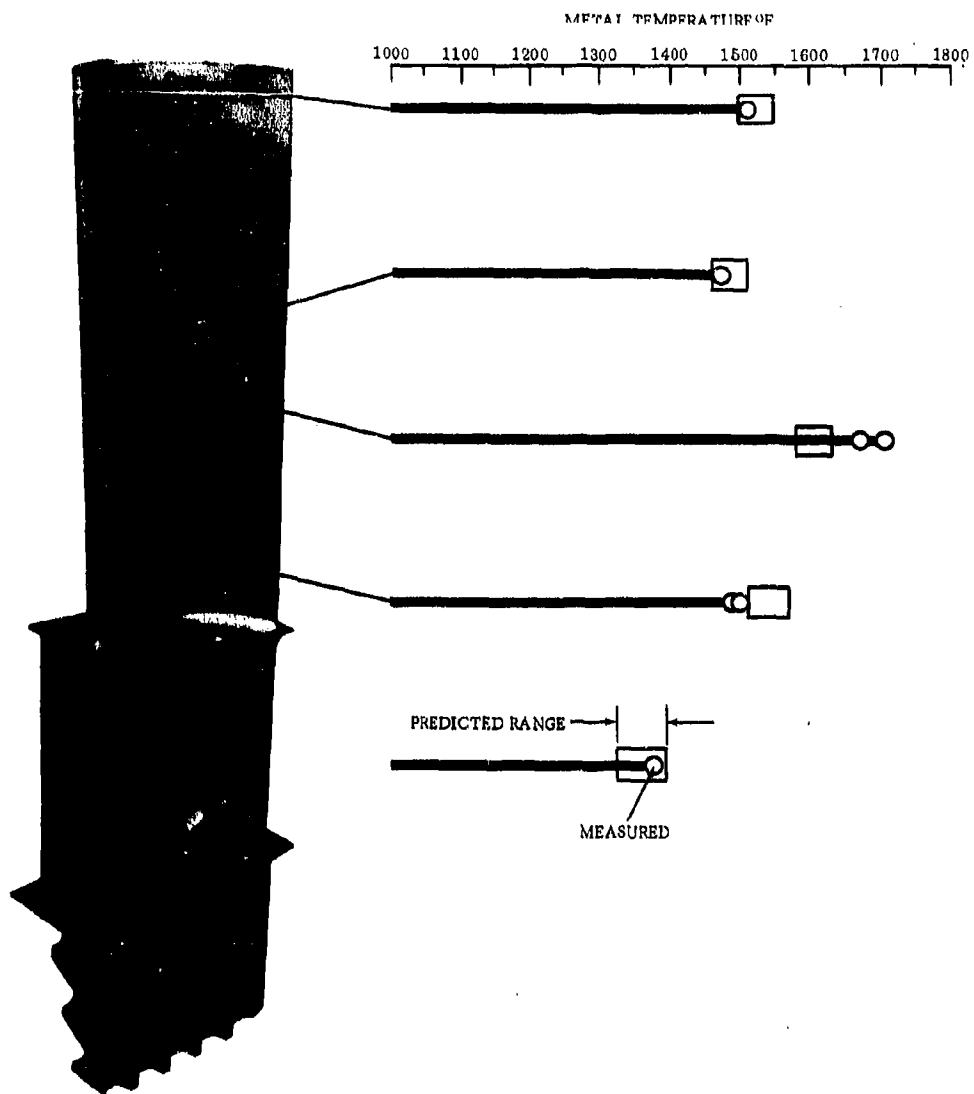


Figure 4.4-5 TURBINE BLADE TEMPERATURES - MEASURED VS PREDICTED. Airfoil temperatures as measured on the GE4 at Sea Level Static are compared with calculated values.

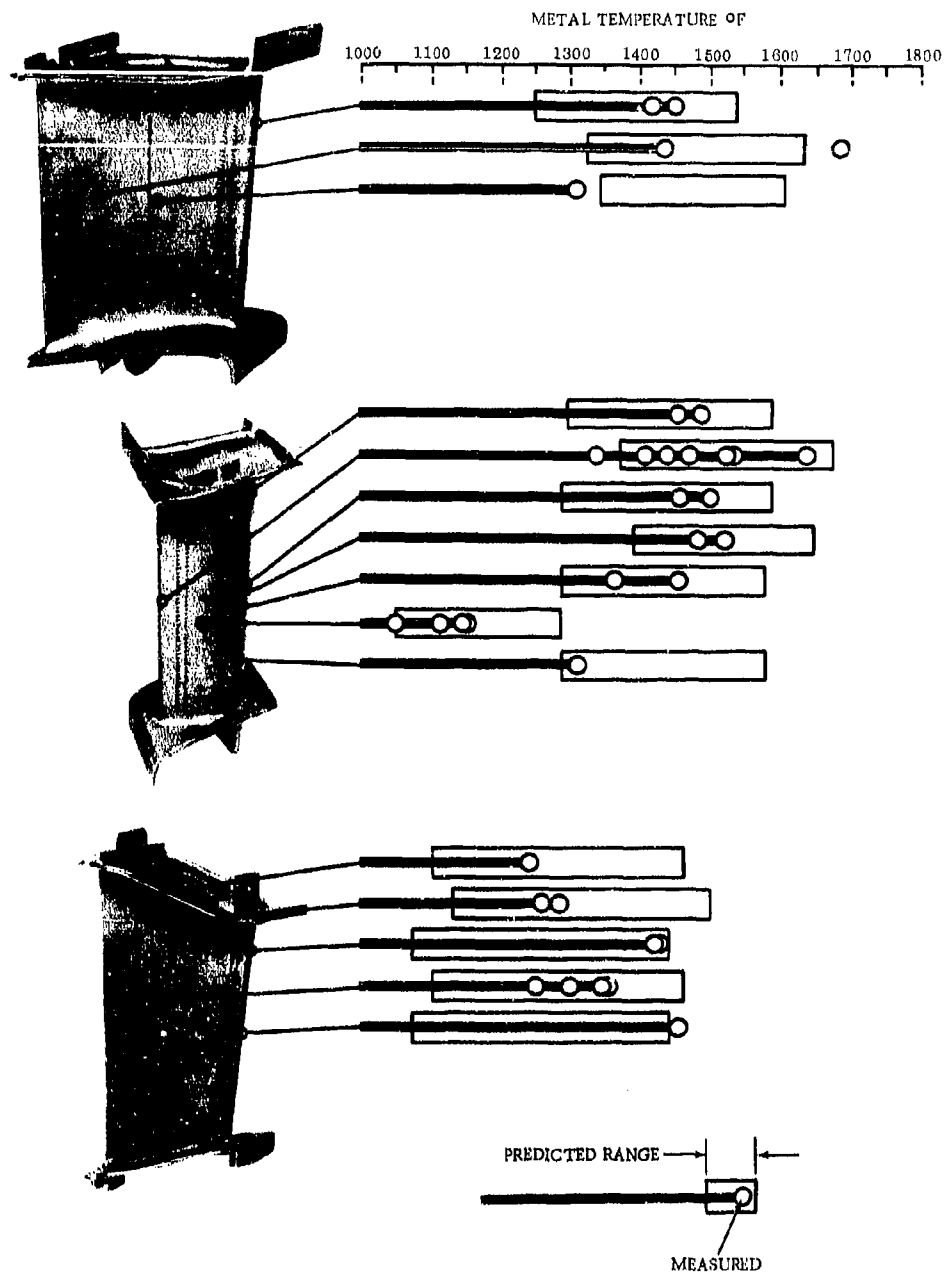


Figure 4.4-6 TURBINE VANE TEMPERATURES - MEASURED VS PREDICTED. Measured vane airfoil temperatures compared to the temperature levels predicted.

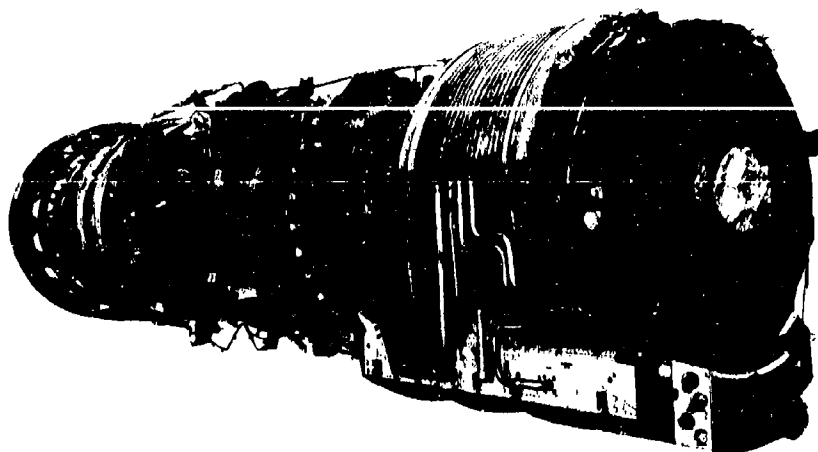


Figure 4.4-7 J93/SST DEMONSTRATION ENGINE. One of the two SST demonstrator engines which have been accumulating extensive high temperature endurance and cyclic test running. Information obtained on these advanced engines has given important guidance and assurance to the GE4 design.

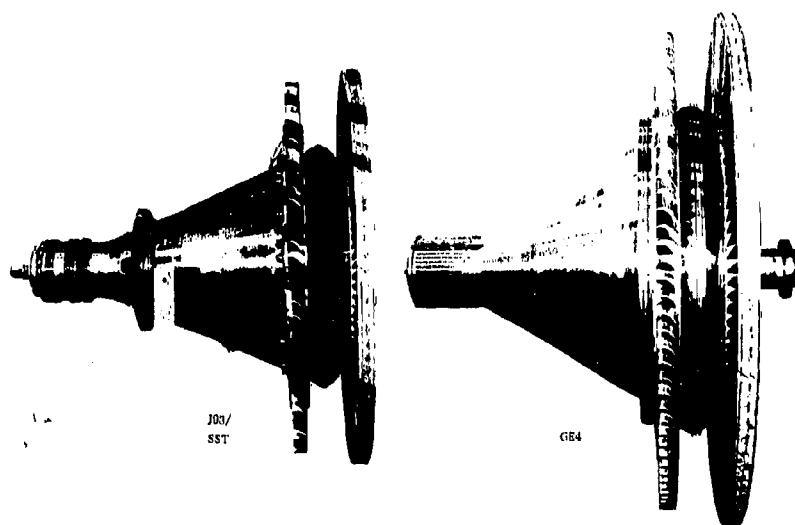


Figure 4.4-8 J93/SST AND GE4 TURBINE. The SST demonstrator turbine is smaller than the GE4 but is in detail very similar to the flight SST design. Not only is the mechanical configuration the same, but details of the cooling system closely simulate the flight SST design.





Table 4-2. (Continued)

RUNNING TIME SUMMARY										
Test Engine	Test Objective	THIS TEST					CUMULATIVE			
		Total	Above 2000°F	2200°F and Above	Cycles	Total	Above 2000°F	2200°F and Above	Cycles	Max. T <sub>4</sub>
7	<ul style="list-style-type: none"> <li>● ALL-COOLED TURBINE CHECK OUT</li> </ul> Shrouded Second-stage blade test	7:30	:32	:21	-	237:45	167:37	166:00	500	2215
8	<ul style="list-style-type: none"> <li>● CYCLIC ENDURANCE TESTING (1000 Cycles)</li> </ul> Accumulate 1000 rapid transient cycles Refined vane design	58:45	26:23	26:12	1000	296:30	234:00	192:12	1500	2210
9	<ul style="list-style-type: none"> <li>● ALL-COOLED TURBINE CRUISE TEMPERATURE CHECKOUT</li> </ul>	10:18	6:34	5:02	-	306:48	240:34	197:14	1500	2215
										<ul style="list-style-type: none"> <li>● All parts in excellent condition</li> <li>● GE4-type all cooled turbine meets all design objectives</li> <li>● Shrouded blade stresses low</li> <li>● Temperature levels achieved throughout turbine</li> <li>● Accumulated 1000 cycles on one set hardware</li> <li>● No cracks on vanes</li> <li>● Blades - Initial leading edge cracks at 540 cycles.</li> <li>● All parts in excellent condition</li> <li>● Temperature predictions met at SLS (T/1) and cruise (M 2.7)<sub>p</sub></li> </ul>

**Table 4-2. (Continued)**



**CONFIDENTIAL**

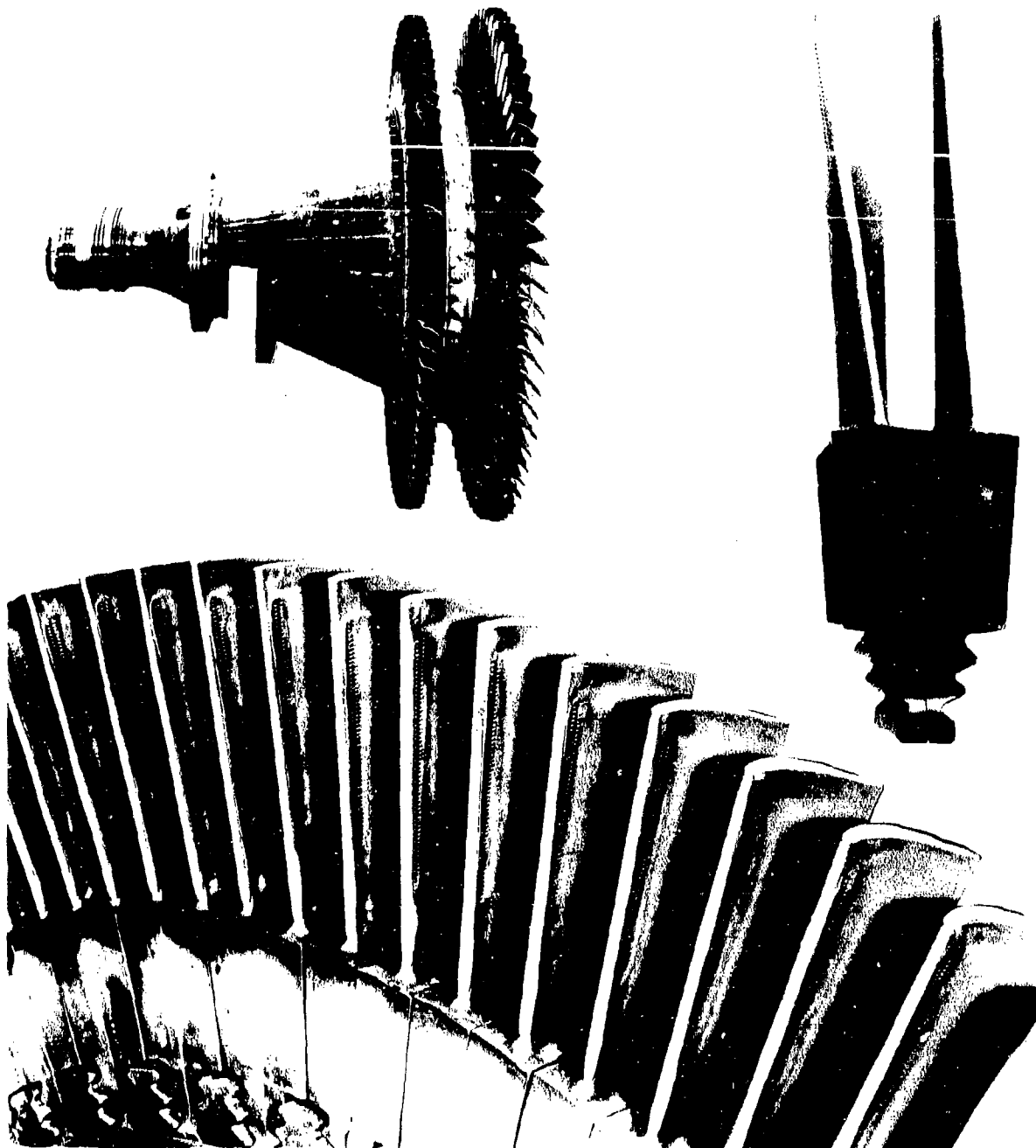


Figure 4.4-9 ACCELERATED ENDURANCE ROTOR PARTS. Turbine rotor and close-up views of the blades from the extra severity engine test program. The parts have been subjected to repeated cyclic transient and high temperature endurance conditions which simulate 1000 hours of SST operation.

4-85

**CONFIDENTIAL**

K

**CONFIDENTIAL**

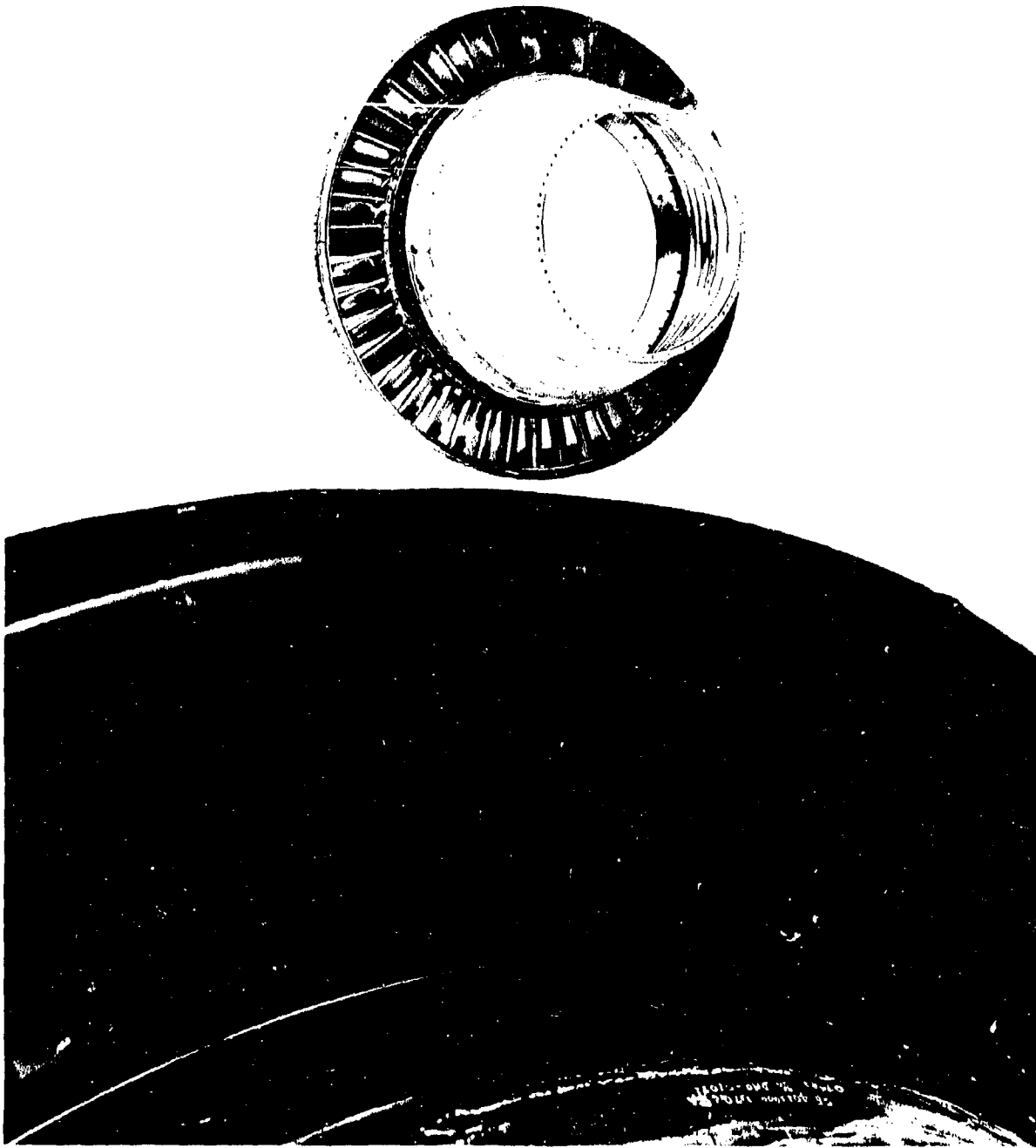


Figure 4.4-10 STATOR PARTS AFTER EXTRA SEVERITY TESTING. Photographs of the nozzle assembly and vanes show the turbine stator to be in good condition after extensive cycle and high temperature test exposure which simulates 1000 hours of SST operation.

4-86

**CONFIDENTIAL**

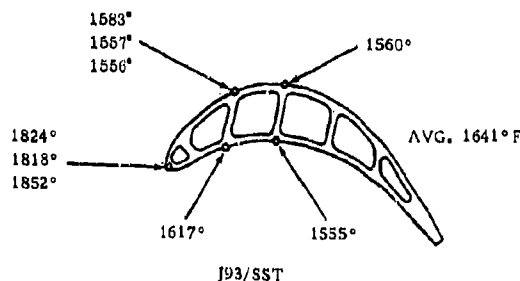
#### 4.4.3.1 J93/SST Temperature Measurements

Figure 4.4-11 and -12 show the measured metal temperatures at specific points on the blade and vane airfoil. Actual measured temperatures are compared with the predicted range. Good correlation between predicted and measured temperature is noted. Temperature analysis and prediction techniques are the same for the GE4 as they are for these J93/SST tests. Actual levels of metal temperatures for comparable gas temperatures are lower for the GE4 because of a more effective internal convection cooling path. The GE4 blades are structurally the same as the J93/SST parts, but they use a serpentine path for the internal cooling. The higher velocities in the serpentine concept mean important improvements in cooling effectiveness and significant reductions in metal temperature.

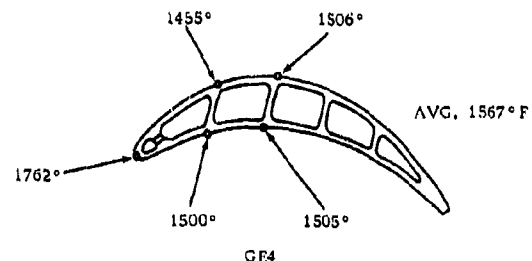
#### 4.4.3.2 Accelerated Cruise Testing

In order to reduce the amount of time needed to demonstrate hundreds of hours of simulated SST cruise operation, it has been necessary to increase the severity of the test. This portion of the test is actually made many times more severe by increasing metal temperatures throughout the turbine. The accelerated cruise test is actually run at conditions simulating Mach 3.0 operation on the J93. As one can see from Figure 4.2-9, a 100° difference in metal temperature is a 10 to 1 factor on life. On the creep limited blade airfoil, the testing on a percentage-of-creep-life-used basis is even more severe in the J93 when considering the creep strength effect of the actual materials used. The initial cruise endurance objective was to demonstrate 1000 hours of typical route structure operation. For the 12,000 hour GE4 design, this is 1000/12,000 or 8.3 percent of the blade life on a time: temperature basis.

The measured J93/SST temperatures compare with the calculated GE4 temperatures as follows:



J93/SST



GE4

Other J93/SST conditions:

Inlet gas temperature	2200°F
Coolant temperature	1074°F
Stress (effective)	18,750 psi
Creep life (See Fig. 4.2-9)	340 hours
8.3% of 340 hours	30 hours

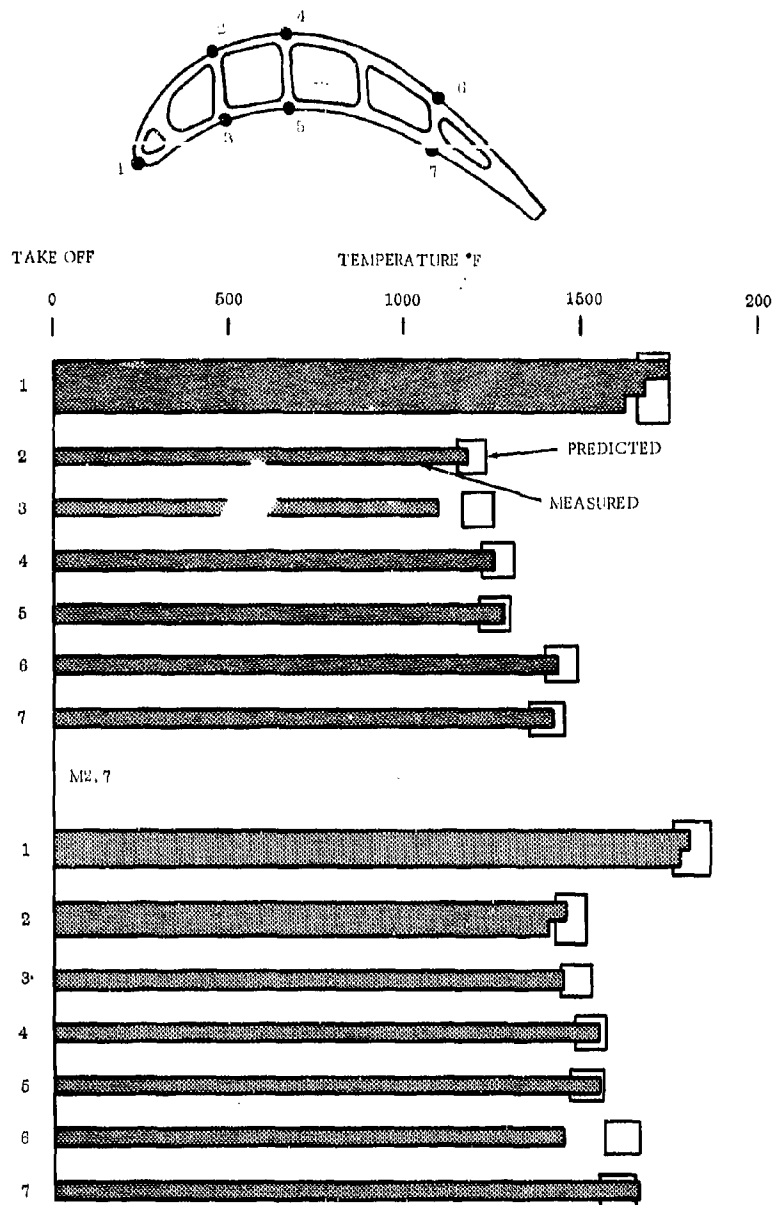


Figure 4.4-11 BLADE TEMPERATURES — J93/SST. Blade temperature summary showing measured and predicted Temperature levels.

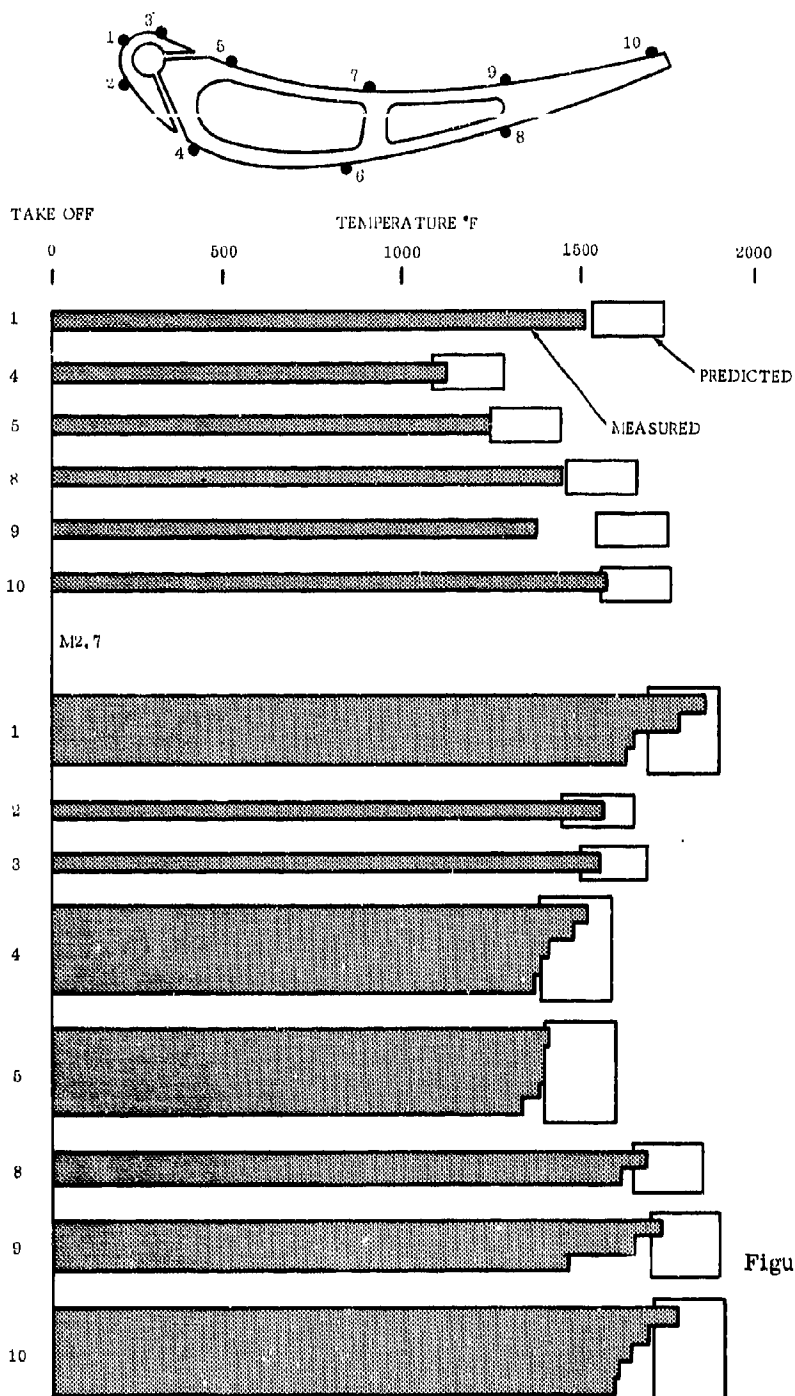


Figure 4.4-12 VANE TEMPERATURES - J93/SST. Plots showing Vane Temperatures as Measured on Demonstration Engines.

The cruise endurance test was run for 30 hours, then the parts were carefully inspected. There was no visible distress of any kind. It is important to note that some of the blades and vanes in this endurance run had previously completed the 1000-cycle engine test and, like the rest of the turbine, showed no sign of wear or distress.

#### 4.4.3.3 Cyclic Endurance Testing

Cyclic operation forms a strenuous and important portion of the simulated 1000-hour life proof-test. Figure 4.4-13 displays the acceleration and throttle-chop transients imposed on the engine. There are actually about 375 cycles in 1000 hours of SST operation. This number was increased to 540 cycles for the J93/SST test to take into account starting and reverser cycles, although starting is not a severe problem on air-cooled airfoils. (See Figure 4.3-24.) The actual cyclic engine test has run to 1000 cycles, and is continuing. Thermal fatigue checking has started on the leading edge of the J93/SST blades as predicted. (Refer to Section 4.3.3.1.) This running has provided important design assurance to the GE4 turbine design, and will continue to be a valuable method of obtaining accelerated proof testing.

### 4.5 SUPPORTING TECHNOLOGY

#### 4.5.1 MANUFACTURING AND PROCESS DEVELOPMENT

Progress in the turbine design, and the quality and value built into the turbine parts, are largely a result of the advancements made in processing, manufacturing and inspection techniques. These processes have made possible important design breakthroughs that contribute heavily to the advanced performance capability of the GE4 engine, and to the inherent durability and long-life capability of the design.

Figure 4.5-1 through -6 show several of the newly developed techniques for producing new air-cooled designs. Quality and repeatability of these new processes bring machining cost levels to a small percentage of the cost of the basic casting. Figure 4.5-1 shows the electrostream drilling process used to form the edge holes of the blades. The process gives stress-free precision holes with smoothly rounded edges. Automated feed and speed techniques ensure accuracies with 0.001-inch diameter. Multiple drilling and indexing tooling bring costs to pennies a hole. Facilities and tooling costs are lower than for any other form of hole drilling. Figure 4.5-2 shows the STEM drilling operation used for holes in the vane edges where almost an unlimited number of holes can be drilled simultaneously.

Figure 4.5-3 pictures a new technique for the EDM machining of thin slots. Leading edges of the vane airfoil are slotted to relieve thermal stresses and distortions. Tests prove the feasibility of simultaneously sawing as many as fifteen 0.005-inch slots in one pass. Figure 4.5-4 illustrates the EDM drilling techniques used to put the holes in the vane bands and leading edges. Precise holes are drilled in fixtures that produce many holes in one pass.

Figures 4.5-5 and -6 illustrate some of the automated inspection techniques used to provide rapid and dependable quality assurance not possible with more conventional inspection techniques.

New manufacturing and inspection developments are being perfected each day in these rapidly expanding fields. It is reasonable to expect that the day will come when the advanced air-cooled components will cost little more than the solid designs of the past.

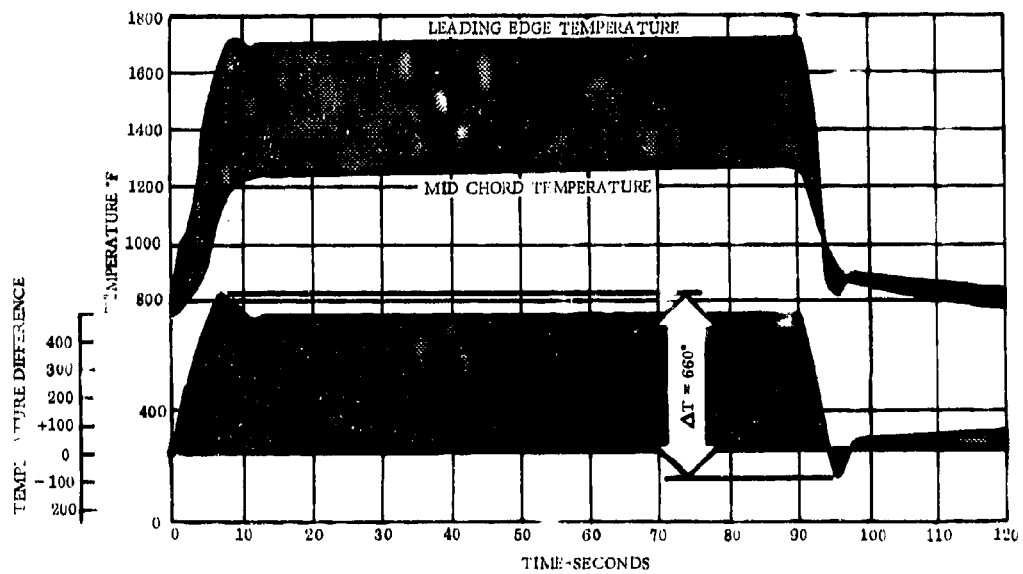
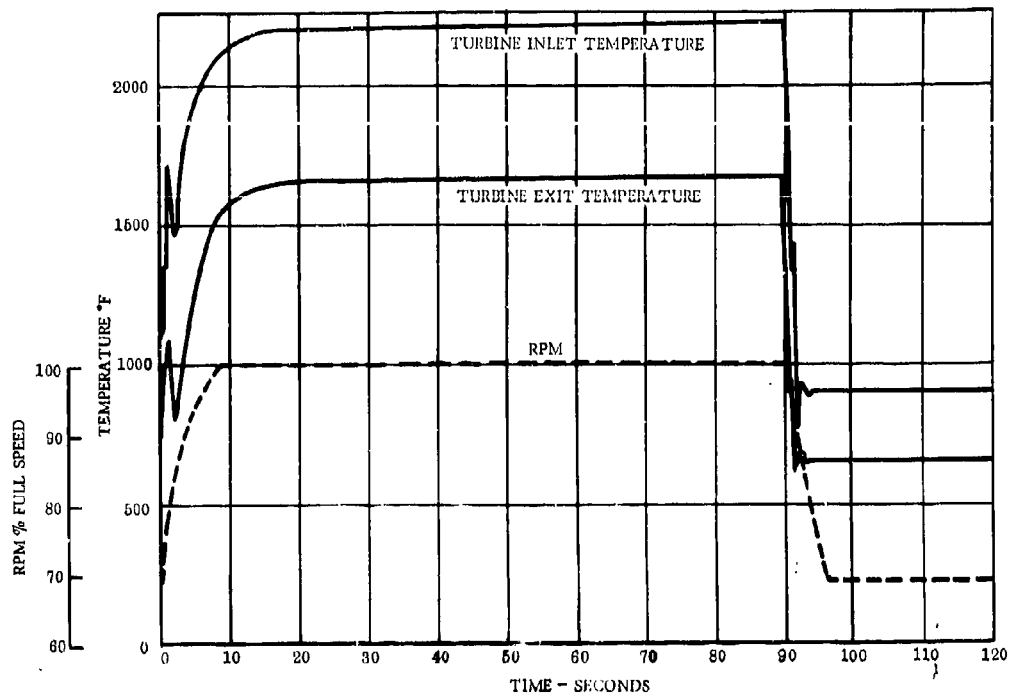


Figure 4.4-13 CYCLIC TEST TRANSIENTS. Plot of the transient gas and metal temperatures during the cyclic fatigue tests on the J93/SST demonstration engine.

**CONFIDENTIAL**

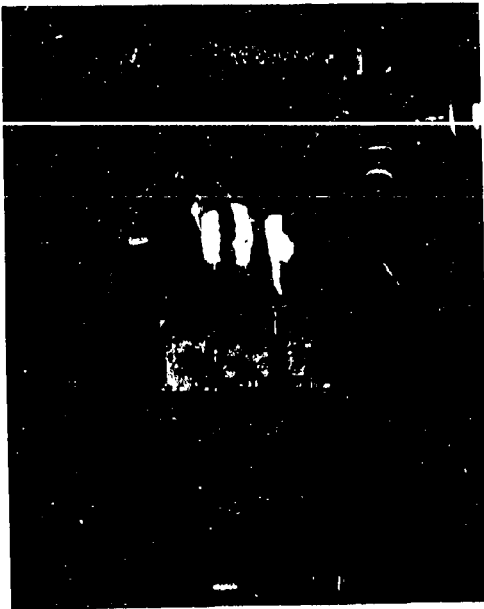


Figure 4.5-1 **ELECTROSTREAM DRILLING.** Advanced, stressfree, precision and low cost hole drilling techniques with new electrolytic machining and processes make possible the reliable film cooled airfoil design of the GE4 Turbine.

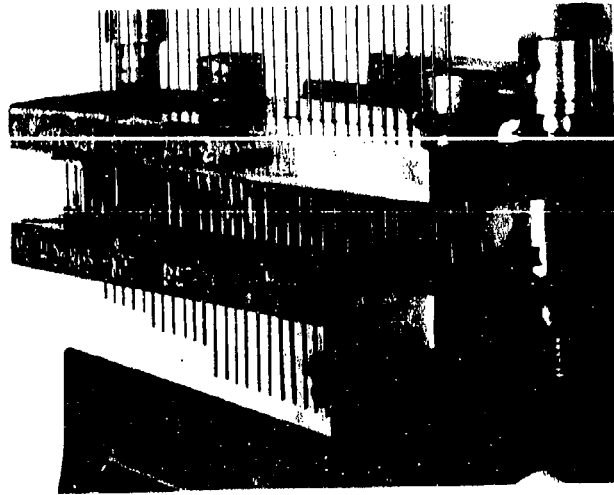


Figure 4.5-2 **STEM DRILLING.** Like electrostream, the stem drilling process makes it possible to economically produce hundreds of low cost, precision cooling holes.

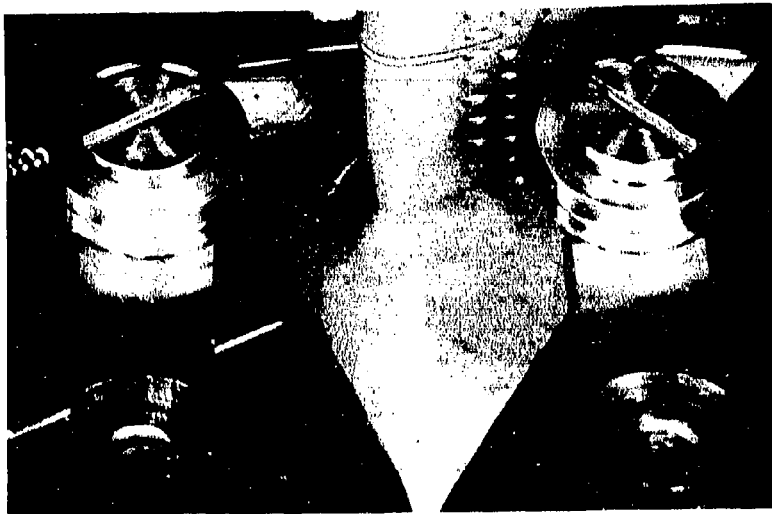


Figure 4.5-3 **EDM SLOTTING.** General Electric breakthroughs in electrical discharge machining techniques have made it possible to produce slots less than .005" in width. New vane structural concepts have been possible with this capability and important design improvements have been realized.

**CONFIDENTIAL**



**CONFIDENTIAL**

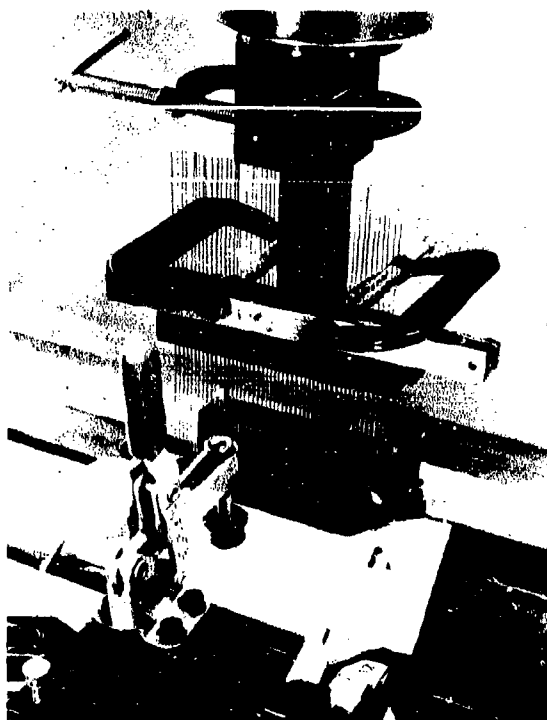


Figure 4.5-4 EDM DRILLING. In low stress areas multiple hole drilling with electrical discharge machining techniques has proven both inexpensive and accurate.

#### 4.5.2 RELATED DEVELOPMENT TESTING

Figure 4.4-1 can show only a portion of the test programs that are concerned with the development and proof testing of the GE4 turbine. Many other related tests have been completed; others still in progress contribute heavily to today's understanding of the GE4 design and to the high level of confidence placed in it.

The TF39 program, and the test programs that support it, are of particular importance to the GE4 engine.

- The TF39 leads the development of the GE4 Phase III engine by approximately 1-2/3 years as measured by first engine to test and FTS. When measured at MQT, the TF39 leads the GE4 Phase III by 4 years.
- The cooling system and mechanical configuration are similar. The temperatures of the TF39 and the GE4 are very comparable.
- TF39 Core Engine Cyclic Testing will provide very important cyclic data for the GE4 program. The core engine of the TF39 is scheduled to complete an extensive program of maximum-severity transient testing including 2000 maximum throttle bursts and chops in 1966 and 15,000 by mid-1968.

Table 4-3 is a summary of some of the important current supporting programs, which will continue to contribute to GE4 turbine design.

**CONFIDENTIAL**

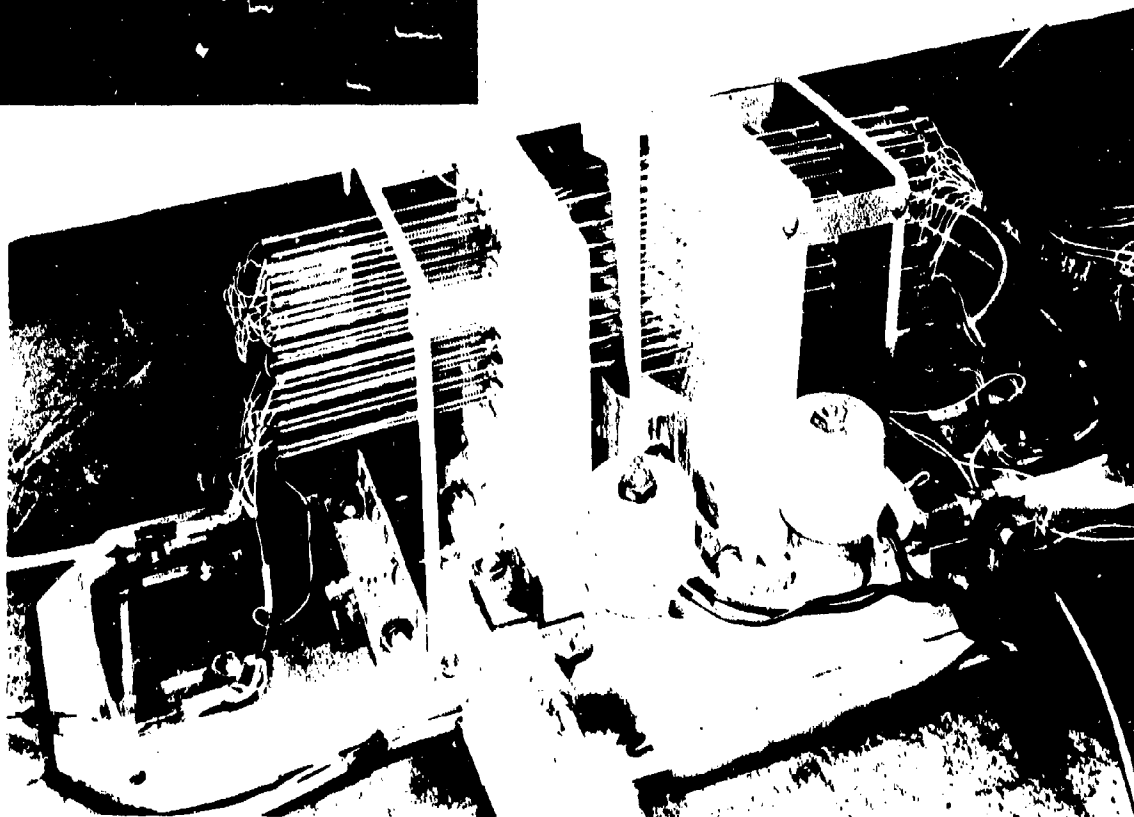
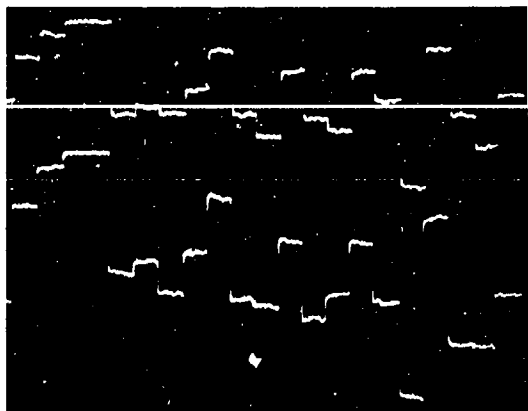


Figure 4. 5-5 **AUTOMATIC INSPECTION - COOLING CIRCUIT.** Equipment for functional testing of the cooling circuit on each blade is under development. This contact thermocouple system senses surface temperature at transient intervals in such a manner as to be able to make photographic printouts of change in temperature. Local hot spots close to restricted holes or dimensional variations are readily discernible.

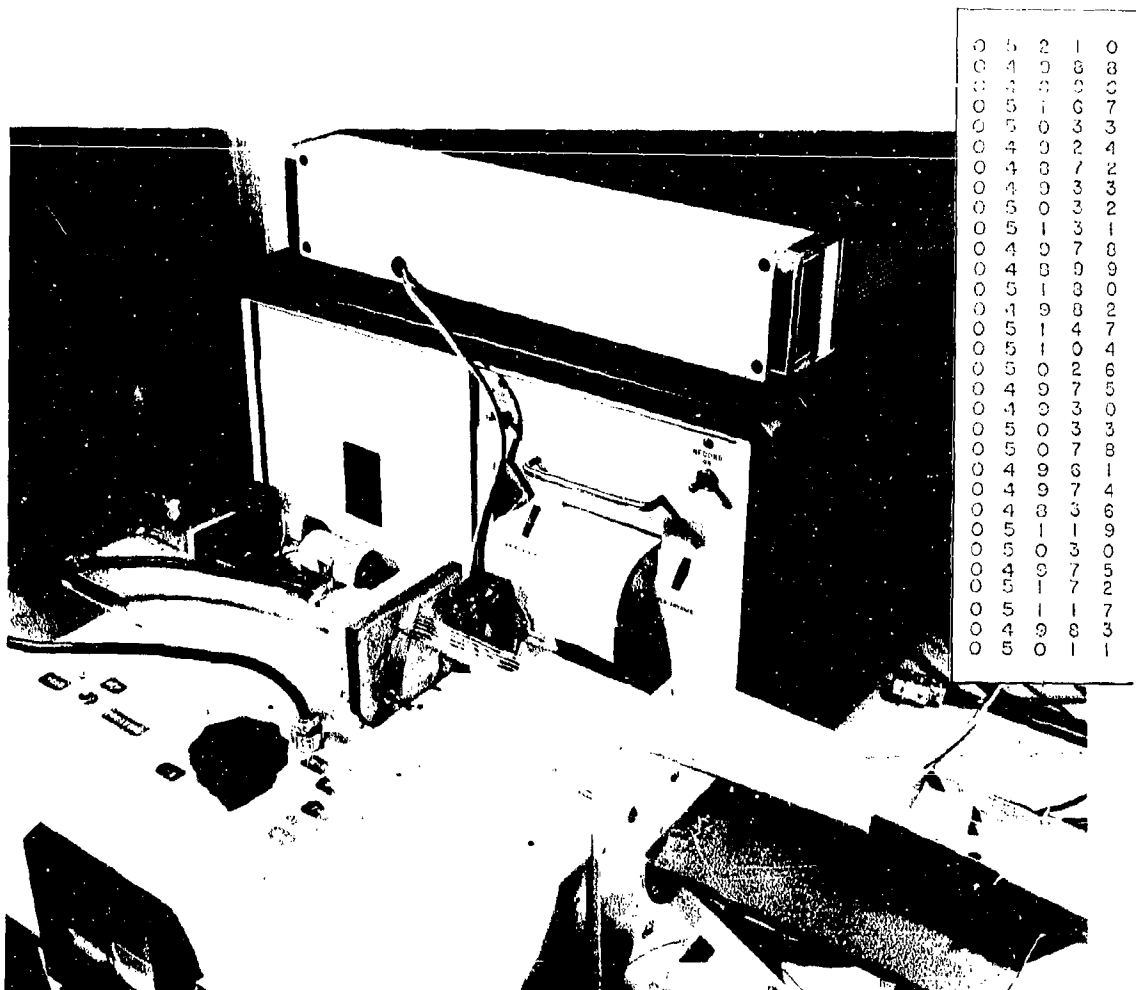


Figure 4.5-6 AUTOMATED INSPECTION - INTERIOR HOLE SIZE. Internal holes are inspected with automatic photoelectric sensing equipment which senses and digitally records each internal diameter with repeatability of closer than .001".



TABLE 4-3. (Continued)

COOLING EFFECTIVENESS									
MATERIALS-COATINGS									
WEAR-EROSION-CORROSION									
MECHANICAL FATIGUE									
THERMAL FATIGUE									
CREEP LIFE									
COST-PRODUCTIVITY									
MAINTAINABILITY									
PERFORMANCE									
PROGRAM									
OBJECTIVES									
FINDINGS									
J93 Engine Testing									
									<ul style="list-style-type: none"> <li>Over 6000 hours total running 7/1/56</li> <li>1360 hours of heated inlet running</li> <li>305 hours at Mach 3.0</li> </ul>
									<ul style="list-style-type: none"> <li>209 transient cycles</li> <li>380+ total hours</li> <li>112 hours over 2000°</li> </ul>
TF39 Engine Testing									
									<ul style="list-style-type: none"> <li>Performance, film cooling effectiveness, producibility and design experience directly applicable to the GE4 design.</li> </ul>
ACTV - Air Cooled Turbine Vehicle Testing									
									<ul style="list-style-type: none"> <li>In a rotating component test: <ul style="list-style-type: none"> <li>Demonstrate cooling effectiveness</li> <li>Verify temperature prediction technique steady-state, transient</li> <li>Cyclic life</li> <li>Endurance capability</li> </ul> </li> <li>Determine film effect on performance in act rotating environment</li> <li>Evaluate cyclic life prediction technique</li> </ul>
									<ul style="list-style-type: none"> <li>Predicted metal temperatures attained</li> <li>T/C temperatures check compared value</li> <li>550 cycles complete</li> <li>3 hours at 2400°F (extra severity)</li> <li>Analytical estimates verified</li> <li>Calculated strains of correct order</li> </ul>

TABLE 4-3. (Continued)

PERFORMANCE MAINTAINABILITY COST-PRODUCTIVITY CREEP LIFE THERMAL FATIGUE MECHANICAL FATIGUE WEAR-EROSION-CORROSION MATERIALS-COATINGS COOLING EFFECTIVENESS	PROGRAM		OBJECTIVES		FINDINGS
	Blade Film Cooling Test Rig		Investigate (in a rotating stage environment). • Effect of "G" field on film cooling effectiveness. • Incidence angle effect on film effectiveness. • Variation of cooling effective- ness with cooling air tempera- ture and flow.		
X			Complete 280 hours of extra severity testing on film-cooled blades at 2400°F.		Leading edge film cooled blades run beyond the ex- tremes of the GE4 inlet tem- perature range without distress.
X			Evaluate film effects on nozzle performance. Study effectiveness of various types of film injection.		Extensive data contributing to further understanding of film-cooling nozzles gathered.

TABLE 4-3. (Continued)

PERFORMANCE MAINTAINABILITY COST-PRODUCTIVITY CREEP LIFE THERMAL FATIGUE MECHANICAL FATIGUE WEAR-EROSION-CORROSION MATERIALS-COATINGS COOLING EFFECTIVENESS				<u>PROGRAM</u>  Film-Cooled Blade Cascade Tests	<u>OBJECTIVES</u>  ● Refinement and verification of earlier blade film studies. ● Study of effect of specific elements of coolant hole design. ● Evaluate aero, performance effects of GE4.	<u>FINDINGS</u>  Results of earlier tests verified. Design methods substantiated. Five cooling configurations compared and select on made. Tests results check predictions.
	X					
				Blade - Thermal Fatigue	Develop background technology and analytical methods for cyclic life prediction in thermal fatigue. Verify cyclic life of GE4 configuration.	550 test hours accumulated as of 7/1/66. Analytical methods developed are in good agreement with test results. Program has made significant contributions toward the understanding of thermal fatigue and ability to predict cyclic life. (Refer to section 4.3.3.1).
				Blade Mechanical Fatigue	Endurance test GE4 blades at temps. to determine runout stress levels and establish engine test limits.	Tests verify satisfactory mechanical fatigue strength. Engine tests confirm adequacy of design margin for blade vibration (Refer to section 4.3.3.2).

TABLE 4-3. (Continued)

PERFORMANCE	MAINTAINABILITY	COST-PRODUCTIVITY	CREEP LIFE	THERMAL FATIGUE	MECHANICAL FATIGUE	WEAR-EROSION-CORROSION	MATERIALS-COATINGS	COOLING EFFECTIVENESS	PROGRAM		OBJECTIVES		FINDINGS
									J79/CJ805 Engine Testing. Wear/Erosion		Evaluate the effects on an engine of dust ingestion typical of thousands of hours of GE4 type operation. Particle size 0-8 microns - 500 pounds, 16-mil particles - 8 quarts.		GE4 Size air-foil cooling holes did not clog. Airfoil erosion matched field experience. GE4 design allowance for blade erosion is realistic. (Refer to section 4.3.3.4.)
									Blade - FOD Testing		Determine strength of hollow GE4 airfoils relative to current commercial blades in controlled laboratory impact tests.		Film-cooled GE4-type airfoils show better resistance to foreign object damage than the smaller CJ805 airfoils. Coolant system is not effected by FCD on the GE4 design.
									Blade-Vane Flame Tunnel Exposure Testing		Subject the cooled vanes and blades to full-temperature, steady-state, and cyclic gas temperature condition to simulate thousands of hours of flight test conditions.		This testing is planned for screening and reliability work on material and coatings. Initial results after 700 hours of blade exposure show no distress. Cyclic temperature exposure testing on the vanes will include gas loading for a creep as well as a thermal fatigue and oxidation evaluation.



## 5. AUGMENTOR

### 5.1 MECHANICAL COMPONENTS

#### 5.1.1 INTRODUCTION

General Electric military turbojets have employed augmentors of the reheat type for efficient thrust increase since 1951. Figure 5-1 shows the continuous experience build-up and advancement in augmentor capability, culminating in the commercial GE4 design. The mechanical durability and reliability have progressively improved as succeeding larger proportions of typical flight spectrums have required augmentor operation; starting with 8 percent on early J47 flights through 13 percent on current J79 flights, to the continuous use of partial augmentor power for all portions of the supersonic flight spectrum of the J93. The important points to note from Figure 5-1 are:

- The 2840°F rating for the GE4 is conservative in comparison with the current in-service capabilities which have progressed from 2800 to 3200°F for military applications.
- The reduction in length by 40 percent contributes to reduced cooled surface and reduced weight.
- Film cooled liner techniques, V-type flameholders and radial spraybars have been used since initial J47 design.

The simplicity of the basic augmentor design is illustrated in Figure 5-2. These general durability and maintainability advantages are cited:

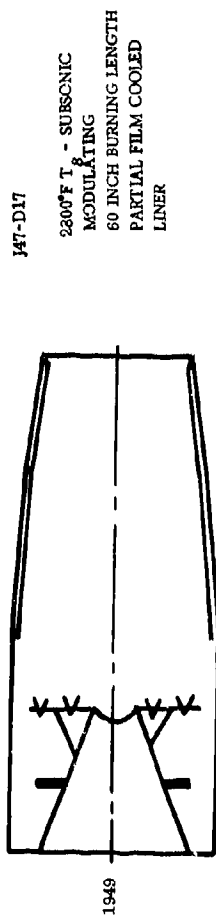
- Cylindrical combustion zone - minimum cooled surface area.
- Short length with diametral dimensions within the basic engine envelope.
- Simple fuel injectors (spray-producing nozzles are not required).
- Simplified flameholders - series of concentric V-shaped rings.
- Ease of augmentor component inspection and replacement through the exhaust nozzle.

The design similarity of the progenitor augmentor designs is illustrated in the actual engine configurations shown in Figure 5-3.

For the proposed GE4 augmentor, this basically simple design approach has been coupled with the two-stage combustion method for broad temperature modulation, illustrated in Figure 5-4. This provides effective isolation of the combustion reaction from the augmentor structure for most of the SST augmentor operation (typical SST flight profile requires 68 percent of the operating time on low augmentation, and only 11 percent with maximum augmentor temperature). An additional contributor to commercial durability is the non-luminous radiation from the exhaust gases which results from the burning of vaporized fuel at low pressures.

Since the turbojet augmentor makes effective use of the total engine airflow, the temperature rise for both cruise and maximum operating conditions is low.

1

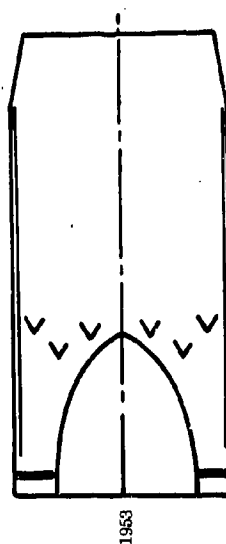


1949

J47-D17

2200°F T - SUBSONIC  
MODULATING  
60 INCH BURNING LENGTH  
PARTIAL FILM COOLED  
LINER

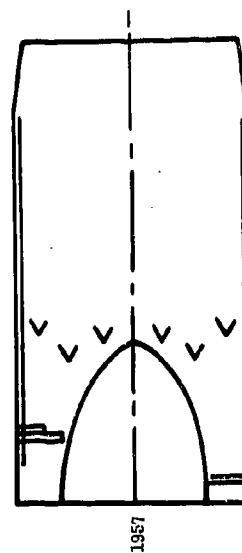
J79-2, 3, 5, 7, & 11



1953

FIRST WIDE MODULATION  
AFTERBURNER (SECTOR  
TYPE)  
3050°F - M<sub>p</sub> 2.0  
54 INCH BURNING LENGTH  
FULL LOUVERED LINER

J79-8, 15



1957

COREBURNER (FOR-  
RUNNER OF GE4 MODULA-  
TION METHOD)  
3150°F - T - M<sub>p</sub> 2.0  
CAPABILITY

J79-10, 17



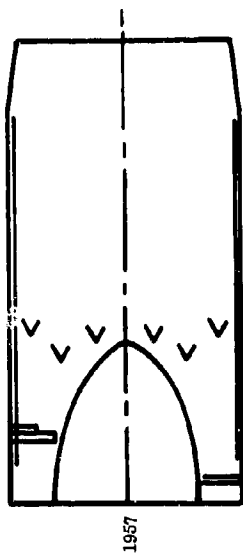
ADVANCED COREBURNER -  
M<sub>p</sub> 2.4 CAPABILITY

Figure 5-1.

K

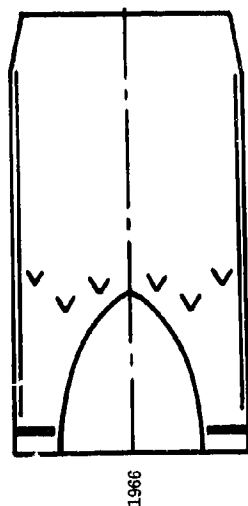
J79-8, 15

COREBURNER (FOR-  
RUNNER OF GE4 MODULA-  
TION METHOD)  
3150°F - T<sub>8</sub> - M<sub>p</sub> 2.0  
CAPABILITY



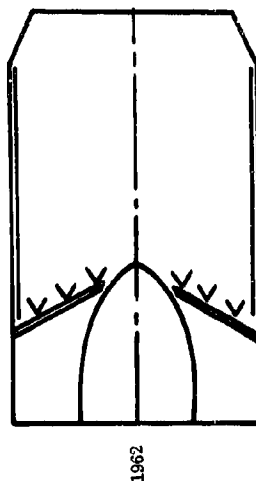
J79-10, 17

ADVANCED COREBURNER ( -  
M<sub>p</sub> 2.4 CAPABILITY



J83

CONTINUOUS REHEAT -  
SUPERSONIC CRUISE  
(97% EFFICIENCY)  
3200°F - M<sub>p</sub> 3.0  
CAPABILITY  
"CONTROLLED FUEL  
DISTRIBUTION" INJECTION  
45 INCH BURNING LENGTH  
CONTINUOUS SLOT (3  
ELEMENT) COOLING



GE4

FIRST COMMERCIAL  
AUGMENTOR  
2840°F - M<sub>p</sub> 2.9  
CAPABILITY  
36 INCH BURNING LENGTH  
CYLINDRICAL COOLING  
LINER

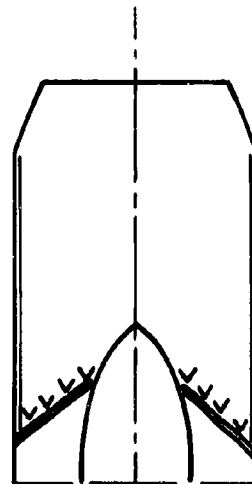


Figure 5-1. AUGMENTOR CHRONOLOGICAL SEQUENCE CHART

5-3/5-4

2

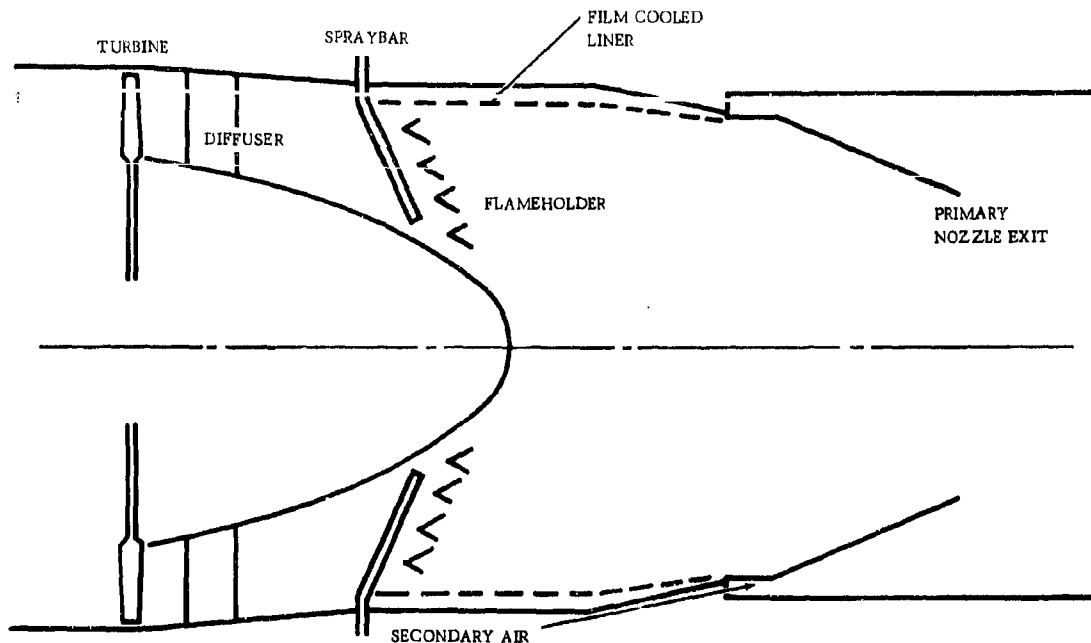


Figure 5-2. TURBOJET AUGMENTOR SIMPLICITY

#### 5.1.2 COMPARISON WITH OTHER GAS TURBINE COMBUSTION

The turbojet augmentor is the simplest of the aircraft gas turbine combustion systems, and, for perspective, should be compared to jet engine main combustors and turbofan duct burners. Its simplicity is principally due to:

- The relatively high inlet temperature, which is fundamentally favorable to dependable light-off flame stability, high efficiency, and low thermal gradients. This provides for simpler fuel injection, flame-stabilizers and ignitors.
- The basic cylindrical shape - one structural casing and one cooling liner.

This simplicity is most readily apparent from comparisons with a typical current cannular combustor like the CJ805 and an annular combustor of the type proposed for the GE4. Figures 5-5 to 5-10 show these configurations and their principal operating conditions.

Figure 5-5 shows the CJ805 combustor in its assembled configuration. In current commercial service the liner has a life between maintenance of 3300 hours, and estimated total life of 8000 hours with replacement of the forward inner liner. This is believed to be at least as good as any combustor liner in service - especially considering that the average flight is only 1.5 hours, resulting in many cycles. During take-off it operates with local metal temperatures of 2000°F with temperature gradients up to 1200°F. At cruise, the maximum liner temperature is 1750°F with the average metal temperature is 1200°F despite the low inlet temperature (609°F). This points out that low inlet temperature alone is not conducive to long life. Thermal gradients, primarily resulting from localized cooling problems at the cross-fire tubes, and the louvered cooling construction limit liner durability.

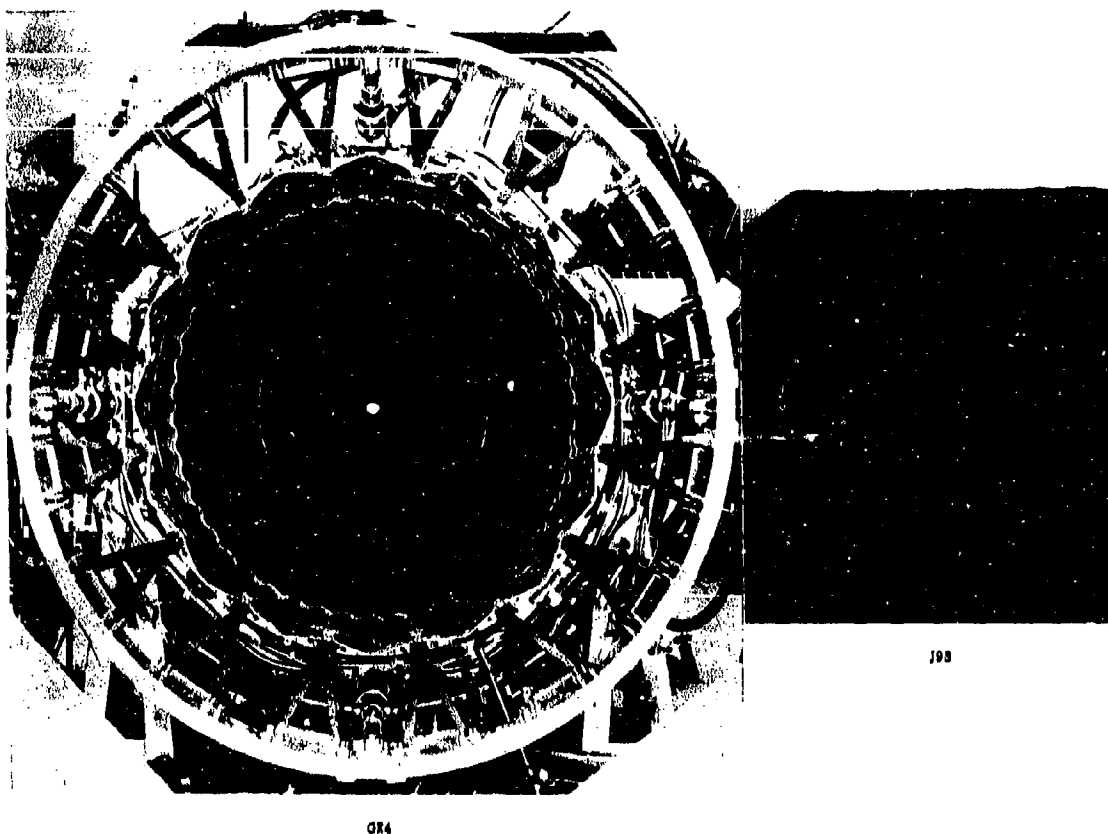
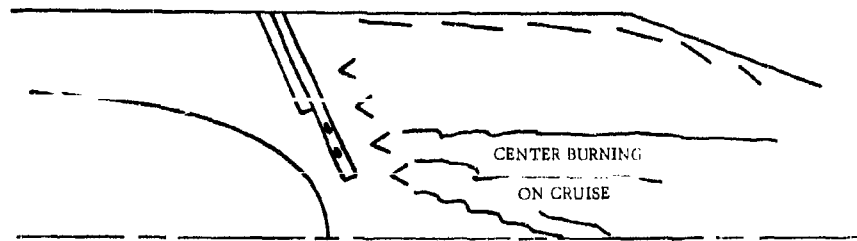


Figure 5-3. J93 GE4 AUGMENTOR

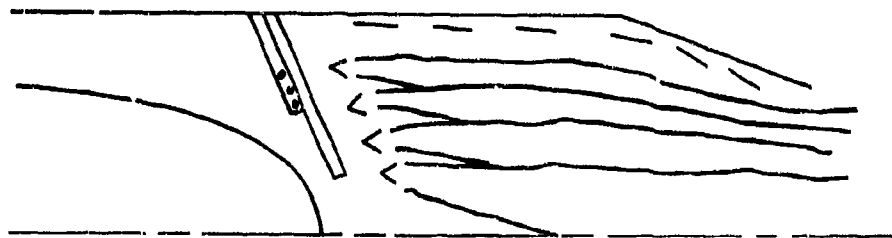
Figure 5-6 shows the CJ805 configuration and its component parts. The important points to note are:

Casing:

- two are required, outer and inner
- they operate at high pressure loading, 165 psi maximum during take-off



1ST STAGE CRUISE POWER SETTING



2ND STAGE TAKE-OFF

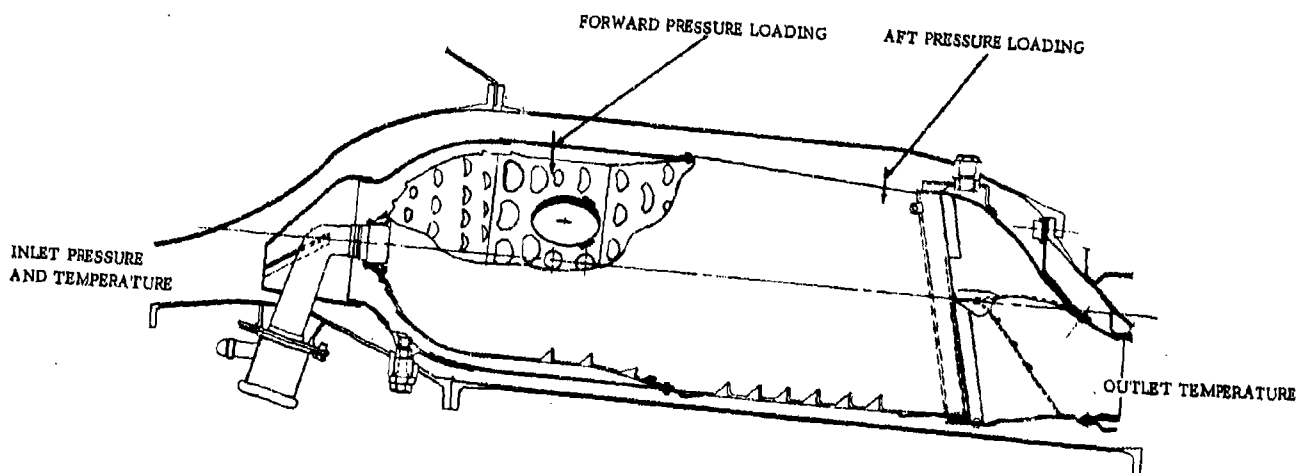
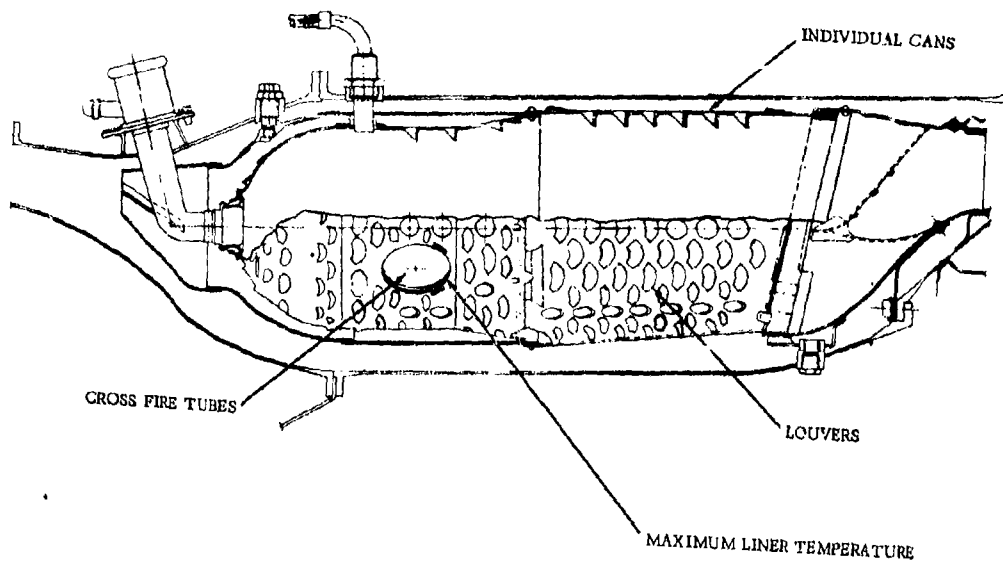
Figure 5-4. GE4 AUGMENTOR TWO STAGE COMBUSTION

#### Combustor Liner:

- Extensive stream-immersed hardware required. High surface area to combustion volume ratio. High blockage - about 50 percent.
- Pressure loading of about 10.8 psi inward differential during take-off.
- Many parts
  - cowl
  - inner liner
  - aft liner
  - transition duct
  - cross fire tubes

5-7/5-8

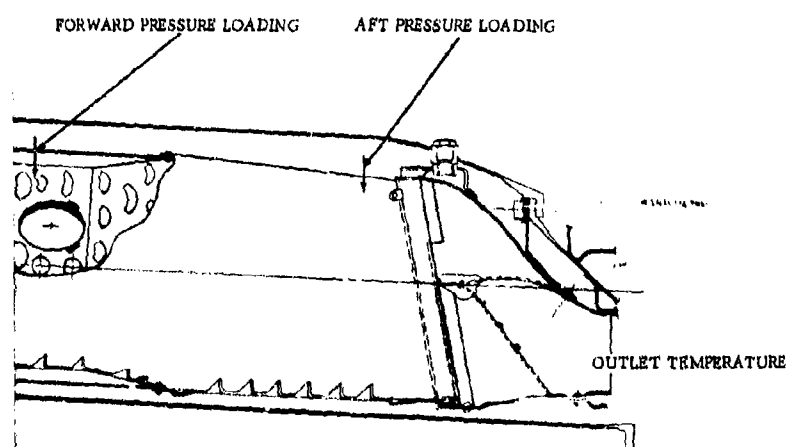
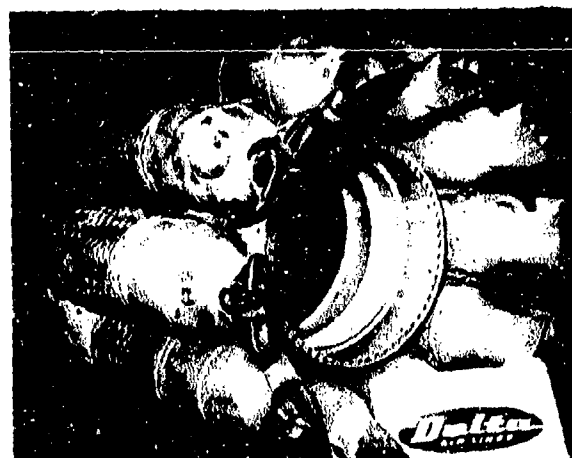
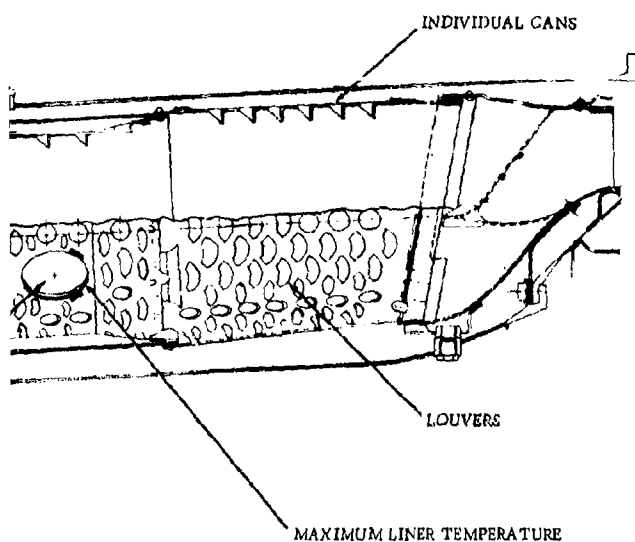
K



1

K

Figure 5-5. CJ805 COM



PARAMETER	SEA	
	LEVEL STATIC	CRUISE
INLET TEMPERATURE, °F	750	810
INLET PRESSURE, PSI	191.6	69
TEMPERATURE RISE, °F	1015	895
OUTLET TEMPERATURE, °F	1765	1805
MAXIMUM LINER TEMPERATURE, °F	2000	1750
AVERAGE LINER TEMPERATURE, °F	1500	1200
LINER THERMAL GRADIENT, °F	1200	1100
FORWARD PRESSURE LOADING, PSI	1.55	.55
AFT PRESSURE LOADING, PSI	10.8	4.10

Figure 5-5. CJ805 COMBUSTOR ASSEMBLY

K

2

5-9/5-10



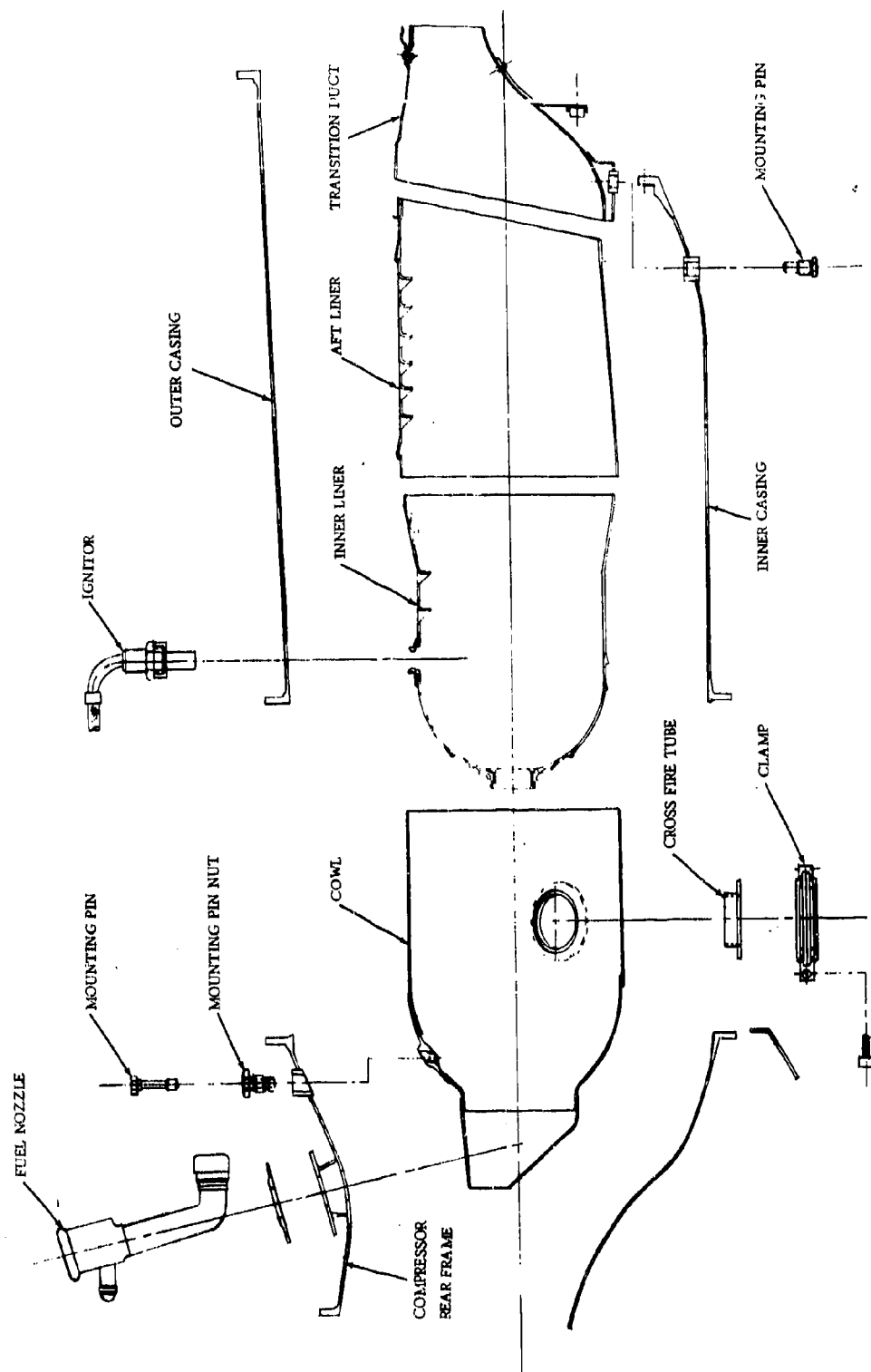


Figure 5-6. CJ805 COMBUSTOR COMPONENTS

- Perforated walls for admission of mixing air.
- Because of the high surface area, a large proportion of the airflow must be used for cooling (about 36 percent).

Although the cannular combustor is a satisfactory part in commercial service, the GE4 main combustor will be much better despite higher inlet temperatures at cruise (1100°F). Figures 5-7 and 5-8 show the GE4 cannular combustor with these advantages over the CJ805 cannular approach:

- More efficient on volume/cooled surface basis, 46 percent of the cooled surface of the cannular liner.
- Lower max metal temperatures due to
  - continuous strip cooling, no louvers
  - absence of discontinuities such as cross-fire tube wakes
- More fuel nozzles - with lower per-nozzle flow schedule requirements - the "compartmented" combustion is eliminated.
- Cross-fire tubes eliminated - a chronic life problem.
- No transition duct between combustion liner and turbine.

The useful life requirement of the GE4 combustor liner is 12,000 hours. Judging from its improvements over current commercial cannular systems, this life is readily attainable.

Figure 5-9 shows the simplicity of design details and lists the operating characteristics of the GE4 augmentor. The fact that the single casing and single non-perforated liner are simpler than main combustors is obvious.

It is also important to illustrate the simplicity of fuel injectors due to the higher augmentor inlet temperature. Figure 5-10 shows a typical CJ805 duplex fuel nozzle in comparison with the GE4 spraybar. For broad fuel-flow range capability, the flow dividing valves in the head sections outside the casing are similar - the advantages of simplicity lie in the stream-immersed part. The combustor fuel nozzle must provide a finely atomized spray in two concentric spray nozzles for starting (at low inlet temperature) and for steady-state operation to obtain the required efficiency and outlet temperature profile. The spraybar, by comparison, simply deposits the fuel in subdivided quantities at the desired radial locations. The vaporization is caused by the high inlet temperature of the air stream, and the distribution is accomplished by the flameholder's mixing action. Efficiency, stability, light-off dependability and durability are not affected by spray quality. The typical turbofan duct burner configuration is basically the same as the annular combustor design but more difficult. It is inherently more complex than the turbojet augmentor.

The following comparison between the GE4 combustor, GE4 augmentor and a typical turbofan duct burner shows the durability and reliability advantages of the augmented turbojet:

K

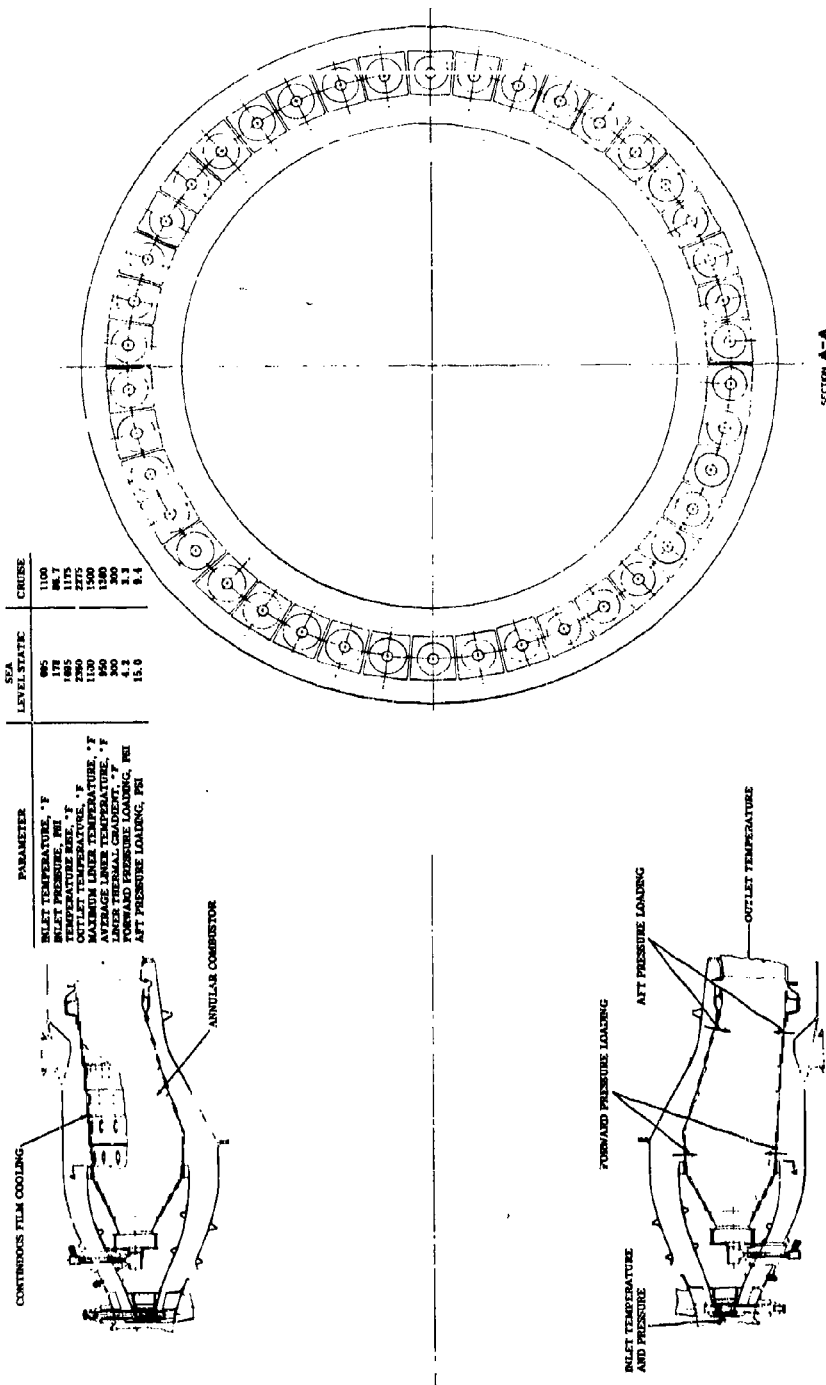


Figure 5-7. GE4 COMBUSTOR

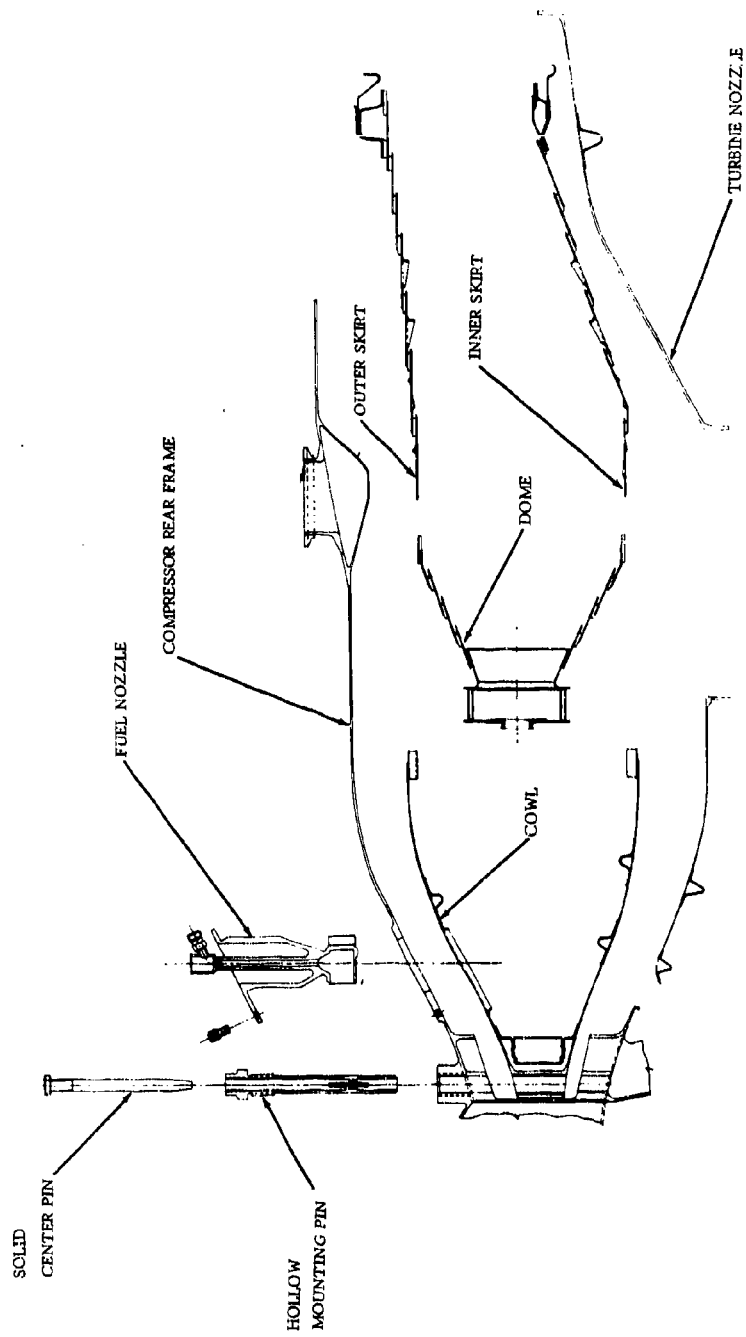


Figure 5-8. GE4 COMBUSTOR COMPONENTS

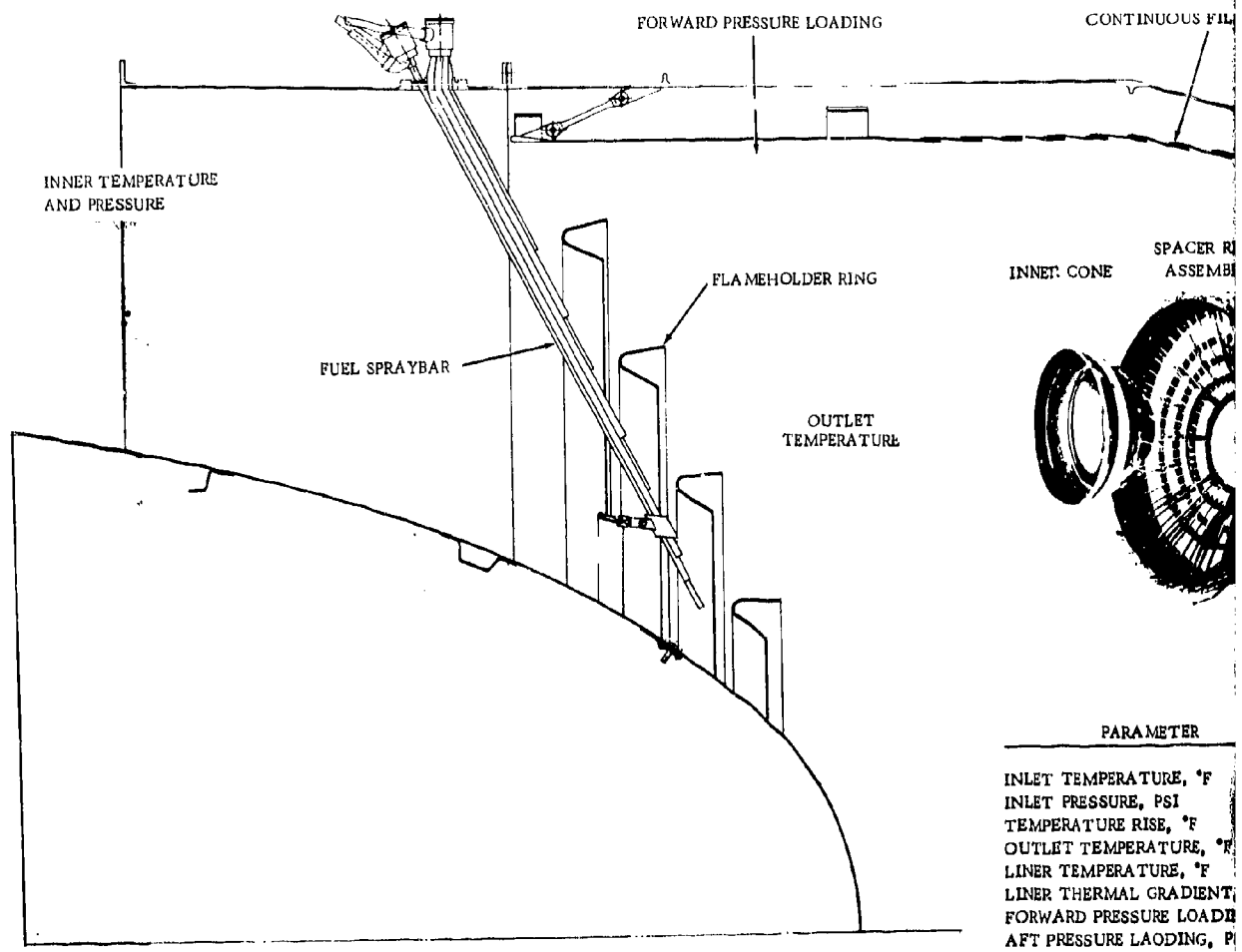


Figure 5-9. GE4 AUGMENTOR

1

K

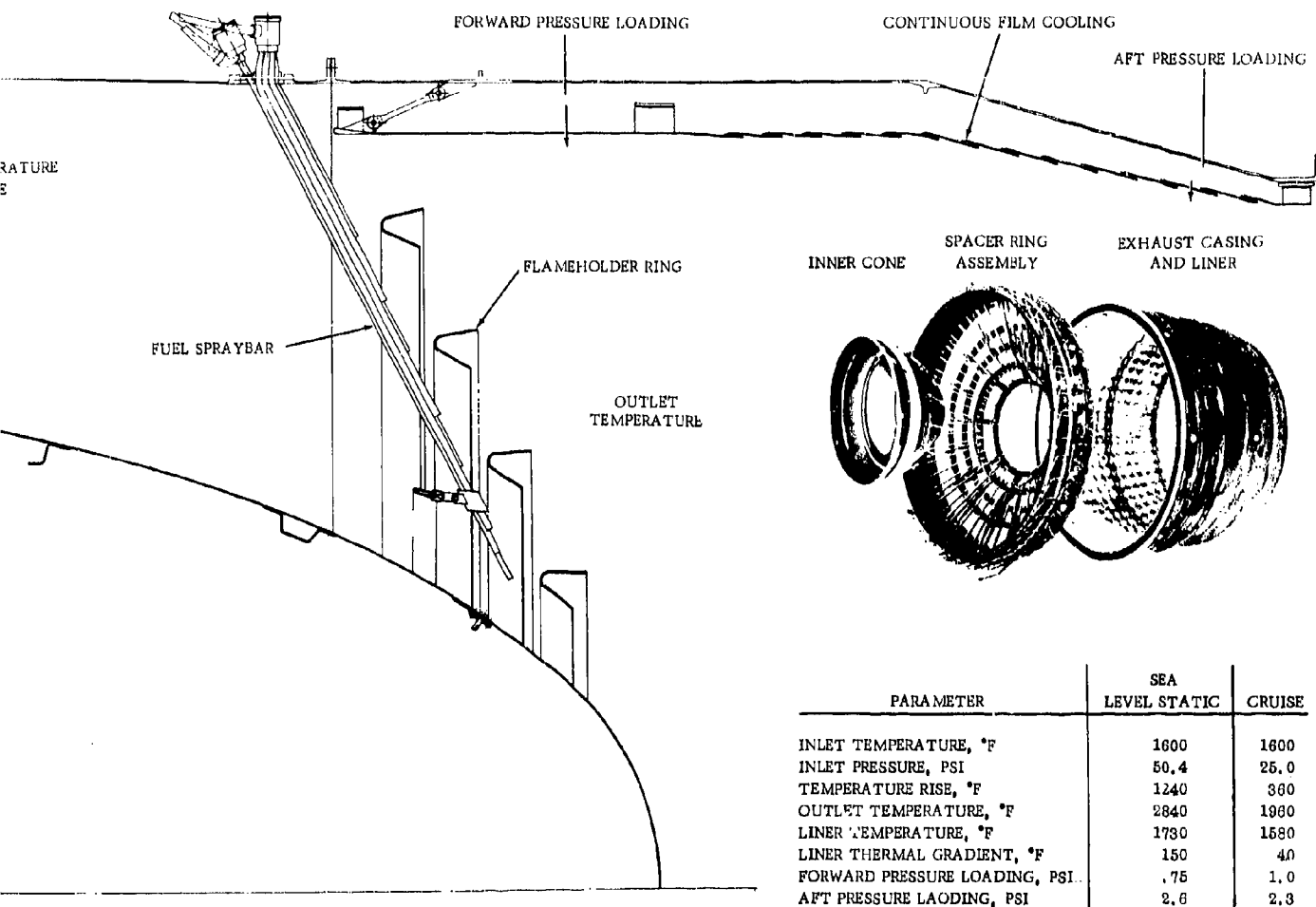


Figure 5-9. GE4 AUGMENTOR

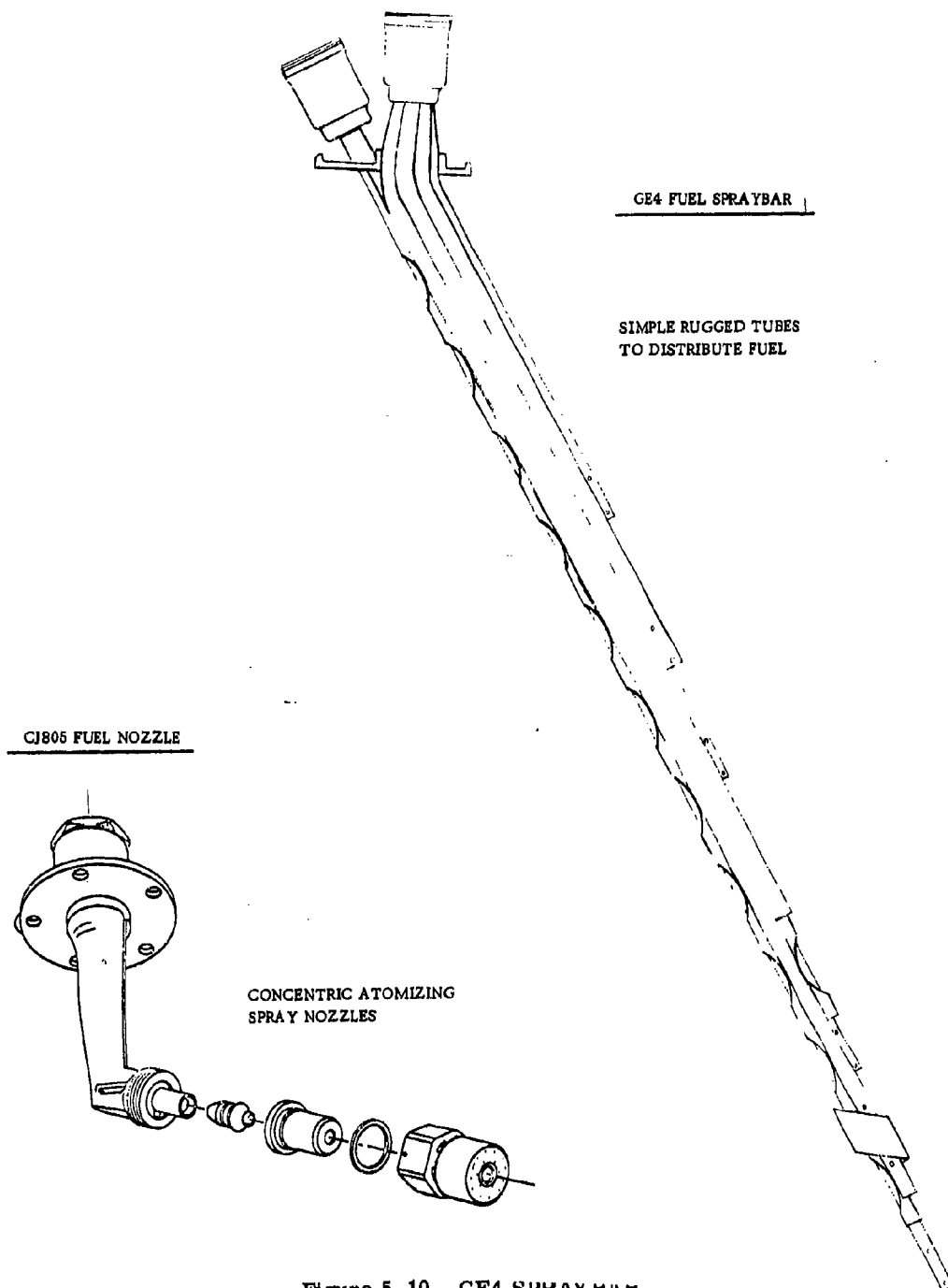


Figure 5-10. GE4 SPRAY BAR

	<u>GE4 Combustor</u>	<u>GE4 Augmentor</u>	<u>Typical Turbofan Duct Burner</u>
• Lower temperature rise at maximum and cruise conditions (Temperature rise is one measure of combustion difficulty, combustion size, and cycle dependence on burner performance.)			
Maximum Take-off $\Delta T$ , °F	1695	1240	2940
Maximum at Mach 0.9, 36,000 $\Delta T$ , °F	1430	1240	3000
Cruise $\Delta T$ , °F (15,000-pound thrust 65,000)	1180	360	1300
• Less liner surface area to cool	250%	100%	300%
• More air available for cooling at maximum temperature rise %	27	24	11
• Lower maximum liner pressure loading, psi	20.6	4.5	7-9
• Lower thermal gradients at cruise, °F	300	40	500
• Simpler parts			
Structural Casing & Cooling Liner	2 required	1 required	2 required
Fuel Injection	Atomizing Nozzle	Simple Spraybar	Atomizing Nozzle
Flame Stabilization	High Stability Dome	Simple Rings	High Stability Dome
Combustion Zone Geometry	Annular	Cylindrical	Annular
Perforated Liner	Yes	No	Yes
• Higher Inlet Temperature			
- Take-off °F	690	1600	264
- Mach 0.9, 3600 ft	575	1380	197
- Mach 2.7, 65,000 ft.	1090	1580	648



- Reduces metal thermal gradients as noted previously.
- Easier to accomplish the required stable combustion process.
- Fuel injection and ignition substantially easier. The GE4 operates at auto-ignition conditions over most of the SST flight path thus reducing dependence on the high energy electrical on torch ignition system.
- More upstream flow distortion attenuation

<u>GE4 Combustor</u>	<u>GE4 Augmentor</u>	<u>Typical Turbofan Duct Burner</u>
9-stage compressor	9-stage compressor + combustion + 2-stage turbine	2-stage fan hi-Mach tip section

The solid base of General Electric experience on the selected augmentor design approach, coupled with the advancements made in the GE4 augmentor, are among the reasons General Electric selected the augmented turbojet for the SST application.

#### 5.1.2.1 Commercial Durability

There are many significant commercial design advancements in the GE4 design which ensure attainment of the expected component life (12,000 to 24,000 hours with flameholder rings at 8,000 hours).

- Simplified exhaust duct - elimination of actuator brackets and cooling liner mounting hardware. (See Figure 5-11.)
- Cylindrical cooling liner with improved continuous slot film cooling. (See Figure 5-11.)
  - Liner design metal temperature less than 125°F higher at maximum reheat than for maximum-unaugmented operation.
  - Liner metal temperature increase 45°F at cruise augmentor power vs non-augmented.
  - Cooling liner maintains exhaust duct at or below the turbine outlet temperature with very little sensitivity to the amount of secondary air flow.
- Radial beam - independent ring flameholder construction, (See Figure 5-11.)
  - The flameholder operates at high metal temperatures (up to 2050°F) - but it is a low stressed part, mounted so it is thermally free. It is made of material with very high oxidation resistance. It will be much easier to attain long life on this part than on the first stage turbine nozzles of current commercial engines for example, which have maximum hot spots of 2000°F and a much more difficult stress and low cycle fatigue environment over typical start, take-off and cruise cycles.

# GE4 EXHAUST CASING

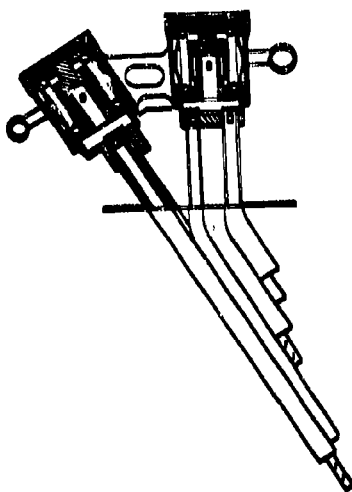
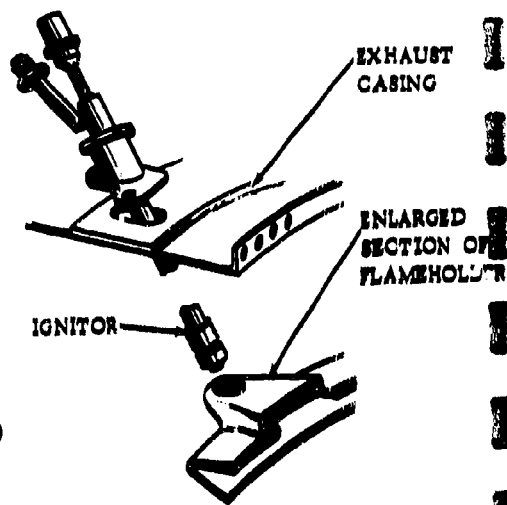
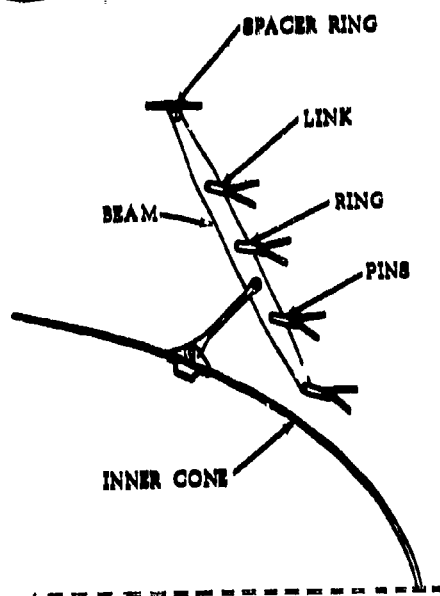
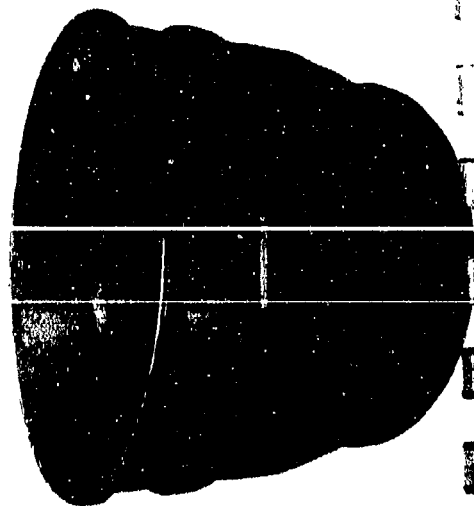
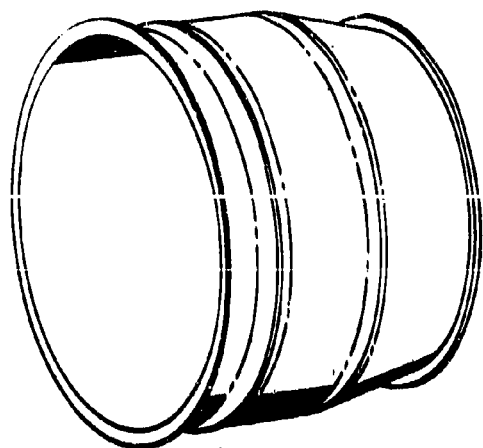


Figure 5-11. GE4 AUGMENTOR DESIGN ADVANCEMENTS

- Rugged spraybar (See Figure 5-11.)
  - Externally metered fuel; no precision parts in flow stream
  - Insensitivity to fuel temperature
  - Compatibility with aviation kerosene
  - Large discharge orifices resist clogging which decreases coke formation
- Simplified air-cooled ignitor (Figure 5-11).
  - Elimination of typical torch ignitor complexity
  - Augmentor auto-ignites for most flight requirements

Most important to the attainment of long life and hardware reliability are low and uniform metal temperatures attained by effective cooling. This capability is clearly illustrated by Figure 5-12 which shows full-scale GE4 predicted and test data of the cooling liner metal temperature as affected by reheat power setting at a simulated  $M_{p2.7}$  - 60K operating condition. The shallow slope with augmentor temperature, only 100°F increase from maximum unaugmented to maximum reheat, is accomplished by a combination of efficient film cooling and temperature profiling in the combustion zone. An additional important point is the excellent agreement between the actual and predicted levels which demonstrates the accuracy of the experience-refined analytical cooling techniques developed by General Electric. These are described in detail in Section 7, Volume III-B, Augmentor and Exhaust Nozzle Cooling. Due to the low SST maximum temperature requirement almost 24 percent of the engine exhaust stream can be applied to cooling. The structural exhaust duct metal temperature is even less sensitive to augmentor temperature than the cooling liner as shown by Figure 5-13, which shows the design levels at  $M_{p2.7}$  55K conditions.

The aforementioned advancement in augmentor component design have been demonstrated in full-scale tests on the GE4 simulator vehicle shown in Figure 5-46.

#### 5.1.2.2 Maintainability

The maintainability advantages are clearly illustrated by Figure 5-14 which shows the three basic flange-connected subassemblies. The concept of the spacer ring subassembly which supports the flameholder, ignitor, fuel spraybars and manifolding separate from the exhaust duct/liner assembly has been well established by J79 and J93 field use. Individual flameholder ring and complete assembly replacement can be made on the airplane.

#### 5.1.3 GENERAL DESCRIPTION

The three major sections of the GE4 augmentor are shown in Figure 5-15:

- Diffuser (which is integral with the turbine rear frame)
- Fuel Injection and Flame Stabilization
- Combustion

# FULL SCALE AUGMENTOR COOLING TESTS

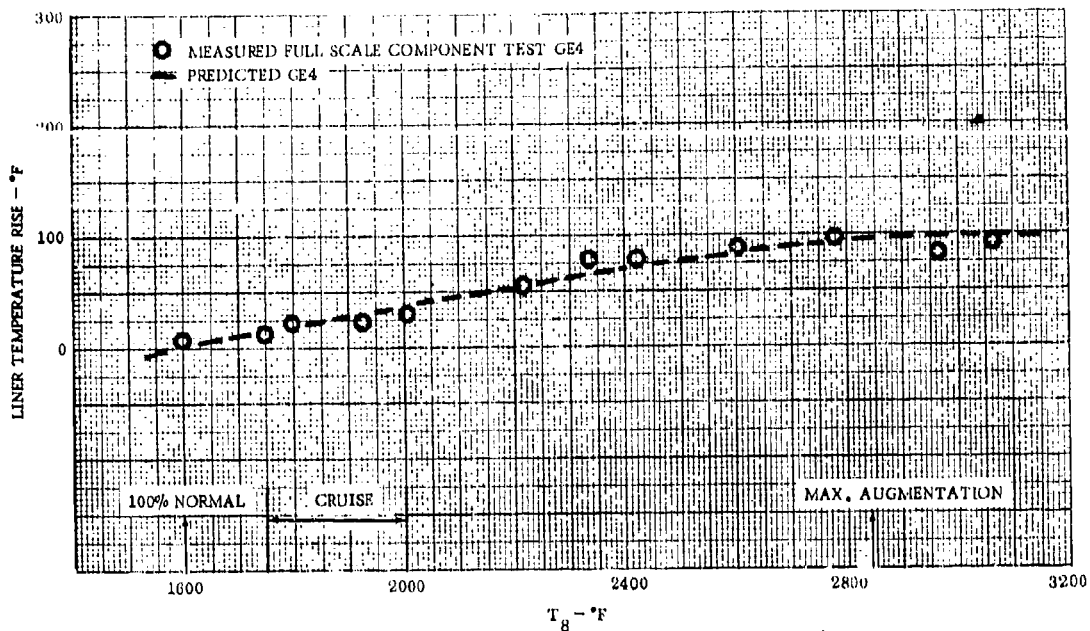


Figure 5-12. GE4 PREDICTED AND MEASURED LINER TEMPERATURE RISE

## GE4 AUGMENTOR COOLING PERF.

M<sub>0</sub> = 2.7 ALT 55,000

(INLET AIR TEMP - °F)

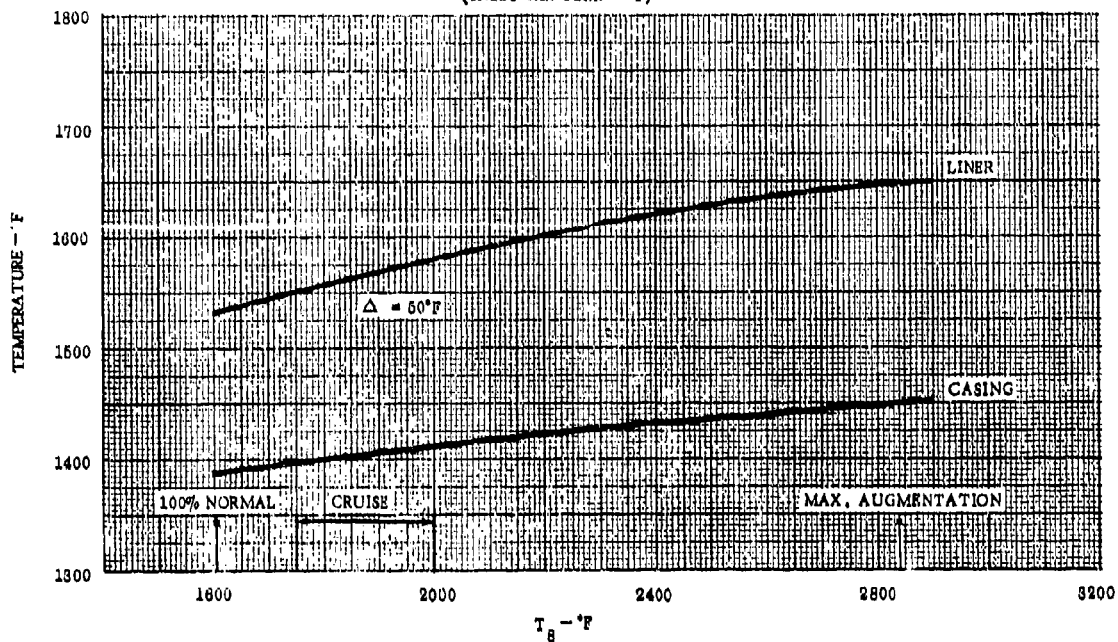


Figure 5-13. PREDICTED SST AUGMENTOR EXHAUST CASING AND LINER TEMPERATURE

- ON AIR PLANE REPLACEMENT OF ALL FLAMEHOLDER SUB-COMPONENTS AUGMENTOR/EXHAUST NOZZLE/THROTT REVERSER ASSEMBLIES
- FUEL DISTRIBUTION AND FLAMEHOLDER SUB-ASSEMBLY PERMITS PRESSURE AND LEAK CHECK OF FUEL SYSTEM
- DUCT SIZE ALLOWS EASY FLIGHT LINE INSPECTION AND NORMAL MAINTENANCE
- REMOVABLE CONE TIP FOR SUMP INSPECTION

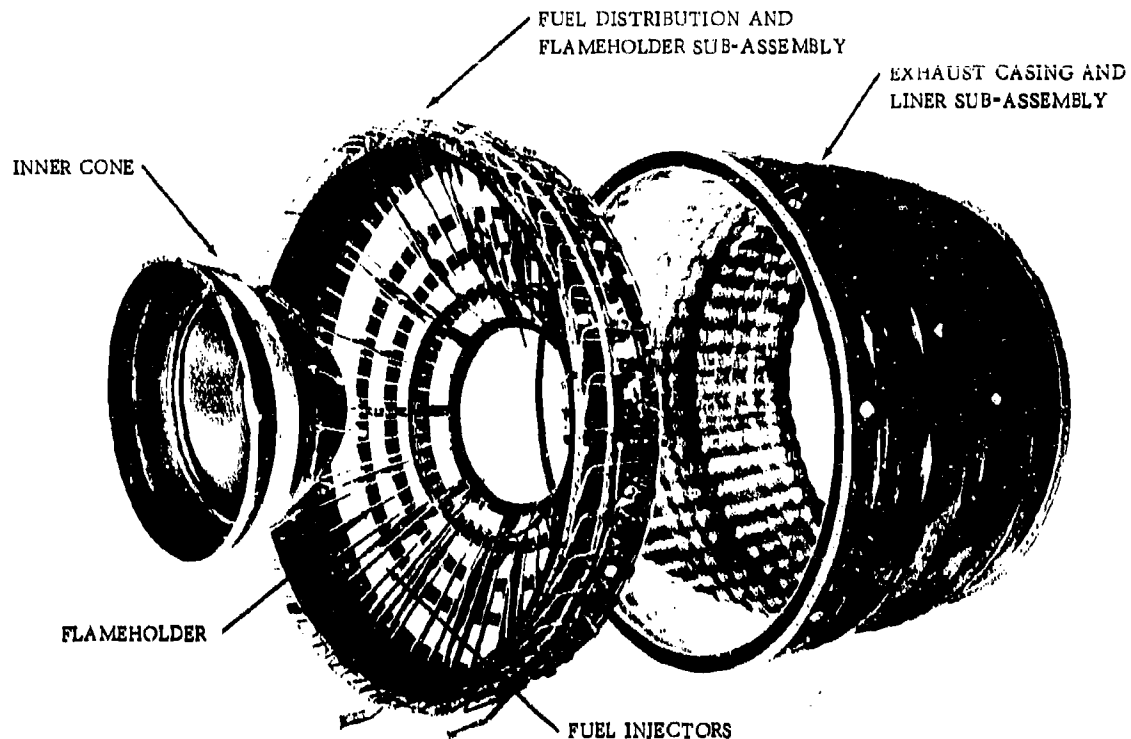


Figure 5-14. GE4 AUGMENTOR ASSEMBLY

The flow discharges from the turbine into the diffuser which has a flow path bounded by the inner cone and spacer ring. Fuel is distributed radially and circumferentially through the 40 fuel injectors, and mixes with the augmentor inlet airflow at the flameholder. Combustion is stabilized and propagates from the wake of the four flameholder rings into the combustion zone. The exhaust casing provides the structural flow-path for the combustion zone, and is shielded from exhaust gas radiant and convective heating by the film-cooled liner. A film of turbine discharge gas, cooled by compressor discharge seal leakage air, maintains the liner at a temperature consistent with durability and long life. The exhaust duct supports the exhaust nozzle/thrust reverser assembly structurally.

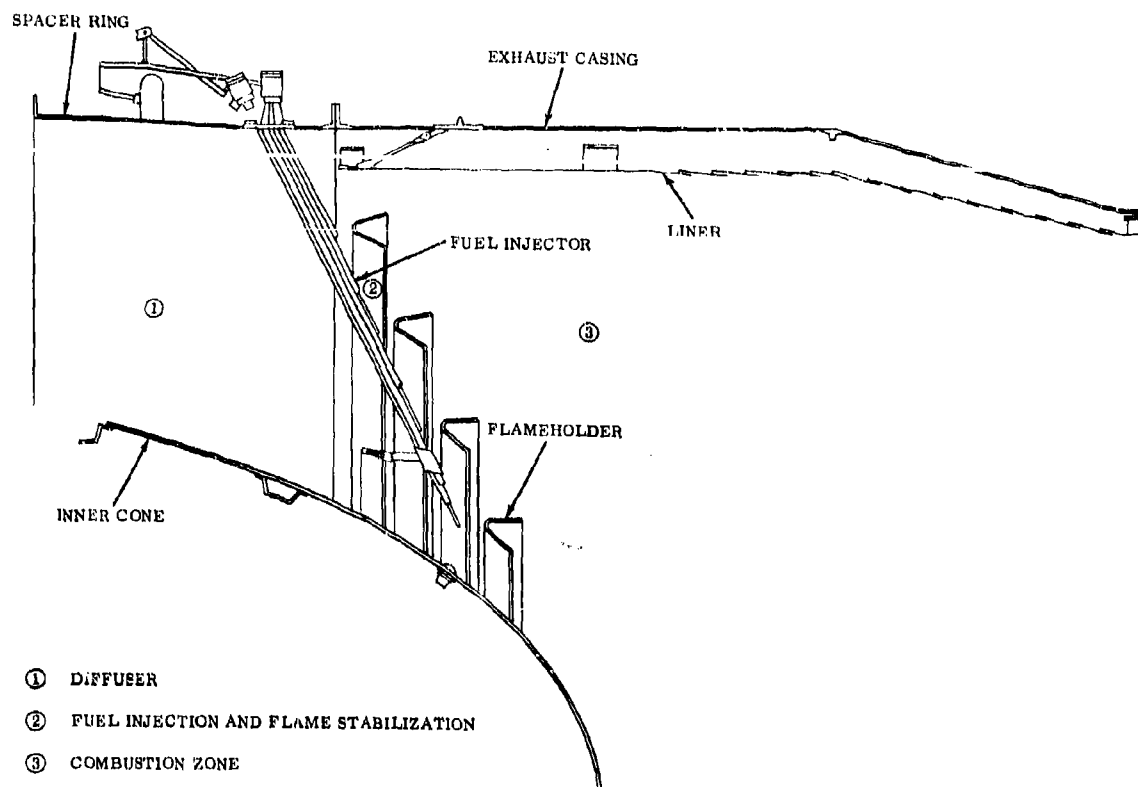


Figure 5-15. GE4 AUGMENTOR

The materials selected for the augmentor components are listed in Table 5-1.

Table 5-1. Augmentor Component Materials

Component	Material
Spacer Ring	Rene'41
Exhaust Casing	Rene'63 and Rene'41
Cooling Liner	Hastelloy X
Flameholder Rings	Hastelloy X
Flameholder Beams	X40
Spraybar Support Ring	Hastelloy X
Spraybar Tube Bundle	TD Nichrome
Spraybar Valve Assembly	N155, INCO 625, INCO X, L605
Ignitor Pylon	Hastelloy X
Inner Cone	Hastelloy X
Mounting Pins	L605

#### 5.1.4 DESIGN REQUIREMENTS

The basic requirement for the mechanical design of the augmentor is to provide components that will meet durability, maintainability, reliability and safety margins under the operating stresses that result from the pressures, temperatures, loads, and time in the SST flight spectrum. Performance requirements are defined in detail in Section 6, Volume III-B. Maintainability, reliability, quality assurance and safety requirements are described in paragraphs 5.1.6.4 through 5.1.6.7 of this section.

##### 5.1.4.1 Augmentor Durability

Life requirements for augmentor parts are established by a comprehensive analysis that considers:

- Measured or calculated stresses and temperatures
- Extensive experience on J79 and J93 parts for SST operating conditions
- Proven material capabilities
- Cooling air trade-off studies
- Processing techniques
- Economy (trade studies of cost versus life)

These studies have established an objective service life for components listed in Table 5-2.

Table 5-2. Component Service Life

<u>Component</u>	<u>Ultimate Life With Repair ~ Hours</u>
Flameholder rings	8,000
Liner	12,000
Flameholder beams	12,000
Fuel injector	12,000
Exhaust duct	12,000
Fuel injector retaining ring	12,000
Miscellaneous hardware	12,000
Spacer ring	18,000
Inner cone	24,000

#### 5.1.4.2 Flight Spectrum

The SST flight spectrum principal requirements for the augmentor design are listed in Table 5-3.

Table 5-3. Flight Profile

<u>Power Setting</u>	<u>Augmentor Temperature Rise, °F</u>	<u>Percentage of Objective Service Life</u>
1.0 Take-off and Transonic Climb Out	1240	11.5
3.5 Partial Augmentation	360	45
2.5 Partial Augmentation	780	19
4.0 Min Augmentation	150	4.0
5.0 100 percent Normal	0	20.5
		<hr/> 100

Each of the assigned time proportions represents a combination of several expected times and power settings. The time proportions shown in Table 5-3 are chosen to represent the expected flight spectrum and to provide the basis for realistic analysis for component life.

#### 5.1.5 DESIGN APPROACH AND CRITERIA

##### 5.1.5.1 Performance

GE4 augmentor performance requires a specific flow-path configuration that is defined by the aerothermo design described in Volume III-A, Section 6, "Augmentor Performance", and shown in Figure 5-16.

The flow-path dimensions in Figure 5-16 are specified for normal operating conditions. All other dimensions shown in this section have been adjusted to room temperature conditions.

##### 5.1.5.2 Augmentor Durability

The GE4 augmentor design approach for durability and safety is based on the following criteria:

- Accurate definition of metal temperatures
- Reduction in thermal gradients and stress concentrations
- Use of well proved design practices based on extensive military experience
- Application of high-strength, corrosion-resistant materials

Specific examples of the attention given to the design factors for durability will be found in paragraphs devoted to the design description of each component.



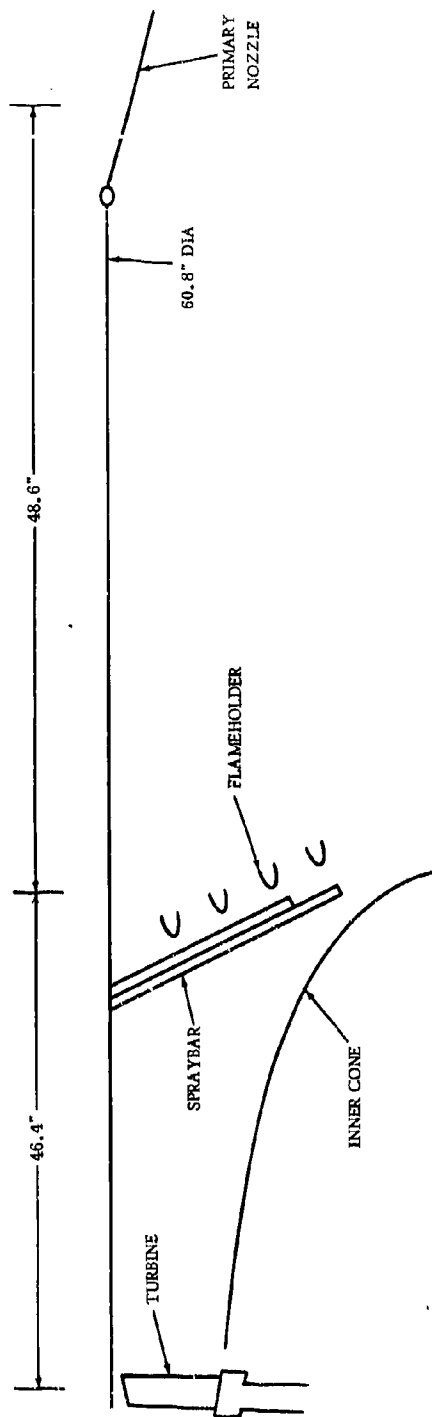


Figure 5-16. AUGMENTOR AERODYNAMIC DESIGN DIMENSIONS

#### 5.1.5.2.1 Metal Temperature

The single most important variable that determines the service life of the augmentor is metal temperature. Figure 5-17 shows the stress-rupture properties of René 63, the exhaust casing material, the effect of temperature on life is evident. Because life is strongly affected by temperature, the cooling system is designed to be insensitive to operating conditions. Figure 5-18 shows the predicted temperatures for the augmentor liner and exhaust casing; it is evident that the liner and casing are relatively insensitive to exhaust gas temperature. For example, at cruise flight conditions, the casing and liner are respectively, only 60° and 120°F higher at maximum augmentation than at 100 percent normal conditions. This highly efficient cooling is possible in the augmented turbojet because of the large quantity of available cooling air. Previous experience on J79 and J93 supersonic augmentor designs has brought progressive confirmation and refinement of the analytical techniques used to predict GE4 temperatures. Because of the importance of accurate temperature definition, Section 7, Volume III-B discusses augmentor cooling and the techniques used for temperature prediction. J93 test data included in Section 7 shows the skin temperature analyses to be accurate within 25°F under conditions very closely allied to the GE4. Preliminary full-scale GE4 tests on the simulator vehicle also show excellent agreement (See Figure 5-19). This agreement provides high confidence in the predicted levels of metal temperatures for the GE4 augmentor. Note that the GE4 design operates between 60° and 150°F lower in metal temperature than the highly successful J93 design because of the increased cooling air available with the lower GE4 maximum temperature and the associated temperature profile.

#### 5.1.5.2.2 Stress Rupture

The components of the augmentor are generally designed on the basis of stress rupture. The stress-rupture criteria relate time with temperature and operating stress, and are used when time-temperature relationships dictate a lower permissible stress than yield strength or other criteria. The augmentor has a variety of temperatures and stresses imposed upon it, depending on the flight condition and power setting. Each of the operating conditions of the flight spectrum consumes stress rupture life at a different rate; the rate of life consumption is higher with increased temperature and stress.

An analysis has been made for each part that is stress-rupture limited, and the method used is summarized in Table 5-4. The typical data shown are for the René 63 exhaust casing.

Table 5-4. Stress Rupture Analysis for Casing

<u>Flight Condition</u>	<u>% of Mission Time</u>	<u>Power Setting</u>	<u>Stress</u>	<u>% 12,000-hour Life Used</u>
Take-off & Climb Out	11.5	1	17,100	41.6
Partial Aug	45	3.5	15,600	26.3
Partial Aug	19	2.5	15,000	29.2
Min Aug	4	4.0	10,800	1.9
Max Non-Aug	20.5	5.0	19,200	0.0
			TOTAL	= 99.0%

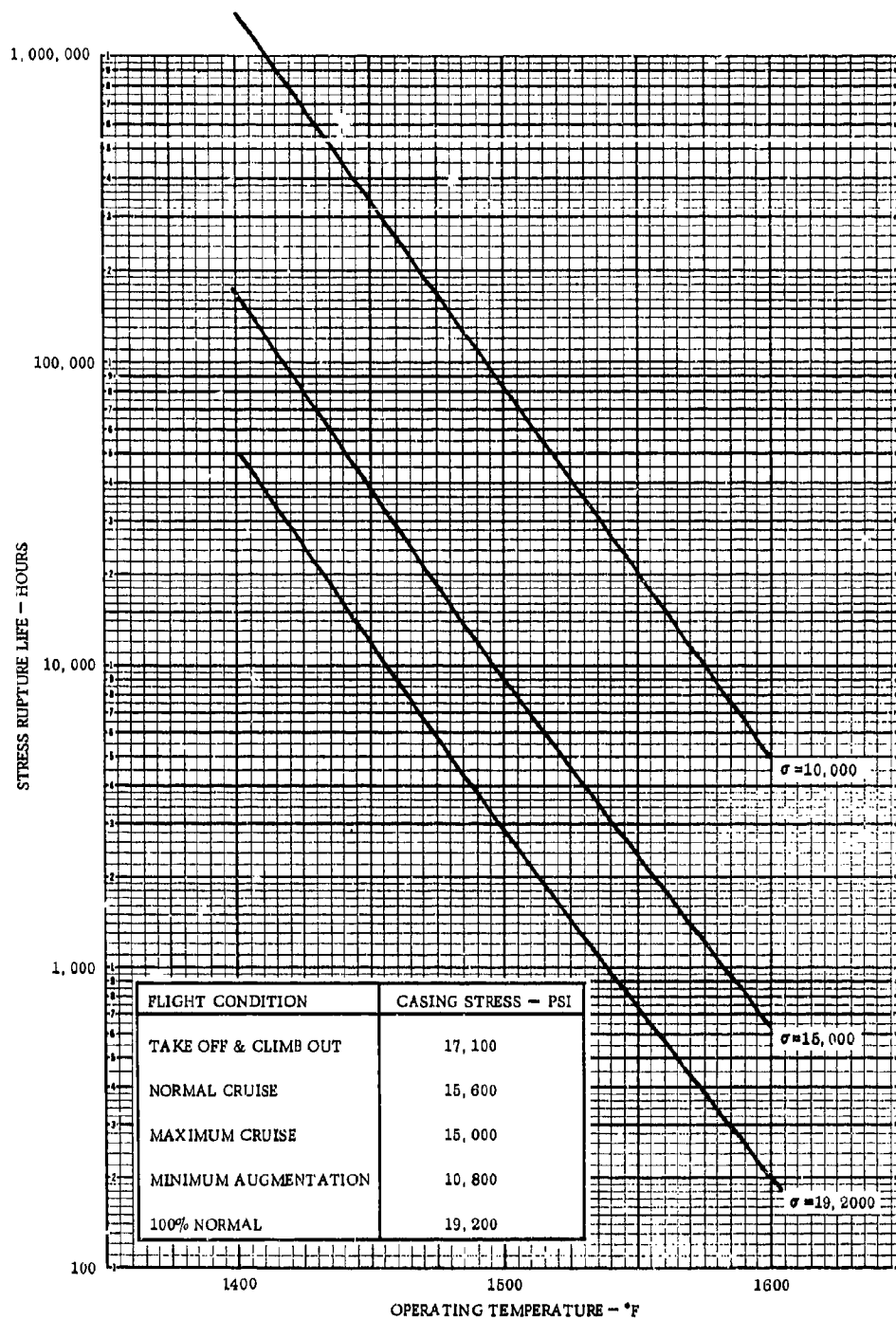


Figure 5-17. RENE 63 STRESS RUPTURE PROPERTIES

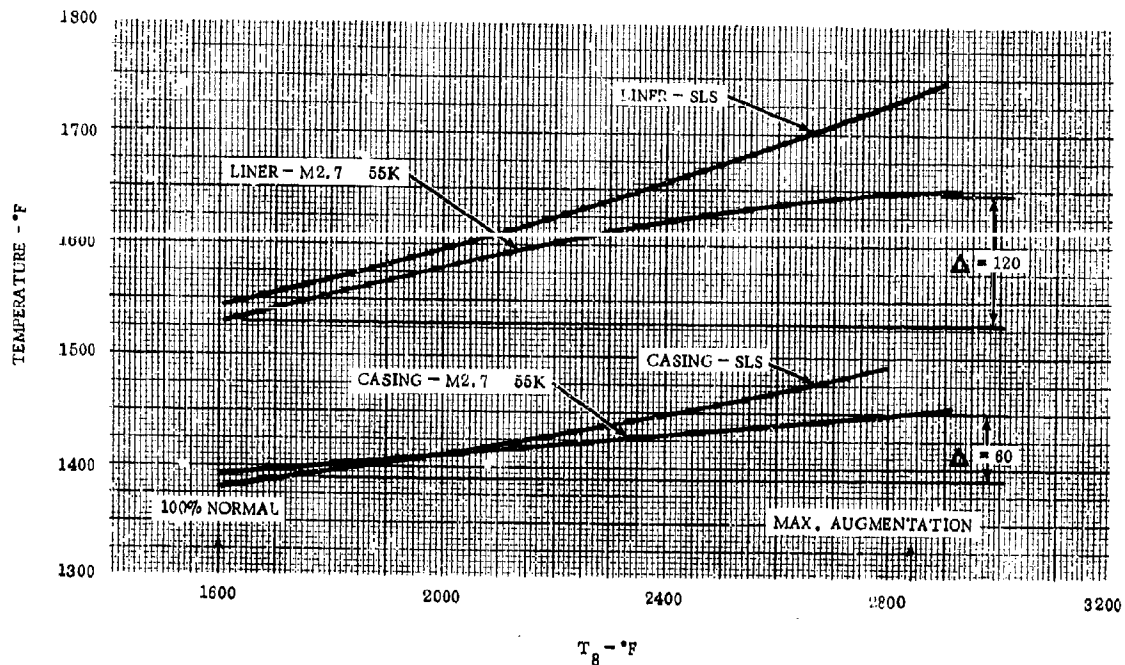


Figure 5-18. PREDICTED LINER AND EXHAUST CASING TEMPERATURES

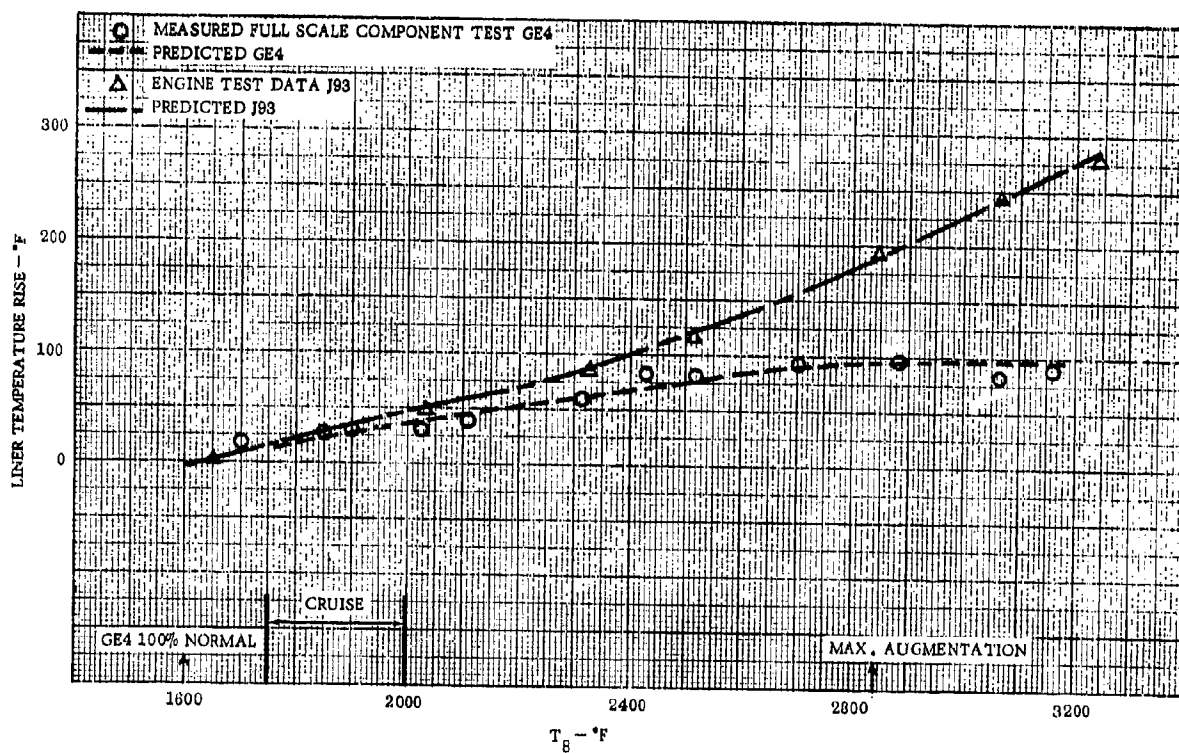


Figure 5-19. J93 AND GE4 PREDICTED AND MEASURED LINER TEMPERATURE RISE

As a general criterion for the casing and all other stress-rupture-limited subcomponents, the stresses used are increased 25 percent over the calculated values, and temperature is 100°F higher than calculated to allow for potential localized hot spots. All components are designed with additional margin by using minimum material properties and stock thicknesses in all analyses.

A summary of the analysis for all parts with stress-rupture-life effects is listed in Table 5-5.

Table 5-5. Stress Rupture Summary

Flight Condition	Take-off & Climb Out	Partial Aug	Partial Aug	Min Aug	100% Normal	
<u>René 41 Spacer Ring</u>						
*Stress, psi	18,500	14,300	13,800	11,700	20,200	
% Life Used	15.8	52.0	23.3	2.4	1.2	Total % 18,000 Hr Life Used = 94.6
<u>K40 Flameholder Beams</u>						
*Stress, psi	2,700	2,650	2,600	1,600	3,300	
% Life Used	6.7	56	30	--	1	Total % 12,000 Hr Life Used = 93.7
<u>Hastelloy X Flameholder 2nd Stage Rings</u>						
*Stress, psi	540	430	440	330	510	
% Life Used	84.6	--	--	14.7	--	Total % 8,000 Hr Life Used = 99.3
<u>Hastelloy X Flameholder 1st Stage Rings</u>						
*Stress, psi	260	200	200	160	300	
% Life Used	6.5	60.0	2.5	0.2	1.0	Total % 8,000 Hr Life Used = 70.2
<u>René 63 Exhaust Casing</u>						
*Stress, psi	17,100	15,600	15,000	10,800	19,200	
% Life Used	41.6	26.3	29.2	1.9	0.0	Total % 12,000 Hr Life Used = 99.0

\*Stresses include 1.25 factor of safety

The stress levels used in the life analysis were obtained from calculations, measured data, or by computer programs developed and successfully used in mechanical designs of the J79, J93, J85 and advanced engines. The methods include computer programs to determine:

- Thermal and hoop stresses in cylindrical shells
- Stresses due to bending moments
- Stresses, deflections, and critical frequencies in dynamic structures.

#### 5.1.5.2.3 Buckling Loads

Due to compressive hoop stress resulting from inward pressure loading, the exhaust casing, cooling liner, and inner cone are designed with sufficient elastic stability margin to prevent buckling. The design procedure, which has been proved by component test of J79, J93 and TF39 hardware, provides assurance that the components will resist three types of buckling:

- Buckling of the entire structure (casing or liner) as a free ring
- Buckling of the structure between the forward and aft stiffening rings (flanges for the casing)
- Individual panel buckling between the various stiffeners

#### 5.1.5.2.4 Maneuver Loads

The GE4 augmentor is designed to withstand aircraft maneuver loads in addition to gas and exhaust nozzle/thrust reverser loads. The most adverse combination of loads yields 6 g's.

#### 5.1.5.2.5 Thermal Stress

Thermal stresses developed during steady-state and transient conditions as one or more local areas of the structure attain different temperatures than adjacent regions. The stresses are caused by differential thermal expansion of the metal. High stresses cause the metal to creep or yield; when the parts are cooled, the plastic deformation may reverse. Repetition of this cyclic operation precipitates thermal fatigue cracking and eventual failure of the components. The methods applied for cooling the structural parts to reduce thermal gradients are discussed in detail in Section 7, Augmentor and Exhaust Nozzle and Thrust Reverser Cooling System. Specific examples of designs for low thermal stress will be found in the paragraphs devoted to the design description of each component.

#### 5.1.5.2.6 Fatigue

The GE4 augmentor has relatively large sheet-metal structures that are subject to vibratory loads induced by the rotation of the engine rotor, pulsations in the gas stream, and by the augmentor combustion reaction. Extensive General Electric experience has shown that structural defects and resultant failures in augmentor components have been largely associated with stress concentrations such as sheared edges, small sheet metal bend radii and abrupt changes in material cross-section. These effects are avoided in the GE4 augmentor design by these typical features:

- The liner has continuous slot cooling construction rather than louvering
- Resistance-welded joints are reinforced with high-temperature braze to eliminate stress concentrations
- All circumferential ring elements are continuous
- Changes in cross-section are gradual
- Sheet-metal bend radii have been maintained at a minimum of three times the stock thickness
- Butt welds are used instead of seam welds in high stress areas

#### 5.1.6 DESIGN DESCRIPTION

Simplicity, reliability, and durability are principle features of the selected GE4 augmentor design. Three major subassemblies in the over-all assembly contribute to the favorable maintainability:

- Spacer ring subassembly; including fuel spraybars, flameholder, and igniter
- Exhaust casing and cooling liner
- Inner cone

Figure 5-20 is a 1/5-scale drawing of the augmentor assembly.

The similarity of some key operating conditions that influence the mechanical design is shown by the data listed in Table 5-6 and compared to the J93 augmented turbojet. The J93 and GE4 engines have very similar inlet temperatures, reference velocities, and Mach numbers. The GE4 temperature-rise is less severe than the J93; a condition favorable to mechanical design and cooling. Emphasis has been placed on the design of the augmentor components for commercial life and safety.

Table 5-6  
Comparative Environmental Parameters for GE4 and J93 (STD DAY)

<u>Take-off</u>	<u>GE4</u>	<u>J93</u>
Ref. Vel. FPS	509	478
Mach No.	.238	.224
Inlet T°F	1596	1589
Temp Rise °F	1244	1611
Exit Temp °F	2840	3200
<u>Cruise M<sub>p</sub> 2.7 @ 65K</u>		
Ref. Vel. FPS	485	490

Table 5-6  
Comparative Environmental Parameters for GE4 and J93 (STD DAY) (Continued)

Take off	GE4	J93
Mach No.	.227	.230
Inlet T°F	1586	1579
Temp. Rise	260	391
Exit Temp °F	1846	1970

#### 5.1.6.1 Spacer Ring Subassembly (Including Fuel Spraybars, Flameholders, and Igniter)

This subassembly includes the augmentor fuel injectors and the flameholder, and consists of the following components:

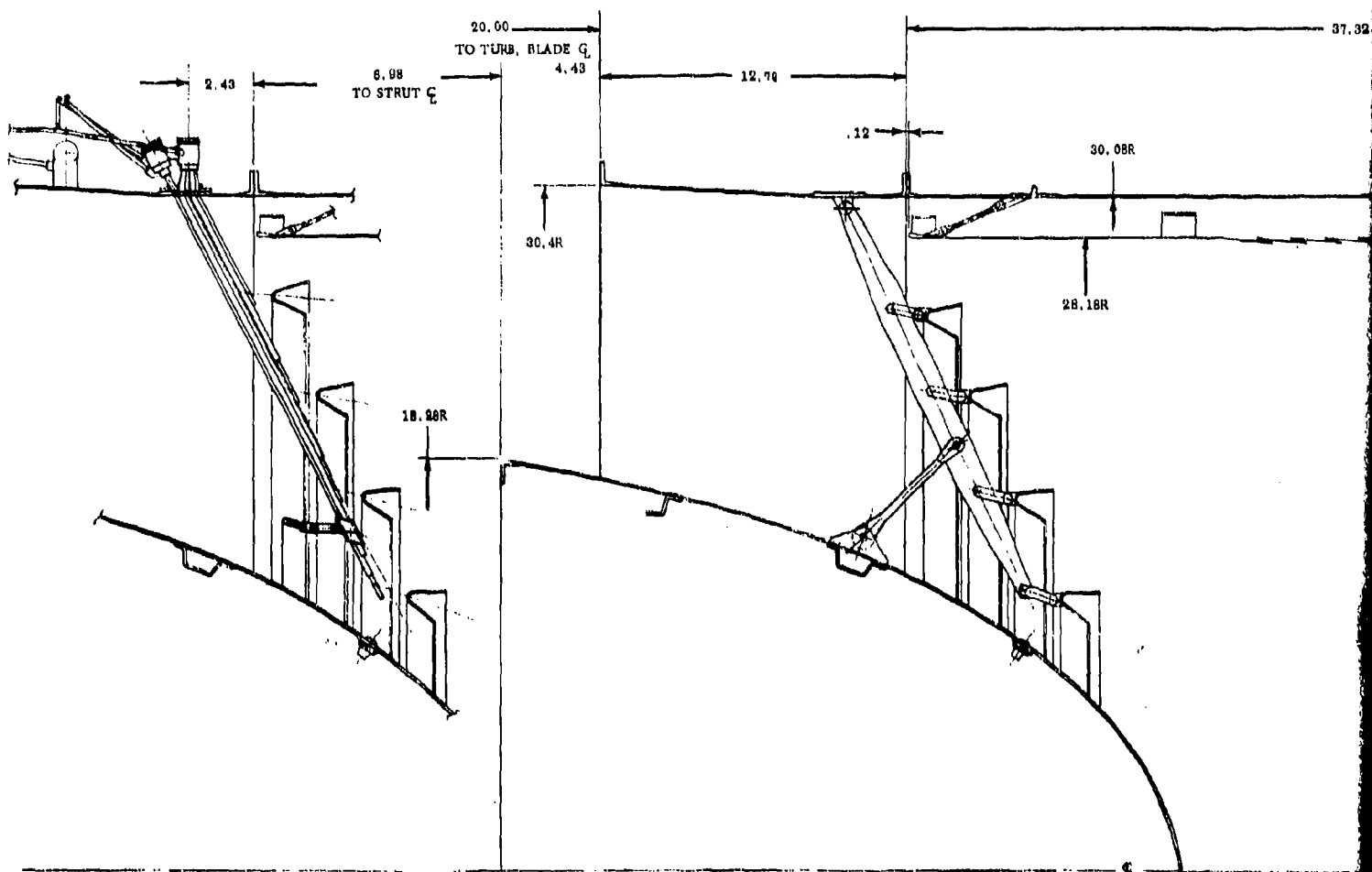
- Spacer ring
- Fuel spraybars (discussed in paragraph 5.2 of this section and paragraph 4.4.3 of Volume III-B, Part II)
- Manifolding (discussed in paragraph 4.4.3 of Volume III-B, Part II)
- Flameholder
- Fuel injector support ring
- Igniter (discussed in Volume III-B, Part II, paragraph 3.9.2.2)

Figure 5-21 is a photograph of the Phase II-C subassembly, showing the removal and replacement of all components.

Features of the fuel distribution and flameholder subassembly, important for maintainability and reliability, are:

- A check for hydraulic leakage can be made with the fuel spraybars and fuel manifolds off the engine
- Individual, as well as complete system, hydraulic flow checks can be made (when coupled with a patternator test stand)
- The key augmentor components can be assembled, checked and stored as a unit
- Flameholder (elements or complete assembly) is replaceable on the aircraft
- Igniter assembly replaceable on the aircraft.





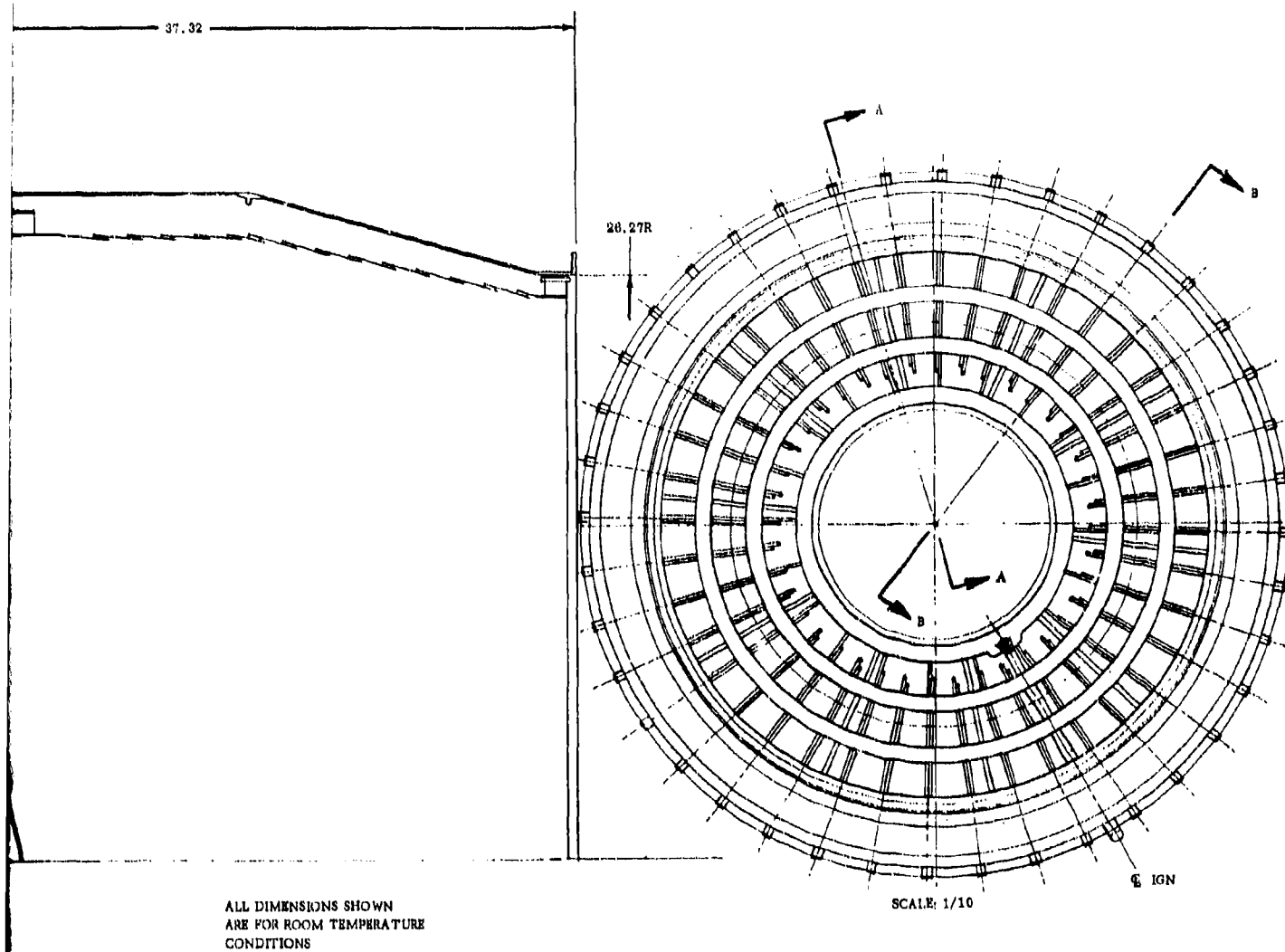


Figure 5-20.

2

5-35/5-38

K

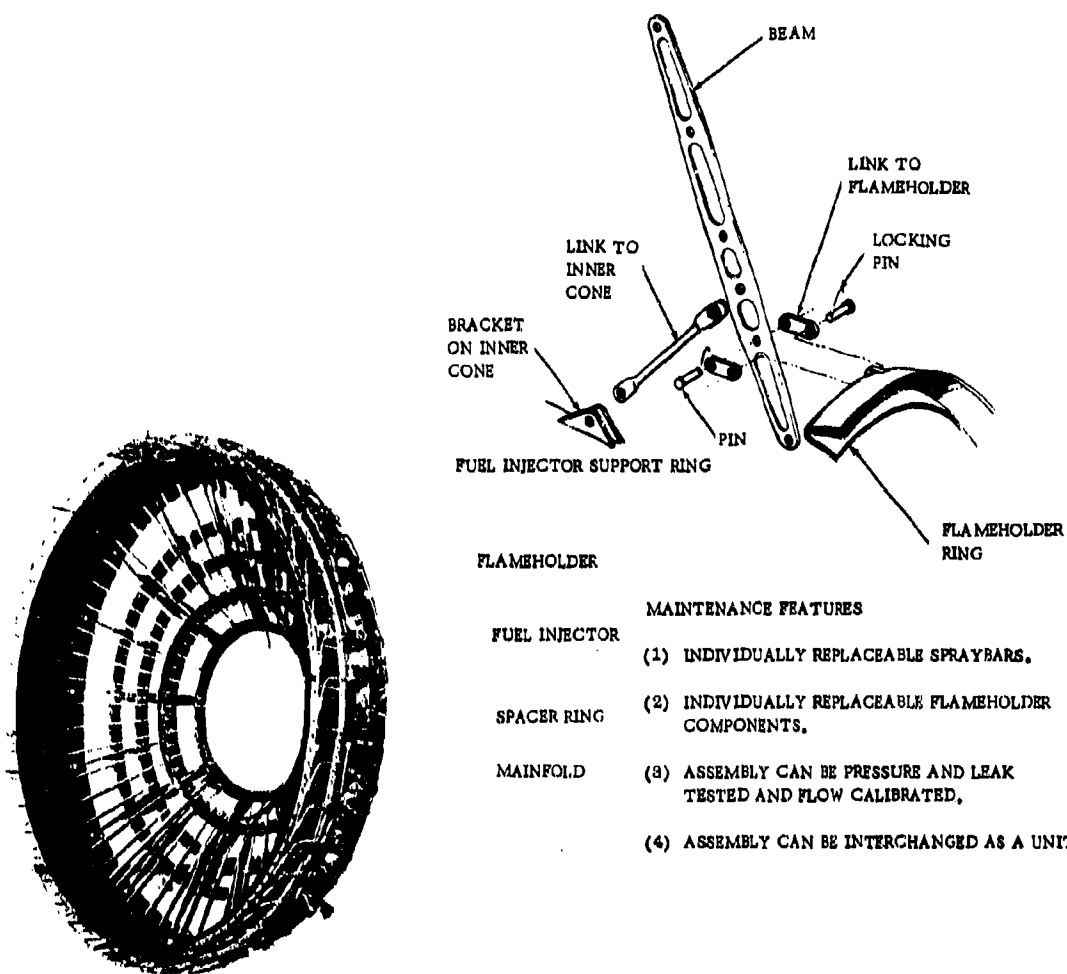


Figure 5-21. FUEL DISTRIBUTION AND FLAMEHOLDER SUBASSEMBLY

#### 5.1.6.1.1 Spacer Ring

The spacer ring is a simple cylindrical component, mounted between the turbine frame and exhaust casing. The spacer-ring structure supports the fuel spraybars and flameholder; it contains the turbine discharge gases, provides the outer boundary of the diffuser flow path, and transmits the bending and axial loads developed by the exhaust nozzle/thrust reverser and augmentor. The inner surface is cooled by compressor discharge seal leakage air, which is discharged forward of the spacer ring from the turbine frame liner.

Figure 5-22 consists of a photograph of the Phase II-C spacer ring and a schematic sketch of the Phase III design. The proposed Phase III spacer ring is larger in diameter and longer than the Phase II-C component. The construction is simple and rugged; all joints are joined with reinforced butt welds. The outer shell is a cylinder of 0.086-inch thick René 41 sheet material, welded to the flanges at each end and to an intermediate fuel injector mounting ring.

The spacer ring concept which provides off-engine flow-check capability is an extension of J79 and J93 experience. All models of the J79 engine utilize such a design. (See Figure 5-23 for the J79 configuration.) The maintainability features of this separate subassembly have been proved in thousands of hours of military operation. The J93 likewise uses a spacer ring, also shown in Figure 5-23. The axially short J93 design encountered durability problems because of temperature differentials between the inner and outer skins, and this design approach has been avoided. The GE4 design employs a single structural skin like the J79, which has been trouble-free. The ring stiffener that supports the flameholder is butt-welded into the skin to minimize thermal gradients and stress concentrations.

The principal structural design criteria for the spacer ring are:

- Stress rupture for the combined hoop stress (developed by the internal gas pressure) and axial stress (developed by the exhaust nozzle/thrust reverser).
- Elastic stability for buckling caused by maneuver loads.
- Elastic stability for buckling resulting from external pressure (under engine-out/windmill brake conditions).

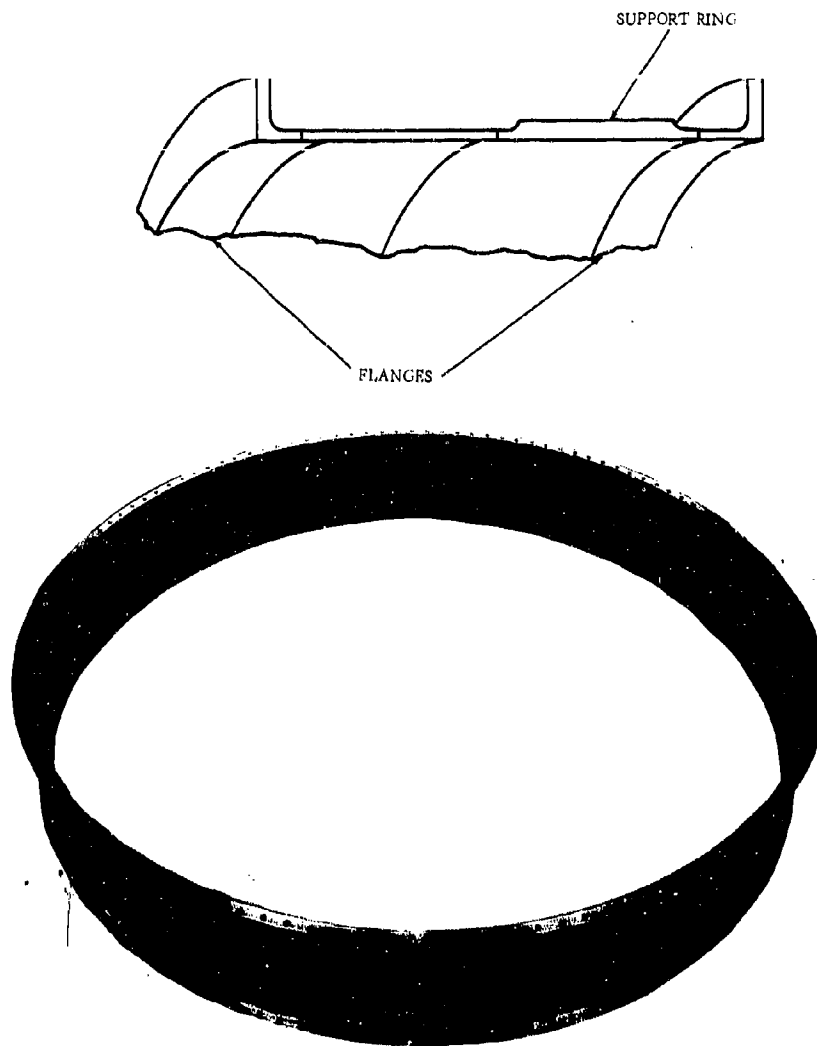
Stress levels and the percentage of design life used by important elements of the flight profile are listed in Table 5-5.

The spacer ring is designed to withstand a bending moment of  $1.2 \times 10^6$  pound-inches due to maneuver loads. The margin incorporated into the design for bending due to buckling is 25 percent above the maximum calculated bending moment.

A 20 psi inward pressure load can be withstood by the spacer ring during transients such as blow-outs or an engine operating at windmill brake conditions. This provides a margin of 235 percent for buckling due to external pressure loading; the pressure load for this flight condition is not expected to exceed 10 psi.

#### 5.1.6.1.2 Spraybar Support Ring

The spraybar support ring connects and supports the tips of all the spraybars. This prevents axial and circumferential vibration of the spraybar assembly in the gas stream. This arrangement maintains stress levels in the tube bundle consistent with those used in the analysis of stress rupture life.



**MAINTENANCE FEATURES:**

- ACCESSIBILITY FROM ALL SIDES FOR CRACK REPAIRS AND INSPECTION.

**DURABILITY FEATURES:**

- BUTT WELDED CONSTRUCTION
- OPERATES AT LOW TEMPERATURE.
- ALL LOAD ATTACHMENTS POINTS ARE ON MACHINED RINGS.

**Figure 5-22. SPACER RING**

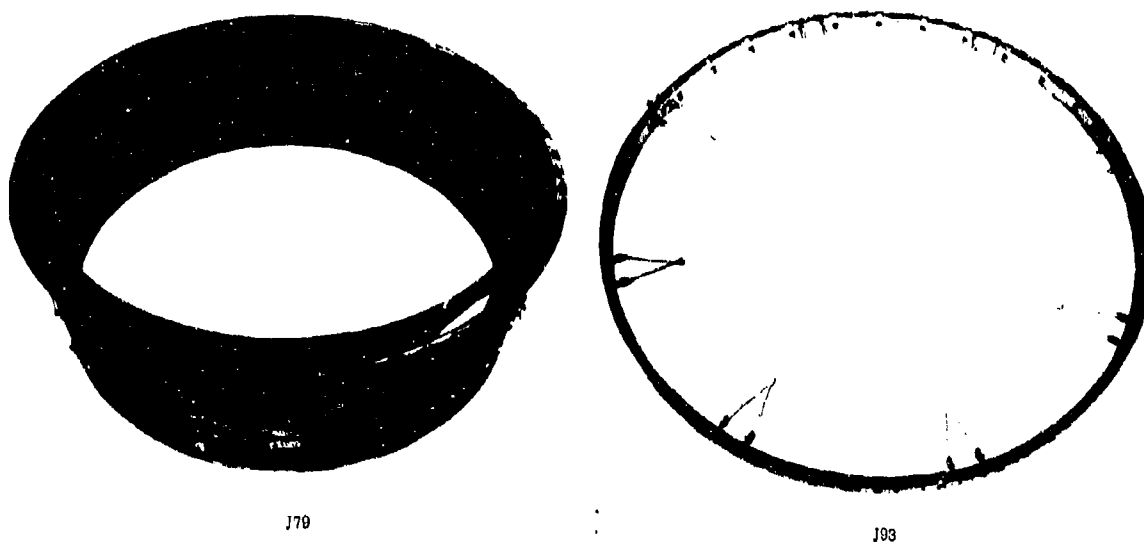
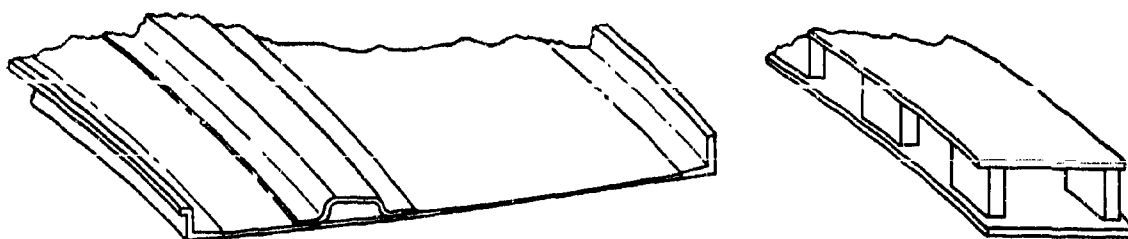


Figure 5-23. J79 AND J93 SPACER RINGS

Figure 5-24 consists of a photograph of the Phase II-C design, and a schematic of the proposed Phase III GE4 support ring, which is fabricated from a flattened butt-welded tube with lugs welded to it. Replaceable connecting links are pinned to the lugs on the ring and to similar lugs on the fuel injector as shown in Figure 5-24. The ring is free to move radially with respect to the fuel injector, when subjected to differential thermal expansion. The similarity of this to the successful J93 design is shown in Figure 5-25. Improvement of the GE4 over the J93 has been made by eliminating the inner cone connection to achieve axial freedom of thermal expansion. This is required because of the large axial (relative) motion between the GE4 inner cone and spacer ring during thermal transients and steady-state operation.

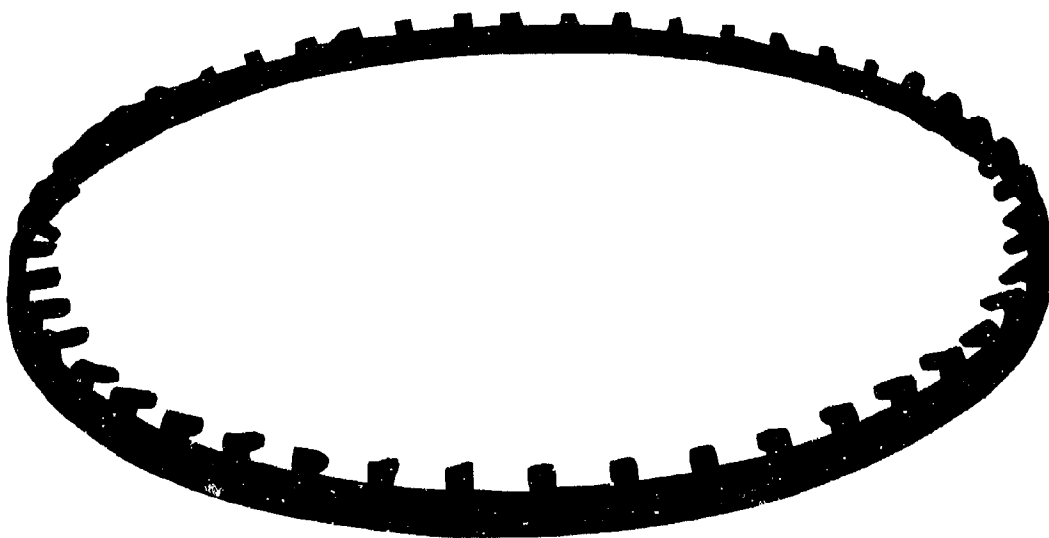
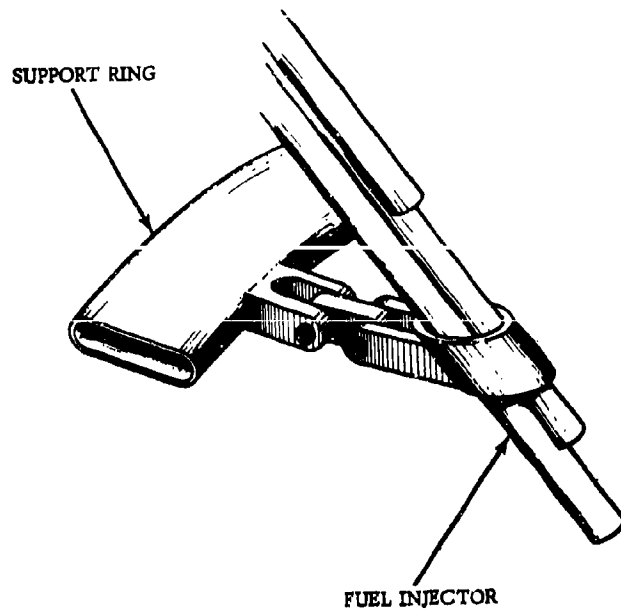


Figure 5-24. FUEL INJECTOR SUPPORT RING

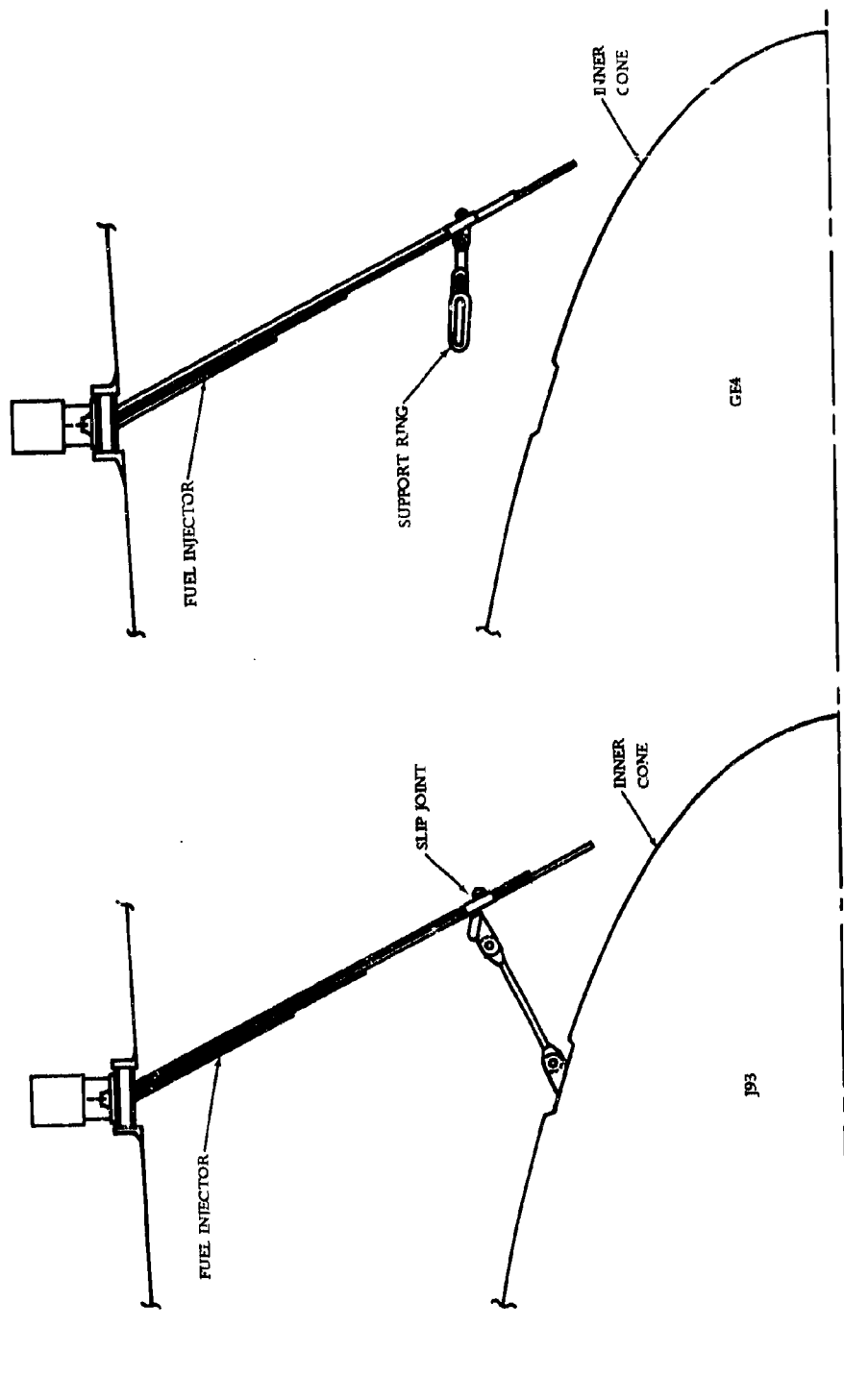


Figure 5-25. COMPARISON OF J93 AND GE4 SPRAYBAR SUPPORT RING SYSTEMS



The primary design criterion for the spraybar support ring, which does not carry any structural load, is resistance to high-temperature oxidation. Hastelloy X has been selected for the tubular ring. This material has demonstrated excellent oxidation resistance in J79 and J93 hot-section components. L605 was selected for the pins and links to provide high-temperature wear resistance at all wear points. The pins and links are easily replaceable for maintenance.

#### 5.1.6.1.3 Flameholder

The mechanical design of the GE4 augmentor flameholder is an extension of the link-pin design approach (proved in J79 and J93 application) with assembly/maintainability features specifically originated for commercial augmentor application. The concept is illustrated in Figure 5-26, and consists of radial structural beams, simply supported between the spacer ring and inner cone, which in turn support the multiple flameholder rings with axial links. The flameholders are formed sheet-metal, butt-welded rings that are fabricated from 0.09-inch-thick Hastelloy X. For ease of ring placement, the rings are mounted on the beams by the link and pin arrangement shown in Figure 5-27. The beams are rugged X40 castings. Spherical bearings and pin joints are employed at rotation points in the assembly, and all surfaces subject to wear are made from L605.

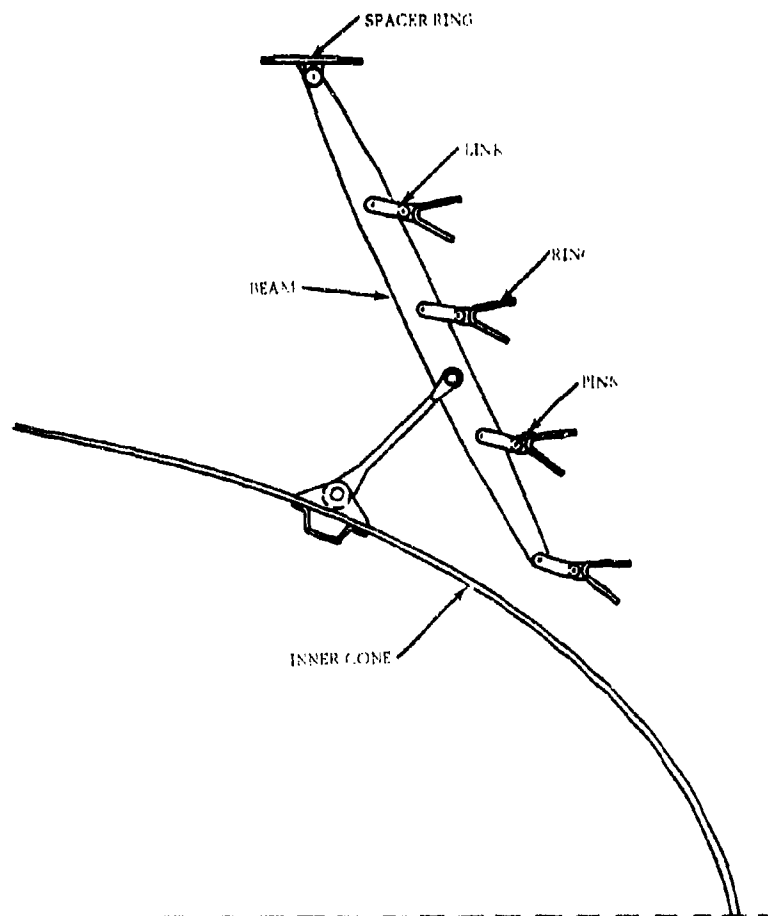


Figure 5-26. GE4 FLAMEHOLDER

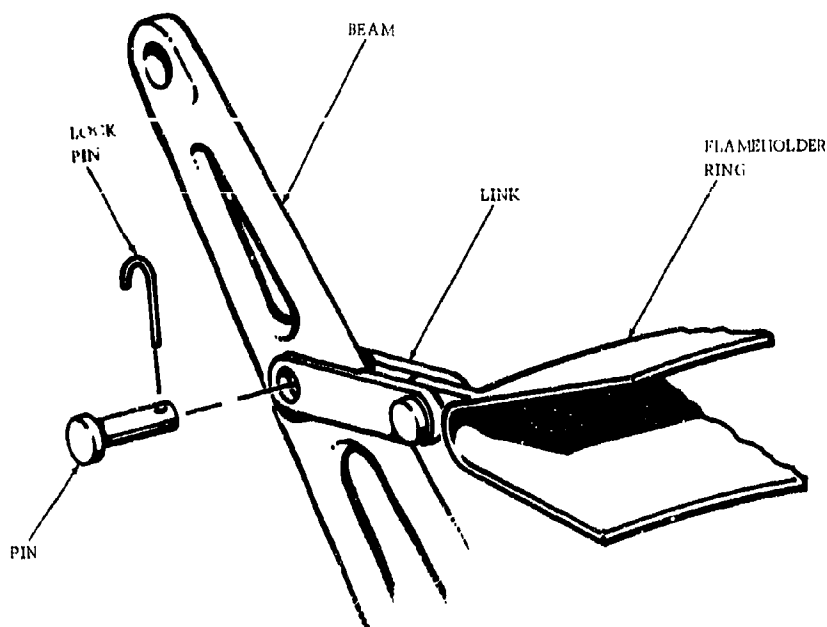
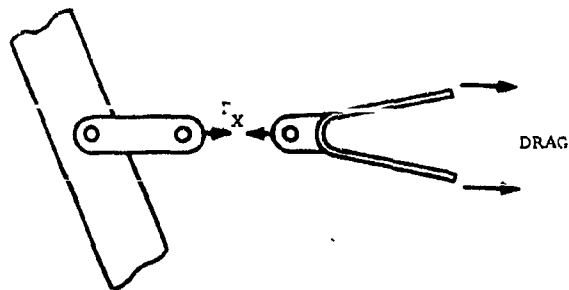


Figure 5-27. FLAMEHOLDER RING MOUNTING ARRANGEMENT

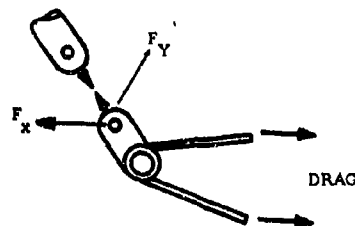
In the J79 and J93 designs, axial drag forces are transmitted to the supporting structure through a series of radial links. The resulting radial loads at each attachment point (Figure 5-28) impose large bending moments and associated high stresses in the flameholder rings. These large bending moments are avoided in the GE4 design because only the axial drag load is imposed on the gutter rings. Loading the rings in the axial direction is fundamentally the most favorable from a stress distribution standpoint. Each flameholder ring supports only its own axial load. The structural beams, which are connected to the spacer ring and inner cone, are not subject to the flame temperatures and are, therefore, capable of accommodating the combined flameholder drag loads. Individual flameholder rings are linked by a double pin that permits radial thermal freedom independent of the supporting beams.

Thermal gradients of the flameholder on the GE4 have been substantially improved from the J79 and J93 designs by providing the change in ring cross-section shown in Figure 5-29. Lack of convective cooling in the area of the flameholder leading edge tube have produced high thermal gradients in the J79 and J93 designs. The GE4 ring has a uniform cross-section with improved convective cooling. Circumferential thermal gradients in the GE4 design have been measured at 200°F, compared to 1150°F measured in the J93 augmentor. The design temperature for the flameholders is based on the thermally similar J93, and this value has been confirmed in the GE4 full-scale augmentor tests summarized in Figure 5-30. The flameholder beam and ring-section properties are established on the basis of stress rupture. Table 5-5 shows the stress levels for typical elements of the flight profile, and the portion of the design life necessary to meet the required component life.

The axially linked design provides for ease in maintenance, in that replacement of any ring or the entire flameholder can be made with the engine installed in the aircraft. The complete assembly or portions thereof can be removed through the primary exhaust nozzle.



GE4



J79 - J93

#### COMPARISON OF J93 AND GE4 FLAMEHOLDER SUPPORT LINKAGE FORCES

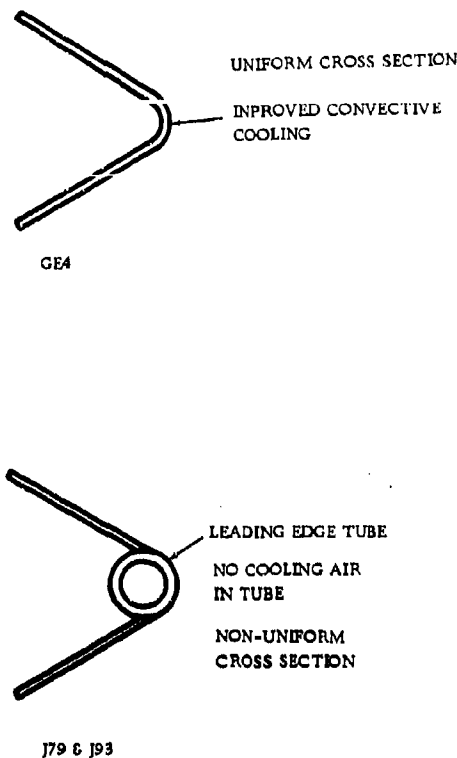
Figure 5-28. COMPARISON OF J93 AND GE4 FLAMEHOLDER SUPPORT LINKAGE FORCES

#### 5.1.6.2 Exhaust Casing and Cooling Liner

This subassembly includes the structural exhaust casing and the film-cooled liner which protects the casing from the high-temperature combustion gases. Figure 5-31 shows the simple Phase II-C subassembly with the liner supported in the casing by links at the forward end.

##### 5.1.6.2.1 Exhaust Casing

The exhaust duct must have prime reliability as a structural, pressure-containing component. These requirements are met by simplified design and construction techniques that eliminate the problems evident in previous configurations.



FLAMEHOLDER RING CONFIGURATION COMPARISON

Figure 5-29. FLAMEHOLDER RING CONFIGURATION COMPARISON

A photograph of the Phase II-C casing and a schematic of the proposed Phase III casing are shown in Figure 5-32. The casing skin is fabricated from 0.08-inch René 63; René 41 has been selected for the stiffening rings and flanges

The previous practice of mounting exhaust nozzle actuation brackets on the exhaust casing of the J79 and J93 engines caused life limitations resulting from low-cycle fatigue. In these previous designs, the actuator loads are transmitted to the exhaust casing through circumferential "hat section" stiffening rings as shown in Figure 5-33. The concentrated actuator loads are, in turn, distributed by the hat sections to the casing skin. Radial thermal gradients (particularly during temperature transients) are inherent with this kind of stiffener, because the top of the hat section operates at a lower temperature than the casing skin. Figure 5-34 shows the J93 steady-state gradient to be measured at 539°F; normal transient gradients up to 790°F were also recorded. High local thermal bending stresses are developed in the casing skin under the hat section, indicated by the dashed lines, and the resulting low-cycle thermal fatigue limits the casing life. In the proposed SST design, the primary nozzle actuators are not mounted on the GE4 exhaust casing. To eliminate the duct problems, as well as to provide more favorable actuator environment and accessibility, the actuators are mounted in the fixed secondary nozzle shroud. The actuator point loads are distributed to the low-temperature shroud structure and then transmitted uniformly to the exhaust casing.

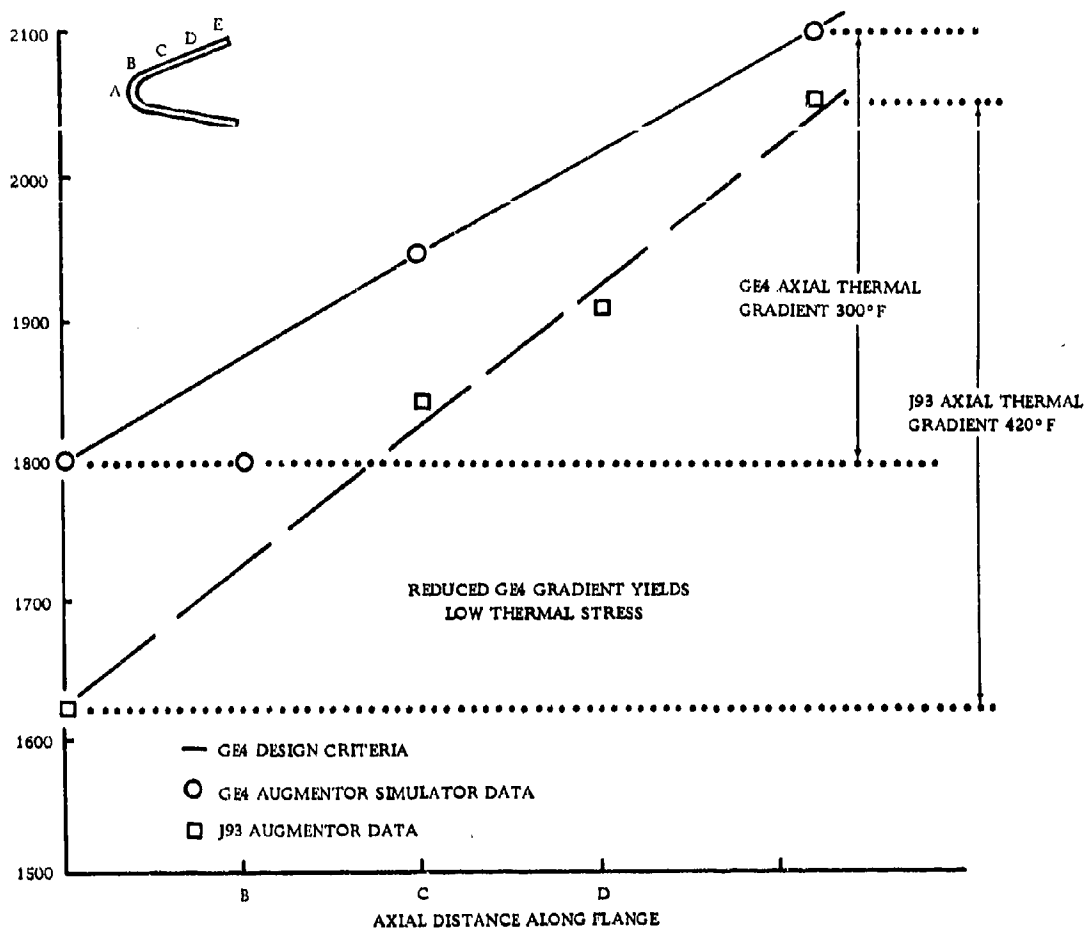


Figure 5-30. REDUCED GE4 GRADIENT YIELDS LOW THERMAL STRESS

Augmentor cooling liner support brackets welded to the skin of the J79 and J93, as illustrated in Figure 5-33, have been a source of fatigue cracks. The GE4 design will not be subjected to this type of failure, because the proposed cylindrical liner design does not require these support brackets.

The skin cracks, originating at seam-welded flange and stiffening ring joints of the J79 and J93 exhaust casings, will be eliminated in the GE4 design, because all joints are butt-welded. It has been widely confirmed that butt welds are more repeatable, more reliable, and more effectively inspected ~~so that they~~, therefore ensure high-quality welds less subject to cracking. Thermal gradients in the exhaust casing stiffeners have been substantially reduced by employing machined rings of T-shaped cross-section with butt-welded attachment to the casing skin. Thermal stresses in these rings are at a sufficiently low level to provide a durable component that will meet the objective service life requirements.

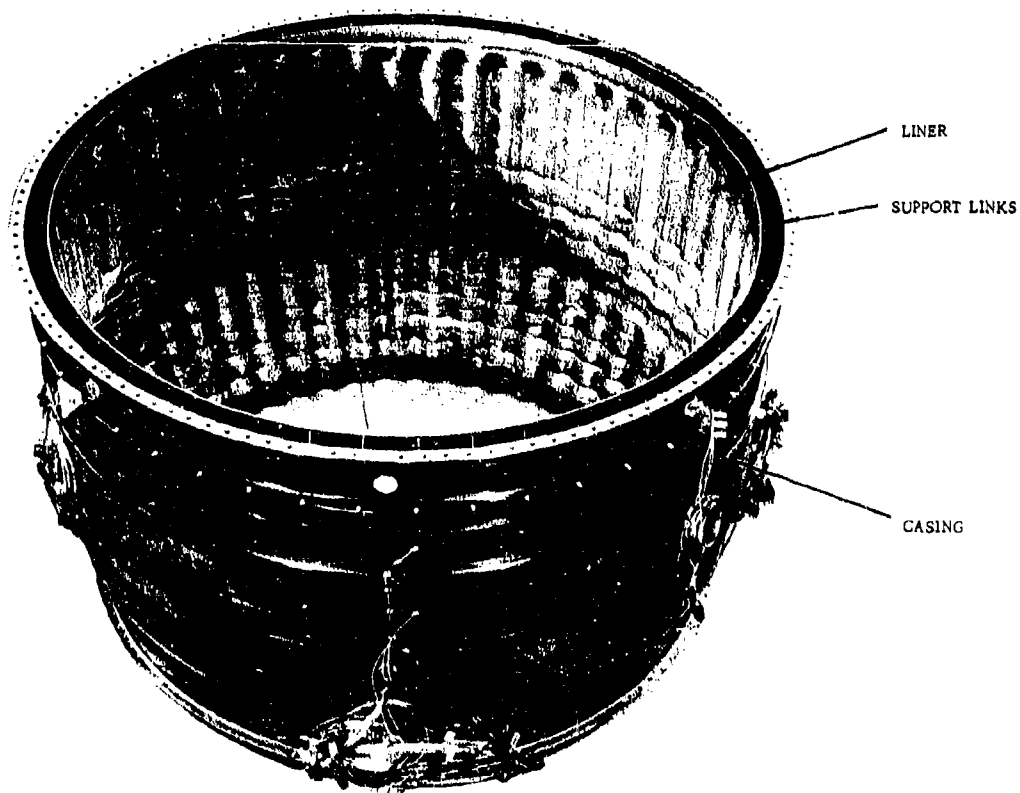


Figure 5-31. PHASE II-C EXHAUST CASING AND LINER SUBASSEMBLY

The principal mechanical-design criteria are:

- Stress rupture due to the hoop stress developed by the internal gas pressure and axial stress developed by the exhaust-nozzle/thrust-reverser.
- Elastic stability for buckling resulting from external pressure loading.



NO LINER SUPPORT  
IN PROPOSED PHASE III  
DESIGN

Figure 5-32. PHASE II-C GE4 EXHAUST CASING

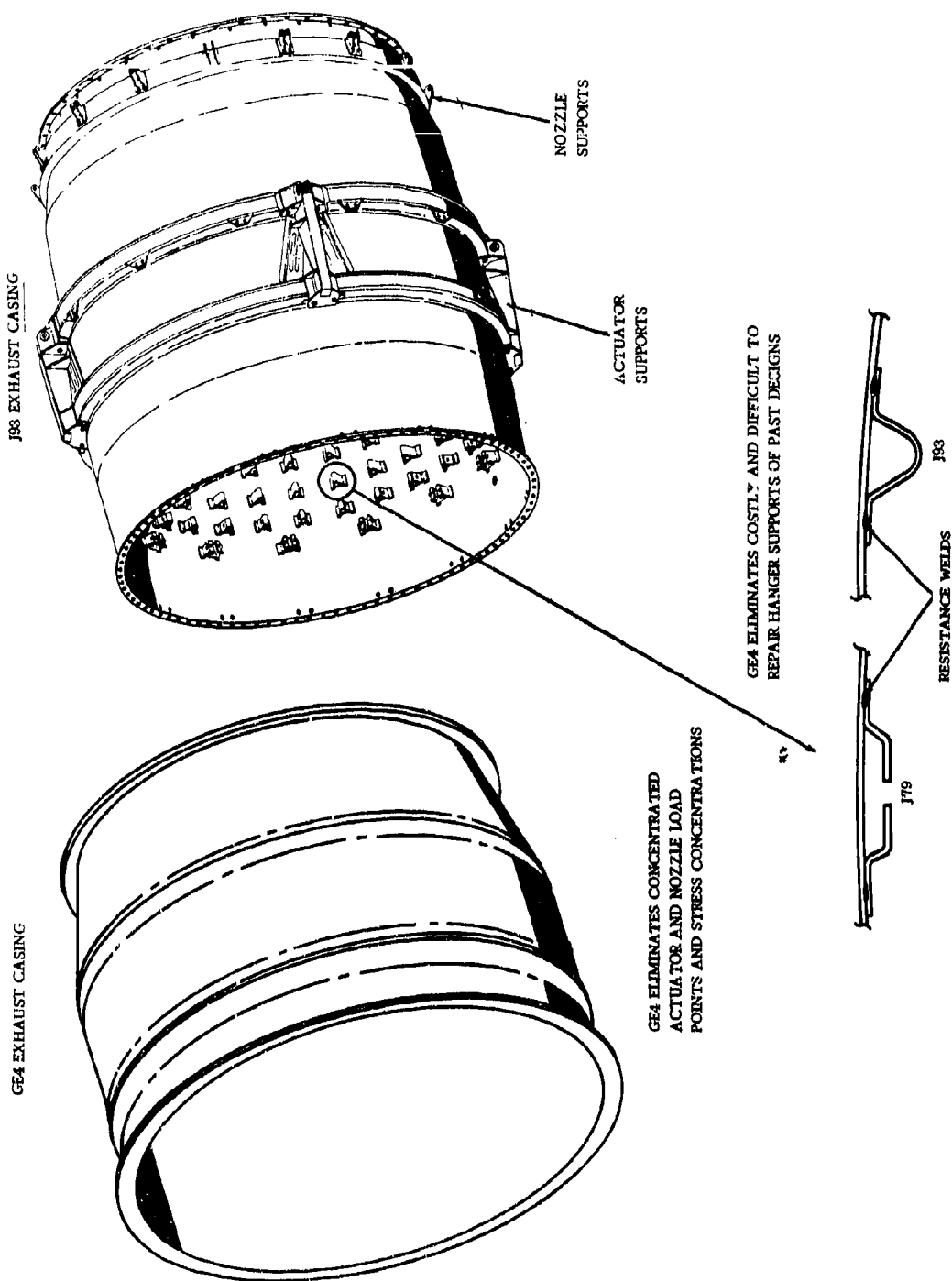


Figure 5-33. GE4 EXHAUST CASING



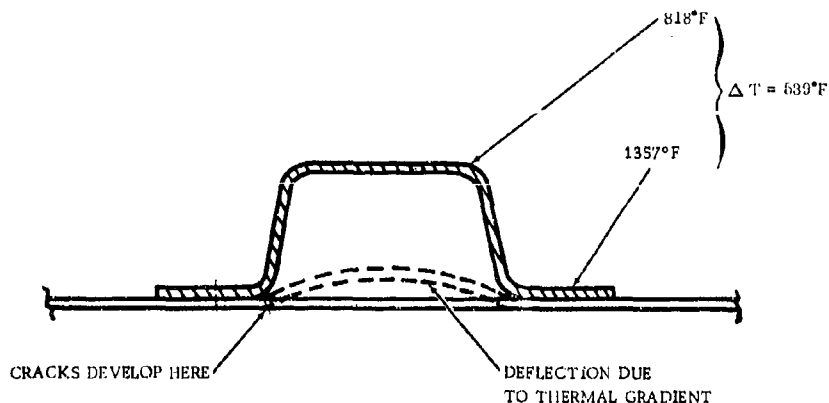


Figure 5-34. J93 EXHAUST CASING HAT SECTION TEMPERATURE GRADIENT

Exhaust casing stress levels, consumed life, and design temperatures for important elements of the flight profile are given in Table 5-5. The casing will also support the required six-psi maximum compressive load caused by external pressure. Proof tests will be conducted to confirm the analyses.

In summary, the simplicity of the exhaust casing is evident; it features reliable butt-weld construction. The casing is clean and free of exhaust nozzle actuator brackets, liner support brackets, and their attendant thermal stresses and concentrated loads.

#### 5.1.6.2.2 Film-Cooled Liner

The high exhaust gas temperatures in augmentors make positive and efficient cooling of the augmentor structure necessary. The proved, common method used to maintain the structural augmentor casing at a low temperature level is the cooling liner. The cooling liner prevents convective heat transfer from the combustion gas to the structural wall, and also intercepts radiation from the combustion gas. Details of the heat transfer, cooling analysis, and temperature predictions are thoroughly discussed in Section 7 of this volume.

The cylindrical liner shown in Figure 5-35 is the Phase II-C design proposed for the Phase III, GE4 augmentor. In the Phase II-C program, two cooling liner designs were evaluated in full-scale tests: the convoluted design shown in Figure 5-36 and an advanced cylindrical design. The cylindrical liner was selected for the following advantages:

- Maintainability, including assembly and repair, is substantially improved.
- Multiple supports are not required on the exhaust casing and liner.

The cylindrical liner employs the continuous circumferential slot cooling and the three-element slot construction of all recent high-performance annular combustors; the J93, GE1, and TF39 as well as the GE4. J79 and J85 combustors and augmentor cooling liners employed sheared louvers for film cooling, and, due to the discontinuous film, there were steep temperature gradients between the louvers. The louvers are formed by shearing a local section of a single-thickness sheet and therefore must have a finite circumferential length; the louver opening and the resulting cooling film are not continuous but interrupted, producing local uncooled areas. The most effective

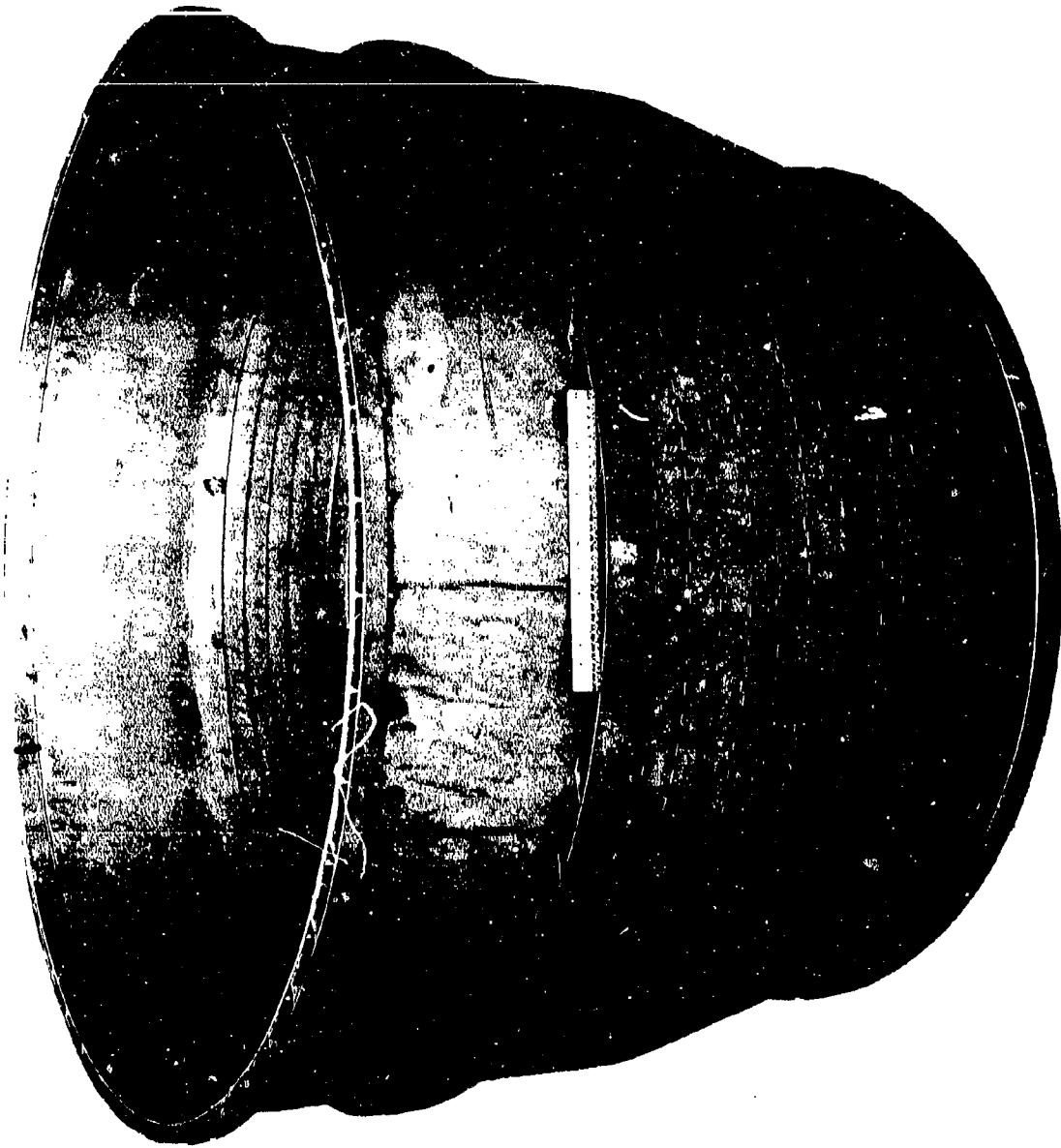


Figure 5-35. CYLINDRICAL AUGMENTOR LINER

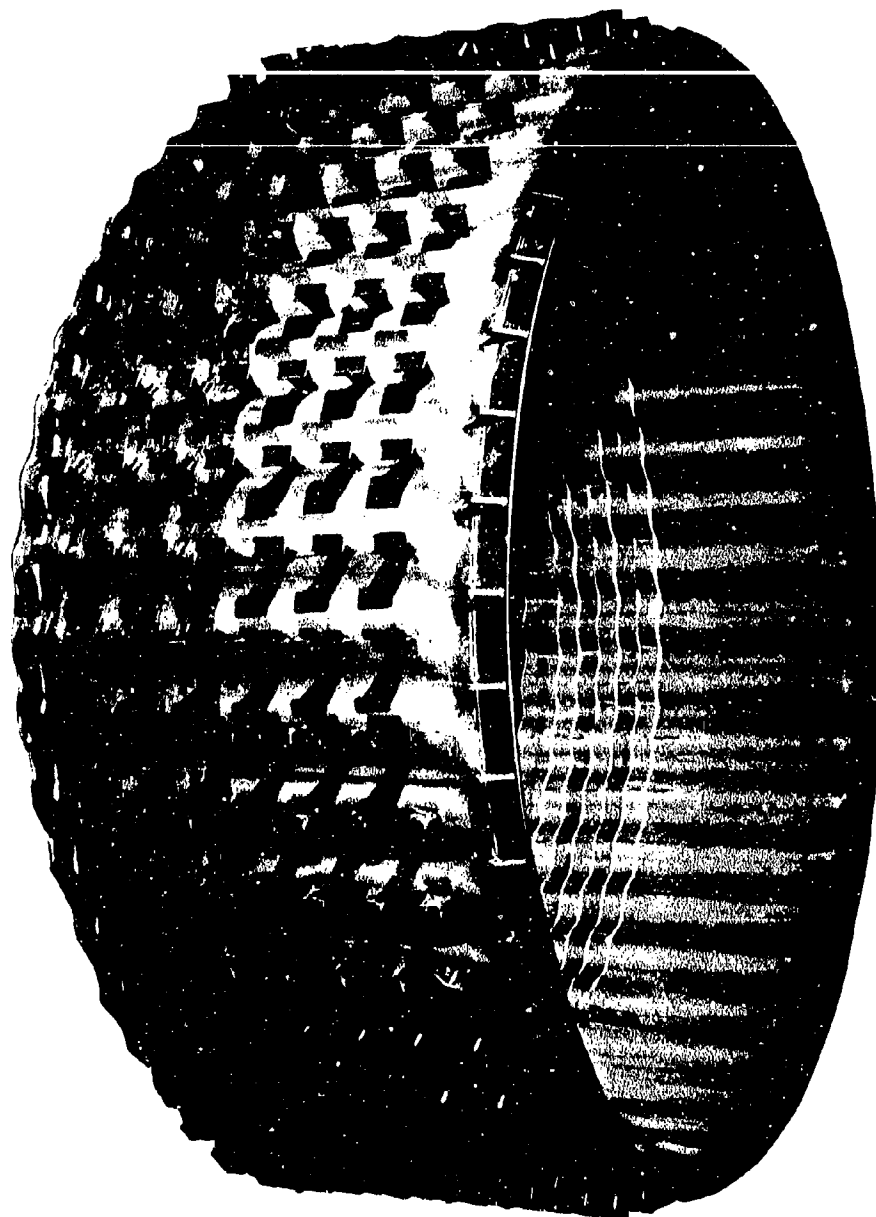


Figure 5-36. PHASE II-C CONVOLUTED LINER

louver pattern, from a heat transfer standpoint, effects a nearly continuous circumferential cooling film, thereby reducing the over-all average metal temperature, the thermal gradients, and their thermal stresses. A typical louver density sufficient for cooling has low mechanical strength because of lack of material/structure between adjacent louvers. An additional compounding problem is that cracks propagate from the stress concentrations formed by the corners of adjacent louvers. It is apparent that a reduction in the number of louvers provides a more adequate cross-section, but has the penalty of higher structural temperature (due to reduced cooling effectiveness). Therefore, a basic limitation of louvered cooling is that it is necessary to compromise temperature and fatigue strength. This has been acceptable for small-diameter combustors and augmentors with a high inherent stiffness. For diameters corresponding to the GE4 augmentor liner dimensions however, the available fatigue strength becomes a more acute problem because of panel and ring vibration.

The three-element cooling-slot design shown in Figure 5-37 was developed for the severe operating requirements of the J93 combustor. Fundamentally, it eliminates the compromise between cooling and strength in that it provides independent control of cooling and mechanical strength and a continuous uninterrupted circumferential cooling film. The cooling-air quantity is controlled by wiggle-strip height, which has no effect on the structural band strength because, as the cooling effectiveness or slot height is increased, the available structural section is retained and stress concentrations are not introduced. This cooling-slot approach has been satisfactorily proved on J93 and TF39 combustors, and has been subsequently applied to combustors and augmentor liners of all advanced General Electric engines.

The cooling liner design is composed of a series of circumferential bands and corrugated strips joined by a combination resistance to welded and brazed joint. The bands and strips are joined initially by spot welding. High-temperature braze is sequentially added to reduce the stress concentration and thermal gradient associated with spot welds. J93 combustor experience has demonstrated that this unique combination weld-braze joint is durable and reliable. The cooling-liner

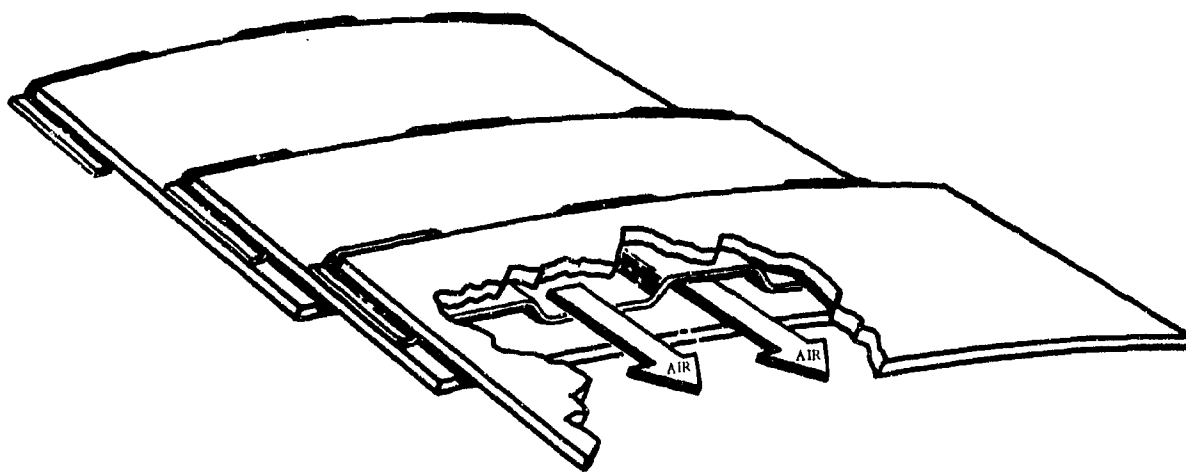


Figure 5-37. GE4 AUGMENTOR LINER COOLING SLOT

metal is protected from the high convective and radiant heat flux generated by the combustion reaction by continuous circumferential film cooling. (Details of cooling design are included in Section 7, Volume II-B.)

Concentricity and positioning of the cooling liner in the casing are maintained by a mounting system consisting of 40 links. The links attach the liner to the exhaust casing at the forward end, and a ring stiffener centers the liner at the aft end as shown in Figure 5-38. This mounting approach provides positive positioning of the liner, concurrent with complete freedom for axial and radial differential expansion.

Table 5-7 is a comparison of augmentor and combustor cylindrical liner design requirements. Note that the requirements for the augmentor liner are like those of the combustion liner. The increase in skin temperature is offset by the large reduction in pressure loading. An additional large advantage of the augmentor case is the lower radiation heat load resulting from the combustion of vaporized fuel and reduced pressure levels. The proposed cylindrical liner for the augmentor makes effective use of experience of successful annular combustion liners for the J93, TF39, and GE1.

Table 5-7. Comparison of Augmentor and Combustor Liner Design Requirements

	<u>Augmentor Liner</u>	<u>Combustor Liner</u>
Required Life, Hours	12,000	12,000
Max Skin Temperature, °F	1730	1500
Skin Temperature at Cruise, °F	1580	1360
Radial Thermal Gradient at Cruise	40	300
Pressure Loading at Cruise, psi	2.3	9.4
Maximum Pressure Loading psi	4.5	20.6
Cooling Air Proportion (of inlet air stream)	24%	22-25%

The principal mechanical design criterion is the need for resistance to buckling, resulting from the external pressure which produces the flow of film-cooling air through the cooling slots. The liner will accommodate the 4.5-psi maximum compressive load with a 50 percent overload capability. This margin is consistent with similar combustor liner designs which have been authenticated by J93 and TF39 hydrostatic load testing. Vibration resistance and high structural integrity is obtained by the incorporation of a trussed leading-edge ring stiffener. General Electric combustor and augmentor experience has shown the need for a stiff leading-edge structure to accommodate the buffeting forces of the high-velocity inlet air stream.

Hastelloy X material of 0.040-inch thickness is used in the liner. This combination provides the operating margin required for durability, and facilitates repair.

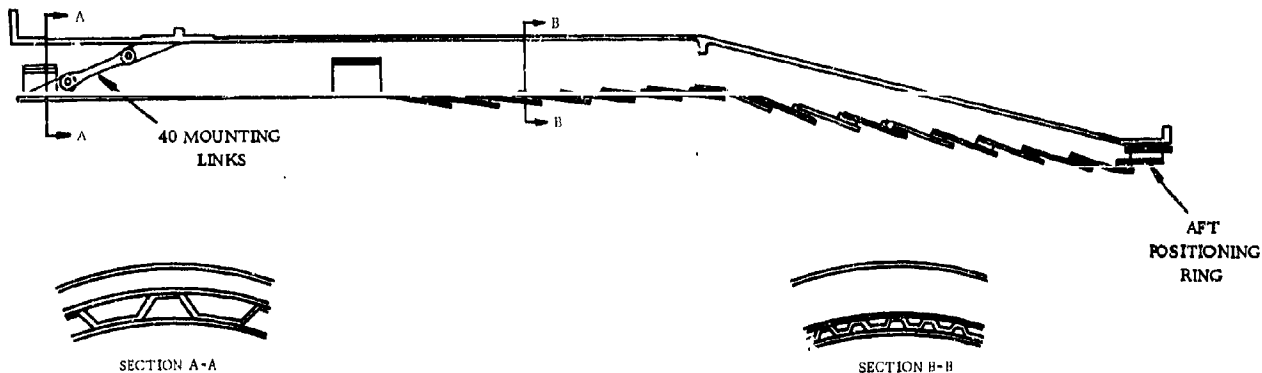


Figure 5-38. GE4 LINER MOUNTING

#### 5.1.6.3 Inner Cone

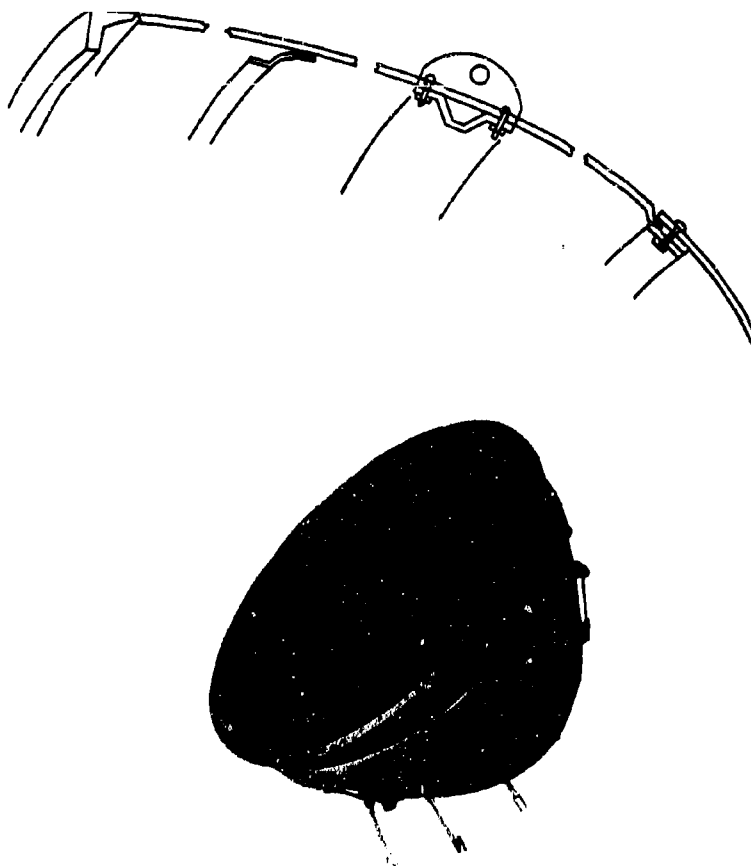
Figure 5-39 shows the Block I design and a schematic of the construction used in the inner cone. The design incorporates a separate (bolted) tip section that can be removed for visual or radiographic-probe inspection of the turbine bearing. The shape of the inner cone provides the inner diffuser flowpath. The inner cone consists of formed, 0.03-inch-thick, sheet metal sections and a forward flange for mounting to the turbine frame. The aft reinforcing ring supports the inner flameholder beam links. A sheet metal ring is resistance-welded to the forward portion to stiffen the skin for the compressive buckling load resulting from an inward pressure differential under conditions of augmentor light-off.

The design criterion for the inner cone skin is elastic stability — to resist inward pressure load. It is designed for a 5.2 psi buckling load with 580 percent overload capability. The material selected for the inner cone is Hastelloy X which has proven oxidation resistance at the operating temperatures of this component.

#### 5.1.6.4 Maintainability

The proposed augmentor design provides "on aircraft" replacement capability for principal sub-components such as the flameholder, as well as the over-all augmentor, exhaust-nozzle, thrust-reverser assembly. The flameholder, igniters, spraybars, and liner are replaceable with minimum disassembly of the augmentor when the exhaust duct is separated from the engine. Figure 5-40 shows how the augmentor can be disassembled into its major components after removal from the engine. Figure 5-41 shows that a mechanic can comfortably enter the exhaust casing to make routine inspections, perform normal maintenance, or replace sub-components.

The cylindrical liner is substantially easier to replace than previous designs, because of the limited number of accessible attachments. J79 and J93 convoluted liners with multiple support tracks and hangers that have to be engaged are subject to handling damage, and require difficult-to-perform inspection for assurance that all supports are engaged. This problem has been eliminated in the GE4 by the self-supported cylindrical liner. All flameholder parts, including the four rings and the support beams, can be replaced with the GE4 engine installed in the aircraft. Other important maintenance and repair features include:



MAINTENANCE FEATURES:

- REMOVABLE TIP FOR INSPECTION

Figure 5-39. INNER CONE

- Removable inner-cone tip for radiographic and visual inspection.
- All mounting pins for the flameholder, liner, and spraybar support ring are easily replaceable and are made from wear-resistant L605 material.
- Butt-welded construction is used throughout the structural spacer ring and duct. This design permits complete inspection and simplified repair. There are no inaccessible or hidden weld joints.
- The spacer ring subassembly permits off-engine flow, pressure, and leak checks of the entire augmentor fuel distribution system.

A durability and maintainability analysis for the Section 5. AUGMENTOR has been completed and is contained in a special appendix entitled "GE4 Durability and Maintainability Analysis", which is available on request as back-up material to the substantiating data submitted.

#### 5.1.6.5 Reliability

To achieve commercial reliability, the following criteria were applied throughout the augmentor design:

- All parts affected by stress rupture are designed for two times required life with a 1.25 to 1 factor of safety.
- All stress analyses are made with temperatures 100°F higher than predicted.
- All stress analyses are made using minimum material properties and minimum material thickness.
- Parts designed for external buckling have a safety factor of 1.85.

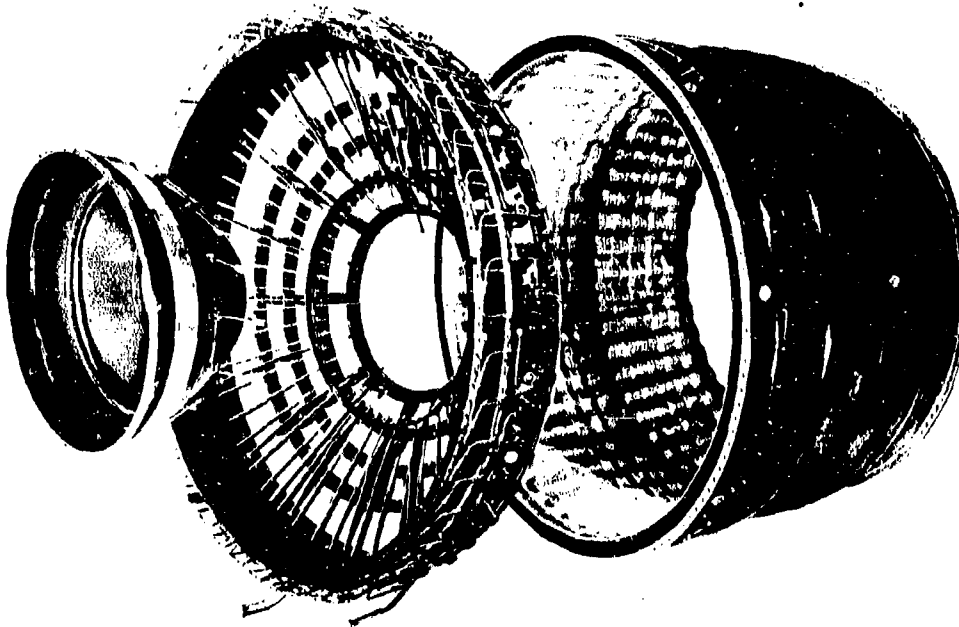


Figure 5-40. MAJOR AUGMENTOR COMPONENTS



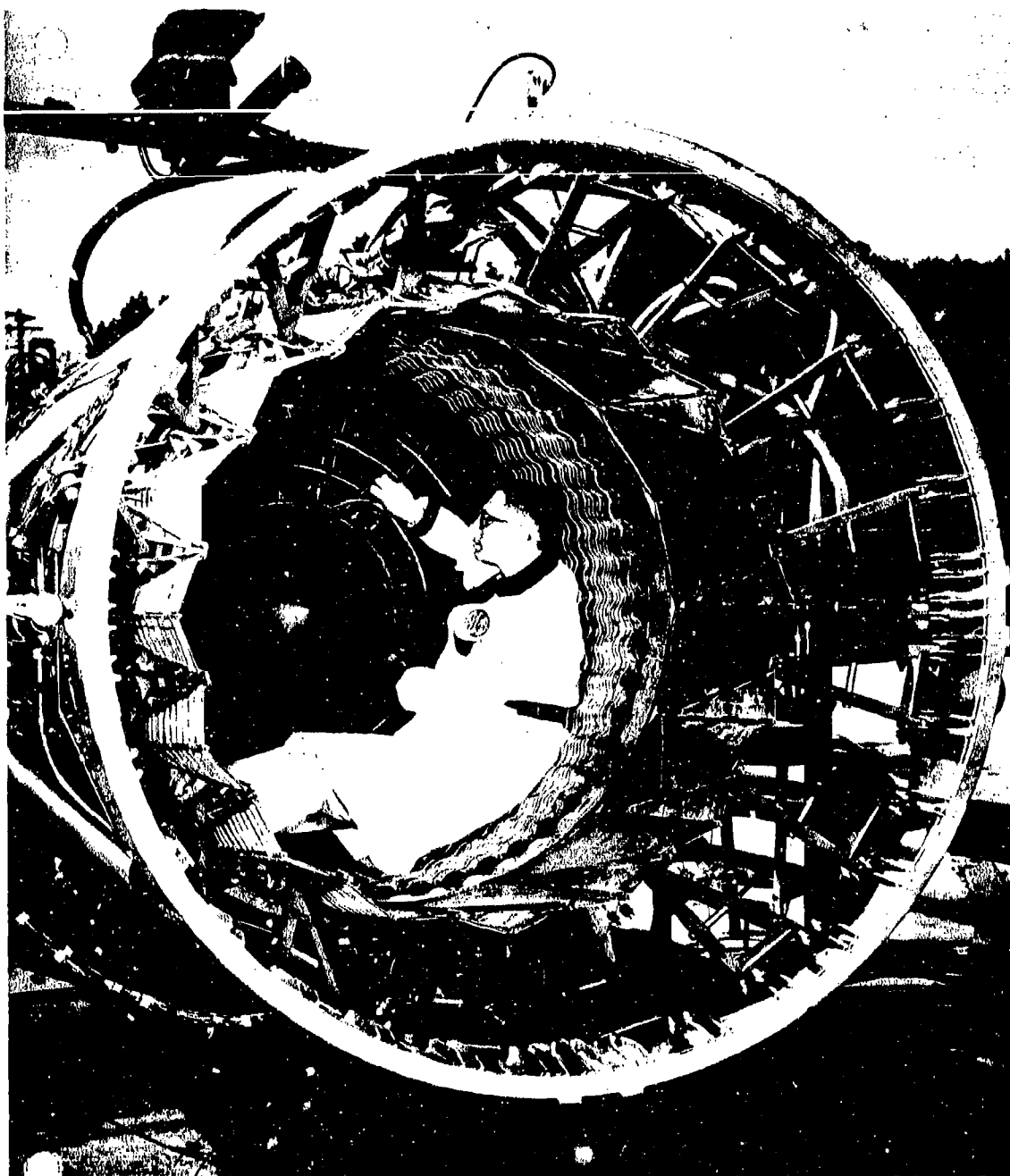


Figure 5-41. SIZE FOR EASY MAINTENANCE

Included in the individual component design description are specific definitions of significant design improvements introduced on the GE4 to improve reliability. Briefly, these are:

- Primary nozzle actuator brackets, hat sections, and liner support brackets are removed from the exhaust casing to eliminate point loads and stress concentrations.
- Butt-welded construction is used for all structural joints.
- Cooling liner resistance-welds are reinforced with braze.
- Thermal gradients are low as a result of the elimination of closed-section stiffeners (hat sections).
- Failure-producing stresses are reduced in the flameholder by independent support for each gutter.
- Spraybars have high valve force for gum-resistance.
- Spraybar metering orifices operate in low-temperature environment.
- Thermal independence exists between "cruise" and "fill" tubes in the fuel injector.

#### 5.1.6.6 Quality Assurance

The proposed augmentor components are produced with conventional welding, casting, forming and machining operations, and process methods that have produced highly reliable parts. Changes that have been made in design or processing to increase the operational quality of the parts are:

- Repeatable and inspectable butt-welds rather than seam-welds; there are no hidden joints.
- Additional application of radiographic inspection to key structural joints.
- The quality control engineering function reviews and approves all drawings and specifications in advance of manufacturing release.
- Material grain size, alloy depletion, and intergranular attack are accurately specified and carefully controlled by macro- and micro-examination.

#### 5.1.6.7 Safety

Safe augmentor operation is achieved primarily by applying dependable, well proved design features and design criteria. The predictable and reliable cooling-air distribution design is essential to safety, and is achieved by minimizing the possibility of liner and casing burn-through. The cooling system is designed to maintain low metal temperatures. During maximum augmentor operation, the liner operates at least 400°F below the burn-out temperature. Augmentor integrity is ensured by the ease of routine visual inspections, since the design is open, and is completely accessible internally for preflight inspection. General Electric's experience with supersonic augmentor operation in three previous designs ensures that the component designs selected for the GE4 will have the required safety.

#### 5.1.6.8 Failure Analysis

A failure mode and effects analysis (FMEA) is being completed on the augmentor design. Specific component or engine overstress margin or vibrational test requirements will be established to evaluate the effectiveness of the design to eliminate or reduce the failures determined by the FMEA. The failures experienced in service on the J85, J79, and J93 have been reviewed, and effective and proven design action taken to reduce or eliminate potential problems.

A task force comprising a five-man team was convened for several weeks to investigate all significant General Electric experience on turbojet augmentors. Problems affecting IFPL, IFSD, delay reliability, VER, and high maintenance were examined. These problems were then classified according to the primary source of difficulty, i.e., controls, augmentor parts, jet nozzle, or systems effects. The most important problems were then compared with corresponding GE4 designs to eliminate or reduce the possible occurrence of such problems on the GE4 augmentor.

Additional failure analyses to be conducted on the augmentor are described in Volume IV, Reliability.

#### 5.1.6.9 Value Engineering

A value engineering team composed of the design engineer, value engineer, manufacturing engineer, and production supervisor has continuously reviewed the design and conducted programs to ensure a low-cost, high-quality component. Team recommendations that have been influential in the design selected are:

- Design of a simple butt-welded spacer ring and exhaust casing without actuator brackets and liner supports



Figure 5-42. J93 SIMULATOR ON J79 ENGINE

- Use of a cylindrical liner
- Design of simplified components compatible with established fabrication methods.

#### 5.1.6.10 Human Engineering

The GE4 augmentor design has been studied for assurance that there are no parts that can be assembled improperly, or that could cause a dangerous situation through human error. Stack-up studies have shown that all parts under all tolerance situations assemble easily. Fuel injectors cannot be put in sideways or backwards because of the bolting pattern, spacer-ring hole size, and fuel piping connections. All parts have clear identifying marks to make sure that they are oriented properly. All assembly and disassembly can be performed by maintenance personnel with normal skills and abilities. There are no sharp edges or other features that would constitute hazards.

#### 5.1.6.11 Standardization

Augmentor casings, liners, flameholders, fuel injectors, and all other sub-components are designed for complete interchangeability.

### 5.1.7 DEVELOPMENT STATUS

#### 5.1.7.1.1 Deleted

#### 5.1.7.1.2 Description and Capability

The SST exhaust system simulator test vehicle is shown schematically in Figure 5-43. It is composed of two J79-2 engines with their augmentors modified for low-temperature-rise operation. The J79 engines normal exhaust gas temperature is increased approximately 450°F by the modi-

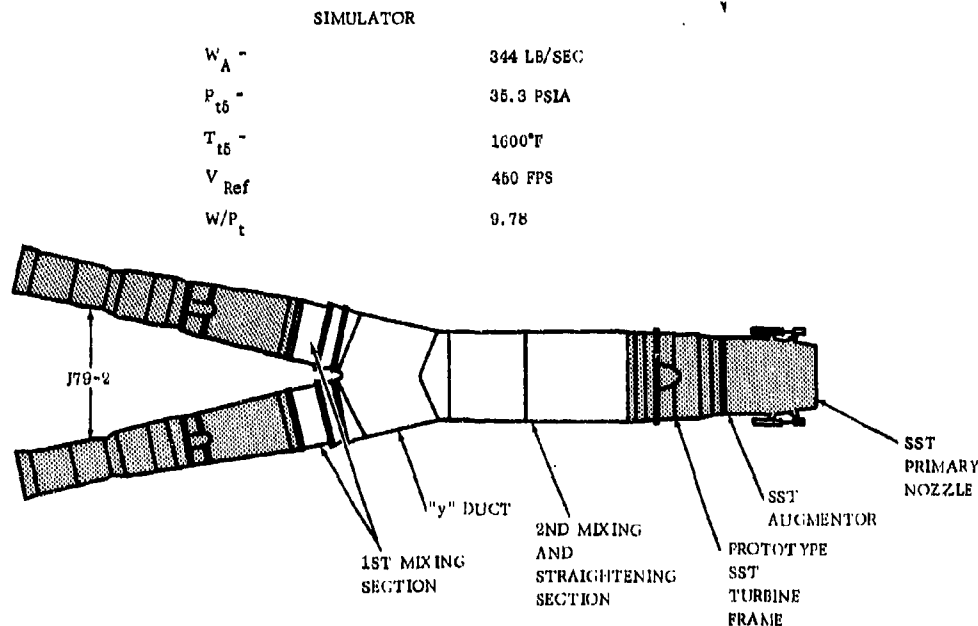


Figure 5-43. SST EXHAUST SYSTEM SIMULATOR

fied augmentors to match the rated GE4 Phase II-C engine cycle. At the discharge of each augmentor, a mixer section is installed to normalize the outlet temperature distribution initially before joining the two augmented exhaust streams with a Y-duct. This is followed by a second stage of mixing (to ensure uniform temperature) and a straightening section which transitions to a prototype GE4 turbine frame. The exhaust system mounts on the prototype turbine frame in the same manner as it will on the GE4 engine. Photographs of the simulator vehicle are shown in Figures 5-44. The combined airflow of the simulator is 305 pps at a GE4 augmentor inlet pressure of 29 psi.

The mixer pressure-drops have been sized to permit exact simulation of the SST augmentor reference velocity and inlet temperature at a pressure level of 64 percent of the Phase II-C cycle for SLS. This pressure level is high enough to permit extensive aero-thermo-dynamic performance investigations, cooling evaluations, and mechanical durability testing. The comparison of the simulator capability with the GE4 cycle conditions is shown in Figure 5-45. It is pointed out that the simulator operating range accurately reproduces the GE4 conditions in the important Mach 2.7, 55-65,000-foot altitude range.

In addition to simulating the correct average turbine discharge conditions, the turbine frame is equipped with a system of variable vanes to permit evaluation of variations in turbine exit swirl angle. The capability for providing average outlet temperatures greater than the rated conditions permits margin testing for cooling system performance and mechanical endurance.

#### 5.1.7.1.3 Phase II-C Program

The Phase II-C exhaust system evaluation program on the SST engine simulator is arranged in several phases.

- Augmentor and variable nozzle thermodynamic and mechanical check-out before engine application
- Augmentor and exhaust nozzle cooling evaluations
- Augmentor performance demonstration
  - Combustion efficiency
  - Temperature modulation range
  - Pressure losses
  - Influence of inlet variables
- Augmentor and variable primary nozzle endurance
- Thrust reverser static and dynamic evaluation

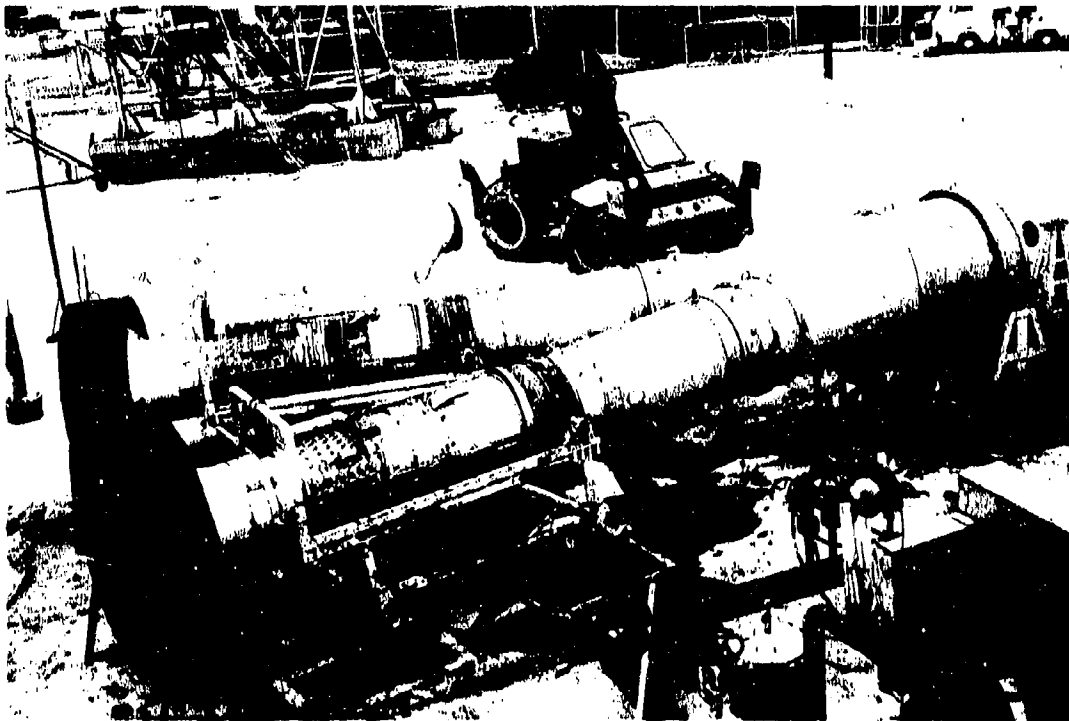
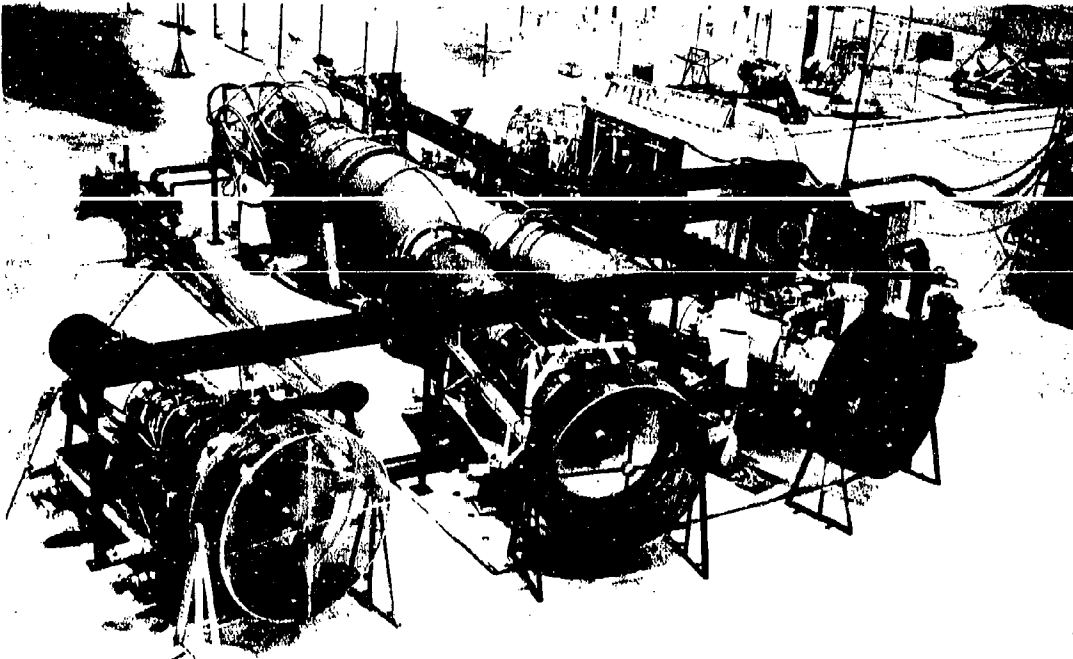


Figure 5-44. EXHAUST SYSTEM SIMULATOR TEST VEHICLE

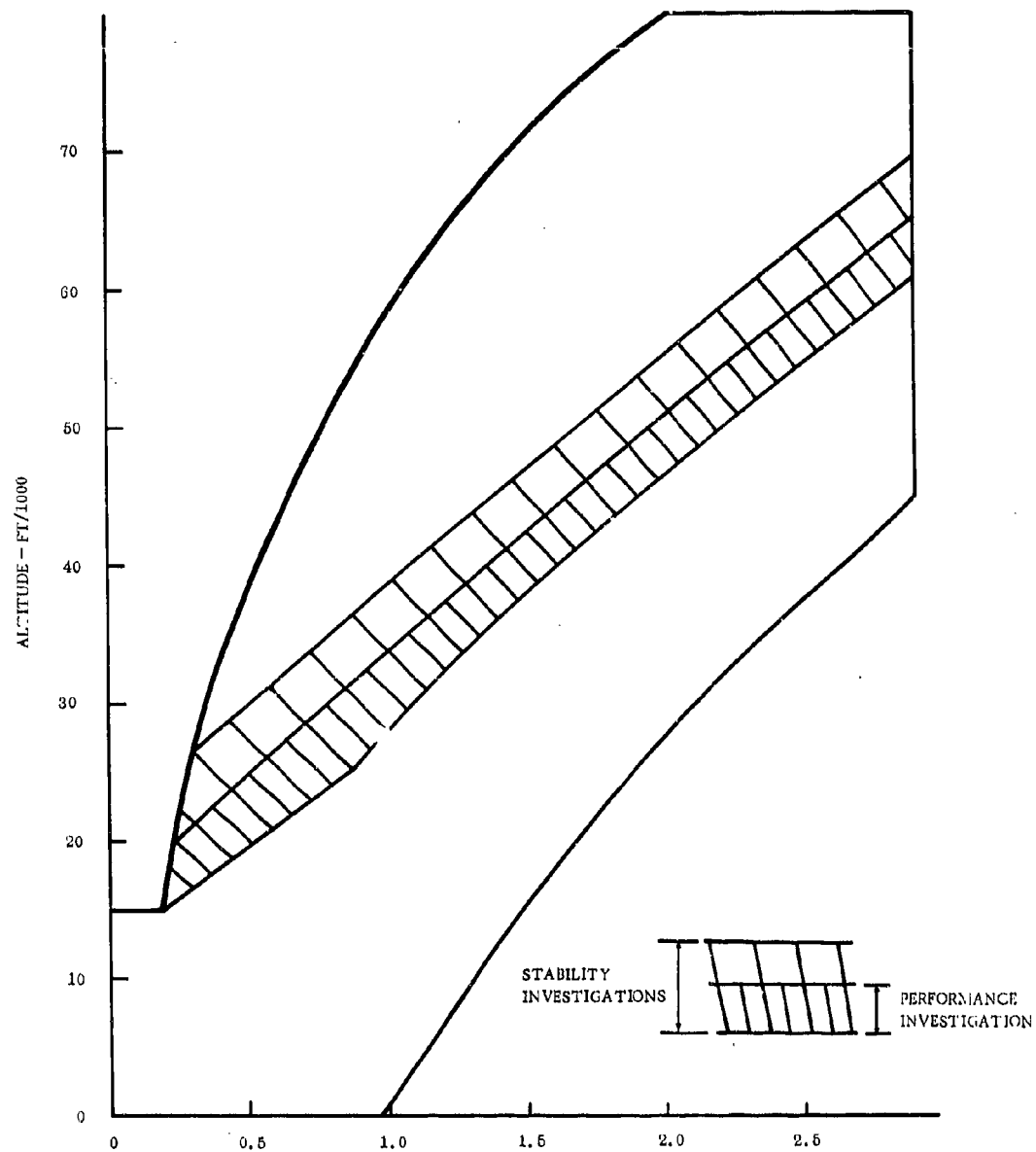


Figure 5-45. SIMULATOR ENVELOPE

At this point, the program has completed the first two phases. In total, 330 hours of test time are planned, including 100 hours of augmentor operation by the end of Phase II-C. The test program has accumulated this testing to date:

85 hours of simulator testing.

32 1/2 hours at rated turbine exit temperature.

17 1/2 hours of augmentor operation.

Figure 5-46 and 5-47 show the simulator vehicle with the Phase II-C augmentor and star-shaped variable area nozzle installed. The third J79-2 engine shown serves as a cooling-air-supply vehicle. Compressor bleed air in the correct proportions for primary nozzle, igniter, and turbine frame cooling is obtained from this additional engine to permit independent cooling airflow control, and to avoid the performance deterioration that bleed would impose on the simulator vehicles.

#### 5.1.7.1.4 Augmentor Test Results

A full-scale augmentor in the simulator at Peebles Proving Ground (shown in Figure 5-46 and described in paragraph 5.1.6.1.3) accumulated 85 hours of operation. 17 1/2 hours were with the augmentor operating including 2 1/2 hours of cruise. The following temperatures were measured during maximum augmentation operation.

Table 5-9. Comparison of Predicted and Measured Component Temperatures

	Measured	Predicted
Liner	<u>1545° F</u>	<u>1555° F</u>
Casing	<u>1320</u>	<u>1300</u>
Flameholder	<u>2100</u>	<u>2150</u>
Inner Cone	<u>1598</u>	<u>1600</u>

#### 5.1.7.2 Flameholder Ring Tests

Figure 5-48 shows a flameholder ring installed in the test facility. A schematic load diagram is shown in Figure 5-49. The objective of this test was to confirm the accuracy of the flameholder gutter stress analysis. A secondary objective was to determine whether an open-section flameholder gutter would rotate about its shear center or centroid when loaded in bending. Figure 5-50 compares the measured stresses with the predicted levels, and shows good agreement. Analysis of the deflections confirmed the design of the flameholder and substantiated that the section rotated about its shear center.



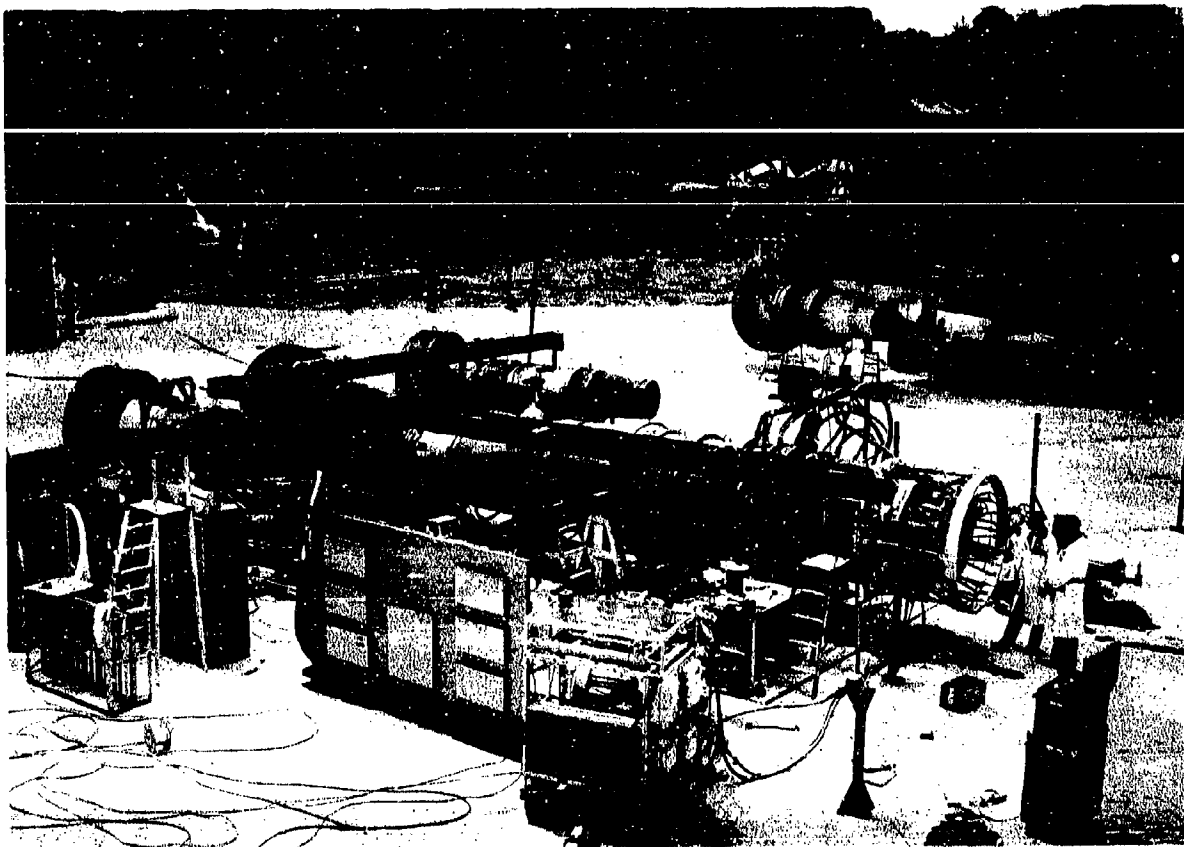


Figure 5-46. EXHAUST SYSTEM SIMULATOR TEST VEHICLE

#### 5.1.7.3 Spherical Bearing Tests

Figure 5-51 shows an exploded view of the spherical bearing test facility used to evaluate leakage and wear on split and standard unibal designs. Such spherical bearings are used in the igniter mounting. The test was performed by establishing a pressure difference, as shown in Figure 5-52, across the bearing and rotating the bearing in relation to the stationary race. This test indicated that leakage was low and constant up to 105 hours and 20.5 million cycles. It was observed that the pressure differential kept the unbals seated throughout the test; this minimized the leakage and kept it constant. Visual inspection revealed no appreciable (or measurable) wear on the test specimens. Leakage results are shown in Figure 5-53.

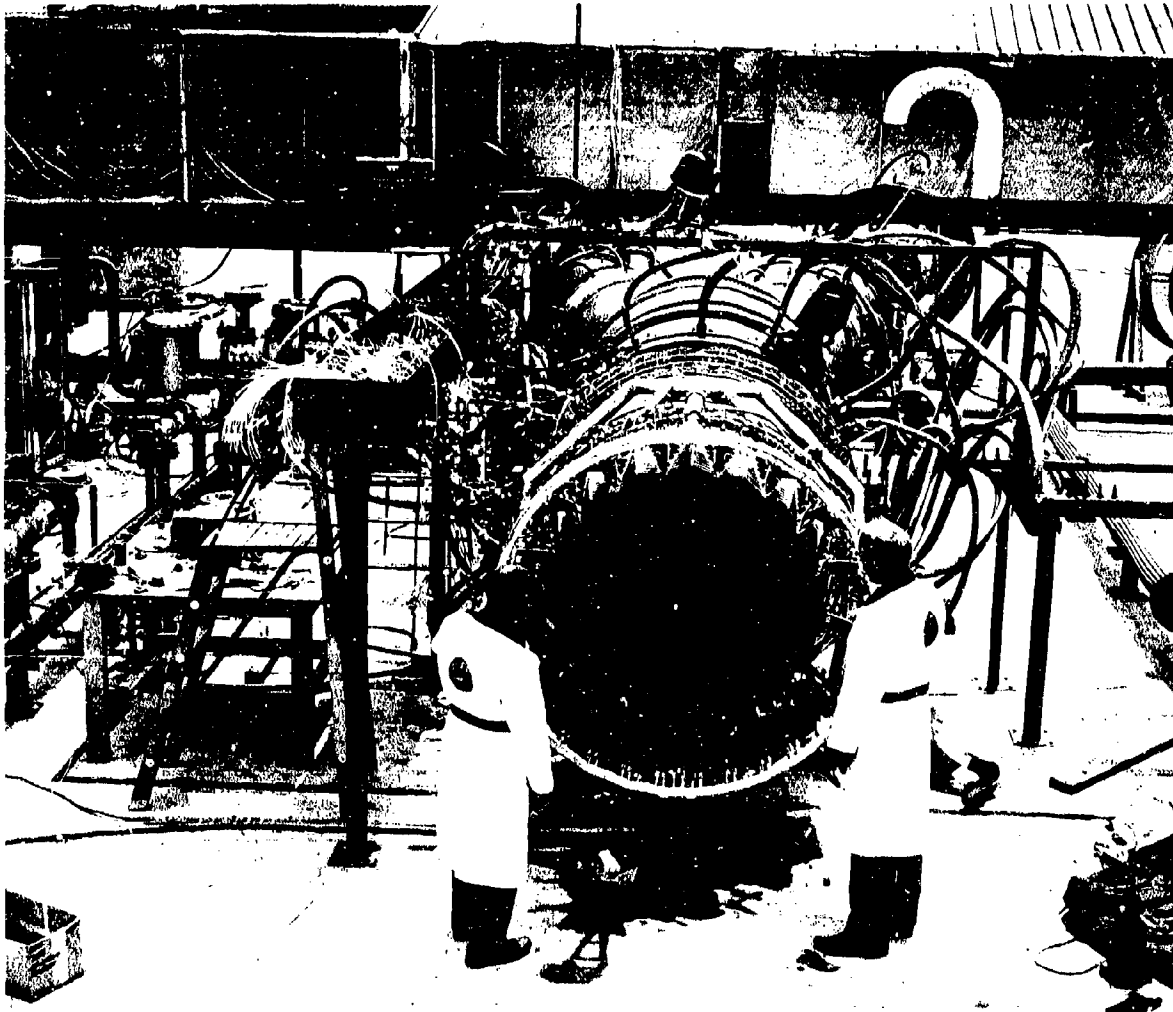


Figure 5-47. EXHAUST SYSTEM SIMULATOR TEST VEHICLE

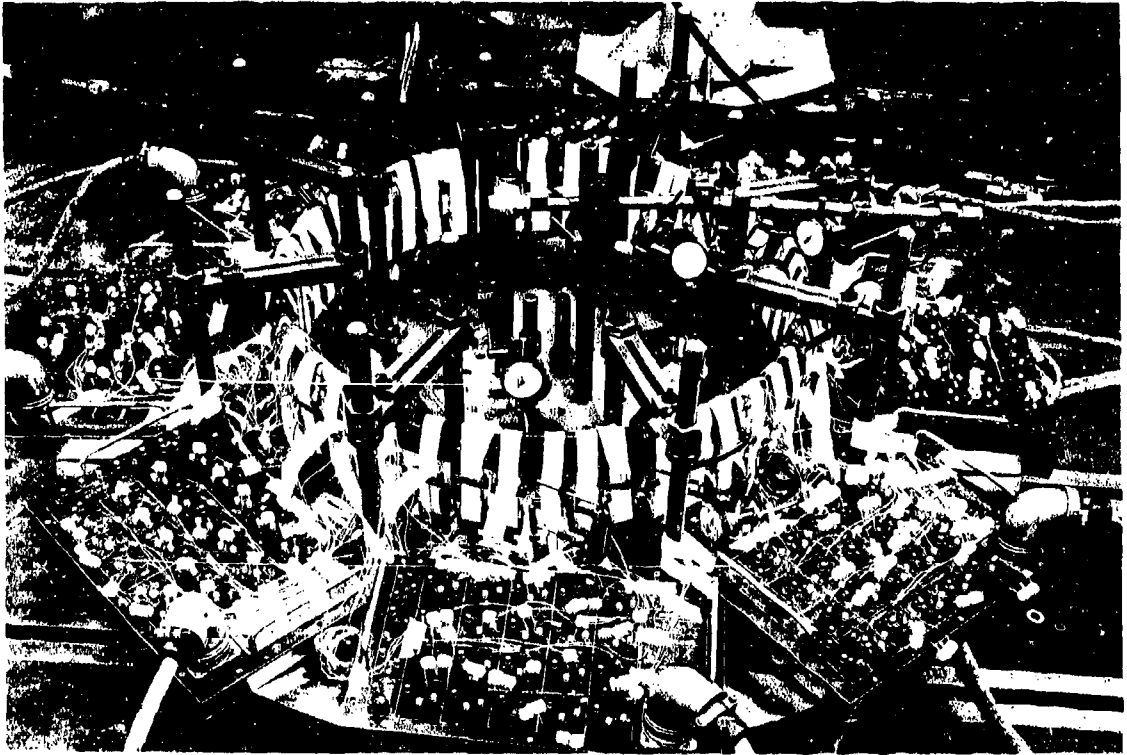


Figure 5-48. FLAMEHOLDER RING LOAD TEST

### 5.1.8 SUPPORTING TECHNOLOGY

The GE4 augmentor is based on J79 and J93 designs for major aerothermodynamic and mechanical features. J93 experience provides a platform of excellent experience from which this augmentor design has evolved. The J93 operates at an augmentor inlet temperature of 1560°F, with an exhaust gas temperature of 3200°F at maximum augmentation 360°F higher than the proposed GE4. More than 5,098 hours of factory engine testing, including 370 hours of simulated Mach-3.0 operation, have been accumulated in full-scale tests on the J93 augmentor. The J93 in the XB-70 aircraft has accumulated 549 hours of augmentor operation. The J93 augmentor's mechanical condition after engine operation has been highly satisfactory. The liner's cooling design has effectively eliminated hot spots, oxidation, and metal-burning.

The GE4 will benefit from experience to be gained on the advanced GE9 and GE10 augmentors. These advanced augmentors use a cylindrical liner and fuel injector mounting arrangement like the GE4. These full-scale augmentors will be evaluated at the Arnold Engineering and Development Center in Tullahoma, Tennessee. This testing will use the AEDC facility air supply to evaluate the augmentor in a manner similar to that employed in the GE4 full-scale simulator. After preliminary testing at AEDC, the augmentors will be operated on their respective engines in late 1966 and early 1967. This experience will be applicable to the GE4.

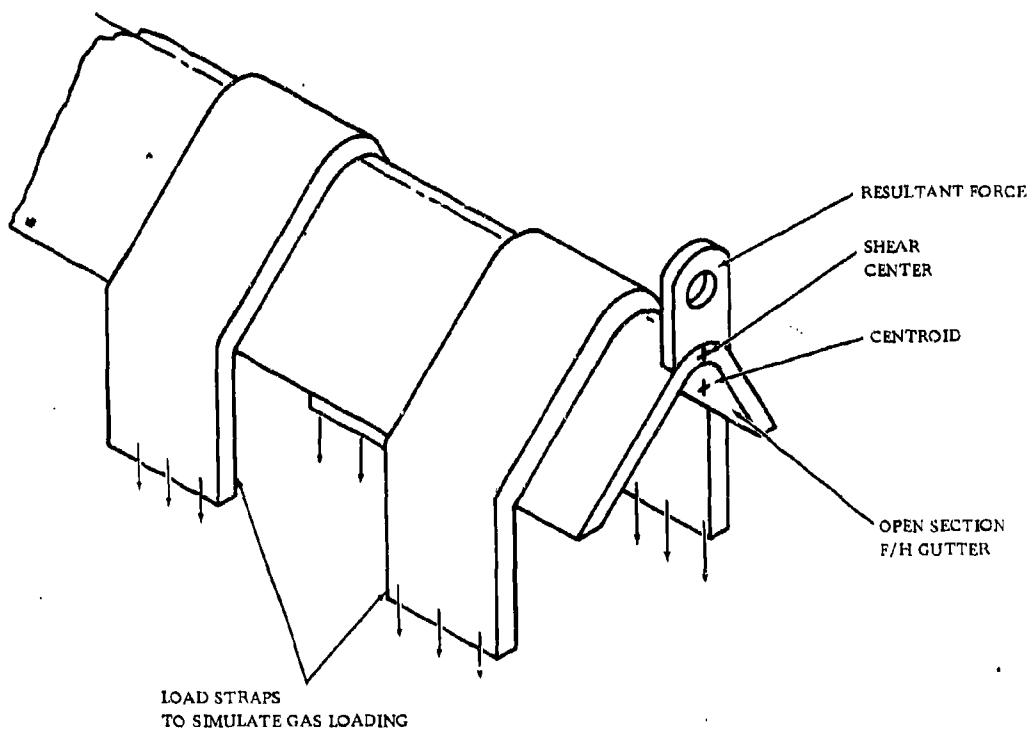


Figure 5-49. FLAMEHOLDER RING LOADING DIAGRAM

K

SPECIMAN	LOAD	MEASURED STRESS			PREDICTED STRESS		
		S ①	S ②	S ③	S ①	S ②	S ③
NO. 1	6# /IN	-765	-765	612	-875	-1000	590
NO. 2	6# /IN	-418	-418	360	-490	-750	424

(STRESSES ARE THE AXIAL MEMBRANE STRESSES AT THE POSITIONS SHOWN IN SKETCH BELOW)



Figure 5-50. FLAMEHOLDER STRESSES

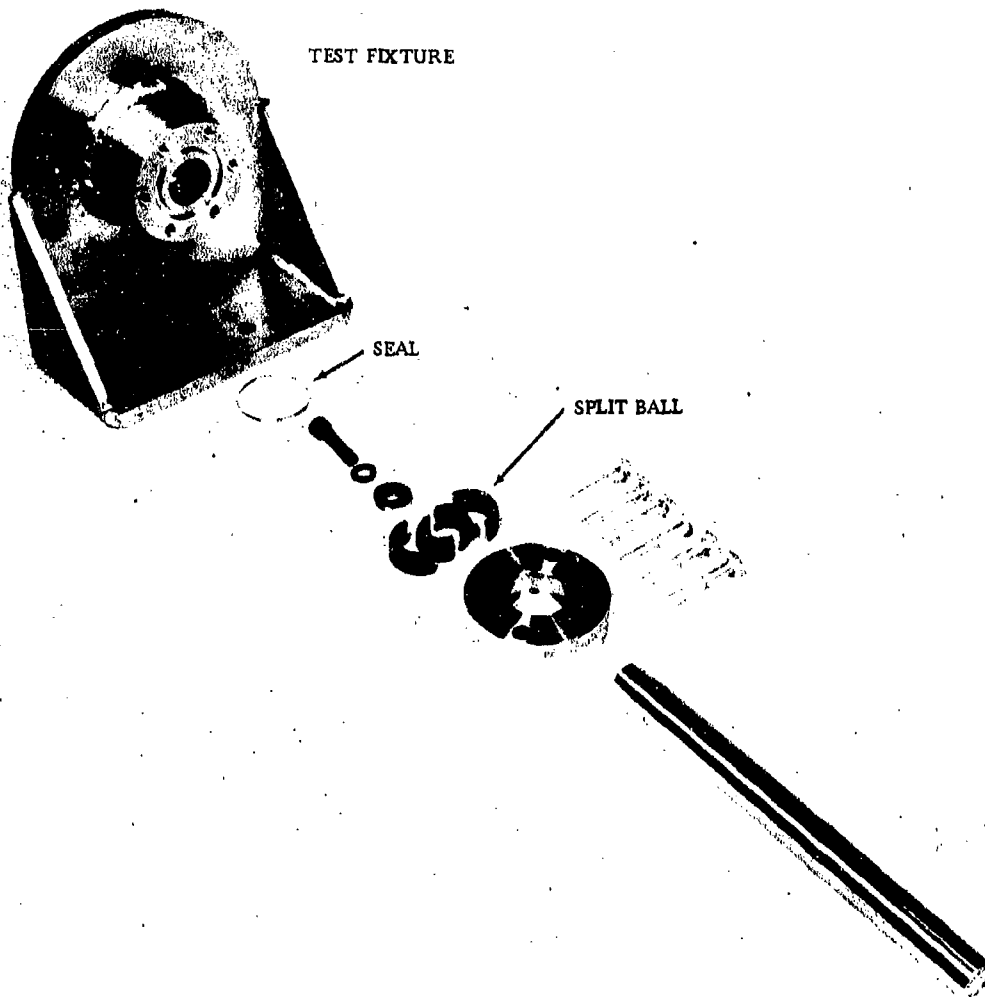
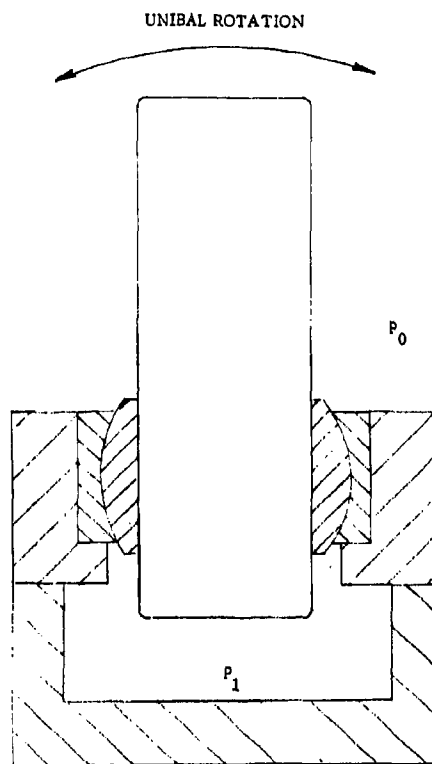


Figure 5-51. BALL JOINT TEST SET-UP (EXPLODED VIEW)



PRESSURE DIFFERENCE =  $P_1 - P_0$

SCHEMATIC - UNIBAL TEST

Figure 5-52. BALL JOINT TEST SET-UP (EXPLODED VIEW) - SCHEMATIC

3/5-74

### 5.1.8 AUGMENTOR SUPPLEMENT

#### 5.1.8.1 Introduction and Summary

The augmentor design discussed in this section is for a straight engine exhaust system. Installation in the aircraft requires a canted exhaust duct. The required installation configuration is accomplished with the retention of a symmetrical augmentor inlet diffuser, fuel injection system, and flameholder as shown in Figure 5-53(B). The six degree angularity change occurs between the flameholders and the first (forward) liner coolant discharge slot. This approach has the following advantages:

- Standard diffuser/flameholder design practices which apply are:
  - No increase in diffuser length
  - Flow direction change easily accommodated in sudden expansion from flameholders.
- Average exhaust duct velocities, Mach numbers retained; No increase in combustion length.
- Cant occurs before introduction of the cooling film
  - Minimum convective heat load zone
  - Liner symmetrical over cooled portion.

Since all critical components are identical to the straight exhaust duct design, the canted augmentor will have the same performance characteristics; i. e., modulation range, combustion efficiency, pressure loss (dry and with heat addition), operating and relight limits, and thrust transition.

The exhaust duct transposition is obtained by the addition of an appropriately located machined ring butt-welded to the duct skins. The change in neutral axis is slight and easily accommodated by this ring. The exhaust duct durability is not affected by the bending due to the cant.

As shown in Figure 5-53(B), the symmetrical liner mounting is retained and the angularity is developed in the liner fabrication.

In summary, the proposed design for accomplishing the installation cant has no effect on augmentor performance, safety, or durability.



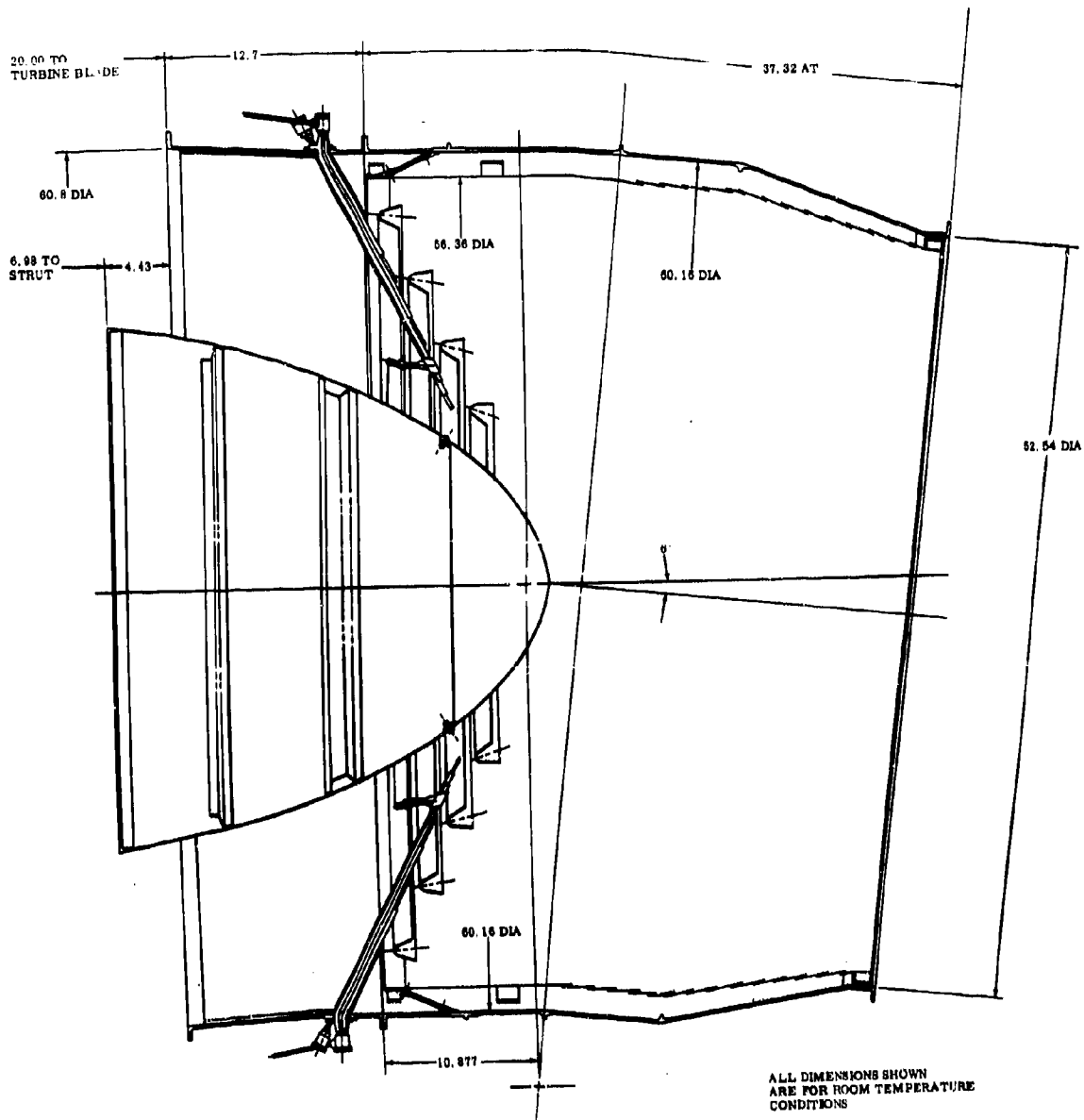


Figure 5-53 (B). UNIBAL LEAKAGE

### 5.1.8 AUGMENTOR SUPPLEMENT

#### 5.1.8.2 Introduction and Summary

The augmentor design discussed in this section is for a straight engine exhaust system. Installation in the aircraft requires a canted exhaust duct. The required installation configuration is accomplished with the retention of a symmetrical augmentor inlet diffuser, fuel injection system, flameholder as shown in Figure 5-53(L). The 4-degree angularity change occurs between the flameholders and the first (forward) liner coolant discharge slot. This approach has the following advantages:

Standard diffuser/flameholder design practices which apply are:

- No increase in diffuser length
- Flow direction change easily accommodated in sudden expansion from flameholders.
- Average exhaust duct velocities, Mach numbers retained; No increase in combustion length.
- Cant occurs before introduction of the cooling film:
  - Minimum convective heat load zone
  - Liner symmetrical over cooled portion.

Since all critical components are identical to the straight exhaust duct design, the canted augmentor will have the same performance characteristics; i.e., modulation range, combustion efficiency, pressure loss (dry and with heat addition), operating and relight limits, and thrust transition.

The exhaust duct transposition is obtained by the addition of an appropriately located machined ring butt-welded to the duct skins. The change in neutral axis is slight and easily accommodated by this ring. The exhaust duct durability is not affected by the bending due to the cant.

As shown in Figure 5-53(L), the symmetrical liner mounting is retained and the angularity is developed in the liner fabrication.

In summary, the proposed design for accomplishing the installation cant has no effect on augmentor performance, safety, or durability.

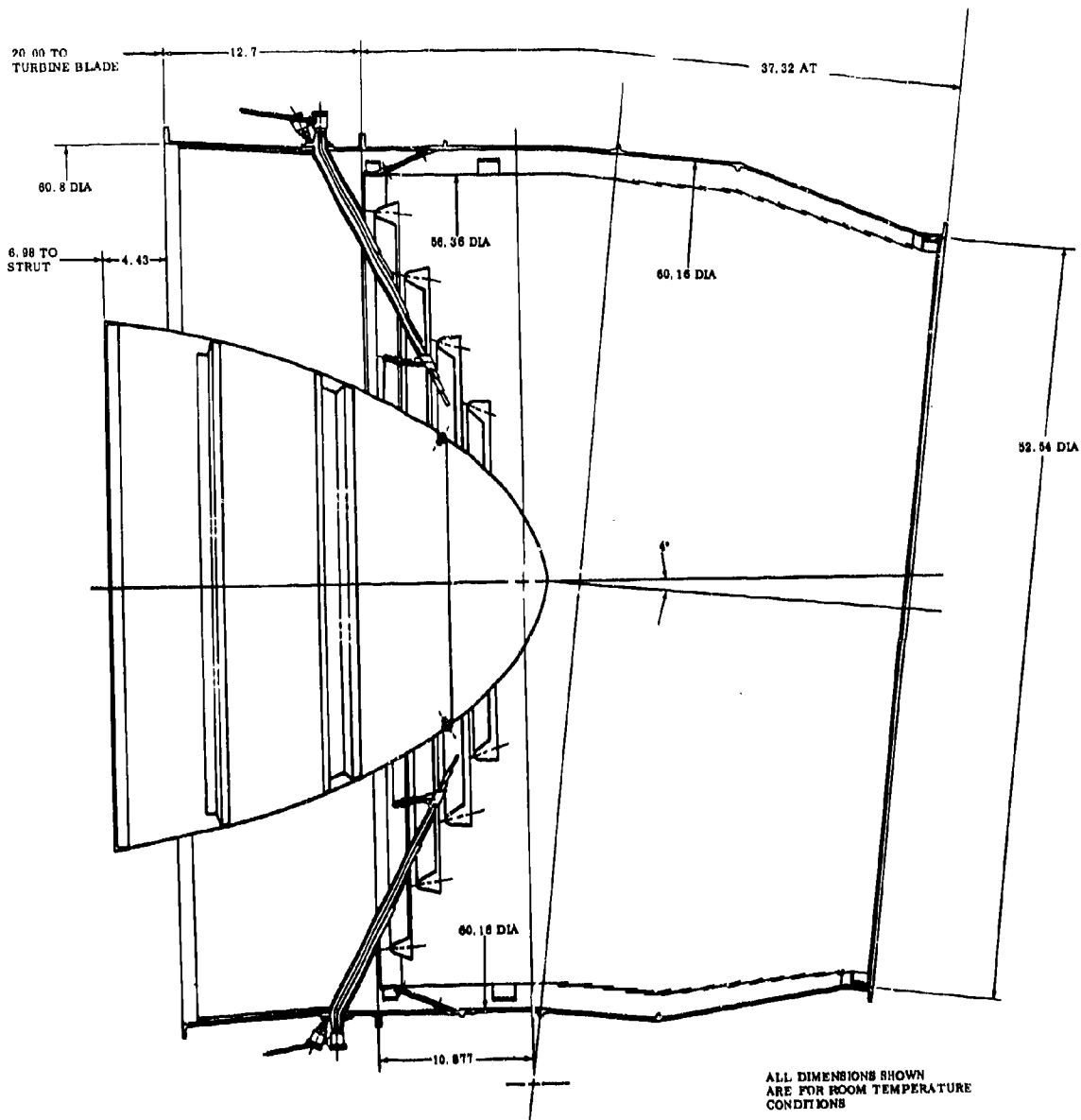


Figure 5-53 (L). UNIBAL LEAKAGE

## 5.2 FUEL INJECTION SYSTEM

The fuel injection system is discussed in detail in Volume III-B, Part II, Section 4.4.3.

5-79/5-80

K

## 6. EXHAUST NOZZLE AND THRUST REVERSER

### 6.1 INTRODUCTION AND SUMMARY

Since 1953 and the advent of supersonic flight, the General Electric Company has designed, produced, and serviced supersonic exhaust nozzle systems as integral components of the J79, J85 and J93 turbojet engines. This experience with progressively superior supersonic nozzles is shown schematically in Figure 6-1, and installed on engines in Figure 6-2. Major mechanical design features incorporated to ensure the operating success of the nozzles shown in Figure 6-1 are:

- J78 Ejector Nozzle, 1953 - First exhaust nozzle with variable-area ejector shroud. Both primary nozzle area and shroud area controlled by single actuation.
- J79-5 Low Base Drag Nozzle, 1956 - First guided expansion nozzle, incorporating low boat-tail angle to minimize nozzle boattail drag.
- J93, 1959 - First fully variable, three-finger nozzle design with secondary nozzle area positioned by throat area and  $P_8/P_0$ .
- 1964 - Advanced J79 nozzle combining simplicity of single actuation system with performance advantage of guided expansion and low boattail angle.

The thrust reverser for the GE4 makes use of General Electric's experience with the CJ805-3 commercial turbojet and the CJ805-23 commercial turbofan designs. These General Electric thrust reverser designs are shown in Figure 6-3. The CJ805-23 has a clamshell type blocker, and the CJ805-3 combines a clamshell with cascades.

The diverse and extensive supersonic and thrust reverser experience has been effectively applied to the proposed GE4 commercial design with advancements in simplicity, durability, and reliability.

The mechanical design of the GE4 exhaust nozzle provides for four major functions:

- Primary Jet Nozzle - Control of the engine turbine inlet temperature.
- Secondary Jet Nozzle - Efficient expansion of the engine exhaust over broad pressure ratio range with minimum afterbody drag.
- Exhaust sound suppression.
- Efficient thrust reversal with capability for ground or in-flight use.

The major features of the GE4 design which make it possible to accomplish the required functions efficiently are:

- Hinged primary flaps and seals in a "star" design to obtain the wide range nozzle area variations for both thrust reversal blockage and throat variation for efficient forward thrust.
- No separate thrust reverser blocker.
- A three-hinge secondary flap to provide stable aerodynamic positioning for the exit throat area variation.

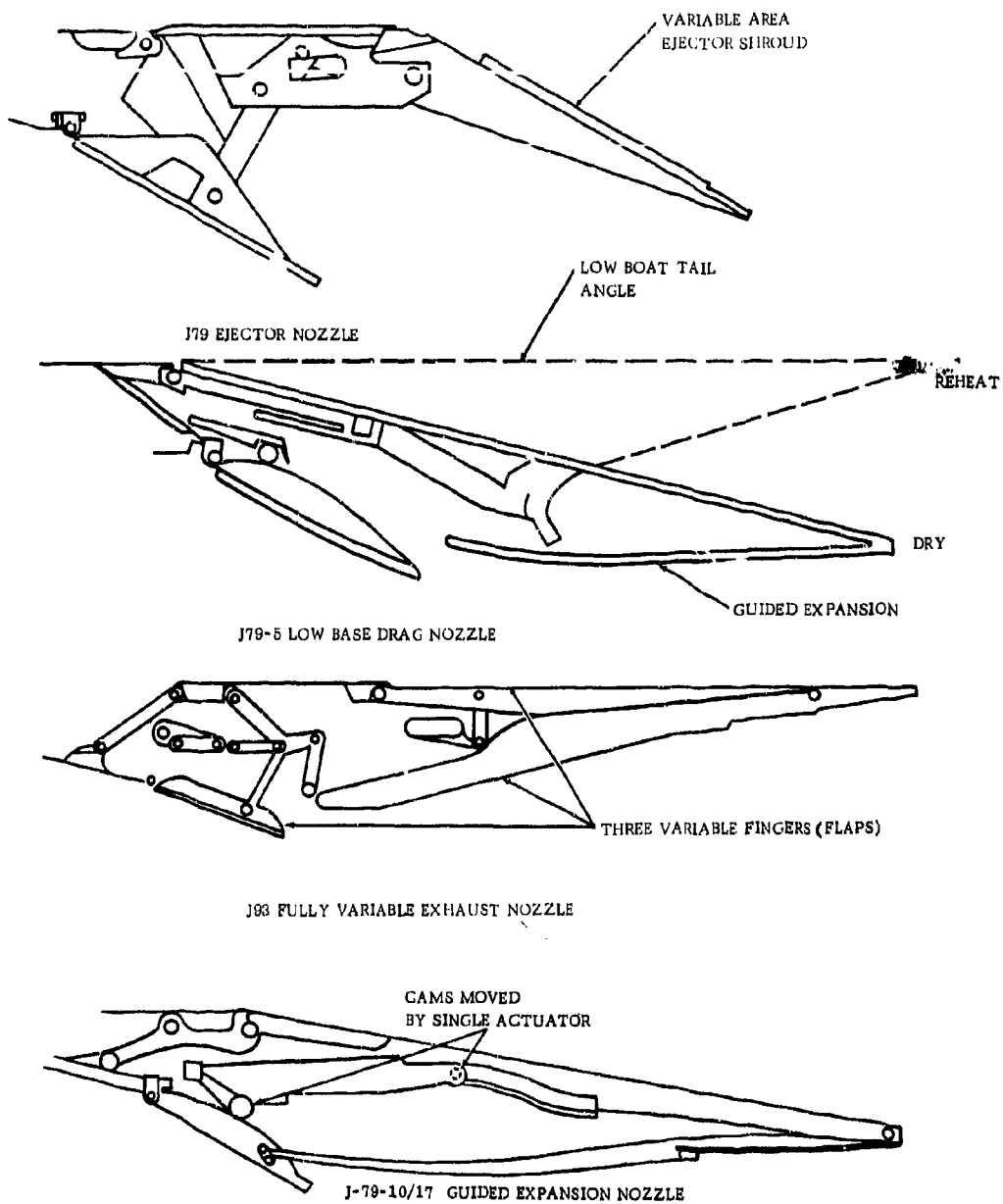
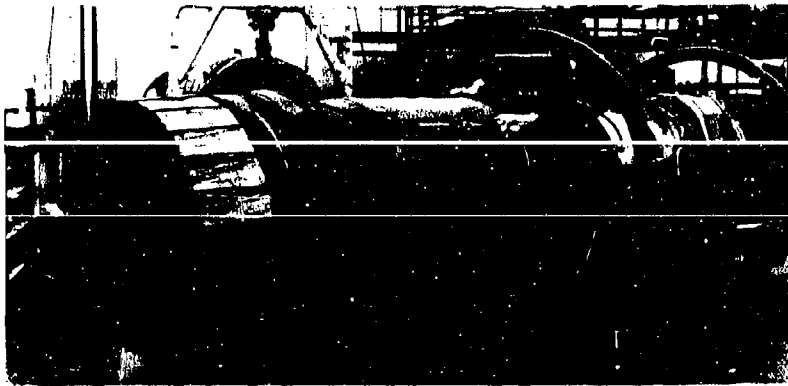
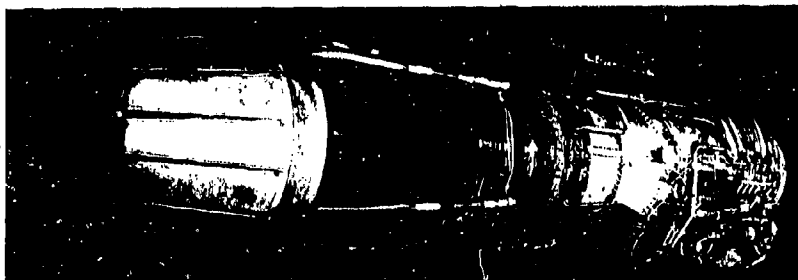


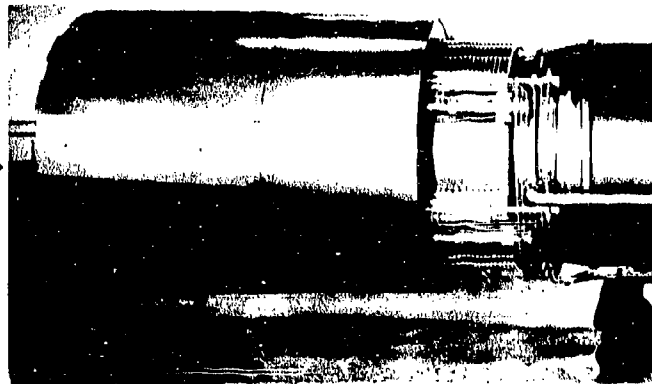
Figure 6-1. SUPERSONIC NOZZLE EVOLUTION



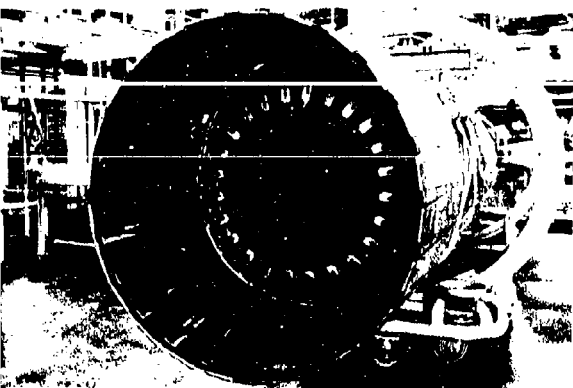
J79-3



J70-10/17



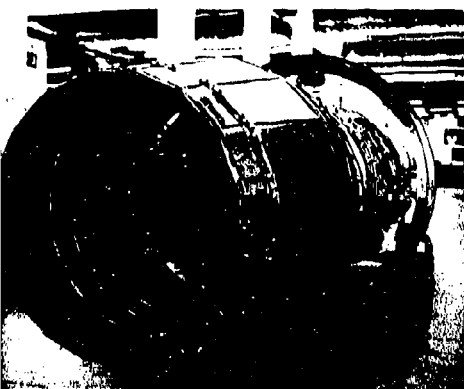
1



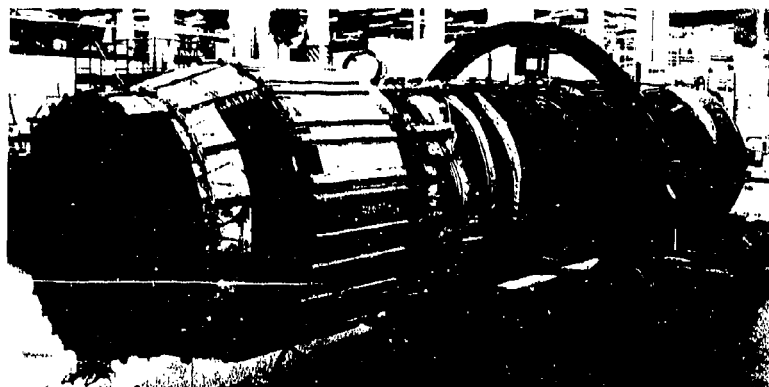
J70-5



J86



J83



J83/SS1



GE4

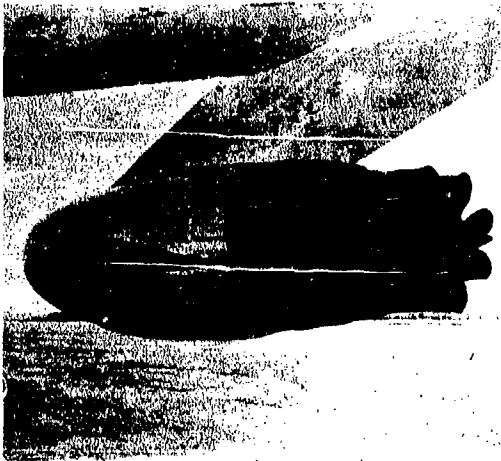
Figure 6-2. GE4 EXHAUST NOZZLE PROGENITORS EP16979

K

2

6-3/6-4





- TURBOJET REVERSER
- CASCADE TYPE
- CV 880
- 56% REV. THR.



- TURBOFAN REVERSER
- TARGET TYPE
- CV 990
- 38% REV. THR.

Figure 6-3. THRUST REVERSER EVOLUTION

The basic elements of the exhaust nozzle/thrust reverser are shown in the key operating modes for SST in Figure 6-4.

- Supersonic cruise
- Take-off and subsonic
- Reverse

In the supersonic cruise mode:

- The secondary nozzle is aerodynamically positioned in the full open position.
- The full range of primary nozzle areas are available for required power settings through operation of the primary nozzle actuating system.
- The auxiliary inlets are closed, and cooling air for the engine and nozzle is provided from the inlet.
- The thrust reverser cascades are stowed forward.

In the take-off mode:

- The secondary flap is positioned full closed for the reduced pressure ratio at take-off.
- The primary flap is in the open position for augmentation, or partially closed for dry operation depending on the airframe take-off power requirements.
- The auxiliary air inlet doors are open to admit high supplementary flow which provides effective noise suppression.
- Thrust reverser cascades are stowed forward.

This geometry also applies to the loiter and subsonic conditions.

When the nozzle is in the reverse mode:

- The primary nozzle translates aft, rotating into the blocker position.
- The auxiliary inlet doors translate aft to provide an opening for the reverse exhaust gases.
- The reverser cascades translate aft into the radial exits provided by the primary nozzle translation and turn the exhaust gases to the required angle for reverse thrust.

All three functions are accomplished by the motion of the reverser actuation system.

The proposed primary nozzle/reverser design incorporates these specific advantages for SST application, which are emphasized in Figure 6-5.

- ① Actuator mounting on reverser frame
  - high exhaust duct mechanical reliability
  - favorable actuator environment
  - ease of accessibility

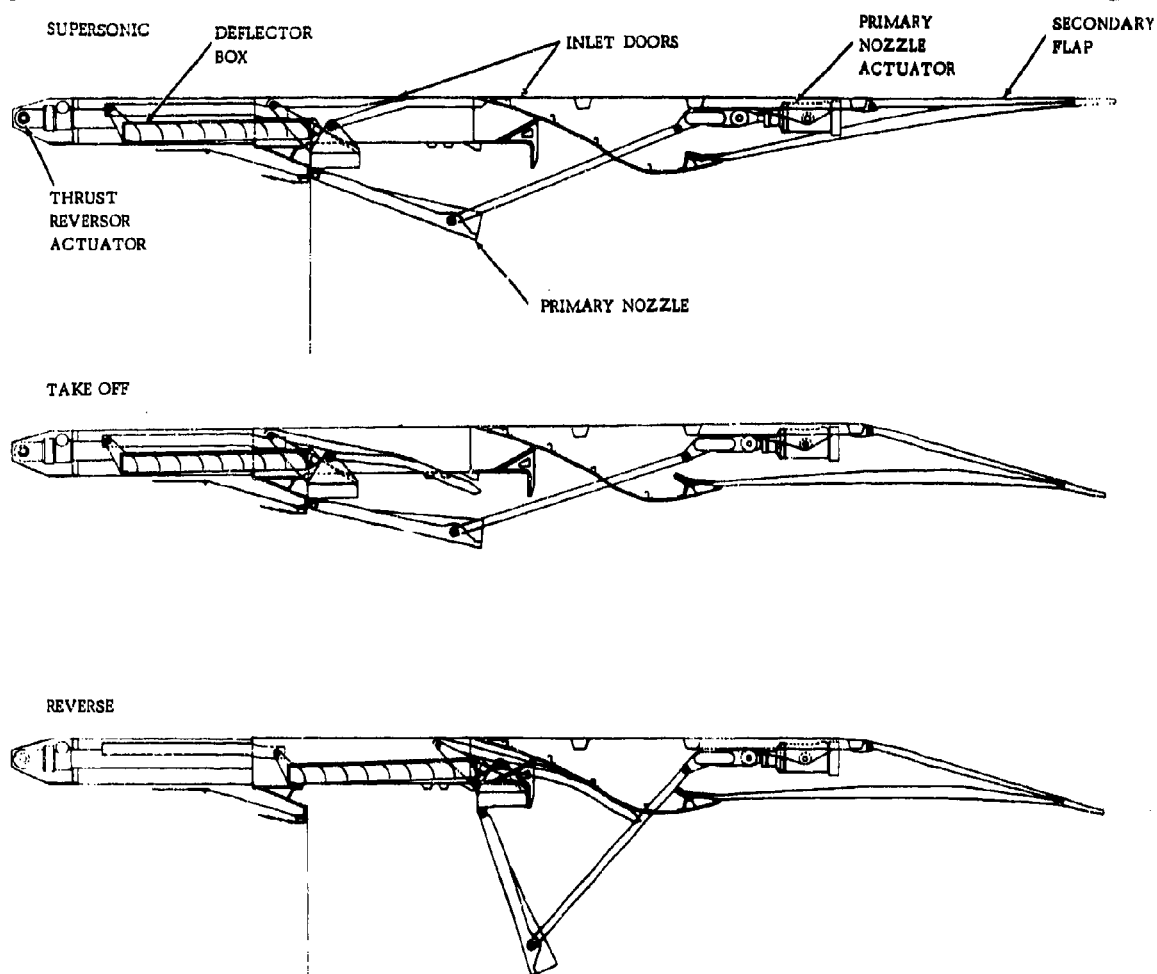


Figure 6-4. EXHAUST NOZZLE OPERATING MODES

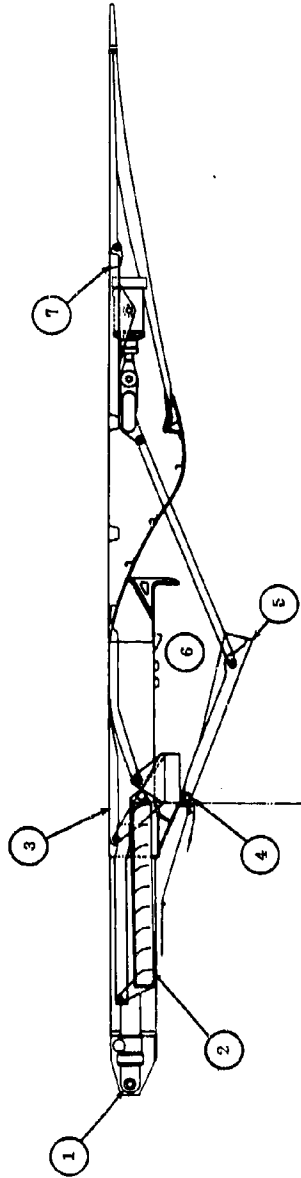


Figure 6-5. GE4 EXHAUST NOZZLE THRUST REVERSER AND SOUND SUPPRESSION CONFIGURATIONS

- ② Cascade-type thrust reverser with
  - high turning effectiveness
  - jet wake directional control
  - symmetrical blocker arrangement - cascade exit flexibility
- ③ Integral cascade cover/auxiliary inlet doors
  - integrated with nozzle/reverser
  - no additional actuation required
- ④ Compressor bleed-air-cooled star primary nozzle with these features
  - durability - low metal temperature on augmentation
  - elimination of sliding wear of conventional primary nozzle designs
  - star shape for noise suppression (in conjunction with supplemental airflow)
- ⑤ Integrated reverser function, which utilizes the primary nozzle as the reverser blocker, with benefits in
  - system simplicity
  - reliability
  - safety
- ⑥ High supplemental airflow at take-off for exhaust noise suppression.
- ⑦ Aerodynamically positioned secondary nozzle actuated by secondary pressure with demonstrated
  - stability
  - performance

The commercial life of the parts design is assured by effective metal cooling (discussed in detail in Section 7 this volume) and use of proven currently employed materials.

- Use of currently employed materials
  - René 41
  - Inco 718
  - René 77 (Udimet 700)

The major design features have been evaluated in Phase II-C:

- The air-cooled star primary nozzle has operated in conjunction with the augmentor in full-scale tests on the engine simulator.
- Assembly of full-scale thrust reverser hardware for static and dynamic testing on the simulator test vehicle is in the final stages, and is shown in Figure 6-6. The variable-star primary nozzle which is an integral part of the reverser is also shown.
- A J93-size model (Figure 6-2) of the aerodynamically positioned secondary nozzle was successfully tested under simulated flight conditions at the AEDC altitude test facility in early 1966.

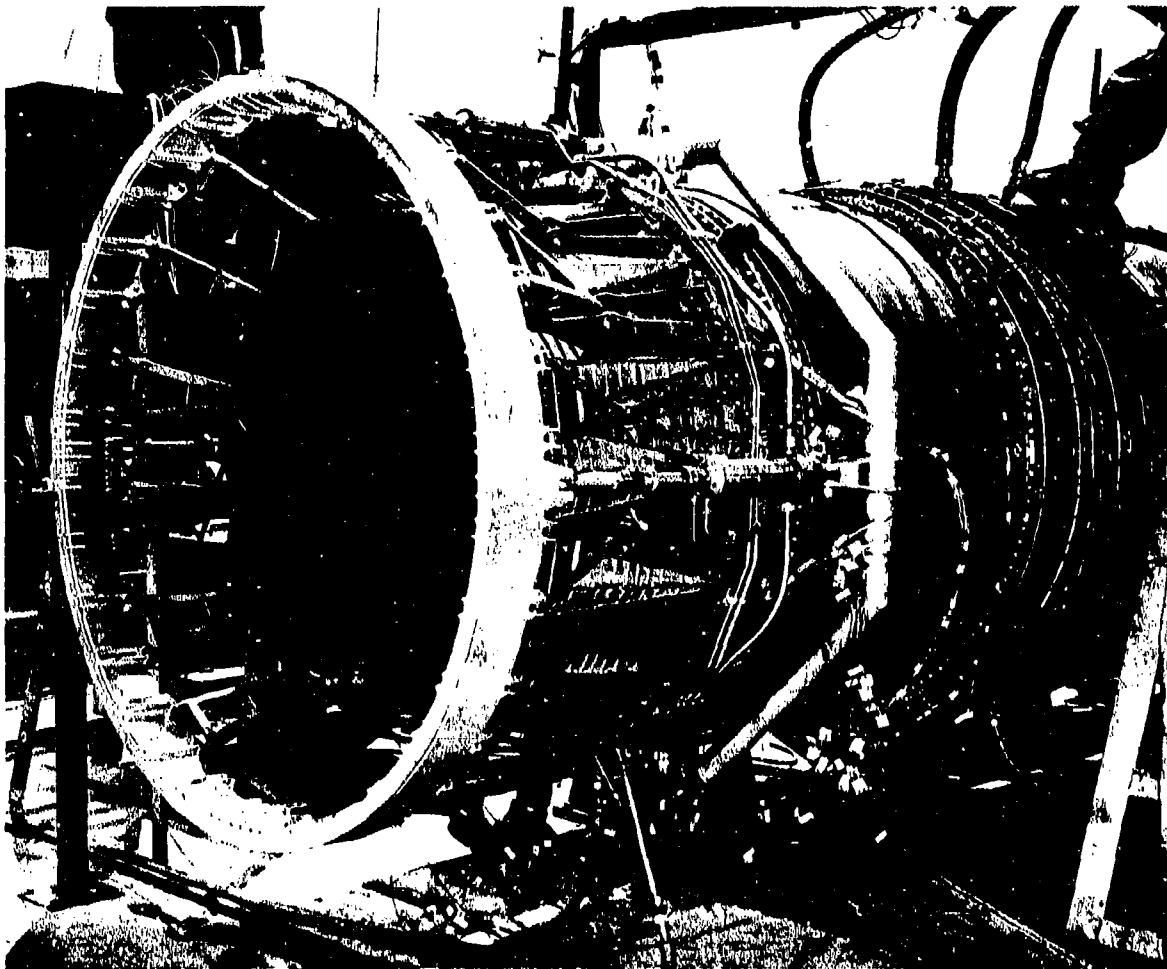


Figure 6-6. NOZZLE TEST AT PEEBLES

## 6.2 GENERAL DESCRIPTION

Figure 6-7 shows a cross-section of the GE4 variable - area supersonic nozzle with an integrated thrust reverser. Major components of the design are indicated on the drawing.

The star primary nozzle design is shown in Figure 6-8. The illustration includes a photo of a scale-model of the design to show the nozzle in two operating modes. In order to function as a reverser blocker, the throat area must vary from approximately 7 to 1850 square inches, or an area ratio of 280 to 1. This is substantially higher than the capability of conventional primary nozzles, which have area ratios limited to approximately 3.2 to 1. This increase is accomplished with extended-length flaps and axially-hinged seals. This arrangement has important reliability and life advantages over the typical sliding overlap flap and seal design currently in use on military nozzles. (See figure 6-9.)

- Positive retention of the seals to the flaps.
- Retention of the flap in event of link or actuation pin failure.
- Elimination of sliding seal wear by low-friction pivot joints.

The primary nozzle is actuated with two sets of hydraulic actuators; one set for nozzle throat modulation and one set for reverser actuation. This provides reliability and safety advantages:

- Each actuator system can operate within its mode, independently of the other system.
- Use of common hardware for the primary nozzle and reverser blocker eliminates the possibility of interrelated malfunction (i. e. primary throat area cannot be at wrong position in reverser mode).

Figure 6-10 is a photograph of the full-scale Phase II-C star primary nozzle which illustrates the complete accessibility to all parts provided by this design. This allows for:

- Complete and easy inspection of all parts in the installation.
- Simple disassembly and low replacement time.

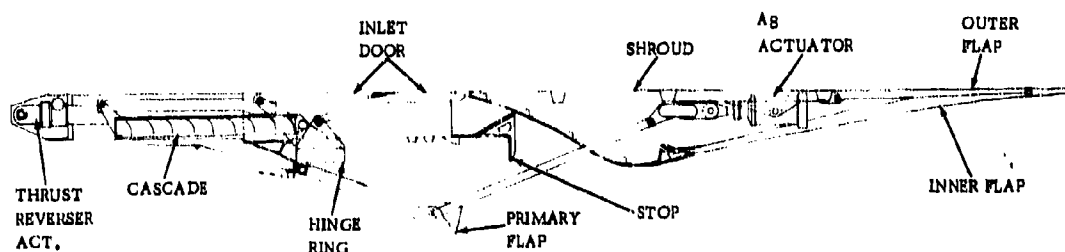


Figure 6-7. GE4 EXHAUST NOZZLE AND THRUST REVERSER

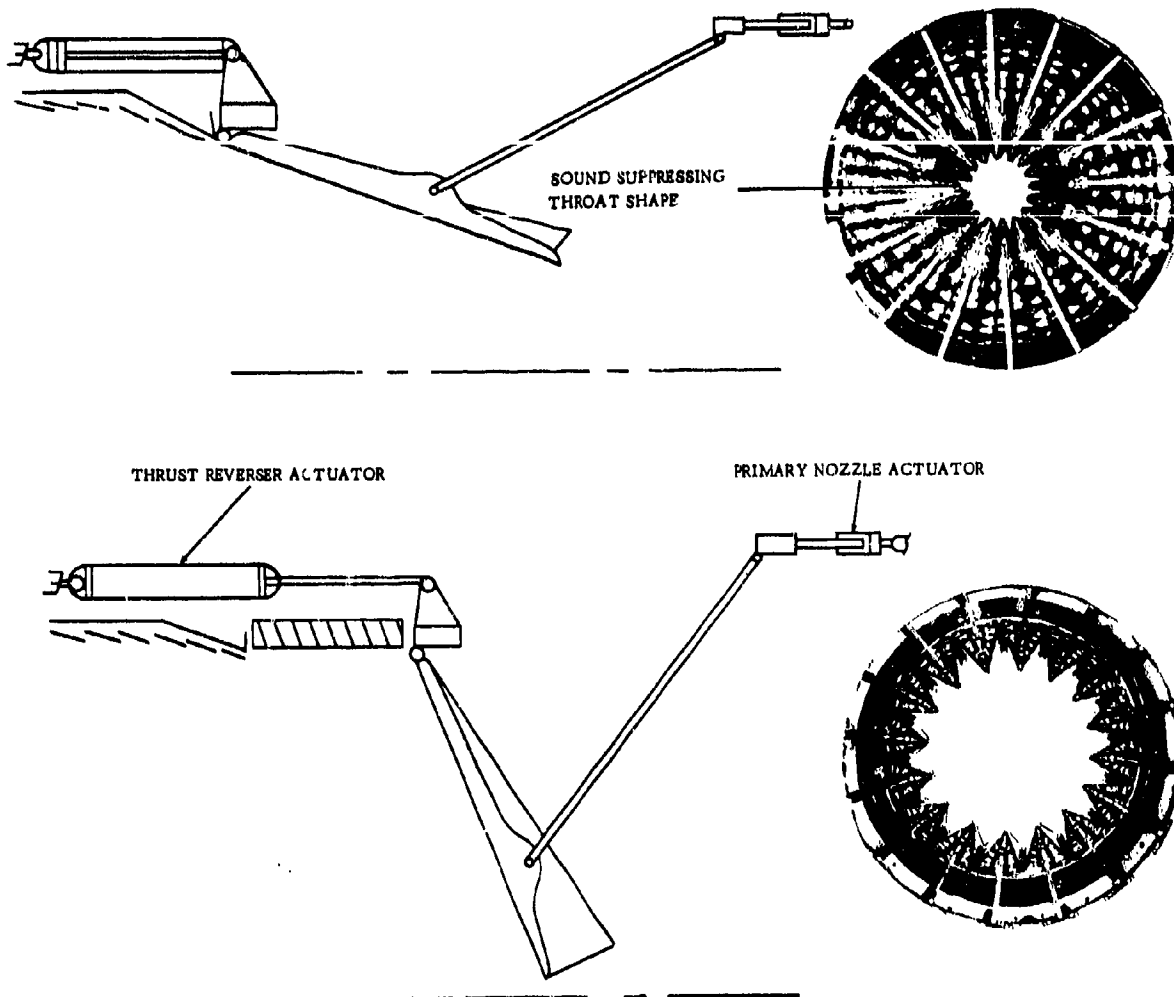


Figure 6-8. MULTIPLE FUNCTION STAR NOZZLE

The thrust reverser is an integrated element of the over-all exhaust system, which is used to achieve rapid aircraft deceleration. The reverser function consists of two separate phases:

- The engine forward thrust is canceled by blocking the normal discharge path for the engine exhaust. (This is equivalent to an engine shutdown without application of any aircraft braking device.)
- Discharge gases are turned so that flow is in a forward and radially-outward direction. The forward force component provides the reverse thrust.



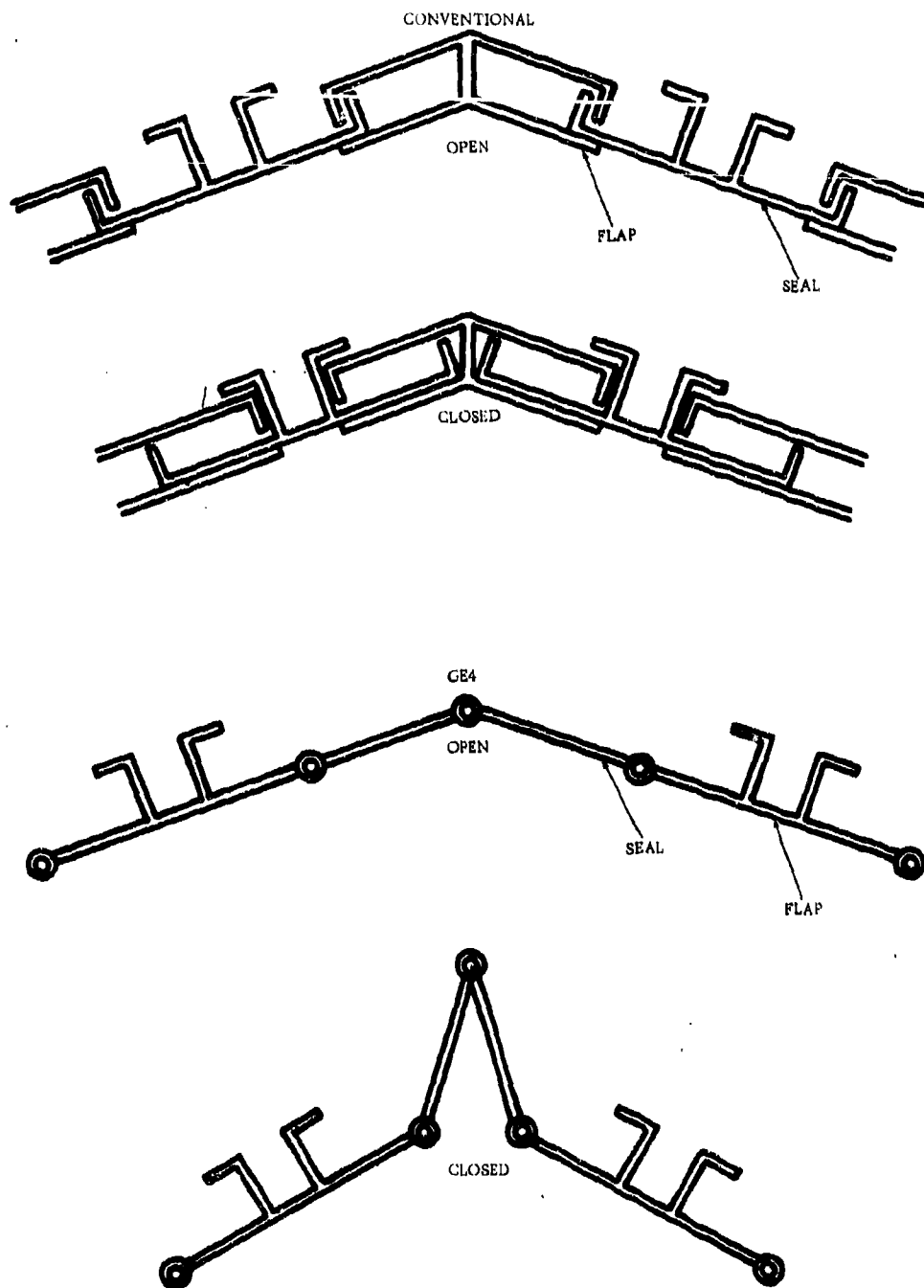


Figure 6-9. FLAP SEAL CONFIGURATIONS

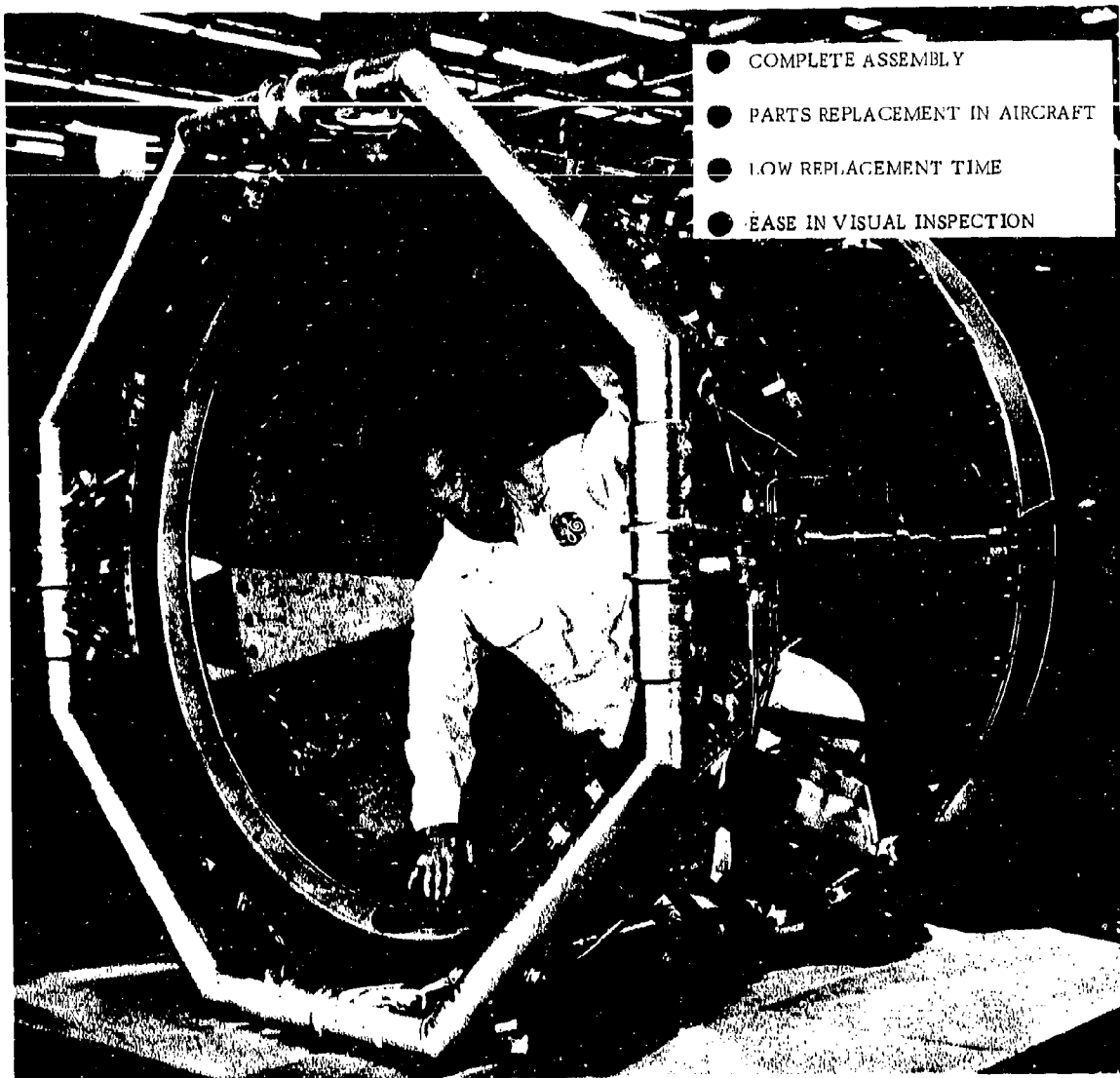


Figure 6-10. GE4 PRIMARY NOZZLE ASSEMBLY

The basic elements of the reverser illustrated in Figure 6-11 are:

- Primary nozzle - blocker
- Hinge ring
- Cascade boxes
- Frame and beam assembly

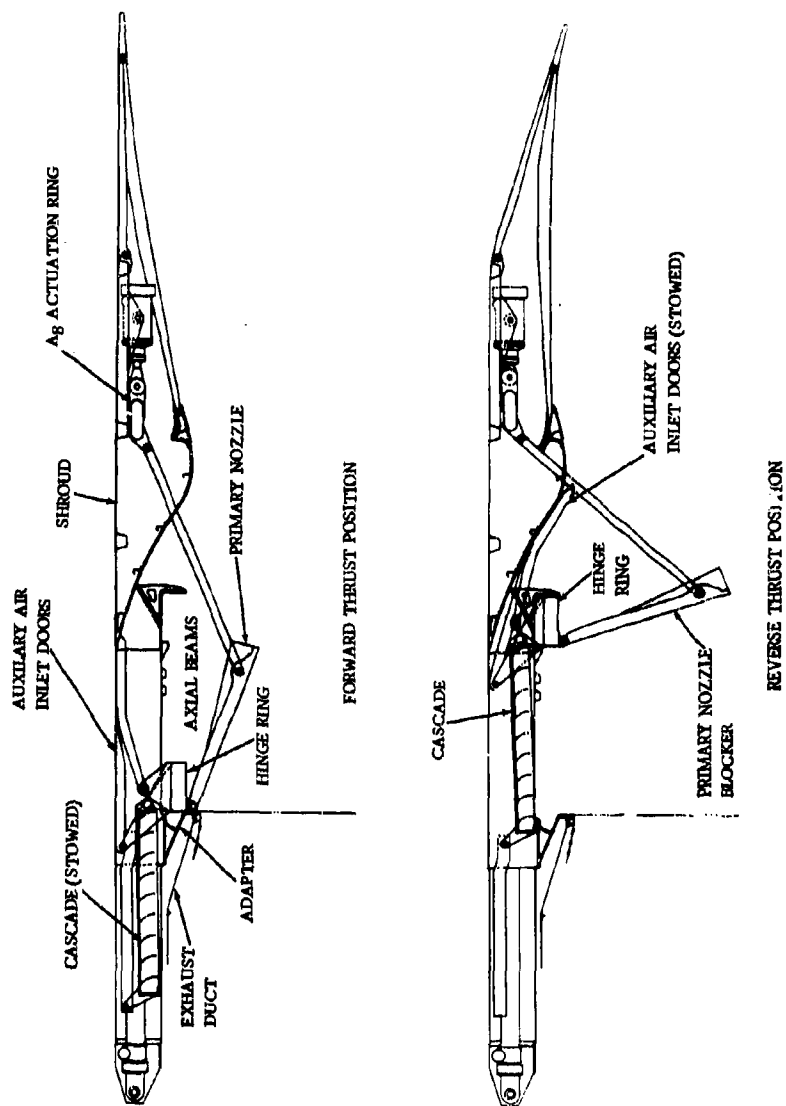


Figure 6-11. GE4 THRUST REVERSER

The cascade boxes and auxiliary air inlet doors for the second-stage ejector are also mounted to the hinge ring. In the forward thrust mode, the cascades are stowed forward over the exhaust casing. As the hinge ring translates aft, the cascades are moved from the stowed to the thrust reverse position, and auxiliary air inlet doors are moved from the functional to the stowed position. The axial translation of these three components is accomplished with the single reverser actuation stroke. Figure 6-12 shows the scale model of the Phase II-C thrust reverser in forward and reverse position and in transition

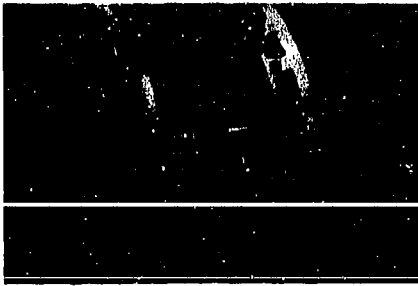
For the proposed design, there are 14 inlet doors spaced on the basis of 16 total (See Figure 6-13) (doors at the typical nacelle/wing juncture at the approximate ten o'clock and two o'clock positions are omitted). Eleven of the 14 door positions are used as reverser exits. Details illustrating this scheme are included in Section 6.5.3.

The shroud and beam assembly Figure 6-13 consists of the secondary nozzle shroud, 16 axial beams, and an adapter section which is attached to the tailpipe. This assembly is the prime supporting structure for the entire nozzle and reverser system. The 16 axial beams join the shroud and adapter into one rigid frame, which is attached to the exhaust duct by bolting adapter and duct together.

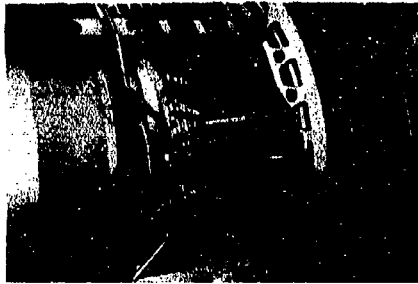
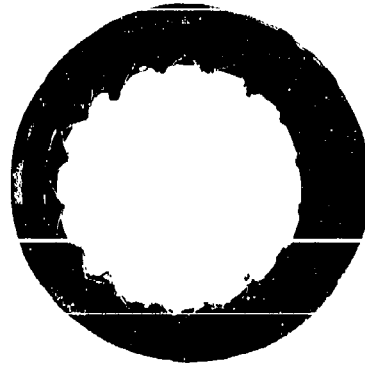
The secondary nozzle aerodynamic surfaces, both internal and external, are composed of 16 sets of flaps and seals as illustrated in Figure 6-7. The flap and seal assemblies are supported from the fixed shroud, and are designed to provide an exit area varying from 2280 square inches to 4300 square inches. The exit area is varied and controlled aerodynamically by the secondary pressure forces on the individual flaps and seals. The general secondary nozzle configuration is shown in Figure 6-7 which illustrates the external/internal flap, tripple-hinged arrangement. For aerodynamic positioning, the external flap is approximately 0.70 of the length of the inner divergent flap. This double-flap concept provides significant positioning advantage over the simple single-flap, single-pivot approach; the positioning forces are about two times higher than those corresponding to the single flap (which is positioned by a balance of external and exhaust-stream pressures only, without the influence of the secondary pressure). The principal of aerodynamic positioning and a description of the development testing accomplished to date are discussed in detail in Section 7.4.2.

The secondary nozzle is designed to minimize air leakage through the outer flap seals, and concurrently to provide the aerodynamic features of area variability, low boattail angle, minimum base area and self-positioning or balance. Seal leakage inward (into the exhaust stream) through the inner flap assembly is not a performance penalty. Ventilation of this surface is accomplished with secondary airflow for cooling and stability. All leakage paths are pressure sealed, utilizing the differential pressure between the nacelle pressure and ambient pressure. Figure 6-14 illustrates the sealing arrangement made to ensure that the seals "seat": retainer clips hold the seals close to the flap so that sufficient pressure differential exists at low flows to seat the seal. The retainers serve to center the seal between adjacent flaps. In the GE4 nozzle, the sealing also includes an additional gland, or labyrinth, to ensure sealing when the differential pressures are low. Figure 6-15 describes the leakage characteristic of the outer seal.

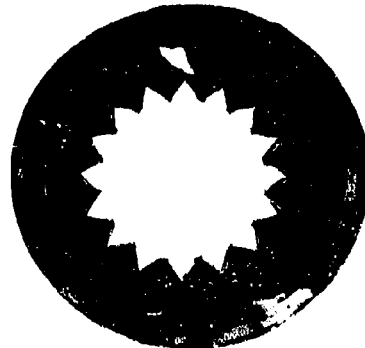
The leakage across the secondary outer flap and seals results in a loss in thrust which is most important at the supersonic cruise condition. This loss of secondary flow is a direct loss in net thrust, since no gross thrust is obtained for the flow and the penalty is equal to the ram drag of the flow lost. Many tests of flap and seal secondary nozzles have been made for leakage as a function of the pressure differential across the secondary. Typical data are presented in Figure 6-15 for a J93 engine nozzle, and these levels of leakage area were taken as attainable in the GE4 design. Note that seal leakage area is presented in the form of a gap height or the leakage area



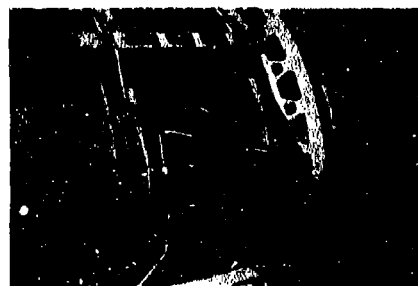
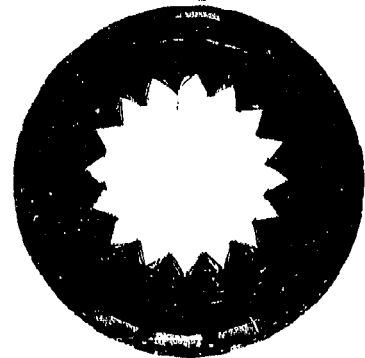
**Forward Thrust Max Area**



**Forward Thrust Min Area**



**Transition to Reverse**



**Reverse Thrust**

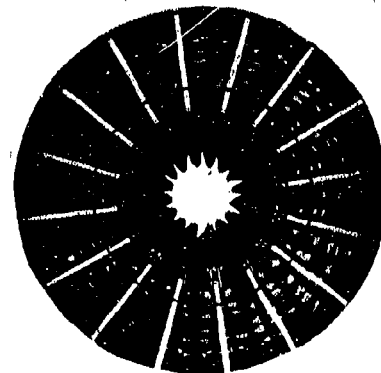


**Figure 6-12. GE4 THRUST REVERSER MODEL**

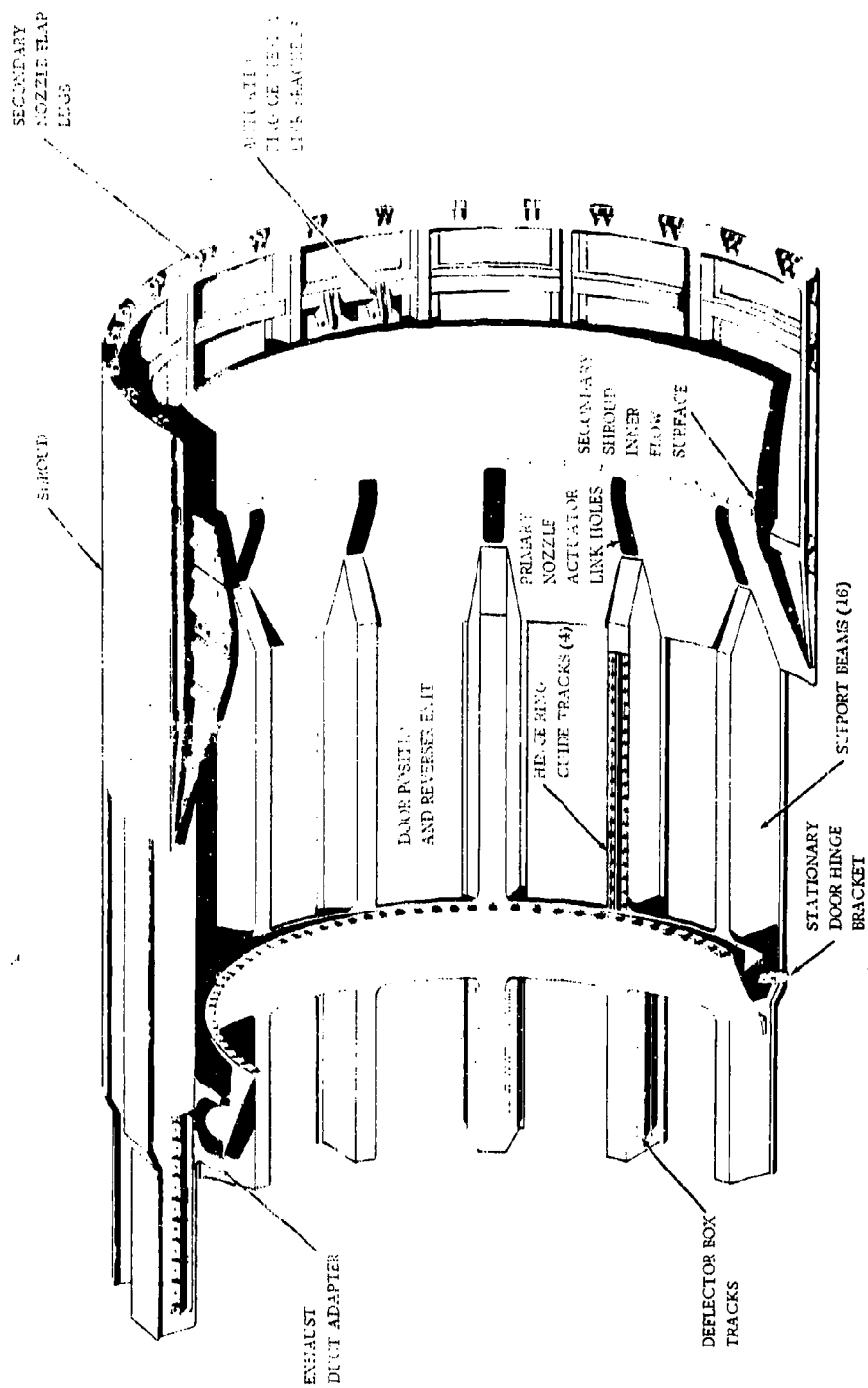


Figure 6-13. SHROUD AND BEAM ASSEMBLY

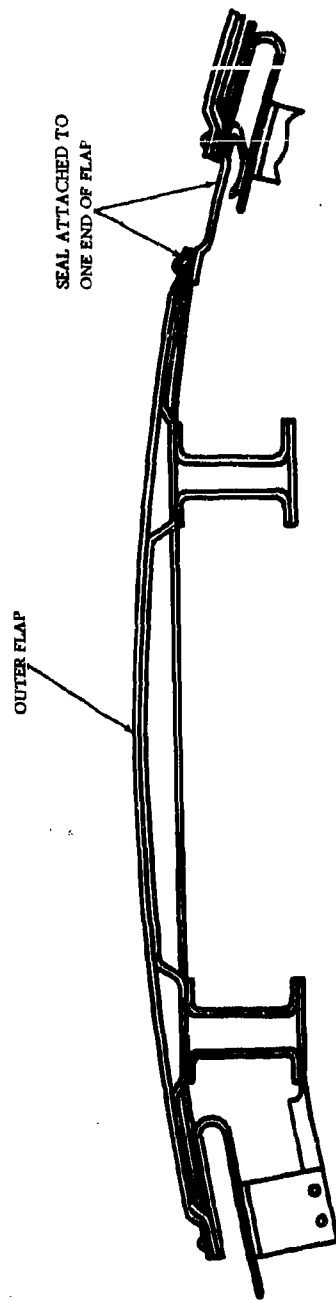


Figure 6-14. OUTERFLAP SEAL

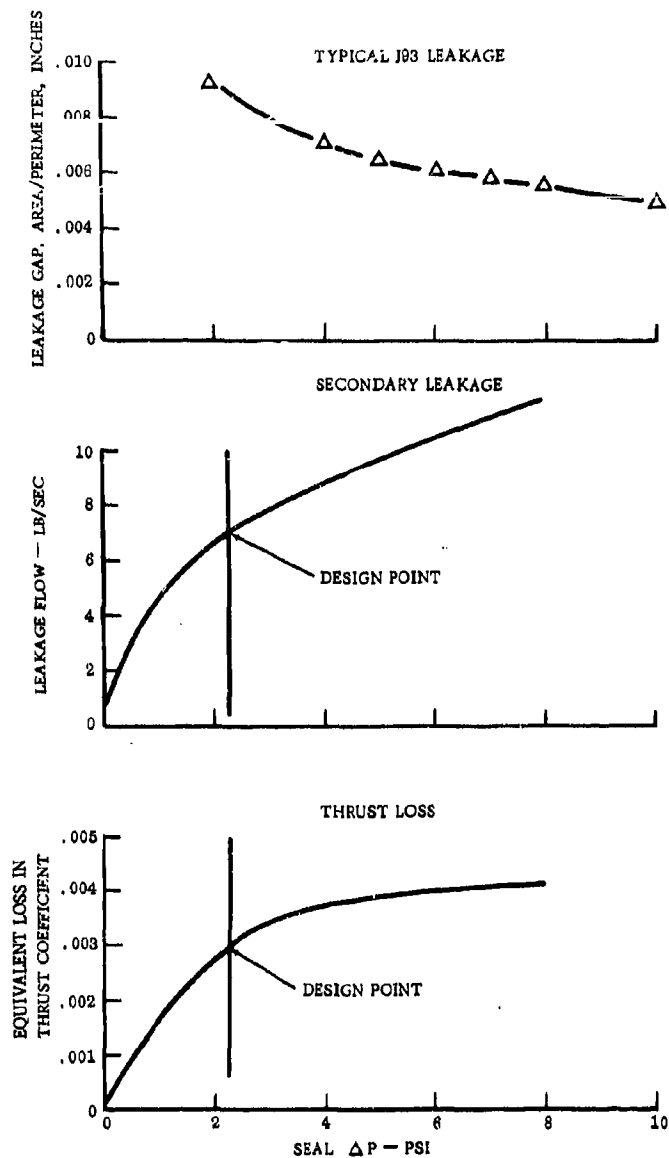


Figure 6-15. SECONDARY NOZZLE LEAKAGE LIMITS

divided by the perimeter. The resulting loss from a given gap is found by multiplying the appropriate gap by the total leakage perimeter to obtain an area, and by using the area with the compressible flow functions to find flow. The resulting flow for the GE4 design point is presented in Figure 6-15, and 0.7 pounds per second for 2.5 psi flap pressure differential. The associated loss in thrust is evident from lower Figure 6-15 as 0.003 points in gross thrust coefficient. This amount is taken as a subtractor from the nozzle thrust coefficient and was used in the aerodynamic design of the GE4 nozzle.



An important feature of the design approach to the secondary nozzle was to eliminate the need for hydraulic actuation forces to control the exit area. The respective forces are adjusted to a point where the nacelle pressure levels position the nozzle without the need of a separate hydraulic actuation system. The proposed GE4 secondary nozzle exit area schedule, utilizing secondary pressure for control, is as follows:

<u>M<sub>p</sub></u>	<u>Position</u>
0 to 0.7	Closed
0.7 to 0.9	Within 4 degrees of Minimum Stop
0.9 to 1.1	Transition Outward
1.1 to 1.8	Within 4 degrees of Maximum Stop
1.8 to 2.7	Open

The internal nozzle performance estimates are based on the above area schedule.

The materials selected for the exhaust nozzle components are summarized in Table 6-1.

TABLE 6-1. EXHAUST NOZZLE COMPONENT MATERIALS

<u>Component</u>	<u>Material</u>
Primary Flap	R41
Primary Seal	R77 (U 700)
Hinge and Pin	R41
Hinge Ring	R41
Actuator Ring	Inco 718
Links, Primary	Inco 718
Shroud	Inco 718 & Hastelloy X
Inlet Doors	Inco 718
Inner Flap	R41
Inner Seal	R41
Outer Flap	Inco 718
Outer Seal	Inco 718
Bushings	S - Monel

### 6.3 DESIGN REQUIREMENTS

#### 6.3.1 COMPONENT DURABILITY (LIFE)

The component life requirements are summarized in Table 6-2.

TABLE 6-2 COMPONENT LIFE REQUIREMENTS

<u>Component</u>	<u>Minimum Life Without Repair (hours)</u>	<u>Ultimate Life With Repair (hours)</u>
Pins and Bushings	4,000	4,000
Primary Flap Seals	4,000	8,000
Primary Flap Shields	4,000	8,000
Secondary Seal - Inner	4,000	8,000
Primary Flaps	8,000	12,000
Secondary Flap - Inner	8,000	12,000
Secondary Seal - Outer	4,000	12,000
Cascade Box	8,000	12,000
Hardware	12,000	12,000
Hinge Ring	12,000	36,000
Actuation Linkage	12,000	36,000
Secondary Flap - Outer	12,000	36,000
Fixed Shroud Structure	12,000	36,000
Actuation Ring	12,000	36,000

These life requirements provide the basis for selecting materials, operating stress levels and temperatures for each component. The service life varies, depending on individual component characteristics. Experience has shown that the useful service life of some components is limited by considerations such as wear rather than stress rupture. In actual practice many of the nozzle components have essentially unlimited service life from a stress rupture standpoint. However, by setting a specific life requirement, the best selection of materials and operating temperatures is ensured.

#### 6.3.2 THRUST REVERSER

The thrust reverser is designed to meet the following requirements:

- Operation in the full reverse thrust position at 100 percent speed according to these specified periods.

<u>Utilization Period Per Occurrence (Seconds)</u>	<u>Reverse Cycles (Percentage)</u>
30	1
20	19
15	60
10	20

- The specified number of normal ground thrust reversals made from idle forward thrust are:

	<u>Number of Cycles</u>
Frame and Beam Assembly	19, 500
Cascade Box	8, 500

- Translation of the blocker can be made at engine speeds between ground idle and 85-percent speed (rpm).
- Engine thrust transients will be as follows:
  - From maximum augmented forward thrust to maximum reverse thrust (take-off abort) = 5.5 seconds
  - From idle forward thrust to maximum reverse thrust = 6 seconds.

#### 6.4 DESIGN APPROACH

##### 6.4.1 GENERAL

The mechanical design approach to the exhaust nozzle emphasizes a reliable and maintainable system that meets performance and that employs the proven exhaust nozzle technology demonstrated in 780,000 hours of variable-area nozzle experience in military J47, J79, J85 and J93 engines. Initial design studies concluded that a separate variable primary nozzle and thrust reverser system was much too complex when integrated with a variable divergent section. Studies of systems employing a separate reverser blocker indicated lower but still unacceptable complexity as well as reliability problems. Design effort was aimed at combination of functions. These studies led to the arrangement of the proposed GE4 system:

- Combined primary nozzle/reverser blocker
- Combined tertiary inlet/cascade covers
- Self-actuated, aerodynamically positioned secondary nozzle

The primary nozzle has also been designed to perform the function of thrust reverser blocker, with the forward-thrust area variation function and the reverser function controlled by separate actuating systems. A malfunction in the thrust reverser system does not prohibit use of the unit as a primary nozzle, and vice versa. The integrated nozzle/blocker also results in a symmetrical

reverser flow-path that permits flexibility in locating the cascade boxes circumferentially without altering the design approach to the blocker design.

The reverser cascade boxes are designed to be covered, when not in use, to eliminate the aerodynamic drag penalty. These covers are the auxiliary inlet doors, which are opened for supplementary air-flow in take-off and subsonic operation.

The secondary nozzle is completely variable to provide the required area variation. It has been designed for aerodynamic positioning by the secondary pressure. This feature has been incorporated to improve reliability by eliminating an additional divergent-section actuating system, an area control, and the mechanical interlocks between the exit of the secondary nozzle and the throat of the primary.

#### 6.4.2 DESIGN ANALYSIS AND CRITERIA

The thrust reverser/nozzle components are designed mechanically on the basis of the pressure distributions and the predicted metal temperature of each component. The pressure distributions are derived from scale-model aerodynamic test data and previously established correlations with full-scale prototypes. The metal temperatures are derived from extensive computer applied heat transfer analyses, which have been confirmed and refined by current and previous augmentor nozzle experience. The load and temperature analyses for the nozzle system are prepared in computer form so that SST flight plan studies can readily be performed to determine component life requirements. With the component life, load, and temperature determined the detailed mechanical design including material selection, stress analysis, and design for manufacturability was made. The components are analyzed for yield under maximum loading, usually encountered on the maximum "q" line. Under the long-term load conditions, each component is analyzed for stress-rupture or creep, depending on the function of the component. In general, the seals between flaps are creep-limited, whereas the flaps are stress-rupture-limited. Pins and clevises are sized for low wear by designing for low (and uniform) bearing pressures.

Allowable working stresses for the material used are based on the laboratory average properties minus three standard deviations. All loads are increased by a factor of 1.25 as margin between the operating stress and the allowable working stress. In special cases, a larger factor is used if the stress analysis required does not have the desired statistical verification. In the design of a stress-rupture-limited component, the design is made for twice the required life, to account for the fact that the loadings are repeated, cycling from no-load to full-load throughout the useful life of the component. (See Figure 6-16)

Early in the development of the nozzle and thrust reverser, tests to evaluate thermal strain loads are conducted, especially during transients, and also to determine what fatigue and/or acoustic problems might be encountered. These problems are generally resolved by component tests, once sufficient information has been obtained from development engine tests. Experience has led to construction details and to material proportions that have essentially eliminated acoustic damage as a mode of failure in General Electric exhaust nozzles and thrust reverser.

Two of the clearest lessons learned from experience with commercial exhaust components have been the thermal stress damage and excessive wear that occurs in long-service parts. This knowledge has been used in the design of our recent military exhaust nozzle, the J79-10 nozzle, as well as in the GE4 exhaust system. All wear points have been designed to be free of a stress limit. Typical components continue to function despite wear, and operation is interrupted only to replace the wear element. The mechanical design ensures that normal wear cannot cause a hang-up or jammed condition.

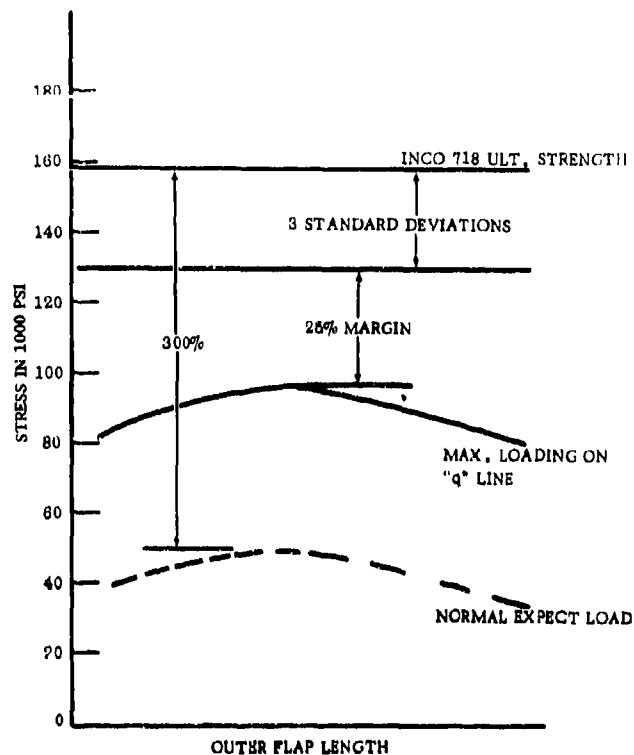


Figure 6-16. DESIGN CRITERIA

Thermal stress damage to the flaps is essentially eliminated by incorporating a heat shield on the flap to act as a buffer against random streaks and large temperature changes during starts and augmentor lights. In addition, the primary flaps and seals are air-cooled at all power settings above augmented cruise.

## 6.5 DESIGN DESCRIPTION

### 6.5.1 PRIMARY NOZZLE

The major components of the primary nozzle described in this paragraph are shown in Figure 6-17. The 16 primary flaps are hinged to the translatable hinge ring, at the forward end. The flaps are positioned by links, pivoted to the flap (approximately two-thirds of the flap length) aft of the forward hinge. The opposite ends of the links are attached to the actuation ring, which is translated in forward and aft directions. The translation of this ring provides synchronized movement of the primary flaps and seal to set exhaust throat area. Translation of the hinge ring aft causes the flaps to move aft, which opens the reverser exhaust area. The links simultaneously cause the flaps to rotate inward to the reverser blocker position.

In order to keep exhaust gases confined to the primary nozzle throat, two axially hinged seals are used between each pair of the sixteen flaps. These seals are positively attached to the flaps by the

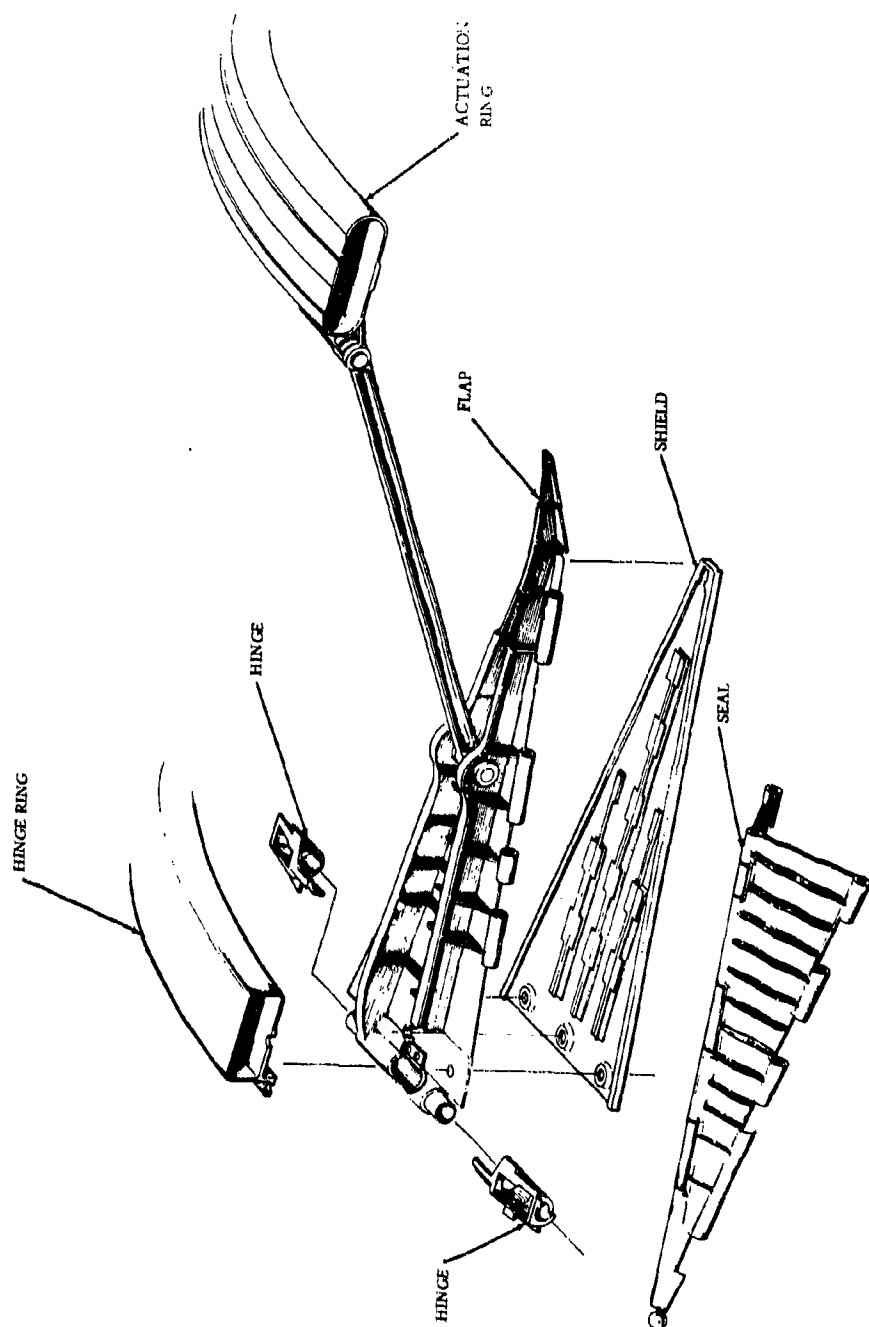


Figure 6-17. PRIMARY NOZZLE

hinge lugs on the edge of the flaps and seals. The two seals are also attached to each other by similar connections. A pin is inserted through the center of the hinge lugs, and engages the alternate lugs on the flaps and seals. The mounting and axial pivots are not lubricated. Experience with J93 nozzles, in which similar hinges are used for flap to exhaust duct attachment, confirms that low wear and long life is obtainable in the nozzle hinge environment without lubrication.

Each of the primary flaps and the primary seals are one-piece castings. This construction avoids structural, thermal, and dimensional problems that would occur with the extensive welding required to make the parts as fabrications. Figure 6-18 illustrates the comparable features of the J79, J93 and GE4 primary flaps. Note the favorable transitions from base sheet to structural ribs provided by the casting approach.

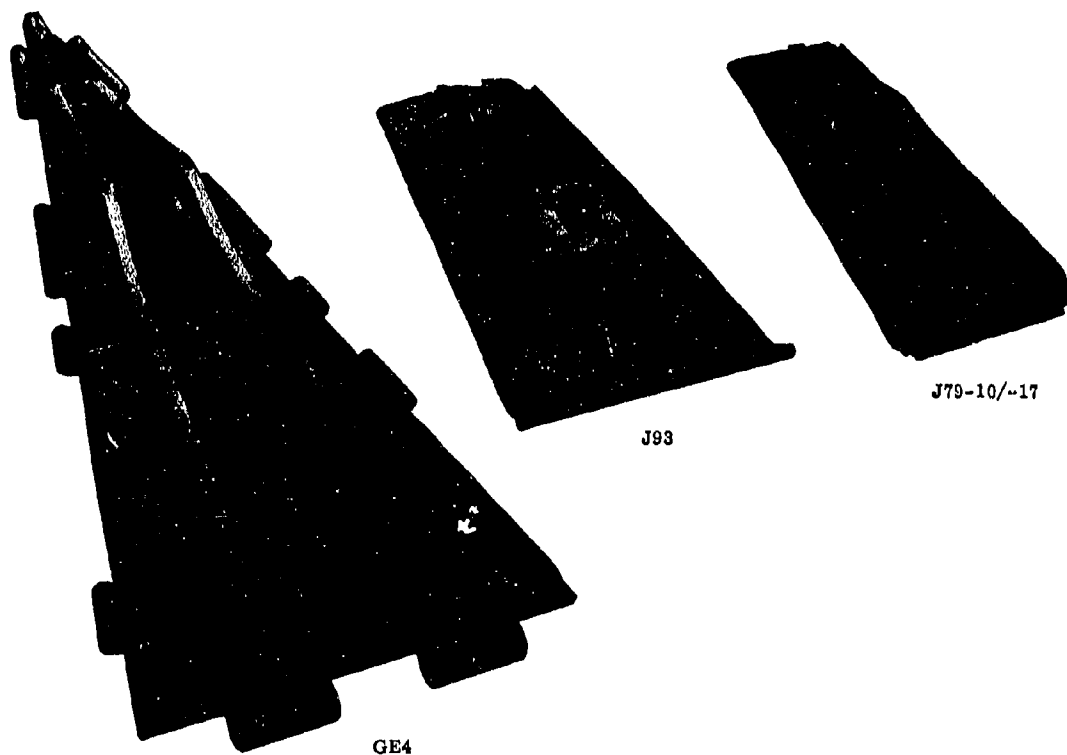


Figure 6-18. J93, J79-10/17 AND GE4 PRIMARY FLAPS

#### 6.5.1.1 Material

The flap is cast to provide the required structural, thermal, and dimensional properties on the part at a low cost. The material employed is René 41 which has high strength-to-weight ratio at elevated temperature, plus good repairability. As shown in Figure 6-19, which is a photograph of the Phase II-C design, the flap base is reinforced with a backbone structure that extends the full length of the flap. Transverse ribs extend from the edge of the flap to the backbone. These ribs are located to provide maximum support to the seal attachment lugs which are integrally cast on the edges. Castings are used in this area to obtain high joint efficiencies and to avoid stress-concentrations in weld areas. Low thermal stress also results from the high conductive properties of cast sections. Clips riveted to the base of the primary flap engage the mounting rails on the heat shield. These clips in conjunction with three bolts (for axial retention) hold the shield to the flap.

The primary seals are made of cast René 77 (Udimet 700 turbine blade material) because of its exceptional strength capabilities at high operating temperatures. René-77 seals are currently being used in the J79-10 and J93 engines. The primary seals have lugs integrally cast on their edges which mate with the flaps. There are two seals for each flap connected (flaps to seals and seals to seals) by axial pins inserted through the respective hinge lugs. For axial retention, the pins between the flaps and seals are bolted together at the aft end of the flap. This arrangement prevents relative motion between the flap and pin, and eliminates wear on the flaps. Each axial pin that connects the two seals is riveted to one seal, which further prevents relative motion and wear. The seal lugs are bushed with replaceable bushings at the points where there is relative motion between the pin and lugs.

Figure 6-20 illustrates the Phase II-C flap and shield system. The shield rails engage the clips on the flap. The flap and shield are aligned with the clips, axially out of phase so that sliding the shield forward on the flap causes the clips on the flap to interlock with those on the shield. Three bolts are inserted through the holes on the forward end, and are secured with lock nuts to hold the flap and shield together. The shield is formed from Hastelloy X material for its high-temperature oxidation resistance and repairability. The clips are strip sheet-metal stampings that are attached to the shield by resistance welding. The shield distributes the compressor discharge cooling air over the face of the flap, and radially across the seals, through intermittent slots along the edge. The slots are of variable, experimentally determined dimensions, to provide the most effective coolant distribution for uniformly low seal and flap metal temperatures. The shield also absorbs the radiation heat-load from the augmentor gas stream, thereby keeping the structural flap at a low temperature. As described in Section 7, Volume IIIB, the metal temperature differential (shield to flap) is about 250°F. The compressor air also convectively cools the shield as the airflows between it and the flap base. An additional function of the shield is to insulate the flap from abnormally high local temperatures which might occur due to hot streaks.

The hinges that hold the flaps to the hinge ring are cast from René 41 material because of its high strength-to-weight ratio. The hinges form a gas seal when bolted to the ID of the hinge ring. As illustrated in Figure 6-17, the hinge casting slides over the hollow shaft that is cast integrally on the flap. A cavity is formed by the end of the flap shaft, the closed end of the hinge, and the ID of the hinge ring, which is vented to the hinge ring to permit cooling air-flow into the flap.

Each primary flap has a forged René 41 link pinned to it. These (sixteen) links positioned in unison by the axial stroke of the actuating ring sets the flaps at the proper position to form the throat of the exhaust system. The links also resolve the primary flap gas force, and transmit the gas force reaction to the actuating ring. Each link is pinned to the flap on one end and to the actuating ring on the other.



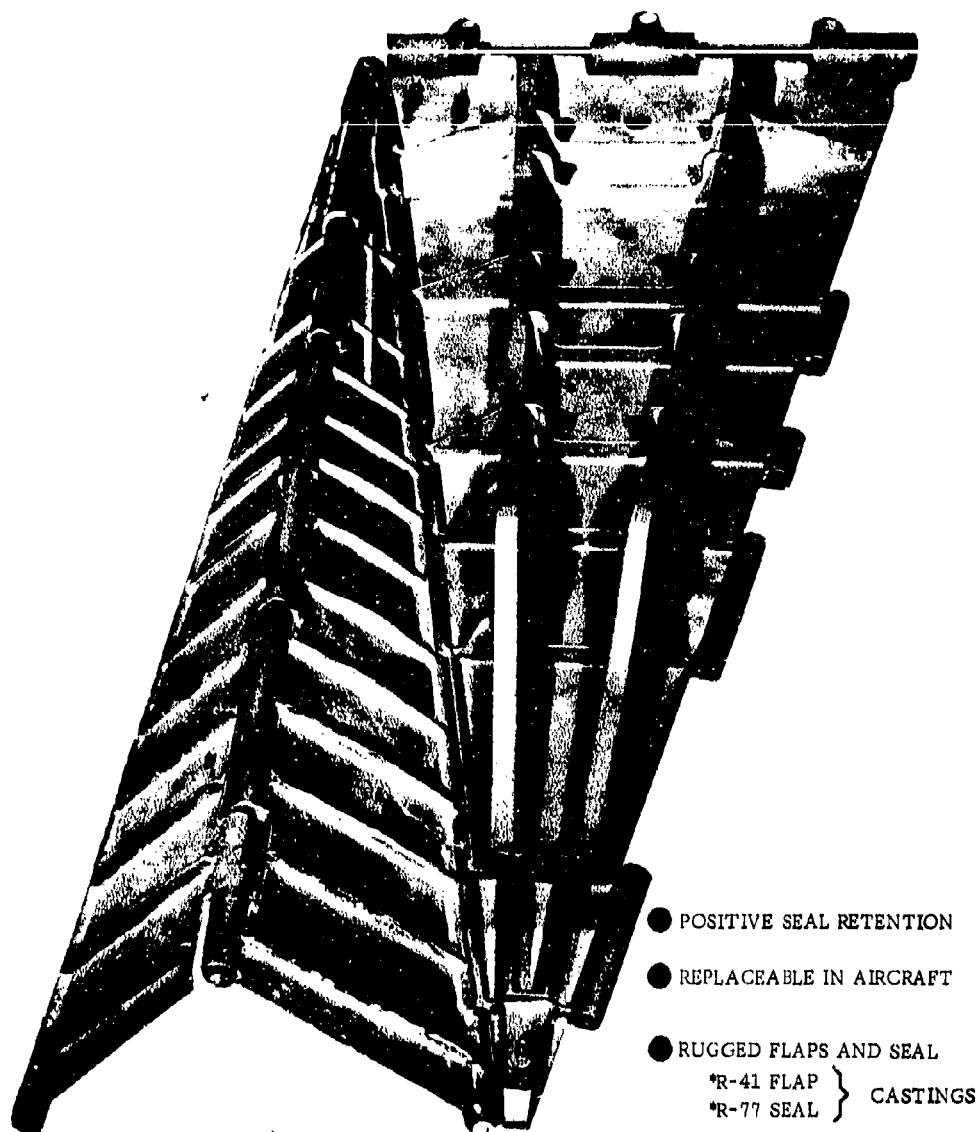


Figure 6-19. GE4 FLAP DESIGN

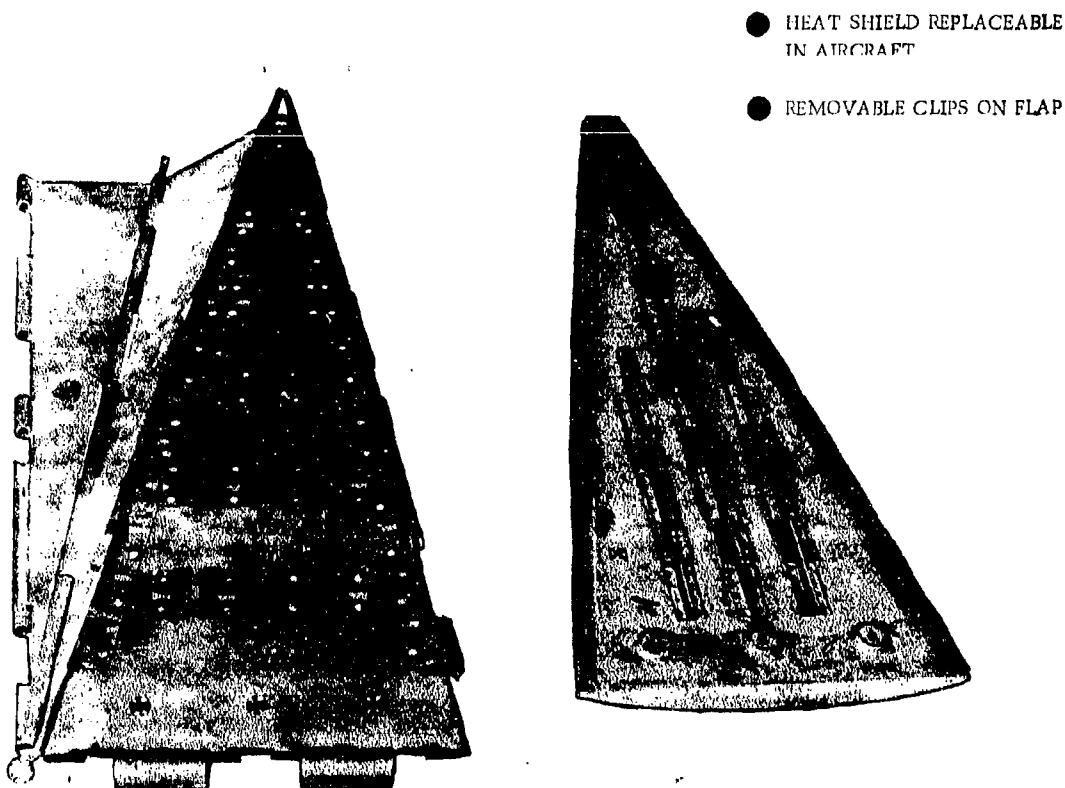


Figure 6-20. GE4 FLAP AND SHIELD SYSTEM

All pivot points in the primary nozzle system have been designed so that the pins are stationary with respect to the major components - i.e., primary flap, actuation ring. The links are provided with replaceable bushings for repairability, and each link can be removed from the engine by simple disassembly of the pin from each end of the link.

The actuation ring Figure 6-21 is an Inconel 718 fabrication made from two semi-circles of tubing. The tubing is shaped to an oval cross-section, then roll-formed into the two segments which are butt welded together. The OD and ID of the ring are jointed by welded stiffeners to stabilize the cross-section, which would otherwise be subjected to secondary buckling that would result in low efficiency (shear lag). The ring has 16 link-bracket castings made of Inconel 718 for attachment of the flap links. It also incorporates four actuator bracket castings made of Inconel 718, for attachment of the primary nozzle hydraulic actuators.

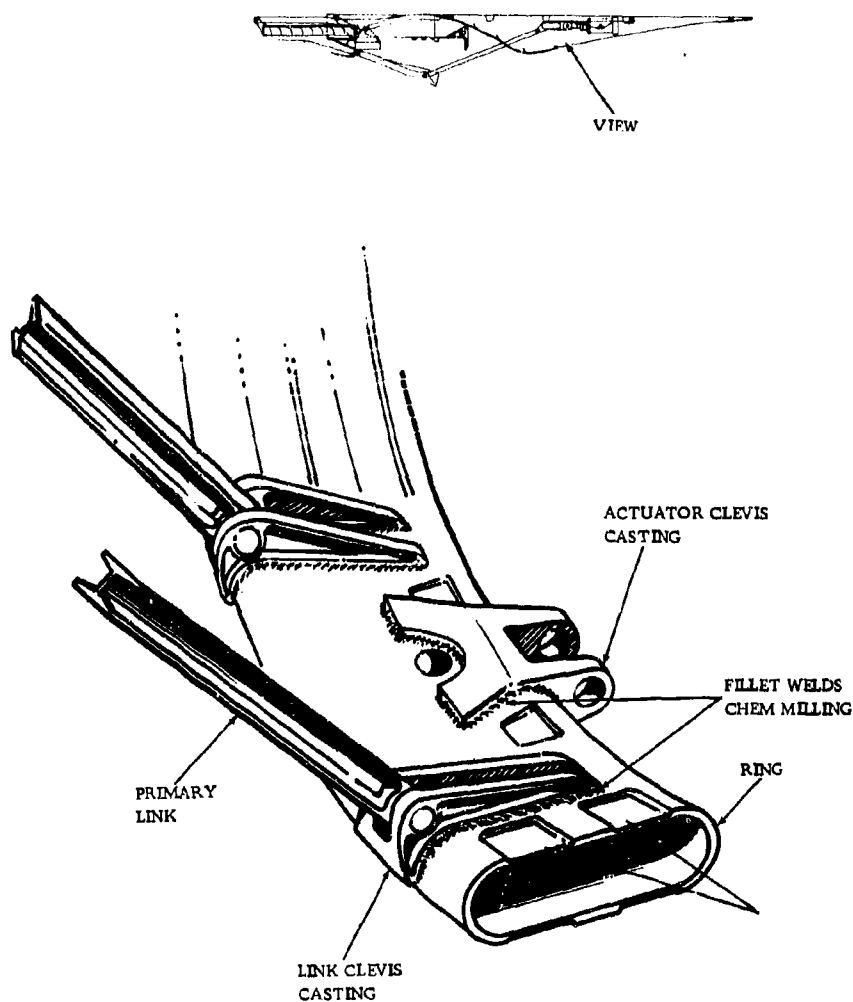


Figure 6-21. ACTUATION RING STRUCTURAL DESIGN

#### 6.5.1.2 Load Analysis

The primary nozzle loads are calculated from an integration of:

- Static pressure inside the nozzle, resulting from the primary gas flow.
- Static pressure on the outside of the flaps, resulting from secondary air flow.

These loads acting on the flap and seal surfaces develop reaction forces at the flap hinge and actuator link as shown in Figure 6-22.

When the engine is in forward thrust, the axial hinge reaction is applied to the hinge ring to keep it sealed against the exhaust duct. When the engine is in reverse thrust, the axial hinge reaction is applied to the hinge ring to keep it against the reverser stops. This design provides the fail-safe characteristics.

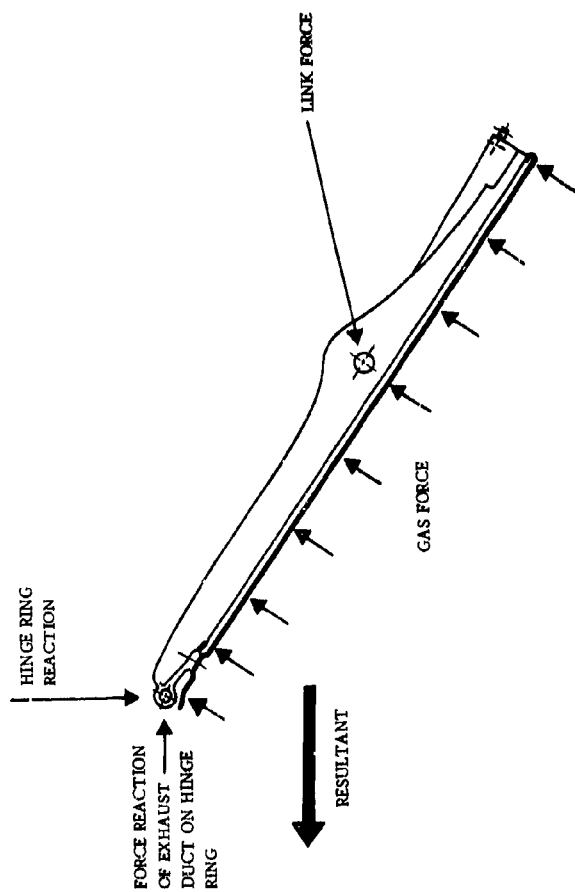
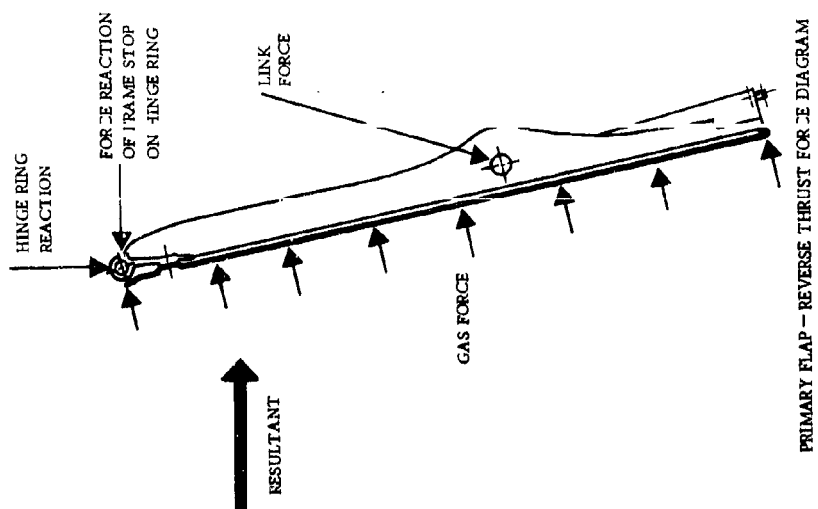


Figure 6-22. FLAP FORCES

### 6.5.1.3 Design Analysis and Criteria

A computer program is used to evaluate the gas loads of the exhaust nozzle for each flight condition. This program provides primary flap bending moment at approximately 30 stations along the axis of the flap. The program also calculates link loads and flap reactions at the hinge ring. The loads on the nozzle components are dependent on nozzle position, engine cycle pressure, and altitude ambient pressure. These loads generally tend to be maximum in high dynamic-pressure regions of the flight map. Each required flight condition is evaluated, and the flap (and seal) stresses are calculated and compared with the material capability. The primary flap and seal are stress-rupture limited. Each flight condition uses a certain percentage of the stress-rupture life. The sum of all flight conditions does not exceed 100-percent of life when based on twice the flight times and a temperature deviation (approximately 100°F) above expected temperatures to account for local hot spot conditions. Thermal stresses are evaluated on the basis of experimentally measured gradients, and are added to the gas load stresses when additive. All calculations are based on minimum stock thickness, and the stress calculations are based on a 1.25 margin of safety. Stress levels are limited to the 0.2-percent yield capabilities with three standard deviations from the average properties. Pin and bushing bearing stresses are designed to be low (2000 - 4000 psi).

The stress in the primary flaps and seals are presented in Figure 6-23. The data shows that -

- Insignificant time is spent at maximum stress conditions.
- Maximum stress level is only 60 percent of the strength of the material.

The link connecting the primary flap with the actuation ring is an I-beam in cross-section. It is loaded as a column during steady-state conditions; however, during transient conditions the pin friction applies end moments which induce bending stresses as well as column stresses.

The radial components of the 16 link loads are reacted by hoop tension in the actuating ring. In addition, the point loading produces bending stress in the ring as a result of the tendency of the ring to deform from a circular shape to a 16 sided polygonal shape. This stress is maximum at the point of load application and acts about the neutral axis that is parallel to the engine axis.

The axial component of the link load is carried by the ring in flexure from the 16 points of load application to the four actuators, as shown in Figure 6-24. The axial load has the major influence on the ring size and cross-sections. The associated high axial bending moment also produces large torsional shear moments in the curved structure. For this loading, a closed, hollow shape is most efficient for adequate torsional shear strength and stiffness.

The J93 nozzle employs a ring of uniform wall-thickness, sized by the axial section requirements. Two circumferential butt welds are used to close the cross-section. (See Figure 6-25). The GE4 ring design (See Figure 6-21) is similar in concept to the J93, except that the two circumferential welds were eliminated by forming the ring section from a flattened seamless tube.

### 6.5.2 THRUST REVERSER

#### 6.5.2.1 Hinge Ring

The hinge ring provides all required thrust reverser motion with a single actuation system stroke. It provides these simultaneous functions:

- Translates primary nozzle aft and concurrently closes the nozzle for thrust reverse.
- Translates the reverser cascade boxes aft from the stowed position into the gas stream for reverse thrust.

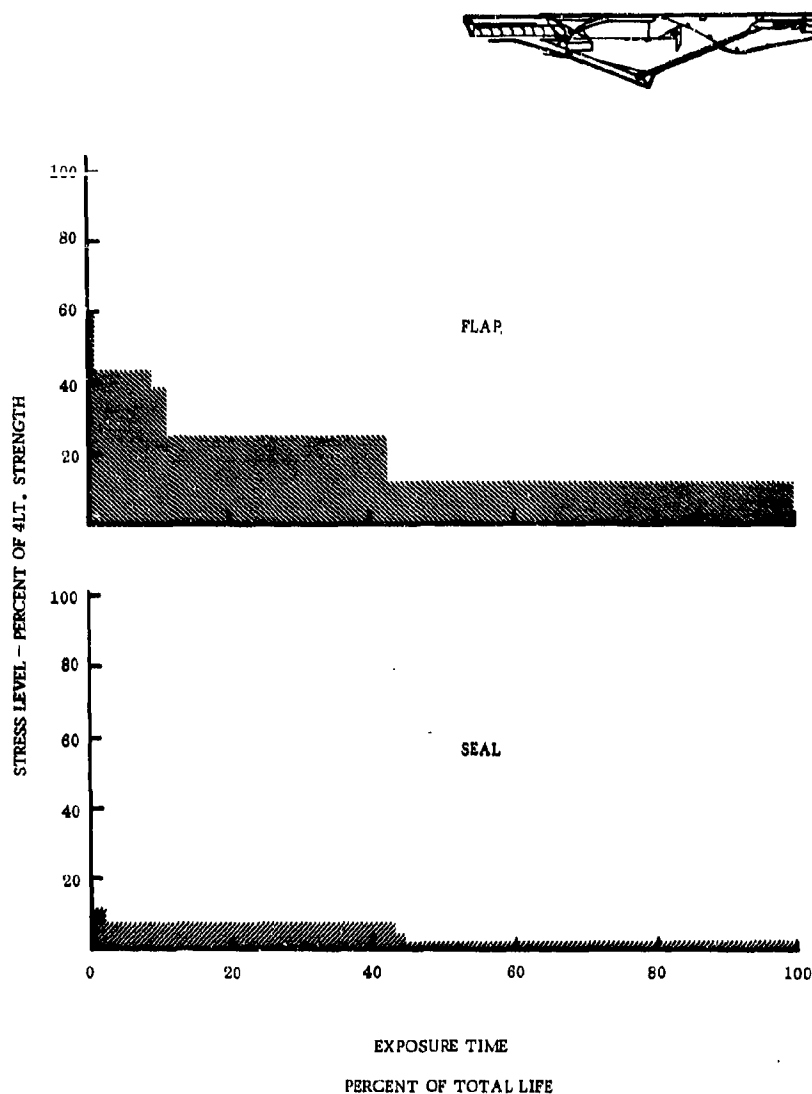


Figure 6-23. FLAP AND SEAL STRESS LEVELS

- Translates the auxiliary inlet doors aft, uncovering the reverser openings. It is noted that in this arrangement these doors uniquely function as cascade covers.
- It functions as the primary nozzle cooling air manifold.

These functions are shown in more detail in Figure 6-26.

The hinge ring is a basic structural member, axially positioned by four hydraulic actuators, which function only during transition from forward to reverse thrust and vice versa. The flaps are positioned during forward thrust by  $A_8$  actuators and actuation ring. (See Figure 6-26.)

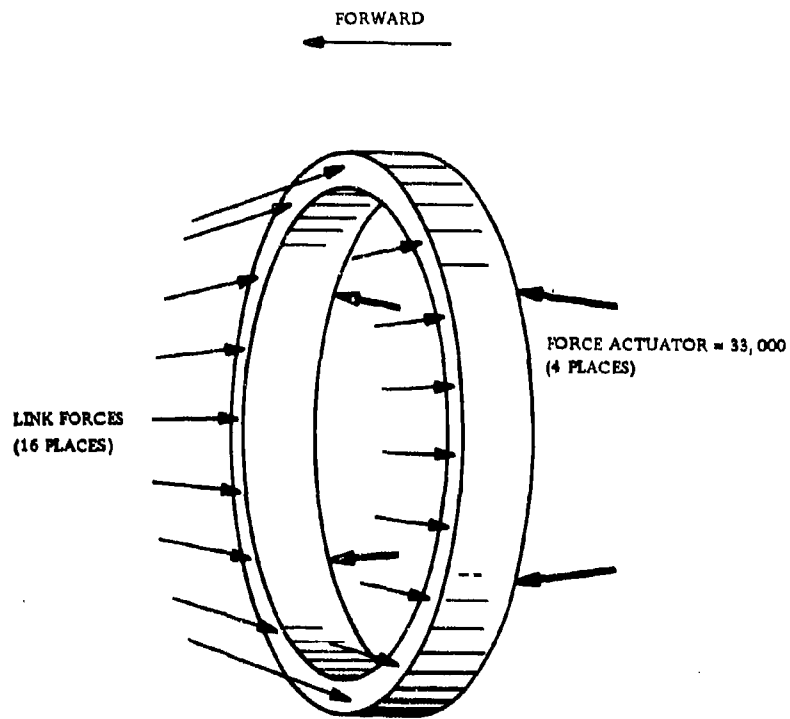


Figure 6-24. RING LOADING

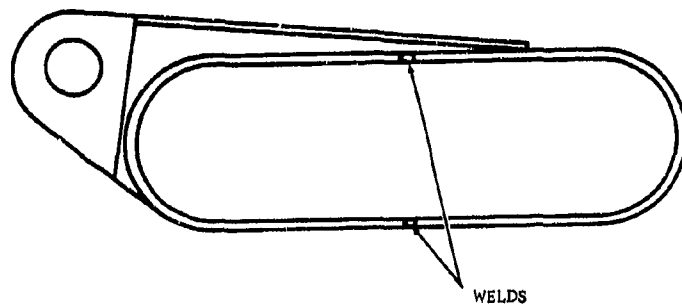


Figure 6-25. J93 ACTUATOR RING CONSTRUCTION

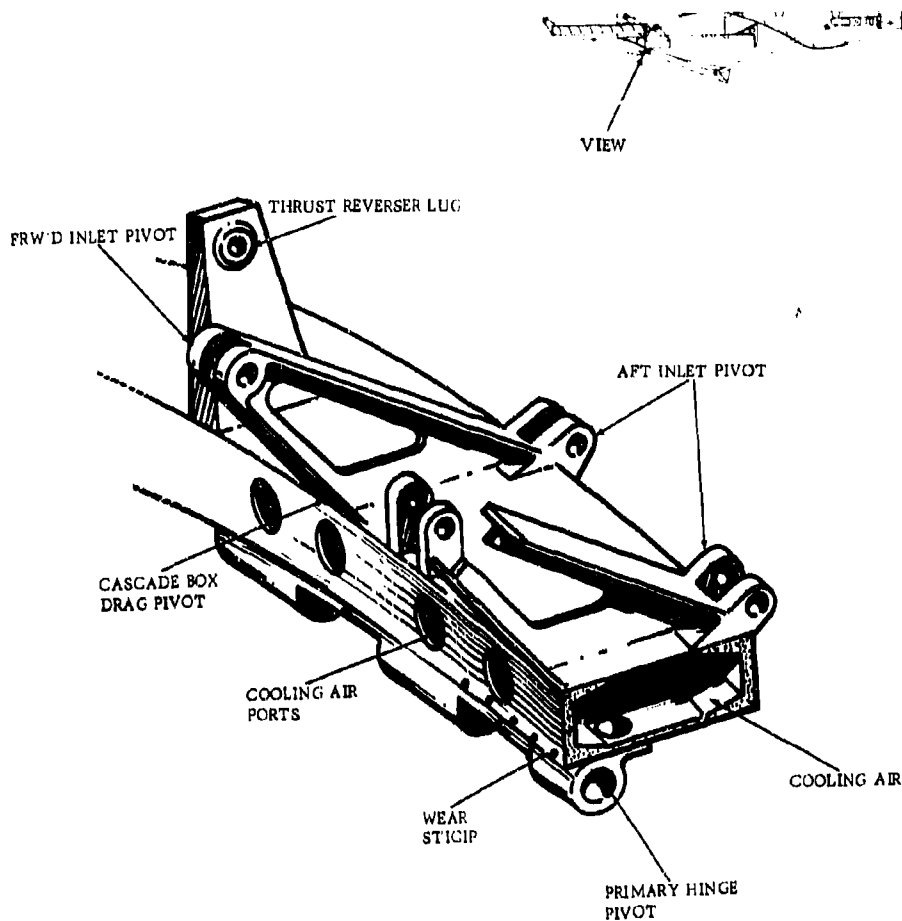


Figure 6-26. Hinge Ring

The four radial actuator attachment brackets are tangentially supported on guide rails in the axial beams of the thrust reverser frame. Radial support is provided by tangential constraint imposed on the brackets by the sides of the guide rails; freedom for differential thermal expansion between ring and rails is provided by freedom of the bracket arm to slide radially on the rails. (See Figure 6-27 and 6-28.) These guide rails incorporate replaceable wear-strips for simplified maintenance.

The hinge ring is moved axially by four axially synchronized hydraulic actuators. These actuators are mounted in spherical bearings at the forward end, to extensions of the secondary nozzle support beams as illustrated in Figure 6-29. This mounting permits the actuator to swivel, in order to compensate for thermal expansion and mechanical deflection. The rod-ends of the four actuators are attached to the hinge ring actuator brackets, as shown in Figure 6-30. Actuator synchronization holds the hinge ring perpendicular to the axial beams during translation from forward to reverse thrust modes. Internal leakage is provided in the actuators for cooling. The maximum hydraulic fluid temperature is 444°F and metal temperature, 470°F (Refer to table 5.0-2 in volume III-B, part 2.)



The primary flaps are mounted to the inside surface of the hinge ring (In typical military augmentors, the primary nozzle is similarly mounted directly to the exhaust duct.) In the forward-thrust mode, the ring bears against the exhaust duct, forming a gas seal and allowing the forward axial load to transfer directly and uniformly to the exhaust duct. The radial load is absorbed by the ring. Since the primary flaps and seals are positioned on the inner diameter of the hinge ring they serve as a radiation shield for the ring, resulting in low operating temperature of the ring. The proposed arrangement of flap shielding in conjunction with CDP air cooling accomplishes this effectively.

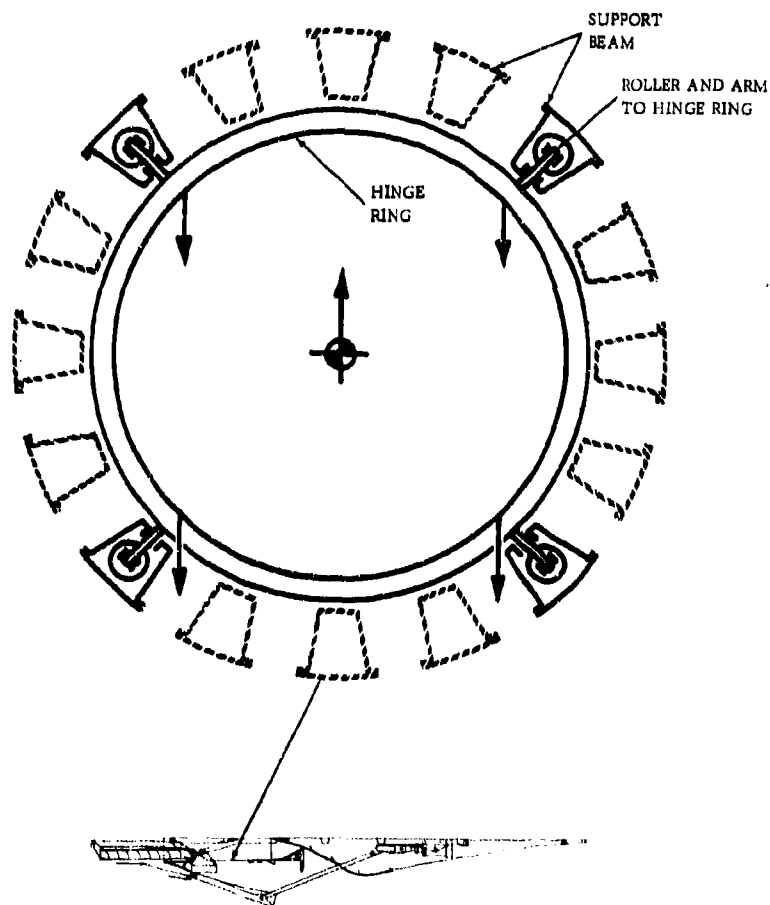


Figure 6-27. Hinge Ring Support

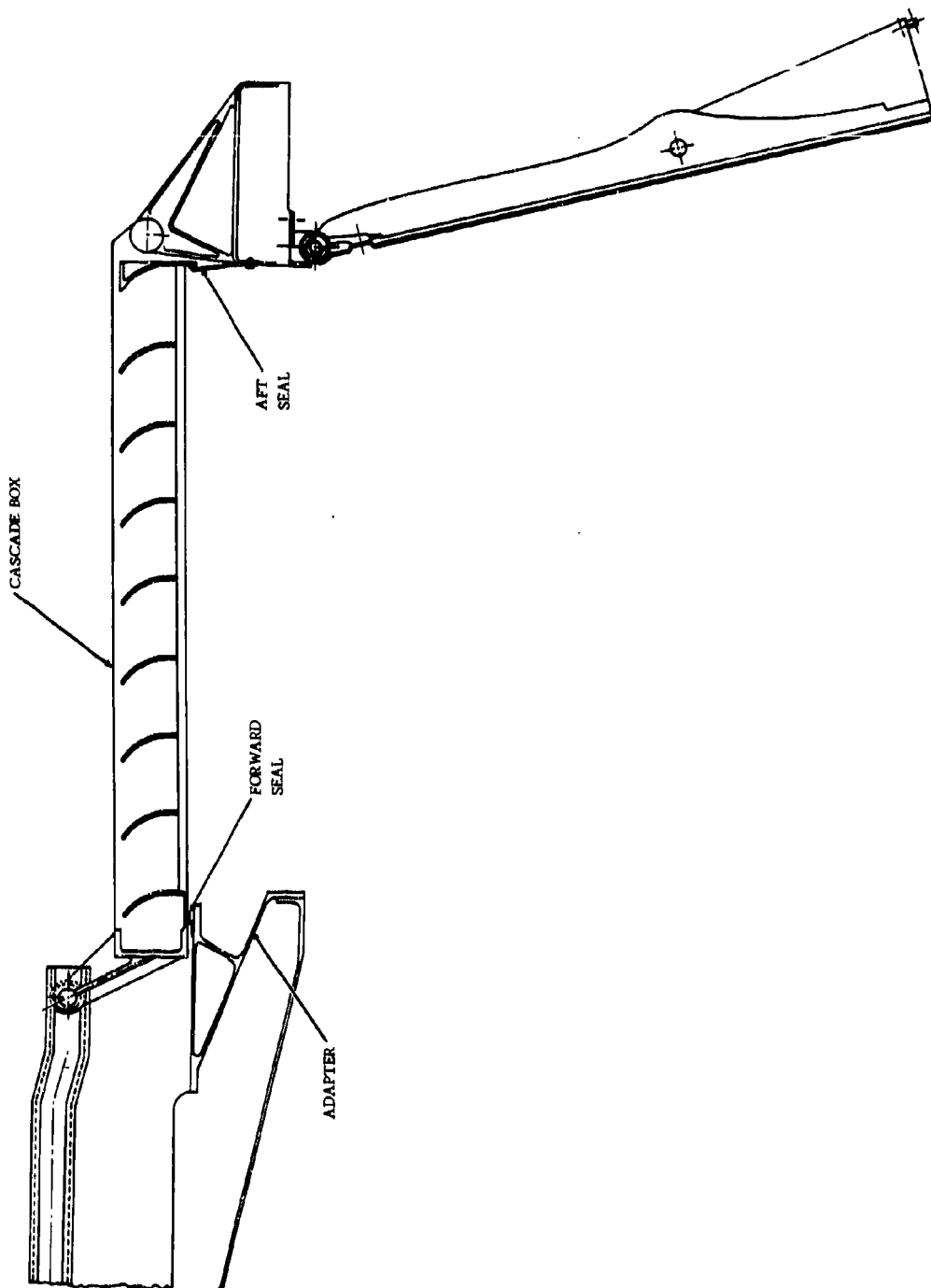


Figure 6-28. SECTIONAL VIEW CASCADE BOX IN THRUST REVERSER POSITION

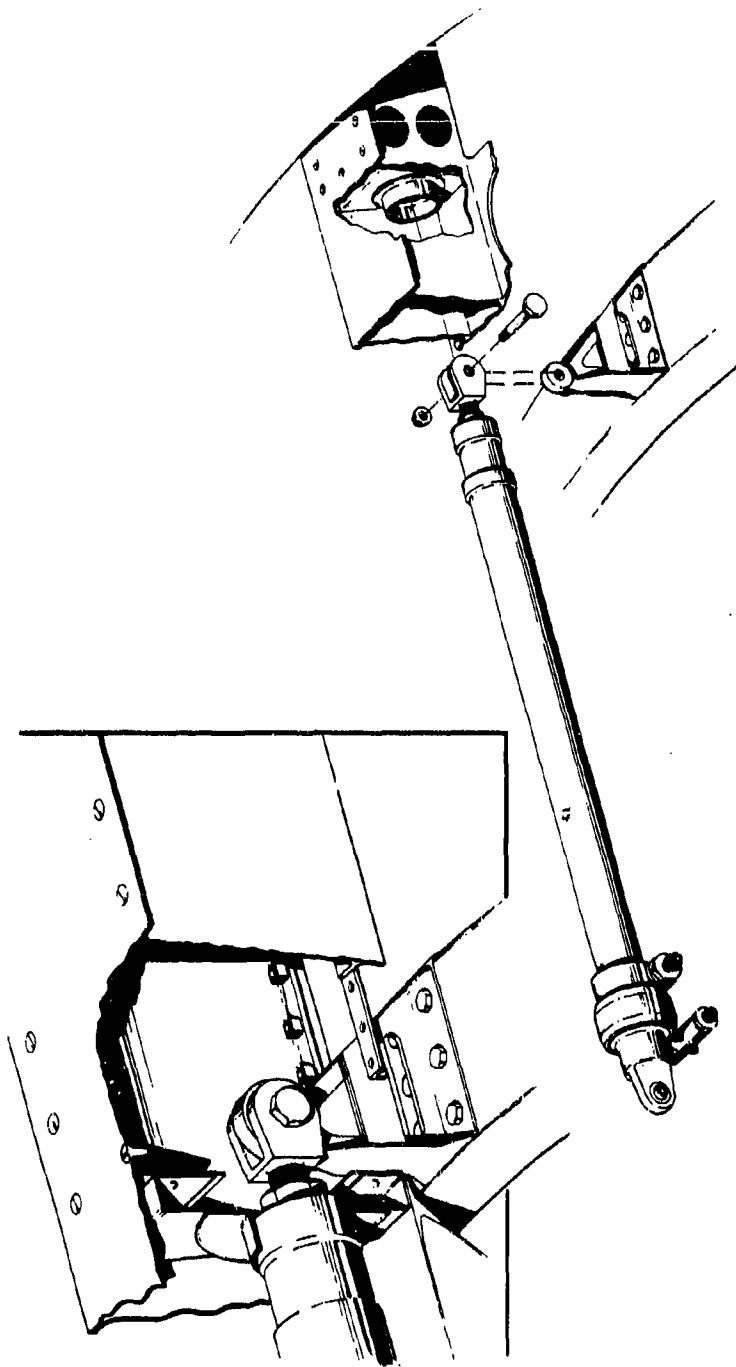


Figure 6-29. ACTUATOR MOUNT TO HINGE AND RING

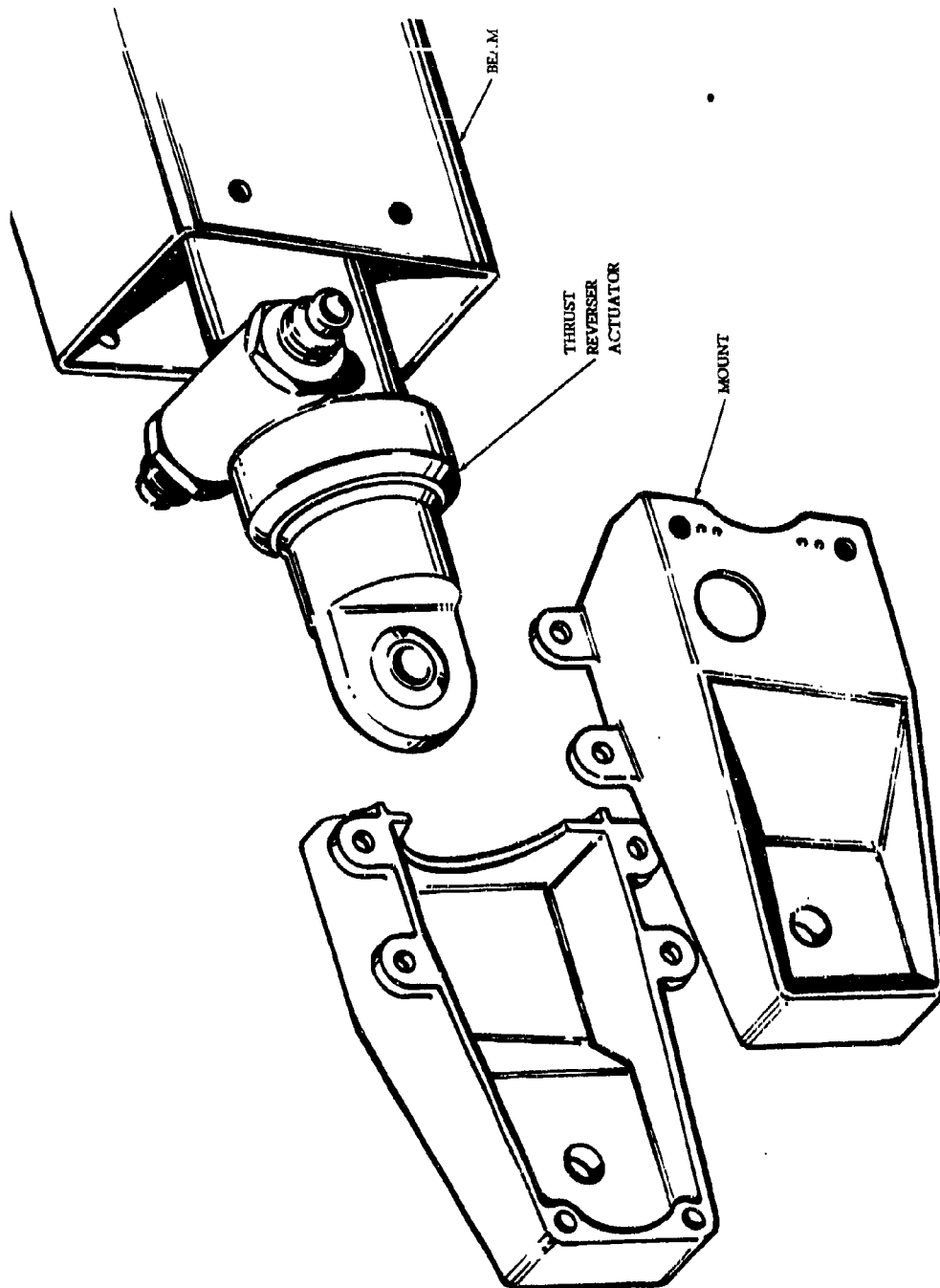


Figure 6-30. REVERSER ACTUATOR MOUNT

For reverse-thrust operation, the hinge ring moves aft, rotating the primary flaps inward to the blocker position. This system provides an important build-in fail-safe feature. If the hydraulic system of the actuator fails, the reverser blocker remains in the committed position.

Figure 6-31 shows a force diagram of the reverser system during translation near full forward and near full reverse thrust positions. Note that the thrust reverser actuator force changes from compression to tension during the translation from forward to reverse thrust. This change in load direction on the hinge ring/primary nozzle assembly occurs at 5.0 inches or approximately 25 percent of the reverser stroke (axial translation). This is further illustrated by Figure 6-32 which shows reverser actuator force as a function of hinge-ring travel. Point (A) represents forward thrust position at initiation of movement to reverse. Point (C) is the nozzle position just before the reverser engages the hinge-ring stops. Point (B) represents the intermediate point at 2.0 inches of reverser stroke at which the load direction on the hinge ring/primary nozzle assembly reverses. At position aft of this point the reverser actuators act as restraints since the loads on the flaps and cascades are axially aft. In addition to this fail-safe feature, each thrust reverser actuator contains an integral built-in-latch to prevent inadvertent in-flight reversal. The latch prevents rotation of the synchronizing screw in a direction which allows translation of the blocker to the reverse position.

To provide for low-impact loads at either extremity of the hinge-ring stroke, the actuation system provides the velocity/stroke relationship shown in Figure 6-33 for the forward-to-reverse transition (engage) and from reverse to forward thrust (disengage). A maximum stop engagement velocity of 27 inches per second is provided.

Interfaces of the cooling air duct connections are provided between the stationary duct part and the inlet to the hinge ring at two locations, approximately 180° degrees apart, allowing separation as the ring is translated to the reverse thrust position. (See Figure 6-34.) Compressor discharge air is piped aft from the compressor to the plane of the primary nozzle and through the skin of the reverser frame. The axial locations of the air inlet port interfaces are closely controlled dimensionally with respect to the exhaust duct aft flange.

The aft end of each reverser cascade box is attached to the ring at a single clevis, and the boxes are moved into reverse-thrust position by the aftward movement of the ring. The radial reaction is carried by the ring, and the aft axial reaction is transmitted directly to the beams through the stops. The auxiliary air inlet doors are mounted on radial brackets on the hinge ring. As the hinge ring moves aft for reverse thrust operation, the doors translate aft to uncover the openings through which exhaust gas is discharged.

#### 6.5.2.1.1 Design Criteria and Stress Analysis

The loads transmitted through the ring are applied at points other than the centroid of the ring. The cascade boxes are not located symmetrically with respect to the horizontal ring centerline and actuators are not located symmetrically with respect to the cascade boxes. A computerized approach to the distribution of these unsymmetrical loads and the resulting stresses has been developed. The General Electric MASS program was used to simulate the ring, and provided bending, torsional, shear and direct stresses, as well as all deflections and reactions. An investigation of the pertinent flight conditions indicated that the highest loading occurs when the four actuators are holding the ring just before it engages the stops in the reverse thrust mode during a cold day take-off abort condition. This condition therefore defines the hinge ring section requirements.

The ring acts as a pressure vessel when the primary nozzle cooling air is ducted through it. This effect and the effect of thermal gradients were simulated by the General Electrical Multishell computer program for a more comprehensive analysis of the ring stress patterns.

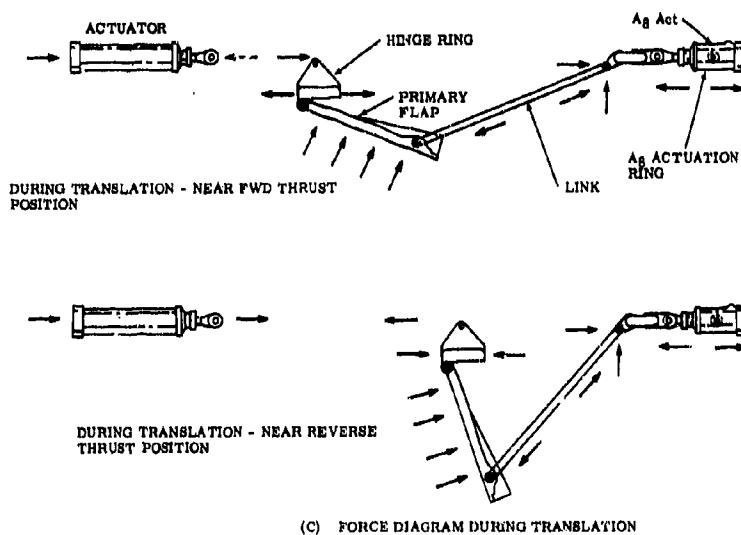
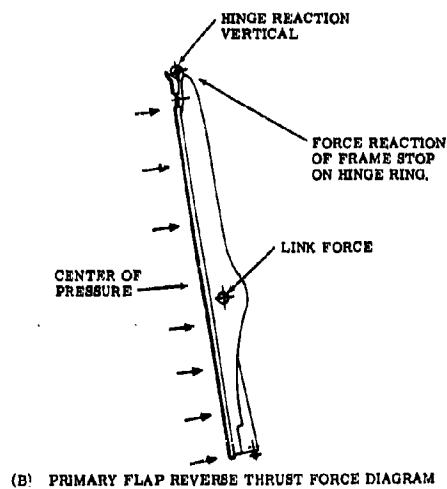
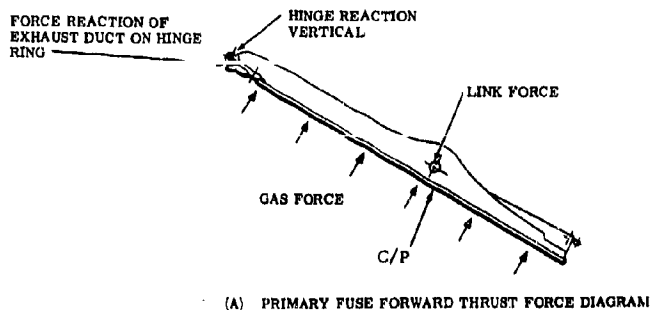


Figure 6-31. FORWARD AND REVERSE THRUST LOAD DIAGRAMS

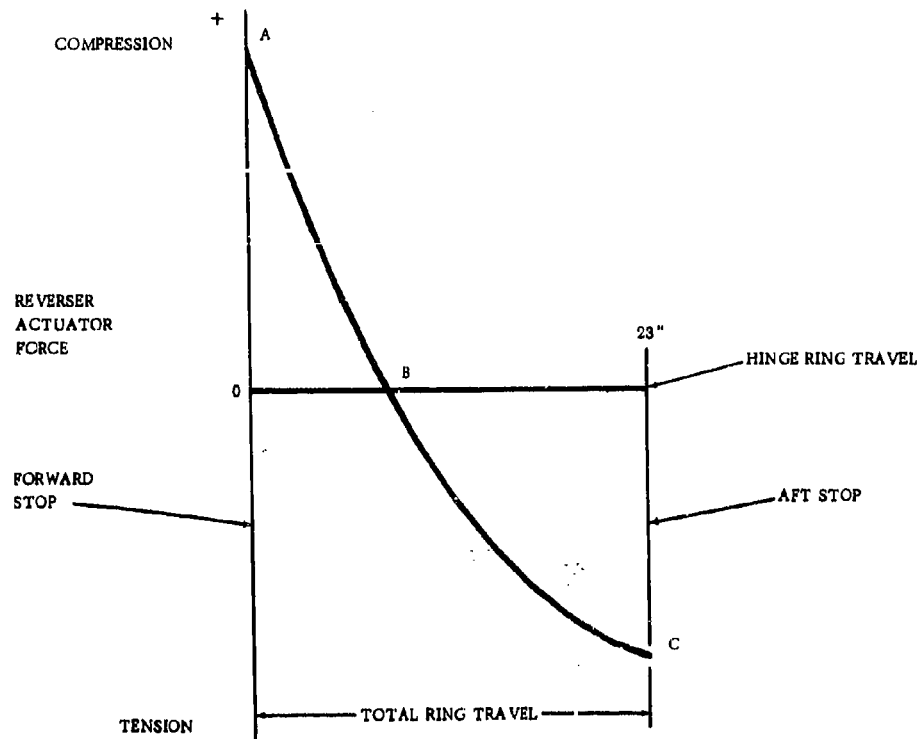


Figure 6-32. ACTUATOR FORCE AS A FUNCTION OF TRAVEL

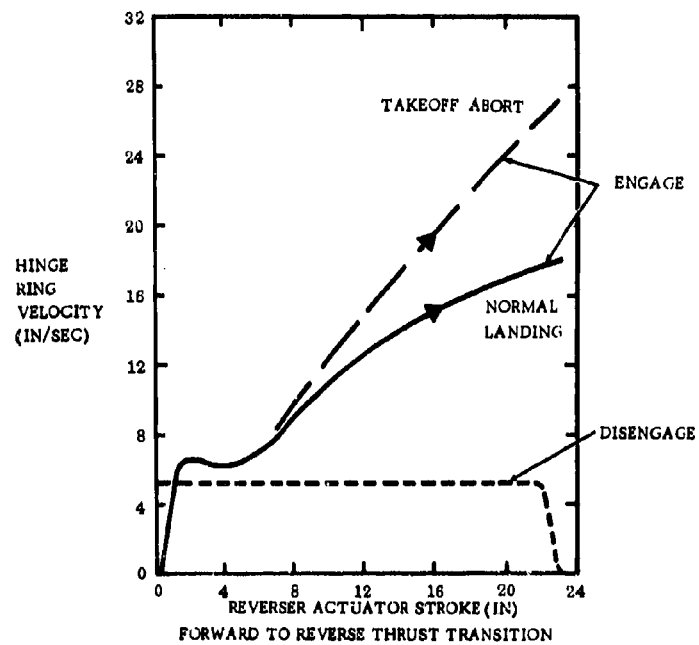


Figure 6-33. FORWARD TO REVERSE THRUST TRANSITION

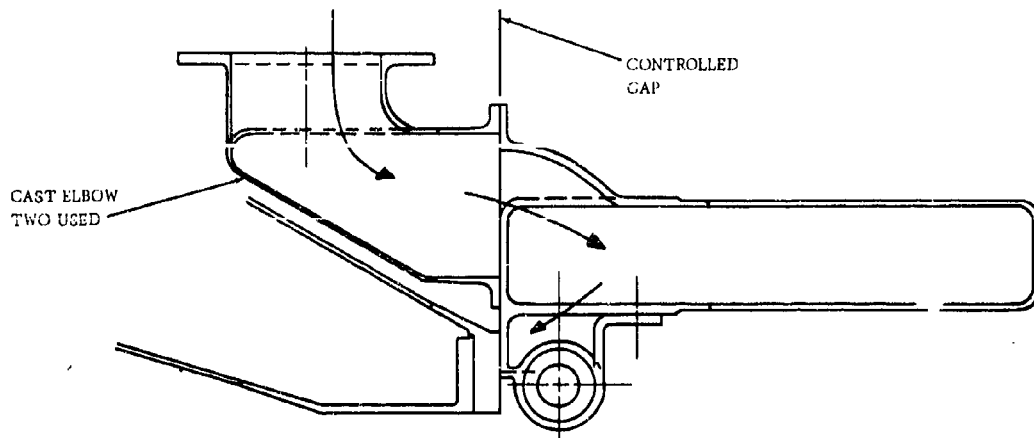


Figure 6-34. COLLING AIR INLET PRIMARY

#### 6.5.2.2 Cascade Boxes

The cascades are integrally cast boxes containing turning vanes. The cascade box is nominally 8.7 inches wide and 28.6 inches long, with 12 vanes. The eleven cascade boxes that make up the total reverser exit area translate axially between the secondary nozzle shroud support beams. (See Figure 6-35.) The box translation and radial mounting is accomplished with the track and roller design shown in Figure 6-36, which also illustrates the axial seal approach. The forward and aft seals are illustrated in Figure 6-. All reverser seals are pressure loaded outward to the mating surface to minimize leakage. The tracks, rollers and box attachments are designed so that the radial seal at the forward edge of the box is in contact only when in the reverse thrust position. During translation and stowing, the box is lifted from the seal to eliminate rubbing and to minimize wear.

Each cascade box is mounted at three points; a single aft attachment to the hinge ring (with a simple clevis joint) and by the two rollers at the forward end. Note that the roller and track system is mounted forward of the cascade box in the reverse thrust position, and is not subjected to the direct impingement of the exhaust gases.

Figure 6-37 illustrates the circumferential orientation of auxiliary air inlets and the proposed reverser exits. Inlets are located between the axial beams of the frame in 14 of the 16 equally-spaced spans. Inlets, omitted at the wing positions, are located at positions 1 to 14. The eleven proposed cascade exits are shown in positions in the typical wing opening on the top and symmetrically on each side of the lower nacelle. The blocker arrangement provided by the primary nozzle flaps and seals in the thrust reverse position is symmetrical with respect to the exhaust stream, thus providing aerodynamic flexibility for cascade exit positioning. Cascades can be located at any of the 14 positions used for inlet doors. Since the frame assembly is composed of 16 equally spaced beams, a revision in cascade location from one position to another would have no effect on the basic design concept nor on the frame structural analysis.

The cascade box detail is shown in Figure 6-38 and consists of three axial beams with turning vanes located at right angles to and between the beams. The vanes are shaped to provide turning of the discharge gases to obtain the required exit angle and reverse thrust. Figure 6-39 shows the Phase II-C cascade box which illustrates the configuration. Since the cascades are held radially at three points, a predictable load at the suspension points is assured. It also provides simplicity of mounting, because the removal of only one bolt is required to remove a box.



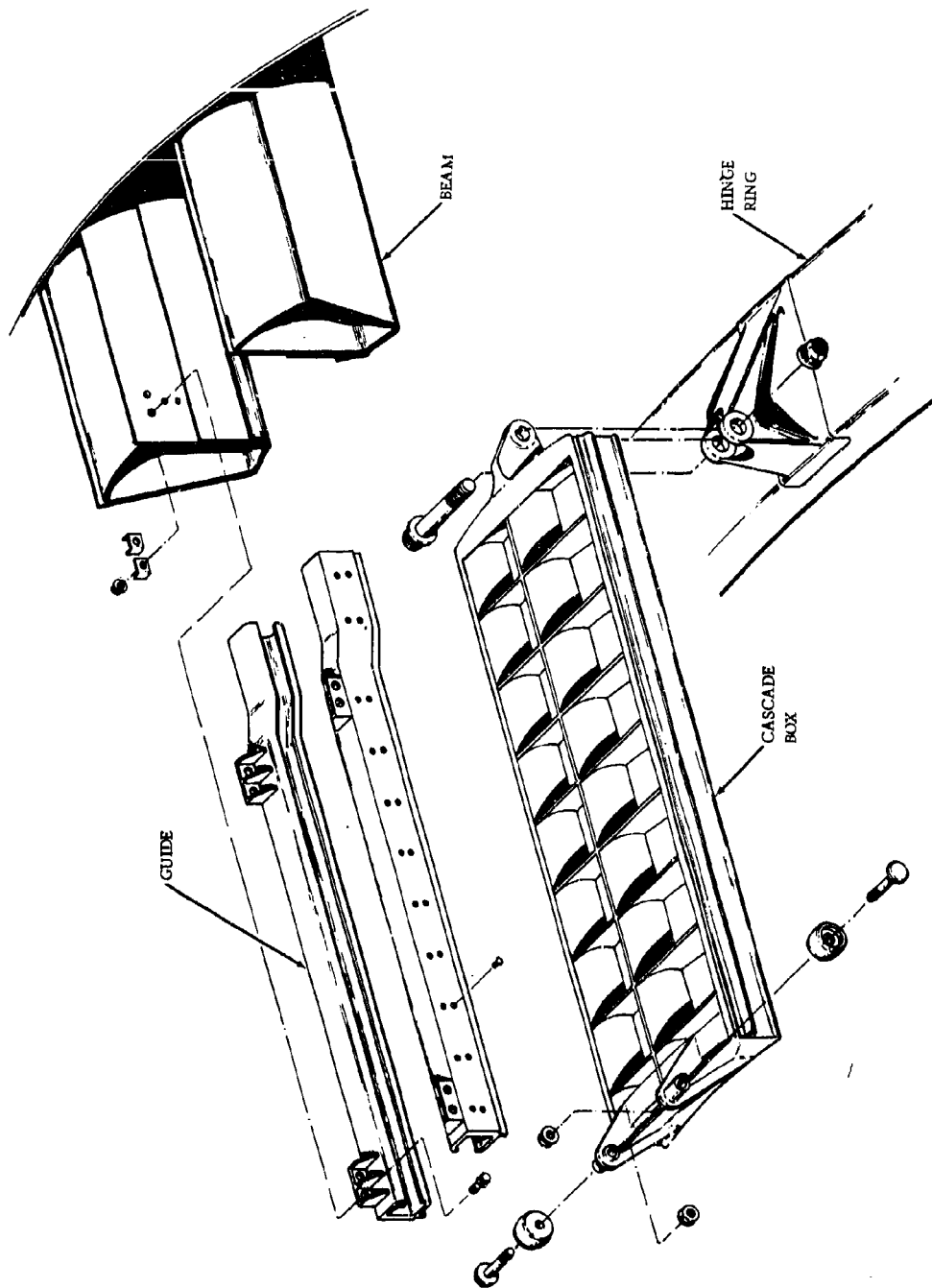
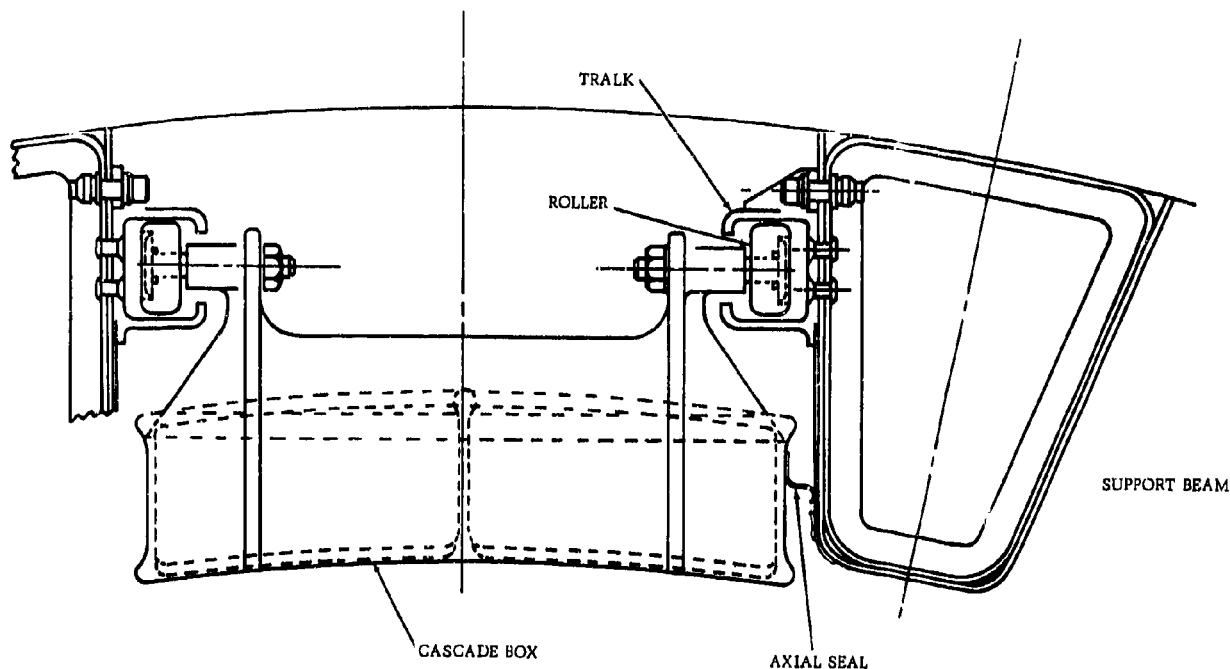


Figure 6-35 HINGE RING AND CASCADE BOX ASSEMBLY



VIEW LOOKING AFT SHOWING FRONT OF CASCADE BOX IN T/R POSITION

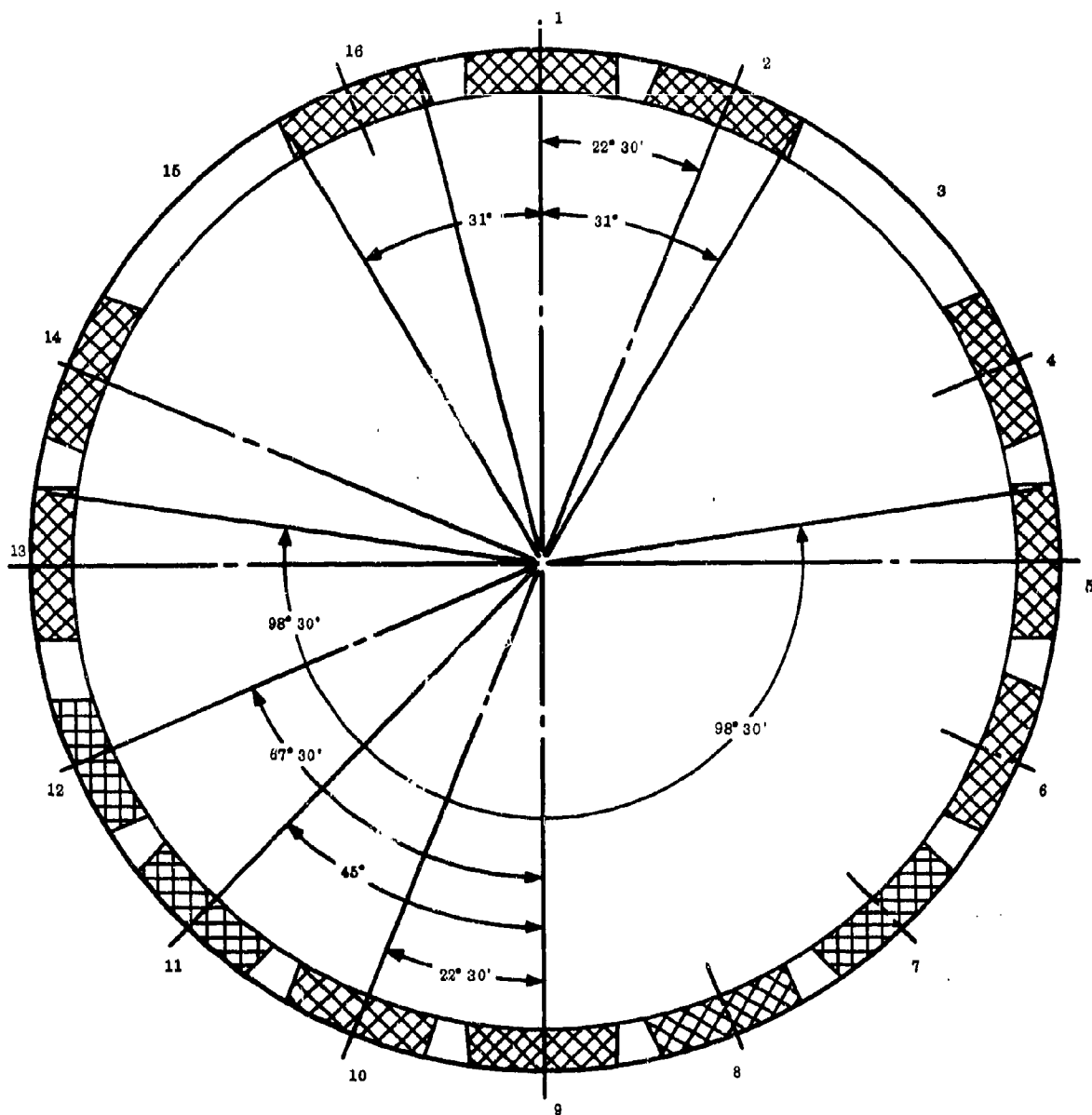
Figure 6-36 BOX TRANSLATION AND RADIAL MOUNTING

The cascade box is designed as an investment casting of RENE-41 material. This provides excellent structural (section) properties and aerodynamic surfaces. The roller supports and aft lug (for attachment to the hinge ring) are integrally cast extensions of the box beams. The entire cascade casting is designed for optimum stress/material distribution.

#### 6.5.2.2.1 Design Criteria and Stress Analysis

Results of a heat transfer analysis of the cascade box are shown in Figure 6-40. The lower curves show the vane and beam temperature as a function of time for a normal reversal. The upper curves show the same parameters, but for an extended reversal. The principle loads for which the cascade box and its mount are designed are gas loads exerted by the engine exhaust upon the vanes and beams. The steady-state loads have been used in defining the proposed design.

Thermal transients and thermal gradients between beams and vanes will be evaluated experimentally in the Phase II-C full-scale reverser test program. This program will provide:



POSITIONS 16, 1, 2, 4 thru 14 ARE INLETS

POSITIONS 16, 1, 2, 4 thru 8, 10 thru 13 ARE CASCADES

Figure 6-37 EXTERNAL DOOR ARRANGEMENT

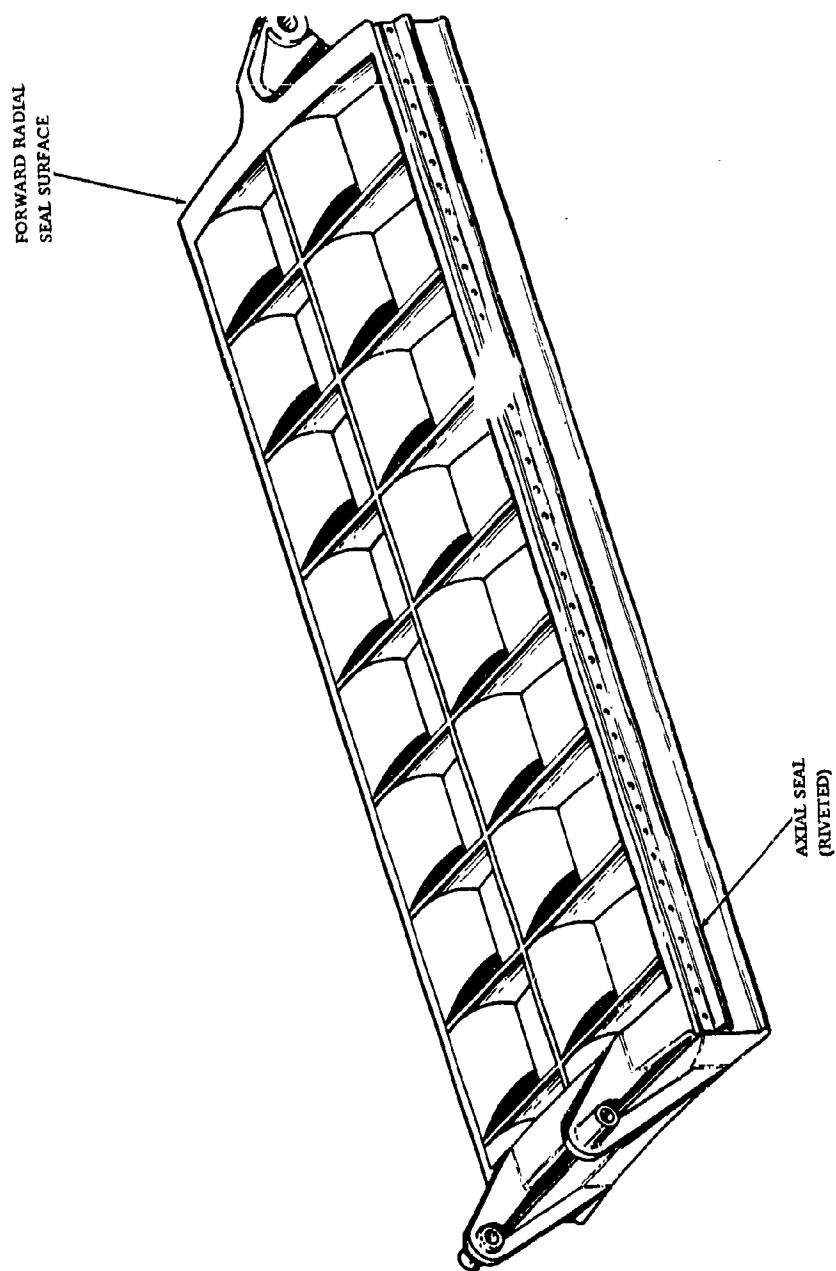


Figure 6-38 CASCADE BOX

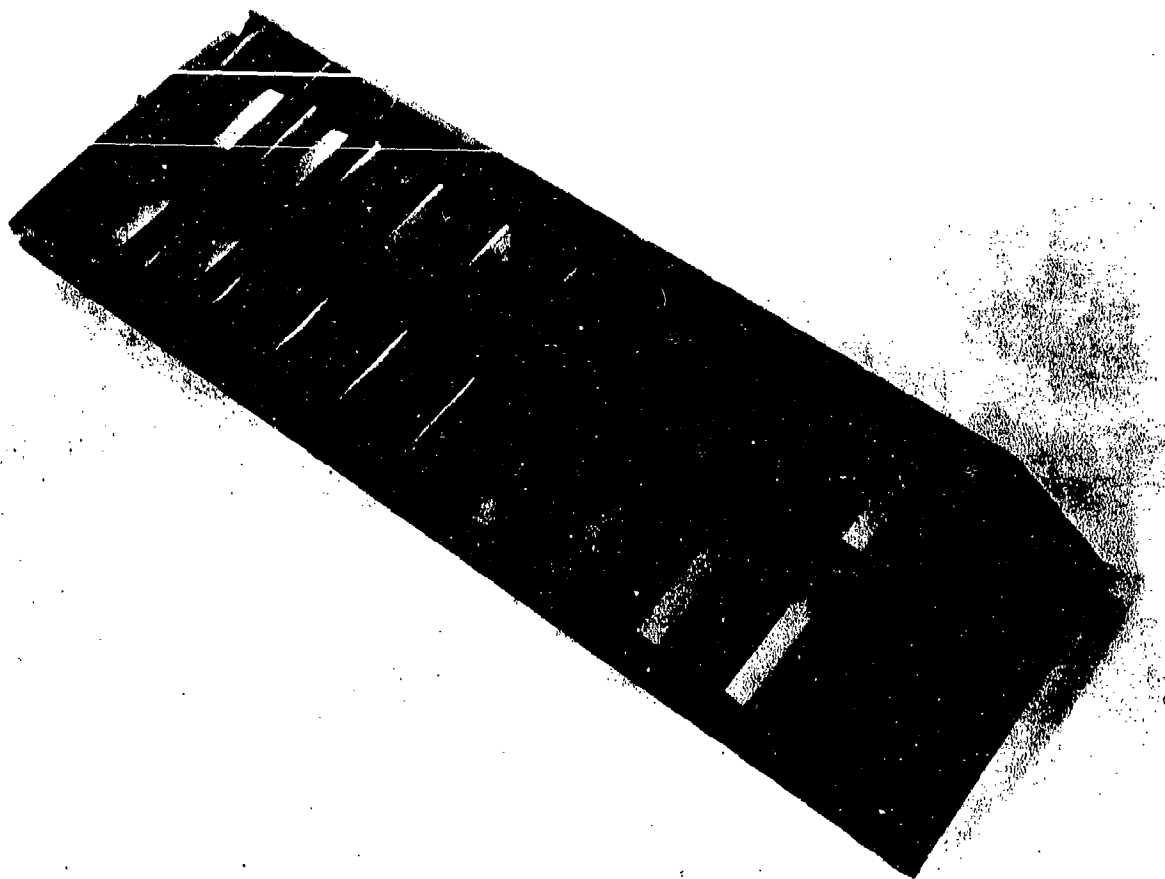


Figure 6-39 CASCADE BOX (PHOTO)

- Verification, and adjustment if necessary, of transient heat transfer analysis.
- A verification of thermal stress distribution.
- Evaluation of box life versus number of cycles.

Since the cascade box is an investment casting, it is ideally suited to an experimental design refinement to minimize thermal gradient effects and achieve the objective life.

#### 6.5.2.3 Frame and Beam Assembly

In addition to the blocker and cascade components, the reverser consists of a basic frame which guides the nozzle/blocker/hinge-ring, supports the translating cascade boxes, and provides a mount for the thrust reverser actuators. The frame is the main structure for supporting the secondary nozzle and the auxiliary air inlet doors. It includes the secondary nozzle shroud, 16 axial

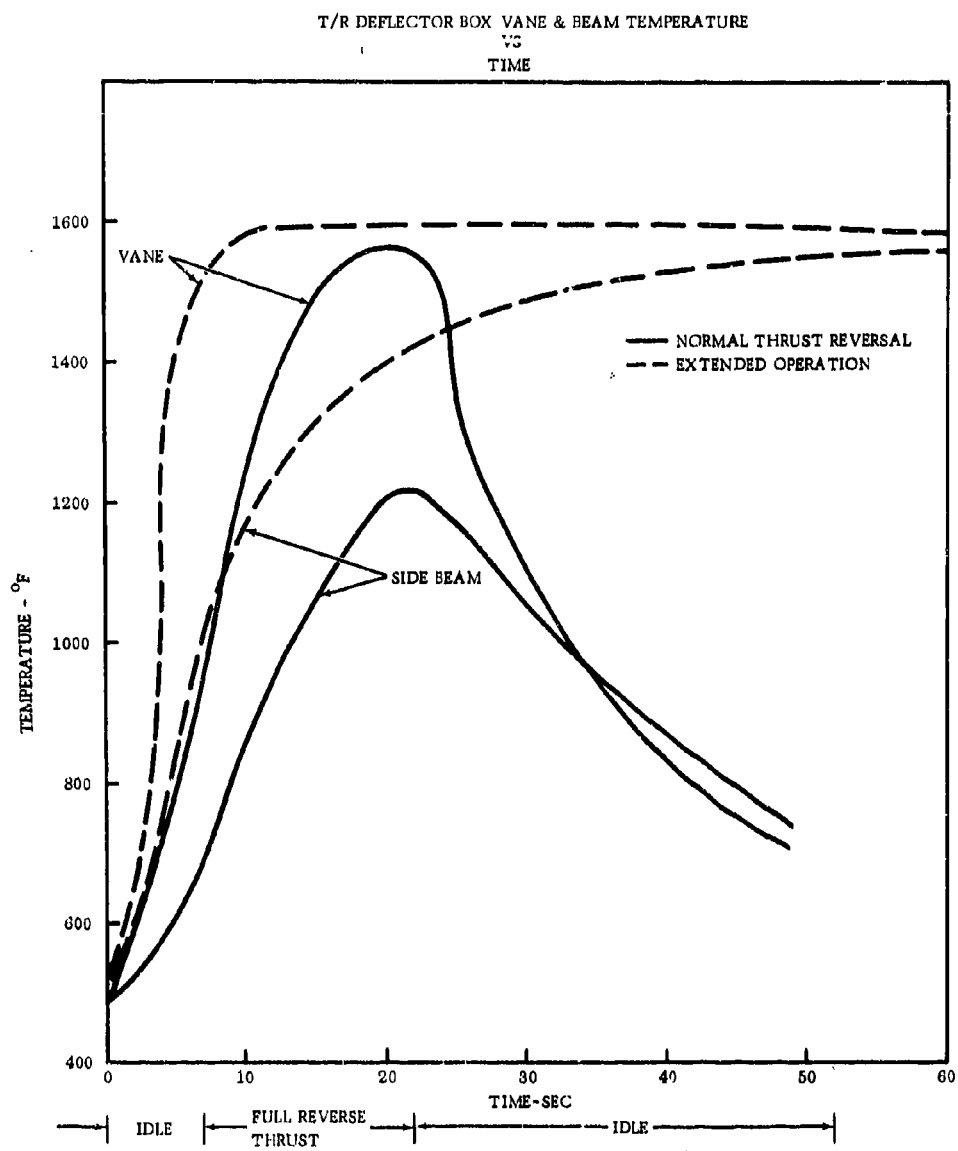


Figure 6-40 CASCADE BOX, VANE AND BEAM TEMPERATURES

beams, and an adapter ring section which connects to the tailpipe. The 16 support beams provide the connection between the secondary nozzle shroud and the exhaust duct adapter. This general arrangement is shown by Figure 6-13. These beams provide the tangential support for the primary nozzle hinge-ring in both forward- and reverse-thrust positions.

Each of the beams incorporates an aft stop for the hinge-ring in the reverse-thrust position. The stop is a simple radial inward protrusion of the beam body illustrated in Figure 6-41.

The exhaust casing adapter design is illustrated in Figures 6-42 and 6-43. The 16 axial beams are joined to the adapter by a cast-and-welded transition joint. This provides a gradual change from axial to circumferential structural members. The adapter inner flange is bolted to the exhaust duct aft flange. Differential thermal gradients between the duct and adapter beam assembly are accommodated by deflections in the flange joint, in the adapter cone, and in the axial beams between the adapter and shroud.

#### 6.5.2.3.1 Design Criteria and Stress Analysis

The basic frame structure, consisting of secondary nozzle shroud, axial beams, and adapter, is analyzed for stress and deflection. Analysis is made by utilizing two digital computer programs: (1) MASS - a digital computer program for static and dynamic analysis of general structures, and (2) PAPA - a digital computer program for the static and dynamic analysis of structures made up of plate and panel elements.

In this analysis, the entire structure is modeled to the computer program by utilizing sections of straight and curved beams and panels. Gas load forces, maneuver load forces, and thermal differences are applied to the structure for computer analysis; forward and reverse thrust load conditions are calculated. Results obtained consist of uniaxial stresses and deflection. Combined, effective stresses are then calculated and compared to allowable working stresses. (Refer to Section on nozzle summary for general design criteria.)

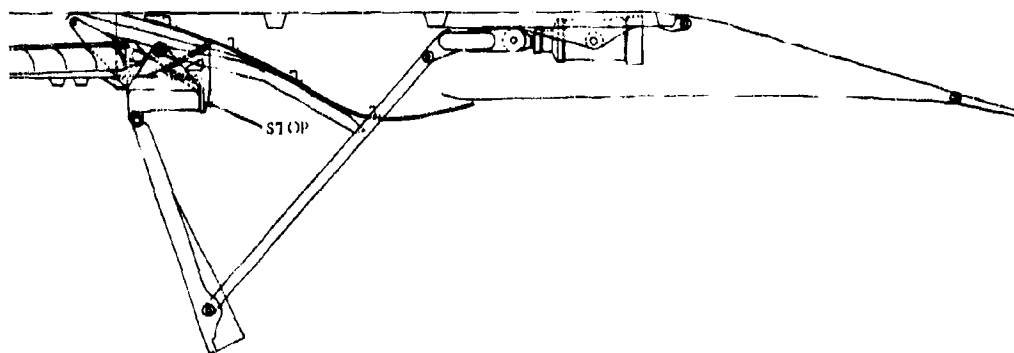


Figure 6-41 HINGE RING STOP

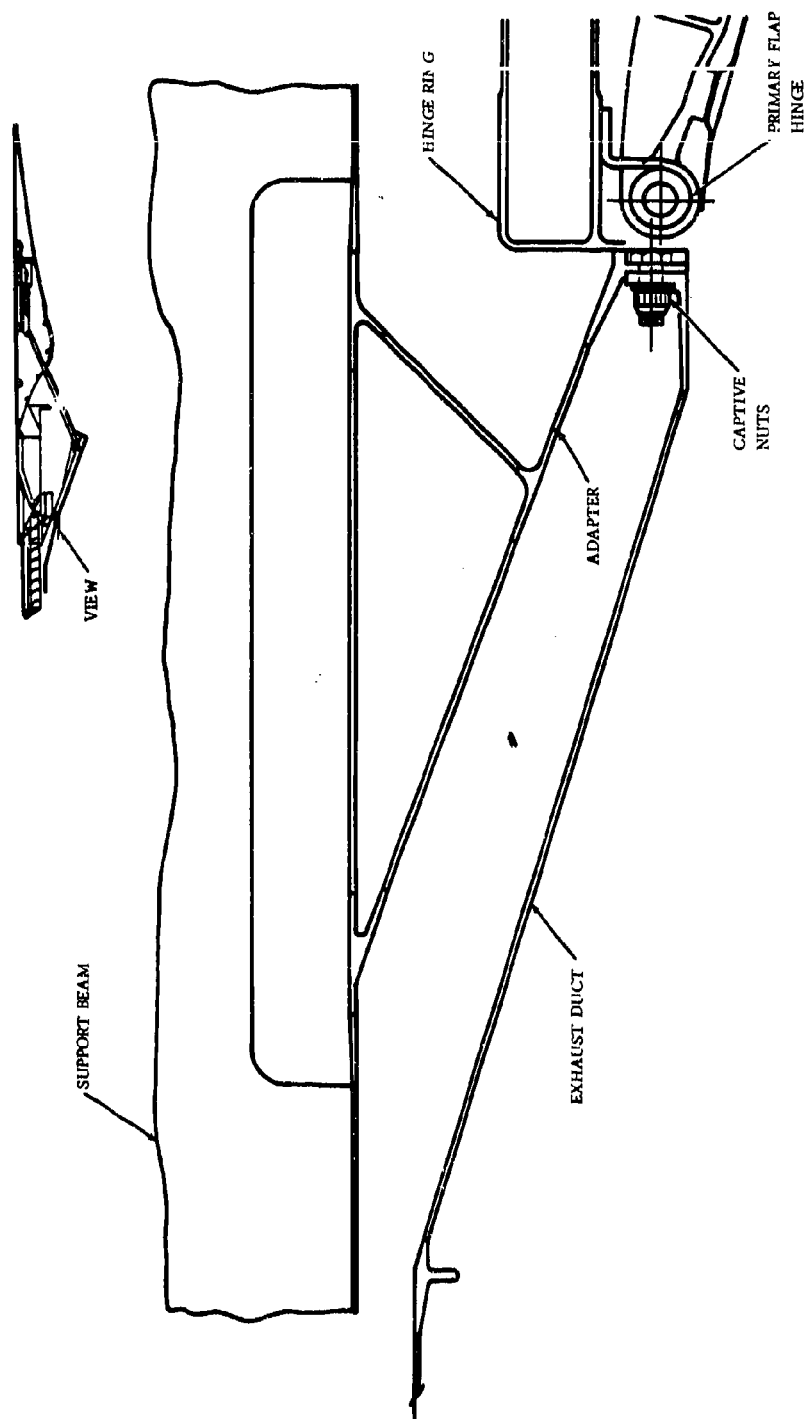


Figure 6-42 ADAPTER DETAIL



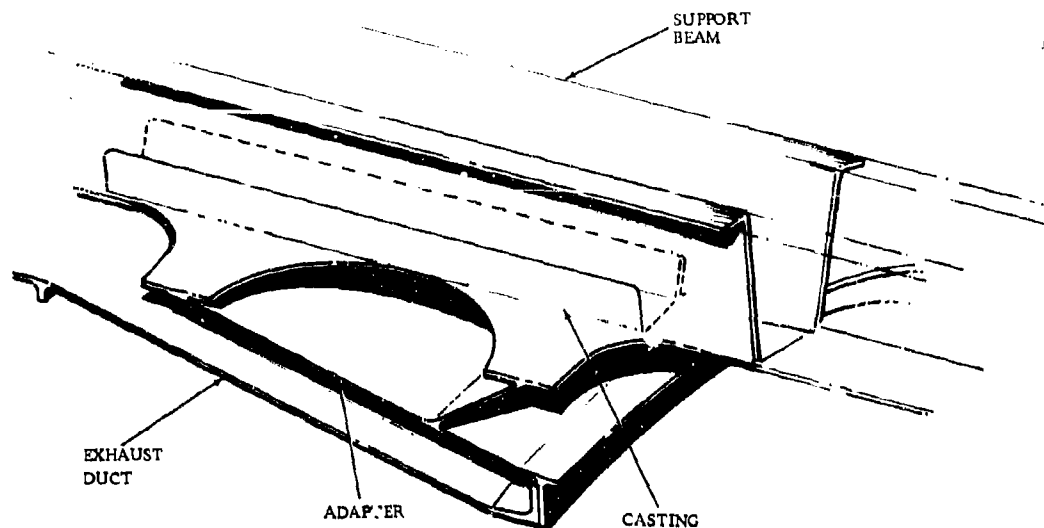


Figure 6-43 ADAPTER, BEAM, EXHAUST DUCT ATTACHMENT

### 6.5.3 SECONDARY NOZZLE

The secondary nozzle is comprised of 16 sets of flaps and seals assemblies supported by a fixed shroud illustrated in Figure 6-44. No alternatives are required to move the flaps to vary because of the previously described aerodynamic positioning concept.

#### 6.5.3.1 Outer Flap and Seal

The peak operating temperature of the outer flap and seal is 900°F. This limit is based on heat transfer analysis coupled with correlations with J93 experimental results obtained from XB-70 flight-test instrumentation, as well as from extensive testing at AEDC. Inconel 718 material has been selected for its excellent strength properties coupled with relatively low cost, good weldability, and repairability. Recent modification of the heat-treat cycle has resulted in improved yield strengths that are 15 percent higher than René 41. On a strength: weight ratio it is equal to titanium alloys in yield properties, but is superior in creep strength. This relationship is shown in Figure 6-45, which compares Inconel 718, René 41 and titanium (Ti 679) on the basis of a strength to weight ratio. Strength is defined as the allowable working stress, which is the average material property minus the three sigma deviation limit. In choosing the working stress, an average design temperature of 750°F was used as representative of engine cruise conditions; a total part life of 36,000 hours was a condition. The 0.2-percent yield strength is shown for all three materials. The 0.2 percent creep strength is shown for titanium only; creep strengths for Inconel 718 and René 41 are greater than their respective yield strengths. The same trend in relative material properties continues up to the 900°F peak expected operating temperature. Inconel 718 remains superior to René 41; however, the allowable stress/density for titanium drops quickly as temperature increases.

The aerodynamic loads imposed on the outer flap are a combination of the pressure differential across the outer surface (10 psi maximum) and an end load applied at the aft hinge that results

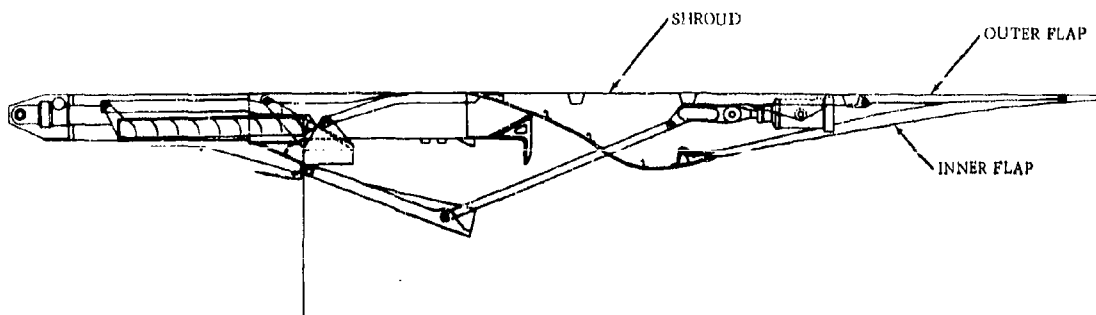


Figure 6-44 GE4 SECONDARY NOZZLE CONFIGURATION

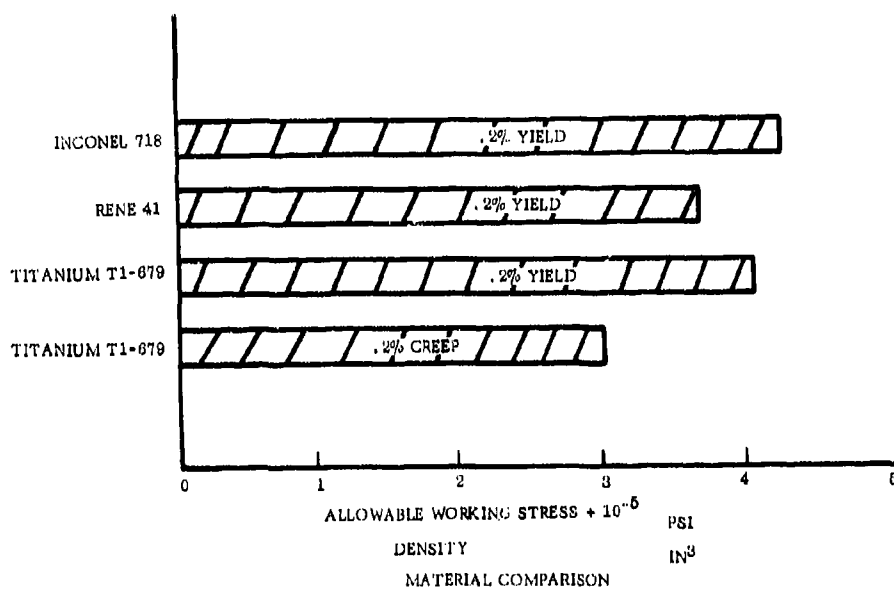


Figure 6-45 MATERIAL COMPARISON

from the pressure loading on the inner flap. This loading is illustrated schematically in Figure 6-46. The hinge loads and flap bending moments are determined from the exhaust nozzle load computer program. With the addition of the maneuver load effects, the required section properties of the flap are determined.

The exhaust nozzle computer program was used to calculate nozzle loads with the aerodynamically-positioned secondary nozzle. The program uses two types of input:

- Variable

Primary Nozzle - Area

Total Pressure

Total Temperature

Flight Mach Number

Altitude Ambient Pressure

Secondary Pressure or Weight Flow

- Fixed Input

Nozzle Linkage Kinematics

Dimensionless

Characteristics of:

Nozzle Pumping of Secondary Air

Divergent Flap Pressures

Outer Flap Pressures

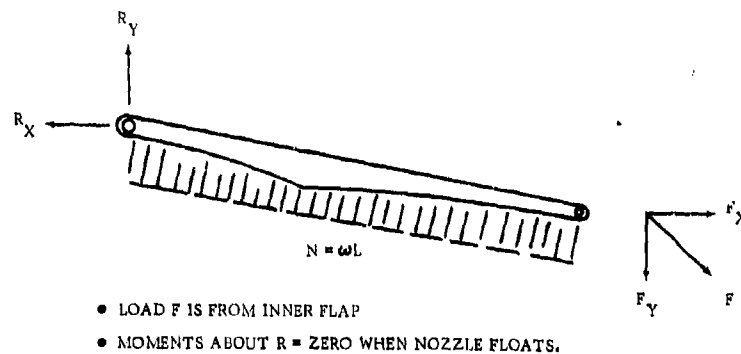


Figure 6-46 OUTER FLAP LOAD ANALYSIS

The program initiates the calculation with the secondary nozzle at minimum area, and the flap pressure calculations are based on the secondary pressure or weight flow (pressure limits are based on nacelle pressure limiting doors). The flaps are checked for equilibrium. If the flap system is found to be out of equilibrium the calculation is repeated with the nozzle at maximum area. The program iterates until the nozzle is in equilibrium or at the open or closed area limit.

With the flight position of the secondary nozzle defined, the secondary total pressure, the divergent flap static pressure distribution, and the outer flap static pressure are established. The pressure/area information is integrated over the inner and outer flap surfaces, which establishes the flap loading. The flap bending moments are calculated at 40 positions along each of the flaps, and are used to size the flap structure. The reaction loads at the ends of the flaps are the loads applied to the links and shroud. These are used for the stress analysis of the link and shroud.

Due to the relatively low operating temperature of the outer flap and seal the 0.2-percent yield strength is the design criterion. A 25-percent safety margin on allowable stress is used, and 100°F is added to the peak calculated temperature for additional margin of safety.

The well proved analytical techniques used to define the flap loads at each axial station permit the design of a mechanically efficient, simple outer flap structure. The embossed plate and beam construction approach illustrated in Figure 6-47 which is a photograph of the J79-10 outer flap, has been applied to the proposed design. The aerodynamic positioning concept in conjunction with the high auxiliary flow capability (for sound suppression) has substantially simplified the secondary nozzle by elimination of such components as actuating rings and links, and gap scheduling linkage.

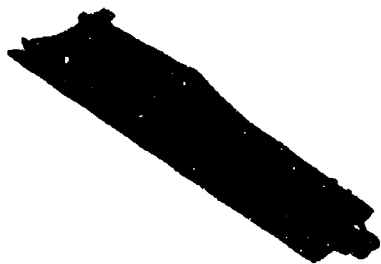


Figure 6-47 J79 OUTER FLAP

### 6.5.3.2 Inner Flap and Seal

The peak temperature of the secondary inner flap and seal is 1360°F and occurs at the Power Setting 1 - SLS operating condition. René 41 material is selected for these components because of its excellent strength in this temperature range. The aerodynamic loads imposed on the inner flaps and seals result from the pressure differential between secondary air pressure and the exhaust pressure in the expanding jet. The nozzle load computer program described earlier is used to determine hinge loads and bending moments. The design and analysis are similar to those used for the outer flap and seal. The secondary inner flap and seal are constructed with a transverse step slot that forms a cooling slot midway along the flap and seal inner surface. This detail is shown in figure 6-48.

Because of the higher operating temperature of the inner flap and seal during afterburner operation, stress rupture is the limiting the design criterion. The same stress and temperature margins described for the external flap are employed.

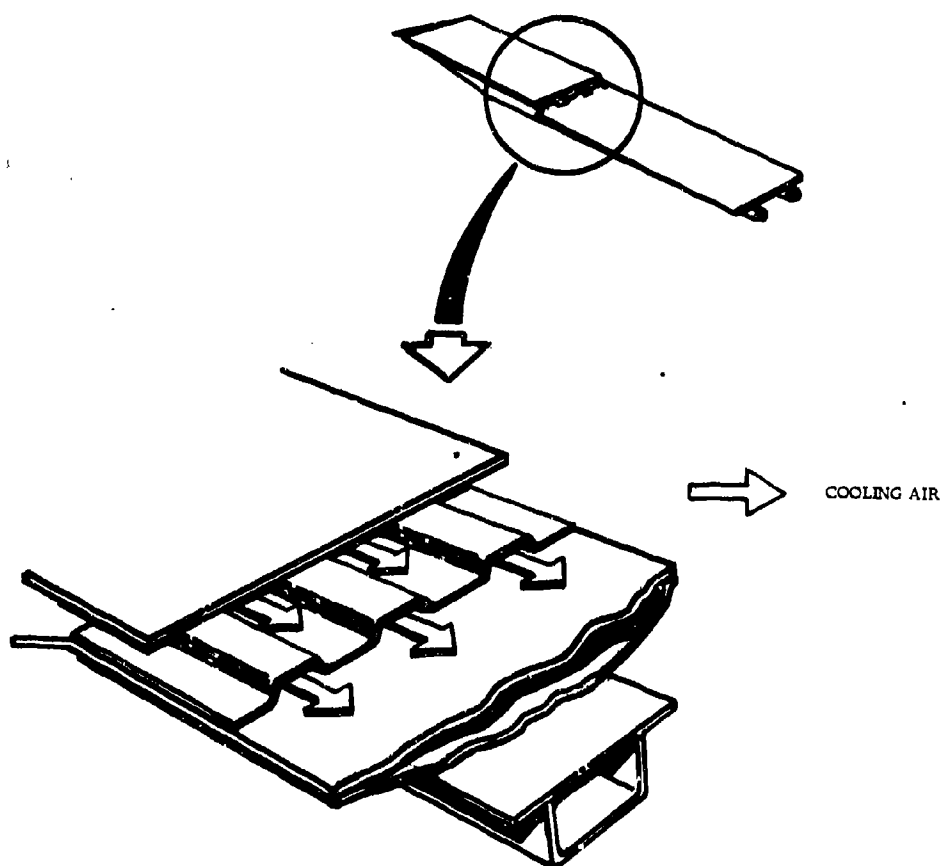


Figure 6-48 INNER FLAP COOLING

Because of the higher operating temperature of the inner flap and seal during afterburner operation, stress rupture is, the limiting design criterion. The same stress and temperature margins described for the external flap are employed.

#### 6.5.3.3 Shroud

The secondary nozzle shroud is a fixed cylindrical shell structure that forms the outer surface of the nacelle forward of the variable flaps, the aft inlet ramp of the second-stage ejector inlet, and the forward section of the diverging nozzle. The shroud supports the variable secondary flaps and the primary nozzle actuating ring, and is supported from longitudinal beams of the frame assembly. This general configuration is illustrated in Figure 6-44.

The shroud is basically a sheet-metal fabrication. Castings are used at the mounting hinges for the flaps and at the beam attachment points. The four primary nozzle actuators are clevis-mounted on the shroud.

Access panels on the outer surface of the shroud are provided for access and adjustment of the primary nozzle actuators. The shroud construction consists of a sheet metal outer cylinder with internal circumferential hat-section stiffeners and longitudinal beams. A sheet metal cone with circumferential Z-stiffeners form the inner surface. The construction of the secondary nozzle shroud is shown in Figure 6-49.

The loads imposed on the shroud structure are secondary flap hinge and link loads, pressure differential across the outer shell (10 psi maximum), pressure differential across the inner wall, and flight maneuver loads ( $6g$  vertical and  $9g$  horizontal). The secondary flap hinge and link loads and the exhaust static pressure distribution along the diverging wall are determined over the flight spectrum by the nozzle computer program. In addition, a digital computer program for static and dynamic analysis of general structures (MASS) is used in the stress analysis of the shroud structure.

The outer shell and stiffening members of the shroud have a maximum temperature of  $900^{\circ}\text{F}$ . Inconel 718 material is selected for these members, which are designed to the 0.2-percent yield strength with a 25-percent margin on stress and  $100^{\circ}$  margin on temperature. The inner diverging surface, attains a temperature of  $1350^{\circ}\text{F}$  during maximum augmentor operation. Hastelloy X material was chosen for the internal surfaces, for its excellent oxidation resistance. High tensile strength or stress rupture properties are not required, since the critical load condition is buckling.

#### 6.5.4.4 Ejector Inlet/Cascade Cover Doors

The auxiliary air inlets for the second-stage ejector also serve as the cascade covers for the thrust reverser. This inlet system is composed of 14 sets of double doors, equally spaced on the basis of 16. The inlets have been omitted in the two o'clock and ten o'clock positions, which correspond to the typical wing/nacelle juncture. Figure 6-37 is a cross-section schematic which illustrates the inlet door arrangement. It also identifies the 11 positions that correspond to the thrust reverser exits.

Each inlet door is a double-hinged configuration (Figure 6-50) to provide the required inlet angles for high-performance air induction. The doors are designed to provide an initial inlet ramp angle of 10 degrees and a final angle of 22 degrees at the maximum open position. These inlet doors are actuated by secondary pressure, and remain open at flight speeds from sea level up to flight Mach number ( $M_p$ )  $\sim 1.2$ . Each set of doors is mounted on the nozzle/reverser hinge-ring (as illustrated in Section 6.5.2.) and is moved aft with the thrust reverser to uncover the reverser exits.

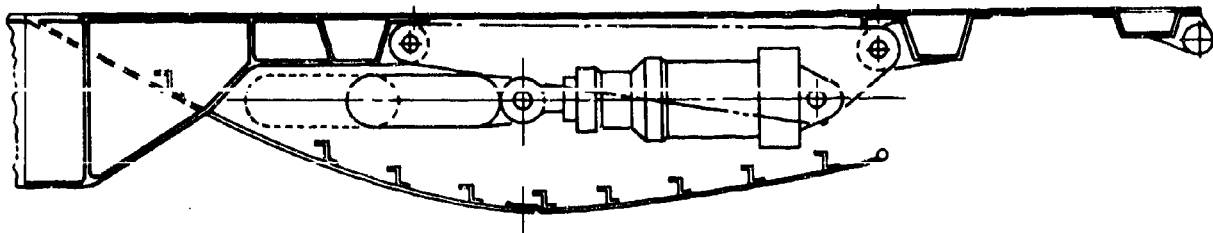


Figure 6-49 SHROUD

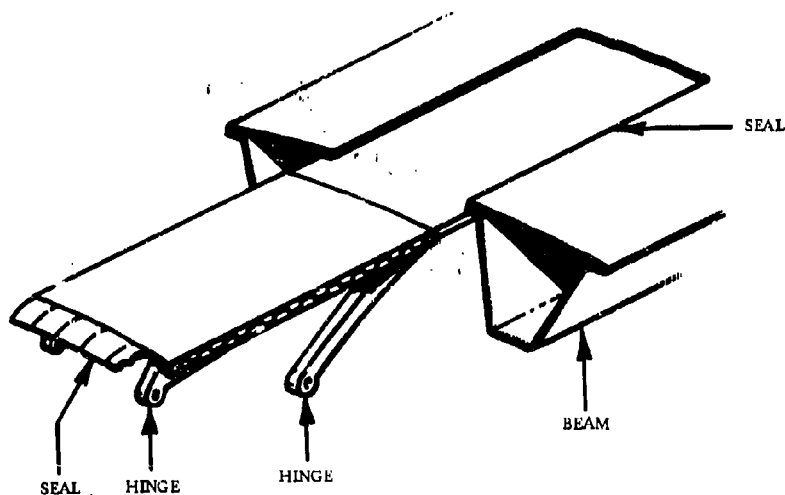


Figure 6-50 INLET DOORS

The mechanical design of the inlet door is like that of the external secondary flaps. The design approach is depicted by Figure 6-50. The doors are constructed of sheet metal with cast hinge elements. The door panels are stiffened transversely by a corrugated sheet that is resistance-welded to a smooth outer skin. Longitudinal ribs are attached to the doors to support the hinges. The pressure loads on the inlet doors are determined by nozzle scale-model tests. This data is programmed in the nozzle load computer program for determining door position and pressure differential at all flight conditions. On the basis that these doors have essentially one sealing position, it is concluded that the leakage problem is substantially less than that in the external flaps which must seal effectively over a range of seal positions with secondary flap radial movement. During operation with these inlets closed, the seals are forced against a lip on each side of the support beams by secondary pressure. Replaceable seals and hinge bushings are provided for maintainability.

The Inconel 718 door material was selected on the basis of the low operating temperature. This material is the best choice for strength: weight ratio as previously described in the secondary external flap discussion.

## 6.6 MAINTAINABILITY

Heavy emphasis has been placed on maintainability in the design of the GE4 exhaust nozzle and thrust reverser assembly. Complete accessibility for inspection and component replacement has been provided so as to permit on-condition, on-aircraft maintenance as opposed to fixed-time overhauls for this assembly. General Electric turbojet nozzles in military service are currently maintained in this fashion, with repairs performed on an as-required basis.

It is possible to inspect all nozzle components of the GE4 engine on the aircraft. It is also possible to replace most parts without removal of the engine from the aircraft. Further, replacement of the complete assembly on the aircraft can be performed easily and quickly. A minimum amount of ground handling equipment and only standard mechanics tools are required to perform all maintenance. The reverser/nozzle actuation system can be checked and rigged by means of a ground hydraulic supply cart.

Specific maintainability features for the three major components of the nozzle/reverser assembly are as follows:

### Primary Nozzle

- Flaps, seals, heat shields, hinges and links replaceable on aircraft.
- All pivot points have replaceable bushings.
- Cast flaps protected by low-cost heat shields.
- Clips on the flaps to attach the heat shield are replaceable.
- Thrust washers are provided on all journals.
- S-Monel bushings and Rene 41 pins result in maximum bearing life.

### Thrust Reverser

- Cascade boxes are interchangeable and replaceable by removing one bolt.
- Cascade boxes can be assembled only one way.
- Low bearing stresses eliminate the need for lubrication of pivot points.
- Replaceable wear-strips on reverser track.
- Actuators are accessible for inspection and replacement while installed.

### Secondary Nozzle

- Flaps and seals are interchangeable and replaceable on the aircraft.
- Individually replaceable auxiliary air inlet doors.
- Access panel in shroud for primary nozzle actuators.



- Bushings in hinge pivot points.
- All sheet materials are repair weldable.

A Durability and Maintainability Analysis has been conducted on the major components of the nozzle and reverser assembly section and is contained in a special appendix entitled "GE4 Durability and Maintainability Analysis", which is available on request as back up material to the substantiating data submitted. The purpose of this analysis is to make sure that all aspects of maintainability have been given full consideration in the design of the component. For each potential failure mode, the following information is given:

- Design features to minimize likelihood of failure.
- Design features that make the maintenance easy to perform.
- Method of repair.

In addition, the technique for monitoring the condition of the component in service is given, along with diagnostic means to isolate the deterioration or failure. Finally, the frequency of checking the parameter is given; information for this column will be determined during the GE4 development program.

#### 6.7 RELIABILITY

Commercial reliability is being assured for the exhaust nozzle and thrust reverser by the application of the following criteria:

- All parts affected by stress rupture are designed for twice the required life, with a 1.25 to 1 factor of safety.
- Stress analyses are made with temperature 100° F higher than predicted.
- Minimum material properties and thickness are used in stress analysis.
- Parts designed for buckling have a factor of safety of two.

Significant design improvements in the GE4 exhaust nozzle and thrust reverser will increase reliability.

- Actuation loads are transmitted to sturdy beams and rings (See Figure 6-30.)
- Simplification of design, and reduction of number of parts by combining functions.
  - Primary nozzle flaps vary throat area for forward thrust and act as blocker doors for reverse thrust. (See Figure 6-11.)
  - Second-stage ejector air inlet doors also serve as cascade covers. (See Figure 6-11.)
  - Translating hinge ring is also the manifold for primary nozzle cooling air distribution. (See Figure 6-34.)

- One simple actuation stroke provides translation of primary nozzle flap, air inlet door and cascade box for reverse thrust. (See Figure 6-11.)
- Secondary nozzle shroud and reverser frame are integrated into one static structure. (See Figure 6-31.)
- Axial beams of the reverser frame provide a mounting support for the reverser actuator.
- Secondary nozzle flaps and seals combined
- Aerodynamic positioning eliminates need for actuation system and attendant linkage.
- Positive discharge flow angle control during reverse thrust by virtue of multi-vane cascade boxes ensures consistent magnitude of reverse thrust.
- One-piece castings are used for cascade boxes, primary flaps and primary seals. (See Figures 6-19, 6-39.)
- Actuators are mounted directly on the reverser structure for favorable thermal environment, elimination of separate mounting brackets, and freedom for circumferential and radial deflection.
- Stability of secondary flap position ensured by use of balance of secondary air and cycle pressure on pinned inner and outer flap, as opposed to single-pinned secondary flap.

#### 6.8 QUALITY ASSURANCE

The proposed exhaust nozzle and thrust reverser components are produced with conventional welding, casting, forming, and machining operations and process methods that have produced parts of high quality on all General Electric engines. Specific designs or processes that increase the operational quality of the parts are:

- Maximum use of repeatable butt-welds rather than seam welds to eliminate hidden joints.
- Use of ASTM radiographic inspection standard for key structural joints.
- Use of tape-controlled resistance welds.
- Design reviews are made with quality engineering function before release to processing.

#### 6.9 SAFETY

Safe nozzle operation is achieved primarily by applying dependable well-proved design pictures and design criteria to all elements of the nozzle. Special attention has been given to key areas that affect safety. These areas include:

- The maximum force level of the thrust reverser has been limited so that inadvertent actuation of the thrust reverser during augmentor operation will result in no movement of the blocker.
- A residual force on the reverser actuator ensures that the hinge-ring remains in contact with the exhaust duct. This is in addition to a latch mechanism built into the actuator.

- The nozzle will function properly without the compressor cooling air in the event of a duct failure, but some reduction in life will occur if extended operation were to take place before the failure was discovered.
- Primary seals are positively retained by the flaps - not subject to disengagement from the flap by deflection or distortion.
- In the event of hydraulic failure, the thrust reverser blockers remain in the committed position.

#### 6.10 FAILURE ANALYSIS

A failure mode and effects analysis (FMEA) is being completed on the exhaust nozzle design. Specific component on engine overstress margin on vibrational test requirements will be established to evaluate the effectiveness of the design in order to eliminate or reduce the failures determined by the FMEA.

Significant General Electric experience on turbojet exhaust nozzle and thrust reversers was investigated by a special task force. Problems affecting in-flight power loss, in-flight shutdown, delay reliability, UER and high maintenance were examined. These problems were then classified according to primary source of difficulty i.e., controls, exhaust nozzle and thrust reverser parts on system effects. More important problems were then compared to related GE4 designs, and recommendations were made to eliminate or reduce the possibility of the occurrence of similar problems on the GE4. Additional failure analyses to be conducted on the augmentor are described in Volume IV, Reliability.

#### 6.11 VALUE ENGINEERING

A team including representatives of Manufacturing, Design and Evaluation Engineering, and Purchasing has continuously reviewed the design to ensure that low-cost designs that can be produced with high quality are provided. Some of the primary features included for low cost are:

- Combining functions in a single part or system, already reviewed under reliability.
- Improvements in conventional welding methods, such as using automatic techniques and special fixturing.
- Designing for rolled pre-shaped sections in the hinge and actuation rings.
- Simplified castings are used for primary flaps and seals and thrust reverser cascades.

#### 6.12 HUMAN ENGINEERING

Extensive design reviews are carried out, as well as trial assemblies and operation with mockups, molds, and actual parts, to make sure that designs can be satisfactorily assembled and operated by the personnel involved with the SST.

- Stop-bolts are provided where necessary at pivot and hinge points to prevent binding.
- Blind assembly points, e.g. rabbets, bolt and nut attachments, have been reviewed and eliminated.

- Means have been provided to ensure that rollers, seals, hinges, and other similar parts, must be put on right-side-to and right-side-up.
- Accessibility has been provided to adjust actuator strokes and stops.

### 6.13 STANDARDIZATION

In addition to the practice of using national, military and General Electric standard parts wherever possible, special design considerations have been made for standardization in the exhaust nozzle and thrust reverser parts. All flaps, seals, linkages, pins, bushings, rings and other components are fully interchangeable. In no case is a matched sets of parts necessary for performance on mechanical assembly.

### 6.14 DEVELOPMENT STATUS

#### 6.14.1 FULL-SCALE COMPONENT TEST

The primary nozzle has been on test since early June on the GE4 test simulator at the General Electric outdoor test site near Peebles, Ohio. During the evaluation of the system performance of the augmentor, the metal temperatures of the nozzle were measured for comparison with calculated values and compressor discharge airflow rates, and distributions were compared with design intent.

The flaps, seals, shields, links and rings were mounted on the exhaust duct as shown in Figure 6-51. The simulator was operated over a range of nozzle inlet temperatures up to 3140° F, which is 200° F above the maximum rated exhaust gas temperature. The compressor discharge air (supplied by a separate J79 engine) was supplied to the system at the proper flow and inlet temperature (1.5 percent flow at 600° F). The flap, seal, and shield temperatures were recorded during operation over the full range of dry and augmentor operation.

Evaluation of the data showed that the flap, seal, and shield temperatures were approximately as predicted by the analysis. The test also confirmed that the compressor discharge air was highly effective in cooling the seal; this results in a low seal temperature. The specific test data are included in Section 7, Volume III-B, Cooling.

Detailed examination of the Peebles test hardware has shown no deterioration of the nozzle's component parts. No thermal distortion or buckling has taken place on the shield, and disassembly can be made without difficulty. The flap and seals continue to operate freely and without any apparent binding, as evidenced by the fact that actuator forces have remained constant throughout the testing. Nozzle actuation is smooth, responsive, and free from hang up. There is no local thermal or mechanical distress exhibited on any of the parts.

#### 6.14.2 PRIMARY FLAP COMPONENT TEST

(Note: This test is still in progress at the date of this writing.) The primary flap component test was conducted to evaluate the stress and deflection characteristics of the flap when the part is subjected to simulated gas loads.

The flap was mounted in a suitable test fixture which duplicated normal mounting in the engine. The flap base was loaded to simulate the gas pressure-differential across the flap. Loading the flap in such a fashion imposes stresses and deflections that are identical to those encountered on

the engine. Loads were applied from 0 to 100 percent in progressive increments to establish the point at which permanent set is induced. After 100 percent load was applied, the loading was continued to establish the ultimate capacity of the system.

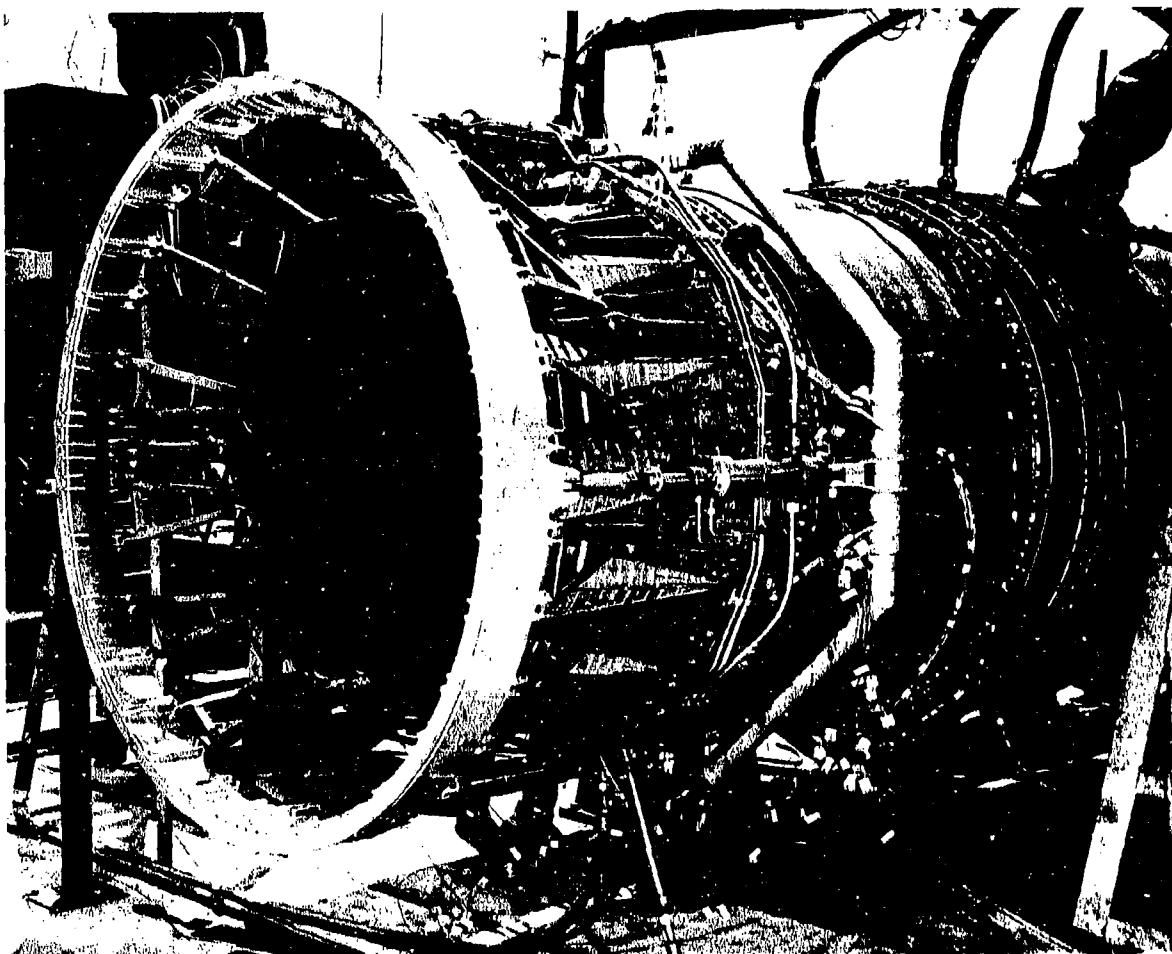


Figure 6-51 NOZZLE TEST AT PEEBLES

6-000-66

## 6.7 NOZZLE/REVERSER MECHANICAL DESIGN SUPPLEMENT

### 6.7.1 BOEING DESIGN SUPPLEMENT

The exhaust nozzle for the Boeing SST aircraft is a two-stage ejector nozzle, including a thrust reverser and sound suppressor. The characteristic dimensions are shown in Figure 6-52. The external shape of the nozzle shroud is a basic four degree conical surface, originating at the 74.2-inch diameter exit and extending forward approximately 121.5 inches to clear the tertiary inlet door mechanism. The external shape is then modified to conform to the forward nacelle cone at a plane 148 inches forward of the nozzle exit. At the 148-inch plane, provisions are made for alignment of the shroud, a thermal expansion allowance and a secondary air seal. Details of this arrangement are shown on Installation Drawing No. 4013019-471. (Refer to Volume III-D.)

Figure 6-53 illustrates the tertiary inlet arrangement and the thrust reverser discharge arrangement. Eleven of the tertiary inlets serve the dual purpose of reverser discharge openings. The proposed thrust reverser discharge arrangement is preliminary, pending a definition of radial thrust balance requirements and reingestion requirements. Figure 6-54 illustrates the Boeing aircraft exit door requirements.

A maximum boattail angle of 15 degrees relative to the four degrees cone has been incorporated. The projected boattail area is the same as the GE4 Phase III nozzle proposal.

Figure 6-55 is a schematic of the nozzle showing the internal flow path for the three principle modes of operation. Weight additions for this nozzle have been included in the GE4/J5P engine weight summary, Volume III-A.

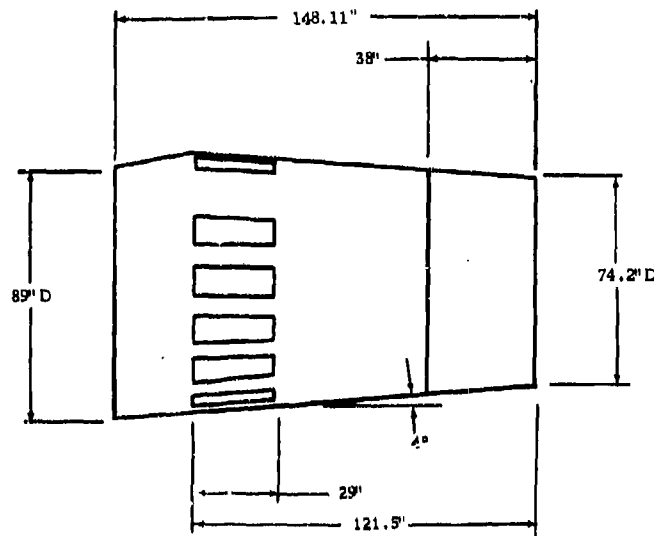


Figure 6-52(B). Exhaust Nozzle and Thrust Reverser Configuration

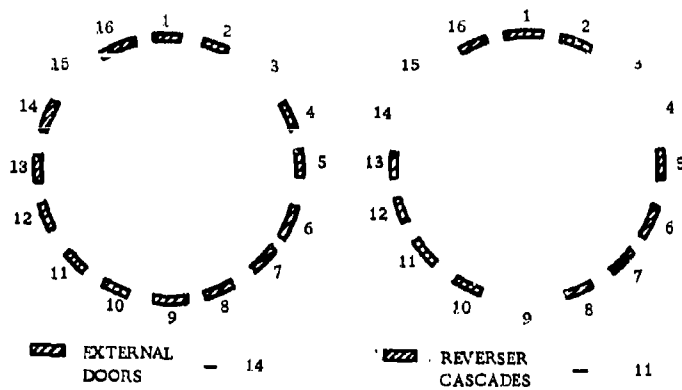


Figure 6-53(B). External Doors on Reverser Cascade

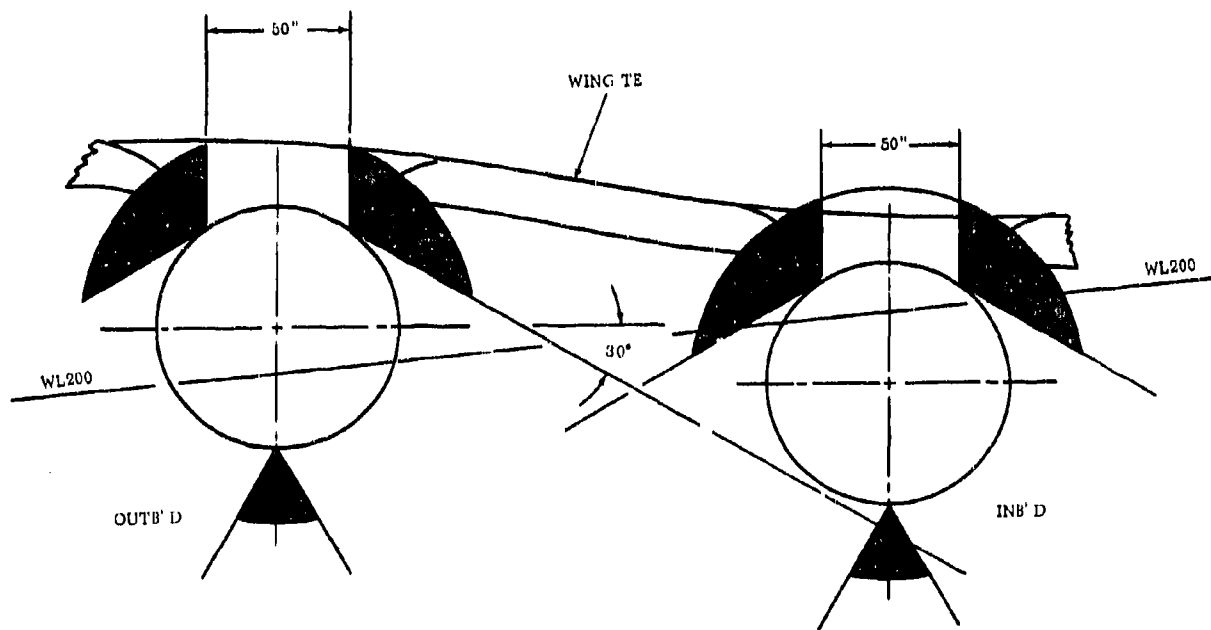
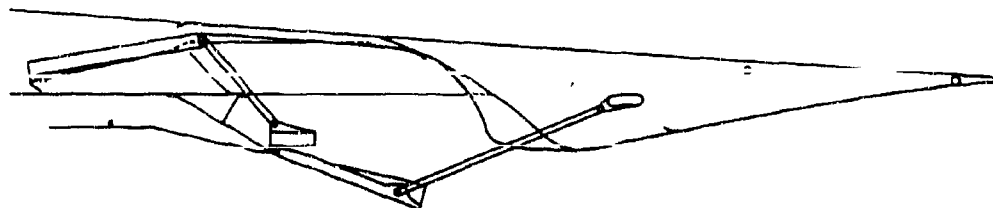
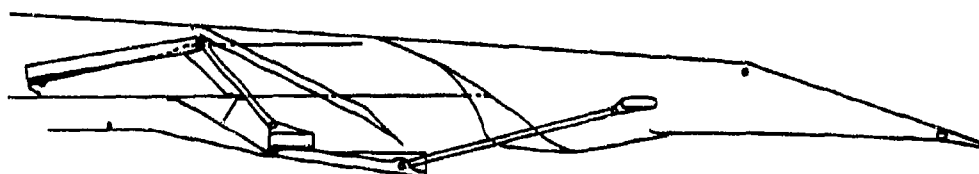


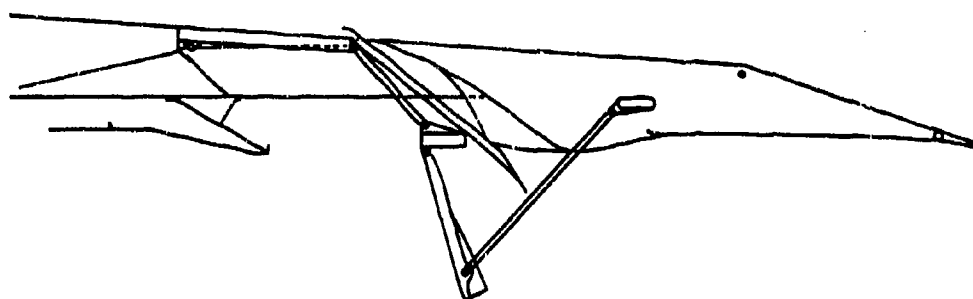
Figure 6-54(B). Thrust Reverser Exit Requirements



SUPERSONIC



TAKE OFF



REVERSE

Figure 6-55(B). Exhaust Nozzle and Thrust Reverser

6-69/6-70

K



## **6.7 NOZZLE/REVERSER MECHANICAL DESIGN SUPPLEMENT**

### **6.7.2 LOCKHEED DESIGN SUPPLEMENT**

The exhaust nozzle and thrust reverser for the Lockheed SST aircraft will be as described in the foregoing paragraphs, except that the thrust reverser cascades and external door arrangement will be as shown in Figure 6-56(L).

REVERSER DISCHARGE OPENING LOOKING FORWARD

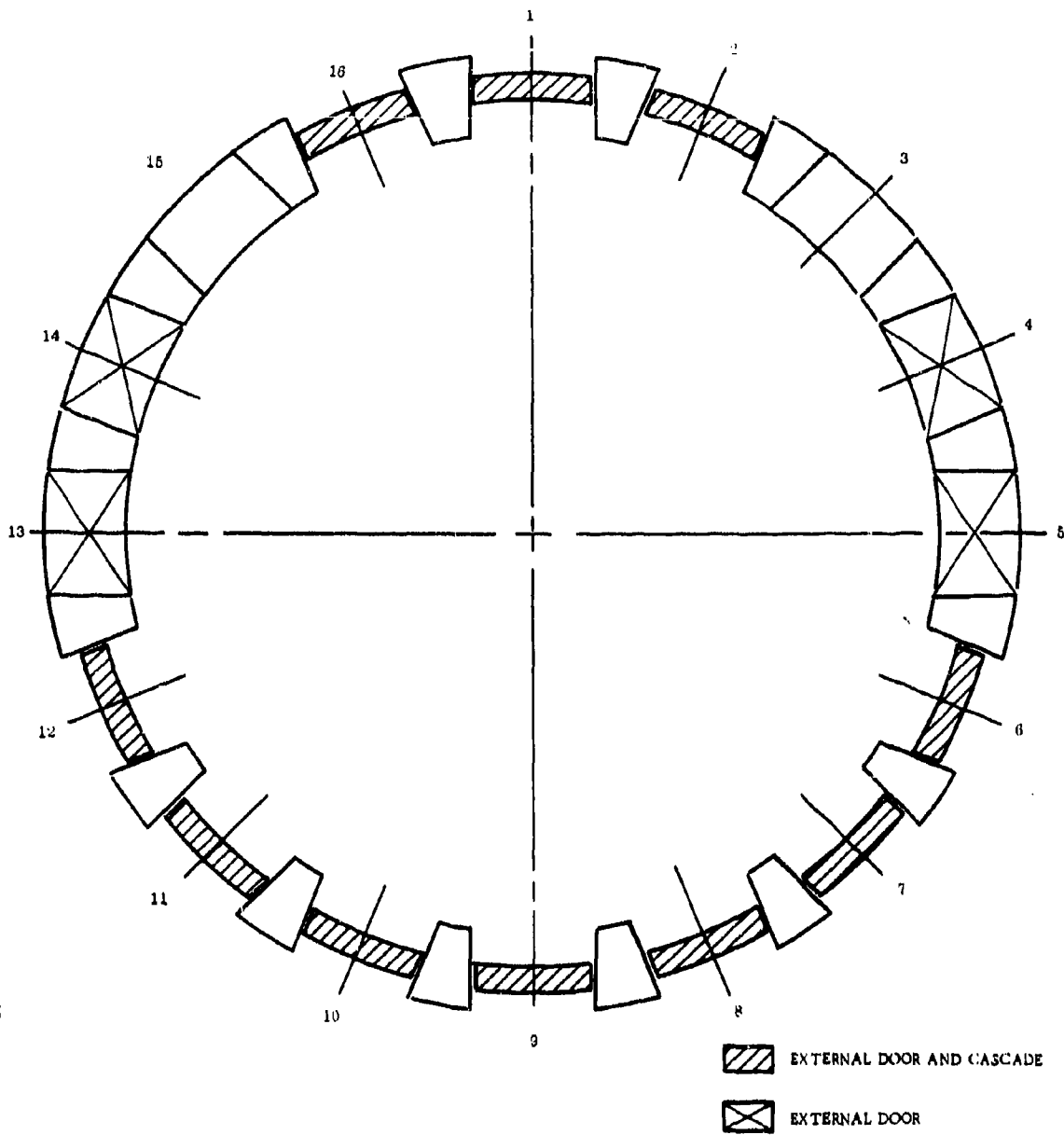


Figure 6-56(L). External Door and Reverser Cascade Arrangement

## 7. AUGMENTOR AND EXHAUST NOZZLE COOLING

### 7.1 INTRODUCTION AND SUMMARY

The relatively high gas temperature in turbojet augmentors and exhaust nozzles requires an effective cooling design for the combined characteristics of high performance and long endurance life. All augmented turbojets now in service are cooled internally by using a portion of the turbine discharge gas stream for film-cooling the exhaust duct and primary nozzle, and externally by secondary air as shown in Figure 7-1. The well established concepts of film-cooling, the addition of cooling liners or shields to protect structural parts, and techniques of distributing augmentor fuel selectively to obtain low convective heating at the combustion boundaries have been proven by demonstration on the J79 and J93.

Substantial improvements in the proven cooling methods are utilized in the GE4 design to keep metal temperature well within the selected materials capability to ensure commercial augmentor durability.

Important differences in the GE4 augmentor cooling are:

- Continuous slot liner design as used in the J93 instead of the spaced design used in the J79 as shown in Figure 7-2.
- Dilution of the turbine discharge gas used for liner cooling with compressor seal leakage air.

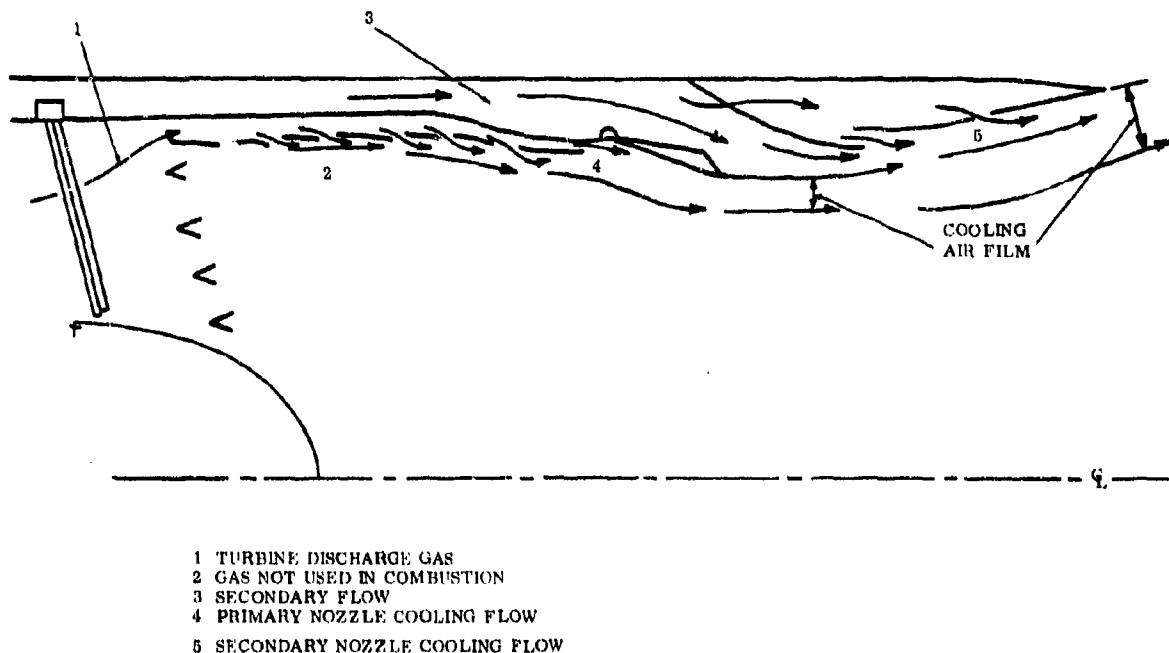
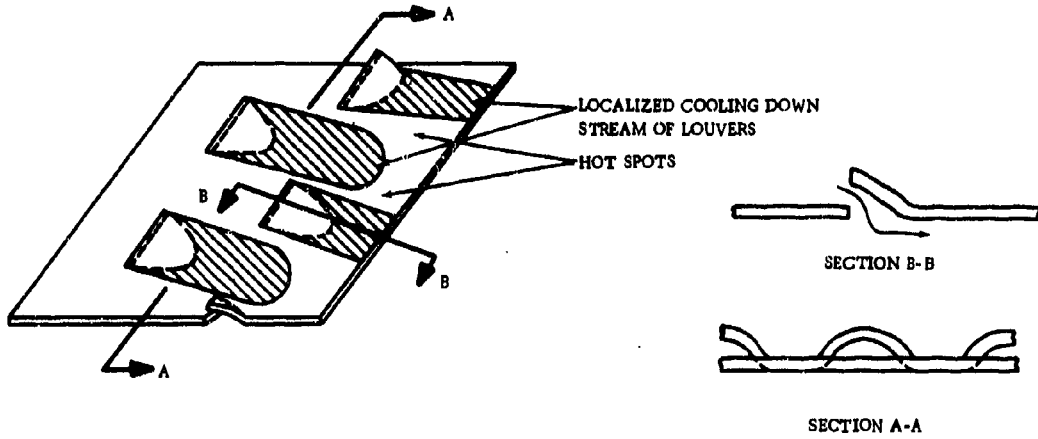


Figure 7-1. AUGMENTOR AND EXHAUST NOZZLE COOLING SYSTEMS

LOUVERED LINER J85 - J79



SHINGLED SLOT LINER J93

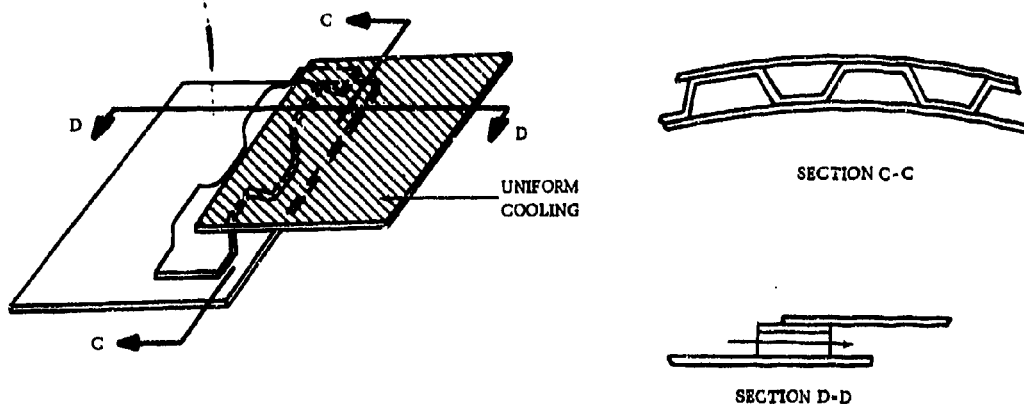


Figure 7-2. AUGMENTOR COOLING LINER SLOT CONFIGURATIONS

- Fuel distribution that effectively avoids combustion in the region close to the augmentor cooling liner, especially at the long-time cruise condition when operation is limited to the inner two flameholder rings. Figures 7-3 and 7-4 show the effectiveness of the cooling improvements.

Figure 7-3 shows that the maximum liner metal temperature increase over non augmented operation for the GE4 will be 177°F as compared to 265°F for the J93 and 480°F for the J79.

Effective shielding of the exhaust duct and the duct's relative insensitivity to augmentor gas temperature is shown in Figure 7-4. The structural augmentor casing has a maximum temperature of 1450°F, 200°F lower than the non-structural cooling liner.

The effectiveness of the augmentor liner cooling design has been demonstrated on a full-scale simulator test. The predicted and actual liner metal temperatures are shown in Figure 7-5. It should be noted also in Figure 7-5 that the total temperature increase from non-augmented to maximum augmentation resulted in a liner temperature increase of approximately 100°F indicating a low sensitivity of liner temperature to augmentor gas temperature.

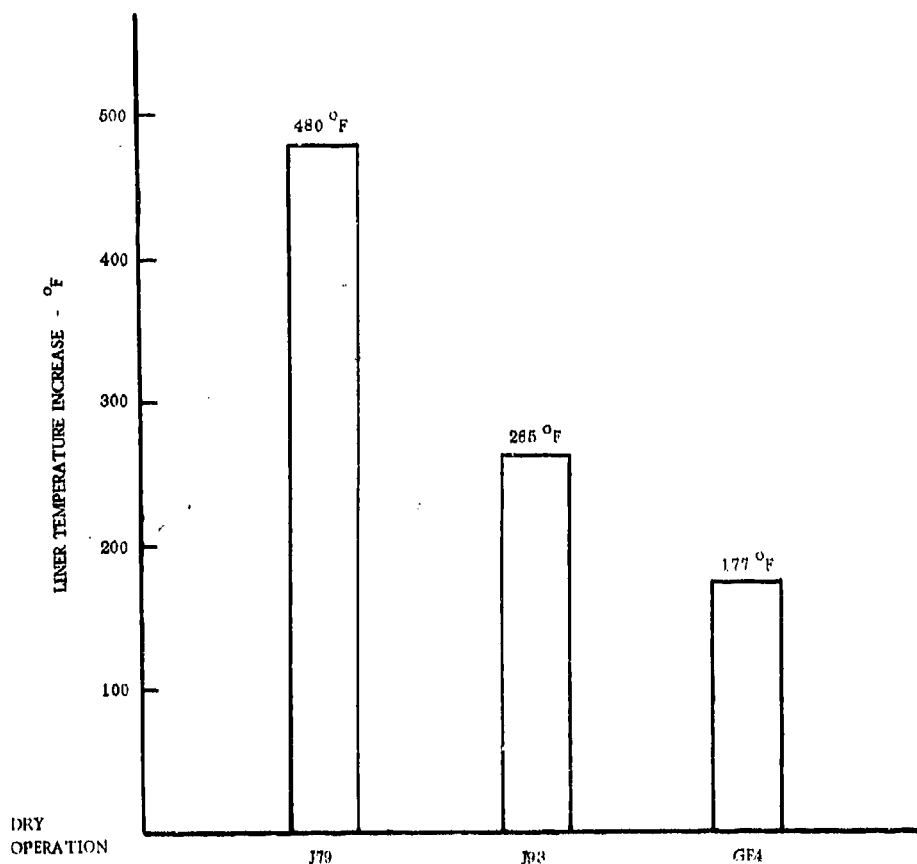


Figure 7-3. AVERAGE AUGMENTOR COOLING LINER TEMPERATURE INCREASE OVER DRY OPERATION FOR MAXIMUM AUGMENTOR OPERATION

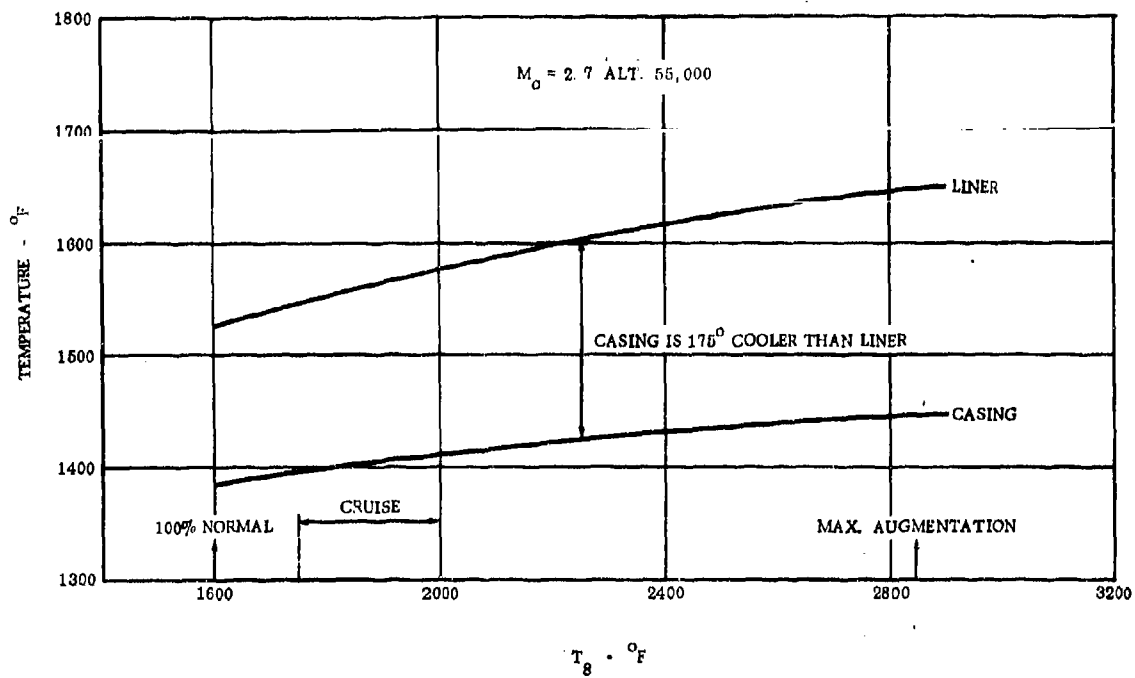


Figure 7-4. EFFECT OF COOLING LINER ON CASING TEMPERATURE

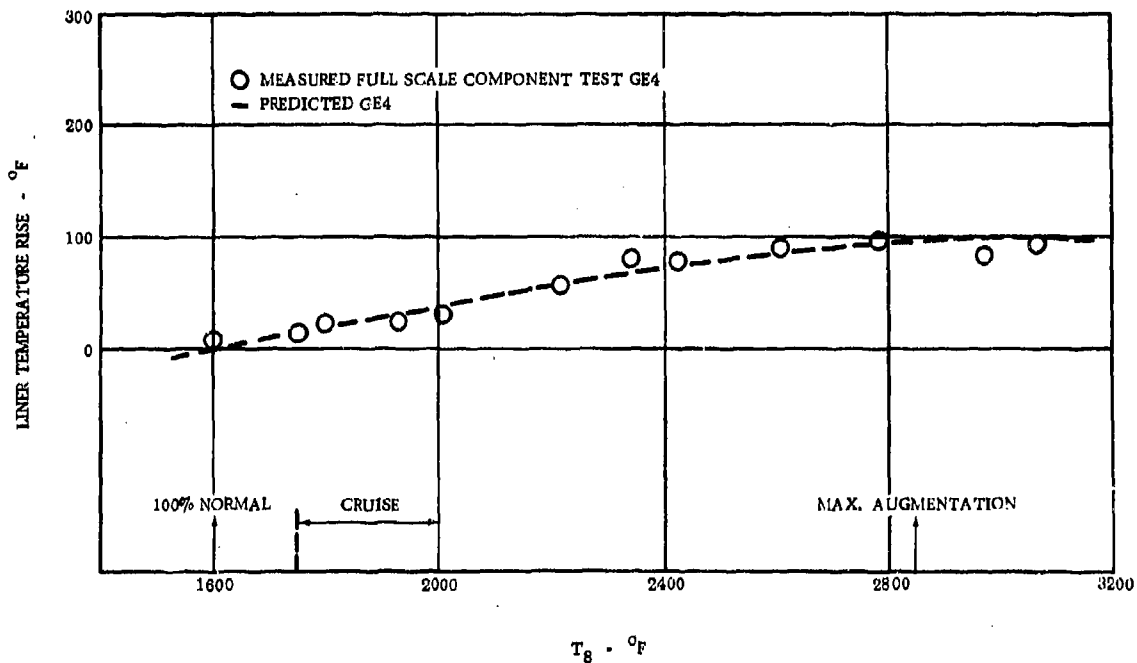


Figure 7-5. GE4 AUGMENTOR LINER METAL TEMPERATURE RISE

As shown in Figure 7-1, the basic coolant for the primary nozzle flap is the relatively thick cooling layer created by the multiple cooling liner slots and the discharge annulus on the augmentor liner. The film of coolant proceeds past the primary nozzle flap and joins the wide stream of secondary flow that enters at the gap between the primary and secondary flaps. The cooling effectiveness is further increased by flow through the slots in the secondary flaps to cool the downstream nozzle inner surface.

Major improvements have been made in the GE4 design to ensure commercial durability of nozzle parts:

- A shield has been added to the primary flap to protect the structural parts from radiation similar to the protection provided by the cooling liner in the augmentor. (See Figure 7-6.)
- Primary nozzle flaps and seal cooling is increased by completely separate compressor discharge air flowing behind a shield on the flap as shown in Figure 7-6.
- The compressor discharge cooling air is subsequently discharged along the edges of the primary flap to cool the hinged primary nozzle seals effectively. (See Figure 7-6.) The resulting primary flap temperatures (Figure 7-7) are lower on maximum augmentor operation than for maximum-unaugmented conditions. Full-scale simulator tests have shown that without compressor discharge cooling air the metal temperature increases are only:

Shield - 190°F

Seal - 150°F

Flap - 120°F

- Large amounts of second-stage ejector air (> 20 percent of engine airflow) flows into the nozzle cooling stream at takeoff, transonic acceleration, and loiter to increase secondary nozzle coolant.

The augmentor and exhaust nozzle cooling system for the GE4 has been designed by using a heat balance computer program and empirical techniques that have evolved by the design and development of exhaust cooling systems for the J79 and J93. Data is presented in this section which shows that:

- Augmentor and nozzle temperatures can be predicted within 50°F using the heat balance program.
- The designs have resulted in low increase in augmentor cooling liner metal temperatures with augmentor temperature rise.
  - Approximately 50°F from non-augmented to typical augmented cruise.
  - 177° from non-augmented to maximum augmented operation.
- A relative insensitivity in augmentor and primary nozzle temperatures to variation in secondary flow rates.

In summary, the augmentor and exhaust nozzle are cooled by well proven principles of using turbine discharge air and secondary air. To ensure commercial durability, this is supplemented by selective use of compressor bleed air for augmentor operation above cruise levels. The proposed approach maintains metal temperatures for all flight conditions at low levels to ensure durable, reliable, and safe operation.

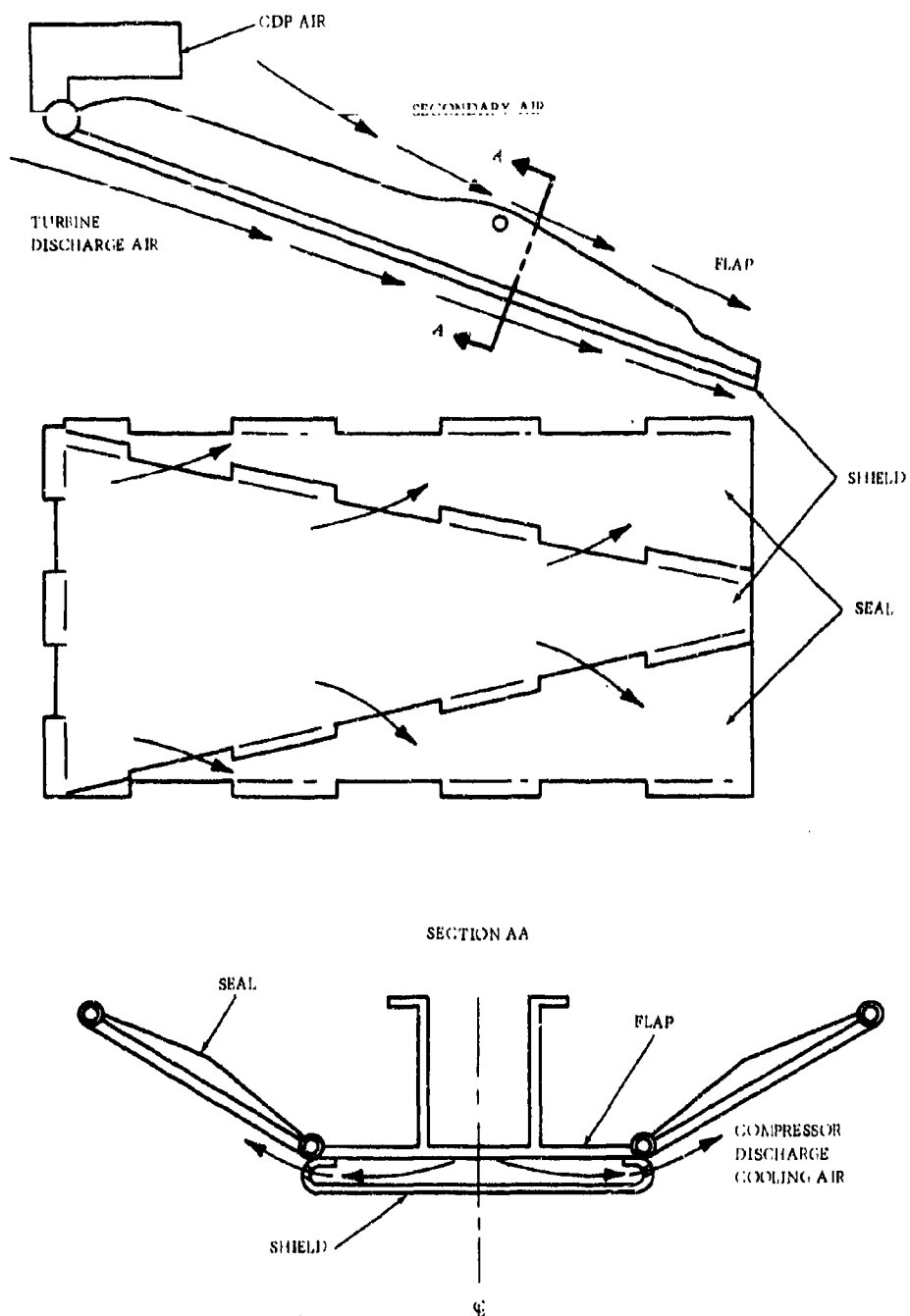


Figure 7-6. CROSS-SECTION PRIMARY FLAP AND SEAL SHOWING COOLING AIR PATH



## CONFIDENTIAL

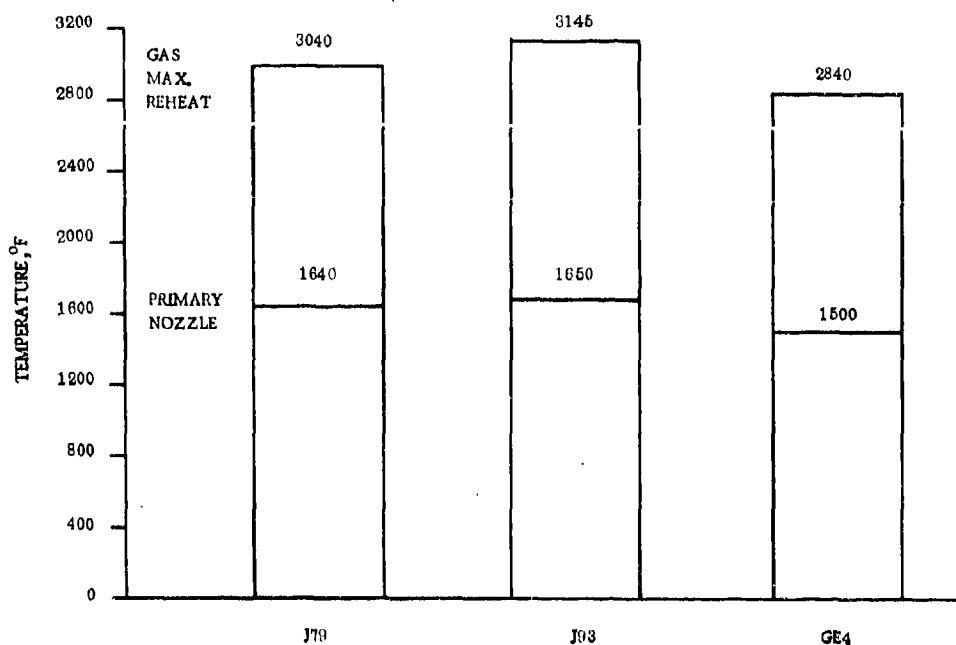


Figure 7-7. EXHAUST NOZZLE METAL TEMPERATURES AT MAXIMUM AUGMENTATION

### 7.2 GENERAL DESCRIPTION

Figure 7-8 shows, schematically, the GE4 exhaust system and the sources and quantities of cooling air. Evident in this figure are the augmentor liner and primary flap heat shield, non-structural parts that shield the structural exhaust casing and primary flaps from convective and radiation heating by the combustion gas. Highly efficient and well proven film and convection cooling techniques maintain the temperature of the structural walls below the temperature of the turbine discharge gas, as indicated below at maximum augmentation:

- Turbine Discharge Gas - 1600°F
- Augmentor Casing - 1500°F
- Primary Nozzle Flap - 1385°F

The cooling liner and nozzle shield are non-structural (low stress) parts, and can operate at higher temperatures than the structural casing and flap.

The exhaust casing and augmentor liner are cooled by turbine discharge air mixed with compressor seal leakage to reduce the coolant temperature, as shown in Figure 7-8. The external or secondary air flowing over the outside surface of the engine provides supplementary convective cooling to the exhaust casing and nozzle flaps. The primary nozzle is cooled by compressor bleed air in addition to film cooling from the cooled-boundary layer that persists downstream of the augmentor cooling system, typical of existing J79 and J93 systems. This exhaust cooling design is a highly effective innovation for nozzle cooling, and is applied to the GE4 to ensure commercial life and reliability.

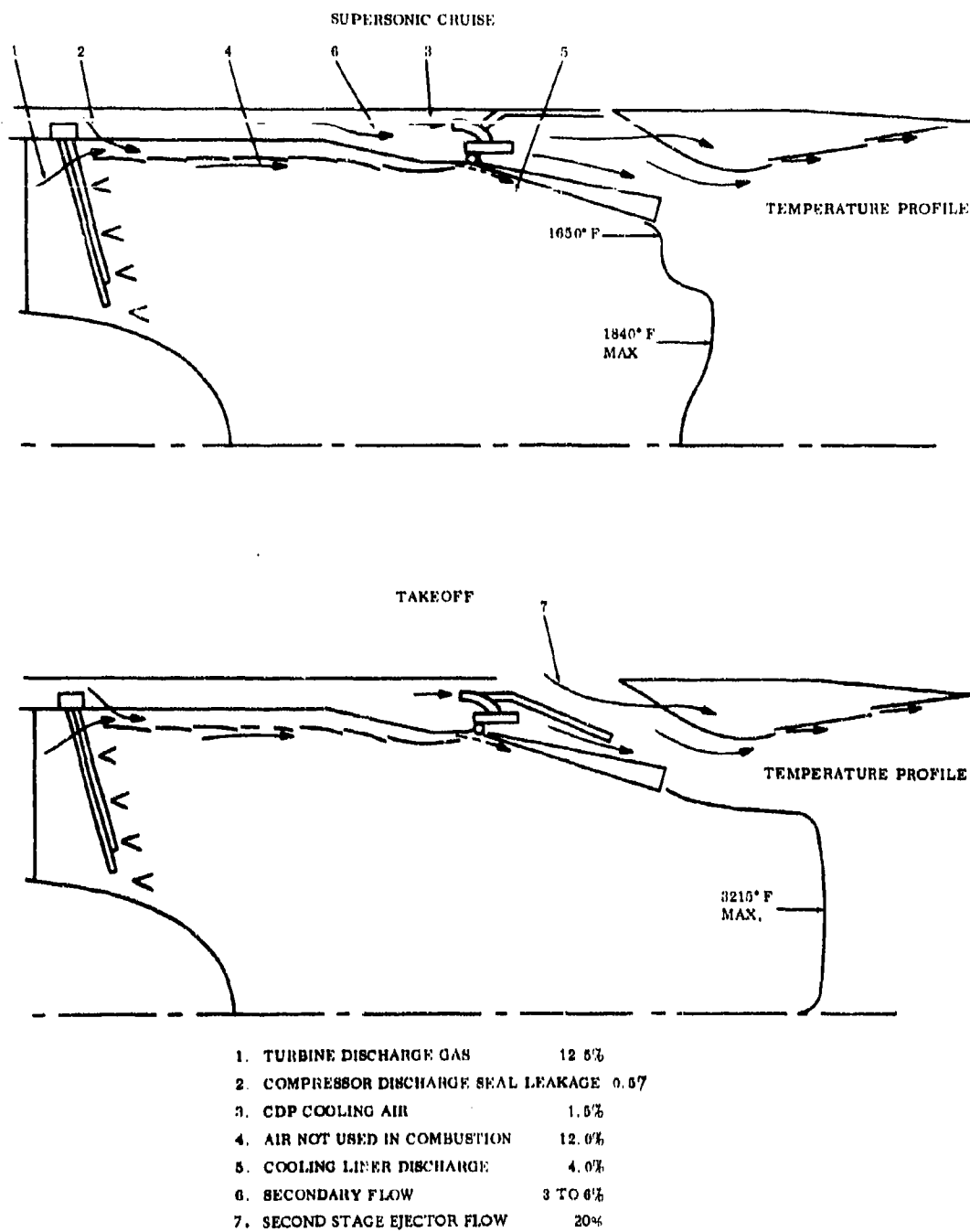


Figure 7-8. GE4 AUGMENTOR AND EXHAUST NOZZLE COOLING SYSTEM

The augmentor liner cooling air flows axially along the annular passage between the cooling liner and exhaust casing, and is discharged through slots in the liner. This creates a low-temperature film between the liner and the combustion gas. The film is continuously regenerated or reinforced by repetitive coolant admission through circumferential slots spaced axially for the most efficient use of the cooling air and the lowest metal temperature. Highly refined methods for spacing and sizing of the cooling slots maintain the liner at a temperature required for long life. This technique, from both a cooling and mechanical design standpoint, is identical to that employed in the combustor. The thickness of the film-cooled boundary is sequentially increased as the coolant flow is admitted through the series of cooling slots. The relatively thick coolant film persists downstream of the last slot in the cooling liner, providing a cooled boundary layer of air along the inner surface of the primary nozzle.

A portion (four percent) of the turbine exit cooling air is discharged at the end of the liner to supplement the film from the upstream cooling slots for cooling the primary nozzle, flap, shield, and seals.

For substantially improved cooling of the primary flap during power settings above cruise conditions, one and one-half percent of compressor bleed air is injected between the primary nozzle structure and the non-structural heat shield. The compressor bleed air cooling is similar in principle to that employed in the turbine section of current (J79 and J93) and advanced (TF39) engines, and is a unique feature of the GE4 nozzle design to ensure durability requirements of the commercial augmentor application.

Secondary air in quantities up to six percent of the inlet flow, cools the secondary inner flap. As shown in Figure 7-8, part of the secondary air cools the forward section of the divergent shroud; the balance of the flow passes through two slots in the inner aft flap to augment the main film.

A large proportion of the turbine discharge flow is available for cooling the GE4 augmentor and nozzle with negligible effect on augmentor performance. This is because the augmentor maximum temperature is low in relation to current military designs. Compared to the J93, the GE4 augmentor exit temperature is 360°F lower at maximum and 200°F lower at cruise. This results in a liner temperature, at supersonic cruise power settings, only 50°F higher than that for dry operation. It is pointed out that this occurs for 68 percent of the total time of a typical SST flight plan.

The high proportion of available cooling flow allows the favorable temperature profile at the nozzle exit shown on Figure 7-8. Note the low wall gas temperature as compared to an average peak temperature of 3215°F for an over-all cycle average of 2840°F. At the cruise augmentor power setting, this profiling is even more advantageous as combustion is concentrated in the core of the augmentor with the indicated temperature distribution.

For operation at takeoff, subsonic, and initial supersonic acceleration, the secondary nozzle cooling is substantially increased by the introduction of large (in excess of 20 percent) auxiliary flows through the two-stage ejector. This mode of operation is illustrated in Figure 7-8.

### 7.3 DESIGN REQUIREMENTS

#### 7.3.1 COMPONENT SKIN TEMPERATURES

The maximum metal temperatures to achieve the required life for the selected materials are shown in Table 7-1.

# CONFIDENTIAL

Table 7-1. Maximum Design Metal Temperature

Component	Material	Metal Temperature, °F at Maximum Augmentation	Metal Temperature, °F at Cruise
Cooling Liner	Hastelloy X	1750	1600
Exhaust Casing	Rene 63	1500	1410
Primary Flap Shield	Hastelloy X	1770	1500
Primary Flap Structure	Rene 41	1275	1280
Secondary Flap Inner Face	Rene 41	1380	1160
Secondary Flap Structure	Rene 41	1180	980

## 7.3.2 INTERNAL COOLING AIR - FROM ENGINE CYCLE

The augmentor and exhaust nozzle internal cooling system design is based on the criteria shown in Table 7-2 for the engine cooling air sources at different flight conditions and power settings. The cooling air sources and distribution are illustrated in Figure 7-8.

Table 7-2. Cooling Air Properties

Source	Flows* lb/sec				Pressures* lb/in <sup>2</sup>				Temperatures* °F			
	1	2	3	4	1	2	3	4	1	2	3	4
Compressor Discharge	9.31	6.48	4.23	4.31	165.8	116.3	77.3	79.3	694	652	735	1097
Compressor Discharge Seal Leakage	4.093	2.79	1.80	1.866	49.07	34.8	23.4	24.24	661	630	710	1075
Turbine Discharge	602.8	429.2	280.3	288.5	50.41	35.61	24.19	25.01	1596	1520	1596	1586

\*Data shown are averages at conditions:

1. Sea Level Static
2. 15,000 ft, Mach 0.5
3. 45,000 ft, Mach 1.5
4. 65,000 ft, Mach 2.7

- Power setting No. 1
- Power setting No. 1
- Power setting No. 1
- Power setting No. 3.75

The cooling air sources and approximate proportions are:

Internal Cooling Flow

- Turbine discharge gas (12.5 percent of engine flow)
- Seal leakage air (0.5 percent of engine flow)
- Compressor discharge air (1.5 percent of engine flow)

All of the internal cooling flows discharge into the engine upstream of the nozzle throat, resulting in a minimum of performance effect due to the cooling process.

### 7.3.3 EXTERNAL COOLING AIR - SECONDARY AND TERTIARY AIRFLOW

At all flight speeds, secondary airflow from the inlet of the engine is introduced into the secondary nozzle to cool the secondary nozzle inner flaps and seals. The quantity of secondary air is shown in Table 7-3.

The major portion of the secondary air is introduced concentrically around the primary gas stream at the end of the primary nozzle. This secondary flow provides an additional film that reinforces the low-temperature boundary air, leaving the inner face of the primary flap in the same regenerative manner as previously described. This provides film cooling for the inner

Table 7-3. Secondary Air Properties

	Quantity* pounds/second	Pressure* psi	Temperature* °R
1. Sea Level Static Power Setting 1	86.9	14.7	552
2. 15,000 ft, Mach 0.5 Power Setting 1	21.2	7.61	556
3. 45,000 ft, Mach 1.5 Power Setting 1	13.2	3.71	598
4. 65,000 ft, Mach 2.7 Power setting 3.5	9.9	5.14	1064

\*Data shown are average.

surface of the secondary flaps. The remainder of the secondary air (50 percent) flows through, and convectively cools, the secondary flap structure discharging through circumferential cooling slots into the gas stream, and provides additional film cooling for the aft sections of the inner flap surfaces.

Cooling of the secondary nozzle is discussed in detail in paragraph 7.5.4. The secondary airflow is supplemented by high proportions of tertiary air entering the exhaust nozzle for noise suppression and engine performance improvement at low pressure ratio operating conditions such as takeoff, climb-out, loiter, and subsonic cruise. This additional (external) air is beneficial for secondary nozzle cooling of subsonic and low-supersonic portions of the flight map.

#### **7.4 DESIGN APPROACH**

The design approach for the cooling system establishes a configuration of cooling airflow passages and distributing slots that provides the maximum utilization of the cooling capacity available to maintain the low exhaust system metal temperatures necessary for durability, reliability, and safety. The cooling method is similar to that demonstrated on in-service supersonic augmented turbojets where utilization of the turbine discharge gases is made for internal cooling and secondary air for external cooling. This cooling system is supplemented with compressor bleed air for nozzle cooling margin. The relative quantities of air obtained from the different sources are based on extensive trade-off studies on cooling effectiveness and performance. The heat transfer analysis for the cooling system utilizes methods developed for the J79 and J93 and other more advanced engines to calculate the surface temperature distribution for augmentor liners, ducts, and more convergent-divergent-type exhaust nozzles. In the analysis, the surface temperature of the ducts, liner, nozzle flaps, seals, actuating mechanism, and surrounding aircraft structure are systematically balanced. The cooling air flows through the various passages, and is heated by radiation and convection.

The surface temperatures at multiple axial locations on the exhaust system are obtained by localized and over-all heat balance calculations of the effect of the cooling air on the augmentor and the convergent-divergent nozzle components. Heat-balance equations are solved to obtain metal temperature at:

- The entrance and exit of the augmentor liner, primary flap, and secondary flap
- Each intermediate cooling slot
- Other special points of selected axial spacing along the liner and flaps

A heat balance is obtained between the incoming cooling air and discharge flow from the cooling slots. The quantities of cooling air and the individual slot flows are computed with the aerodynamic friction losses in the system considered. By computer iteration methods, a flow balance is attained between cooling air supplies and slot flows consistent with the heat balance at each slot, using the local flow results and integrating the total radiation and convection heat transfer. The emissivity of the surface of each wall is defined to evaluate combinations of materials and surface finishes. Figure 7-9 is a schematic representation of the heat balance calculation at a typical slot in the augmentor liner. The primary steps in the heat balance calculations are:

- Evaluate convection coefficients
- Establish surface and gas emissivities
- Establish gas stream temperature
- Write heat balance equations
- Solve for metal temperatures

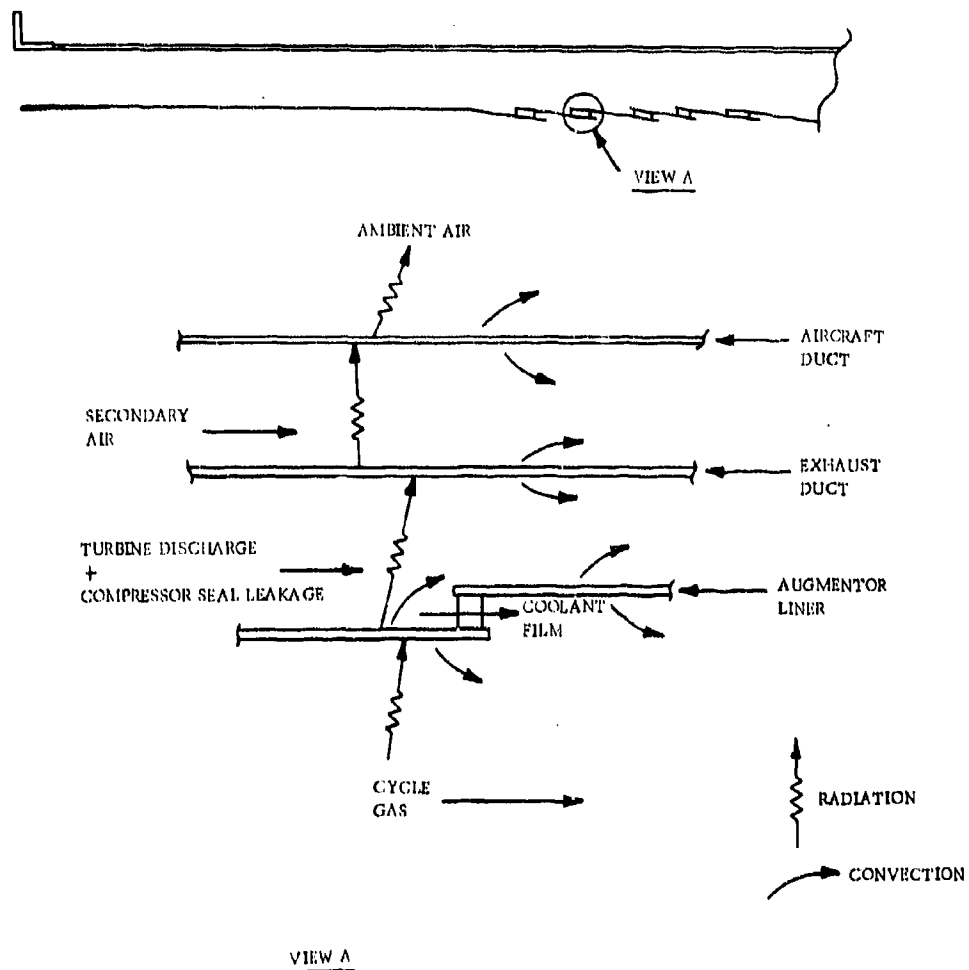


Figure 7-9. HEAT TRANSFER ANALYSIS SCHEMATIC

The analytical methods described above have been extensively refined and verified in J79 and J93 engine tests with heavily instrumented hardware. Figure 7-10 shows a comparison of the axial distribution of calculated and measured augmentor liner temperatures for the J79-10 engine operating at maximum augmentation under sea level static conditions. Note that the agreement is within 3 percent. Figure 7-11 compares the calculated and measured J93 augmentor liner temperatures over the full range of augmentation. These data are particularly significant because of the similarity in operating conditions and liner construction of the J93 and GE4 engines. Particularly emphasized is the low metal temperature increase between typical augmented cruise and non-augmented operation. Figure 7-12 shows corresponding calculated and measured primary flap temperatures for the J93 exhaust nozzle. Figure 7-13 indicates good agreement between predicted and actual results during the 1959 engine test.

More recently, in 1965, extensive data have been obtained from an instrumented J93 nozzle run at the Arnold Engineering Development Center. An example of the kind of data obtained with thermocouples on all 16 nozzle flaps is shown in Figure 7-14. Even though the gas used to supply film cooling is at 1540°F and the primary exhaust gas flow is at 3141°F, the average metal temperature was maintained below 1550°F.

Similar data obtained on the J79-10/-17 nozzle are shown in Figure 7-15. Temperatures measured during flight tests on the XB-70 airplane subsequent to the AEDC tests are compared with predicted temperatures in Figure 7-16. There is good agreement between measured and predicted temperatures.

In Figure 7-17, the J93 calculated and measured values for the augmentor liner and casing temperatures show the effect of secondary airflow. Note the essentially negligible dependence of liner temperature on secondary flow, and the relatively low effect on the duct temperature. This shows that the augmentor components are insensitive to secondary flow variations.

The foregoing test data (Figures 7-11 and 7-12) show:

- Augmentor liner and nozzle temperature prediction capability within 50°F
- Low increase in liner metal temperature with augmentor temperature rise:
  - Approximately 50°F from dry to typical augmented cruise
  - 265°F from dry to maximum
- Relative insensitivity to secondary flow rates

It also confirms that General Electric has the proven cooling technology required to design augmentors and nozzles to operate at the predicted low temperatures which will result in high durability and long, trouble-free life. Using well-established analytical techniques, accurate temperature predictions of augmentor casing, liner, and exhaust nozzle hardware can be made at all operating conditions. The predictions include axial distribution, effect of power setting, and all other significant variables that are involved, as typified by the examples of calculated and measured temperature for the J79 and J93 shown here. Substantial progress to demonstrate this capability further has already been made during the Phase II-C, full-scale, GE4 augmentor tests.



SEA LEVEL STATIC  
MAXIMUM AUGMENTATION

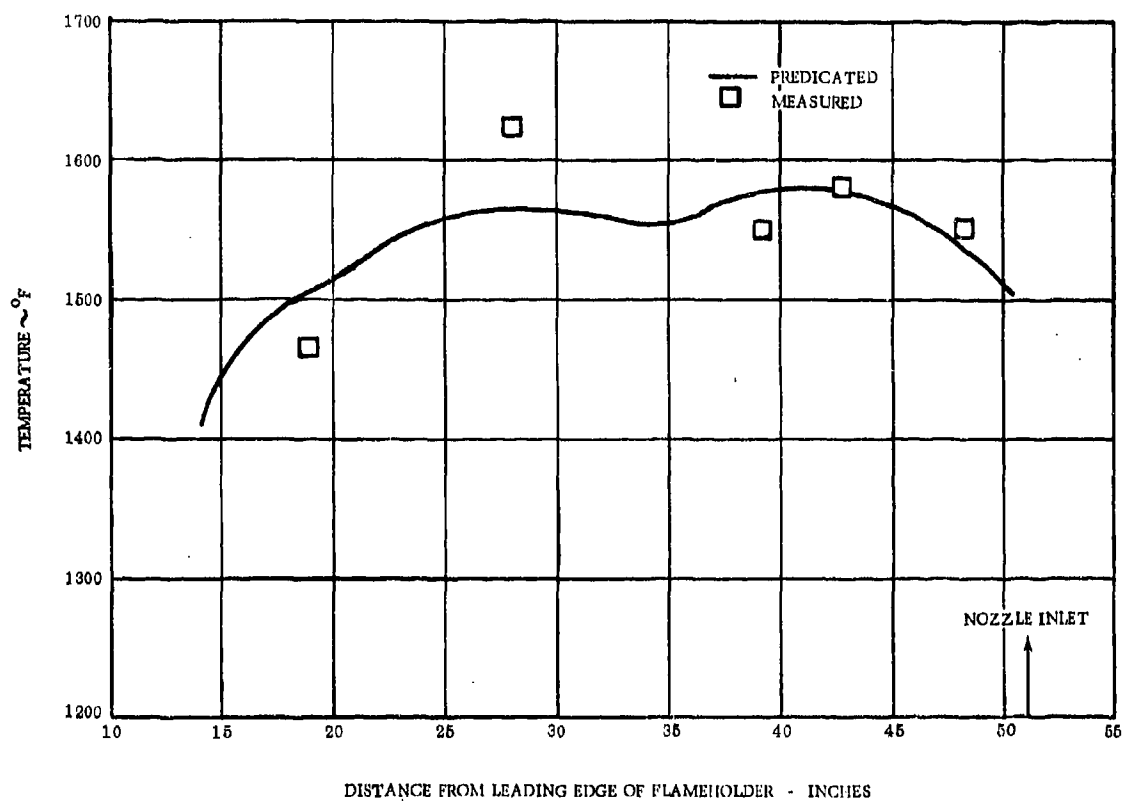


Figure 7-10. J79-10/17 AUGMENTOR LINER TEMPERATURES

TEST DATA FROM J93 ENGINE 508-6 SEA LEVEL STATIC

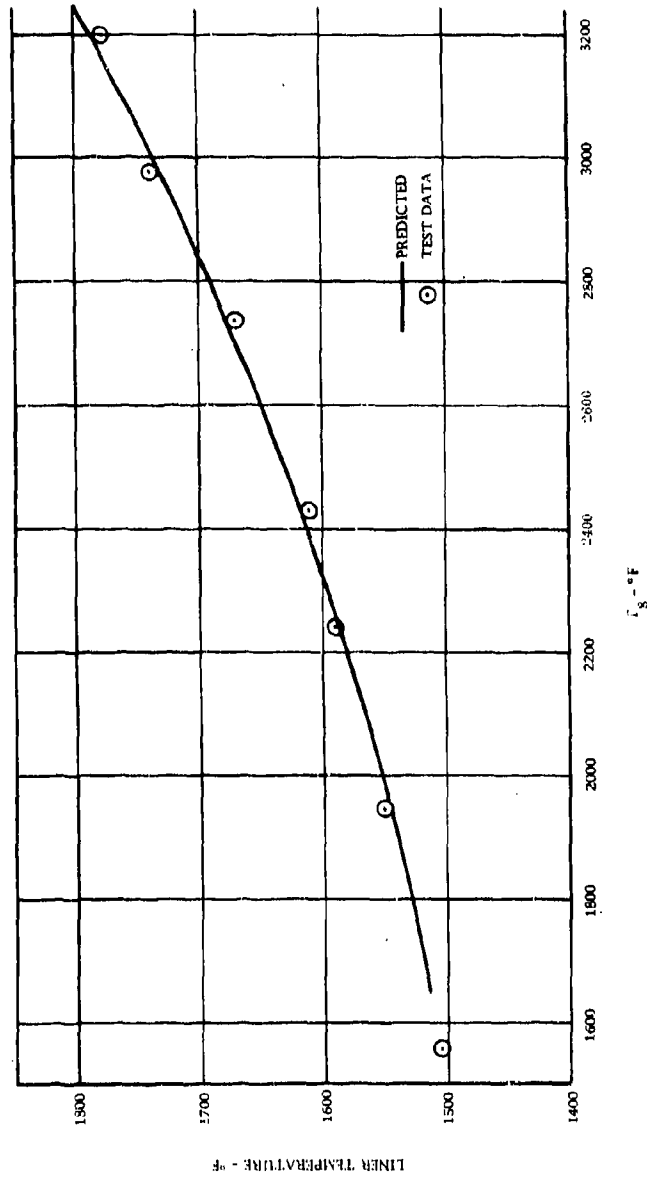


Figure 7-11. J93 AUGMENTOR LINER PREDICTED AND ACTUAL TEMPERATURE

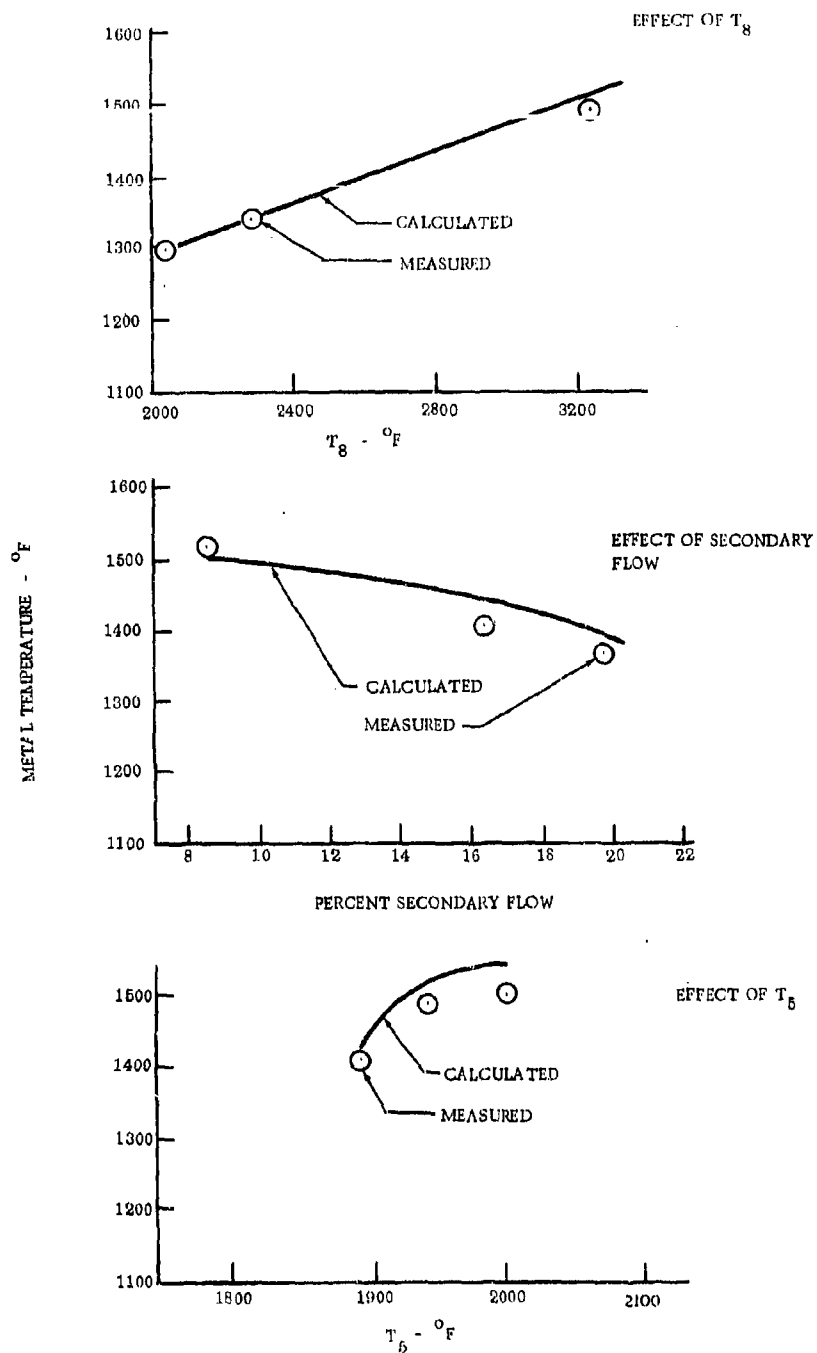


Figure 7-12. J93 NOZZLE PRIMARY FLAP CALCULATED AND MEASURED TEMPERATURES

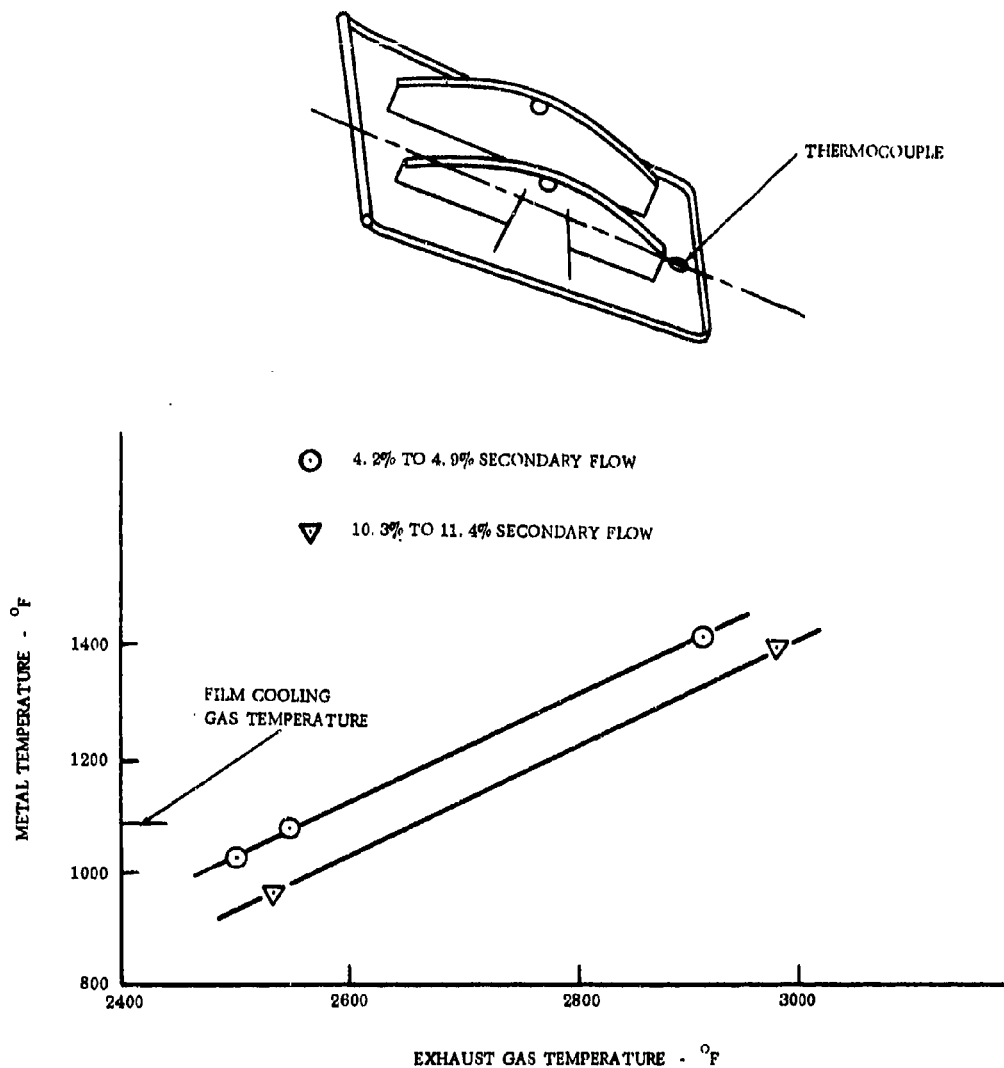


Figure 7-13. J79 EJECTOR NOZZLE, MEASURED PRIMARY FLAP TEMPERATURES

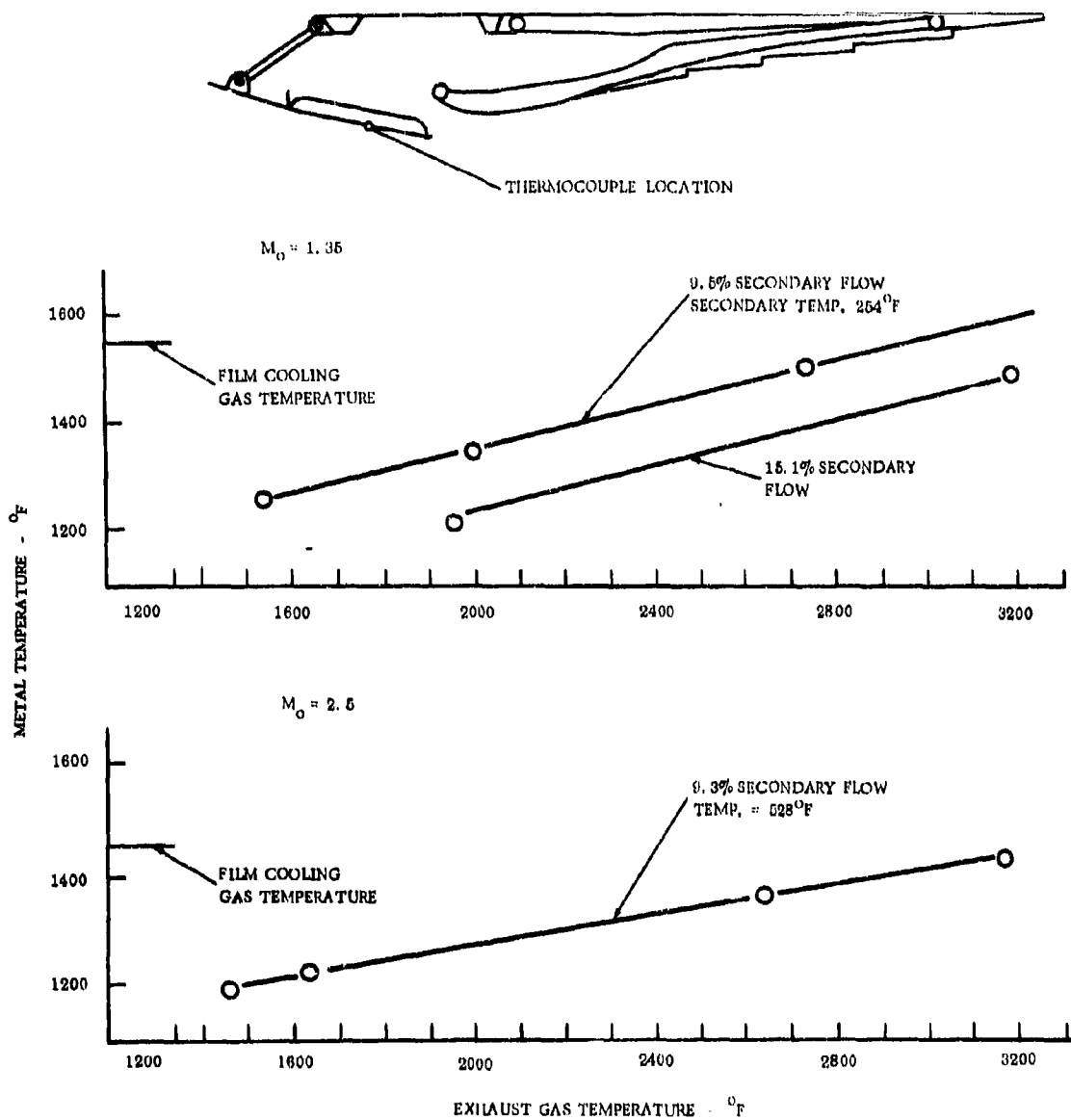


Figure 7-14. J93 NOZZLE, MEASURED PRIMARY FLAP TEMPERATURES

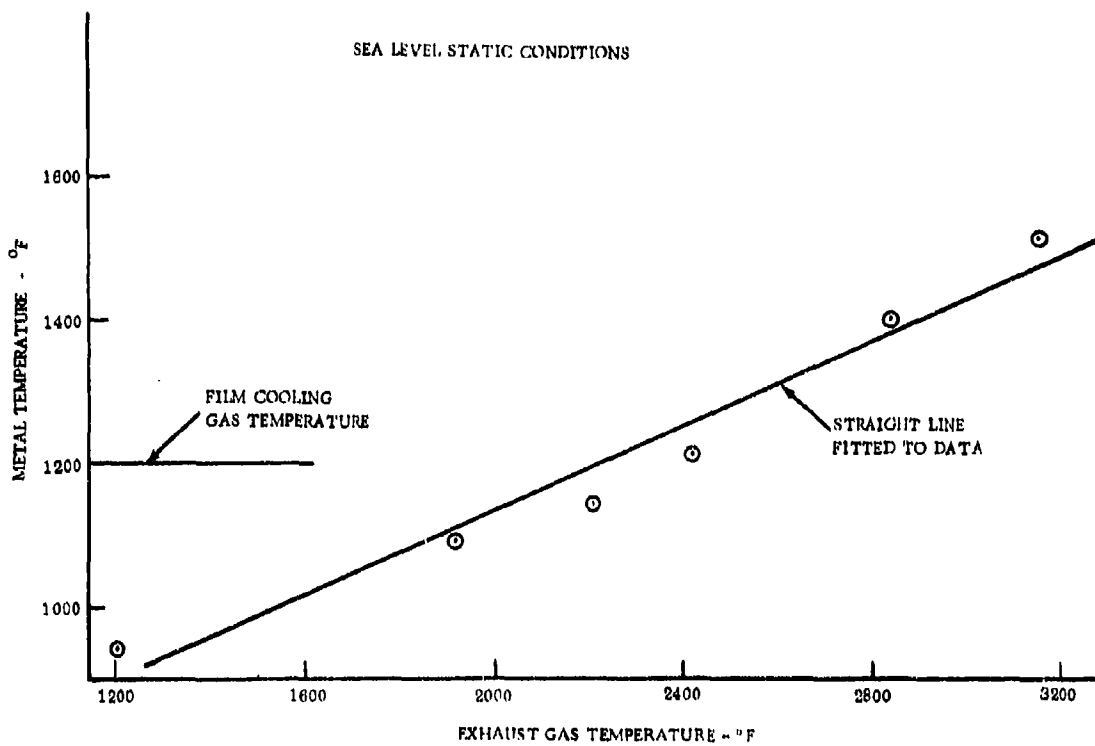
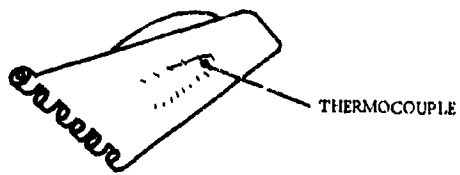


Figure 7-15. J79-10/-17 NOZZLE MEASURED PRIMARY FLAP TEMPERATURES

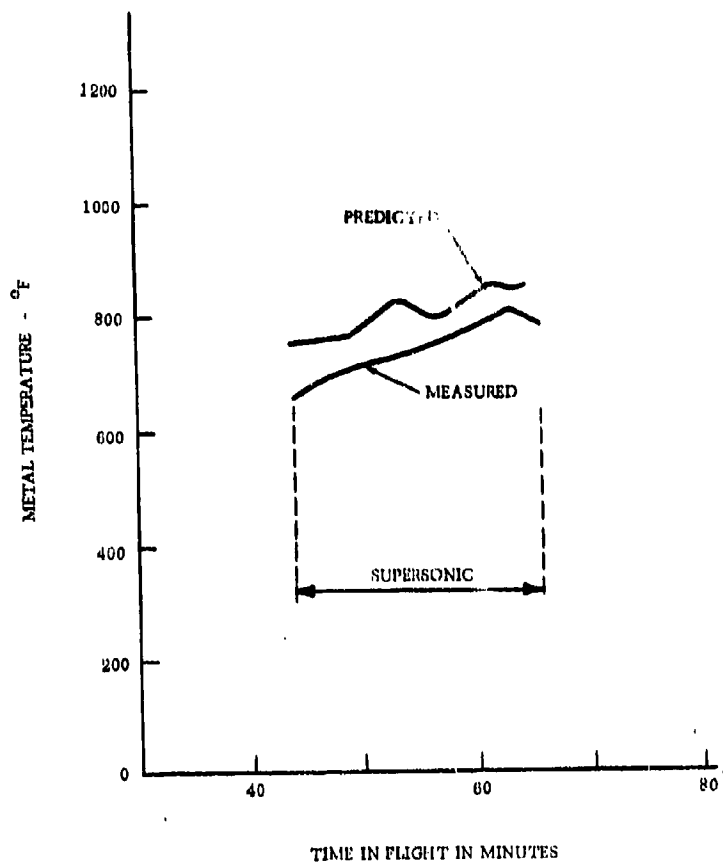
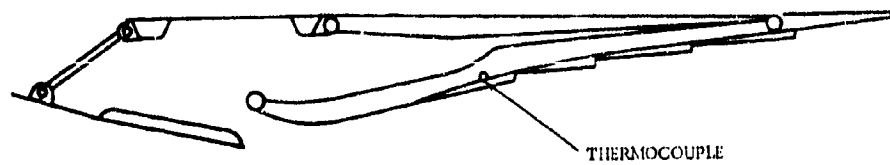


Figure 7-16. J93 NOZZLE METAL TEMPERATURES IN FLIGHT

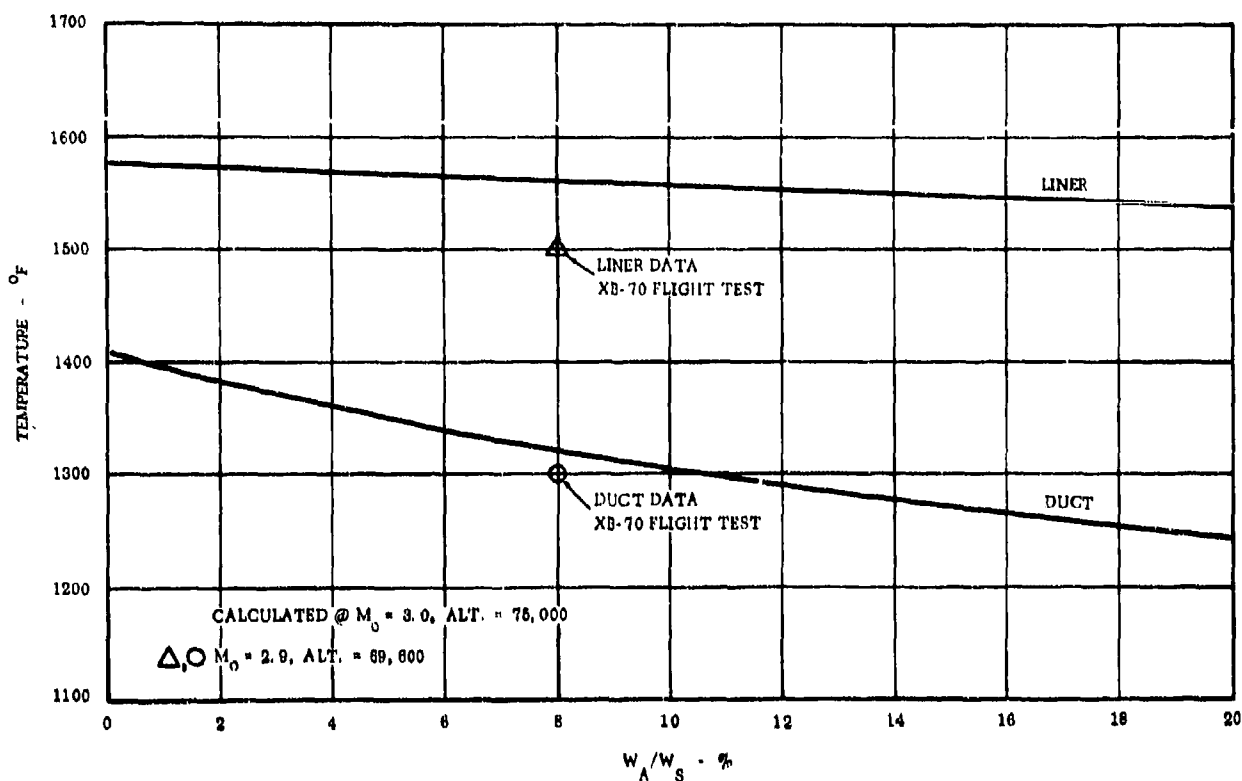


Figure 7-17. EFFECT OF SECONDARY AIR FLOW ON J93 AUGMENTOR LINER AND DUCT TEMPERATURES

General Electric's total experience with combustor and augmentor liner durability has focused on cooling techniques to maintain a low thermal stress in the liner as well as low maximum temperature. Thermal stresses are minimized by these factors:

- High cooling effectiveness or efficiency of the cooling slot design
- Uniformity in coolant distribution
- Low temperature difference between the cooling air and the combustion gas temperature
- Location of fuel injection (and the corresponding combustion reaction) relative to the liner

Low thermal stress is easier to obtain in an augmentor liner than in a main combustor, because of the lower heat flux radiating from the gases (due to lower gas pressures) and the smaller differences between the cooling air temperature and the local combustion gas temperature, as regulated by the location of the fuel injection holes relative to the liner. Figure 7-18 shows the metal temperature gradients measured on various General Electric combustion systems.

The higher gradient in the J79 augmentor liner is due to the less effective cooling of the distribution louvers in contrast to the continuous circumferential slots in J93 and GE4 construction.



**CONFIDENTIAL**

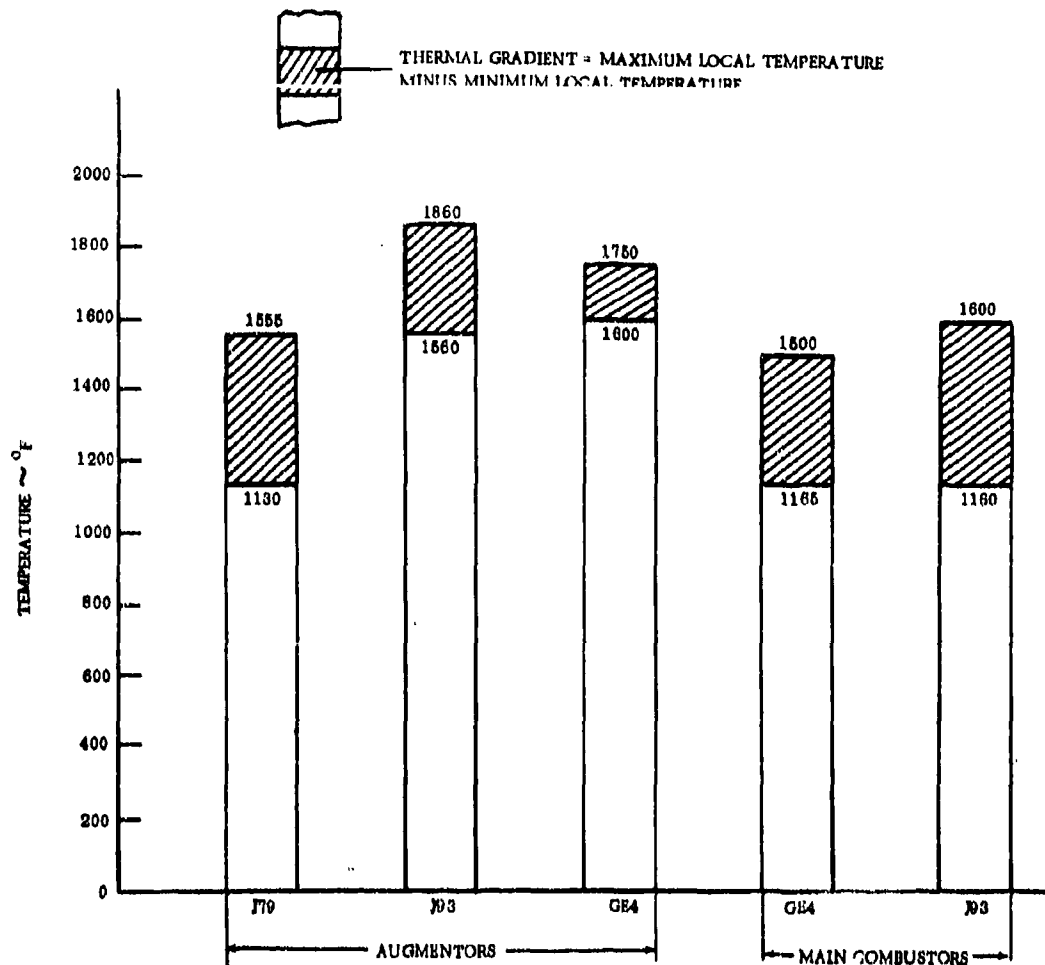


Figure 7-18. COMPARISON OF COMBUSTOR AND AUGMENTOR LINER TEMPERATURE GRADIENTS

The further reduction in temperature gradient on the GE4 relative to the J93 is due primarily to a larger amount of cooling air and the location of the fuel relative to the liner. This has been achieved by injecting the fuel no further outboard than the outer flameholder ring, instead of between the outer ring and the liner as on the J93. This is possible because of the reduced maximum GE4 temperature which is 360°F lower than for the J93.

**CONFIDENTIAL**

# CONFIDENTIAL

## 7.5 DESIGN DESCRIPTION

### 7.5.1 SYSTEM SUMMARY

The GE4 cooling system is designed for the cooling flow quantities summarized in Table 7-2. The coolant flow passages are sized for these coolant quantities, and are summarized in Table 7-4.

Table 7-4. Coolant Flow Passages

	Slot Heights Inch	Area Sq. In.	Spacing Inch
1. Exhaust Duct Liner - Inlet		307	
2. Exhaust Duct Liner - Exit		93.5	
3. Augmentor Cooling Liner Slots (each)	0.05	8.15	1.5
4. Primary Nozzle Flaps - CDP Air Slots	0.080	0.48	3.0
5. Secondary Nozzle Flap Cooling Slots	0.25	105	16

The predicted surface temperatures for augmentor and exhaust nozzle and thrust reverser parts are shown in Table 7-5 for typical flight conditions:

Table 7-5. Surface Temperatures

Part	Material	Temperatures* °F			
		1	2	3	4
Liner Skin	Hastelloy X	1730	1615	1648	1540
Casing	René 63	1495	1400	1408	1396
Primary Flap	René 41	1275	1270	1385	1280
Primary Flap Shield	Hastelloy X	1770	1690	1735	1500
Primary Hinge Mounting Ring	René 41	900	900	1100	1100
Actuating Ring	Inco 718	700	700	650	600
Actuating Linkage	René 41	1000	1000	1100	1190
Secondary Inner Flap	René 41	1360	1350	1295	1160
Secondary Inner Seal	René 41	1470	1540	1425	1220
Secondary Outer Flap, Outer Surface	Inco 718	300	100	120	420
Secondary Outer Seal, Outer Surface	Inco 718	440	150	210	450
Outer Shroud	Inco 718	460	230	380	550

Reverser Cascade in Reverse Power - 1650°F.

Primary Flap in Reverse Power - 1200°F.

\*Temperature Conditions:

1. Seal level static, power setting No. 1
2. 15,000 ft, Mach 0.5, power setting No. 1
3. 45,000 ft, Mach 1.5, power setting No. 1
4. 65,000 ft, Mach 2.7, power setting No. 3.5 percent secondary flow.

### 7.5.2 AUGMENTOR LINER AND CASING

The outer boundary of the turbine discharge flow is mixed with seal leakage air to reduce the average temperature. The cooling liner leading edge splits 12 percent of the total flow at station A-A (Figure 7-15) for cooling air. The augmentor liner employs the three-element slot design shown in Figure 7-19. A similar design is used for the GE4 combustor (Reference Section 4, Volume III-B Part I), which evolved from the design proven on the Mach-3.0-capable J93 combustor. The locally admitted cooling air quantity is controlled by the wiggle strip height and is discharged in axial stations spaced every 1.5 inches. Highly effective convective cooling on the exhaust casing side of the liner is provided by the high velocity (380 ft/sec) air stream. This, in combination with the insulating effect of the film on the inside surface, maintains the liner at the predicted low-temperature level. The temperatures for the GE4 augmentor liner and casing are given in Figure 7-20, and show the relationship of these temperatures at two typical operation conditions. Figure 7-21 shows the liner and casing temperatures for these same two conditions as a function of  $T_g$ . Notice that the liner temperature is only 45°F higher during cruise than during maximum dry conditions. This is accomplished by the effective use of large quantities of cooling air and the fuel distribution that provides combustion on only the two innermost flameholder rings during these conditions. It is to be noted that the liner and casing temperatures are relatively insensitive to power setting or exhaust gas temperature, i.e., the liner temperature increases only 100°F with an exhaust gas temperature increase of 1000°. Thus, the design has insensitivity to other variables, including local high-temperature streaks or secondary flow. This is indicated in more detail in Figure 7-22 which relates the casing and liner temperature with the quantity of secondary air between the exhaust casing and the aircraft shroud or nacelle. The effect on liner temperature is imperceptible and the duct shows only minor reaction.

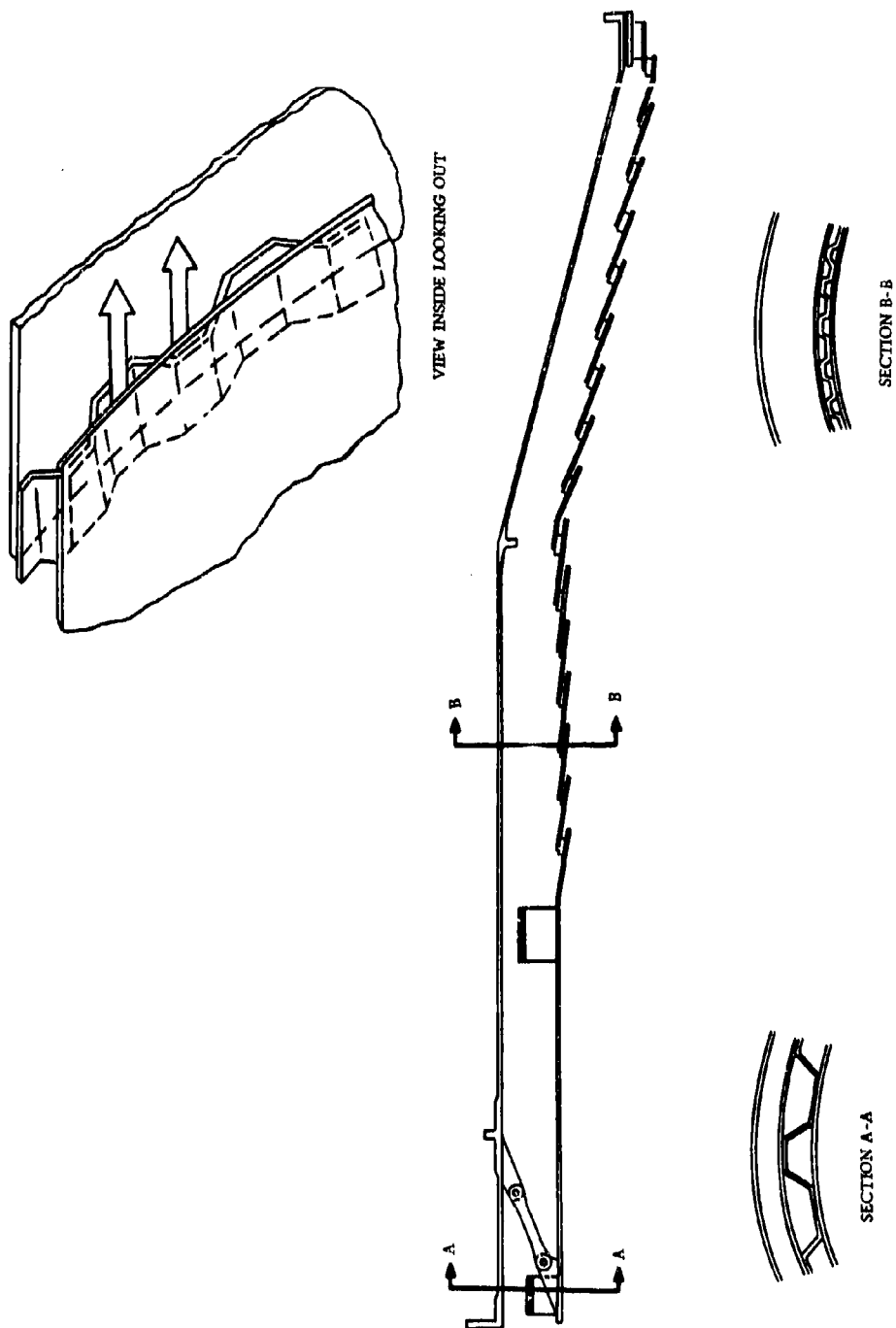
### 7.5.3 PRIMARY NOZZLE

Several advantages in the GE4 design permit the primary nozzle to operate at temperatures well within the range of typical nozzle materials. The temperature profile of the primary gas stream is one of the most important of these factors. Figure 7-23 shows the profile for approximately 68 percent of the augmentor operation and in excess of two-thirds of the total engine operation. Combustion occurs on the innermost flameholders only; therefore, the gas that contacts the nozzle flaps is at a much lower temperature than either the core temperature or the average exhaust gas temperature. Even during full augmentor operation, the temperature profile drops off steeply in the vicinity of the nozzle flaps as shown in Figure 7-24. Therefore, under all augmentor conditions there is a thick boundary of lower-temperature gas adjacent to the primary nozzle flaps.

This temperature profiling concept is not new. Figure 7-25 shows the profile for a typical J79 engine at the nozzle inlet plane. For the GE4 design with the reduced maximum temperature, the degree of profiling is substantially increased.

The lower-temperature gas layer adjacent to the metal wall results not only from the flameholder position, but also from the cooling air introduction from the augmentor cooling liner. As previously described, the sequential addition of coolant along the liner produces a lower-temperature boundary at the nozzle inlet. For assured cooling, a special slot at the end of the liner provides cooling flow for the nozzle flaps and seals equal to approximately 4 percent of the primary gas flow. Although this degree of cooling has been adequate for military nozzles, the GE4 nozzle design incorporates an additional compressor-bleed air-cooling system to ensure long life for the commercial augmented engine.

The distribution of the compressor discharge air (1-1/2 percent) is shown in Figure 7-26. In this diagram, the letters A, B, and C refer, respectively, to stations on the stiffening rib, the base plate of the flap, and the heat shield. Compressor discharge cooling air is admitted to the hinge



7-26

Figure 7-19. GE4 AUGMENTOR LINER AND COOLING SLOT

K

CONFIDENTIAL

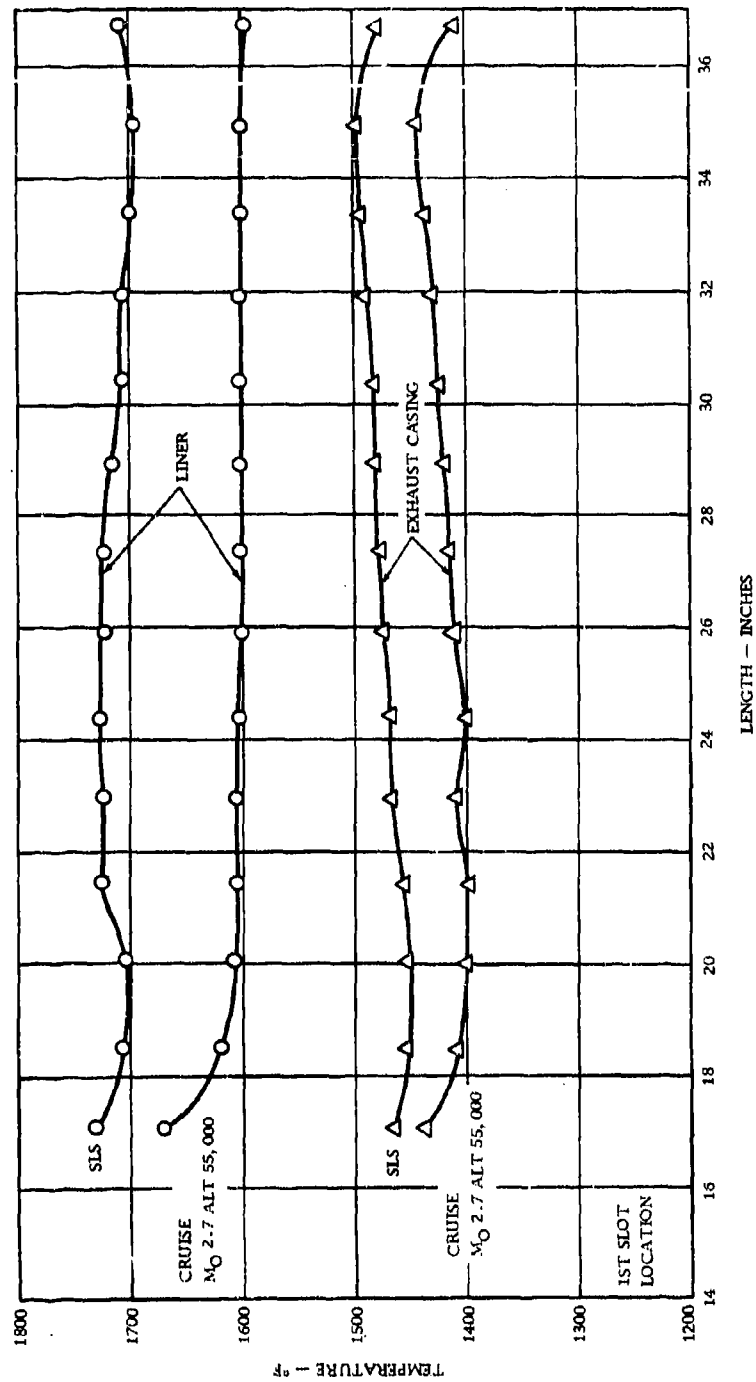


Figure 7-20. AUGMENTOR LINER AND CASING CALCULATED TEMPERATURES

7-27

CONFIDENTIAL

K

**CONFIDENTIAL**

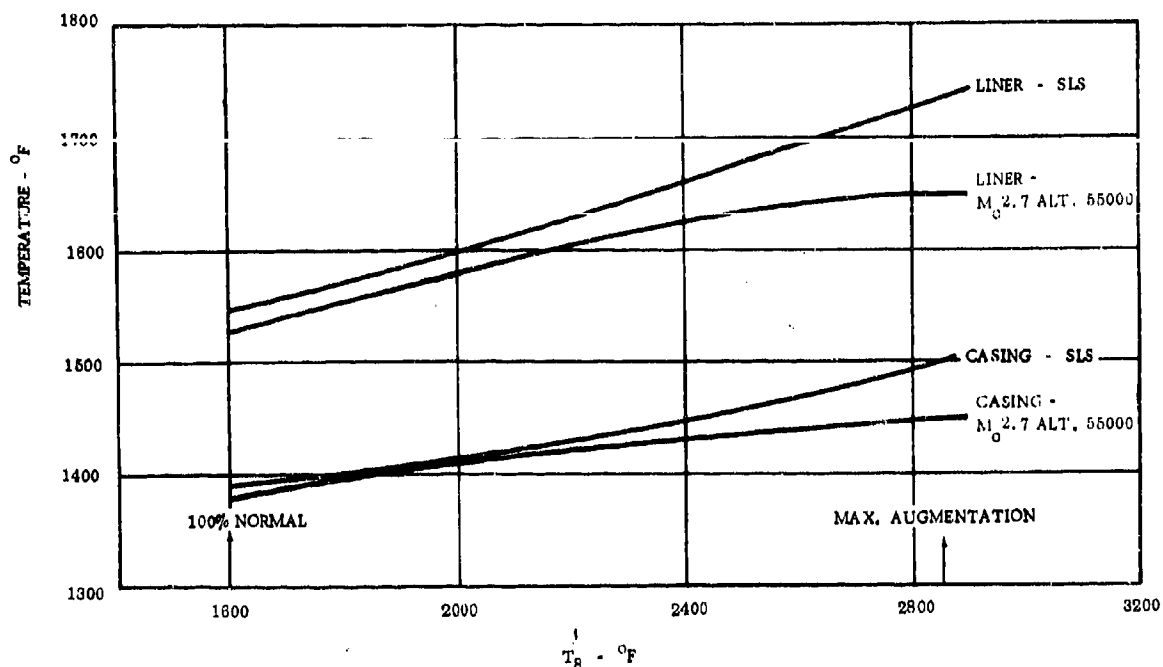


Figure 7-21. PREDICTED AUGMENTOR LINER AND EXHAUST CASING TEMPERATURES

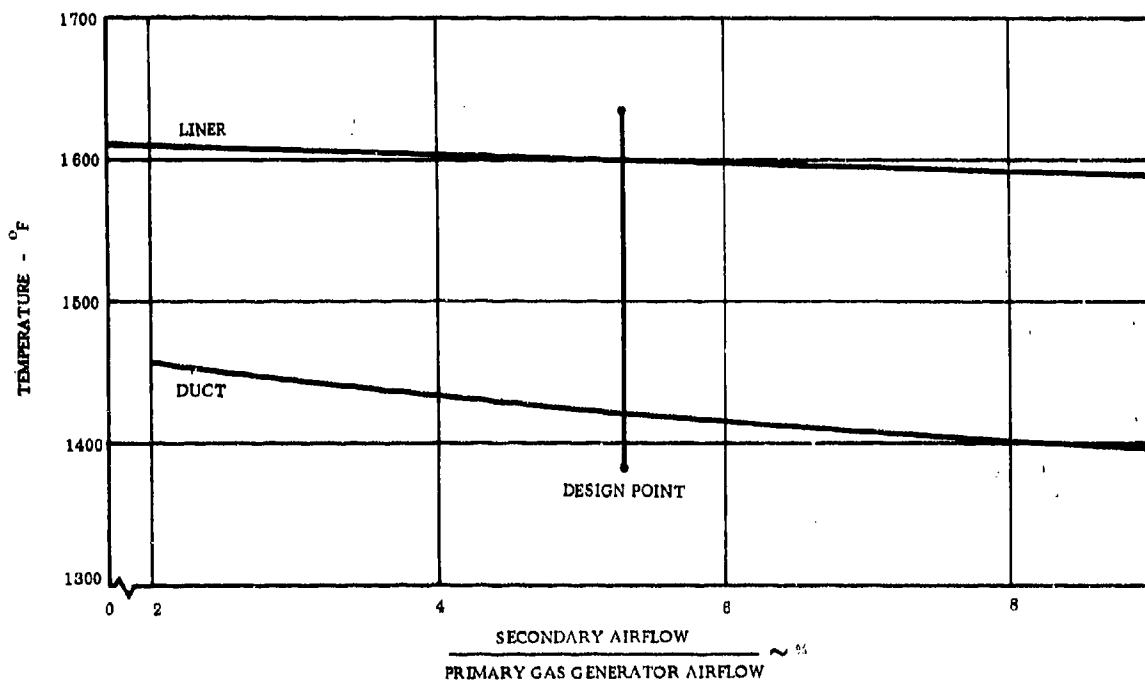


Figure 7-22. EFFECT OF SECONDARY AIR ON GE4 LINER AND CASING TEMPERATURES

**CONFIDENTIAL**

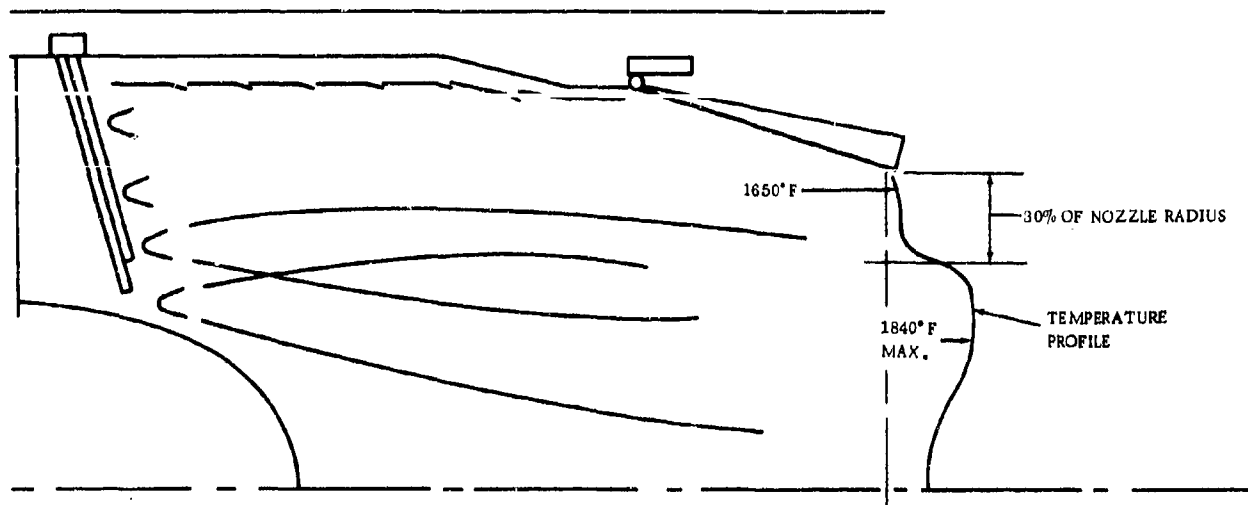


Figure 7-23. CRUISE AUGMENTOR TEMPERATURE PROFILE

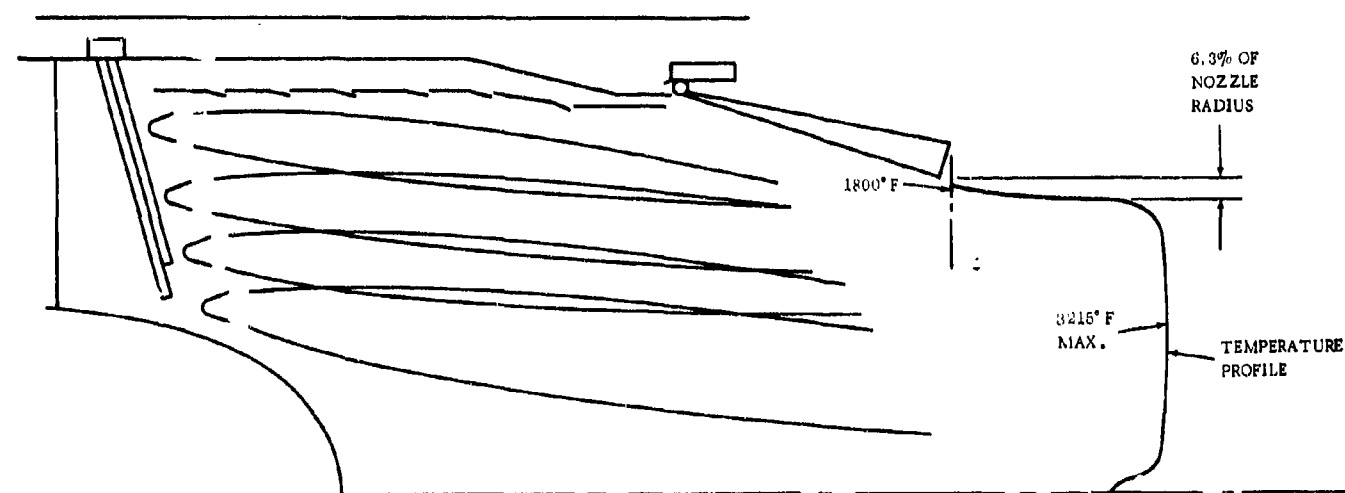


Figure 7-24. MAX AUGMENTATION TEMPERATURE PROFILE

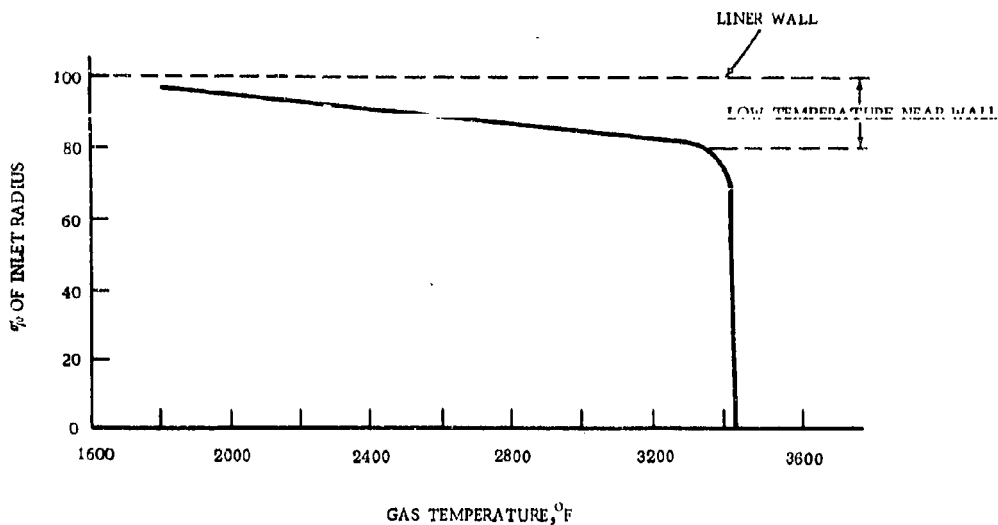


Figure 7-25. GAS TEMPERATURE PROFILE AT END OF AUGMENTOR FOR J79

ring, which serves as a distribution manifold. From the hinge ring, the cooling air flows into the space between the base plate and the heat shield as indicated by the curved arrows. The small arrows and the adjacent percentage numbers along the edge of the flap define the distribution of the cooling air from the slots along the edge of the heat shield. These are percentages of the total flow supplied to one-half the flap. To provide high film-cooling effectiveness along the hinge seals, 55 percent of the total flow is introduced at the forward end.

This approach has been evaluated in full-scale GE4 augmentor tests to maximum exhaust gas temperatures, and nozzle temperature distributions have been recorded. The strong cooling effect of the compressor bleed air is shown by the transverse sectional diagram of a primary flap in Figure 7-27. For dry operation and augmentor settings up to  $360^{\circ}\text{F } \Delta T$ , the cooling air is shut off. The left side of the diagram shows the metal temperatures for this condition. For augmentor operation above  $360^{\circ}\text{F}$ , the nozzle cooling valve opens as a function of throttle position. The right side of the diagram shows the temperatures for the maximum exhaust temperature of  $3040^{\circ}\text{F}$ , which is  $200^{\circ}\text{F}$  higher than the rated GE4 temperature. The base of the flap is  $416^{\circ}\text{F}$  cooler with augmentation than without, due to the 1.5 percent compressor discharge air flowing between the flap and the heat shield. The gradient across the flap structure without augmentation was  $393^{\circ}\text{F}$  compared to  $109^{\circ}$  during augmentation.

The proposed primary nozzle cooling design has noteworthy insensitivity to variations in the principal inlet conditions. The effects of secondary and liner cooling airflow quantity on primary nozzle temperatures are given in Figure 7-28. It should be noted that the component metal temperatures are relatively insensitive to secondary airflow rate. A 50 percent reduction in secondary flow results in an increase of only  $45^{\circ}\text{F}$  in flap temperature at maximum augmentor power and  $10^{\circ}\text{F}$  at cruise. The other parts are affected even less.

An increase of  $100^{\circ}\text{F}$  in the turbine discharge cooling air temperature from the augmentor liner only slightly affects the film cooling of the primary flap and seal. The magnitude of the effect does not exceed  $45^{\circ}\text{F}$  in metal temperature as shown in Figure 7-23.



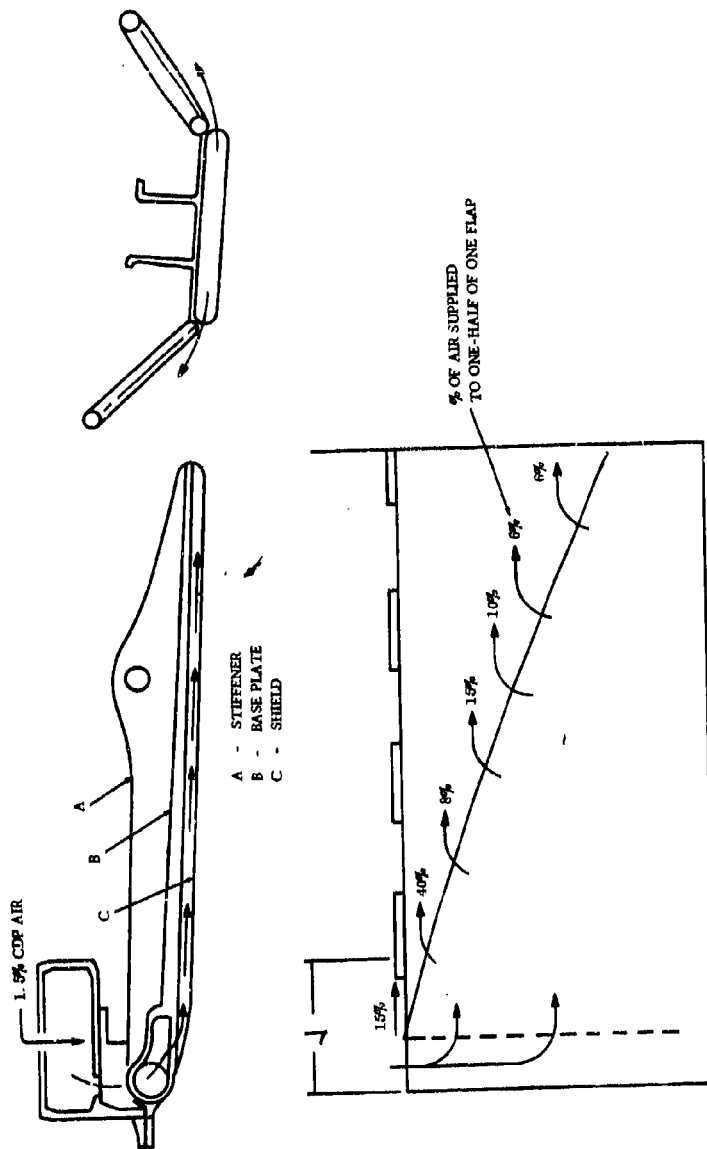


Figure 7-26. PRIMARY FLAP COOLING AIR DISTRIBUTION

CONFIDENTIAL

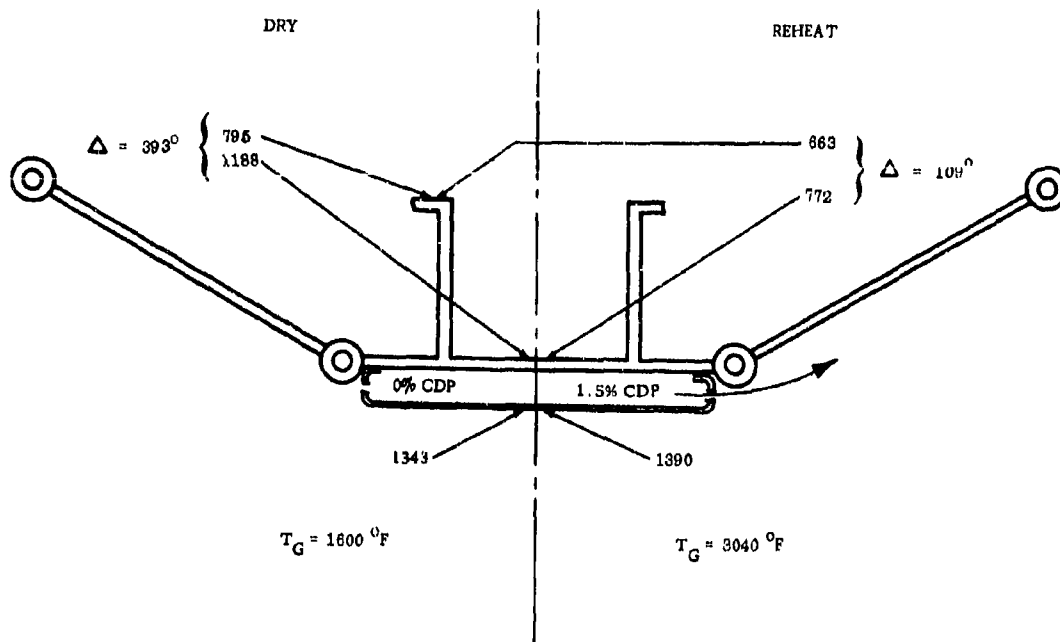


Figure 7-27. EFFECT OF COMPRESSOR DISCHARGE COLLING AIR

This insensitivity is the result of using compressor bleed air as the principal coolant.

The heat shield, in conjunction with the compressor discharge cooling air, makes the flap temperature relatively insensitive to hot streaks in the gas. The plot of metal temperature versus gas temperature in Figure 7-29, shows that the change in flap metal temperature is only about 10 percent of the change in primary gas temperature. A similar effect is evident for the seal temperature.

Refined techniques for heat transfer analysis of exhaust nozzles have been developed and confirmed by previous engine experience. Temperatures predicted by these methods for the GE4 test conditions agree very favorably with the measured temperatures as shown in Figure 7-29. These analyses have been applied to other significant operating conditions.

Figures 7-30 and 7-31 show the calculated flap and shield temperatures for sea level static conditions and Mach 2.7, 55,000 ft, respectively. The shield is not a structural member and, therefore, may operate at a higher temperature than the flap. The shield is similar to the augmentor liner that protects the tailpipe.

The primary flaps operate at favorably low temperature in comparison with existing commercial engine parts as shown in Figure 7-32. At takeoff power, the primary flap temperature is 1320°F compared to a measured reverser duct skin temperature of 1107°F on CJ805-3, 3A, and 3B thrust reversers. This reverser duct experiences the highest temperature at takeoff power.

CONFIDENTIAL

INCREASE IN METAL TEMPERATURE  
DUE TO:

50% LESS SECONDARY  
AIR

100% HIGHER LINER  
COOLING AIR

CRUISE	TAKEOFF	CRUISE	TAKEOFF
0°	15°	40°	45°
10°	45°	25°	45°
10°	40°	40°	45°

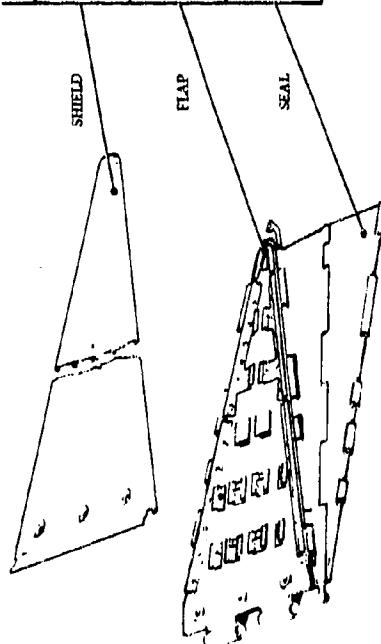


Figure 7-28. EFFECT OF SECONDARY AIR FLOW AND LINER COOLING AIR ON  
PRIMARY FLAP TEMPERATURE

CONFIDENTIAL

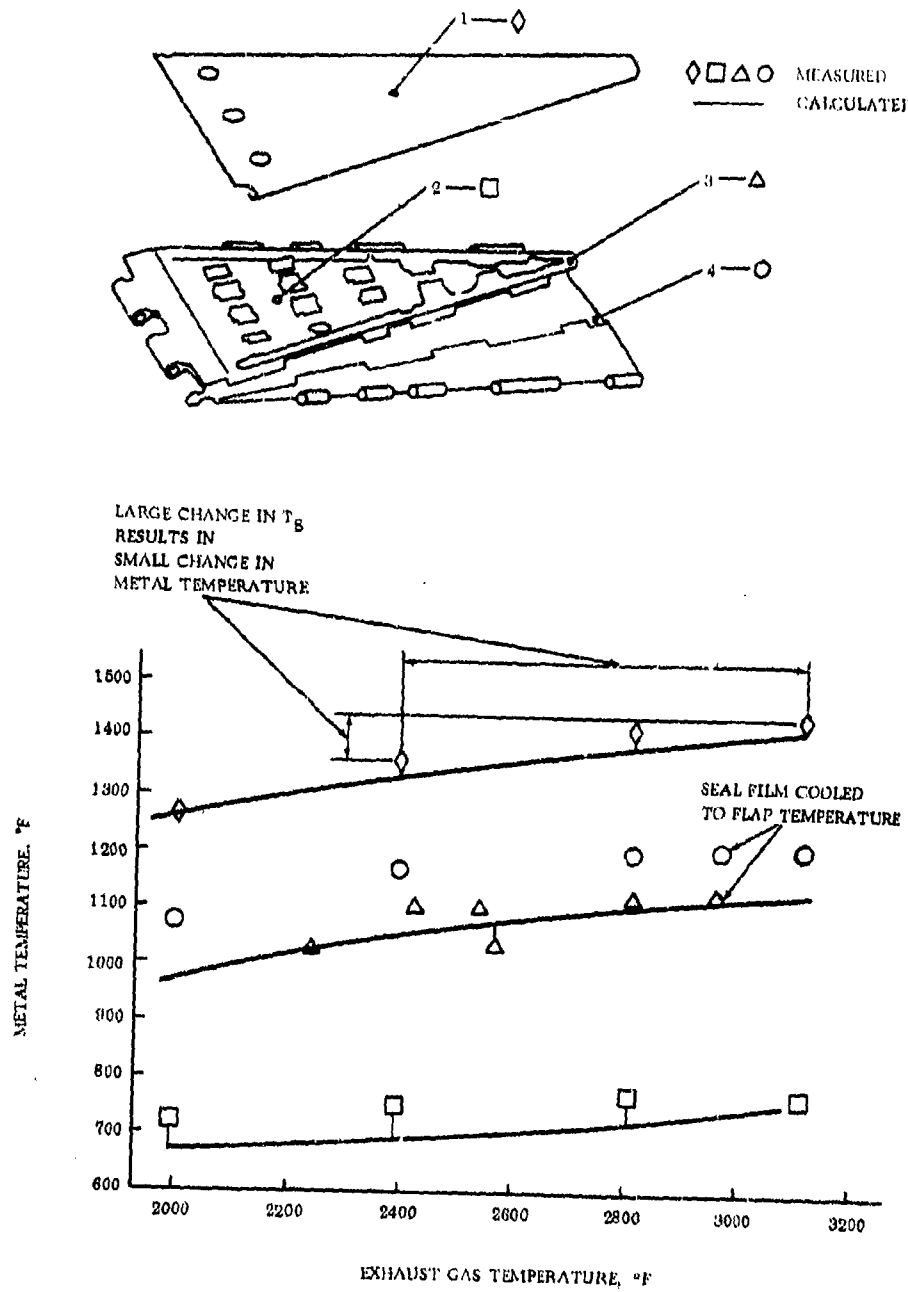


Figure 7-29. GE4 PRIMARY NOZZLE MEASURED AND CALCULATED TEMPERATURES - FULL SCALE TEST

7-34

CONFIDENTIAL

K

CONFIDENTIAL

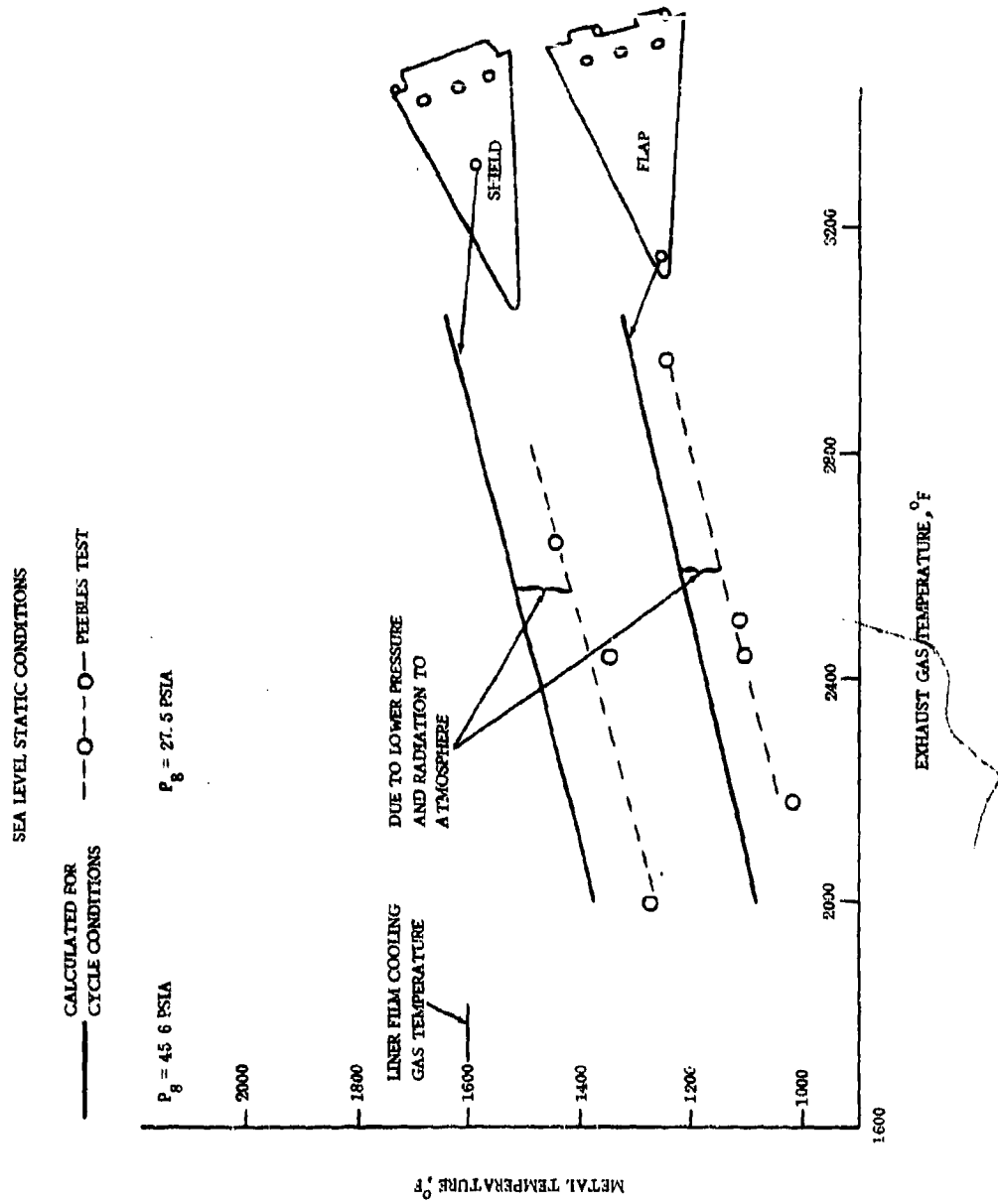


Figure 7-30. GE4 PRIMARY NOZZLE CALCULATED TEMPERATURES, SEA LEVEL STATIC

CONFIDENTIAL

CONFIDENTIAL

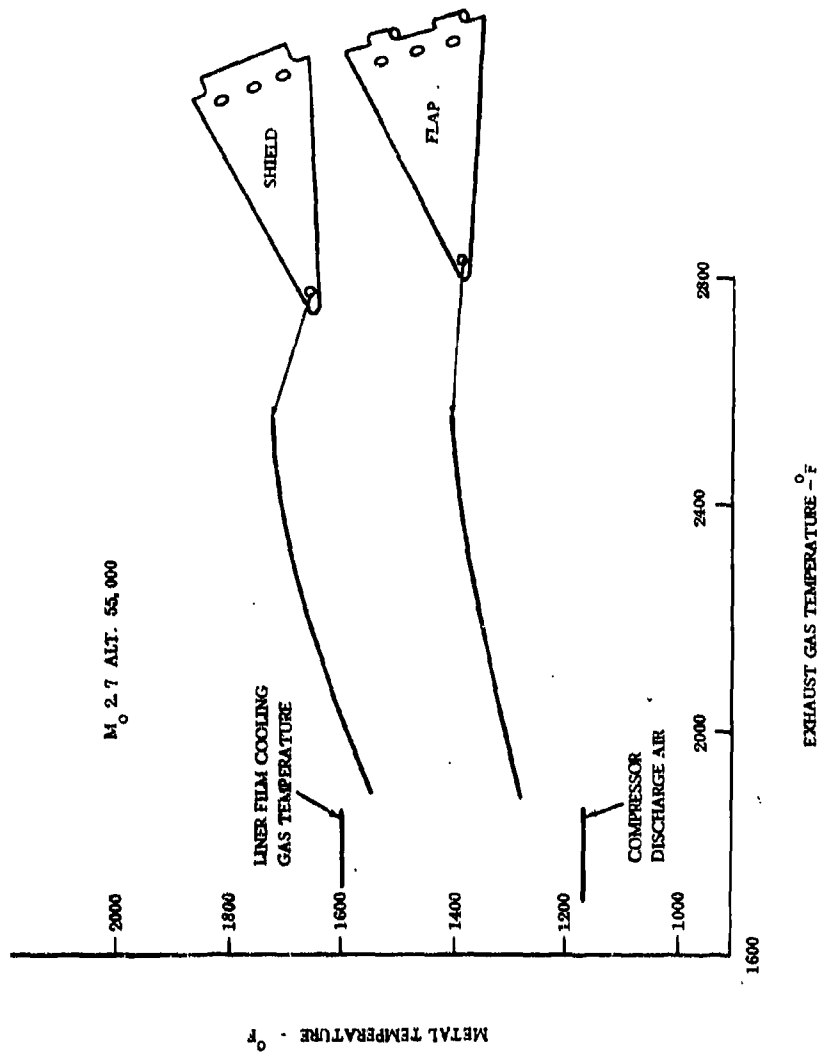


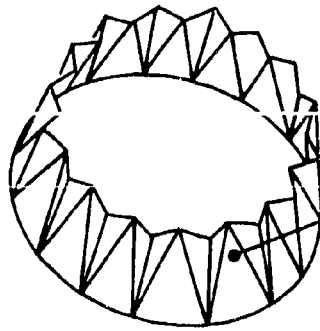
Figure 7-31. GE4 PRIMARY NOZZLE CALCULATED TEMPERATURES -  
MACH 2.7 55,000 FT.

CONFIDENTIAL

CONFIDENTIAL

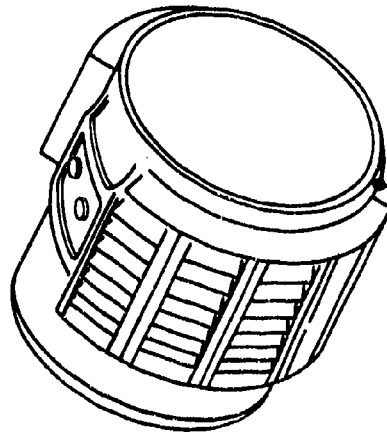
TAKEOFF POWER  
SST FLAP TEMPERATURE COMPARABLE TO  
COMMERCIAL ENGINE TEMPERATURE  
CR05 - 3, 3A, 3B

SST



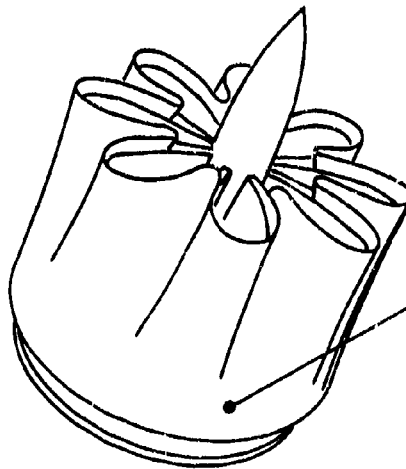
1320 °F

REVERSER DUCT



1107 °F

SOUND SUPPRESSOR



1024 °F

7-37

CONFIDENTIAL

Figure 7-32. COMPARISON OF METAL TEMPERATURES

## CONFIDENTIAL

The hinged seal is film-cooled by the CDP air distributed as shown in Figure 7-26. Test data from the full-scale evaluation are plotted in Figure 7-29. The aft end of the seal was cooled to within 100°F of the aft end of the flap.

It is appropriate to define the margins in the proposed design that enhance safety. Without CDP air for film-cooling, the hinged seals will operate below the yield point of Udimet 700 at maximum augmentor conditions as shown in Figure 7-33. Loss of CDP air will not result in loss of the seal. The primary flap is capable of operating without CDP air because of the protection provided by the shield.

If the shield is lost, the CDP air will provide sufficient film-cooling to prevent loss of the flap. At cruise, the loss of both the shield and the CDP air will not cause loss of a flap. The flap temperature will rise from 1280°F to 1520°F in the event of such a double failure. The safety factor based on 0.2 percent yield strength is 1.9.

### 7.5.4 SECONDARY NOZZLE COOLING

The secondary nozzle, like the primary nozzle, is shielded from the high-temperature exhaust gas by a boundary of coolant adjacent to the flaps and seals. Some of this coolant is provided as a residual film from the primary nozzle. Figures 7-29 and 7-30 illustrate the cooling film that leaves the primary nozzle and persists into the secondary nozzle.

Secondary airflow introduced through the large gap between the primary and secondary nozzles make the principle contribution to cooling of the secondary inner shroud flaps and seals. Secondary flow for the supersonic cruise configuration is shown in Figure 7-34. During takeoff and subsonic climb, the auxiliary air inlets located above the secondary nozzle gap open and admit large amounts of additional flow. The nozzle configuration in this operation mode is shown in Figure 7-34.

The effectiveness of the cooling provided by the gap flow decays exponentially with distance downstream of this point. To maintain a high cooling effectiveness along the entire length, cooling air slots are incorporated in the secondary inner flap aft of the gap to regenerate the cooling film and to compensate for the exponential decay of the gap flow. Air is supplied to these slots from the cavity between the inner and outer flaps. Secondary air enters this cavity through the hollow beams that support the nozzle shroud.

The method of cooling the secondary nozzle on the GE4 is similar to that used on J79 and J93 exhaust nozzles, as shown on Figure 7-35. The J79-10 and the J93 nozzles have gap flow and cooling slots in the secondary. Figures 7-36 and 7-37 show these two nozzles. Earlier nozzle-employed secondary flaps were cooled by the secondary flow entering between the primary and secondary nozzles only.

The effectiveness of the cooling has been demonstrated on the J93 nozzle by flight test evaluations on the XB-70. In-flight measurements of metal temperature on the secondary flap are plotted in Figure 7-34. The predicted temperatures were determined from data taken at AEDC.

Predicted temperatures in the GE4 secondary nozzle inner flaps are determined from heat balance equations that account for film cooling, radiation from the hot gas, radiation from the flap to the surrounding atmosphere, radiation to surrounding structure, and convection on the back side of the flap. Similar to the method defined for the augmentor, predicted temperatures for selected points are listed below in Table 7-6.



**CONFIDENTIAL**

**PRIMARY NOZZLE SEAL TEMPERATURE  
WITHOUT CDP AIR FILM COOLING**

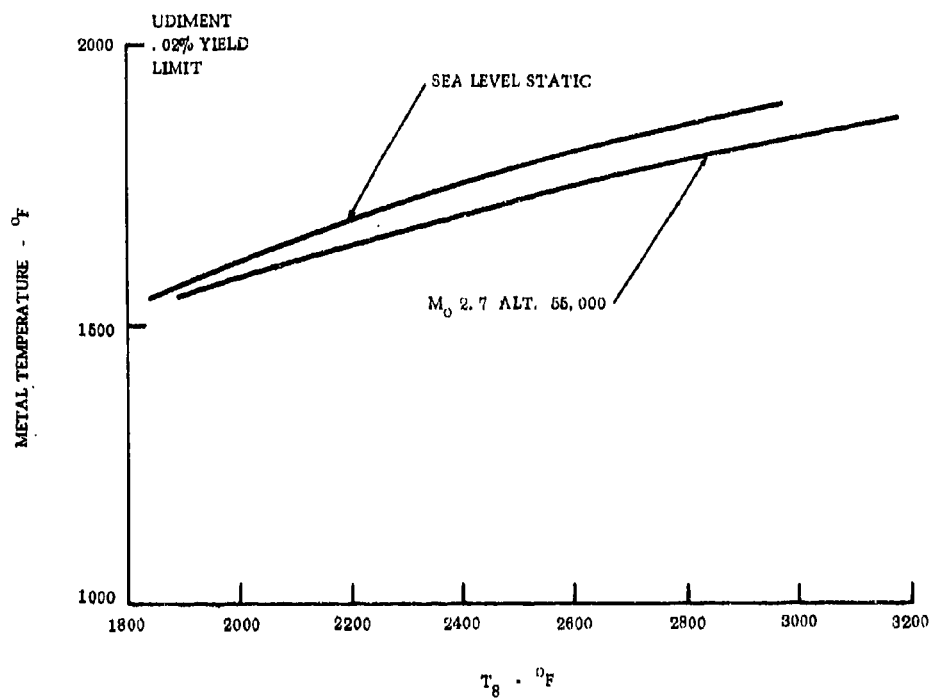


**Figure 7-33. PRIMARY SEAL TEMPERATURE**

**CONFIDENTIAL**

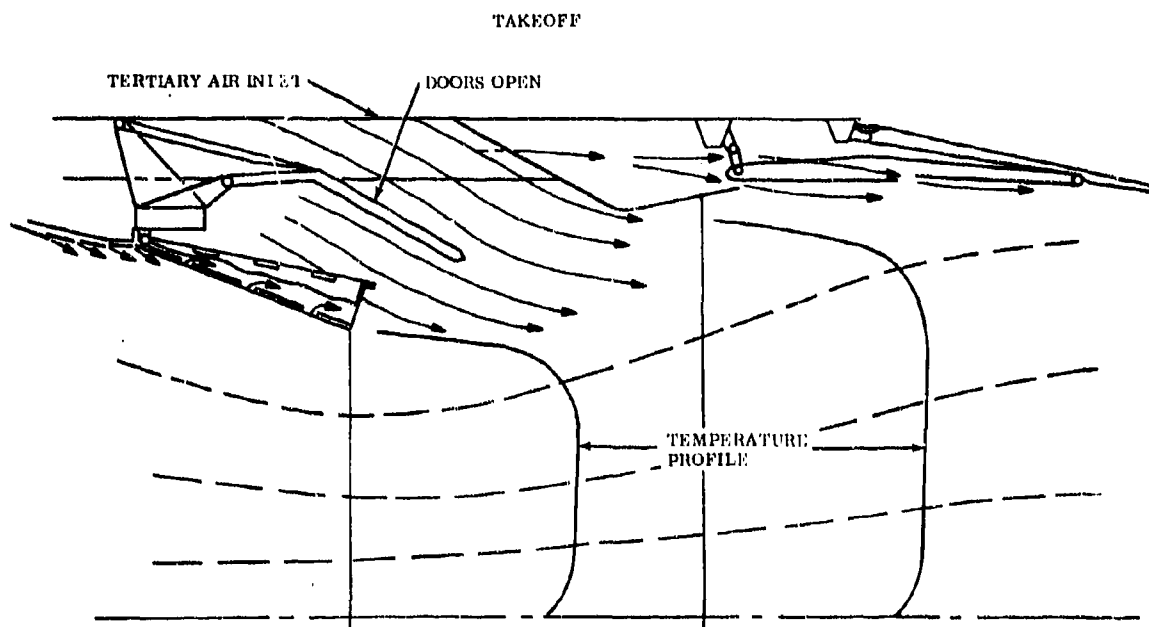
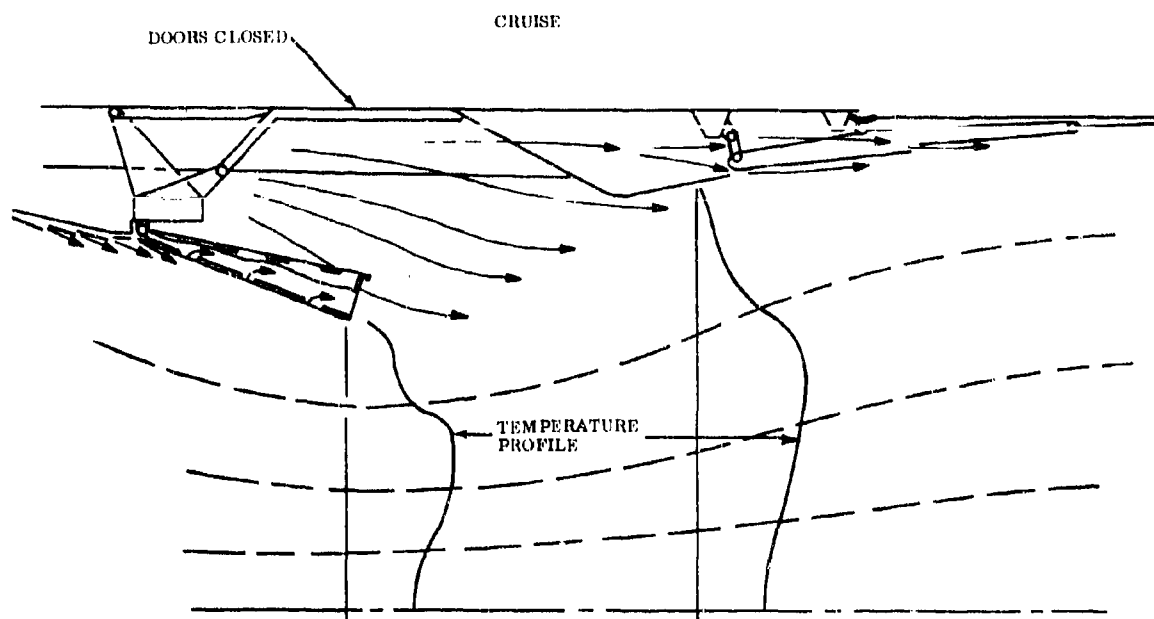


Figure 7-34. SECONDARY NOZZLE FILM COOLING  
AT CRUISE AND AT TAKE-OFF

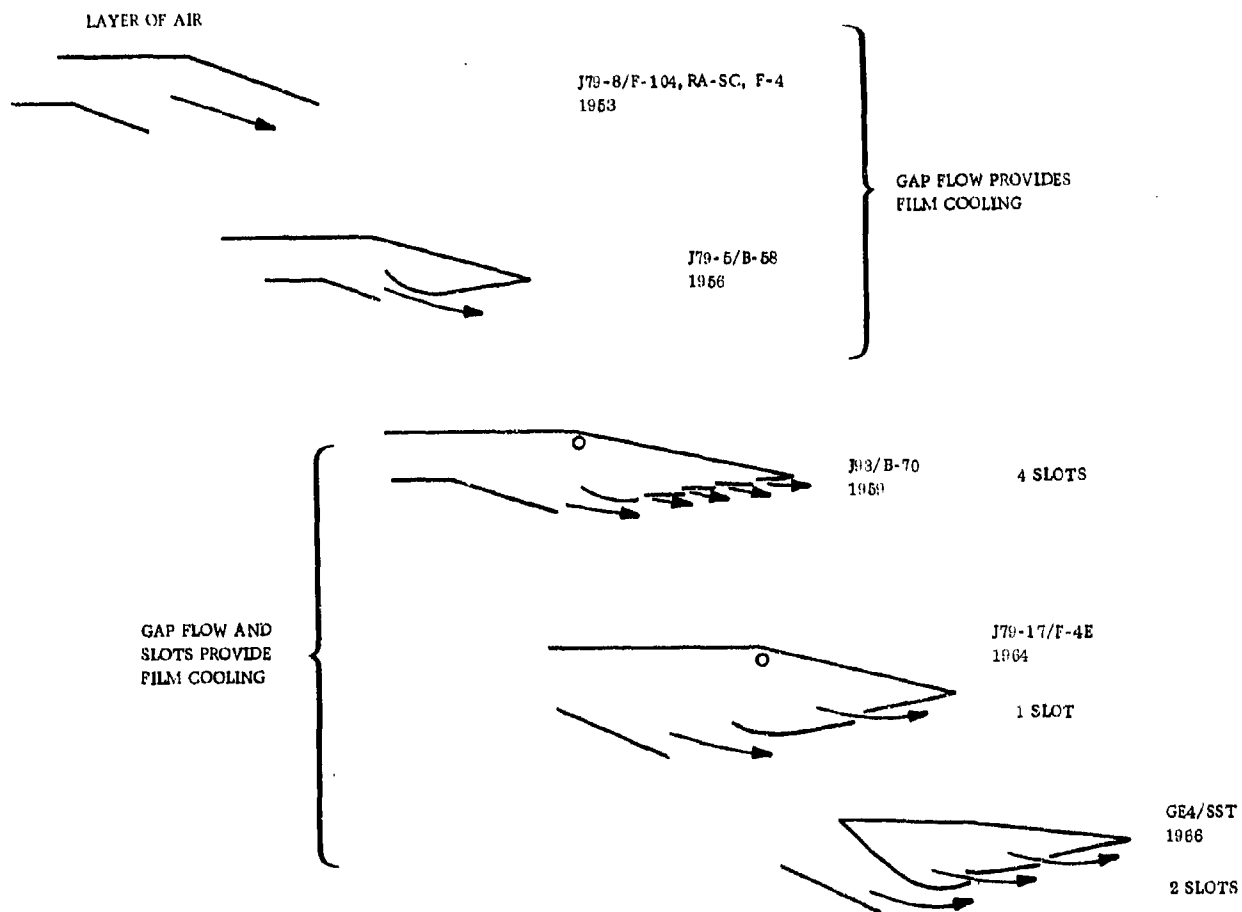
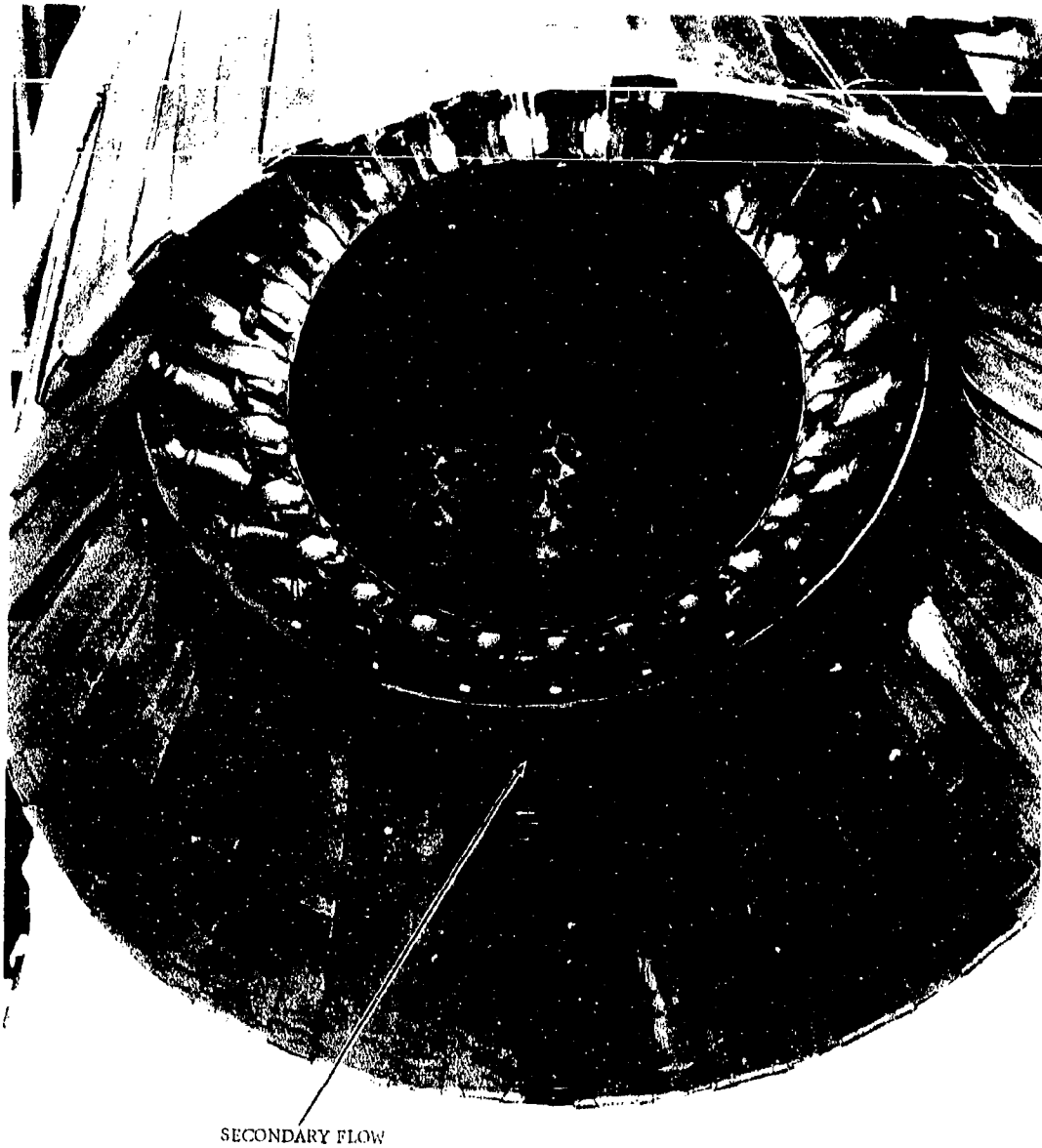


Figure 7-35. COMPARISON OF SECONDARY NOZZLE COOLING SYSTEMS



SECONDARY FLOW

Figure 7-36. J79-10 EXHAUST NOZZLE

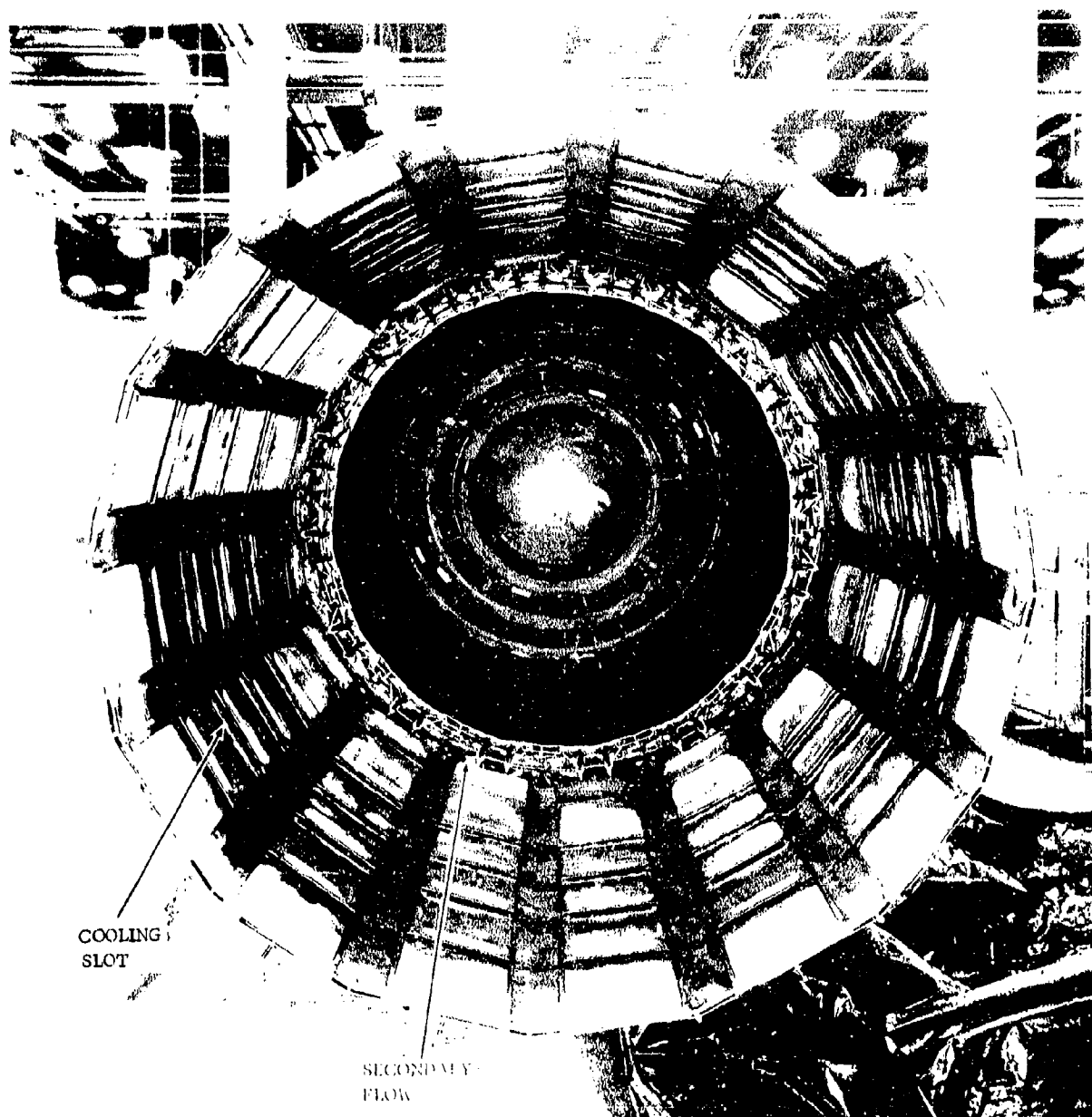


Figure 7-37. J93 EXHAUST NOZZLE

# CONFIDENTIAL

Table 7-6. Secondary Nozzle Metal Temperatures

Macn NO.	0	0	0.5	1.5	2.7
Altitude	0	0	15,000	45,000	65,000
T <sub>8</sub> °F	1850	2840	2535	2840	2840
Inner Flap °F	890	1420	1350	1330	1230
Inner Seal °F	990	1560	1540	1460	1370

Note that the maximum flap temperature is well below corresponding values for the combustor, augmentor liner, and typical current commercial engine hot-section temperatures.

## 8. MAIN SEALS AND BEARINGS

### 8.1 SUMMARY

The GE4 engine has a standard three-bearing system to provide short bearing span for rotor stability and excellent clearance control. Bearings are located:

- Forward of the compressor
- Between compressor and turbine
- Aft of the turbine

This stable system provides vibration control and uses existing bearing technology. Application of existing bearing technologies, i.e. bearing speeds, loads, materials and construction, will ensure meeting the reliability and maintainability goals as well as avoiding vibration difficulties.

Hydrostatic "floating face" carbon seals and a tandem circumferential seal are used in the GE4 engine to provide:

- Long seal life
- Minimum friction heat and resulting wear
- Restriction of air leakage into the sump cavity to help the lubricant achieve the long life required by a commercial supersonic transport

The engine has three basic sumps as follows:

- No. 1 Sump - contains the front main engine roller bearing and tandem oil seal
- No. 2 Sump - contains the engine thrust bearing and two hydrostatic oil seals
- No. 3 Sump - contains the aft engine roller bearing and two hydrostatic oil seals.

A cross-section view of the engine, showing each of the main bearing sumps is shown in Volume III-A, Figure 1-3.

### 8.2 DESIGN REQUIREMENTS AND APPROACH

The major design requirements for the seals and bearings are:

- Long life
- High reliability
- Ease of maintenance

Two major seal features are minimum heat generation and long life. The larger engine size affects shaft and bearing size so that the No. 2 sump seals must be larger in diameter than previous designs. However, the relatively low rotor speeds keep the seal rubbing velocities within reason.

Requirements are satisfied in the No. 1 sump by a conventional tandem circumferential seal because this sump is surrounded by relatively cool compressor inlet air (550° F) as compared to hotter fifth-stage compressor air (850° F) in the No. 2 and No. 3 sumps. This conventional-type seal meets the life and reliability requirements of the GE4 engine, and is lower in cost and weight than the seals required in the No. 2 and No. 3 sumps. The No. 2 and 3 sump uses a floating-face seal which eliminates face rubbing contact. The seal uses an air film and acts much like a gas bearing. Therefore two basic approaches to the thrust-type gas bearing seal have been taken.

- Hydrodynamic face with a velocity generated film.
- Hydrostatic face with a pressure generated film.

Seals of both types have been designed and converted into flight-type, full-scale hardware, then tested and evaluated. Seals of both types have successfully been demonstrated, but the hydrostatic version has the potential advantage of greater life and lower heat generation and therefore was selected for the engine. The minimum required life of the oil seals is 4000 hours, however considerably longer life is expected from this seal design.

Throughout the seal design program, the concepts of maintainability, reliability, human engineering, and standardization were given careful attention.

All machining and manufacturing processes are standard. Seal internal components are well contained within the seal housing to prevent damage in assembly and handling.

Long life and reliability are the prime design criteria for the bearings. The bearing designs are calculated to provide a B10 life of 20,000 hours for the ball bearing and in excess of 30,000 hours for roller bearings. Average bearing lives will be approximately five times these values. The basic designs are similar to the J79, J805 and J93 engine bearings, which have proven completely successful at operating conditions similar to those of the GE4.

Sumps have minimum volumes and lengths that permit the use of one scavenge port, and still have excess passage for all attitude and altitude scavenging conditions. Adequate flow area has been provided across the bearing support cone in each sump to prevent front and rear side pressure differentials and ensure flow of oil to each scavenge port.

The design lives of all other sump components are as follows:

- Air Seals - 18,000 hours
- All Other Parts - 36,000 hours

### 8.3 DESIGN DESCRIPTION

#### 8.3.1 SEAL DESIGN PHILOSOPHY

Figure 8-1 illustrates a cross-sectional view of the hydrostatic face seal used in the No. 2 sump.

The stationary carbon face and the rotating collar form a hydrostatic gas film on the hydrostatic seal. A small controlled flow of fifth-stage compressor bleed air passes in a radial direction between the carbon face and the mating ring surface, thus blocking all other flow and forming a non-rubbing seal. The two surfaces are separated by an air film approximately 0.0004 inch thick. Rubbing friction is reduced by this minimum of face contact; therefore, low heat generation results. The above conditions apply throughout engine operation except during starting, shutdown and



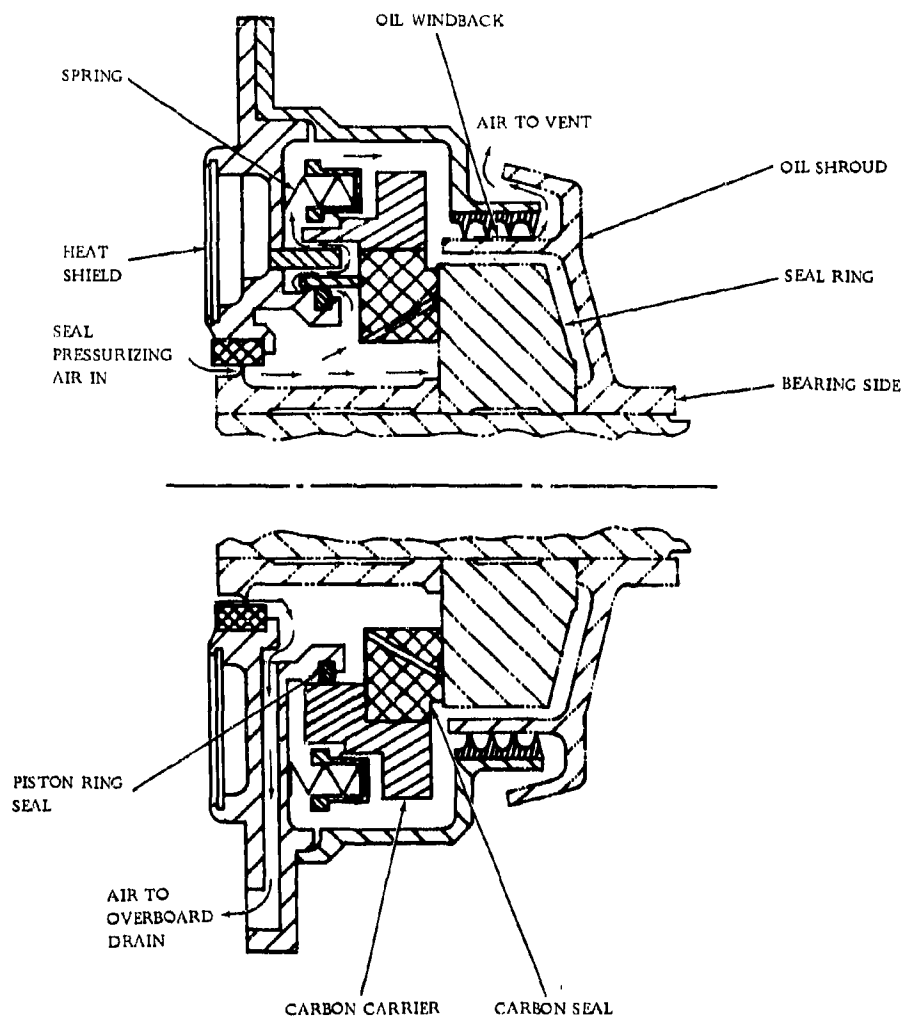


Figure 8-1. CROSS SECTION OF NO. 2 SUMP FLOATING FACE SEAL

windmilling conditions when compressor bleed pressure is low. During that brief period, a light spring force will cause the carbon face and mating ring to come in contact. In this state the seal acts as a standard, lightly-loaded, face seal and thereby prevents oil leakage. Component testing on this seal has successfully demonstrated the transition capability of operating at zero pressures and at normal operating pressures.

The seal uses a single piston ring for the secondary seal. A pressurizing air plenum is provided next to the seal (See Figure 8-2.) This pressurizing plenum is used to surround the entire sump with air considerably cooler (approximately 200° F) than the prevailing environmental air, which is at compressor discharge air temperature.

The following are the advantages of the hydrostatic type seal:

- Capable of operating at high environmental temperatures, pressure differentials, and face velocity.
- Low heat generation and wear resulting in long life.
- Low breakage rate at assembly.
- Has a relatively high face-load to reduce sensitivity to "hang up" from oil deposits or thermally induced rotor movements.

The use of labyrinth-type seals was not considered adequate for the GE4 engine for the following reasons:

- At flight speeds above Mach 1.0, the hot fifth-stage compressor air used for seal pressurization and that surrounding the sump, would result in the greatly increased hazard of sump fires and oil coking.
- The substantially increased hot air sump vent flow, associated with labyrinth seals, would reduce the lubricant life to unacceptable levels. The lubricant life is dependent upon bulk oil temperature, ambient air temperature, and oxygen content all of which are excessive using labyrinth seals on a supersonic application.

### 8.3.2 NO. 1 SUMP

The aft end of this sump is separated from the compressor cooling air by the NO. 1 oil seal, and the forward end of the sump opens into the inlet gearbox. (See Figure 8-3.) Due to the relatively low-temperature air surrounding the No. 1 sump (550° F) compared to the No. 2 and 3 sump, and the long thermal and mechanical axial travel required, a tandem circumferential seal was selected. (See Figure 8-4.) This seal is lower in cost and weight than the floating-face seals required in the No. 2 and 3 sumps. The tandem circumferential type of seal has been used very successfully in the J93 and CJ805 engines at rubbing velocities approximately the same as on this application (Refer to Table 8-1.) Tests have shown that this seal operates successfully under simulated GE4 conditions. A comparison of GE4 temperatures and pressures with the J79 and J93 engines are shown as part of Figure 8-3.

The tandem seal uses two segmented carbon rings, with the segments separated by a compression spring, mounted in the seal housing. (See Figure 8-4.) An oil windback is attached to the front of the seal housing to keep oil from contacting the carbon segment and producing coke. A pressurization cavity is attached to the aft side of the seal housing. Pressurizing air is bled from a plenum at the fifth stage of the compressor, through a pipe in the compressor front frame to the

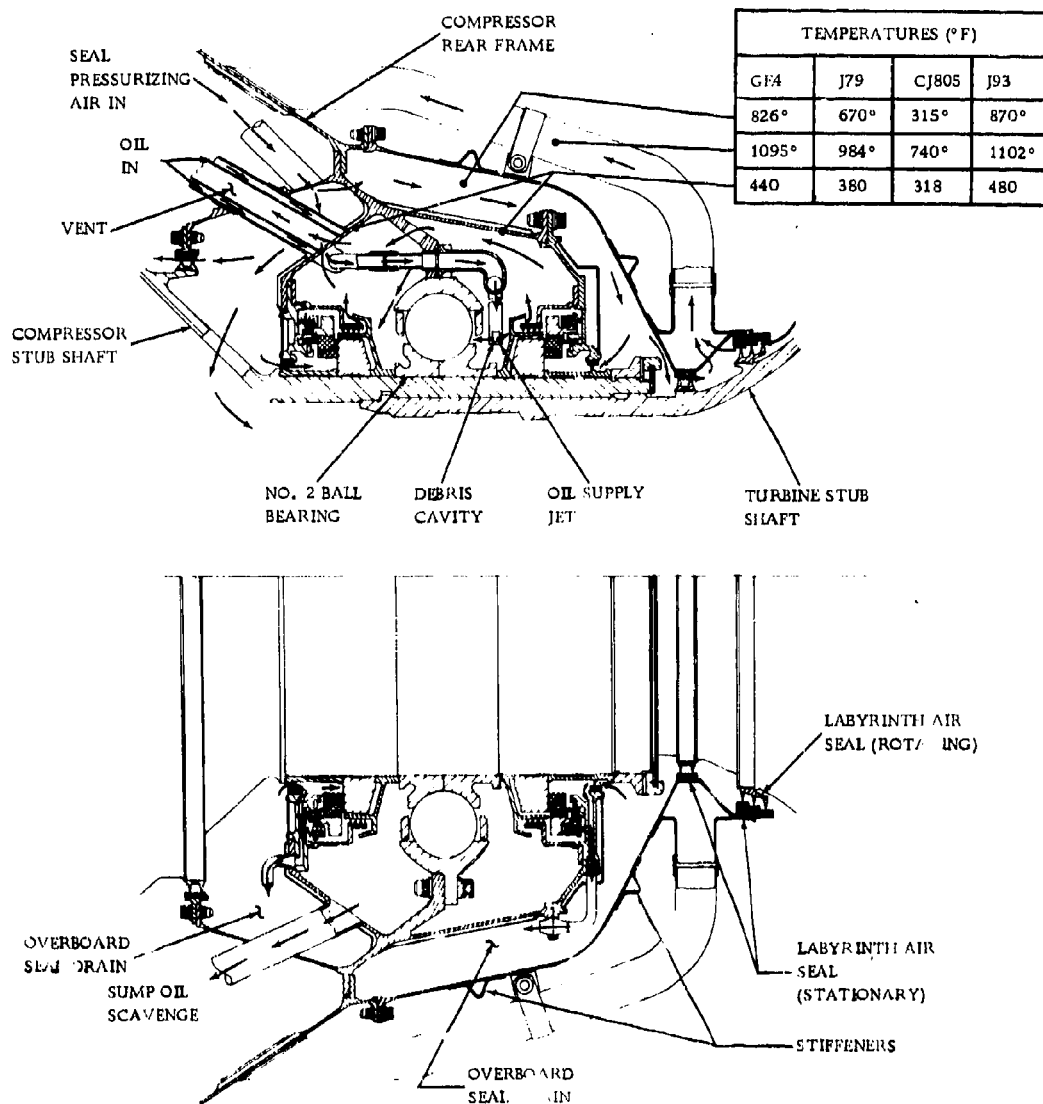


Figure 8-2. LAYOUT AND SCHEMATIC NO. 2 SUMP

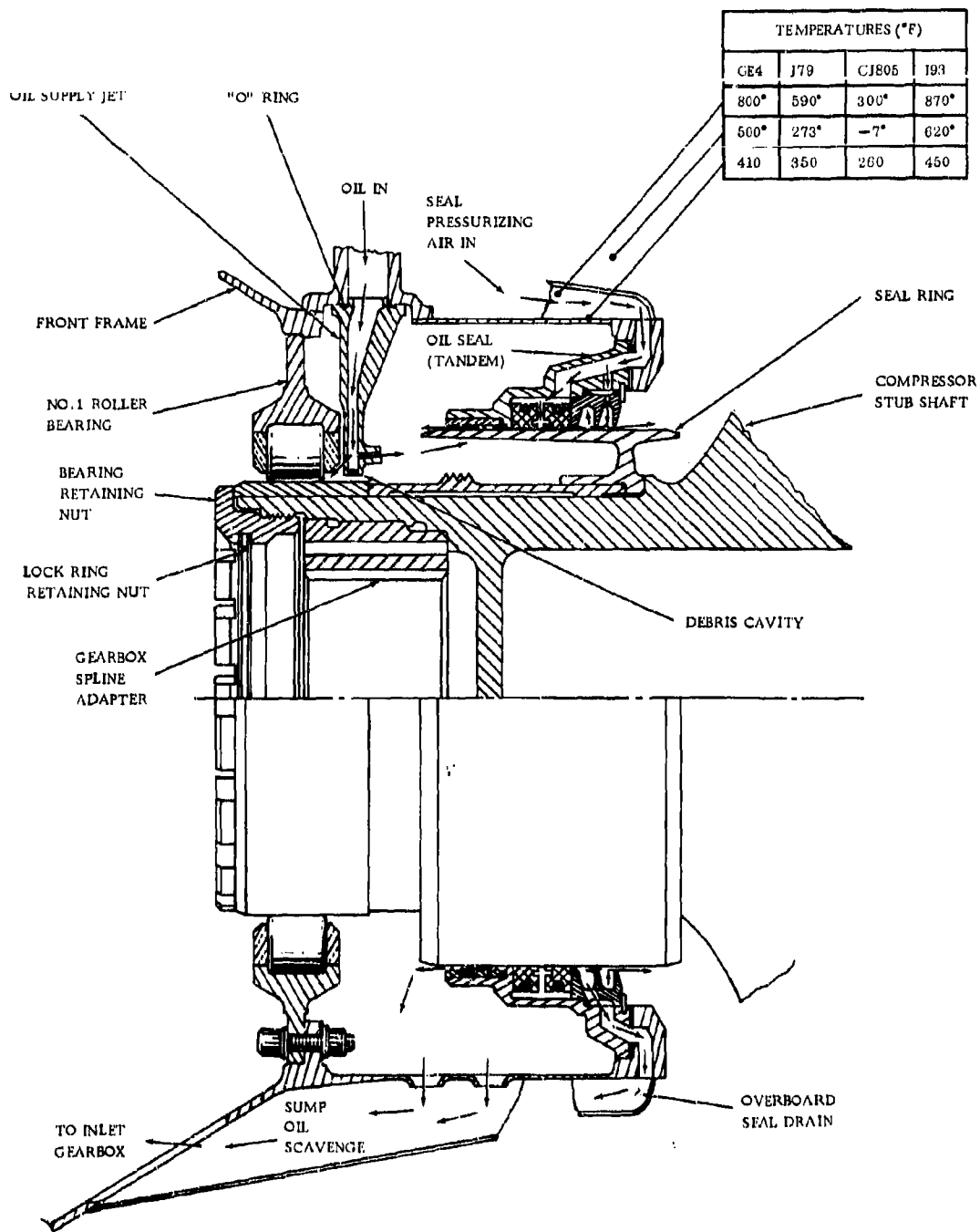


Figure 8-3. LAYOUT AND SCHEMATIC NO. 1 SUMP

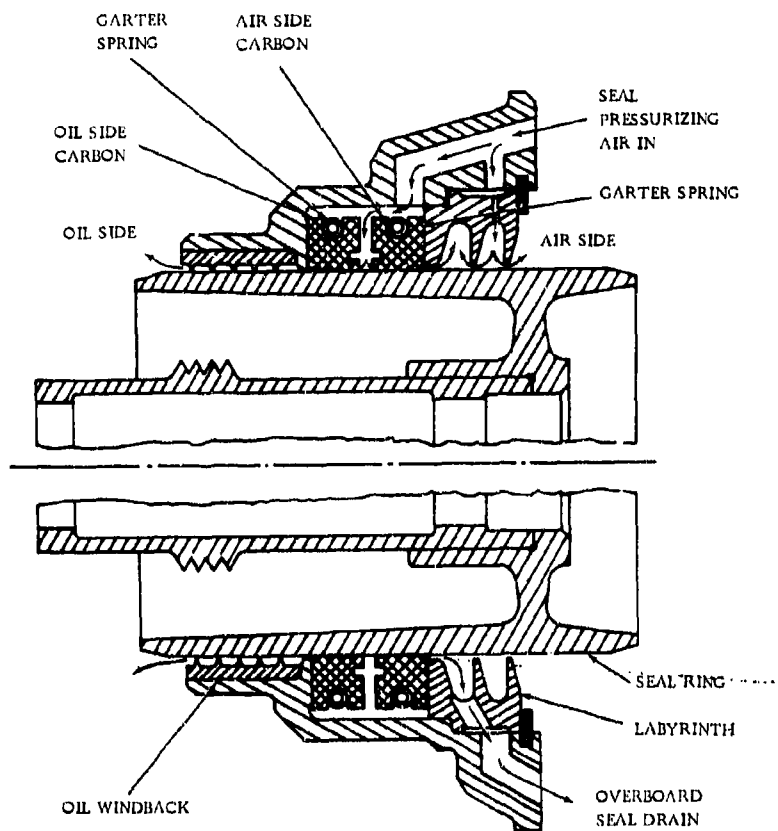


Figure 8-4. CROSS-SECTION OF NO. 1 SUMP TANDEM SEAL

Table 8-1 Main Shaft Seal Data

Location	Type	Pitch Diameter (Inches)	Velocity * (Ft/Sec)		Rubbing Surface Material	
			J93	GE4	Stationary	Rotating
No. 1 Sump	Tandem	6.250	141	138	USG Grade 2821**	Chromium Plate
No. 2 Sump	Forward-Hydrostatic	11.250	182	248	USG Grade 2821**	Tungsten Carbide
	Aft-Hydrostatic	11.250	182	248	USG Grade 2821**	Tungsten Carbide
No. 3 Sump	Forward-Hydrostatic	7.750	117	170	USG Grade 2821**	Tungsten Carbide
	Aft-Hydrostatic	7.750	—	170	USG Grade 2821**	Tungsten Carbide

\*At 5050 rpm engine speed.

\*\*Or improved grade from continuing development program.

seal pressurizing annulus between the two carbon rings. The pressurization air then leaks through the forward carbon ring into the sump, forming a barrier against oil leakage. The air leaking past the seal is discharged overboard after passing through a rotary air-oil separator on the accessory gearbox. The pressurization air also leaks through the aft carbon ring and out the seal drain. The seal drain is provided to prevent any oil from entering the compressor and contaminating compressor air in event of any seal malfunction. A summary of pressures around all sump cavities, including the most adverse pressure conditions, is included in the lube system Section III-B, Part III.

A pressurized cavity provides a continuous flow of air into the seal drain, continually purging the drain of any leakage oil. Because of the rubbing contact of this type of seal, cooling oil is provided under the seal race to ensure long life.

The No. 1 sump (Figure 8-3) uses a roller bearing of conventional design, except for the integral flange on the outer race. The flanged outer race is bolted directly to the front frame for positive prevention of bearing outer race rotation. The inner ring is press-fitted on the shaft, and is retained and clamped by a locked spanner nut. The bearing races and rolling elements are constructed of vacuum-melted M50 tool steel. The roller retainer is of one-piece, non-separable construction and made from S-Monel. (Refer to Table 8-2.) The DN value of  $0.61 \times 10^6$  for the No. 1 bearing is conservative when compared with maximum values on other established engines. (Refer to Table 8-3.)

The single oil jet is one-piece construction for increased reliability. (See Figure 8-3.) Two oil jets are provided for the bearing to increase reliability by providing redundant lubrication for this critical area. (See Figure 8-6.) A special cavity for catching debris which may have lodged in the oil supply tubing has been provided in each of the three sump oil jets.

Table 8-2. Main Shaft Bearing Data

Bearing No.	No. 1	No. 2	No. 3
<u>Bearing Type</u>	Cylindrical roller with flanged outer ring	Angular contact ball split inner rings and flanged outer ring	Cylindrical roller with flanged outer ring
<u>Cage</u>	Outer land riding, one piece construction	Outer land riding, one piece construction	Outer land, riding, one piece construction
<u>Anti Rotation Features</u>	Outer ring bolted to frame, inner ring pressed on plated shaft and clamped axially by spanner nut.	Outer ring bolted to frame Inner rings pressed on plated shaft and clamped axially by spanner nut.	Outer ring bolted to frame inner ring pressed on plated shaft and clamped axially by spanner nut.
<u>Bore (mm)</u>	120	245	160
<u>DN x 10<sup>6</sup></u>	0.61	1.24	0.81
<u>Roller or Ball Size</u>	17 mm x 17 mm	1.625 inches	18 mm x 18 mm
<u>No. of Ball/Roller Elements</u>	22	21	28
<u>Maximum Load (lb) and Operating Condition</u>	21,914 (Maximum Instant Maneuver Load)	90,000 (Emergency Descent)	30,672 (Maximum Instant Maneuver Load)

Table 8-3 DN\* Value General Electric Experience

Engine	Max DN Value X 10 <sup>6</sup>	
	Balls	Rollers
J79/CJ805	1.12	0.82
J93	0.92	0.55
T64	1.45	1.62
J85/CJ810/CF700	1.24	1.32
GE1	1.30	1.45
T58/CT58	1.19	1.19
TF39	1.55	1.59
GE4	1.24	0.81

\*D - Bearing bore diameter in (MM)

N - Speed in rpm

### 8.3.3 NO. 2 SUMP

The No. 2 sump, which contains the ball thrust bearing, is located between the compressor and turbine. (See Figure 8-2.) To minimize thermal growth and stack-up effects, the thrust bearing is located at the midpoint of the engine. The bearing is enclosed on each end by a hydrostatic face seal. The above components have been compactly assembled into a sump with a minimum amount of surface area and can be cooled adequately with a minimum of oil flow.

A comparison of GE4 temperatures and pressures with the J79 and J93 engines is shown as part of Figure 8-2. Pressurizing air for the seal is ducted to the area around the sump. (See Figure 8-2.) It flows past a single-tooth labyrinth seal through a 100-mesh screen located within the seal, and then through three 0.023-inch-diameter orifices into the hydrostatic pad area of the seal face. The seal face has three unconnected static pad sections of equal area that provide compensating forces to counteract any disturbing influence such as runout of the mating ring. Excellent performance has been demonstrated during tests when excessive mating ring runout as high as 0.006 inch was deliberately introduced. The air passing through the hydrostatic face pad flows radially outward through the face, through the windback and into the sump. This helps prevent oil from entering the seal windback. Air also flows from the cavity between the labyrinth tooth and the face through the seal drain, providing a positive blow-down drain to prevent accumulation of any oil in this cavity. Additional protection against oil leakage is obtained by using oil shrouds with slinging lips combined with the windback. The windback is a cylindrical spiral groove located adjacent to a rotating cylinder which forces the leakage oil back into the sump. Windbacks have demonstrated good effectiveness for preventing migration of oil along cylindrical surfaces on component tests and are used in the J93 and J85 engines.

A single-row ball bearing is used with its flanged outer-race bolted directly to the mid-frame to prevent outer race rotation. (Refer to Table 8-2.) The choice of a single-row bearing eliminates the load-sharing problems and mounting complexities common to the duplex type. Also, since the bearing thrust load is designed to change from forward to aft at different parts of the flight segment, bearing life is extended by using both sides of the races. This philosophy of using both fore and aft loading on the thrust bearing has been highly successful on the CJ805 and J93 engines and no bearing deterioration has ever been found as a result of this transient operation during the thrust crossover from forward to aft load. The criteria for size and configuration of the bearing design are straight forward and are like those proven on the CJ805 and J93 engines.

Vacuum-melted M50 steel has been selected for bearing races and balls because of its excellent fatigue properties, especially in the 500°F operating range. This material is used on current General Electric engines such as the CJ805 and J93. Bearing cages are of S-monel material which has had extensive use on the J93 engine and in component testing.

Experience shows that the vent lines are often plagued with coking or gumming of oil vapors. The GE4 vent design (Figure 8-2) avoids such buildups by surrounding the vent line with the oil supply line (concentric lines) thus controlling the temperatures of the metal in the vent line. Tests on the full-size Phase II-C No. 2 sump (Figure 8-5) have shown complete freedom from coke in the vent system.

### 8.3.4. NO. 3 SUMP

The No. 3 sump is located just aft of the turbine and is surrounded by fifth-stage compressor air. (See Figure 8-6.) This air is used to cool the turbine frame and the sump walls, and to pressurize the oil seals located at each end of the sump. Two oil seals are required in this sump to permit recouping compressor seal leakage from the No. 2 sump inside the engine shaft. This arrangement eliminates large external recoup lines on the outside of the engine. (See Figure 8-7.)



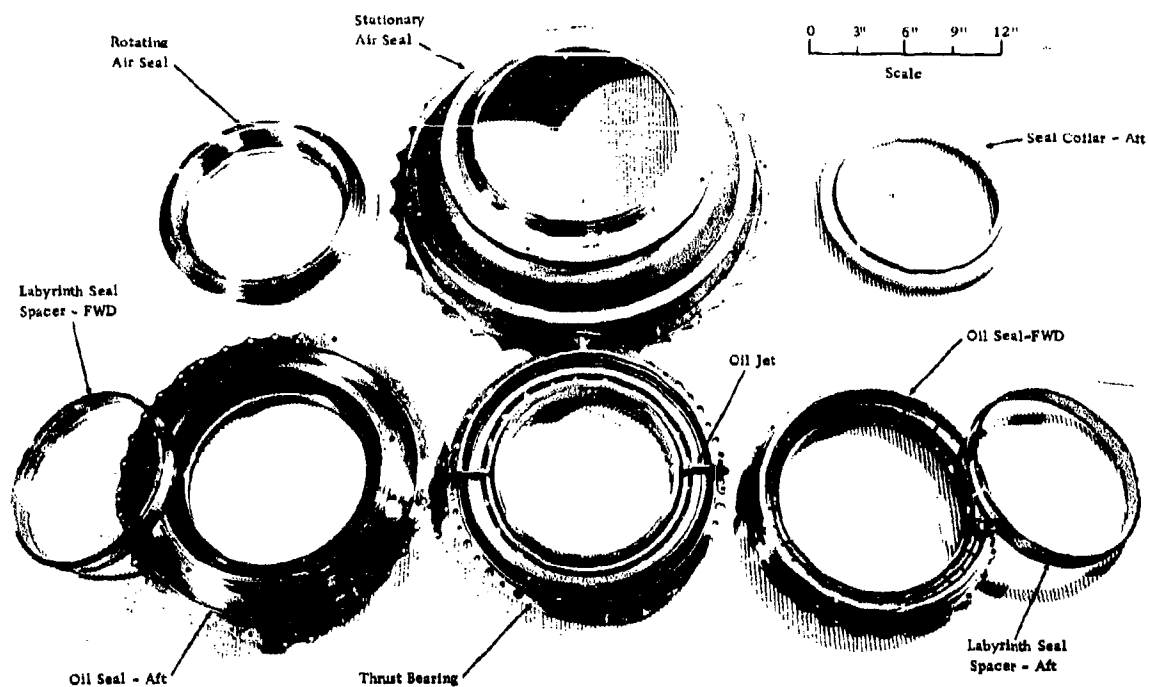


Figure 8-5. PHOTO OF PHASE II-C NO. 2 SUMP COMPONENTS

A hydrostatic seal, similar to those in the No. 2 sump, is used in this area. The features described for the No. 2 sump seals are present in the No. 3 sump seals. Figure 8-7 shows a cross-section of the No. 3 seal. A comparison of GE4 temperatures and pressures with the J79 and J93 engines are shown as part of Figure 8-6.

The roller bearing used in the No. 3 sump is similar to the No. 1 bearing, except for the large diameter required due to internal recouping (Refer to Table 8-2.) The lubrication and vent system are similar to those used in the No. 2 sump.

### 8.3.5 ROTOR THRUST BALANCE SYSTEM

#### 8.3.5.1 Introduction and Approach

Major improvement in thrust bearing life is obtained by careful design of a thrust balancing system to minimize bearing loads. The inherent aerodynamic loads on the turbine and compressor act in opposite directions with different magnitudes. The local static pressures throughout the engine act on projected areas of parts such as disks and cones, causing large, but predictable loads. For any given operating condition, the loads can be balanced by controlling the areas exposed to these pressures. However, these pressures vary with flight conditions, and system trades must be evaluated to establish the best balancing arrangement for the total use of the engine. The optimum balance was achieved by choosing appropriate diameters for the compressor discharge pressure seal (just inside the turbine first-stage nozzle) and for the compressor discharge rotor seal behind the compressor. The configuration results in a low load and provides a thrust bearing life in excess of 4000 hours.

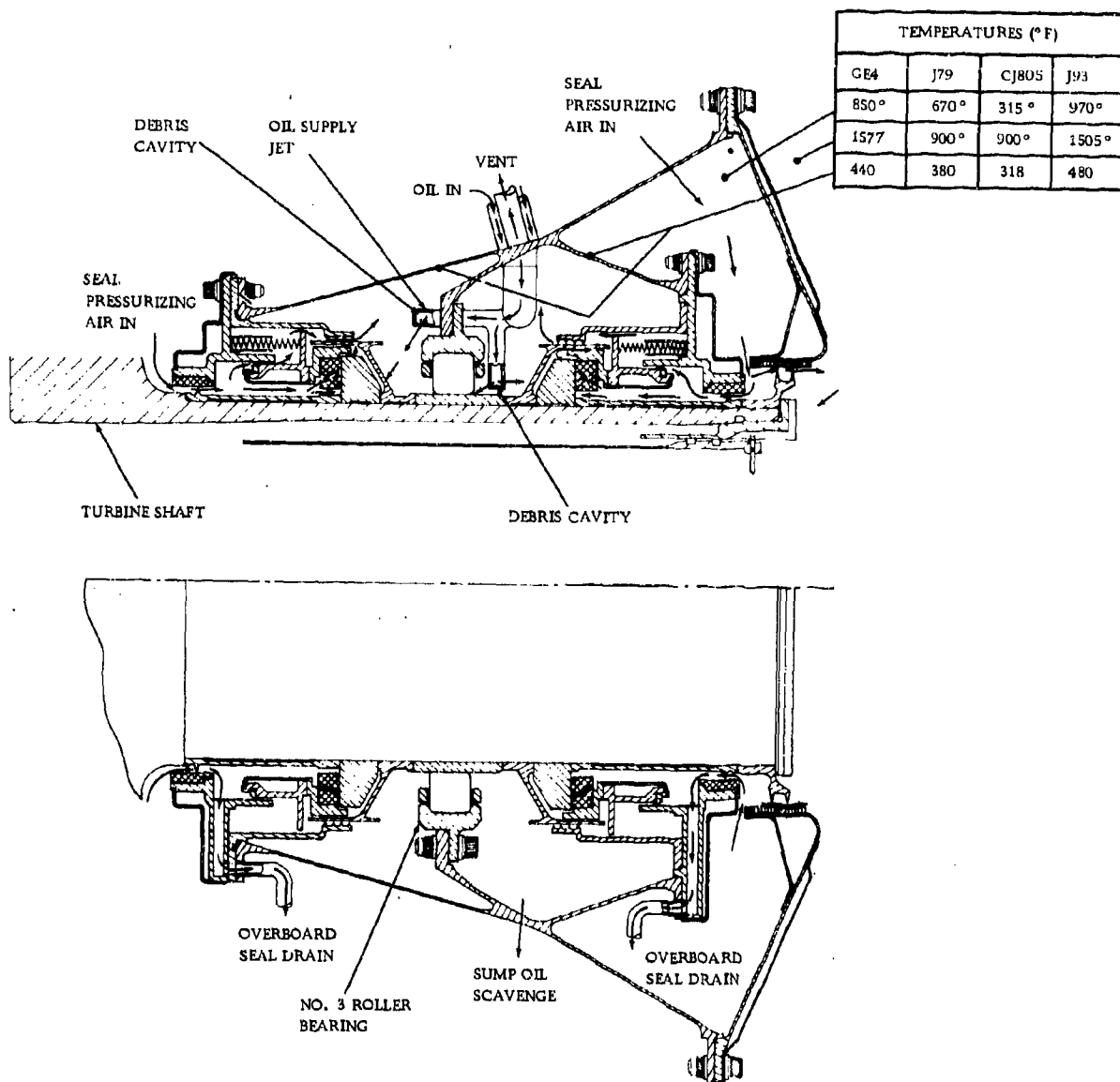


Figure 8-6. LAYOUT AND SCHEMATIC - NO. 3 SUMP

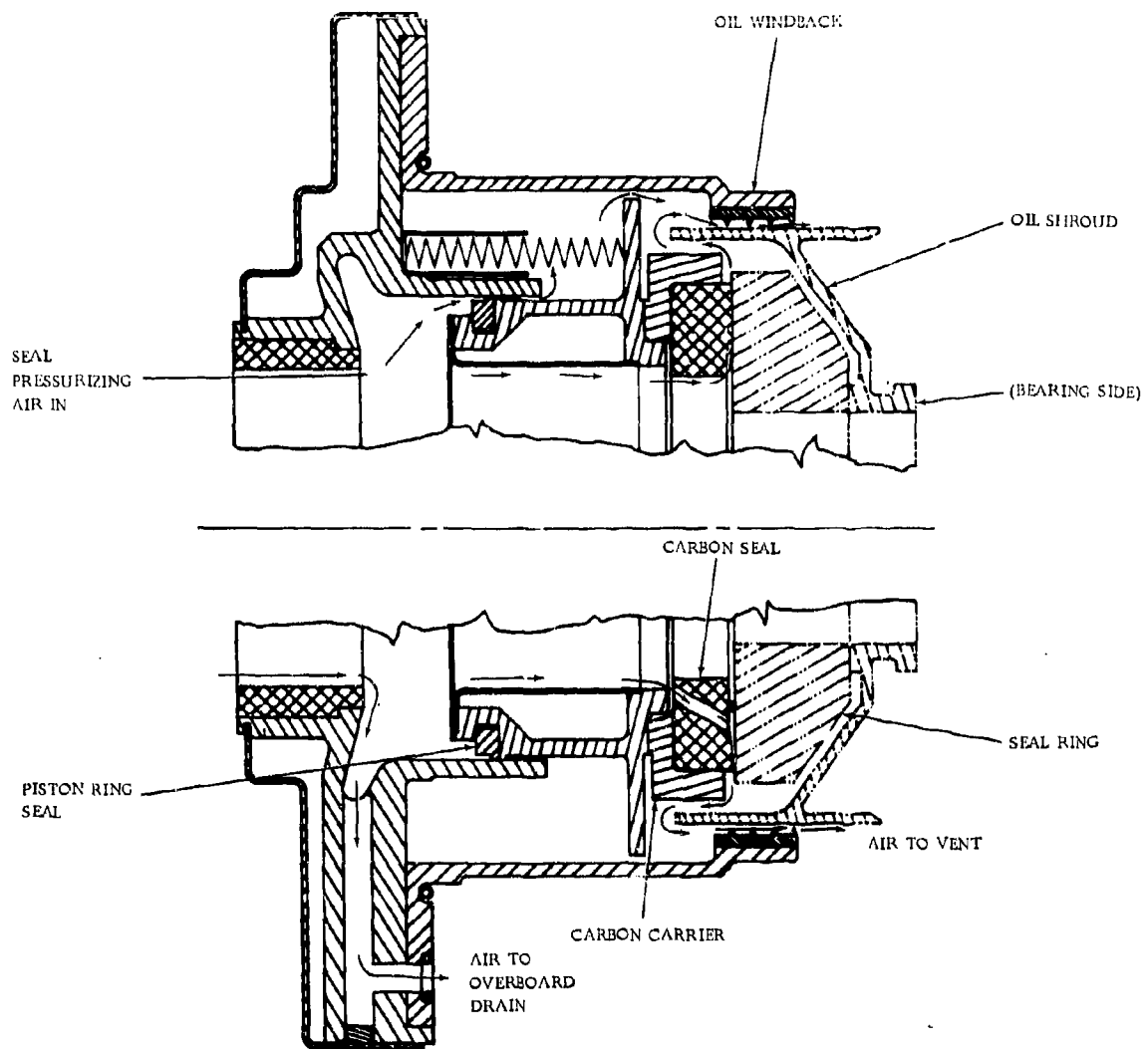


Figure 8-7. CROSS-SECTION OF NO. 3 SUMP-FLOATING FACE SEAL

The procedure used for finding bearing load is similar to the analysis used and thoroughly tested in the J79 and J93 engines. Thrust measurements on a J79 engine were made during flight tests on an F-104 aircraft, and a good correlation was obtained between analysis and test data.

The magnitude of the thrust loads on the bearing is related to the speed and altitude of the aircraft, and to the power setting of the engine. A satisfactory bearing life for a specified flight segment can be achieved by properly sizing the diameters of seals inside the engine with respect to the cavity pressures. A plot of corrected rotor thrust versus corrected speed ( $F/S_2$  versus  $N/50$ ) is given in Figure 8-8 for the GE4 rotor. Seal diameters, determined from the analysis, provide the low loads required to maintain the bearing life.

### 8.3.5.2 Description of Thrust Balance Design

The major load vectors contributing to the axial load on the bearing are shown in Figure 8-9. All load vectors except No. 111 are functions of cycle pressure and are unaffected by changes in air-flow through the labyrinth seals. However, vector No. 111 varies with the leakage air quantity through the compressor discharge seals. Flow through this seal is relatively independent of the pressure in the leakage cavity because the seal usually operates above the critical pressure ratio. Since the flow path out of the cavity does respond to air-flow rate, a larger pressure may develop in the seal leakage cavity as the rate of air leakage increases. The effect of this leakage variation has been minimized in order to prevent overloading of the bearing as the compressor discharge seal wears. The force vector in the cavity is associated with a large area on the rotor (830 square inches) so each psi of pressure variation causes an 830 pound change in bearing load. This effect is held to a minimum in the GE4 engine by providing 18.8 square inches of bleed area from the vent cavity in the compressor rear frame. Rotor thrust bearing loads for two flight conditions are given in Table 8-4.

Seal diameters selected to obtain the rotor balance are designed to minimize the parasitic leakage while maintaining the required rotor thrust bearing loads. Leakage from the compressor discharge seal is vented back into the cycle at the turbine discharge. The turbine seal leakage re-enters the cycle at the turbine inlet. Air that is vented overboard, or to the turbine exit, is more expensive to the cycle in terms of engine performance than is leakage to the turbine inlet, because the latter contributes work to the turbine.

The analysis of rotor thrust is important for determining the loads on shafts, nuts, bolts, and other parts. The GE4 analysis is also used for determining heat rejection of the thrust bearing and for the sizing of its lube supply system.

### 8.3.6 MAINTAINABILITY

Maintainability has been a prime consideration in the design of the sump bearings and seals. Emphasis has not only been placed on ease of performing continued maintenance tasks but on minimizing the need for total maintenance through the initial design of the component/system.

The following are specific features to minimize the need for maintenance:

- Lock rings are used on all bearing lock nuts after the torque is applied. No "sandwich" locking keys are used between the bearing and locknut. No bending of tabs is required with the locking ring system used, and all locknuts are designed to tighten in the event of race spinning.
- M50 bearing material is used to ensure long bearing life.
- Sumps are easily drained so wear debris can be carried to the scavenge screen for easy detection, and all oil can be easily drained from the engine at overhaul.

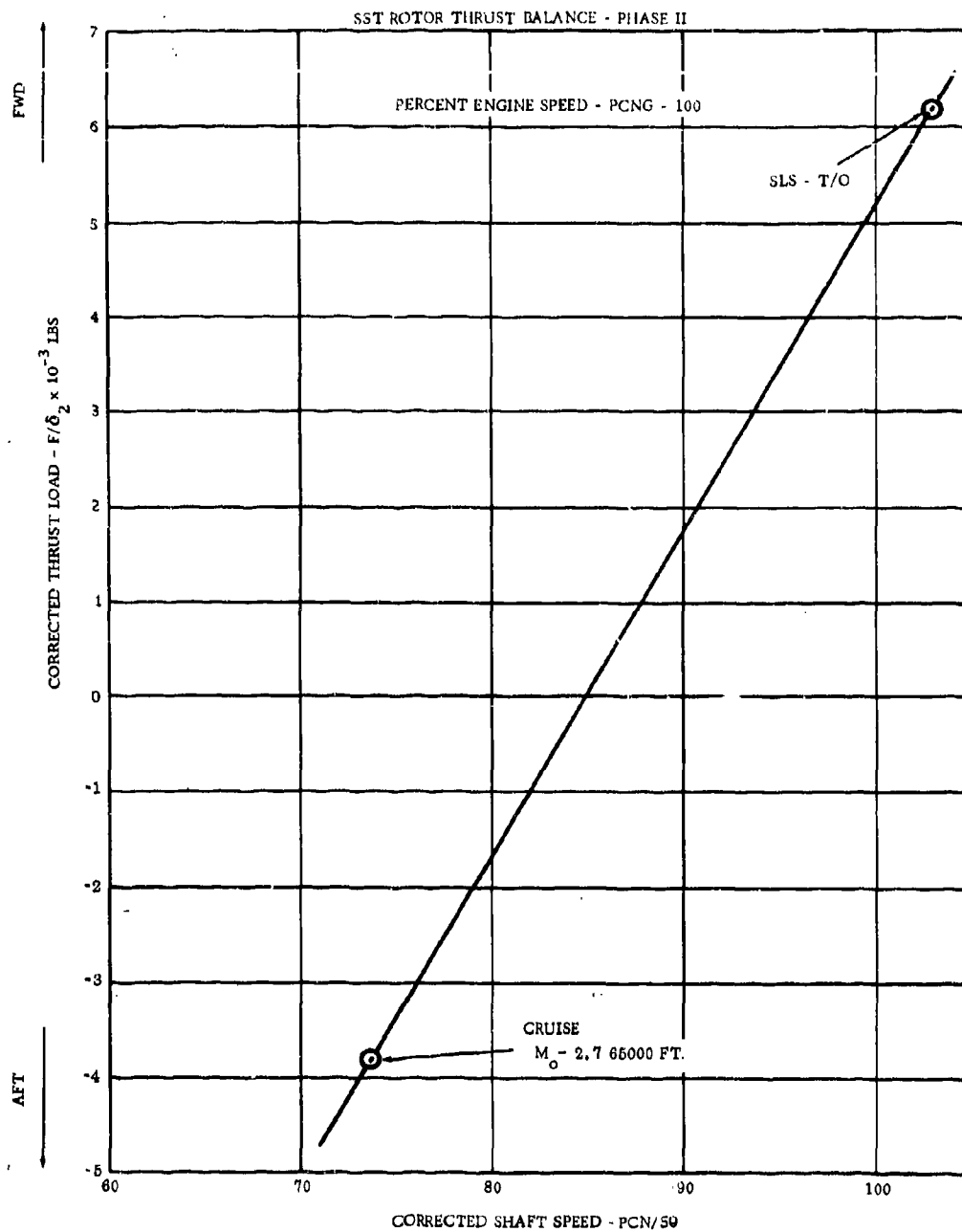


Figure 8-8. CORRECTED ROTOR THRUST VERSUS CORRECTED ENGINE SPEED

100

Table 8-4. Rotor Thrust Balance Forces

Load Vector	Flight Map Condition	
	Cruise	S.L.S.
-101	-7800	-5100
102	40800	74800
-103	-22800	-33400
104	40800	78200
-105	-25700	-49700
-106	-15100	-30400
107	18300	35300
-108	-4100	-8400
109	26600	54400
-110	-900	-1500
111	19400	40200
112	2500	4300
113	200	500
-114	-78600	-157400
115	2000	4000
	-4400	+5800

Total Brg. Thrust Load

- Aft Load, lbs  
+ Fwd Load, lbs

- All bearing outer races are bolted to eliminate race rotation that might cause wear in the bearing and frame rabbets.
- Hard chrome plated surfaces are provided at each main bearing inner diameter journal.
- All bearing inner races are clamped, and use a high press fit to prevent inner race rotation.
- The materials not in contact with oil are corrosion resistant and do not require painting.

- Debris cavities have been incorporated in every oil nozzle to catch and retain particles before they enter the lube nozzle.
- The piston ring secondary seals are chrome plated to prevent wear.
- The oil seals are designed to run without cooling oil internally and, therefore, prevent coking and hang-up during operation.
- No internal pumps are used for sump scavenging.

The following features facilitate maintenance:

- All bearing rollers and balls are retained in the outer race for ease of handling.
- Lead-in chamfers are provided for ease of assembly.
- The sump scavenge lines can be used for borescope inspection of the internal sump cavities without engine disassembly.
- Jack-screws, used for ease of disassembly, are a part of all bearing and seal housings.
- All sump wall heat shields are removable for ease of replacement and frame inspection.
- Flange holes are offset to prevent errors in assembly of parts requiring specific circumferential orientation.
- Puller grooves are incorporated on seal and bearing races that fit tightly.
- The seals are easily disassembled to permit replacement of internal parts, such as carbon faces and piston rings.
- Chrome plated journals and seals can be resurfaced.
- All sump flanges are thick enough to permit rework or repair at overhaul.
- The materials used in all parts can be repair welded.
- The sump support cones on the frames are removable and replaceable.
- Captive nuts are used in all blind assemblies.
- Standard nuts and bolts are used.

A durability and maintainability analysis for the main engine bearings has been completed and is contained in a special appendix entitled "GE4 Durability and Maintainability Analysis", which is available on request as back up material to the substantiating data submitted. The normal failure modes are identified, as well as the design approach employed to avoid the failure mode. Fault detection and maintainability features for the various conditions are listed. The frequency of inspection will be determined during the development program.



### 8.3.7 RELIABILITY

Features described in Section 8.3.6, Maintainability, which enhance reliability are M50 bearing steel, flanged outer races, clamped inner races, and debris cavities in the oil jets. Features in the design that were chosen specifically to enhance life and reliability are as follows:

- \*Heat generated by floating-face seals is very low compared to face contact seals.
- The two oil jets in the No. 1 and 3 sumps are of one piece construction, eliminating brazed and welded joints in the lube tubes. The No. 2 sump thrust bearing area uses a thick wall tube fabricated assembly adequately clamped and damped.
- Two oil jets are provided for each main bearing to provide redundant lubrication for these critical parts.
- Seal drains have been provided at each seal location so that any inadvertent oil leakage from the sump will be immediately drained overboard to prevent sump fires.
- All bearing journals are plated to eliminate fretting and generation of wear particles.
- \*Sump mounting flanges are either external to the sump cavity or use blind holes to prevent oil leakage out or hot air into the sump cavity through the mounting holes.
- The vent lines are surrounded by oil-in lines to prevent coke build-up inside them. (See Figures 8-2 and 8-5.)
- \*In event of a partial seal failure for any reason, the single-tooth labyrinth drain seal and the windback threads provide a restriction of hot air flow into the sump, minimizing internal sump coking.

### 8.3.8 QUALITY ASSURANCE

Seals and bearings are produced by qualified vendors possessing highly specialized skills. Responsibility for quality of product is delegated to the source with close coordination and surveillance. Audits are performed by this General Electric inspector, both initially and periodically (and/or lot-by-lot), to ensure the vendor's understanding of, and compliance with, the product drawing and specification requirements. Special emphasis is placed upon material and process control to preclude the slightest possibility of degradation of strength or life. Functional acceptance tests will be employed for the seals. Quality Assurance tests may be employed for verification of control of material and process variables affecting product life. The design has been made to simplify this activity and to enhance final quality by the following types of actions:

- Datum axis and datum planes have been established on all part drawings consistent with functional needs and manufacturing methods.
- Maximum advantage of shop-run tolerances have been taken where possible without compromising functional requirements.
- Appropriate specifications, such as magnetic particle and fluorescent penetrant inspection, are used wherever required.

\*Items designed specifically for the GE4 engine.

- Use of corrosion-resistant materials, wherever possible, have eliminated the requirements for hard-to-control platings.
- Standard industry bearing tolerances are used.

#### 8.3.9 SAFETY

Features described in Sections 8.3.6 and 8.3.7 Maintainability and Reliability, which enhance safety include: angled outer and clamped inner bearing races, seal drains, debris cavities in the oil jets, closed vent lines, two redundant oil jets to each bearing and fold-away sump flanges. Features in the design that were specially chosen for maximum safety, both during assembly and during operating conditions, are as follows:

- The inner seal components are designed to be completely enclosed and protected and the carbon face is protected during handling by the overhang of the windback flange.
- A windback has been incorporated on all carbon seals to prevent oil, which could cause coking, from entering seal housing, and also acts as an emergency labyrinth seal in the event of carbon seal failure.

#### 8.3.10 FAILURE ANALYSIS

A failure mode and effects analysis was performed on each main bearing and seal component utilizing the mechanized reliability program (RAP). The purpose of this analysis was to determine all possible failure modes and their effect on engine operating performance, and to ensure meeting or exceeding the objective levels of reliability, maintainability, and safety consistent with the technology of bearings and seals design.

All failure modes resulting from a particular failure mechanism were identified for each main bearing and seal component and the component effect was then traced from the systems level to the engine level.

Catastrophic failure modes were then eliminated by design changes, and critical hazards were minimized. The design confidence level of each main bearing and seal component based on design calculations and material properties was analyzed and evaluated separately to determine the need for testing.

General results from the study of failure analysis and effects are contained in Section 4.2.3.5 and other failure analyses to be conducted on the seals and bearings are described in Volume IV, 4.2 Reliability.

#### 8.3.11 VALUE ENGINEERING

Both the total concept and the design details of the main seals and bearings indicate application of manufacturability and value engineering. Features described in Sections 8.3.6 and 8.3.7, Maintainability and Reliability, which apply to value engineering are as follows:

- Bearings are basically of standard design with outer race flanges and inner race puller grooves.
- Sumps and seals are made of corrosion-resistant material to eliminate painting in initial manufacture and overhaul.

- Seal faces and mating rings can be re-lapped to correct for moderate amounts of wear.
- All overboard drain labyrinth seals are sleeves on the main shaft, and are easily replaceable.
- Many identical parts have been used in the sumps, such as various seal components in the No. 2 sump.
- General drawing tolerances and processes are no more severe than used in previous gas turbine design.

### 8.3.12 HUMAN ENGINEERING

Throughout the development of the design, human engineering objectives were considered to ensure both components and sump assemblies with safe, humanly engineered manufacturing and assembly capabilities. Features described in Sections 8.3.6 and 8.3.7, Maintainability and Reliability, which simplify human tasks are offset oil-seal flanges for correct angular orientation, puller grooves and jacking screws, lead-in chamfers, retained bearing balls and rollers, and interference-fitted assemblies controlled to limits of ease of assembly. Features in the design specifically chosen based on human engineering, are as follows:

- All sharp external corners on parts incorporate a radius or chamfer to prevent "knife edge" hazards to assembly personnel.
- Shafts have been designed with stepped diameters in areas of several fitted sleeves, thus, reducing the axial travel required to remove the part and therefore to lessen the likelihood of both assembly and removal damage.

### 8.3.13 STANDARDIZATION

Considerable effort has been used to ensure the standardization and control of design practices for the main seals and bearings. Design Practice Manuals have been used to improve consistency and technical excellence in the designs.

Examples follow of Standards and Specifications applied in the main bearings and seals design that have resulted in a high quality product at a low cost:

- Standard parts such as bolts, nuts, and washers were used wherever possible.
- The use of drafting standards ensures uniform, more easily understood drawings for the main seals and bearings.
- The use of standard specifications, for clearly specifying various main seal and bearing parts, ensures doing it correctly the first time.

A general specification for all ball and roller bearing designs is used to ensure that vendors meet consistent, approved general design requirements. In spite of the highly specialized design standard materials, methods of manufacture and processes have been used throughout the seals and bearings designs.

#### 8.4 DEVELOPMENT STATUS

Testing has already been completed and a continuing effort is underway extending through all phases of the engine program. The major areas of activity are:

- Seal Design and Test.
- Bearing Design and Test.
- Sump Component Design and Test.
- Simulated Lube System and Sump Test.

##### 8.4.1 WORK ACCOMPLISHED

A major break-through has been made in the field of long-life, low-heat-generating face seals. The newly developed concept has led to a new generation of seals particularly suited to air-breathing engines for high-Mach flight conditions.

The bearings are conventional types, tailored to the GE4 application. Proper materials have been selected, and close attention has been given to details to ensure their success.

The over-all sump design combines the seals, bearings and lube system parts into a functional unit. Full-scale tests have demonstrated the potential of the equipment.

##### 8.4.1.1 Component Seal Tests

Component evaluation tests have been run on all seal designs considered for the engine, including back-up designs. This testing has been performed on full-size flight-type seal components using special test equipment simulating the entire range of operating conditions and fulfilling the Phase II-C schedule as originally planned. To date 2145 hours of test have been accumulated. A portion of this time, 700 hours, was accumulated on the J93 simulated sump facility. (See Figure 8-10.) The remainder, 1445 hours, was on special seal component test rigs at Stein Seal Company, Philadelphia, Pa. (See Figures 8-11, 8-12 and refer to Table 8-6.)

##### 8.4.1.2 Component Bearing Test

Approximately 1000 hours of component testing have been completed on the GE4 No. 2 thrust bearing. This testing was conducted in a fatigue tester specifically designed to simulate bearing speed, thrust loads, radial loads, oil flows and oil temperatures the GE4 bearings will encounter. Figure 8-13 shows the tester.

Two bearings are mounted in the tester so that a thrust and radial load is applied to one bearing by a mechanical system, and the reaction opposed by the other bearing.

Three hundred hours of the 1000-hour total were at 10 percent overspeed conditions and 760 bearing hours were at an oil-inlet temperature of 400° F. (Refer to Table 8-7.) Oil shut-offs of 90 seconds at cruise conditions and 60 seconds at descent (max thrust load) conditions were demonstrated successfully. The tester is currently being modified to apply loads equivalent to those encountered during emergency conditions.

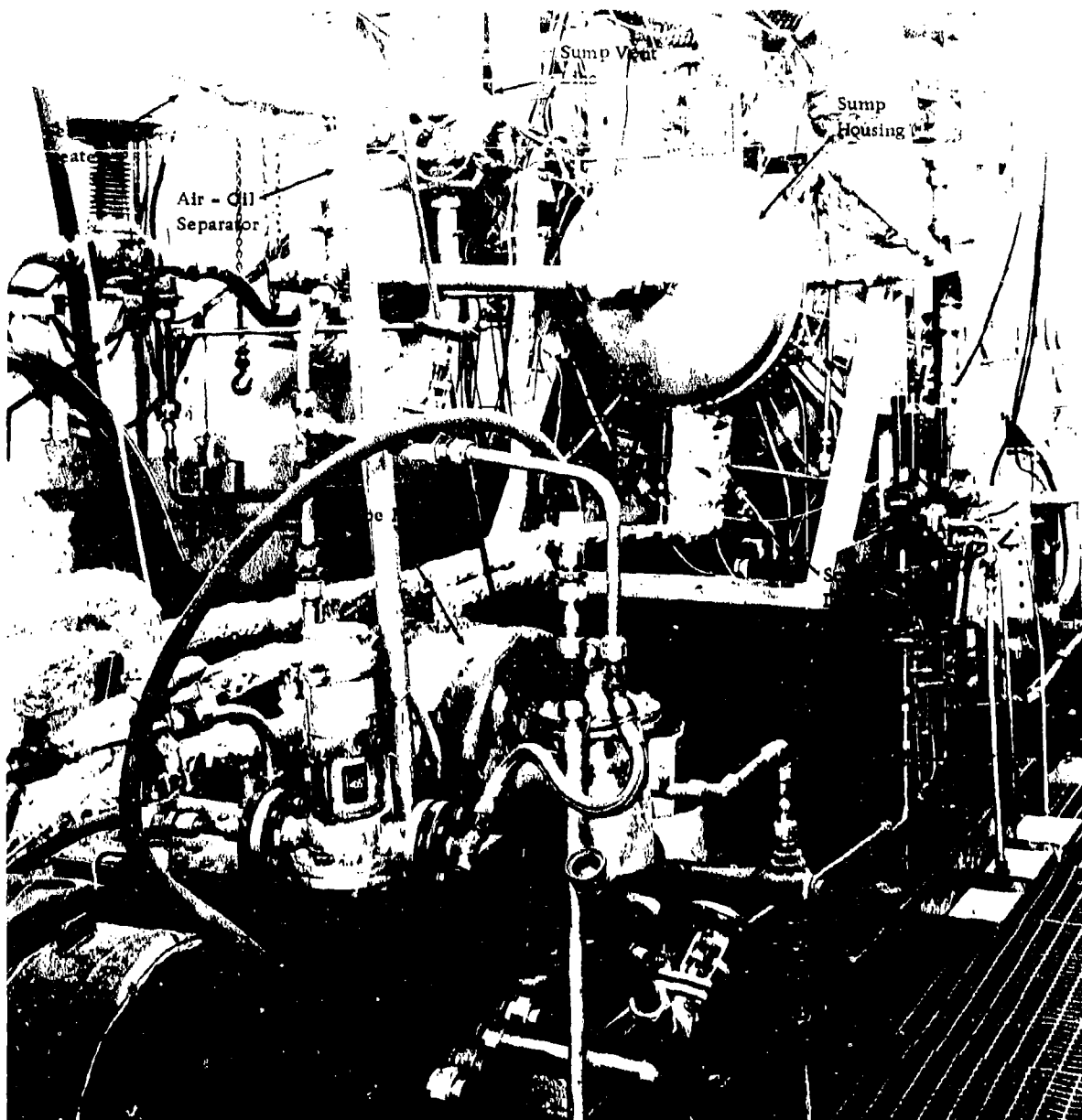


Figure 8-10. NO. 2 SUMP TEST FACILITY

Table 8-6. Main Shaft Seal Component Tests

<u>Sump</u>	<u>Seal Type</u>	<u>Test Parameters</u>	<u>Dura- tion Hr.</u>	<u>Purpose</u>		
No. 1/No. 3	Hydrostatic	Mach 2.7-3.0 & No. 2 PTV*	500	● Initial seal evaluation		
				● Collar development		
				● Initial carbon selection		
				● Windback evaluation		
No. 1/No. 3	Hydrostatic	Mach 0-3.0 & No. 1 PTV*	100	● Compressor bleed pres- surization		
				● Flight type seal		
				● Performance & initial life		
		Mach 0-3.0 & No. 3 PTV*	100	● Performance & initial life		
				Shop air	50	● Compatibility with pre- liminary engine operation
				Low pressurization	50	● Performance at altitude idle conditions
		Medium pressurization	50	● Performance at various power settings		
		Zero pressurization	50	● Performance & initial life at extreme low engine RPM conditions		
Collar run-out	45	● Performance at extreme collar run-out up to 0.006 FIR				
No. 1/No. 3	Hydrodynamic	Mach 0-3.0 & No. 3 PTV*	100	● Flight type seal		
				● Compressor bleed pres- surization		
				● Performance & initial life includes axial travel		

<u>Sump</u>	<u>Seal Type</u>	<u>Test Parameters</u>	<u>Duration Hr.</u>	<u>Purpose</u>
No. 1	Tandem	Mach 0-3.0 & No. 1 PTV*	100	<ul style="list-style-type: none"> <li>• Flight type seal configuration</li> <li>• Performance includes axial travel</li> </ul>
No. 2	Hydrostatic	Mach 0-3.0 & No. 2 PTV*	100	<ul style="list-style-type: none"> <li>• Flight type seal</li> <li>• Compressor bleed pressurization</li> <li>• Performance &amp; initial life</li> </ul>
No. 2	Hydrodynamic	Mach 0-3.0 & No. 2 PTV*	100	<ul style="list-style-type: none"> <li>• Flight type seal</li> <li>• Sump ambient pressurization</li> <li>• Performance &amp; initial life</li> </ul>
No. 2	Hydrodynamic	Mach 0-3.0 & No. 2 PTV*	100	<ul style="list-style-type: none"> <li>• Flight type seal</li> <li>• Compressor bleed pressurization</li> <li>• Performance &amp; initial life</li> </ul>

\*PTV - Pressure, Temperature, and Velocity

Two problems that did not restrict bearing operation were found as a result of these tests: 1) noticeable discoloration of the cage opposite the lube jets indicates a high thermal gradient occurred across the width of the cage; and 2) burnishing of the cage land-riding surface opposite the oil jets during normal running and pick-up between the cage and outer race during "oil off" testing.

The solution to the first problem is to add an oil jet to the forward face of the bearing. This modification is being done, and will be incorporated in the Phase III engine design. The solution to the second problem requires additional testing, using modified cage-to-race clearances and platings if necessary.

#### 8.4.1.3 Simulated No. 2 Sump Test

No. 2 sump test vehicle (Figure 8-10) was designed and constructed to permit evaluation of full-size sump components. The new equipment is capable of testing a complete sump including seals, bearings, wall configuration, shaft components and plumbing such as jets, drains, supply, scavenge, and vent lines. Auxiliary equipment is capable of duplicating the flows, temperatures, pressure differentials and bearing thrust of actual engine operation.

Table 8-7. Summary of No. 2 Bearing Tests

<u>Flight Condition</u>	<u>Bearing Time (hr)</u>	<u>Thrust Load (lb)</u>	<u>Radial Load (lb)</u>	<u>Speed (rpm)</u>	<u>Oil Temp. (° F)</u>
Take-off	103.4	8,230	2,500	5050	250
Normal Climb	45.0	6,600	2,500	5050	250
Maximum Climb	73.8	6,764	2,500	5050	250
Mach 2.7 Cruise	272.6	4,380	2,500	5050	400
Descent	55.8	21,300	2,500	5050	400
Landing	55.0	10,210	2,500	5050	400
Taxi-Idle	104.4	5,115	2,500	5050	400
Overspeed	300.0	4,380	2,500	5500	400
4 Oil Shutoffs	4.5 min	4,380	2,500	5500	250
2 Oil Shutoffs	1.5 min	4,380	2,500	5500	350
3 Oil Shutoffs	2.5 min	10,210	2,500	5500	250
2 Oil Shutoffs	1.5 min	21,300	2,500	5500	350

The initial test of 100-hour duration demonstrated the sump's capability to perform under engine condition. Major items evaluated were:

- Flight-weight hydrodynamic seals
- Flight-weight ball bearing
- Lube system performance
- Heat transfer
- Vent and scavenge performance

Certain areas of desired improvement to maintain performance throughout the extended life required of GE4 engines were noted, including heat transfer resulting in oil degradation and seal wear. Additional tests run on the J93 size facility are listed in Table 8-8.

#### 8.4.1.4 Lube Tube and Cone Vibration Tests

The lube tubes for the various sumps and the conical stationary labyrinth seal from the No. 2 sump for Phase II-C engine were tested for vibratory response. The test pieces were mounted at the same points used in the engine, and were electromagnetically excited while being scanned for response, amplitude, and nodal pattern. In all cases the components were well out of the one-per-



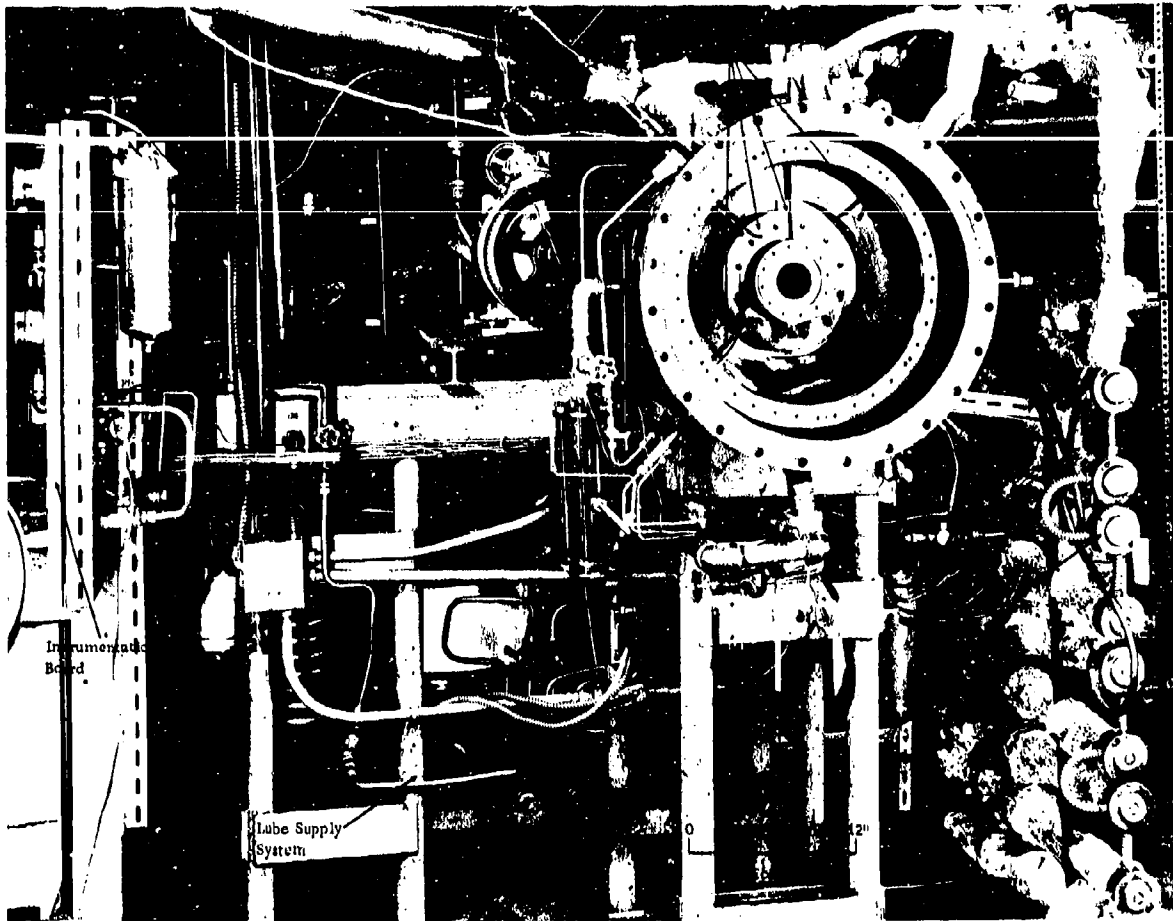


Figure 8-11. COMPONENT SEAL TEST FACILITY

revolution exciting frequency. Response frequencies, therefore, were limited to bearing rolling element passing frequencies.

Changes to some of the hardware will be made on the Phase III engine where appropriate tests will be rerun.

#### 8.4.1.5 Simulated Lube System Test

A test of all components of the engine lubrication system is in process. This test will simulate actual GE4 operating conditions, and combines the operation of the bearings, seals, sumps and gearbox system with that of the actual engine lube, vent and scavenge sump system. Actual engine locations for the system parts are duplicated and provisions will be made to simulate altitude and attitude conditions. Refer to Volume III-B Part III for additional details on the lube system simulator.

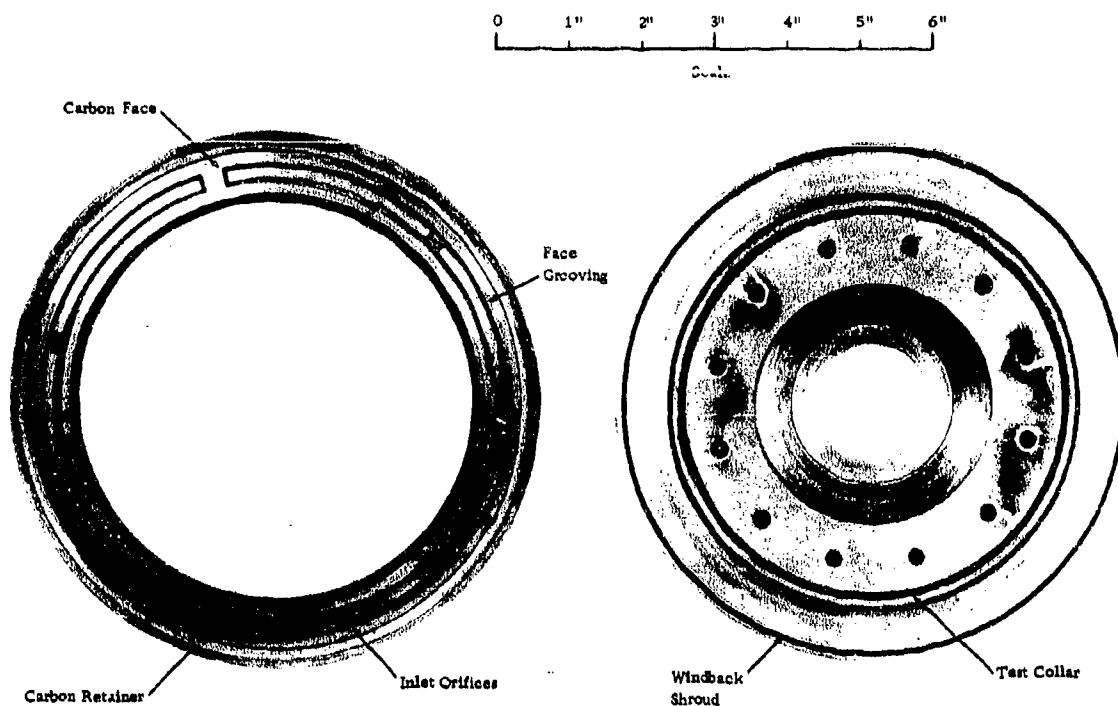


Figure 8-12. FLOATING FACE SEAL AFTER 400 HR. ENDURANCE TEST

Table 8-8. Simulated Sump Tests - J93 Test Facility

<u>Sump</u>	<u>Seal Type</u>	<u>Test Parameters</u>	<u>Duration Hr.</u>	<u>Purpose</u>
No. 1/No. 3	Hydrostatic	Mach 2.7-3.0 & No. 2 PTV*	150	● Initial evaluation
No. 1/No. 3	Hydrostatic	Mach 3.0 & No. 2 PTV*	150	● Redesign evaluation
No. 1/No. 3	Hydrostatic	Mach 2.9 & No. 2 PTV*	200	● Redesign evaluation ● New oil evaluation
No. 1/No. 3	Hydrostatic	Mach 2.7 & No. 3 PTV*	200	● Redesign evaluation

\* PTV - Pressure, Temperature and Velocity

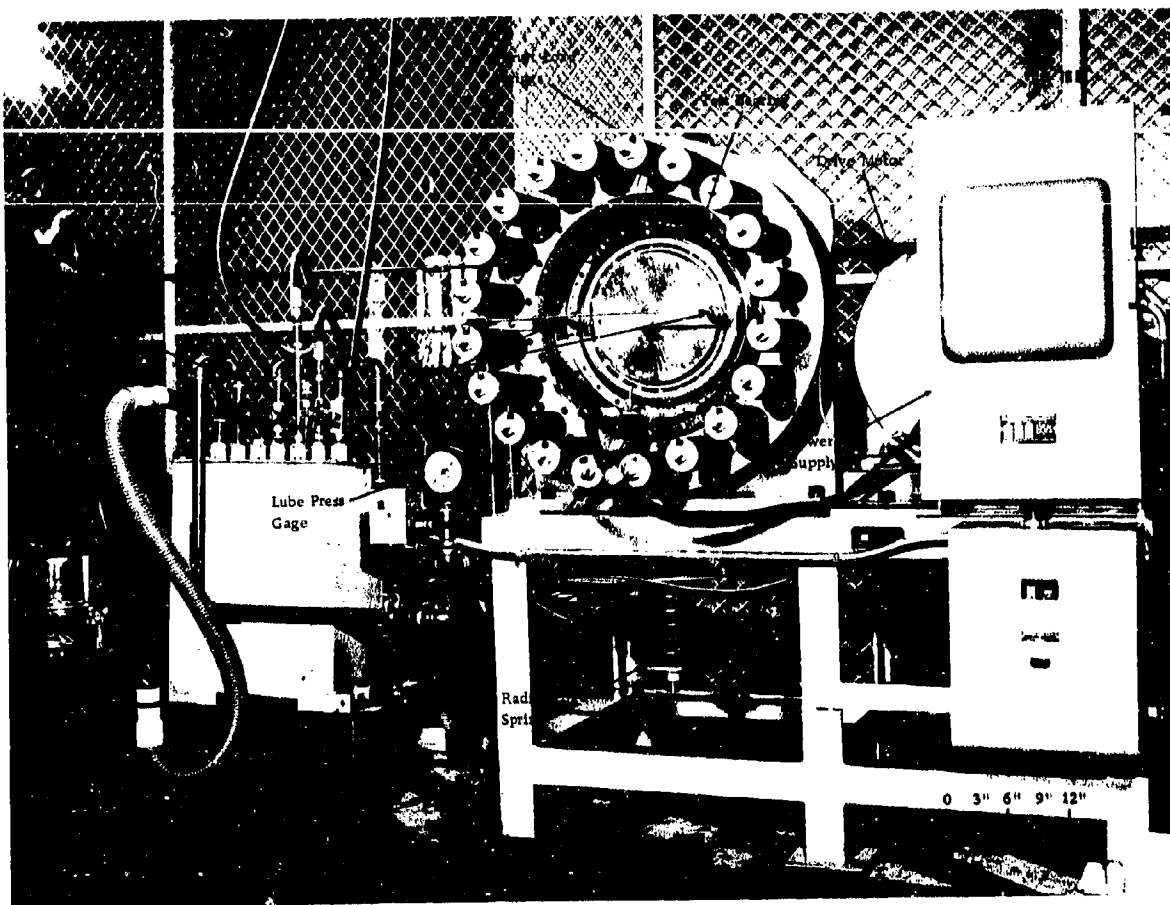


Figure 8-13. THRUST BEARING TEST FACILITY

#### 8.4.2 WORK IN PROGRESS

Work remaining to be accomplished consists mainly of completing programs in progress.

##### 8.4.2.1 Component Seal Tests

A continuing program of seal improvement is under way. Presently defined tests for Phase II-C are:

- No. 1/No. 3 Sump hydrostatic seal:
  - 1) Vibration tests - seal will be exposed to accelerations of three to six and Mach 0-3.0 and No. 2 seal pressures, temperatures, and velocities (PTV) for 100 hours.
  - 2) Contamination tests - seal exposed to high humidity, water, and oil-laden air as well as dust contamination while operating at Mach 0-3.0 & No. 2 P. T. V. conditions for 50 hours.

- No. 2 sump hydrostatic seal:

- 1) Endurance test - seal operated at Mach 0-3.0 and No. 2 Sump PTV conditions for 200 hours. (Note: a portion of this test is completed and reported in paragraph 8.4.1.1.)
- 2) Marginal pressurization test - seal operated at low, medium and zero pressurization levels for 150 hours, of which 100 hours is at Mach 0-3.0 and No. 2 sump temperature and velocity conditions.
- 3) Collar run-out test - seal operated with abnormal collar run-out up to 0.006-inch FIR at Mach 0-3.0 and No. 2/sump PTV for 45 hours.
- 4) Vibration test - refer to No. 1/No. 3 sump test 1) above.
- 5) Contamination test - refer to No. 1/No. 3 sump test 2) above.

## 8.5 SUPPORTING TECHNOLOGY

The design of the bearings and seals for the GE4 engine is based largely on data and experience gained from the design and operation of similar types of components in other General Electric engines, and extensive company and government supported research and development programs during the past five years.

### 8.5.1 CARBON FACE SEALS

The choice of the carbon face and tandem circumferential seals is consistent with the experience obtained on the supersonic J79 and J93 engines. The experience obtained from these seals has clearly indicated their excellent high-temperature capability and their ability to be designed for large pressure differentials. Examples of supporting technology in main shaft seal design and operation are:

- General Electric experience in the design of supersonic seal applications in the J79 and J93 engines.
- NASA sponsored seal and sump development programs.
- Development testing completed (paragraphs 8.4.1 and 8.4.2) and planned for the GE4 seals.

### 8.5.2 BEARINGS

Bearing designs for the GE4 engine have been chosen to make maximum use of existing technologies. Examples of supporting technology in the area of main shaft bearing design and operation are:

- General Electric's experience on high-temperature, M50 consutrode, vacuum-melt material for use on the balls/rollers and races. This material is used on the J79 and J93 engines, and has shown excellent bearing performance.
- General Electric's experience on flanged outer race design on the J93 engine.
- Development testing completed (paragraph 8.4.1.2), and planned for the GE4 main bearings.
- NASA sponsored bearing development programs.

## 9. ACCESSORY DRIVES

### 9.1 SUMMARY

The accessory drive system is a mechanical drive used to transfer engine power to the following engine and aircraft accessories and controls:

- Main fuel pump and control
- Augmentor fuel pump
- Lubrication and scavenge pump
- Hydraulic pump
- Tachometer generator and control alternator
- Aircraft alternators, hydraulic, and air conditioning pumps.

Figure 9-1 shows a cross-section of an entire accessory drive system. The drive system transmits power from the compressor stub-shaft to bevel gears in the inlet gearbox. The power is then transmitted from this gearbox to the various other gearboxes by means of radial and horizontal drive-shafts. The major subsystems and important position features of the accessory drives are as follows:

- Inlet Gearbox - A right-angled bevel gearbox located inside the engine front frame. This location permits easy access and removal without any main engine disassembly.
- Transfer Bevel Gearbox - A right-angled bevel gearbox located at the bottom of the front frame. This location and design permits its removal without removal of either the inlet or accessory gearbox. Because it is on the bottom of the engine and outside the accessory capsule it is very accessible for inspection.
- Accessory Gearbox - A spur-gear gearbox inside the accessory capsule. This location permits the smallest over-all engine envelope because it is mounted in the area of smaller compressor casing diameter.
- Power Take-off Gearbox - A right-angled bevel gearbox located at the top of the front frame. This location was defined by airframe requirements to permit the best packaging of their driven accessories and starter.

### 9.2 DESIGN REQUIREMENTS AND APPROACH

The basic requirements for power ratings, pad type, gear sizes, accessory weights, moments and other details are shown in the gearbox system schematic layout in Figure 9-2.

### 9.3 DESIGN DESCRIPTION

The design philosophy described in this section applies to both the Boeing and the Lockheed accessory drive systems. Section 9.6 outlines basic differences and specific features incorporated in the Boeing and Lockheed design.

## BEVEL GEAR DATA

POSITION	NO. OF TEETH	DIAMETRAL PITCH	PITCH DIA (IN.)	PRESS. ANGLE (DEGREES)	SPIRAL ANGLE (DEGREES)	PITCH LINE VELOCITY (FT. /MIN.)	FACE WIDTH (IN.)	LIFE (HOURS) MIN.
PTO HORIZ	19	3.95	4.8101	20	ZEROL	11640	1.634	12000
PTO VERT	42	3.95	10.6329	20	ZEROL	11640	1.634	12000

POSITION	NO. OF TEETH	DIAMETRAL PITCH	PITCH DIA (IN.)
INLET HORIZ	29	3.65	7.9452
INLET VERT	35	3.65	9.5890

## BEARING DATA

POSITION	TYPE	BEARING SIZE (MM)	SPECIFIC DYNAMIC CAPACITY	CALC. $B_{10}$ LIFE
PTO HORIZ	BALL ROLLER	70 x 150 x 35	17940	12300
		40 x 90 x 23	17226	13500
PTO VERT	BALL ROLLER	80 x 140 x 28	17750	16500
		70 x 110 x 20	18105	18900

BEARING DATA  
SPUR GEARS

POSITION	TYPE	BEARING SIZE (MM)	SPECIFIC DYNAMIC CAPACITY	CALC. $B_{10}$ LIFE
CONTROL ALTERNATOR	BALL ROLLER	16 x 32 x 9	965	812000
		15 x 32 x 9	2030	23 x 10 <sup>6</sup>
TACH, LUBE AND SCAV PUMP	BALL ROLLER	30 x 55 x 13	2610	2.4 x 10 <sup>6</sup>
		20 x 42 x 12	3731	8.8 x 10 <sup>6</sup>
MAIN HYDRAULIC PUMP	BALL ROLLER	40 x 80 x 18	5640	18872
		50 x 80 x 16	9182	15570
MAIN FUEL PUMP	BALL ROLLER	40 x 80 x 18	5640	12500
		40 x 80 x 18	11512	16374
AIR/OIL SEPARATOR	BALL ROLLER	30 x 55 x 13	2610	13906
		30 x 55 x 13	4840	26414

## BEARING DATA

POSITION	TYPE	BEARING SIZE (MM)	SPECIFIC DYNAMIC CAPACITY	CALC. $B_{10}$ LIFE
TRANS VERT	BALL ROLLER	60 x 110 x 22	9100	17000
		50 x 90 x 20	15165	12200
TRANS HORIZ	BALL ROLLER	65 x 140 x 33	24400	12500
		35 x 62 x 14	6092	13700

## SPLINE DATA

POSITION	NUMBER OF TEETH	DIAMETRAL PITCH	PITCH DIA.
PTO HORIZ.	32	16/32	2.000
PTO VERT	35	16/32	2.1875

## SPLINE DATA

POSITION	NUMBER OF TEETH	DIAMETRAL PITCH	PITCH DIA.
TRANSFER VERT DRIVE SHAFT	25	16/32	2.1875
TRANSFER HORIZ DRIVE SHAFT	25	16/32	1.5675

# BEVEL GEAR DATA

OF H	DIAMETRAL PITCH	PITCH DIA (IN.)	PRESS. ANGLE (DEGREES)	SPIRAL ANGLE (DEGREES)	PITCH LINE VELOCITY (FT./MIN.)	FACE WIDTH (IN.)	LIFE (HOURS) MIN.
	3.65	7.9452	20	0	10500	1.743	12000
	3.65	9.6890	20	0	10500	1.743	12000

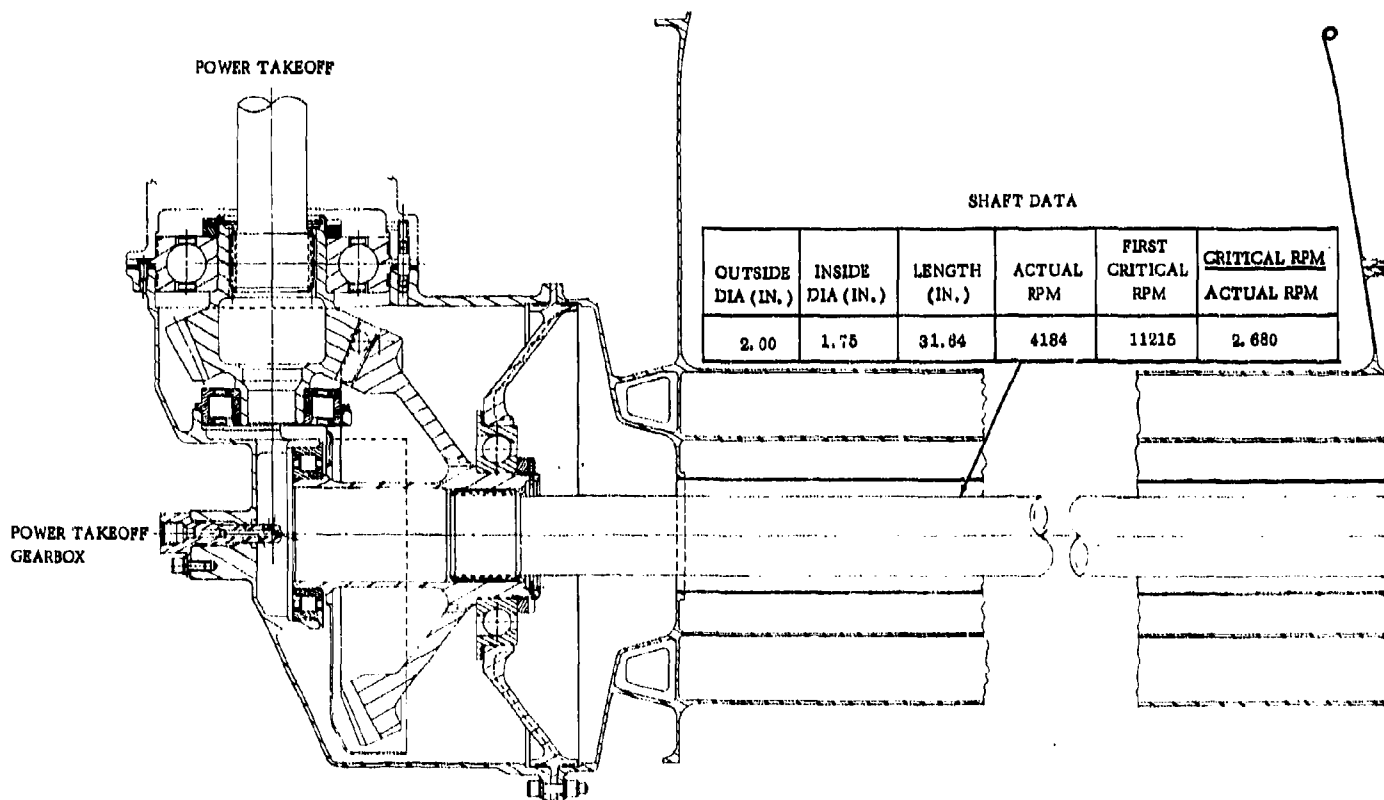
# SPLINE DATA

POSITION	NUMBER OF TEETH	DIAMETRAL PITCH	PITCH DIA.
INLET HORIZ DRIVE SHAFT	35	16/32	2.1875

POSITION
INLET HORIZ
INLET VERT

CALC. $B_{10}$ LIFE
812000 $23 \times 10^6$
$2.4 \times 10^6$ $8.8 \times 10^6$
18872 15570
12500 15374
19906 26414

# POWER TAKEOFF



# SHAFT DATA

OUTSIDE DIA (IN.)	INSIDE DIA (IN.)	LENGTH (IN.)	ACTUAL RPM	FIRST CRITICAL RPM	CRITICAL RPM ACTUAL RPM
2.00	1.75	31.84	4184	11215	2.680

PITCH DIA.
1875
5675

2

# BEARING DATA

POSITION	TYPE	BEARING SIZE (MM)	SPECIFIC DYNAMIC CAPACITY	CALC. $B_{10}$ LIFE
INLET HORIZ	BALL ROLLER	95 x 170 x 32	25430	13480
		70 x 125 x 24	25483	13000
INLET VERT	BALL ROLLER	95 x 170 x 32	25500	13000
		50 x 110 x 27	22795	13700

DIAMETRAL PITCH	PITCH DIA.
16/32	2.1875

CONT

OUTSIDE DIA (IN.)	INSIDE DIA (IN.)
1.10	.90

OUTSIDE DIA (IN.)	INSIDE DIA (IN.)
1.380	1.060

COMPRESSO

## T DATA

ACTUAL RPM	FIRST CRITICAL RPM	CRITICAL RPM ACTUAL RPM
4184	11215	2.680

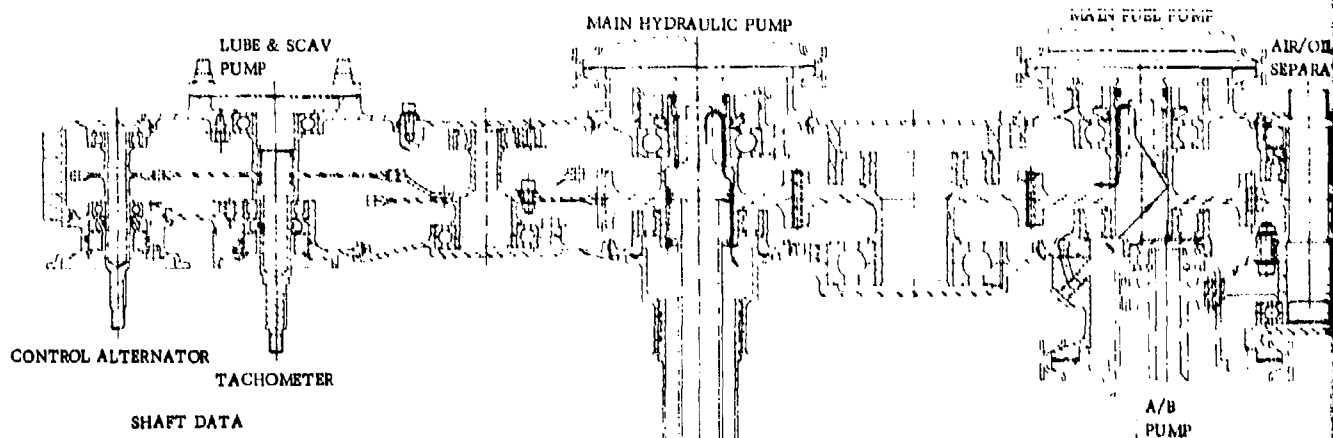
SHEAR SECTION

SHEAR SECTION

INLET GEARBOX

3





SHAFT DATA

OUTSIDE DIA (IN.)	INSIDE DIA (IN.)	LENGTH (IN.)	ACTUAL RPM	FIRST CRITICAL RPM	CRITICAL RPM ACTUAL RPM
1.10	.90	19.00	6025	16633	2.76

ACCESSORY GEARBOX  
(ROTATED 90°)

SHAFT DATA

OUTSIDE DIA (IN.)	INSIDE DIA (IN.)	LENGTH (IN.)	ACTUAL RPM	FIRST CRITICAL RPM	CRITICAL RPM ACTUAL RPM
1.380	1.000	34.00	4184	8360	1.620

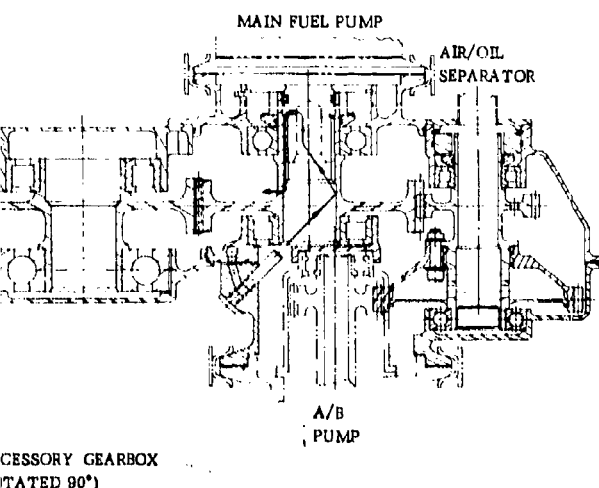
COMPRESSOR FRONT FRAME

TRANSFER GEAR BOX

POSITION	NO. OF TEETH
TRANS VERT	30
TRANS HORIZ	25

4

K



SPUR GEAR DATA

POSITION	NO. OF TEETH	DIAMETRAL PITCH	PITCH DIA (IN.)	PRESSURE ANGLE (DEGREES)	FACE WIDTH (IN.)	LIFE (HOURS) MIN.
CONTROL ALTERNATOR	21	10	2.10	20	.18	12000
LUBE & SCAV PUMP TACHOMETER	59	10	5.90	20	.26	12000
MAIN HYDRAULIC	49	10	4.90	20	1.53	12000
A/O SEPARATOR	29 51	10	2.90 5.10	20	.88 .60	*12000
A/B PUMP	21	10	2.10	20	.65	12000
MAIN FUEL PUMP	56	10	5.60	20	1.35	12000

SPLINE DATA

POSITION	NO. OF TEETH	DIAMETRAL PITCH	PITCH DIA
LUBE & SCAV PUMP	16	20/30	.800
MAIN HYD PUMP	24	20/30	1.200
MAIN FUEL PUMP	24	20/30	1.200

TRANSFER GEAR BOX

BEVEL GEAR DATA

POSITION	NO. OF TEETH	DIAMETRAL PITCH	PITCH DIA (IN.)	PRESS. ANGLE (DEGREES)	SPIRAL ANGLE (DEGREES)	PITCH LINE VELOCITY (FT./MIN.)	FACE WIDTH (IN.)	LIFE (HOURS) MIN.
TRANS VERT	36	5.125	7.024	20	25	7690	1.411	.12000
TRANS HORIZ	25	5.125	4.878	20	25	7690	1.411	.12000

Figure 9-1. LAYOUT OF GEARBOX ASSEMBLY

9-3/9-4

5

K

K

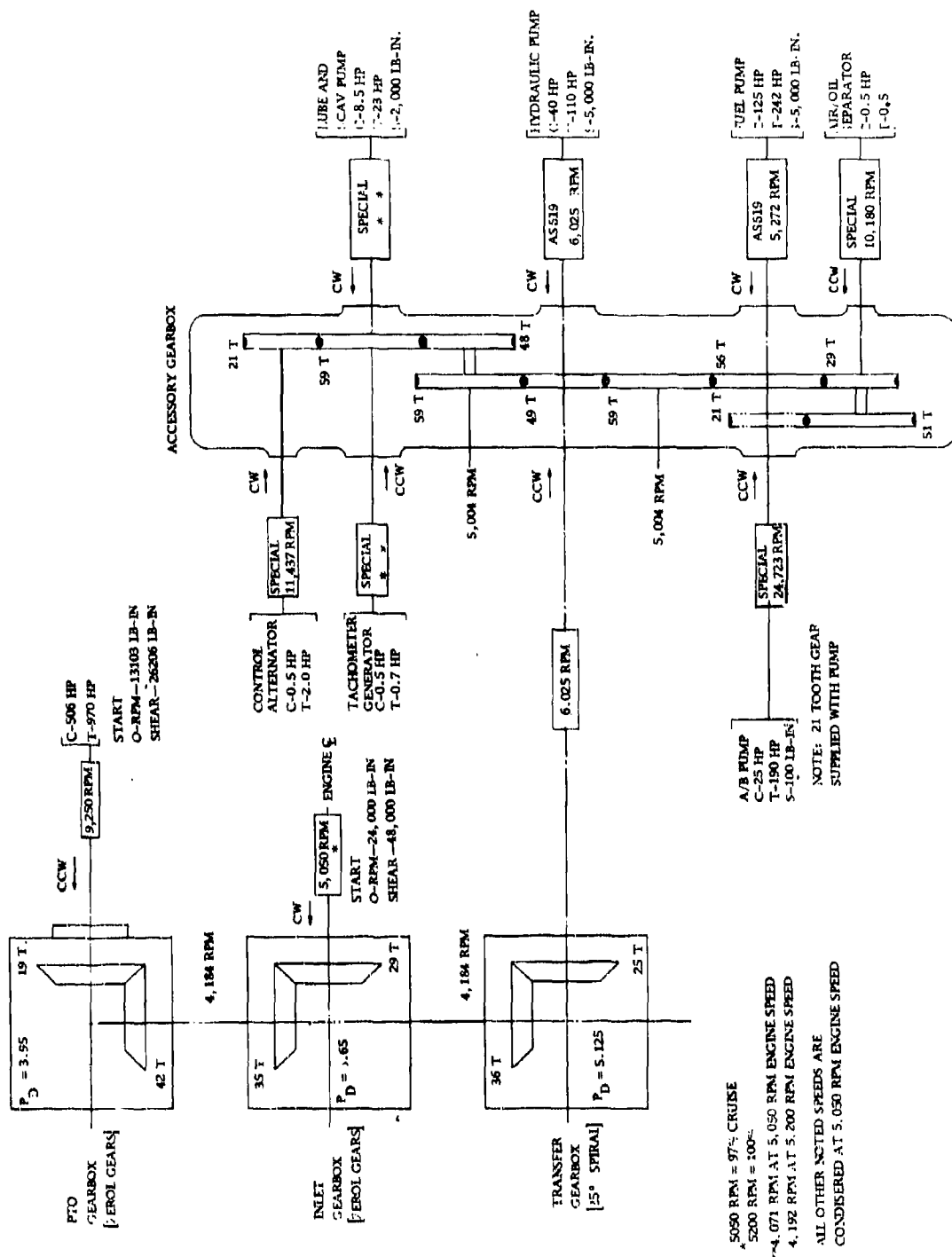


Figure 9-2. SCHEMATIC-GEARBOX ASSEMBLY

### 9.3.1 GEARBOX ACCESSORY ARRANGEMENT

All driven engine accessories and controls are mounted on the engine accessory gearbox. The customer power take-off (PTO) is located on the top of the engine to meet specific customer installation requirements. This POT position permits extraction of customer power at any horizontal angle from the engine centerline, and permits the gearbox to be used easily on either the right- or left-hand engine installation. However, the PTO can be located anywhere a front frame strut is located, or all customer accessories may be mounted on a modified engine accessory gearbox.

Such arrangements have been successfully incorporated on the J93 and J79 engines, and permit high flexibility in installation. Either configuration contains the maintenance and accessibility features required for the GE4 engine.

#### 9.3.1.1 Engine Accessory Location

Accessory components have been located on the engine in a manner that permits the accessory to be integrated easily into the engine system that it supports. Their locations are as follows:

- Hydraulic pump and fuel pump and control - on the rear of the gearbox and adjacent to the augmentor fuel pump, thereby simplifying piping between the components.
- Control alternator and tachometer generator - on the front of the gearbox, in order to use available space on that side.
- Main lubrication and scavenge pump - on the rear end of the gearbox, in order to reduce the size and length of piping required to scavenge and supply the No. 2 and No. 3 sumps.
- Augmentor fuel pump - on the front of the gearbox adjacent to the main fuel pump in order to reduce the width of the gearbox and to simplify piping.

Careful consideration of accessory component placement has reduced the complexity of piping, and has distributed the accessory weight and power-flow through the gearbox.

To minimize the over-all engine diameter, the engine accessory gearbox driving these components is located remotely behind the transfer bevel gearbox. This permits the use of the smaller engine diameter behind the front frame, and easier incorporation of the accessory gearbox within the accessory capsule. The gearbox is contoured to the inner capsule wall, and all accessories and controls are arranged close to this wall. The accessory capsule is described in Volume III-B, Part 2.

#### 9.3.1.2 Accessory Mounting

All driven accessories are mounted on the gearbox by pads which incorporate lubricated female drive splines to accept accessory quill shafts and a pilot to locate the accessory with respect to the spline centerline. The attachment of the various accessories is as follows:

- Hydraulic and Fuel Pumps - quick attach/detach (QAD) clamp couplings.
- Main Lube and Scavenge Pump - stud mounted to seal the flange scavenge port that scavenges the accessory gearbox.
- Control Alternator and Tachometer Generator - bolt mounted because of light weight and infrequent removal.

### 9.3.2 GEARBOX MOUNTING SYSTEM

The gearboxes are mounted by the following method:

- Inlet Gearbox - Bolted to a large diameter vertical mounting pad on the engine centerline of the front frame.
- Transfer Gearbox - bolted to a vertical pad on the accessory capsule, and centered in a locating rabbet at the 6 o'clock position on the front frame.
- PTO Gearbox - bolted to a horizontal pad at the 12 o'clock position on the front frame. This position satisfies all airframe requests and permits location of the customer accessory gearbox in the engine wing.
- Accessory Gearbox - mounted inside the accessory capsule and attached by its ends to a beam support.

### 9.3.3 BEVEL AND SPUR GEARS

The accessory drive system uses zerol, spiral bevel and involute spur gears (Figure 9-1). The zerol gears were used in both inlet and PTO gearboxes to minimize bearing loads and to prevent load reversal on the bearings during the transition from engine starting to engine running. Spiral bevel gears with a 25-degree spiral angle were selected for the transfer gearbox. This spiral angle permits bearings on the vertical bevel gear to be smaller, and permits a shorter vertical engine dimension.

All bevel and spur gears are straddle-mounted between bearings, rather than overhung from bearings, to reduce bearing loads and to provide better gear support. Gears are manufactured from "Super Nitralloy" material that has greater strength than the Nitralloy "N" commonly used. This improved material was chosen as a result of extensive gear development by General Electric. This material is currently used in the T58 Engine speed-decreaser gearbox with good results. All highly loaded bevel gears are manufactured in one piece to prevent any possibility of fretting, wear or fracture at a separate mounting joint.

A high press-fit spline is used in the transfer gearbox horizontal shaft to minimize fretting. This design eliminates bolt and dowel arrangements and their associated problems.

Spur gears are used throughout the accessory gearbox because pitch line velocities are relatively low. The spur-tooth configuration is lower in manufacturing cost and eliminates larger costlier bearings associated with the use of helical gears. General Electric has had extensive experience with aircraft spur gears under similar tooth loadings in aircraft engines through use on all production engines for the past 15 years.

Gear tooth profiles are manufactured to aircraft precision standards. Meshing gears are designed with "hunting tooth" ratios, to prevent repetitive contact during each revolution between the same teeth in the gear mesh. This principle is used throughout the gearboxes for improved life and reliability.

#### 9.3.4 SPLINES

Splines used in the gearboxes (Figure 9-1) are aircraft standard ASA B5.15-1960 involute type, and are manufactured to aircraft precision standards. The aircraft standard pad configurations used on the accessory gearbox incorporate a smooth bore to accept an O-ring at the accessory end of the internal drive spline.

An O-ring seal is used to permit oil lubrication of the spline from inside the gearbox (Figure 9-1). Lubricated splines display superior life and resistance to fretting, when compared to unlubricated splines, this is evidenced by the absence of any significant spline wear when splines are located inside the gearbox where they are bathed in oil.

The splines are sized by criteria developed from test and the design principles have been proven in many applications such as the J79/CJ805 and J93 engines.

#### 9.3.5 Bearings

Ball and roller bearings of anti-friction type are used to support the gears in the accessory drive system. Standard bearing configurations are specified in sizes that meet the capacity of the driven accessories (Figure 9-1). All gears are supported with both a ball bearing and a roller bearing to improve axial positioning, to permit thermal expansion, and to facilitate assembly. All gear shafts with axial seals are provided with a ball bearing adjacent to the seal rotor to provide axial seal positioning and better stack-up control. To ensure bearing reliability, all bearings have been sized to give at least 12,000 hours minimum B<sub>10</sub> life, based on Anti-Friction Bearing Manufacturers Association ratings, (AFBMA), before applying a 4:1 factor for M50 material.

Bearing race rotation is minimized or eliminated by the following means:

- Bearings are press-fitted to the shaft journals.
- Nitrided journals with a hardness of Rc 58-62 are used to prevent shaft damage under the bearing races.
- Outer races of all spur-gear bearings are positively retained by the accessory casing.

Bearings are of ABEC-5 or RBEC-5 precision quality. The races, - balls/rollers and cages are manufactured of consutrode, vacuum-melted M50 tool steel and "S" Monel, respectively. This race and ball/roller material was chosen because of its excellent fatigue life as demonstrated by component testing and by engine experience on the J79/CJ805 and J93.

#### 9.3.6 OIL SEALS

All gearbox oil seals are carbon-face rubbing seals similar to those used on the J93 engine. These seals employ a metal bellows secondary element which is also used to spring load the carbon face. The metal bellows was selected in preference to an elastomer O-ring secondary to ensure meeting the life requirements at the temperature of the GE4 engine. For ease of removal, each seal is retained from outside the gearbox and can be replaced externally without disassembly of the gearbox assembly. This arrangement has worked well in the J93 gearbox.

The mating rings will be shaft-driven with a very light press fit on the shaft. This prevents axial movement of the ring during the plug-in assembly into the gearbox casing. The use of press-fitted mating rings has been successful on previous General Electric component tests.

### 9.3.7 SHAFTS AND MISCELLANEOUS PARTS

Splined drive-shafts (Figure 9-1) are manufactured from Super Nitralloy material. Minimum web wall thickness of 0.100 inch is used to reduce cost and problems of manufacture. A shear section in the radial shafts has been incorporated near the engine centerline end to prevent shaft whip in the event of a shaft failure. Critical speed of the shafts has been set so that calculated values are not less than shaft speed at 120 percent engine speed.

Various other miscellaneous parts, such as lube jets and gear shrouds, are manufactured of aluminum to reduce cost while maintaining adequate strength margin for operation.

### 9.3.8 GEARBOX CASINGS

The gearbox casings are investment castings of 17-4PH stainless steel. This construction gives good corrosion protection and permits light weight consistent with required strength at operating temperatures.

The accessory casing will be cast as a one-piece construction with "plug in" gears at each accessory location (See Figure 9-3). One-piece construction will eliminate the possibility of conventional "split line" oil leakage and will permit easy disassembly of the entire gearbox without removal from the engine. The "plug in" design was evaluated as the best approach considering cost, manufacturing, and maintainability.

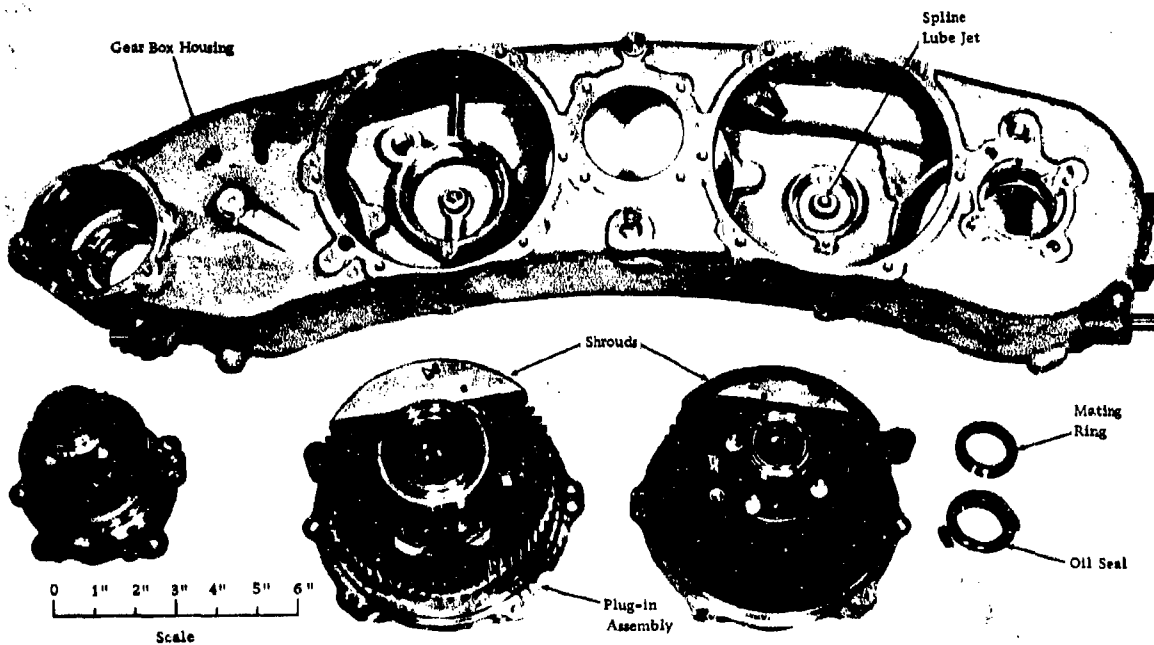


Figure 9-3. PHASE IIC ACCESSORY GEARBOX

### 9.3.9 MAINTAINABILITY

Maintainability requirements have been stressed throughout the design of the accessory drive system. Special emphasis has been given to ease of maintenance. For example, it is possible to replace specific components or to disassemble the entire accessory drive gearbox completely while the engine is installed in the aircraft.

Specific design features that minimize the need for maintenance are:

- All splines lubricated to minimize wear.
- Elimination of split line oil leakage by providing one-piece casing.
- \*The gearboxes can be individually removed from the engine.
- \*A pad is provided on the transfer gearbox housing to mount a tool for turning the gas generator rotor through the radial drive-shaft, for use during borescope inspection of the compressor rotor.
- Avoiding the use of conventional tab-washers subject to tang fatigue.
- Main bevel gears and shafts are integral, to prevent mating joint fretting, wear, or fracture.

Features facilitating maintenance are:

- Rotation of the rotors through a pad on the transfer gearbox to facilitate borescope inspection.

\*Items designed specifically for GE4 engine.

- Independent removal of either the inlet, transfer, accessory or power take-off gearboxes.
- "Plug-in" concept of the accessory gearbox permits a given drive assembly to be independently removed, which allows inspection or replacement of the gears, bearings, oil seals and attaching hardware.
- All lube jets can be removed from outside the gearbox.
- Each gearbox has an accessible magnetic drain plug for fault isolation or complete draining.
- Casing flanges are thick enough to permit remachining or applying metal spray during major maintenance.
- Hydraulic and fuel pumps are mounted with QAD clamps for ease of replacement.

A durability and maintainability analysis for the accessory drive system has been completed and is contained in a special appendix, entitled "GE4 Durability and Maintainability Analysis", which is available on request as back up material to the substantiating data submitted. The purpose of this analysis is to ensure that all aspects of maintainability have given full consideration in the design of the components. For each potential failure mode, the technique for monitoring the condition of the component in service is given, along with diagnostic means to isolate the deterioration or failure. Inspection frequencies will be determined during the GE4 development program.



### 9.3.10 RELIABILITY

The life of each major part in the gearbox system has been checked, and meets the reliability requirements of the GE4 engine. Specifically, bearing life analyses shows a minimum bearing B<sub>10</sub> life of 13,000 hours with a range of individual lives between 12,000 and 10<sup>6</sup> hours as tabulated in Figure 9-1.

The design life of bevel and spur gears has been calculated in excess of 12,000 hours. Manufacturing methods are similar to those used in the J93 engine.

Stress levels and material chosen for the gearbox casings result in no degradation of life during the required 36,000 hour life of the casings. Care has been taken to eliminate all loose parts that can precipitate wear and reduce life.

Life of current gearboxes used in J79/CJ805 and J93 engines was initially limited by such items as casing fatigue, tab-washer failures, bearing spinning, lube jet failures, and spline wear. In every case, a methodical review has been made of the GE4 design against the CJ805 design experience and has incorporated the long life corrections required:

- \*Reduction of gearbox mounting stresses and increased material properties available with the use of cast 17-4PH stainless steel to eliminate casing fatigue.
- The use of all tab-washers has been eliminated.
- Bolted bevel-gear flanges are eliminated to preclude bolt failures. Highly loaded bevel gears are of one-piece construction and the lower loaded transfer bevel gear is mounted on a heavy press-fit spline; outer race bearing spinning and chip generation are eliminated by bolted, flanged, or keyed outer races. Inter race bearing spinning is controlled by axial clampup of locknuts and high press fits. All journals are nitrided to RC-58-63.
- Spline wear, a problem in some installations, is controlled by lubrication of all splines (see Figure 9-1)
- QAD pads are used for easy accessory removal
- \*All external flanges have two O-rings for redundancy in the event of one ring failure
- The use of a one-piece accessory casing eliminates the possibility of conventional split-line oil leakage.

\*Items designed specifically for GE4 engine.

### 9.3.11 QUALITY ASSURANCE

The accessory drive system has incorporated many items to reduce quality problems in the final design:

- Use of "plug-in" gearbox design has reduced casing complexity and tolerances.
- Standard vendor bearing sizes are used.
- Tolerance allowances and use of wider face-widths has eliminated the need for complicated profile modification on gear teeth, and the problems of inspection that go with them.

- Datum axis and datum planes have been established on all part drawings consistent with functional needs and manufacturing methods.
- Ample stock allowance has been provided on all gearbox casting drawings to ensure machining clean-up.
- Maximum advantage of shop run tolerances has been taken where possible without compromising functional requirements.
- Appropriate specifications are used where required, such as pressure testing, repair welding and magnetic particle and fluorescent-penetrant inspection.
- Tolerances used throughout the accessory drives design permit the use of standard gaging practices.

Close liaison during the design phase between quality control personnel and design personnel has resulted in better, more precise drawing requirements.

### 9.3.12 SAFETY

The accessory drives have been designed with assurance of maximum safety, both during flight and ground inspection. The following significant safety items have been incorporated:

- All individual drive pads incorporate shear sections to protect the drive train from overload in the event of accessory failure.
- Shear sections are incorporated on the drive end of the radial drive-shafts to protect the front frame from shaft whip in the event of shaft failure.
- Magnetic drain plugs are incorporated in the transfer and accessory casings for quick inspection of the system.
- Gearbox casings are of extra rigid wall construction to retain any failed or disassociated part within it.
- All external flanges have two O-rings for redundancy in the event of a single O-ring failure, and to ensure fire safety in the hot ambient cavities.
- Accessory gearbox located in accessory capsule to ensure fire safety.

### 9.3.13 FAILURE ANALYSIS

The failure analysis for the accessory drives has been completed to the same extent as the seals and bearings explained in paragraph 8.3.10. Similarly, additional failure analyses will be conducted on the accessory drives as described in 4.2, Reliability, Volume IV.

### 9.3.14 VALUE ENGINEERING

The accessory drive system has incorporated many items to reduce cost of manufacture and maintenance. Follow-up work on the original design has resulted in significant cost reductions:

- Use of the "plug-in" gearbox design has reduced casing cost.
- Use of standard and existing tooling for gears and splines has reduced tooling cost.
- Tolerance allowances and use of wide-face-width gears has eliminated need for costly profile modifications on gear teeth, and problems of manufacture and inspection that go with them.

Close liaison among the design engineering and the shop manufacturing people has been an integral part of the program from its inception.

#### 9.3.15 HUMAN ENGINEERING

Various human engineering principles were integrated into the design and test of the accessory drive system, such as the following:

- All main mounting flanges that require particular angular positioning have been "Murphy-proof" designed to ensure correct angular positioning.
- Oil jets have been "Murphy-proof" designed to ensure correct angular positioning after assembly.
- All sharp external corners on parts incorporate a radius or chamfer to prevent "knife-edge" type hazards to assembly personnel.
- Magnetic drain plugs incorporate oil drain stops that prevent oil drippage during and after their removal.
- Gear "plug in" adapters are designed to engage the roller-bearing races prior to the adapter rabbets to give the assembler a "feel" of proper bearing alignment and prevent bearing damage during assembly.
- Roller drop dimensions have been made consistent with bearing lead-in chamfers to prevent damage at assembly.
- All closely fitted mating diameters are adequately chamfered to ease assembly and prevent assembly damage, and incorporate jacking screws to ensure proper and easy disassembly.
- All O-ring diameters are adequately chamfered to prevent damaging the O-ring during assembly.
- Adequate test programs have been set up to ensure that operation of all components meet human performance requirements.
- All bearing rollers and balls are retained in the inner or outer races for ease of handling and assembly.

#### 9.3.16 STANDARDIZATION

The standardization practices for the accessory drives are the same as described for the seals and bearings in paragraph 8.3.13.

## **9.4 DEVELOPMENT STATUS**

### **9.4.1 WORK ACCOMPLISHED**

Phase II-C design has shown the feasibility of casting and machining complex thin wall 17-4 PH steel castings. No major problems were encountered at the various casting vendors and sound castings were achieved, in some cases on the very first pour. Minimum stock allowance is resulting in minimum machining time, and the close tolerances of investment castings are keeping excess weight associated with casting shift to reasonable limits. Surface finishes of 32 micro-inches have been achieved in O-ring grooves with ordinary turning, and the material has been found stable in and out of holding fixtures.

Super Nitralloy is the primary material for all gears and shafts. The higher aluminum content of Super Nitralloy makes this material more easily machined than the Nitralloy N used in the J93 gearboxes. Minor grinding wheel filling occurred early in the program, but was easily remedied by proper selection of grinding wheels. Most gears were machined with numerically-controlled, single-point tooling, and accuracy and quality of finish has been extremely good. The low temperatures (975°F) associated with the nitriding process have made heat-treat distortion negligible.

### **9.4.2 WORK IN PROCESS**

#### **9.4.2.1 Gearbox Dynamometer Test**

An initial 100-hour accessory gearbox proof test will be completed by the end of 1966. The lube simulator facility will be the vehicle for this test. Actual hardware, fuel pump, hydraulic pump, and lube pump will be used in this test to simulate normal operating conditions. The actual capsule and accessory mounting will be used so the flanges will be loaded as in conventional engine configuration. The "plug-in" concept used in this gearbox design makes this test set-up extremely feasible because the highly loaded gear meshes can be inspected by simply removing the two forward adapter assemblies.

#### **9.4.2.2 Gear Scoring Test**

Data is being obtained on the load-carrying capacity of the primary engine lubricant used with Super Nitralloy gears under GE4 engine conditions. For comparison, data is also being obtained on M50 through hardened gears. The evaluation is being accomplished on a WADD high-temperature gear machine. Basically, this is a standard Ryder gear scoring test with high-temperature capabilities required by the GE4 engine. A large body of comparison data are available for other oils, from previous tests run under Air Force and FAA contracts.

## **9.5 SUPPORTING TECHNOLOGY**

Design of gearboxes for the GE4 engine employs features based on over 5 million flight-hours of J79, J93, and CJ805 turbojet engine experience. The GE4 accessory drive system is based on design criteria used on these General Electric engines, which have had good gear and bearing life. Mechanical improvements have been incorporated in the design where military and commercial experience has shown them to be necessary. The manufacturing processes used in the manufacture of the gears are typical of aircraft practice. Spur-gear designs specify 10-pitch gears that are similar to many gears built for the J93 and the CJ805 family of engines. Quality control procedures that have been developed for our production engines will be used on these components.

The bearings used in the gearbox will be vacuum-melted M50 material, which has proven completely satisfactory on the J93 engine, and which has considerably better fatigue life and hot hardness than the normally used 52100 material. Analysis procedures have been based on duty-cycle analysis and reliability calculations.

The gearbox casing manufacturing techniques are similar to those for the J93 engine, but use a casting instead of a fabrication to eliminate manufacturing problems with cracks and thermal distortion previously encountered.

9-15/9-16

K

## **9.6 AIRCRAFT COMPANY ACCESSORY DRIVE SYSTEM DETAILS**

### **9.6.1 BOEING ACCESSORY DRIVE SYSTEM**

See Figure 9-4 for the schematic of the accessory drive system. This design contains features described in Section 9.3 and shown in Figure 9-1, but is different in its kinematic arrangement. The basic differences are as follows:

- The right-angle drive is eliminated from the top of the engine
- The capsule is moved from a bottom to a side location, which requires a three-gear inlet gearbox.
- Two hydraulic-pump pads are incorporated on the accessory gearbox.

#### **Design Description**

Accessory power is transmitted from the compressor stub-shaft to bevel gears in the inlet gearbox. The power is divided and directed by shafting to a top power-takeoff (PTO) drive-shaft. This top PTO shaft is supported in the engine front frame by a jet-lubricated ball bearing. Lube drainage is returned to the inlet gearbox. A dynamic carbon seal is provided to isolate lubrication from the customer-supplied decoupler. The decoupler is driven through a female spline located in the shaft end. Incorporated in the engine front frame is a quick attach/detach (QAD) flange to which the customer decoupler can be attached.

Power is also directed to a transfer bevel gearbox which is located on the left side of the engine. The speed requirements of the top PTO determine the ratio of the transfer gearbox. This ratio is basically a function of the kinematics of bevel gear design. From this transfer bevel gearbox, a shaft drives aft to the accessory gearbox. The accessory gearbox is enclosed in the capsule.

Mounted on this accessory gearbox are the engine-required accessories and provisions for two customer hydraulic pump drives. These pump drives are on the front face of the accessory gearbox and straddle the input-drive shaft. These drives are designed with QAD flanges, and the splines are provided with positive lubrication. The fuel pump and augmentor pump are located above the horizontal centerline, and the lube and scavenge pump is on the lower end of the accessory gearbox.

Refer to Volume III-D Section 1 for external details and pad information.



**Figure 9-4. BOEING ACCESSORY DRIVE SYSTEM**

## 9.6 AIRCRAFT COMPANY ACCESSORY DRIVE SYSTEM DETAILS

### 9.6.2 LOCKHEED ACCESSORY DRIVE SYSTEM

See Figure 9-5 for the schematic of the accessory drive system. This design utilizes features described in Section 9.3 and shown in Figure 9-1, but is different in its kinematic arrangement. The basic differences are as follows:

- Accessory drive disconnect is mounted to PTO gearbox.
- Three-gear inlet gearbox is necessary to transmit required customer horsepower.
- Transfer gearbox is designed to incorporate LAC compressor drive. This drive includes disconnecting features.

#### Design Description

Accessory power is transmitted from the compressor stub-shaft to bevel gears in the inlet gearbox. For the required powers, this gearbox features a three-gear design to keep gears within the space allowed in the front frame. The power is divided and directed by shafting to the PTO at the top and to the transfer gearbox located on the bottom. The speed of 4184 rpm for the radial drive-shafts was selected to provide a minimum envelope for the transfer gearbox and for the accessory capsule.

Mounted to the PTO is a drive disconnect. This unit can be disconnected in case of an in-flight emergency. Power for disengaging is provided by engine rotation. Re-engagement is easily accomplished on the ground by the ground crew with the engine shut down. Decoupling and recoupling (with the engine shut down) for ground power and check-out is also provided in the design by electro-mechanical means. This coupling is designed for a continuous rating of 268 hp, with transient capabilities of 645 hp for 13 percent of a 12,000-hour design life.

The transfer gearbox incorporates a spur-gear train to provide a 9445 rpm drive, and a 9.00-inch offset for the engine driven environmental control system compressor. A left-side drive is provided to accommodate Lockheed requirements. Included in the design is an emergency in-flight decoupling device that can be manually reset by ground crews. This decoupler is similar to the one mounted to the top PTO, but does not incorporate ground check-out features.

From the transfer gearbox, a shaft drives aft to the accessory gearbox located inside the capsule. The engine-required accessories are driven from this gearbox. The transfer gearbox and the accessory gearbox are separated and connected by shafting to keep the over-all capsule envelope to a minimum.

Refer to Volume III-D Section 1 for external details and pad information.



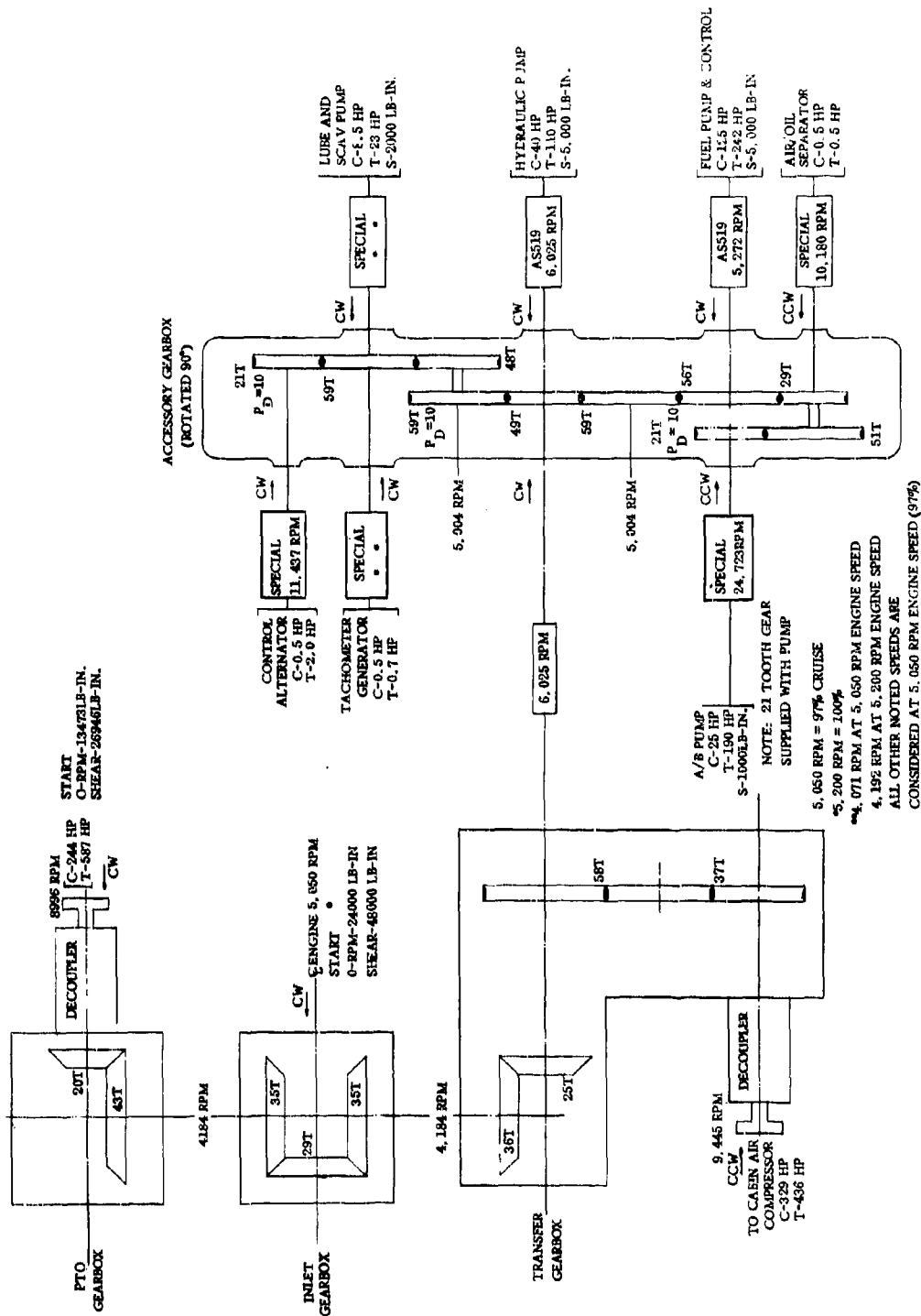


Figure 9-5. LOCKHEED ACCESSORY DRIVE SYSTEM

## 10. FRAMES AND STRUCTURES

### 10.1 INTRODUCTION AND SUMMARY

GE4 engine structure is designed from the outset for a minimum life of 36,000 hours, although, the environment is more severe than that of current commercial engines. It is not as severe as that imposed on the successful structure of the J93 engine. A detailed review of all current commercial frame problems has shown that the life requirements can be met on the GE4 and commercial durability, reliability and maintainability enhanced over current designs.

The GE4 engine shown in Figure 10-1 has three main engine bearing support structures or frames.

- Compressor Front Frame - Including the forward engine mount, provides support for the compressor rotor and stator, accessory capsule support, airframe power take off, airframe inlet adapters, and inlet guide vane support.
- Compressor Rear Frame - Provides support for the engine combustor and midspan support of compressor and turbine rotors, combustor and fuel nozzle support, customer bleed system, and accessory capsule support.
- Turbine Frame - Including the aft engine mount, provides support for the turbine rotor, stator, tailpipe support, and inner diffuser support.

The following criteria were used in designing the main engine bearing support structures to meet the operating objectives:

- The stress caused by maneuver plus steady-state and thermal forces is less than the minimum strength of 0.2 percent yield and less than 80 percent of the (minimum ultimate strength).
- Sump service tubes and flowpath liners are "sized" and supported to prevent detrimental criticals in the operating speed range.
- Stress due to transient and steady-state thermal gradients is less than 50 percent of the stress in the present radial strut frames in commercial service by the use of "partially" tangential struts.
- Casings, rings, and struts, as constructed, give at least 20 percent margin in buckling.
- Steady-state stresses are less than the minimum 0.2 percent plastic creep strength and 80 percent of the minimum rupture strength.
- Maintain aerodynamic flowpath.

The engine mounting system is designed to meet these criteria with an additional load factor of 1.5 minimum, due to the consequence of failure

The design criteria for the thrust bearing is specified in Section 8.3.3.

The general principles employed in the design of the GE4 engine structures that will meet the key goals of safety, durability, ease of maintenance, and repairability are based on the proven concepts of the J79/CJ805 and J93 such as:

- Use of established design practices, standards, and calculation techniques.
- Use of materials that require no coating or special protection to meet corrosive-atmosphere operating requirements
- Selection of structural materials with good repair characteristics, plus adequate strength and life capabilities
- Smooth air passages with area changes designed and tested to ensure minimum pressure loss in the system
- Design emphasis on ease of maintenance, producibility, and quality control
- Removable sump housing on all frames, thus allowing good inspection and repair quality for low-cost maintenance
- Service piping readily serviceable for replacement or repair and designed for durability with:
  1. Slip joints for thermal gradients
  2. Wear sleeves at potential interference points
  3. Tube interface designs which prevent torque damage during assembly or disassembly
  4. Concentric tubes to prevent coking of the vent line
- Butt-welding done in relatively low stress areas away from the strut casing transition joints where stress concentrations are high
- Accessible structural welds for inspection and repair
- Use of casting or forgings for all strut ends.
- Strict attention to the structural problems due to low and high cycle fatigue. Experience has indicated that 95 percent of the past structural problems have been traceable to this factor.
- Design features that control differential thermal stresses in structure and tubing are as follows:
  1. Heating/cooling air is manifolded on outer casing to balance thermal gradient
  2. Semi-tangential struts which rotate the inner hub rings to minimize thermal loading
  3. Redundant heating/cooling circuits which will allow operation with a portion of the system inoperative
- Mounting bosses with surplus stock for rework if necessary
- Piping supports designed to keep detrimental resonant frequencies out of the engine operating range
- Windmill brake system to minimize effects of in-flight shutdown

- Design of the engine frames to a specified deflection coefficient to meet the requirements of the system dynamic studies

Structural dynamic requirements for the total engine as a system have been established. The requirements have been met by establishing bearing positions along with rotor, frame, and casing flexibilities. The dynamics are determined by calculation at the design origin and are monitored throughout the engine development. This effort results in a structurally stable machine free from excessive vibration. This effort aids the safety, reliability, and durability of the engine.

Although main engine structures have adequate structural integrity to withstand a failed blade condition, additional safety is obtained through the use of the windmill brake. The following dynamic analysis of the main engine bearings and the mounts due to a failed blade condition give the resulting loads:

Location	Operating Speed (RPM)	Braked Speed (RPM)	
	5200	1600	1400
No. 1 Bearing	1820	314	252
No. 2 Bearing	19,900	428	278
No. 3 Bearing	24,600	907	618
Forward Mount	2160	543	543
Aft Mount	13,020	1261	960

NOTE: 5200 was used only to calculate loads. Engine will not necessarily operate at this speed.

#### 10.1.1 MANEUVER LOADS

The specific design maneuver loads of components as needed to meet airframe requirements are defined in paragraph 10.7 of this section.

#### 10.2 DESIGN REQUIREMENTS AND DESIGN APPROACH

The GE4 engine structures are designed for 36,000 hours of life, with repair, while meeting the total structures segment requirements specified for reliability and maintainability sections of Volume IV. These requirements are ensured by incorporation of proven design features such as:

- Butt-welded joints - defined load path and smooth transition from strut to rings which minimize discontinuity stresses
- Mechanical arrangement for controlling thermal stresses, using semi-tangential struts and cooling air manifolding, reduces the steady-state stress to 15 percent of allowable stress. CJ05 experience has shown conventional radial struts to be life-limiting due to thermal stresses.
- Replaceable sumps and tubing
- Concentric tubing to prevent coking in the sump vent tube

- Replaceable liners and service tubing improves accessibility of structural welds for inspection and repair. The turbine frame parts are replaceable without welding, cutting, or disassembly of the primary structure.

### 10.3 DESIGN DESCRIPTION

#### 10.3.1 COMPRESSOR FRONT FRAME

##### 10.3.1.1 Front Frame Description

The front frame assembly performs the following important structural and aerodynamic functions: (See Figure 10-2, which appears in paragraph 10.7.)

- Engine-airframe forward attachment point (vertical, side, thrust and torque)
- Front support of engine compressor rotor (No. 1 bearing)
- Support for accessory drives
- Provides piping for lubrication and cooling of the No. 1 bearing and inlet gearbox
- Distribution of front-end anti-icing system
- Enclosure and support of variable inlet guide vane system
- Minimize aerodynamic distortion to compressor inlet

The frame assembly consists of the main frame structure (welded assembly) outer casing, inlet guide vanes and actuation levers, and the No. 1 bearing and sump housing and internal piping. In addition to enclosing the sump for the front bearing, the inner hub supports the inlet nose adapter, the inlet gearbox, and the inner trunnions of the variable inlet guide vane system.

Titanium alloy (5Al-2-1/2 Sn) material was selected for the primary structure of the frame and the inlet guide vanes because of its high strength-to-weight ratio, good ductility (10 percent elongation, 25 percent reduction of area), corrosion resistance, and excellent inservice performance throughout the aircraft industry.

The frame cross-section, strut usage, and tube sizes are shown in Figure 10-3. (See paragraph 10.7.) The basic frame consists of an inner structural ring (Item 1), eight radial struts (Item 2), and a double-hat-section outer structure (Item 3).

The outer structure consists of eight strut-end-castings butt-welded into the outer casing skin. Between the strut-ends are fabricated, sheet-metal sections (hat-shaped) that are butt-welded to the strut-ends and seam-welded to the outer casing. The hats essentially become a continuous structural ring. The strut-end castings have generous radii in the casing-strut transition joint. They are butt-welded to the strut away from this potentially troublesome joint. This design gives minimum stress concentration at the transition and moves the weld-joint to a relatively low-stress area.

The outer casing is a cylindrical shell with machined flanges butt-welded on each end. The forward end supports the inlet duct, and the aft end supports the compressor casing.

Struts of constant section connect the strut-ends of the inner structure with the strut-ends of the outer casing. Cross-members are welded inside the struts to prevent deformation due to internal pressure from anti-icing air. These cross-members divide the struts into three areas. Sheet-metal strut inserts (Item 4) are provided in the leading areas to improve the efficiency of the anti-icing system. The struts at the 6 and 12 o'clock positions are thicker than the other six to accommodate the radial drive shafts that pass through them for the power takeoff and transfer gearboxes.

The inner structural ring or hub is a casting of open-channel-shape with forward and aft flanges to support the No. 1 sump housing, inlet gearbox, engine bullet-nose, and the inlet guide vane inner support. Eight strut-ends are included in the casting, forming a smooth transition for load-carrying similar to the outer joint. The J79 and CJ805 compressor front frames are shown in Figures 10-4 and 10-5 respectively. The sump housing (Item 5, Figure 10-3, paragraph 10.7) is bolted to the hub to facilitate manufacturing and maintenance. The sump housing (of cast titanium material) consists of the No. 1 bearing support, the sump seal support, and the sump service lines (oil, seal pressure, and drain).

The front frame is designed to withstand a minimum of fifty hours operation with an open anti-icing valve at maximum cruise. This feature gives additional margin to the normal frame design. (Figure 10-6.)

The inlet guide vane is fabricated of titanium (5Al-2-1/2 Sn). The inner and outer trunnions, sheet-metal skin, and internal stiffeners are joined by brazing to minimize distortion (Figure 10-7). The inlet guide vanes are supported by sleeve bearings with carbon facing to withstand the high inlet temperature.

#### 10.3.1.2 Stress Summary

The design criteria specifies that stresses resulting from the applied loads shall not cause stresses exceeding the material ultimate strength. The maximum maneuver load stresses in the hub, struts, and casing, and the material minimum allowable stresses are shown in Figure 10-8. When compared with allowable material properties, the calculated stresses are below the yield limit with adequate safety margins. The steady-state stresses are due to pressure, temperature, and nominal G forces with a 4G alternating force superimposed due to rotor imbalance. (See Figure 10-9.)

#### 10.3.1.3 Manufacturing Techniques

The same manufacturing processing used on the TF39 front frames is used in processing the GE4. Most of the structural welding is done by the electron beam method which reduces joint shrinkage by about 10 to 1, as compared to conventional tungsten inert gas methods. By controlling the shrinkage, a high-quality component is being produced with relatively little distortion or built-in stresses and, therefore, susceptibility to cracks in service is minimized.

#### 10.3.1.4 Sump Service Tubing

Sump service tubing is made of 321 stainless steel with sufficient wall thickness and side support to prevent resonant frequencies in the operating speed range. The tubes are attached only at the sump, having replaceable slip joints where the tube passes through the outer strut ends. This arrangement provides for the differential thermal growth between sump service tubing and the surrounding structure that is heated by anti-icing air. Tube interfaces are designed and oriented to prevent torque damage during assembly or disassembly.

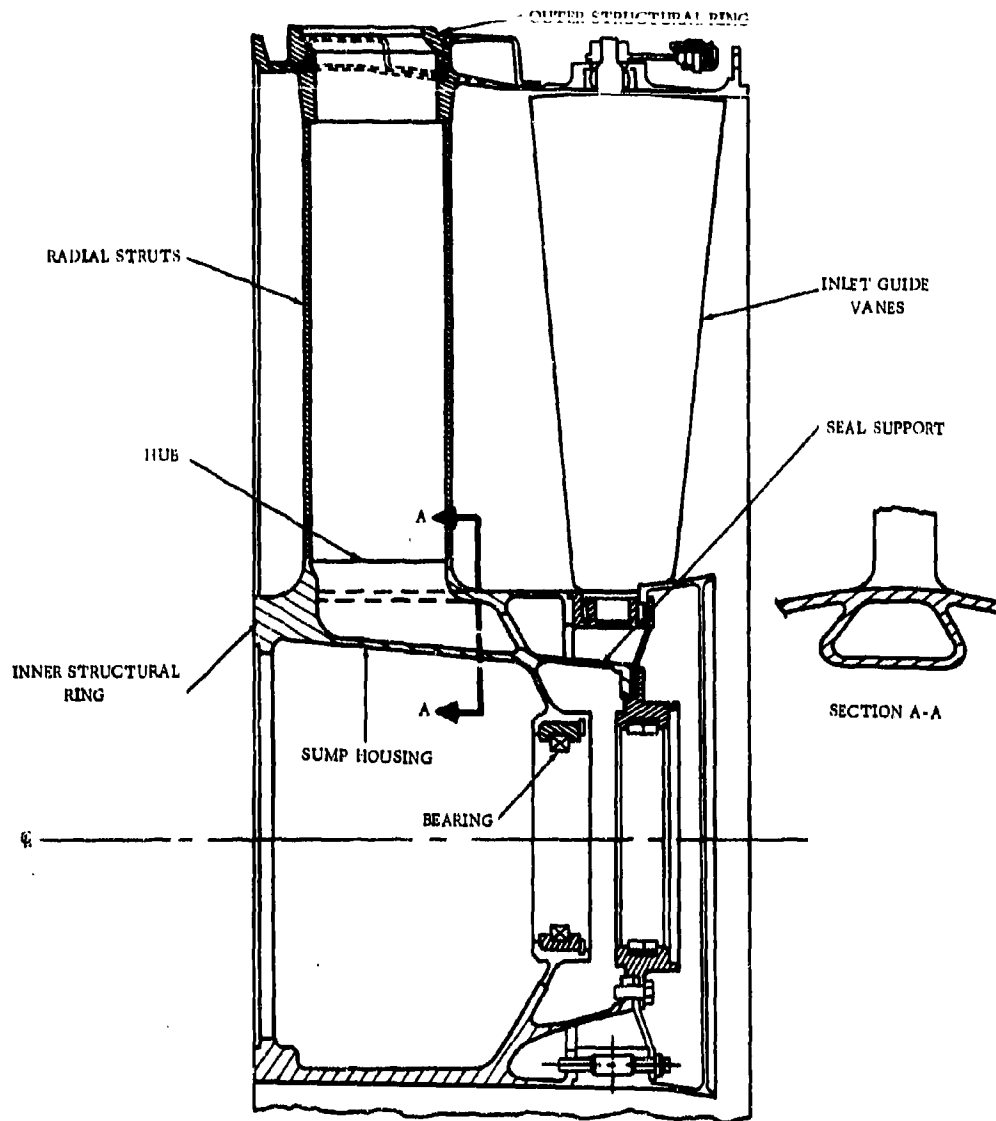


Figure 10-4. J79 COMPRESSOR FRONT FRAME

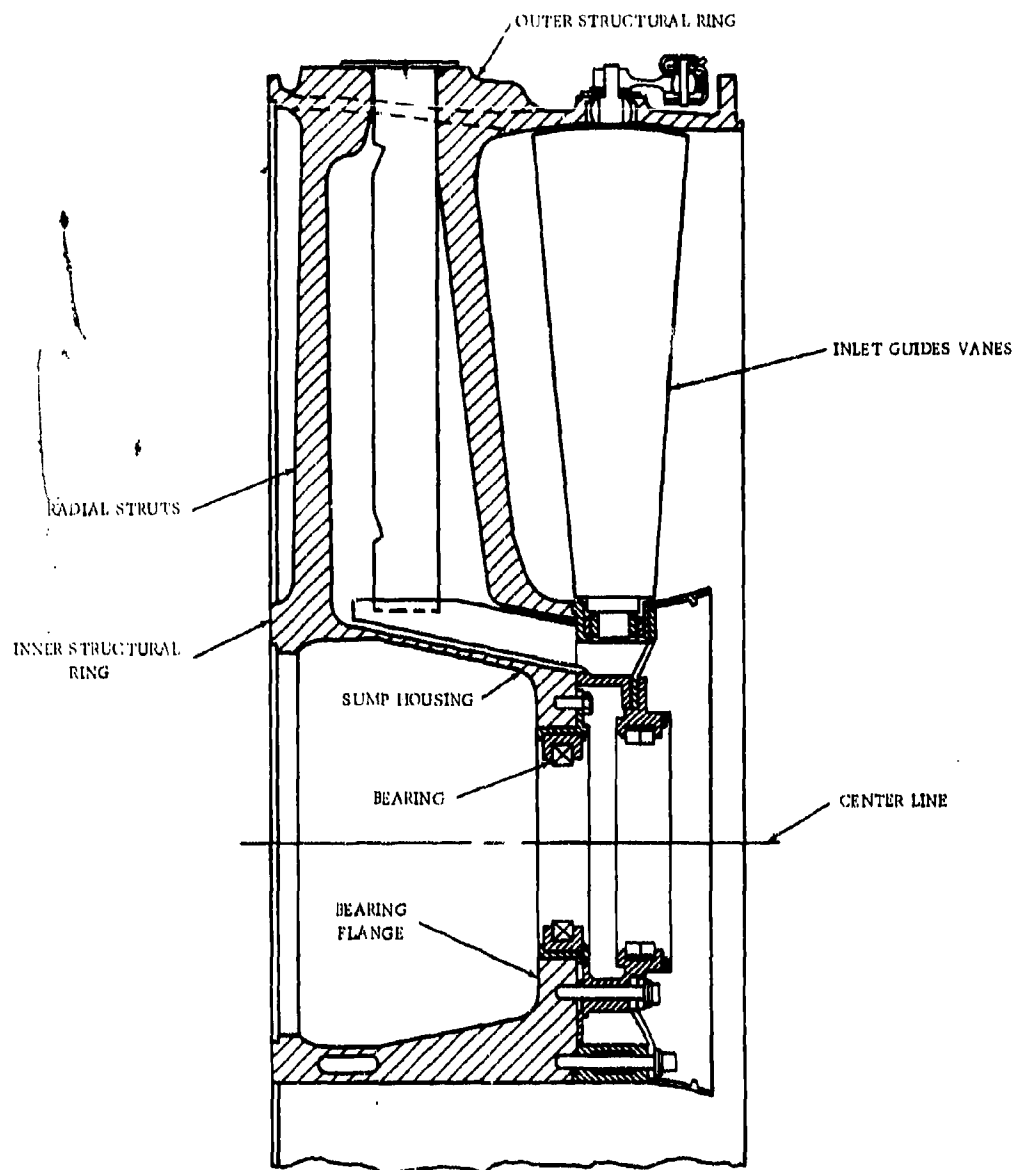


Figure 10-5. CJ805 COMPRESSOR FRONT FRAME



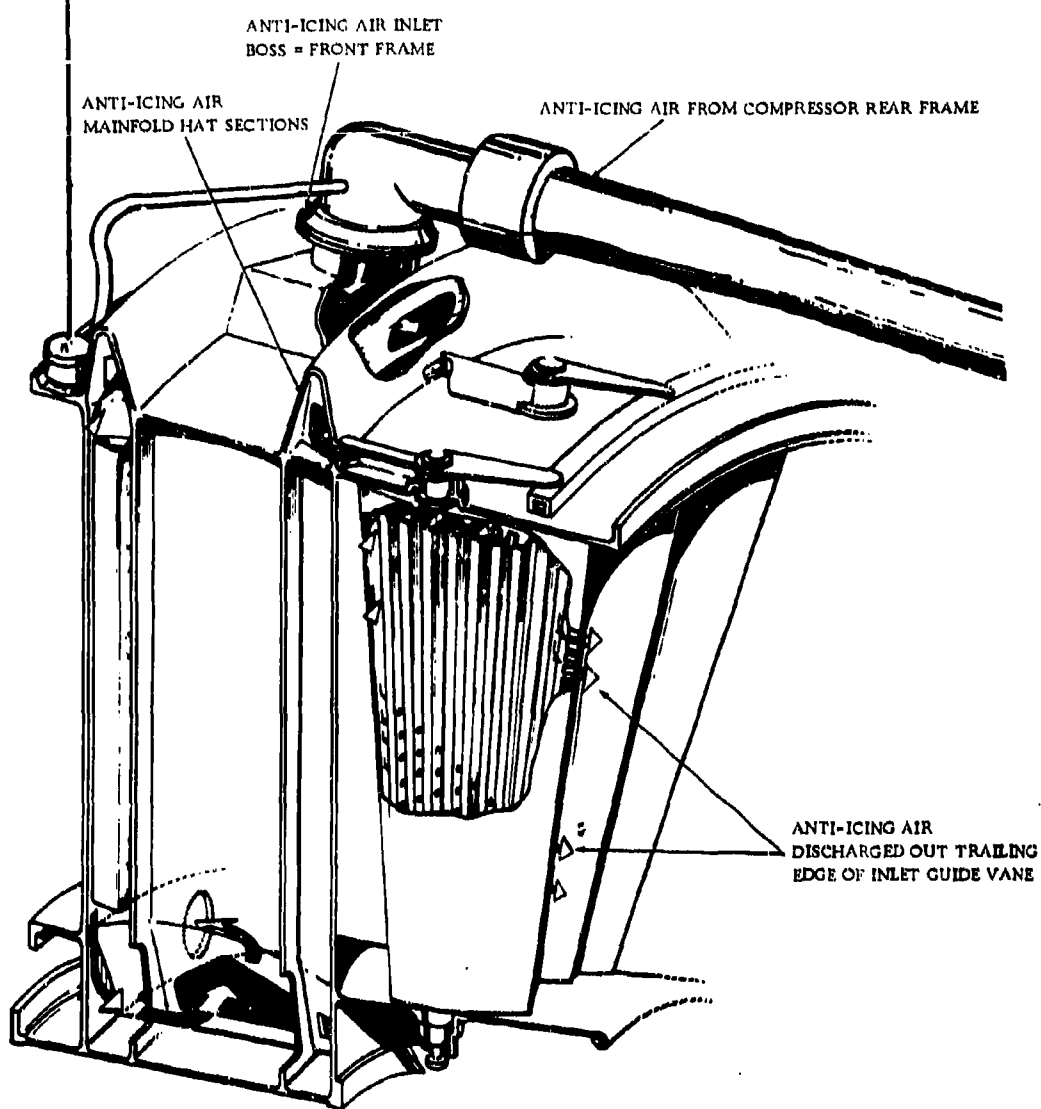


Figure 10-6. ANTI-ICING, COMPRESSOR FRONT FRAME

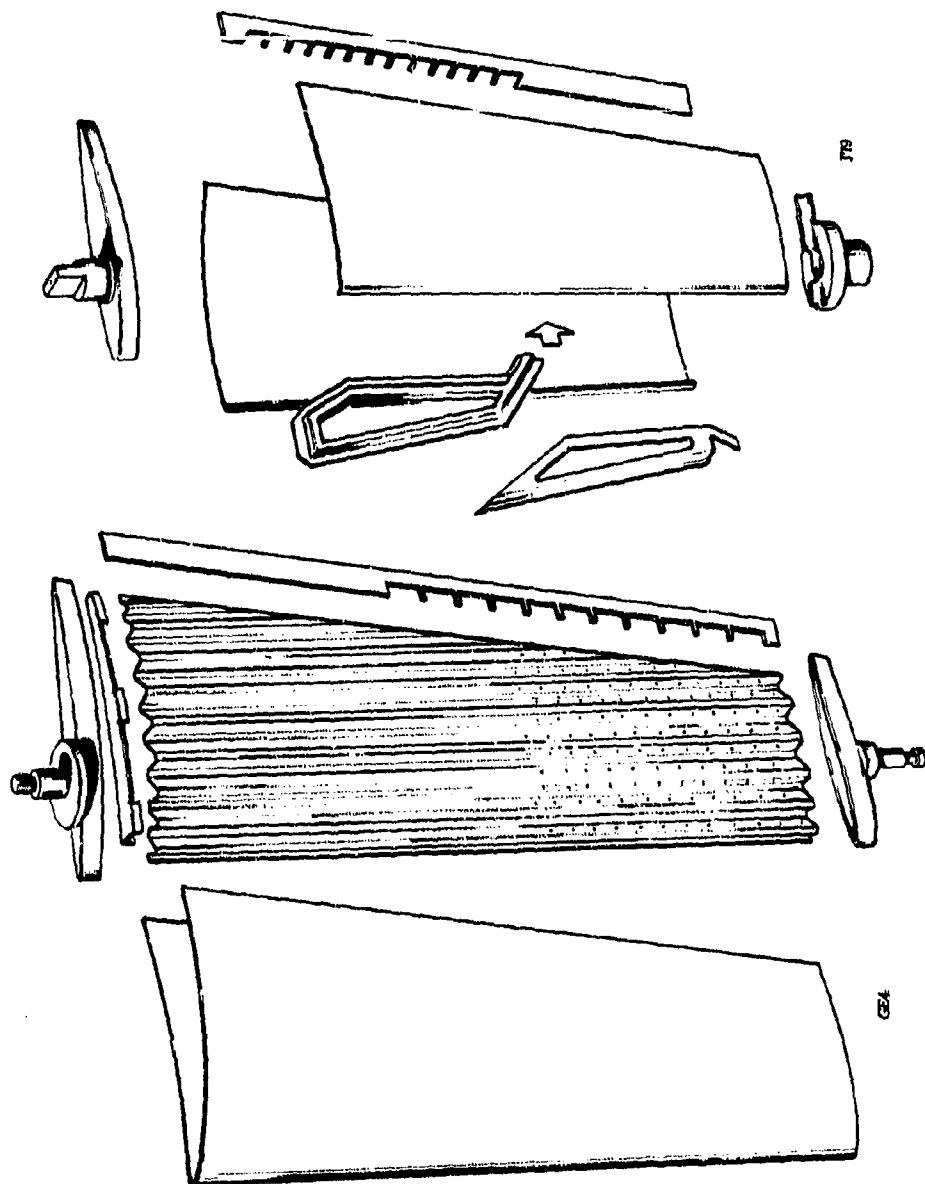


Figure 10-7. FRONT FRAME IGV

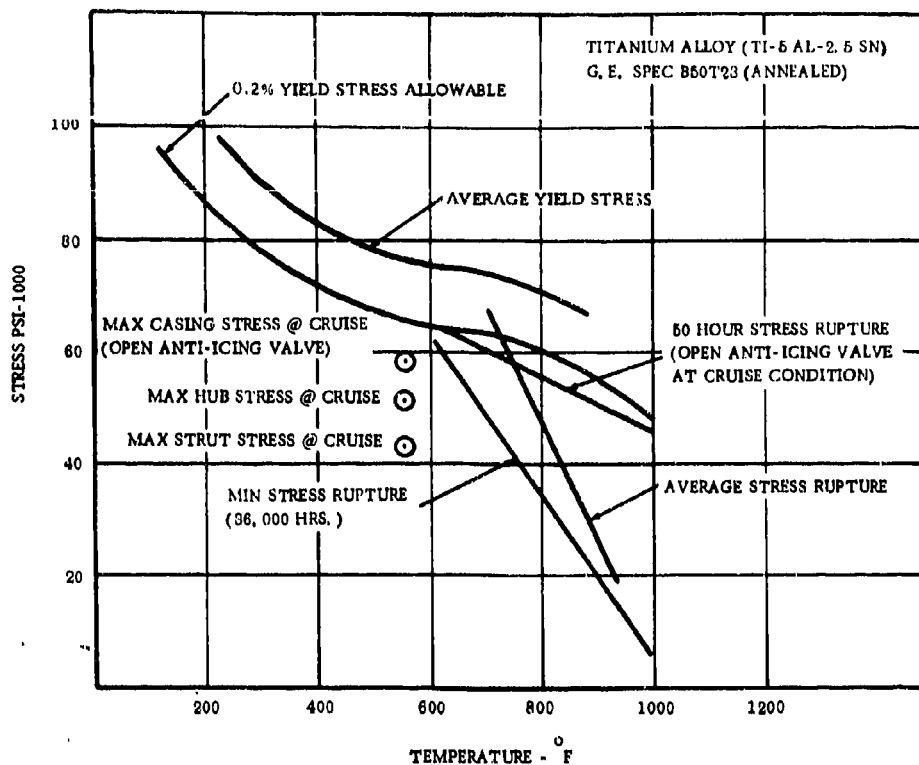


Figure 10-8. MATERIALS ALLOWABLE STRESSES, FRONT FRAME

#### 10.3.1.5 Anti-icing Provisions

Compressor discharge air is used to prevent ice formation on the compressor front frame struts and inlet guide vanes. (See Figure 10-6.) Compressor discharge air is extracted uniformly from the compressor rear frame outer casing and is controlled by external anti-icing valves before entering the compressor front frame manifold. The flow is directed through the struts and the inlet guide vanes in parallel flow-paths, and then discharged into the compressor inlet stream. The anti-icing air flows through the complete outer hat section and every strut, thereby minimizing the temperature gradient in the frame structure, keeping the frame stresses within the specified design criteria. Details of the flow system and the control valve are discussed in the anti-icing systems, Volume III-B, Part II, paragraph 9.5.

#### 10.3.1.6 Front Frame Design Details

The specific details of the front frame design as needed to meet airframe requirements are presented in paragraph 10.7 of this section.

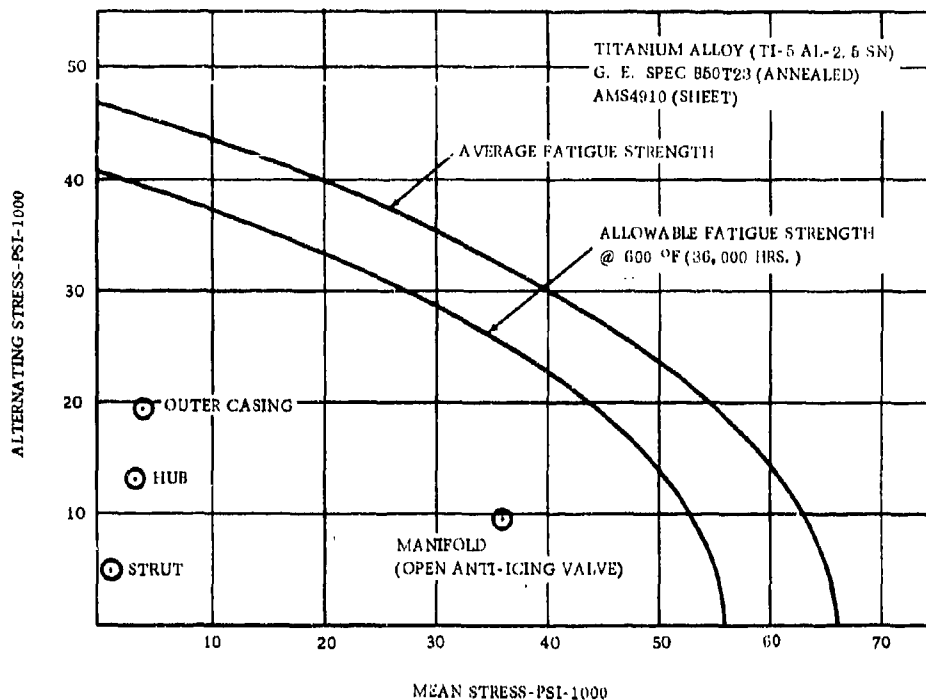


Figure 10-9. COMPRESSOR FRONT FRAME STRESS RANGE DIAGRAM

### 10.3.2 COMPRESSOR REAR FRAME

#### 10.3.2.1 Rear Frame Description

The compressor rear frame assembly performs the following major functions: (See Figure 10-10.)

- Provides mid support for the No. 2 rotor bearing, taking radial and unbalanced rotor thrust loads
- Transmits engine loads and provides for the flow annulus between the compressor and turbine frame
- Supports and positions the combustor, fuel nozzles, and igniters
- Supports for the forward side of first-stage turbine nozzle
- Provides a bleed system for the customer air, engine recoup air, engine anti-icing air and turbine rotor cooling
- Provides a manifold for exhaust leakage from the compressor discharge seal
- Provides piping for lubrication and cooling of the thrust bearing

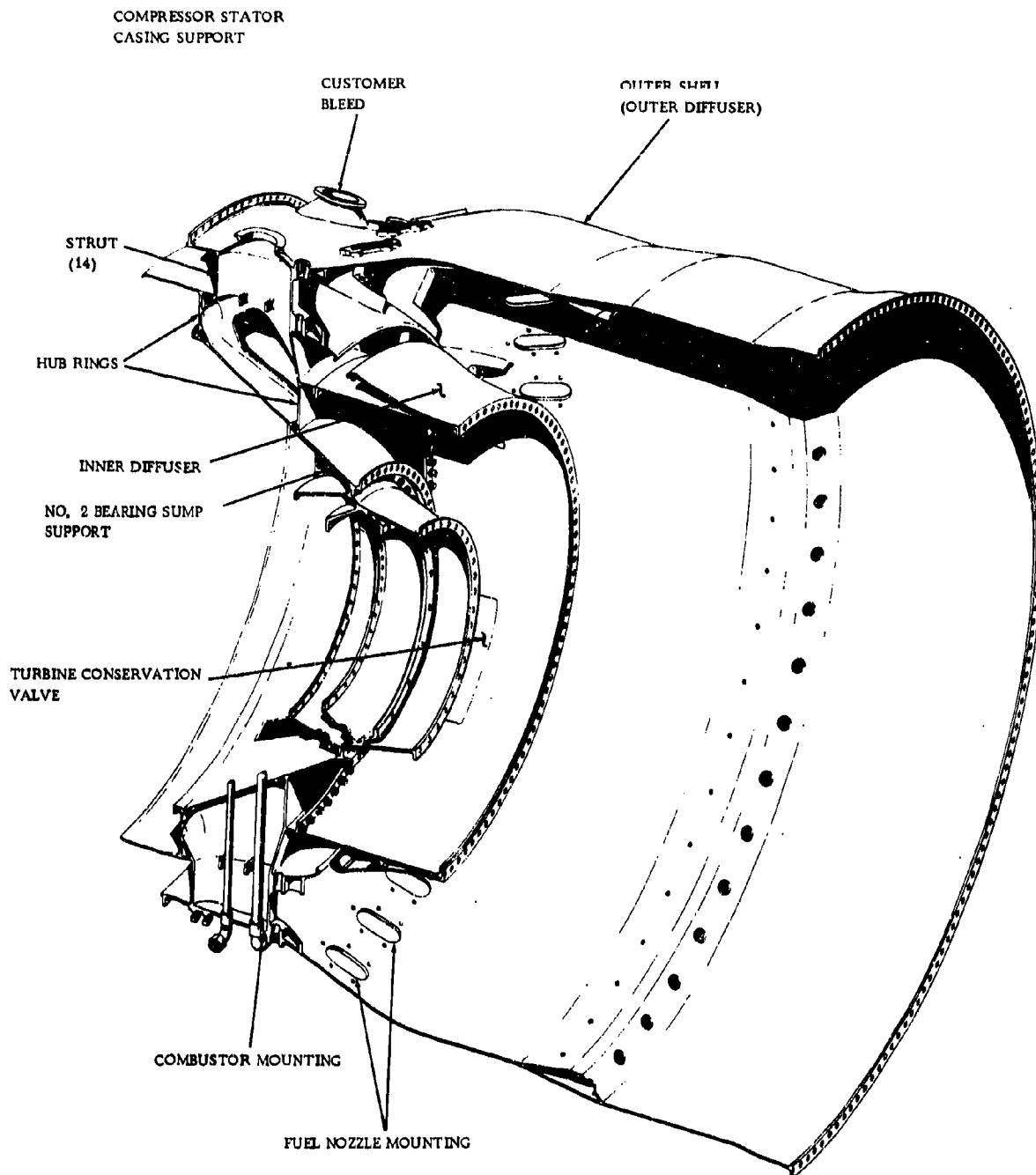


Figure 10-10. COMPRESSOR REAR FRAME ASSEMBLY

- Provides turbine air conservation system. Refer to Volume III-B, Section 3.9.4.2 Part II, and Figure 10-11 of this volume.

The frame assembly consists of the main frame structural weldment and the No. 2 sump housing. The main design is based on the J93, GE1, and TF39 compressor-rear-frame, engine and component test experiences for transmitting loads, but contains tubing and attachment features successfully introduced on the CJ805 frame to obtain long life (see Figure 10-12.) The J79/CJ805 fillet-weld hub construction, with its associated stress concentration factors, has been replaced with cast-strut ends butt-welded into hub rings connected by a shear cylinder. This design concept has been used on the J93, GE1, and TF39 frames.

The material selected for the compressor rear frame is Inconel 718. This material was chosen because of its high strength at temperature, excellent corrosion resistance, and good repairability for a high-temperature alloy. The frame cross-section is shown in Figure 10-13, with the individual pieces called out by item numbers.

Axial and radial bearing loads and a portion of the turbine first-stage nozzle load are taken at the inner structure or the hub and transmitted through 14 radial struts to the outer shell. The hub (Item 1) of the frame is a weldment consisting of cast strut-ends (including approximately one-half of the strut), machined rings and sheet-metal butt-welded together. The rigidity is achieved from two large rings approximately seven inches apart, connected at the inner surface and through the 14 struts. This long axial base provides high stiffness to overturning moment from the thrust bearing.

The outer-strut-ends (Item 2) are welded to the inner-strut-ends to complete the formation of the struts. Combining the hub to the outer casing in this manner forms a smooth strut-to-ring transition. No weld joints exist in the transition area where stress concentration would be a major concern.

The outer-strut ends, which are a part of the outer casing assembly, are turned to a close tolerance diameter, thus providing excellent weld fit-up to the inner-strut ends of the hub assembly. This excellent fit-up minimizes weld distortion and ensures a smooth flowpath into the combustor.

The 14 radial struts are airfoil-shaped to reduce aerodynamic losses, and are sized to provide adequate internal area for sump service lines and bleed airflow. Fourteen struts were selected to provide ample support to the combustor. The outer-strut ends are welded into the outer shell (Item 3). The shell is a sheet-metal and machined-ring weldment defining the outer flow annulus boundary that carries the structural load between the compressor casing and turbine frame. The internal hat section on the outer casing, shown in the aft combustion area, provides a manifold (Item 4) for uniform extraction of anti-icing air and turbine nozzle cooling air from the primary gas stream. The plugs (Item 5) that extend through the outer shell are access ports for borescope inspection of the combustor, first-stage turbine nozzle, and turbine blades.

Experience has shown that deviations in the diffuser contour at the inlet of the frame can affect the turbine-inlet-temperature pattern (Reference paragraph 4.2.2.2, Combustor). To minimize the effects of weld distortion, the 42 fuel-nozzle pads are deep chem-milled from a thick forged ring (Item 6). The inner diffuser flowpath is formed by the outer surface of the hub which consists of the strut and castings and sheet metal welded at the aft end to the combustion casing support flange. The aerodynamic load of the turbine first-stage nozzle is carried by these components.

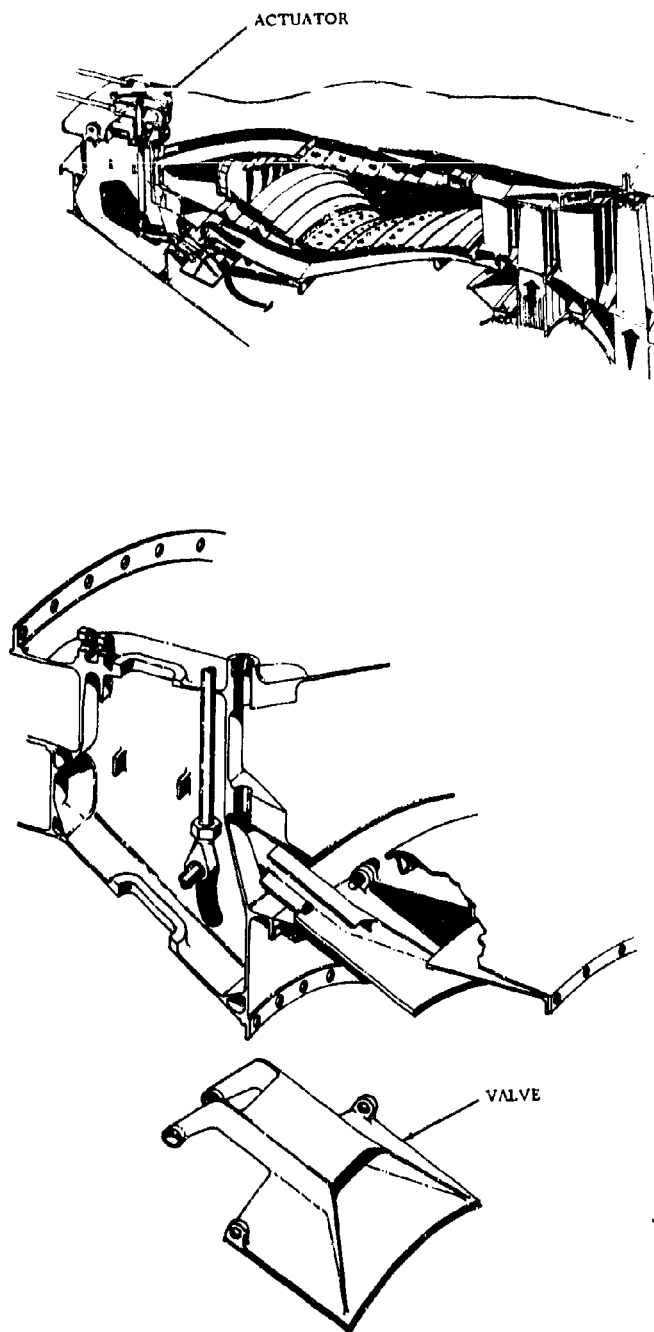
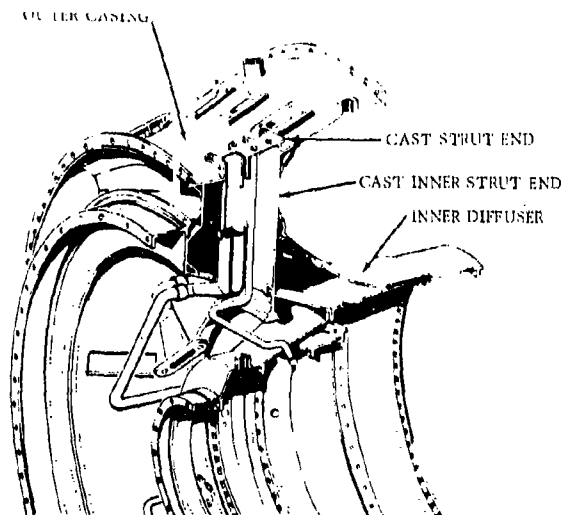


Figure 10-11. TURBINE AIR CONSERVATION VALVE, COMPRESSOR REAR FRAME



J93 COMPRESSOR REAR FRAME SHOWING THE CAST STRUT BUTT WELDED INTO THE OUTER CASING AND HUB RINGS. THE HUB RINGS ARE CONNECTED BY A SHEAR CYLINDER WHICH DISTRIBUTES THE BEARING LOAD TO THE HUB RINGS.

HUB SECTION OF J79/CJ805 COMPRESSOR REAR FRAME SHOWING STRUT CASTING BUTT WELDED INTO OUTER CASING AND FILLET WELDS CONNECTING THE INNER STRUT AND CHANNEL TO THE HUB SECTION.

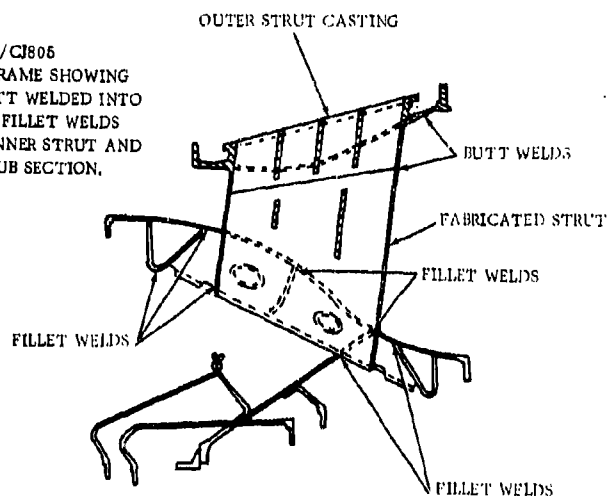


Figure 10-12. J79, CJ805, AND J93 COMPRESSOR REAR FRAMES



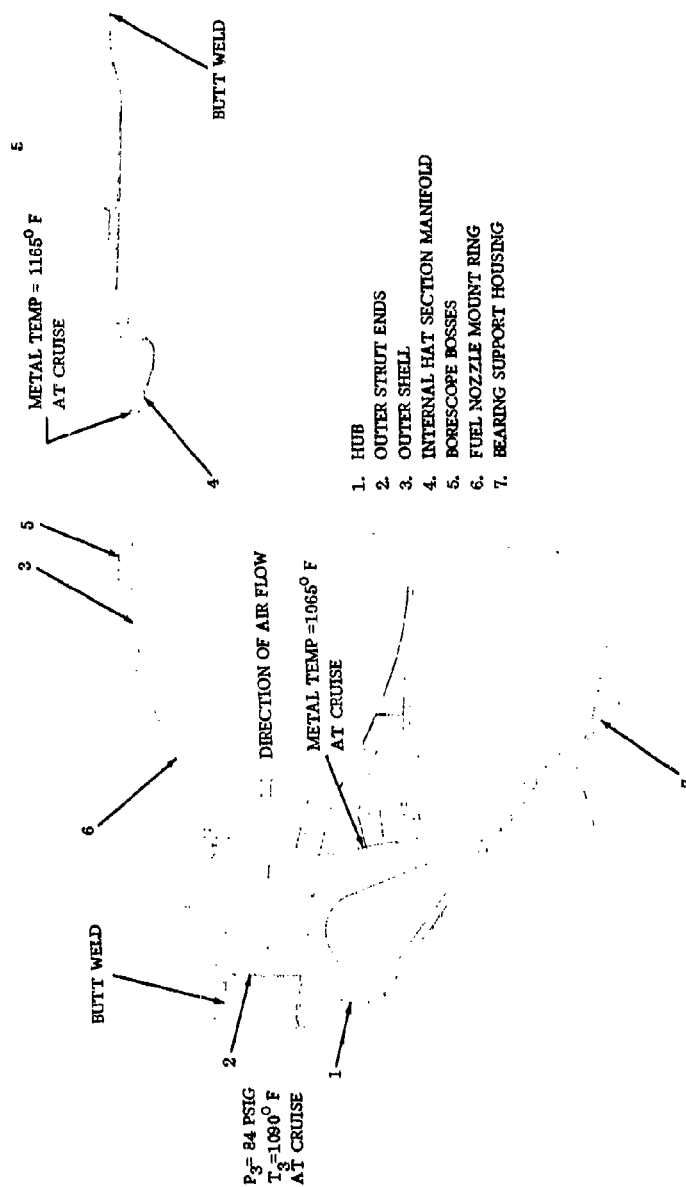


Figure 10-13. COMPRESSOR REAR FRAME CROSS SECTION

The bearing support housing (Item 7) is fabricated from an Inconel 718 casting, sheet support-cones, and machined circumferential flanges. The housing forms the sump cavity and supports the sealing hardware. All parts are butt-welded together. All sump flanges are external to the sump to prevent possible oil leakage through the bolted assembly. The sump housing is removable from the basic frame for ease of maintenance.

#### 10.3.2.2 Stress Summary

The steady-state and maximum maneuver load stresses in relation to material allowable stresses are shown in Figure 10-14. The location of calculated maximum and steady-state-cruise stresses show that the design has adequate safety margins for all conditions. Maximum stress conditions due to maneuver and engine cycle has been analyzed with regard to time at these conditions, and is not subject to a life limit due to rupture or creep properties of the material. The maximum casing stress is based on the compressor discharge pressure limiter. Figures 10-15 and 10-16 show average steady state levels and alternating stresses at Mach 0.5 at sea level and Mach 2.7 at 65,000 ft respectively.

#### 10.3.2.3 Sump Service Tubing

Sump service tubing is made of 321 stainless steel with .049 minimum wall thickness and side support to prevent resonant frequencies in the operating speed range. The tubes are attached only at the sump. Slip joints are used where the tube passes through the outer strut ends. This design permits differential thermal growth between sump, service tubing, and the surrounding structure without damage to the tubes. Wear sleeves are incorporated at the slip joints to ensure that no life impairment results from relative motion. External and internal tube interface are designed and oriented to prevent torque damage during assembly or disassembly. (See paragraph 10.7 for Figure 10-17.)

The sump is made with double-wall construction, and fifth-stage cooling air is used to isolate the inner sump wall from the frame environmental temperature.

Coking in the sump vent has long been a problem in commercial and military engines where the tubes are exposed to high temperature environments. Under this condition coke deposits from oil entrained in vent airflow form on the inside of the vent tube and in time can close off the tube entirely. Such coking can alter the entire system venting characteristics. To eliminate any possibility of this problem, the vent tube has been placed inside the oil-in line, so oil flowing into the sump will maintain the vent tube temperature well below the coking temperature of 540°F. Experience on the J79 and J93 has proven this method to be satisfactory and necessary to solve the problem.

#### 10.3.2.4 Compressor Rear Frame Specific Details

The compressor rear frame strut usage needed to meet airframe requirements are presented in paragraph 10.7 of this Section.

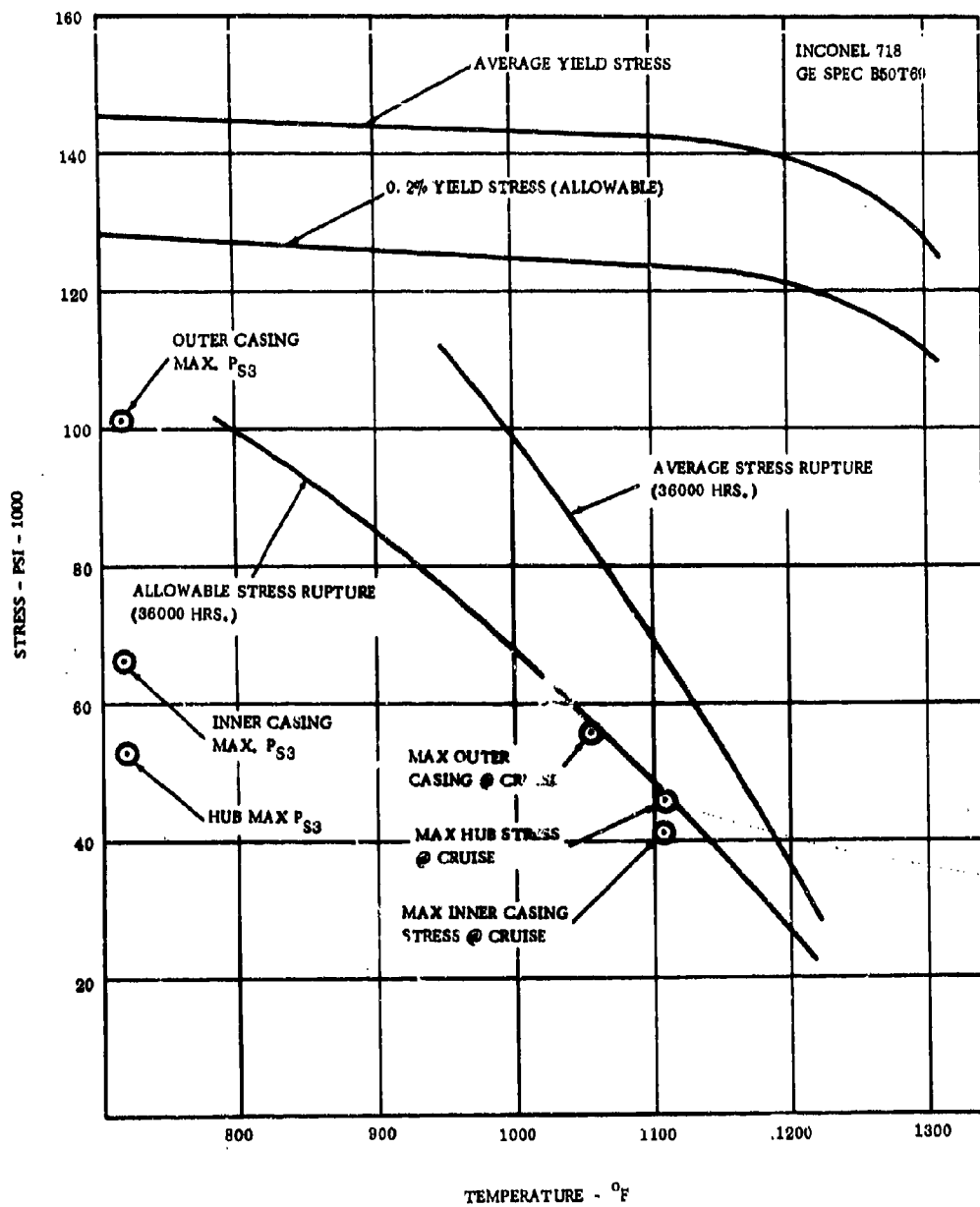


Figure 10-14. MATERIAL ALLOWABLE STRESSES, COMPRESSOR REAR FRAME

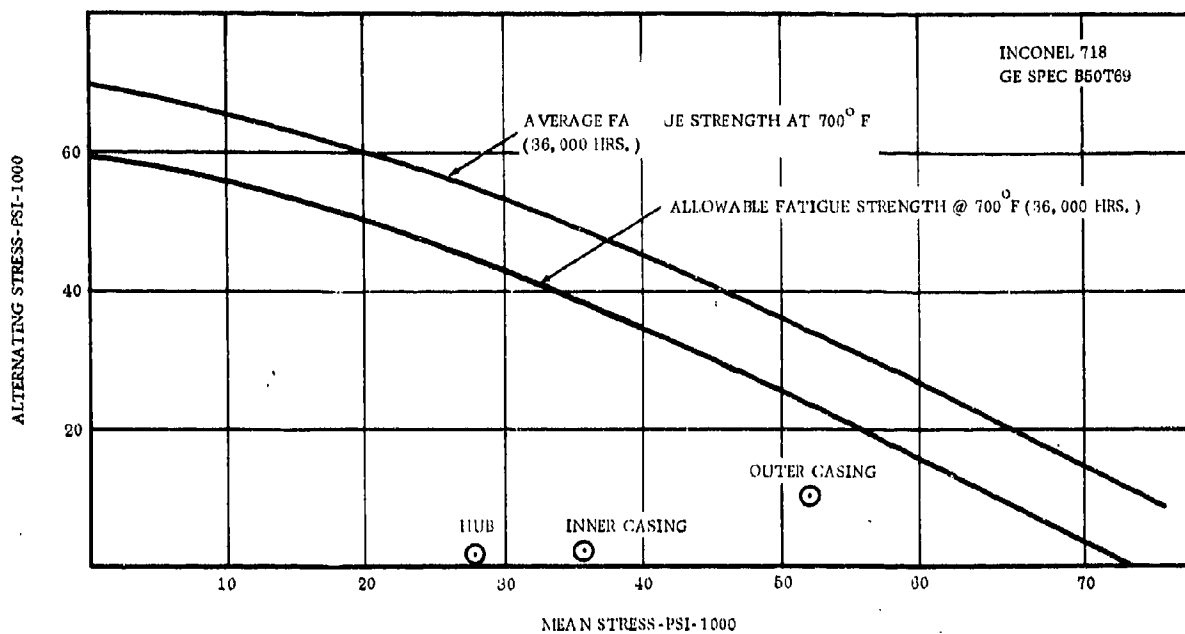


Figure 10-15. COMPRESSOR REAR FRAME STRESS RANGE DIAGRAM AT 700°F

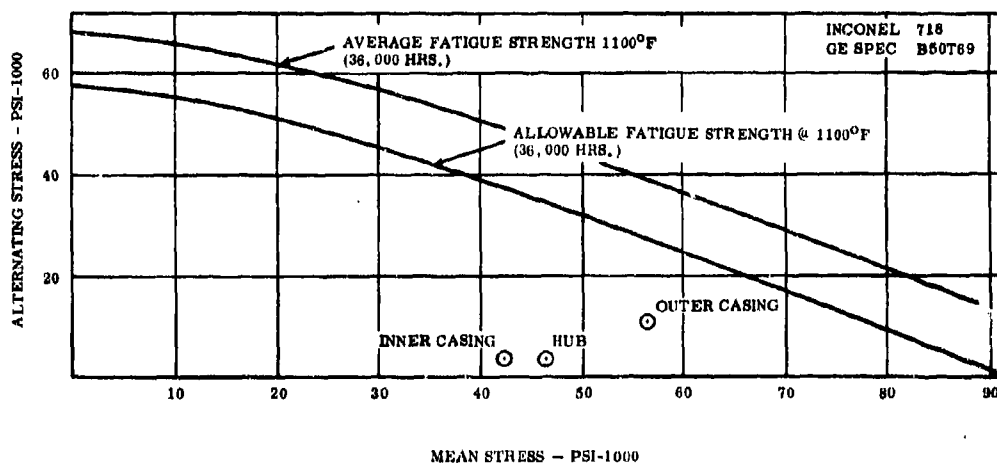


Figure 10-16. COMPRESSOR REAR FRAME STRESS RANGE DIAGRAM AT 1100°F

### 10.3.3 TURBINE FRAME

#### 10.3.3.1 Turbine Frame Description

The turbine frame (Figure 10-18) performs the following major functions:

- Provides rear support for the rotor
- Provides the engine aft attachment point (vertical and side)
- Provides a smooth diffuser flow passage for turbine discharge air into the augmentor
- Provides piping for lubrication and cooling of the No. 3 bearing

The turbine frame assembly is a bolted configuration consisting of an outer casing, struts, inner structure or hub, No. 3 sump housing, piping, gas-passage liner assembly, and the engine rear mounts.

The bolted assembly was selected because of numerous thermal stress problems encountered in the CJ family of engines and frequent manufacturing problems encountered on the J93 engine. This design eliminates weld restraint and thermal distortion during heat treatment, and will provide disassembly for repair or replacement of the struts, hub, gas passages, and the outer casing. Heat-treatment of a complete frame, upon completion of repairs, would never be required. Rene 41 was selected for the outer casing and struts because of its superior strength and ductility at high temperature. Experience with the J93 joining techniques for the engine turbine frame of Rene 41 can be directly applied to the manufacture of the GE4 turbine frame.

The eight frame-struts are secured to the inner and outer structural rings by bolts. This permits of manufacture and maintenance without compromising structural integrity (see Figure 10-19). The semi-tangential struts are used to control thermal stress in the structure. Thermal differentials between the struts and rings cause rotation in the hub and impose bending moments about the strut minor axis. Strut stresses are low because the struts are relatively flexible around the minor axis and permit large deflections at low-stress levels. All major parts of the frame may be replaced or repaired without disturbing any structural welds due to the bolted feature.

The outer structure is fabricated from two rings with hat-shaped cross-sections. (See Figure 10-20). Each ring is butt-welded into the outer casing. Eight castings, which form the attachment points for the struts, are butt-welded into the rings and casing. The hat sections and castings are constructed to form a continuous structure that distributes the load uniformly with a minimum of stress concentration points.

The outer casing (Item 1, Figure 10-19) is conical with a machined flange butt-welded on each end. The forward flange supports the aft end of the compressor rear frame casing and turbine stator. The aft flange provides an attachment point and support for the augmentor fuel injector, flame-holder, and exhaust duct.

The structural struts (Item 2) are fabricated assemblies consisting of a casting at each end, butt-welded to a formed and welded sheet-metal section between the castings.

The inner structural ring or hub (Item 3) is a one-piece Inconel 718 casting with flanges to support the bearing cone, flanges for strut attachment to hub, and stationary seal (see Figure 10-21). The No. 3 air-seal support cone is butt-welded to the seal-support flange and the forward end of the inner structural ring.

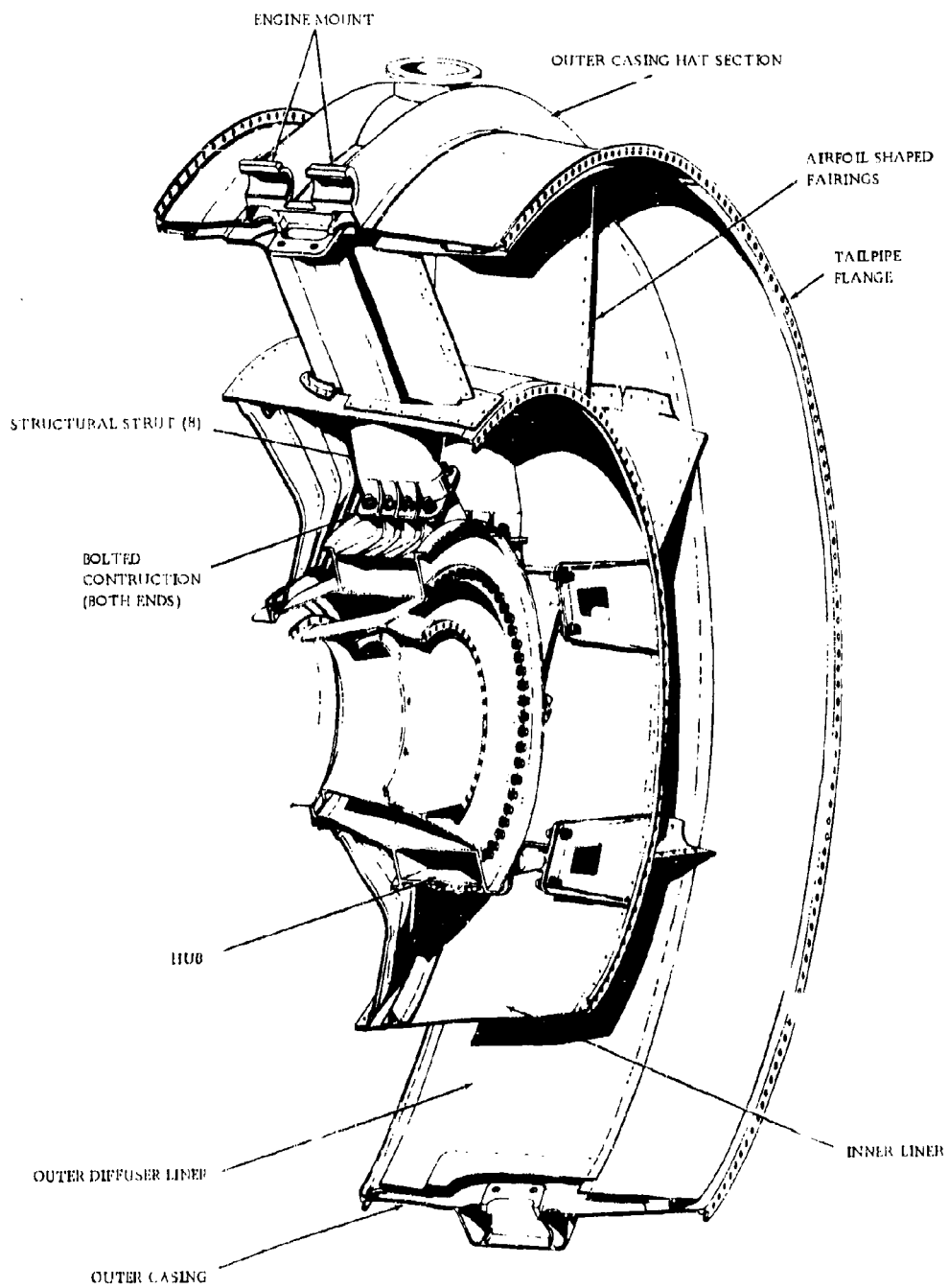


Figure 10-18. TURBINE FRAME ASSEMBLY

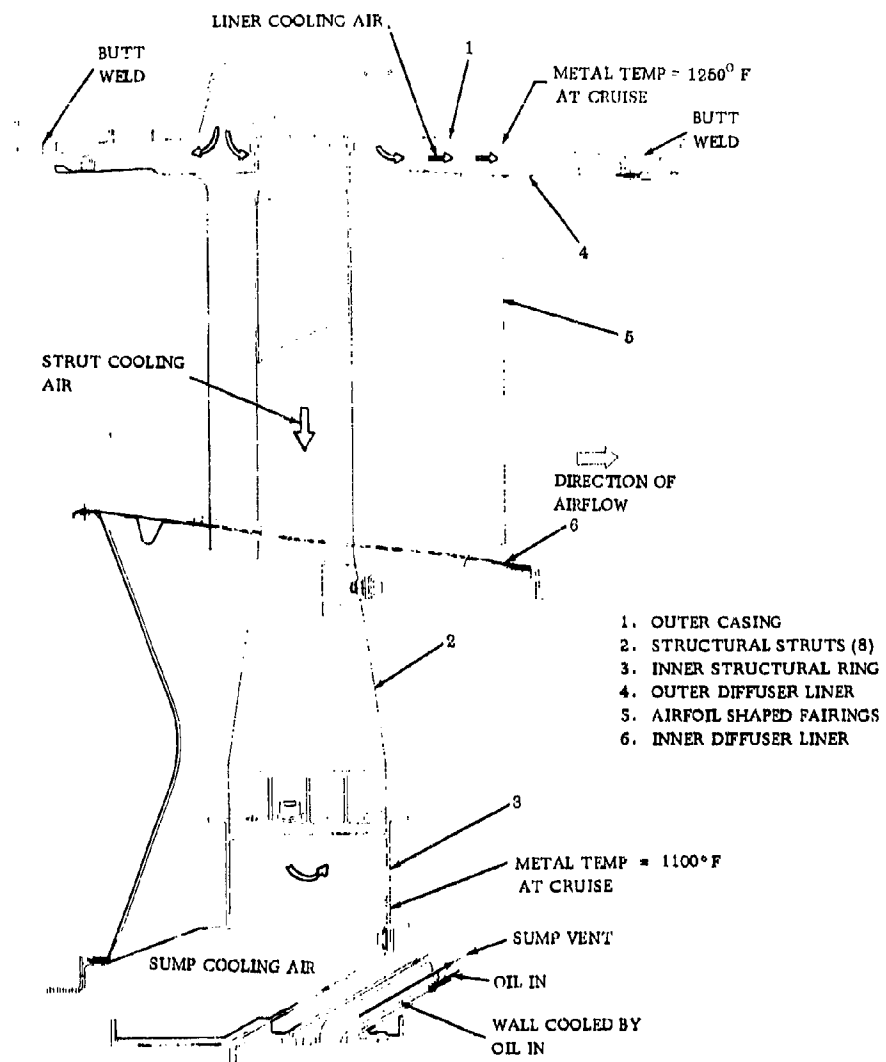


Figure 10-19. TURBINE FRAME CROSS SECTION



J79/CJ805

J93

GE4

OUTER CASING

SOLID RINGS

SHEET METAL  
HAT SECTIONS

## REASON FOR CHANGING:

1. ELIMINATE LOW CYCLE FATIGUE DUE TO THERMAL GRADIENTS.
2. MORE EFFICIENT MANNER OF STIFFENING THE OUTER CASING.
3. SHEET METAL HAT SECTIONS SERVE AS MANIFOLDS FOR AIR THEREBY REDUCING THE STRUT THERMAL STRESSES.

1. MORE EFFICIENT MANNER OF STIFFENING THE OUTER CASING.

Figure 10-20. TURBINE FRAME OUTER CASING

The Hastelloy X flowpath liner assembly consists of the outer gas passage, eight airfoil-shaped fairings, and the inner gas passage and cones. This assembly serves as a flowpath and shields the main structure from high-temperature streaks and temperature transients of the turbine discharge flow.

Hastelloy X was selected for the liner material because it possesses excellent strength up to 2100° F, and exceptional oxidation and hot corrosion resistance.

The outer diffuser liner (Item 4, Figure 10-19) consists of two pieces connected by a circumferential row of bolts. The forward end of the liner is supported by eight links, and each is pinned to a cast clevis which is bolted to the liner and outer casing (See Figure 10-22). The aft end of the outer liner is supported by eight tee rails to the outer casing. Three axial beads are formed in the outer liner between each strut to reduce the panel size as an additional resistance to buckling, and to raise the liner resonant frequency above the engine operating range.

The airfoil-shaped fairings (Item 5, Figure 10-19) are riveted on their trailing edges and riveted and bolted to the outer liner (See Figure 10-23).

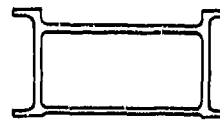
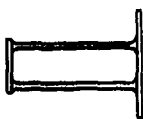
The fairing is damped by wear pads to the inner diffuser liners to limit fairing vibration amplitude.

HUB

J79/CJ805

J93

GE4



## REASON FOR CHANGING:

1. TO ACHIEVE A MORE EFFICIENT CONFIGURATION FOR PROVIDING RADIAL STIFFNESS.

## REASON FOR CHANGING:

1. TO PROVIDE A MORE EFFICIENT CONFIGURATION FOR ACHIEVE OVERTURNING STIFFNESS.
2. TO OBTAIN AN EQUAL RADIAL LOAD SPLIT BETWEEN THE TWO RINGS.

Figure 10-21. TURBINE FRAME HUB

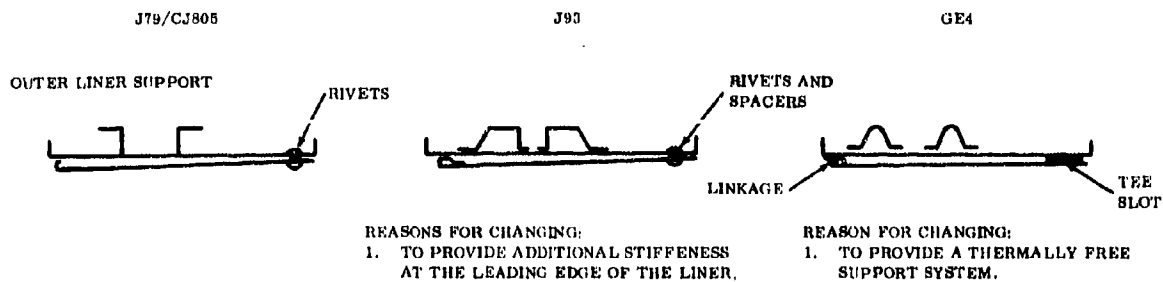


Figure 10-22. TURBINE FRAME OUTER LINER SUPPORT

The inner diffuser liner supports the exhaust inner cone through a riveted flange on the aft end and eight brackets that are bolted to the frame struts. A sheet-metal, double cone of Hastelloy X is riveted to the forward end of the inner liner and extends to the No. 3 sump air seal. Both the inner liner and double cone have formed axial beads to prevent buckling and to reduce vibration. The diffuser flowpath assembly can be completely disassembled for repair or part replacement if required, without disturbing the frame structure.

The life requirements of the liner assembly are met by keeping steady-state liner stresses, including thermal and pressure loading, well within the rupture criteria, and by keeping the calculated critical buckling stresses below the buckling criteria. Also, calculations show that no liner resonant frequencies will exist in the engine operating speed range.

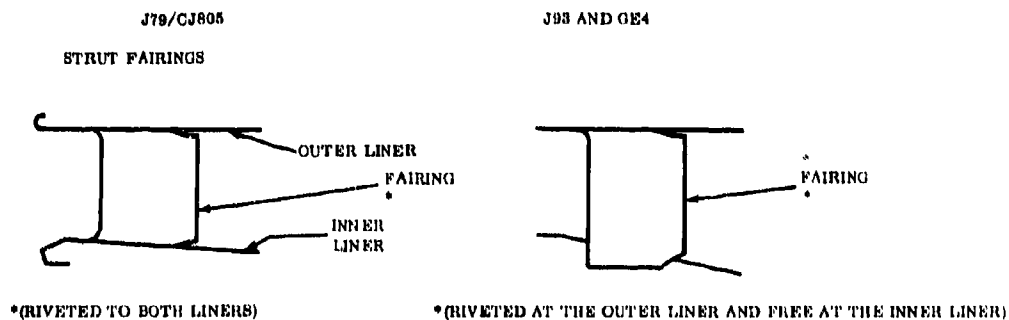


Figure 10-23. TURBINE FRAME STRUT FAIRINGS

The bearing support housing is fabricated from an Inconel 718 casting with Hastelloy X sheet support-cones and machined circumferential flanges. The housing includes the sump cavity and supports the seal hardware. All parts are butt-welded together and all flanges are external to the sump to prevent possible oil leakage. The sump housing is removable from the basic frame for ease of maintenance.

The aft end of the sump is made of double-wall construction and has stage 5 cooling air flowing through it to maintain the sump wall temperature below the 540 F coking limit.

#### 10.3.3.2 Stress Summary

The steady-state and maximum stress levels for the turbine frame in relation to the allowable stresses are shown in Figure 10-24 and 10-25. The maximum and steady-state cruise stresses, due to maneuver and engine operating loads respectively, indicate that the component design is not life-limited because of rupture or creep properties of the material. Figure 10-26 and 10-27 show the average steady-state levels and the alternating stresses in the turbine frame.

#### 10.3.3.3 Sump Service Tubing

Sump service tubing is made of 321 stainless steel and contains the same features as the compressor rear frame tubing as described in paragraph 10.3.2.3.

#### 10.3.3.4 Temperature and Cooling

Thermal stresses have often been a major concern in hot frame structures. Under normal conditions, the outer structure is relatively cool and the struts are hot due to the hot gas passing over them. When these high thermal gradients develop in the structure, high stresses also occur. The semi-tangential struts automatically rotate the inner ring to compensate for differential expansion and thus minimize the thermal stresses. The strut slant angle has been optimized between minimum thermal stress and high radial spring constant for the structure.

In addition to the thermal stress reduction due to semi-tangential struts, cooling air is used in the structure to minimize the temperature difference. Compressor discharge air passes through four struts, flows into the inner structure, and flows out the other four struts into the double-hat section. The air is vented from the double-hat section and flows into the area between the outer casing and outer gas-passage liner. This blanket of air reduces the outer skin temperatures. Stage-5 cooling air is used to isolate the inner sump wall from the frame environmental temperature.

#### 10.3.4 MAINTAINABILITY

The engine structures have been designed with high attention to simplicity for manufacturing and in-service maintainability. The maintainability features are:

- Replaceable sumps (Figures 10-2, 10-10, and 10-18).
- Accessible welds for inspection and repair (Figures 10-2, 10-10, and 10-18).
- Bolted slant struts on the turbine frame (Figure 10-18).
- Removable liners in the gas passage (Figure 10-18).

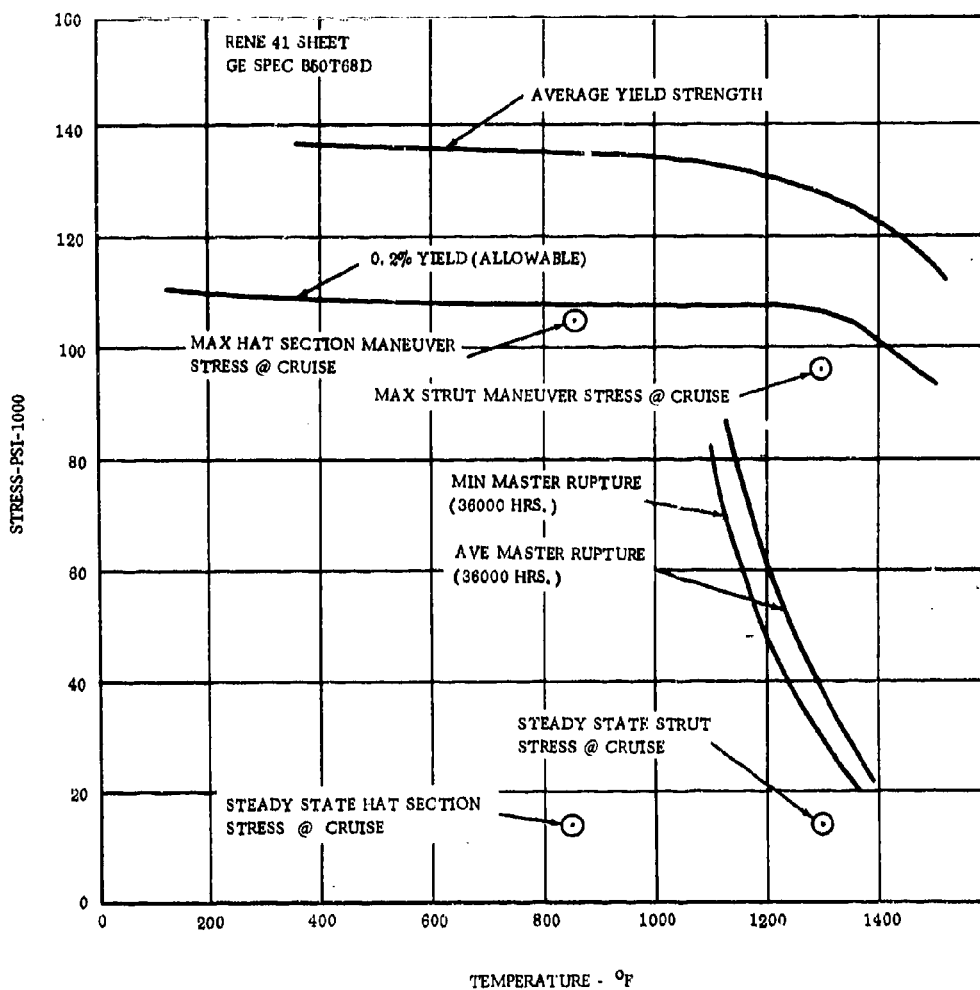


Figure 10-24. STEADY STATE STRESS, TURBINE FRAME (RENE' 41)

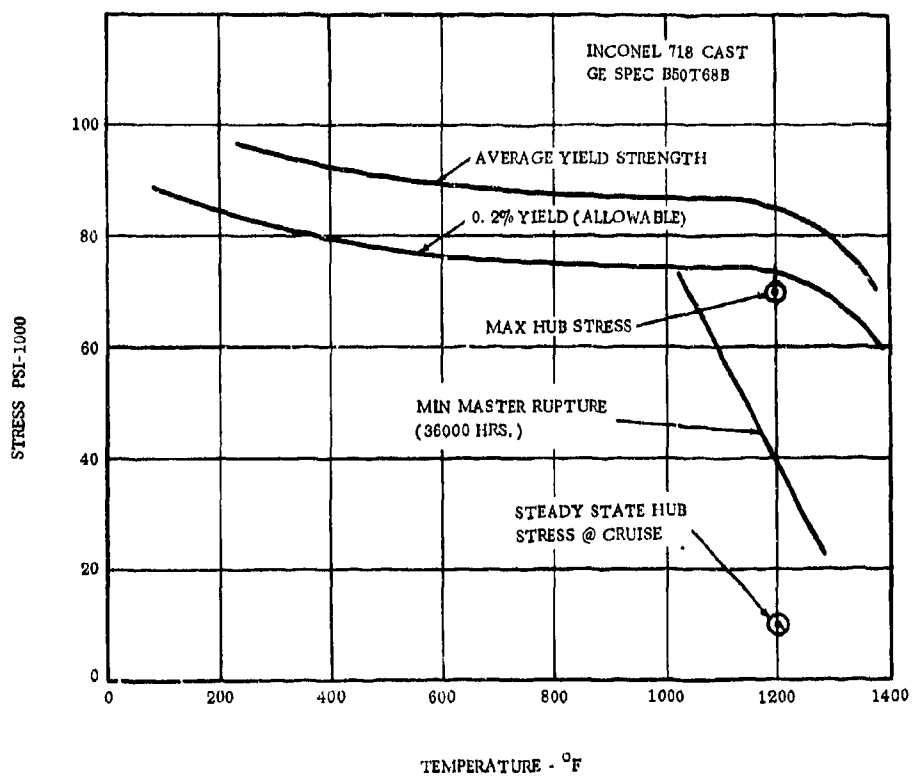


Figure 10-25. STEADY STATE STRESSES, TURBINE FRAME (INCONEL 718)

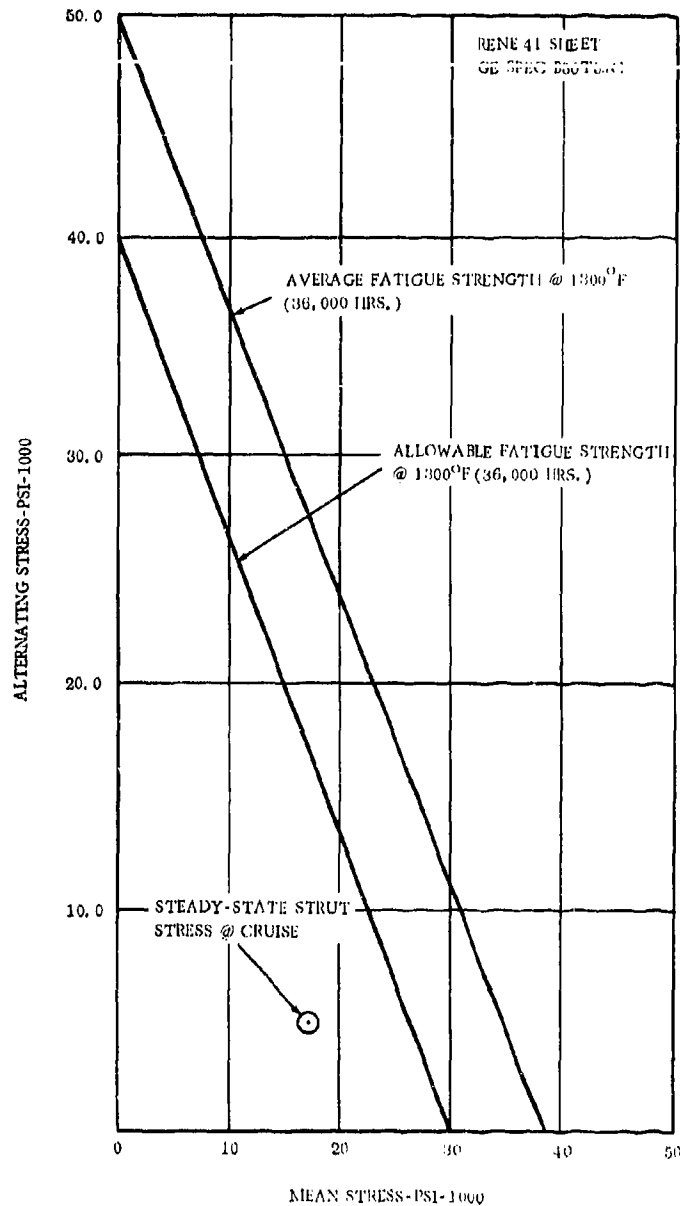


Figure 10-26. TURBINE FRAME STRESS RANGE DIAGRAM (RENE' 41)

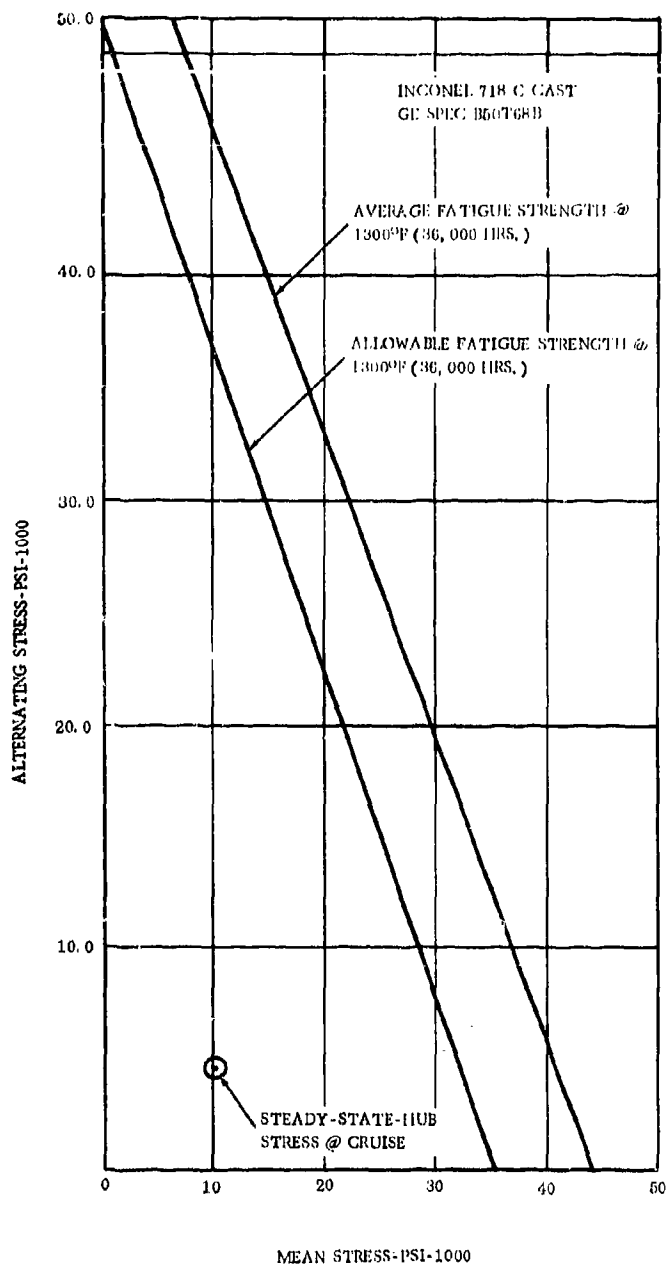


Figure 10-27. TURBINE FRAME STRESS RANTE DIAGRAM (INCONEL 718)

- Extra stock on mounting bosses for damage rework.
- Vent line cooled by concentric oil supply line to prevent coking.
- Use of corrosion-resistant materials
- Use of weldable, repairable frame materials.
- Front frame can be removed with the rest of the engine intact.
- Turbine frame and rotor can be removed as an assembly or individually.
- Access for radiography (X-ray) inspection through (L) center of turbine frame on installed engine.
- Anti-torquing provisions on service lines.

A Durability and Maintainability analysis has been conducted on the major components of the Frame and Structures section (Table 10-2).

In addition to summarizing maintenance and repair features, the technique for monitoring the condition of the component in service is given, along with diagnostic means to isolate the deterioration or failure. Finally, the frequency of checking the parameter is given; information for this column will be determined during the GE4 development program.

#### 10.3.5 RELIABILITY

The engine structures have been designed to meet the Reliability goals specified in paragraph 4.2 of volume IV. An example of this design activity is in the compressor front frame. The structure is designed to operate satisfactorily for a minimum of 50 hours at maximum cruise with an open anti-icing valve. This design adds considerable margin to the compressor front frame for normal operating condition, thereby increasing the reliability of the frame.

#### 10.3.6 QUALITY ASSURANCE

A Quality Control representative is a member of the engine structures design team and his input is continuous throughout the design and development manufacturing process. Examples of the quality features are:

- All structural welds are X-rayed and inspected by fluorescent penetrant to ensure quality.
- Each frame is individually instrumented during heat treatment to ensure control of the heat-treating temperatures.

#### 10.3.7 SAFETY

Refer to paragraph 2.1, Volume IV, for a general discussion on Safety. The following are points of safety incorporated into the frame design:

- The customer bleed manifold on the compressor rear frame takes air from the inner diffuser flowpath, which is the cleanest air available because of engine centrifuging action with respect to fluids, foreign materials, etc.



- The compressor rear frame outer casing ports for engine bleed systems have an aerodynamic jump for foreign material elimination and over-all system cleanliness.
- The inlet guide vane inner trunnion is retained to minimize effects of impact from foreign objects.
- All cooling circuits have redundant flowpaths to minimize effects of single-line loss.
- Compressor discharge pressure limiter.

#### 10.3.8 FAILURE ANALYSIS

Failure mode and consequence analyses have been made on all the engine structures. These analyses have resulted in design changes to ensure that Safety, Reliability, and Maintainability goals are met. The analyses are also being used in component test planning.

Additional failure analyses to be performed on the structural parts of the engine are described in Volume IV, 4.2 Reliability.

#### 10.3.9 VALUE ENGINEERING

The Value Engineer is a member of the engine structures design team. His input is evident in each design and process. Refer to paragraph 4.5, Volume IV, for a general explanation of Value Engineering contributions. Specific decisions affecting the frames are:

- Cast sumps
- Use of electroformed heat shields

#### 10.3.10 HUMAN ENGINEERING

The following are examples of Human Engineering on the frames:

- Service line diameters and direction are such that different functions cannot be interchanged.
- The bolts for assembling the struts in the turbine frame can be seen and reached in a practical manner. Because the bolts are unique, accidental substitution of inadequate bolts is avoided.

Refer to paragraph 2.3, Volume IV, for a general explanation of Human Engineering work.

#### 10.3.11 STANDARDIZATION

The Flight Propulsion Division (FPD) Engineering Manuals are routinely used in the design of the engine structures. The design criteria specified in paragraph 10.2 under Design Requirements and Design Approach were taken from the Mechanical Design criteria of FPD Design Practice 14021, which is one of the Engineering Manuals. Refer to paragraph 4.6, Volume IV, for a detailed explanation of the system.

#### 10.4 DEVELOPMENT STATUS

The development program for the Frames and Structures includes:

- The detailed analysis to size the elements of each component
- The static and cyclic load tests of the components to demonstrate ultimate capability consistent with operating requirements

The GE4 static structures are being analyzed by computer programs that have been thoroughly substantiated by comparison with production engine test and flight experience. Very little development testing should be required to substantiate further the design methods. Detailed testing, described below, will be conducted in the Phase III program to verify that components meet the over-all operational requirements. Phase II-C testing for design checks prior to engine operation is as follows:

- Static load test of all three frames to verify spring constants determined from analysis
- Static load test on the engine mounts to prove integrity of Phase II-C testing

##### 10.4.1 STRUCTURES STATIC LOAD TEST

Refer to Volume III-E, Test and Certification Plan. Each frame will be static-load-tested to confirm its design intent. The loads imposed include force and moment. These tests are conducted to establish the adequacy of the design under the most severe loading conditions that are defined by the requirements. The spring rate for each frame will also be verified. In addition, the compressor rear frame will be hydrostatic-pressure-tested to demonstrate its pressure loading capabilities. The engine mounts on the compressor front frame and turbine frame will be loaded to failure to determine their ultimate capability.

##### Phase II-C Status.

The three main engine bearing support frames were statically loaded at the bearing bores and the mounting pads to demonstrate the structure and mount integrity and to determine the frame spring rates. A typical comparison between the tested spring rate and the calculated value is the compressor front frame deflection-load curve as shown in Figure 10-28.

For summary of completed bearing testing, see Section 8.4.1.

##### 10.4.2 STRUCTURES VIBRATION SURVEY TEST

All tubes, casings, and liners will be excited to determine their natural frequencies in beam, ring, and torsional modes to ensure that no detrimental criticals occur that may be excited by the engine or associated hardware.

##### 10.4.3 STRUCTURES DESTRUCTIVE TEST

All frames will be tested to destruction in high- and low-cycle fatigue to establish design margins where differences of test versus calculated indicate that corrections are required. The results of frequency investigation (paragraph 10.4.2) and engine tests which reveal predominant frequencies will be used to set test conditions. Investigations will be continued until all frames demonstrate the required fatigue life. The frames will also be subjected to cyclic thermal stress to determine their design margin and fatigue limit for this mode.

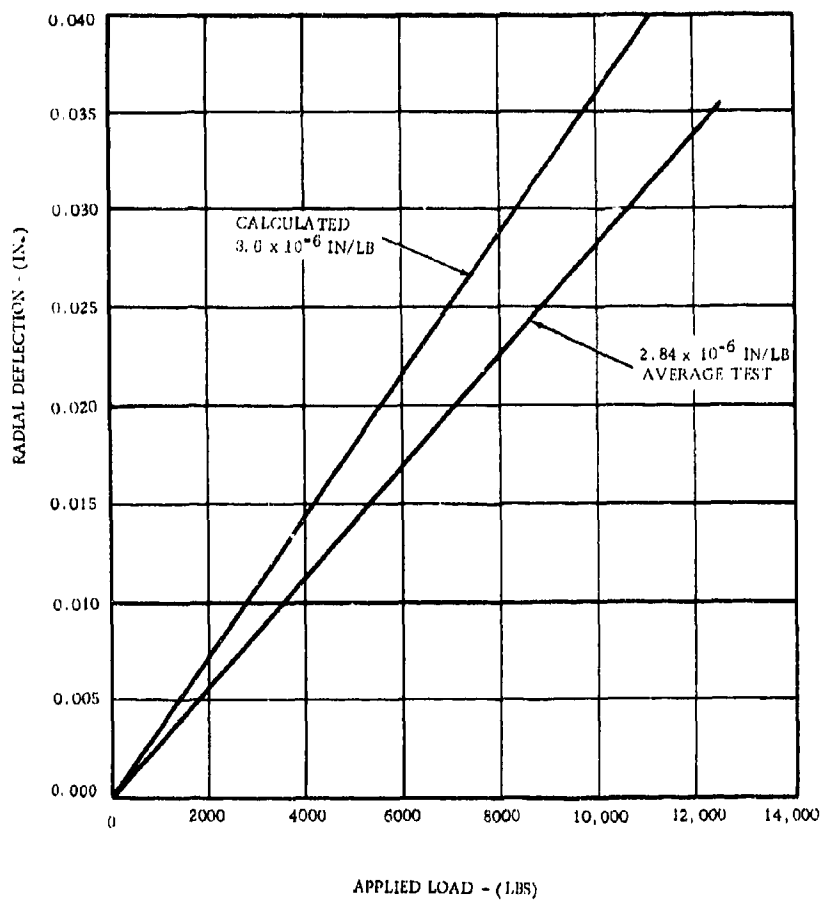


Figure 10-28. COMPRESSOR FRONT FRAME RADIAL SPRING RATE

The main engine mounts will be subjected to cyclic loads equivalent to their maximum loadings, with an operating environment to verify proper design margin.

In addition, the front frame will be used on the dynamometer tests of the inlet and accessory gear-boxes to demonstrate that none of the frame elements are adversely affected by gear-induced excitation forces.

#### 10.4.4 STRUCTURES MAINTAINABILITY AND REPAIRABILITY TESTS

Basic repair techniques developed on the J79/CJ805 and J93 structures will be incorporated in GE4 design when a failure of any structural component occurs during engine or component testing. A repair procedure will be established, the component repaired, and additional tests conducted to establish Repairability limits and the effectiveness of the repair procedure.

#### 10.4.5 FRONT FRAME STRUT AND IGV - ICEBALL AND BIRD IMPACT TESTS

Iceball and bird impact tests will be conducted on the front frame assembly. The iceballs and birds (per FAA regulations) will be shot at the struts and inlet guide vanes to prove the engine's capability to withstand these impact loads and complete the flight safely.

#### 10.4.6 SYSTEM FLOW TEST

System flow tests shall be conducted on the anti-icing system, recoup air system, turbine cooling air system, customer bleed air system, and lubrication system to demonstrate flow capabilities.

#### 10.4.7 EVALUATION OF NOISE SUPPRESSION MATERIALS/OR DEVICE INCORPORATION IN THE COMPRESSOR FRONT FRAME

This evaluation procedure and the compressor front frame effects on it are explained in detail in Volume III-C.

### 10.5 SUPPORTING TECHNOLOGY

The analytical tools available for the detailed design of engine structures have been greatly improved during the last five years. Formerly, many man-weeks of engineering effort were required to "break down" complex structures into elements that could be analyzed with the available procedures. Now, computer programs will analyze complete assemblies after a realistic model is defined. Many advantages are obtained, as follows:

- Design iterations are possible to ensure maximum structural efficiency and optimum weight
- Interaction effects with adjacent components and associated systems are studied in detail
- Computer programs ASIST, FAST, MASS, PAPA, MULTISHELL, developed for jet engine structures analysis, consider redundancy, straight and curved members, three-dimensional effects, and differential thermal expansion.
- Development tests have been used to evaluate and calibrate the theoretical analysis made on the frame spring rates. (See Table 10-3.)
- Additional analysis to establish buckling limits, concentrated factors, and excitation versus response of tubes and shells on campbell diagrams are also conducted to predict the component capability.

The procedures described above are being used in the development of the GE4 engine structures. Much of the long-life experience on commercial engines (CJ805-3 and CJ805-23), military engines (J79, J93, J85, T58, and T64), and the development engine (GE1) applies directly to the design of the GE4 structural components. Some of the significant features included are as follows:

- Castings at strut-to-ring junctions. The smooth transition results in predictable load paths that are readily analyzed.
- Butt-welded joints. They eliminate discontinuities and stress concentration.
- Mechanical control of temperature gradient in the turbine frame. The use of partially tangential struts and the use of cooling air results in significantly more margin between steady state stress and allowable stress (see Table 10-4).
- Replaceable liner and sump service tubing
- Removable sump housings
- Ductile and corrosive-resistant material
- Accessible welds for inspection and repair

Table 10-3. Radial and Overturning Spring Rates for J93 Compressor

	Calculation x 10 <sup>-6</sup> in/lb	Test x 10 <sup>-6</sup> in/lb	Percent Error
Radial Spring Rate	1.22	1.14	7.0
Overturning Spring Rate	4.53	4.46	1.5

Radial and overturning spring rates for the J93 compressor rear frame were obtained from static load test and various methods of analysis.

Table 10-4. Steady-State Thermal Stress Margin at Cruise Condition

	Stress	Percent of Allowable Stress
J79 and CJ805-3 Machine Ring Turbine Frame	47,900 psi	60.0
CJ805-23 Turbine Frame	65,000 psi	81.0
GE4 Turbine Frame	15,000 psi	15

## 10.6 ENGINE STRUCTURAL DYNAMICS

### 10.6.1 DYNAMIC ANALYSIS

The GE4 engine system has been analyzed to determine its dynamic characteristics. The analysis was undertaken at the onset of the design and will continue throughout the engine development. This is to ensure that the engine will be free from destructive vibration and will be structurally efficient.

The effort is guided by criteria which require the finding and avoiding of critical frequencies. It also identifies potential sources of exciting energy, both mechanical and aerodynamic, and indicates how to minimize or avoid these forces. The procedure for establishing vibration levels is also included. The analysis was performed using a special computer program. The cost, accuracy, and convenience of this program aids in obtaining reliable results.

### 10.6.2 DESCRIPTION OF ANALYTICAL METHOD

The analysis was made using the VAST (Vibration and Static Analysis) computer program developed by General Electric. This is a mathematical method for computing the dynamic characteristics of the engine.

The VAST program is capable of determining natural frequencies, mode shapes, and vibration amplitudes for an entire engine system. It takes into consideration all masses and flexibilities of the engine and supporting structure. The mass properties accounted for are: weight, polar moment of inertia, and transverse moment of inertia.

The flexibility properties considered are length, area moment of inertia, shear area, modulus of elasticity, and shear modulus. Additional conditions studied are bearing clearances, misalignment, maneuvers, imbalance, and system damping. The output of the VAST program is a tabulation of the critical frequencies, mode shapes, deflections, bending moments, and shear forces for all components of the engine. Graphs are generated for deflection, force, and moment. An independent calculation is made for the potential and kinetic energy for each of the resulting mode shapes to prove the accuracy of the results.

A thorough understanding of the vibrational characteristics of the engine is essential to an engine development program. All parts of the engine influence its dynamic behavior and, therefore, the entire system must be analyzed to obtain correct results. This analysis can only be accomplished with the aid of a high-speed computer program because of the complexity of the calculations. An optimum structural design can be achieved by conducting parametric studies wherein the bearing locations, structural load paths, and flexibilities are varied.

The GE4 engine-airframe dynamic compatibility has also been studied in detail. The inlet system and the engine nacelle are considered in the over-all installed dynamics. The interaction between the aircraft mounting system, the engine pylon, and the wing structure are included in this analysis. The reason for this total-system evaluation is to avoid a detrimental dynamic coupling between the engine and a component of the aircraft.

The usefulness and accuracy of the VAST program have been proven conclusively on all current production and development engines produced by General Electric - - the J79, J93, CJ805-3, CJ805-23, T58, J85, T64, GE1, and TF39 engines. The average variance between test and calculated frequencies was 2.6 percent during the original accuracy checks made in 1959, when the program was first applied to a complex engine system.

### 10.6.3 DESIGN CRITERIA

The design criteria for GE4 engine system vibrations have been established. Design requirements are specified for flexural, torsional, and axial critical frequencies of the system. Design specifications are also included to avoid the phenomenon of whirl, caused by aerodynamic forces.

The design criteria specifies that major critical frequencies should not be located at a steady-state operating points or at any engine speed where the mode could be easily excited. A major critical frequency is defined as one in which the mode is characterized by a prominent bow or deflection of any of the rotors. The rotor speed ranges where major critical frequencies should be avoided are as follows:

- The region from 15 percent above maximum physical speed to 15 percent below cruise speed
- 40 percent to 55 percent of nominal speed
- $\pm 10$  percent from the rotor thrust crossover speed point
- $\pm 10$  percent from idle speed setting

Criteria have been established to ensure that the engine will be insensitive to aerodynamically excited rotor whirl. Two situations can cause whirl to develop. One is known as torque deflection and the second is seal instability. Both conditions can occur when the deflections of the components involved cause a circumferential variation in pressure loading. Design requirements have been defined using the criteria to avoid these destructive excitations. Vibration limits have been established consistent with design practices to ensure low vibratory stress and to aid in achieving long fatigue life.

All GE4 components have been checked for their vibratory characteristics. These components include shafts, disks, liners, shells, air seals, cones, accessories, and piping. They are analyzed for all potential excitations, meaning, one per revolution  $1/2$  and other multiples of rotor frequency, and passing frequencies of roller and ball bearings, struts, blades, and gear teeth. Aerodynamic excitations considered are "duct buzz" and combustor and tailpipe acoustics. Additional phenomenon considered are ring and bell modes.

### 10.6.4 ENGINE DYNAMIC ANALYSIS RESULTS

The results of the vibrational analysis are illustrated in Figure 10-29. The figure shows the mode shapes and amplitudes of the engine system's natural frequencies. The amplitudes of vibration are based upon predicted damping coefficients and rotor imbalances obtained from experience. The results show that vibration amplitudes are within an acceptable range.

Listed below is a brief description of the predominant modes of vibration at each natural frequency.

The modes of vibration at 8.8 cps and 16.3 cps are the natural frequencies of the rear and front engine mounts, respectively. These frequencies are a function of the engine weight and the flexibility of the engine support structure. These modes are characterized by rigid body translation of the engine. The rotor and stator are in phase and have very small relative motion.

The natural frequency at 43.3 cps is the first flexural mode of the engine shell. This frequency is a function of the engine shell flexural stiffness and the engine weight and its distribution. This mode will not have any detrimental effect on engine operation. It occurs below idle, and the rotor and stator have small relative motion.

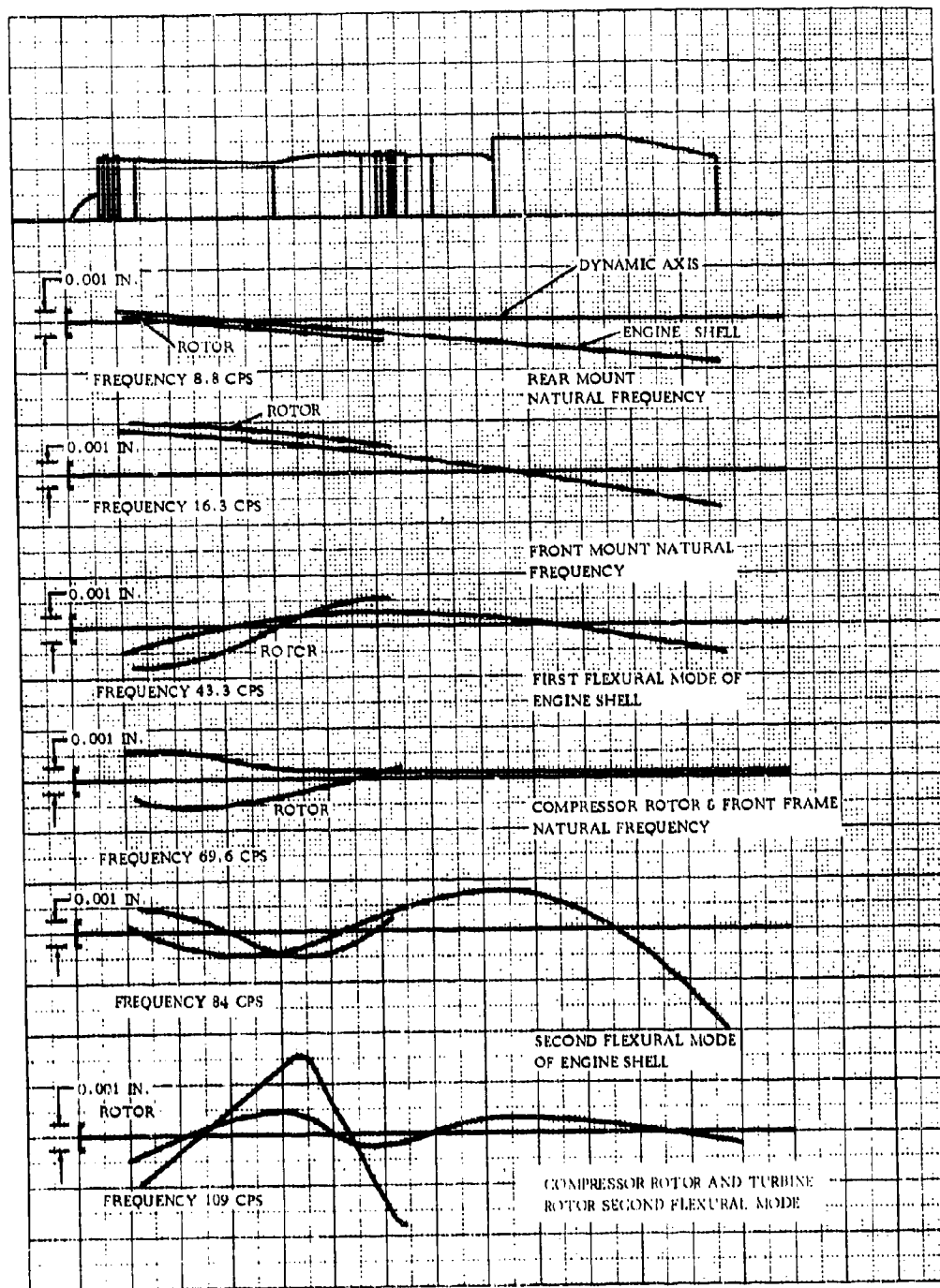


Figure 10-28. NATURAL FREQUENCIES OF OVER-ALL ENGINE SYSTEM



The mode of vibration at 69.6 cps is the natural frequency of the compressor rotor and compressor front frame. This mode is characterized by bending of the compressor rotor and translation of the compressor front frame, resulting in separation between the rotor and stator. This mode has been located at a non-steady state operating point so that it will not have a detrimental effect on engine operation.

The natural frequency at 84 cps is the second flexural mode of the engine shell. The rotor and stator have small relative motion. Similar modes of vibration on previous engines have been shown to be very difficult to excite. No detrimental effect on engine operation is anticipated at this frequency.

The mode of vibration at 109 cps is the second flexural frequency of the compressor and turbine rotor. This mode is characterized by high rotor deflection. It occurs at a frequency approximately 25 percent above the maximum rotor speed and will not be excited.

#### 10.6.5 ENGINE MOUNTING

There are two transverse mounting planes. The forward mount is in the plane of the compressor front frame. The aft-mounting plane is on the centerline of the turbine frame struts.

The GE4 mounting system is designed so that all forces that connect the engine with the airframe structure are statically determinant. All reaction points on the engine have a spherical bearing which is free to rotate about all axes passing through the point of load application. The statically determinant system requires that the thrust force be reacted at one point when side and vertical loads are reacted in two planes, that moments about the engine longitudinal axis be reacted in only one transverse mounting plane, and that there are just two transverse mounting planes in which all mounting loads are reacted. In addition, the mounting system must not restrain the engine with respect to induced effects of the supporting platform, thermal expansion, or relative deflections. The elimination of difficulty to predict secondary or induced stresses at points of attachment to the engine ensures that the engine structure will meet service life requirements.

##### 10.6.5.1 Engine Mounting Design Details

The specific details of the engine mounting system needed to meet airframe requirements are presented in paragraph 10.7.

## 10.7 AIRFRAME COMPANY DESIGN DETAILS

### 10.7.1 BOEING AIRCRAFT COMPANY DESIGN DETAILS

#### 10.7.1.1 Maneuver Loads

The following information supplements paragraph 10.1 of the preceding presentation.

The maximum design maneuver loads of components are defined in Table 10-1 (B). These loads were used in the frames' design to withstand the maximum pressure loads and temperatures of the engine operation cycle, and to withstand maneuver and inertia loads per specifications.

#### 10.7.1.2 Compressor Front Frame

The following information supplements paragraph 10.3.1 of the preceding presentation.

Figure 10-2 (B) is a trimetric view of the B. A. C. compressor front frame. The frame basic structuring is identical to that in Figure 10-3 (B). The frame has been elongated between the outer casing hat sections to accommodate the engine secondary-air system (reference Volume III-B, Part II). The outer casing forward flange supports the engine inlet system through a conical flange with axial attachments at the four 45-degree strut locations. Four frame struts provide the extension of the inlet struts. Refer to paragraph 10.7.1.3 for engine forward mounting arrangement.

#### 10.7.1.3 Compressor Rear Frame

The following information supplements paragraph 10.3.2 of the preceding presentation.

A diagram defining strut usage and tube sizes is shown in Figure 10-17 (B).

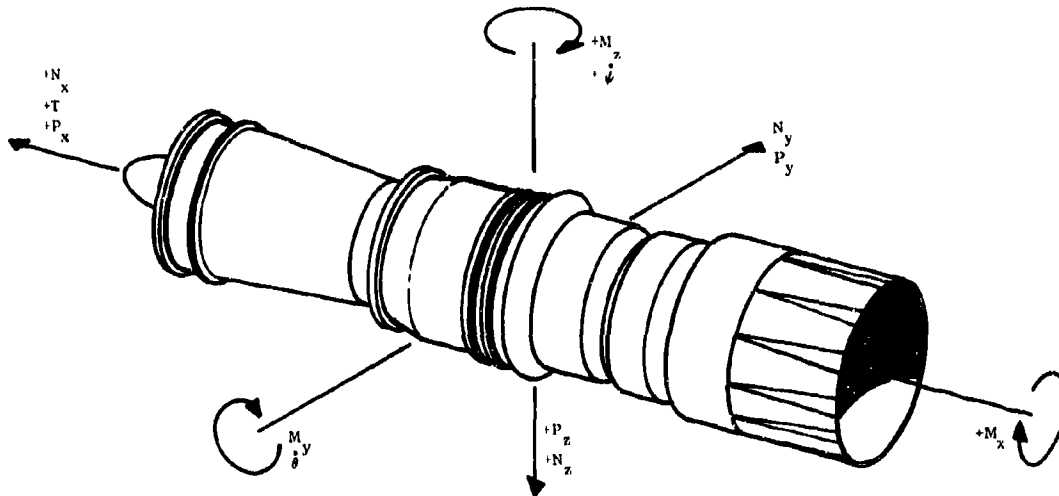
#### 10.7.1.4 Engine Mounting Arrangement

The following information supplements paragraph 10.6.5 of the preceding presentation.

Figure 10-30 (B) is schematic of the Boeing mounting system. The following loads are reacted at the forward mount plane: thrust, vertical, side, and moment about the longitudinal axis. Vertical and side loads are reacted at the aft mount.

The Boeing forward mount consists of two links attaching to the compressor front frame at 45 degrees on either side of the vertical top center. The links form a truss extending down from the support platform. The frame incorporates a spherical bearing at top center which receives a thrust link. The aft mount consists of an inverted saddle that is fitted with a spherical bearing at the engine attachment point. The saddle attachment to the support platform permits fore and aft freedom with respect to the support.

Table 10-1(B). Definition of Maneuver Modes



BOEING LIMIT LOADS

CONDITION	$N_x$	$N_y$	$N_z$	$\dot{\theta}$	$\dot{\psi}$	THRUST
UNITS	g's	g's	g's	RAD/SEC	RAD/SEC	LBS
LANDING	-	-	-	-	-	-
EMERGENCY LANDING OR DITCHING	+6.0 -4.0	-	-	-	-	-
MANEUVER	-	-	-	-	-	-
FATIGUE OR THRUST REVERSE	-	-	+2.0	-	-	136200 - 49100
SUPERSONIC MANEUVER	-	-	-2.68 +4.0	-	-	63200 0
GYROSCOPIC	-	-	-	$\pm 1.0$	-	63200 0
GYROSCOPIC	-	-	-	-	$\pm 1.5$	63200 0

CONDITION	$P_x$	$P_y$	$P_z$	$M_x$	$M_y$	$M_z$	THRUST
UNITS	LBS	LBS	LBS	IN-LBS	IN-LBS	IN-LBS	LBS
MANEUVER AERODYNAMIC	-	23K	15.4K	-	2440K	1630K	63200
MANEUVER -AERODYNAMIC	-	-23K	-15.4K	-	-2440K	-1630K	63200

- NOTE: 1. MAXIMUM TRANSIENT ROLL MOMENT DUE TO ROTOR SEIZURE -3370K IN-LBS.  
 2. ULTIMATE LOADS ARE 1.56 TIMES LIMIT LOADS EXCEPT FOR THE PITCH AND YAW ULTIMATE ANGULAR VELOCITIES WHICH ARE 2.25 RAD/SEC AND 3.0 RAD/SEC RESPECTIVELY.  
 3. GYROSCOPIC LOADS CAN ONLY BE TAKEN WHEN ENGINE IS RUNNING AT A STEADY STATE CONDITION.

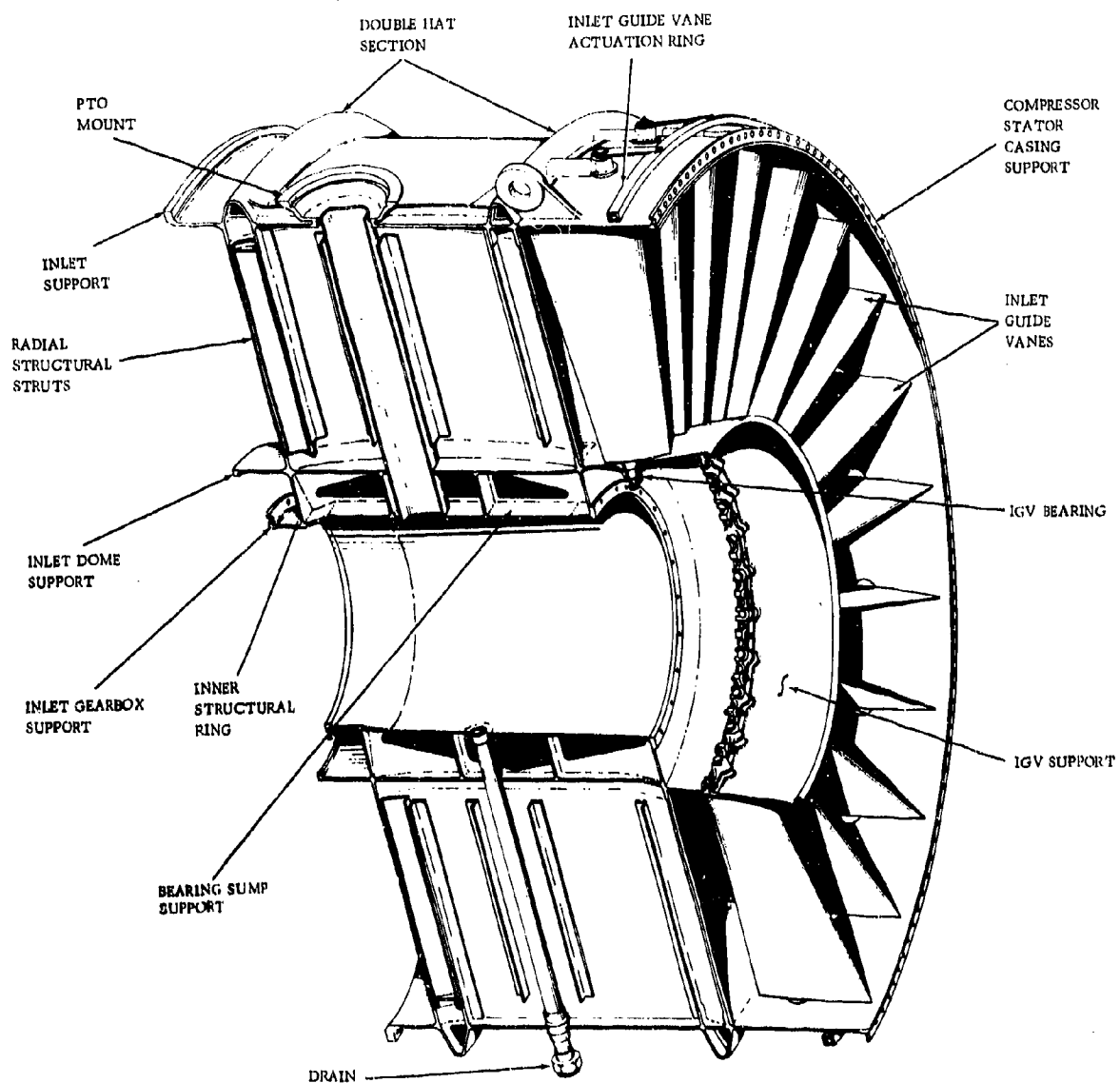


Figure 10-2(B). COMPRESSOR FRONT FRAME ASSEMBLY

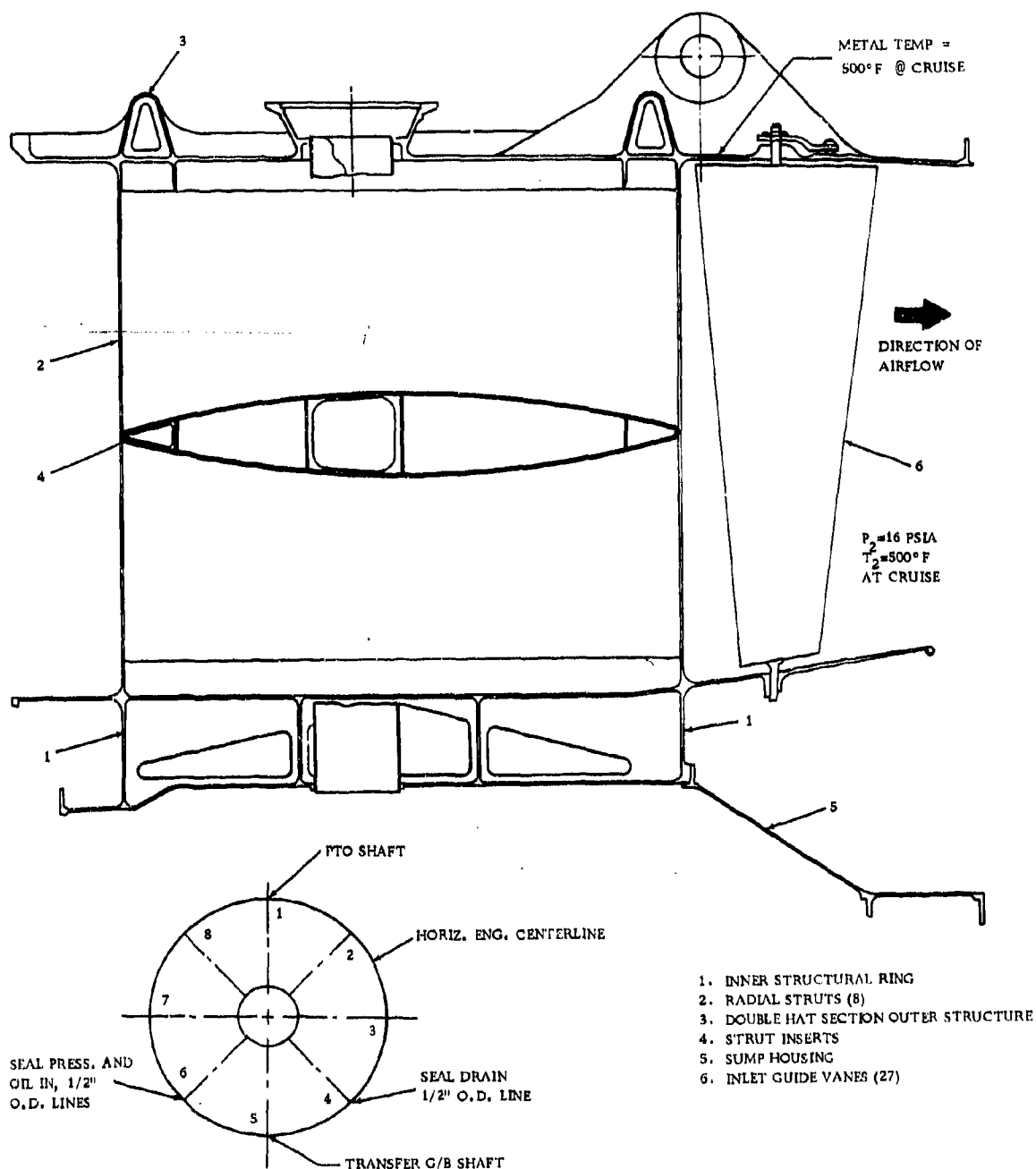
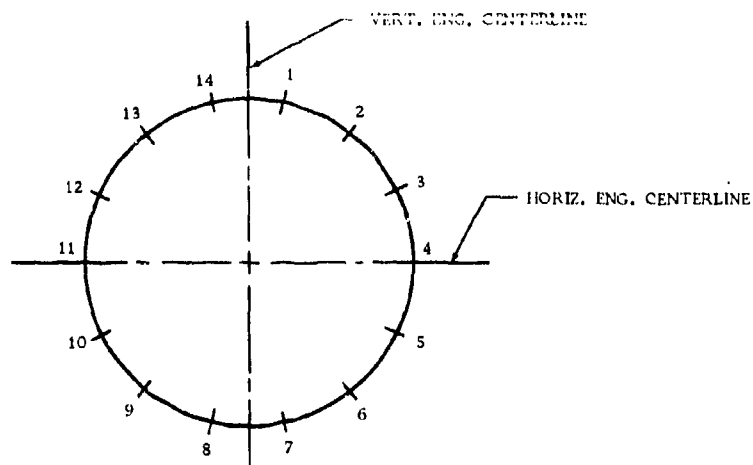


Figure 10-3(B). FRONT FRAME CROSS SECTION, STRUT USAGE, AND TUBE SIZES

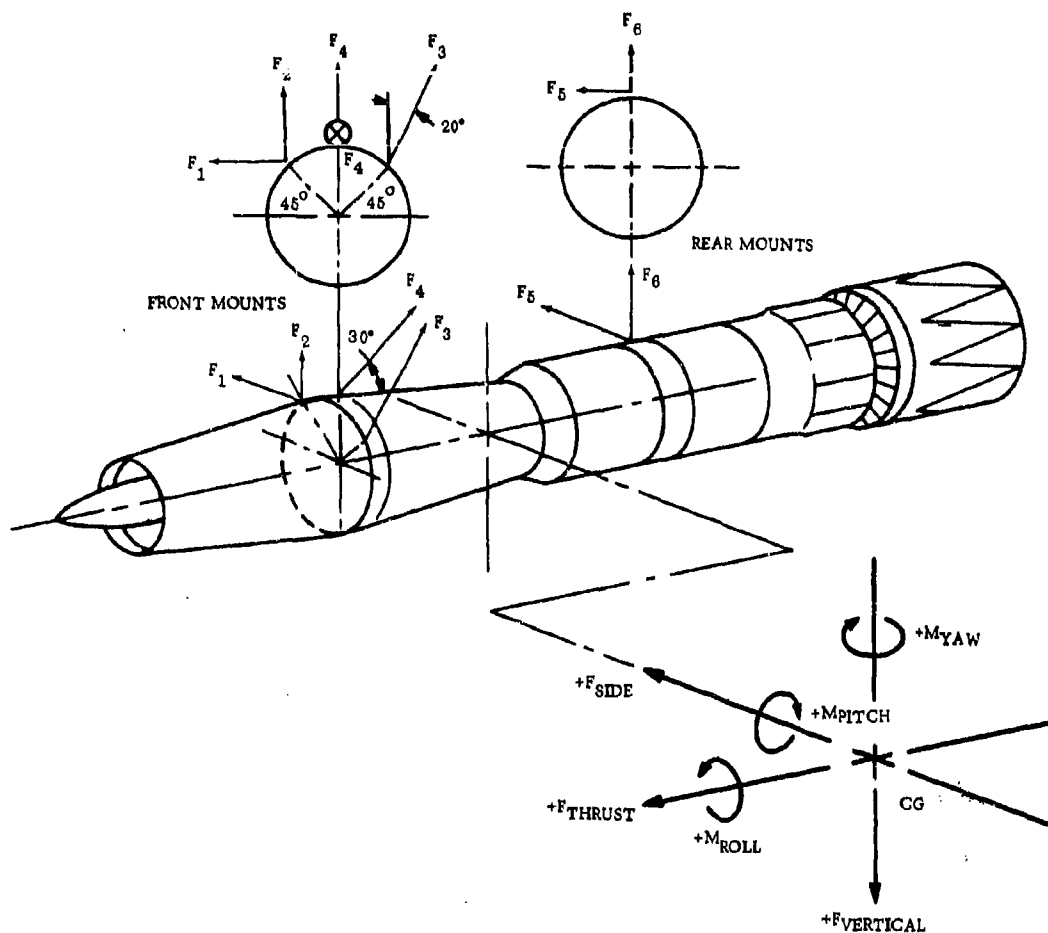


REAR VIEW LOOKING FORWARD

STRUT	USAGE
1	CUSTOMER BLEED
2	TURBINE COOLING, OIL IN & SUMP, VENT
3	CUSTOMER BLEED
4	- - -
5	ANTI-ICING
6	TURBINE COOLING & 5TH STAGE COOLING
7	ANTI-ICING
8	OIL SCAVENGE & SEAL DRAIN
9	TURBINE COOLING
10	5TH STAGE COOLING
11	- - -
12	5TH STAGE COOLING
13	TURBINE COOLING
14	CUSTOMER BLEED

8

Figure 10-17(B). COMPRESSOR REAR FRAME STRUT USAGE AND TUBE SIZES  
(BOEING INSTALLATION)



LOADING CONDITION	$F_1$	$F_2$	$F_3$	$F_4$	$F_5$	$F_6$
UNIT THRUST	-.14994	-.40980	-.43644	1.15489	.00067	.24258
UNIT SIDE	-.18038	-.85065	+.89242	0	-.58279	0
UNIT VERTICAL	.07614	.20810	.22182	0	-.00004	.58363
UNIT ROLL	-.00823	.02253	-.02397	0	.00003	0
UNIT YAW	-.00836	.00197	-.00210	0	.00764	0
UNIT PITCH	.00139	.00380	.00404	0	0	-.00780

FORCES ARE IN LBS. PER UNIT LOAD

Figure 10-30(B). ENGINE MOUNT REACTIONS FOR UNIT LOAD IN-PUT (BOEING INSTALLATION)

## 10.7 AIRFRAME COMPANY DESIGN DETAILS

### 10.7.2 LOCKHEED AIRCRAFT COMPANY DESIGN DETAILS

#### 10.7.2.1 Maneuver Loads

The following information supplements paragraph 10.1 of the preceding presentation.

The maximum design maneuver loads of components are defined in Table 10-1 (L). These loads were used in the frames' design to withstand the maximum pressure loads and temperatures of the engine operation cycle, and to withstand maneuver and inertia loads per specifications.

#### 10.7.2.2 Compressor Front Frame

The following information supplements paragraph 10.3.1 of the preceding presentation.

Figure 10-2 (L) is a trimetric view of the L.A.C. compressor front frame. The frame basic structuring is identical to Figure 10-3 (L). The outer casing forward flange supports the engine inlet system adapter through a quick-disconnect-type flange. See paragraph 10.6.5 for engine forward mounting arrangement.

#### 10.7.2.3 Compressor Rear Frame

The following information supplements paragraph 10.3.2 of the preceding presentation.

A diagram defining strut usage and tube sizes is shown in Figure 10-17 (L).

#### 10.7.2.4 Engine Mounting Arrangement

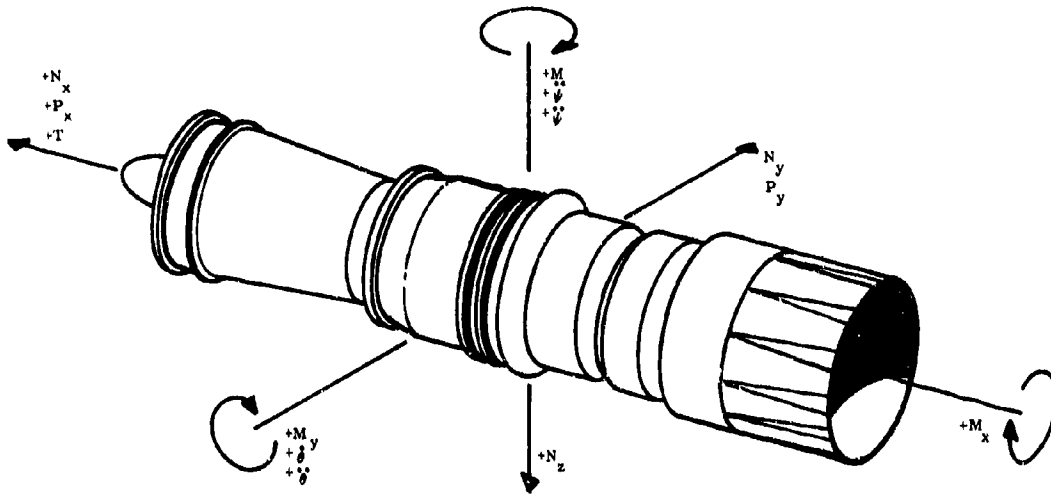
The following information supplements paragraph 10.6.5 of the preceding presentation.

Figure 10-30L is a schematic of the Lockheed mounting system. The following loads are reacted at the forward mount plane: thrust, vertical, side, and moment about the longitudinal axis. Vertical and side loads are reacted at the aft mount.

The Lockheed forward mount consists of spherical bearings and shear pins located at 45 degrees on either side of the vertical top center. The Lockheed aft mounts react vertical and horizontal forces through two links. These attach to the turbine frame by means of spherical bearings and longitudinal shear pins located at 45 degrees on either side of the top vertical. The links are hinged at their upper attachment points in order to eliminate induced effects of the supporting platform.



Table 10-1(L). Definition of Maneuver Molds



LOCKHEED LIMIT LOADS

CONDITION	$N_x$	$N_y$	$N_z$	$\ddot{\theta}$	$\ddot{\psi}$	$\ddot{\phi}$	$\ddot{\gamma}$	THRUST
UNITS	"g"	"g"	"g"	RAD/SEC <sup>2</sup>	RAD/SEC <sup>2</sup>	RAD/SEC	RAD/SEC	LBS
DYNAMIC LANDING	-	$\pm 7$	$\pm 4.75$ $-1.75$	$\pm 10.3$	-	-	-	$\pm 63200$ $-22000$
EMERGENCY LANDING	$\pm 7.0$	-	$\pm 4.75$ $-1.75$	$\pm 10.3$	-	-	-	$\pm 4000$ $0$
ENGINE POWER LOSS	$\pm 30$	$\pm 0.9$	$\pm 2.50$	-	$\pm 12$	-	$\pm 0.0$	$-80000$
VERTICAL DYNAMIC GUST	-	$\pm 8.0$	$\pm 4.78$ $-2.78$	$\pm 8.9$	-	-	-	$\pm 57600$ $-7400$
SIDE DYNAMIC GUST	-	$\pm 0.0$	$\pm 3.27$ $-1.27$	$\pm 3.69$	-	-	-	$\pm 57600$ $-7400$
PULL-UP	$\pm 5$	-	$\pm 2.82$	$\pm 20$	-	$\pm 20$	-	$\pm 63200$ $-8000$
PUSH-OVER	-	-	$-1.40$	$\pm 24$ $-20$	-	$\pm 25$	-	$\pm 63200$ $-80000$
ARBITRARY SIDE LOAD	-	$\pm 2.0$	-	-	$\pm 0.0$	-	-	-

NOTE: ULTIMATE LOADS ARE 1.5 TIMES LIMIT LOADS.

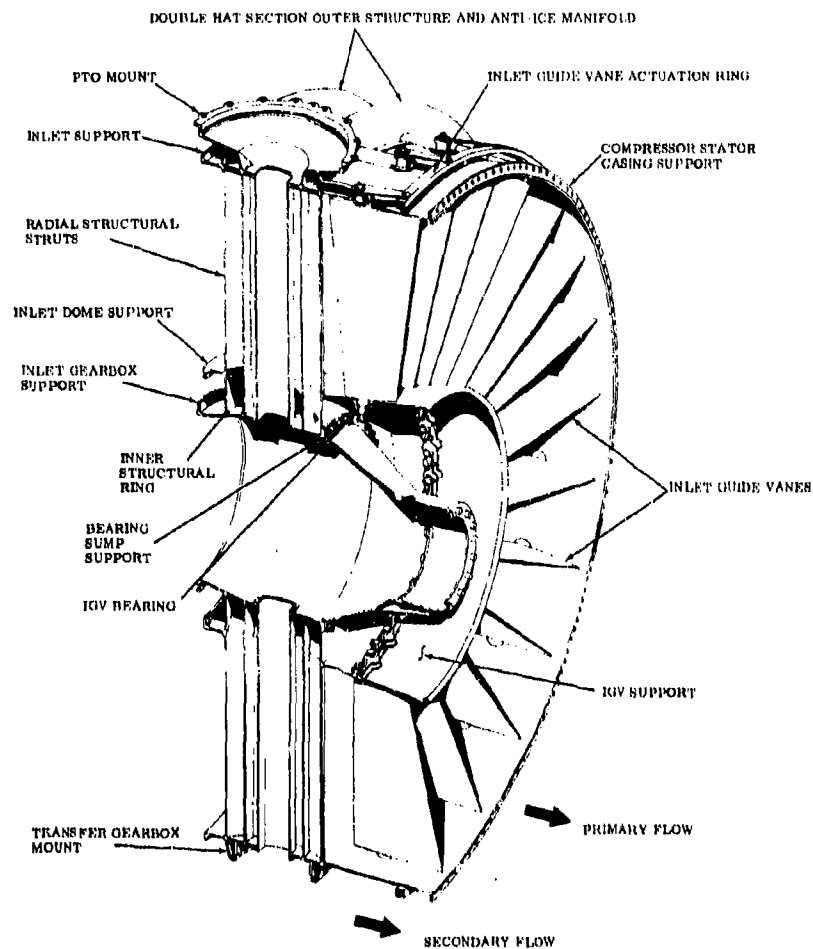


Figure 10-2(L). COMPRESSOR FRONT FRAME ASSEMBLY

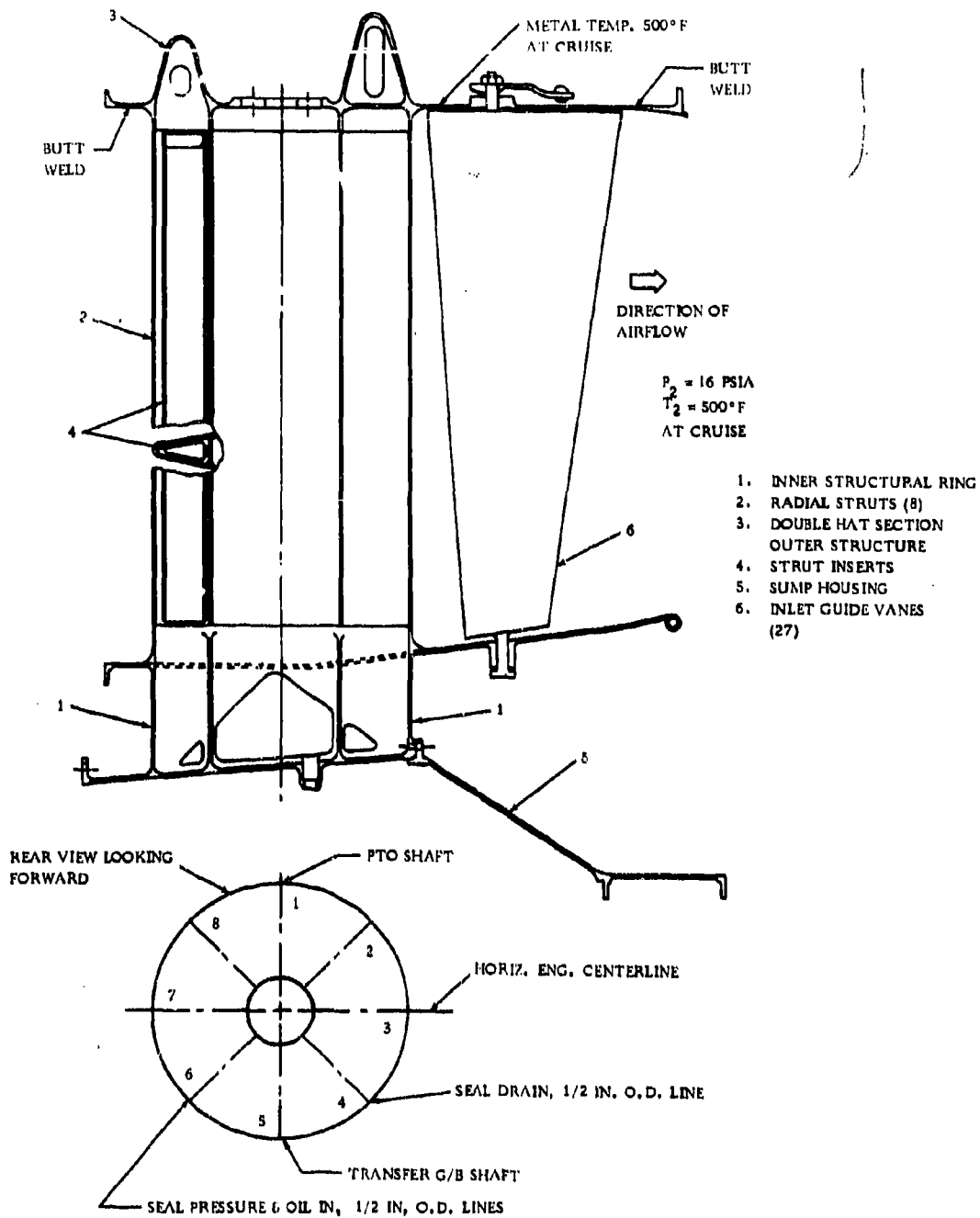
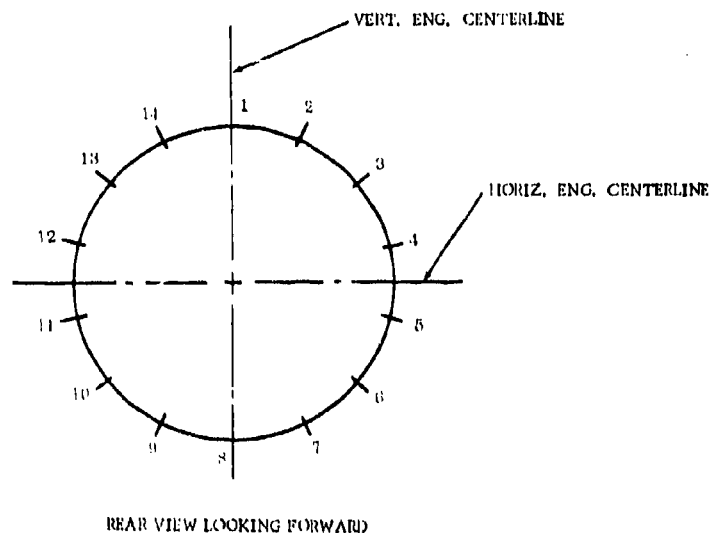
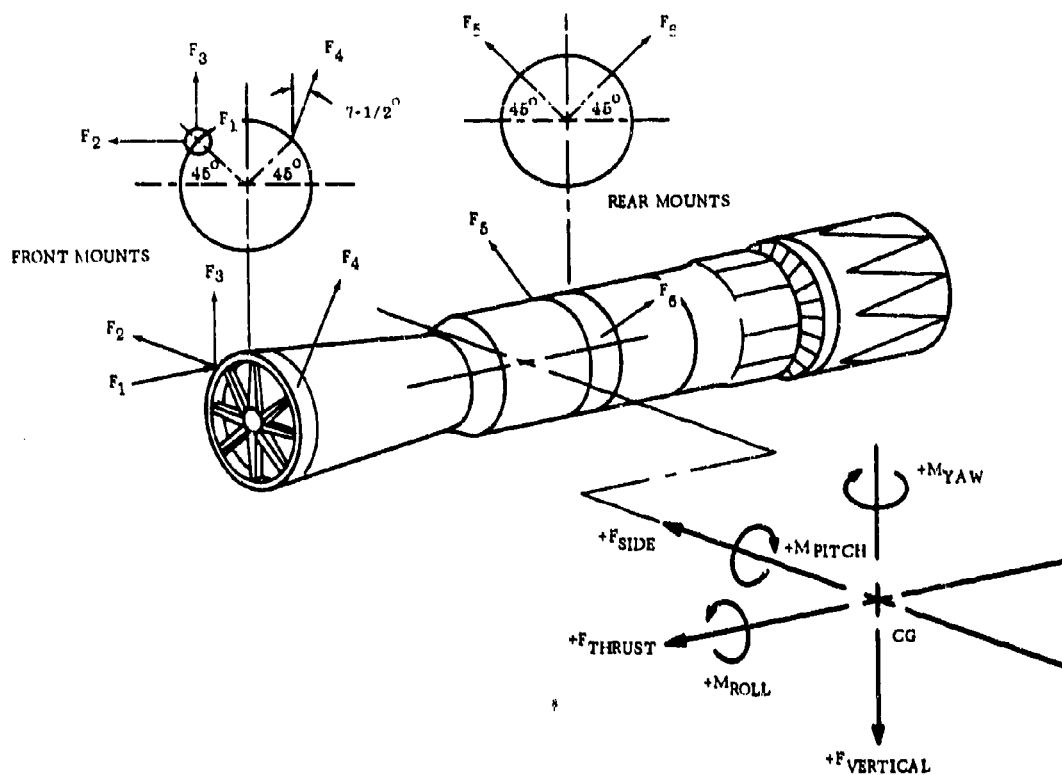


Figure 10-3(L). FRONT FRAME CROSS SECTION, STRUT USAGE, AND TUBE SIZES



STRUT	USAGE
1	ANTI-ICING
2	ANTI-ICING
3	TURBINE COOLING & 5TH STAGE COOLING
4	CUSTOMER BLEED
5	CUSTOMER BLEED
6	TURBINE COOLING
7	OIL SCAVENGE & SEAL DRAIN
8	5TH STAGE COOLING
9	" "
10	TURBINE COOLING
11	CUSTOMER BLEED
12	CUSTOMER BLEED
13	TURBINE COOLING & 5TH STAGE COOLING
14	OIL IN & SUMP VENT

Figure 10-17(L). COMPRESSOR REAR FRAME STRUT USAGE AND TUBE SIZES  
(LOCKHEED INSTALLATION)



LOADING CONDITION	F <sub>1</sub>	F <sub>2</sub>	F <sub>3</sub>	F <sub>4</sub>	F <sub>5</sub>	F <sub>6</sub>
UNIT THRUST	1	-0.1673	-0.0727	-0.0844	+0.2211	0
UNIT VERTICAL	0	+0.0120	+0.0792	+0.0010	+0.5867	+0.5867
UNIT SIDE	0	-0.1703	0	0	-0.5867	+0.5867
UNIT ROLL	0	-0.0033	+0.0281	-0.0253	0	0
UNIT PITCH	0	-0.0005	-0.0034	-0.0030	+0.0052	0.0052
UNIT YAW	0	-0.0073	0	0	+0.0052	-0.0052

FORCES ARE IN POUNDS PER UNIT LOAD

Figure 10-30(L). ENGINE MOUNT REACTIONS FOR UNIT LOAD IN-PUT (LOCKHEED INSTALLATION)

Table 10-2. Durability and Maintainability Analysis

## Part General (All Frames)

Mode of Deterioration/Failure	Design Features to Avoid Failure	Deterioration/Fault Detection During Service	Frequency of Check	Maintainability Features	Repair Method
<u>OUTER CASING/HAT SECTION</u>					
Low Cycle Fatigue	<ul style="list-style-type: none"> <li>Minimized stress concentration factor; low stress</li> </ul>	<ul style="list-style-type: none"> <li>Radiographic, fluorescent-penetrant visual inspection</li> <li>Sonic/vibration analysis</li> <li>Spring rate change analysis</li> </ul>		<ul style="list-style-type: none"> <li>Accessibility</li> </ul>	<ul style="list-style-type: none"> <li>Weld-repair</li> </ul>
High Cycle Fatigue	<ul style="list-style-type: none"> <li>Critical frequency not within steady-state operating points</li> </ul>	<ul style="list-style-type: none"> <li>Radiography, penetrant, visual inspection</li> </ul>		<ul style="list-style-type: none"> <li>Accessibility</li> </ul>	<ul style="list-style-type: none"> <li>Weld-repair</li> </ul>
<u>STRUTS</u>					
Low Cycle Fatigue Between Strut Ends	<ul style="list-style-type: none"> <li>Low stressed part</li> <li>Butt-welded structure</li> <li>Substantial fillet radii at struts</li> </ul>	<ul style="list-style-type: none"> <li>Vibration level trend</li> <li>Visual, radiography-spring rate change analysis</li> </ul>		<ul style="list-style-type: none"> <li>Accessibility</li> </ul>	<ul style="list-style-type: none"> <li>Weld-repair</li> </ul>
High Cycle Fatigue Rupture	<ul style="list-style-type: none"> <li>Low stressed part</li> <li>Butt-welded structure</li> <li>Substantial fillet radii at struts</li> <li>Critical frequency does not occur at steady-state engine operating point</li> </ul>	<ul style="list-style-type: none"> <li>Visual, radiographic, fluorescent penetrant, rate change analysis</li> </ul>		<ul style="list-style-type: none"> <li>Accessibility</li> </ul>	<ul style="list-style-type: none"> <li>Weld-repair</li> </ul>
<u>HUB</u>					
Low Cycle Fatigue	<ul style="list-style-type: none"> <li>Low stresses</li> <li>Minimized stress concentration by substantial fillet radii</li> <li>Butt-welded structure</li> </ul>	<ul style="list-style-type: none"> <li>Radiographic, visual, fluorescent penetrant</li> <li>Spring rate change analysis</li> </ul>		<ul style="list-style-type: none"> <li>Accessibility</li> </ul>	<ul style="list-style-type: none"> <li>Weld-repair</li> </ul>

Table 10-2. (Continued)

## Part General (All Frames)

Mode of Deterioration/Failure	Design Features to Avoid Failure	Deterioration/Fault Detection During Service	Frequency of Check	Maintainability Features	Repair Method
<u>SERVICE LINES</u>					
High Cycle Fatigue	<ul style="list-style-type: none"> <li>Lines clamped at intermediate points</li> <li>Critical frequency out of engine operating range</li> </ul>	<ul style="list-style-type: none"> <li>Visual, fluorescent penetrant, sump pressure analysis</li> <li>Pressure instrumentation</li> </ul>		<ul style="list-style-type: none"> <li>Induction braze joints</li> </ul>	<ul style="list-style-type: none"> <li>Replace line</li> </ul>
Coking or Gumming of Oil, Vent, Seal Drain Lines	<ul style="list-style-type: none"> <li>Heat shields on lines</li> <li>Vent line isolated by oil lines</li> </ul>	<ul style="list-style-type: none"> <li>Oil pressure and temperature trends</li> <li>Sump pressure analysis</li> <li>Radiographic analysis</li> </ul>		<ul style="list-style-type: none"> <li>Induction braze joints</li> </ul>	<ul style="list-style-type: none"> <li>Clean</li> <li>Replace line</li> </ul>
Low Cycle Fatigue	<ul style="list-style-type: none"> <li>Thermal loops provided</li> </ul>	<ul style="list-style-type: none"> <li>Visual, fluorescent penetrant</li> </ul>		<ul style="list-style-type: none"> <li>Induction braze joints</li> </ul>	<ul style="list-style-type: none"> <li>Replace line</li> </ul>
Line Wear	<ul style="list-style-type: none"> <li>Wear sleeves</li> </ul>	<ul style="list-style-type: none"> <li>Visual inspection</li> </ul>		<ul style="list-style-type: none"> <li>Induction braze</li> </ul>	<ul style="list-style-type: none"> <li>Replace wear sleeves</li> </ul>
<u>SUMP</u>					
High Cycle Fatigue	<ul style="list-style-type: none"> <li>Low stressed part</li> <li>Critical frequency not within steady-state operating points</li> </ul>	<ul style="list-style-type: none"> <li>Visual, radiographic, fluorescent penetrant</li> <li>Spring rate change analysis, sump pressurization (AIDS)</li> </ul>		<ul style="list-style-type: none"> <li>Separately removable from frames</li> </ul>	<ul style="list-style-type: none"> <li>Welding</li> </ul>
Low Cycle Fatigue	<ul style="list-style-type: none"> <li>Thermal loops provided where necessary</li> </ul>	<ul style="list-style-type: none"> <li>Visual, radiographic, fluorescent penetrant</li> </ul>		<ul style="list-style-type: none"> <li>Separately removable from frames</li> </ul>	<ul style="list-style-type: none"> <li>Welding</li> </ul>
Coking and/or Gumming	<ul style="list-style-type: none"> <li>Heat shields are used</li> <li>Low temperature plenum around sump</li> </ul>	<ul style="list-style-type: none"> <li>Visual inspection</li> <li>Oil pressure and temperature trend analysis</li> </ul>		<ul style="list-style-type: none"> <li>Separately removable from frame</li> </ul>	<ul style="list-style-type: none"> <li>Clean</li> <li>Replaceable heat shields</li> </ul>

Table 10-2. (Continued)

Part General (All Frame)

Mode of Deterioration/Failure	Design Features to Avoid Failure	Deterioration/Fault Detection During Service	Frequency of Check	Maintainability Features	Repair Method
Warped Flanges	<ul style="list-style-type: none"> <li>Adequate thickness</li> </ul>	<ul style="list-style-type: none"> <li>Visual inspection</li> <li>Sump pressure check analysis</li> <li>Oil pressure analysis</li> </ul>		<ul style="list-style-type: none"> <li>Separately removable from frames</li> <li>Extra material on flanges</li> </ul>	<ul style="list-style-type: none"> <li>Flame-spray - remachine</li> </ul>



Table 10-2. (Continued)

## Part Compressor Front Frame

Mode of Deterioration/Failure	Design Features to Avoid Failure	Deterioration/Fault Detection During Service	Frequency of Check	Maintainability Features	Repair Method
<u>HUB</u> High Cycle Fatigue	<ul style="list-style-type: none"> <li>• Low stresses</li> <li>• Minimizes stress concentration by substantial fillet radii</li> <li>• Butt-welded structure</li> </ul>	<ul style="list-style-type: none"> <li>• Radiography, visual inspection</li> <li>• Sonic/vibration analysis</li> <li>• Spring rate change analysis</li> </ul>		<ul style="list-style-type: none"> <li>• Accessible</li> </ul>	<ul style="list-style-type: none"> <li>• Weld-repair</li> </ul>
<u>IGV'S</u> High Cycle Fatigue Fracture of Skins	<ul style="list-style-type: none"> <li>• Large braze areas critical frequency not within steady-state operating points</li> </ul>	<ul style="list-style-type: none"> <li>• Radiography, penetrant, visual inspection</li> </ul>		<ul style="list-style-type: none"> <li>• Individually replaceable with frame assembly removed</li> </ul>	<ul style="list-style-type: none"> <li>• Replace as required</li> </ul>
Low Cycle Fatigue due to Internal Pressure	<ul style="list-style-type: none"> <li>• Minimized stress concentration factors</li> </ul>	<ul style="list-style-type: none"> <li>• Radiography, penetrant, visual inspection</li> </ul>		<ul style="list-style-type: none"> <li>• Adaptable to material build-up</li> </ul>	<ul style="list-style-type: none"> <li>• Weld-repair</li> </ul>
FOD, Birds, and Ice	<ul style="list-style-type: none"> <li>• Low deflection adequate stiffeners to absorb impact</li> </ul>	<ul style="list-style-type: none"> <li>• Compressors trend performance</li> <li>• Visual, sonic analysis</li> </ul>			<ul style="list-style-type: none"> <li>• Blend out defects</li> </ul>
Bearing Wear	<ul style="list-style-type: none"> <li>• Replaceable</li> </ul>	<ul style="list-style-type: none"> <li>• Visual - looseness check</li> <li>• Sonic/vibration analysis</li> </ul>			<ul style="list-style-type: none"> <li>• Flame-spray</li> </ul>
STRUT ADAPTER ENGINE MOUNT UNIBAL OR PIN					
Galling and Wear	<ul style="list-style-type: none"> <li>• Low stress use of hard material with anti-seize and anti-galling characteristics</li> </ul>	<ul style="list-style-type: none"> <li>• Visual - looseness check</li> <li>• Sonic/vibration analysis</li> </ul>		<ul style="list-style-type: none"> <li>• Removable insert</li> </ul>	<ul style="list-style-type: none"> <li>• Replace as required</li> <li>• Flame-spray</li> </ul>

Table 10-2. (Continued)

## Part Compressor Front Frame

Mode of Deterioration/Failure	Design Features to Avoid Failure	Deterioration/Fault Detection During Service	Frequency of Check	Maintainability Features	Repair Method
Tensile Fracture Failure <u>INNER DIFFUSER</u>	<ul style="list-style-type: none"> <li>Low stresses</li> </ul>	<ul style="list-style-type: none"> <li>Spring rate change analysis</li> </ul>			<ul style="list-style-type: none"> <li>Replace</li> </ul>
Low Cycle Fatigue	<ul style="list-style-type: none"> <li>Substantial fillet radii to prevent stress concentration</li> <li>Butt-welded structure</li> </ul>	<ul style="list-style-type: none"> <li>Visual, radiography, fluorescent penetrant inspection</li> <li>Spring rate change analysis</li> <li>Sonic/vibration analysis</li> </ul>		<ul style="list-style-type: none"> <li>Accessible</li> </ul>	<ul style="list-style-type: none"> <li>Weld-repair</li> </ul>
High Cycle Fatigue	<ul style="list-style-type: none"> <li>Substantial fillet radii to prevent stress concentration</li> <li>Butt-welded structure</li> </ul>	<ul style="list-style-type: none"> <li>Visual, radiography, fluorescent penetrant inspection</li> </ul>		<ul style="list-style-type: none"> <li>Accessible</li> </ul>	<ul style="list-style-type: none"> <li>Weld-repair</li> </ul>

Table 10-2. (Continued)

## Part Compressor Rear Frame

Mode of Deterioration/Failure	Design Features to Avoid Failure	Deterioration/Fault Detection During Service	Frequency of Check	Maintainability Features	Repair Method
<b>TURBINE AIR CON-SERVATION VALVE</b>					
High Cycle Fatigue Failure of Pins	<ul style="list-style-type: none"> <li>• Critical frequency out of operating range</li> </ul>	<ul style="list-style-type: none"> <li>• Actuation force analysis</li> <li>• Radiography, penetrant, visual analysis</li> </ul>		<ul style="list-style-type: none"> <li>• Removable pins</li> </ul>	<ul style="list-style-type: none"> <li>• Replace</li> </ul>
Pin Failure at Valve due to Wear from Vibration	<ul style="list-style-type: none"> <li>• Pin hard-coated to minimize wear</li> <li>• Valve kept from vibration by constant gas loading</li> </ul>	<ul style="list-style-type: none"> <li>• Sonic/vibration analysis</li> </ul>		<ul style="list-style-type: none"> <li>• Removable pins, valves, seats</li> </ul>	<ul style="list-style-type: none"> <li>• Replace pin</li> </ul>
Buckling of Valve Seat Cone	<ul style="list-style-type: none"> <li>• Low stresses with margin for tolerances</li> <li>• Force level margin sufficient to prevent failure in open position only</li> </ul>	<ul style="list-style-type: none"> <li>• Performance</li> </ul>		<ul style="list-style-type: none"> <li>• Removable</li> </ul>	<ul style="list-style-type: none"> <li>• Replace</li> </ul>
<b>LINERS AND FAIR-LINGS</b>					
Fatigue Cracking	<ul style="list-style-type: none"> <li>• Circumferential stiffeners plus dimples to increase rigidity</li> <li>• Low stress concentration factors</li> </ul>	<ul style="list-style-type: none"> <li>• Visual, fluorescent penetrant, radiography inspection</li> <li>• Spring rate change analysis</li> <li>• Sonic/vibration analysis</li> </ul>		<ul style="list-style-type: none"> <li>• Individually replaceable components</li> </ul>	<ul style="list-style-type: none"> <li>• Weld-repair</li> <li>• Replace as required</li> </ul>
Erosion/Oxidation and Buckling	<ul style="list-style-type: none"> <li>• Erosion resistant material selection</li> <li>• Low comb. carbon content</li> <li>• Uniform temperature profile</li> </ul>	<ul style="list-style-type: none"> <li>• Borescope inspection</li> </ul>			

Table 10-2. (Continued)

## Part Turbine Frame

Mode of Deterioration/Failure	Design Features to Avoid Failure	Deterioration/Fault Detection During Service	Frequency of Check	Maintainability Features	Repair Method
<u>STRUT</u> Cracking	<ul style="list-style-type: none"> <li>• Semi-tangential strut</li> <li>• Heated hat sections</li> <li>• Consideration of manufacturing tolerances</li> <li>• Bolted structure</li> </ul>	<ul style="list-style-type: none"> <li>• Visual, fluorescent penetrant, radiography analysis</li> <li>• Spring rate change analysis</li> <li>• Sonic/vibration analysis</li> </ul>		<ul style="list-style-type: none"> <li>• Struts are individually replaceable</li> </ul>	<ul style="list-style-type: none"> <li>• Weld-repair</li> <li>• Replace as required</li> </ul>
<u>OUTER CASING</u> Stress Rupture	<ul style="list-style-type: none"> <li>• Use cooling air to keep operating temperature within acceptable limits</li> </ul>	<ul style="list-style-type: none"> <li>• Time-temperature integration</li> <li>• <math>P_5</math>, <math>T_5</math>, <math>A_8</math> trend</li> </ul>		<ul style="list-style-type: none"> <li>• Individually replaceable</li> </ul>	<ul style="list-style-type: none"> <li>• Weld-repair</li> <li>• Replace as required</li> </ul>

**SUPPLEMENTARY**

**INFORMATION**

# ERRATA SHEET

**AD 378484L**

October 12, 1966

GE4 PHASE III PROPOSAL

VOLUME III - TECHNICAL/ENGINE - B. ENGINE DESIGN REPORT - PART I - MAJOR COMPONENTS

## NOW READS

1. Page 4-79, Fig. 4.4-6
2. Page 8-8, Par. 8.3.2  
"Two oil jets are provided for the bearing to increase reliability by providing redundant lubrication for this critical area. (See Fig. 8-6.)"
3. Page 8-10, Par. 8.3.4  
".....This arrangement eliminates large external recoup lines on the outside of the engine. (See Fig. 8-7.)"
4. Page 8-14, Par. 8.3.5.1  
"A plot of corrected rotor thrust versus corrected speed ( $F/S_2$  versus  $N/50$ ) is given in Figure 8-8 for the GE4 rotor."
5. Page 8-15, Fig. 8-8  
" (On Abscissa) Corrected Shaft Speed -  $PCN/50$ "
6. Page 8-19, Par. 8.3.7  
" . The vent lines are surrounded by oil-in lines to prevent coke build-up inside them. (See Figures 8-2 and 8-5)."
7. Page 9-1/9-2, Par. 9.2  
"....pad type, gear sizes, accessory weights moments and other details.."
8. Page 9-3/9-4, Fig. 9.1  
Chart entitled "Bevel Gear Data"  
(Lower right hand corner)

	Life (Hours) Min.
	.12000
	.12000

## SHOULD READ

- The measured metal point on the second line at 1680°F is printed in error and should be eliminated.
- "Two oil jets are provided for the bearing to increase reliability by providing redundant lubrication for this critical area. (See Fig. 8-2, 8-3 and 8-6.)"
- ".....This arrangement eliminates large external recoup lines on the outside of the engine."
- "A plot of corrected rotor thrust versus corrected speed ( $F/S_2$  versus  $PCN/\sqrt{\theta_2}$ ) is given in Figure 8-8 for the GE4 rotor."
- " (On Abscissa) Corrected Shaft Speed -  $PCN/\sqrt{\theta_2}$ "
- " . The vent lines are surrounded by oil-in lines to prevent coke build-up inside them. (See Figures 8-2 and 8-6)."
- "....pad type, gear sizes and other details...."

	Life (Hours) Min.
	12000
	12000

# ERRATA SHEET

AD 378484L

October 12, 1966

GE4 PHASE III PROPOSAL

VOLUME III - TECHNICAL/ENGINE - B. ENGINE DESIGN REPORT - PART I - MAJOR COMPONENTS

## NOW READS

## SHOULD READ

9. Page 9-3, 9-4

Air/Oil Separator				
Double Idler	Ball Roller	40 x 68 x 15 20 x 42 x 12	3610 3741	$4.79 \times 10^5$ $2.52 \times 10^6$
Idler	Ball Roller	50 x 110 x 27 40 x 90 x 23	10700 17242	12154 12566

10. Page 9-5, Part 1, Fig. 9-2

A/B Pump  
C-25 HP  
T-190 HP  
S-100 Lb-in

A/B Pump  
C-25HP  
T-190HP  
S-1000 Lb-in

11. Page 9-6, Par. 9.3.1

".....requirements. This POT position permits....."

".....requirements. This PTO position permits....."

12. Page 9-7, Par. 9.3.2

"....of the customer accessory gearbox in the engine wing."

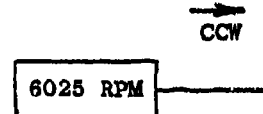
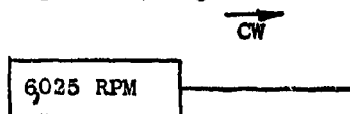
"....of the customer accessory gearbox in the airframe wing."

13. Page 9-9, Par. 9.3.7

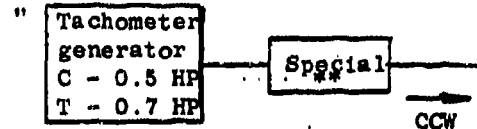
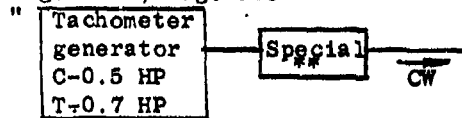
".....Nitralloy material. Minimum web wall thickness of ....."

".....Nitralloy material. Minimum wall thickness of ....."

14. Page 9-20, Fig. 9-5



15. Page 9-20, Fig. 9-5



16. Page 10-23, Par. 10.3.3.1

"...This permits of manufacture and maintenance"

"....This permits ease of manufacture and maintenance"